



NORTH LINK

PRELIMINARY ENGINEERING VIBRATION CONTROL FOR THE NORTH LINK PREFERRED ALTERNATIVE AT THE UNIVERSITY OF WASHINGTON

*Sound Transit
North Link Light Rail Project*

**April 2006
CIN 2911-0604-1679**

**Prepared by
Puget Sound Transit Consultants**





WILSON, IHRIG & ASSOCIATES, INC.
ACOUSTICAL CONSULTANTS

5776 BROADWAY
OAKLAND, CA
U.S.A. 94618-1531

Tel: (510) 658-6719

Fax: (510) 652-4441

E-mail: info@wiai.com

Web: www.wiai.com

**PRELIMINARY ENGINEERING VIBRATION CONTROL
FOR THE NORTH LINK PREFERRED ALTERNATIVE
AT THE UNIVERSITY OF WASHINGTON**

CIN 2100-0604-1679

17 April 2006

Submitted to:

**Puget Sound Transit Consultants
401 South Jackson Street
Seattle Washington
98104-2826**

By:

**James T. Nelson, Ph.D., P.E
Vice President**

**Andrew Jessop
Assistant Consultant**

TABLE OF CONTENTS

1	INTRODUCTION	1-1
2	IMPACT CRITERIA	2-1
3	PREDICTION METHODOLOGY.....	3-1
3.1	Force Density Level.....	3-1
3.2	Line Source Response.....	3-3
4	VEHICLE FORCE DENSITY LEVELS.....	4-1
4.1	Kinkisharyo Force Density Tests at VTA.....	4-2
4.2	Rail Undulation and Wheel Run-out.....	4-4
4.3	Comparison with Other Vehicles.....	4-8
4.4	Uncertainty in FDL	4-11
5	LINE SOURCE RESPONSE DETERMINATION.....	5-1
5.1	Borehole LSR Tests	5-1
	Measurement Locations	5-2
	Procedure	5-3
	LSR Uncertainties	5-8
5.2	Numerically Calculated Line Source Responses	5-16
	Numerical Procedure	5-16
	Calibration with Tests Results	5-17
6	VIBRATION PREDICTIONS FOR STANDARD TRACK AND DESIGN SPEED	6-1
6.1	Assumptions.....	6-1
6.2	Predicted Ground Surface Vibration.....	6-2
6.3	Basement Vibration Levels.....	6-4
6.4	Example of Ground Vibration at Toronto.....	6-4
6.5	Two Trains versus One Train	6-7
6.6	Uncertainty of the Predicted Levels.....	6-7
7	IMPACT MITIGATION	7-1
7.1	Vibration Control Provisions	7-1
	Floating Slab Track.....	7-2

GERB Floating Slab	7-2
16Hz Double Tie Floating Slab	7-5
High Compliance Direct Fixation Fasteners.....	7-9
Moveable Point Frog.....	7-9
Speed Reduction to 30mph	7-10
Rail Grinding and Rail Corrugation Control	7-12
Wheel Truing Machines.....	7-12
Rail Straightness Specification	7-13
7.2 Predicted Ground Surface Vibration with Proposed Vibration Control Provisions ..	7-15
8 GROUND BORNE NOISE IN BUILDINGS	8-1
8.1 Criteria for Ground-Borne Noise	8-1
8.2 Estimated A-Weighted Noise Levels.....	8-1
9 MONITORING.....	9-1
9.1 Pre-Revenue Service Monitoring.....	9-3
9.2 Permanent Monitoring	9-4
10 CONCLUSION.....	10-1
10.1 Ground Surface Vibration.....	10-1
10.2 Ground-Borne Noise.....	10-3
APPENDIX A: LINE SOURCE RESPONSE TESTS	
APPENDIX B: NUMERICAL MODELING OF LINE SOURCE RESPONSES	
APPENDIX C: KINKISHARYO FDL TESTS AT VTA	
APPENDIX D: VIBRATION PREDICTIONS	
APPENDIX E: VIBRATION PREDICTIONS FOR PROPOSED MITIGATION	

TABLES

Table 2-1	UW Requested Thresholds: Vertical Root-Mean-Square Velocity Level - dB re 1 micro-in/sec.....	2-4
Table 5-1	Borehole Test Locations	5-3
Table 6-1	Predicted Velocity Levels and UW Thresholds - Maximum over Train Operating Speed Range – Two Trains - Standard DF Fasteners on Rigid Invert.....	6-3
Table 7-1	Insertion Losses Estimated by GERB for a Continuous Poured-in-Place Floating Slab with Design Resonance 4Hz	7-3
Table 7-2	Vibration Transmission of Proposed Track Vibration Isolation Provisions Relative to Those of Standard DF Track.....	7-9
Table 7-3	Energy Mean and UW Threshold Velocity Levels for Two 30mph Trains	7-17
Table 8-1	FTA Ground-Borne Noise Impact Criteria	8-1
Table 8-2	Adjustment Factors in Decibels to be Added to Ground Surface Vibration Velocity Levels in dB re 1micro-in/sec to Obtain Ground Borne Noise Level Estimates ..	8-2
Table 8-3	Maximum Ground Borne A-Weighted Noise Levels for Various Buildings for 4-Car Trains at 30 to 55mph – dBA re 20 Micro-Pascal.....	8-3
Table 10-1	Comparison of Predicted Exterior Ground Surface Vibration Velocity Levels with UW Threshold for Two Trains	10-4

FIGURES

Figure 1-1	Map of Campus.....	1-3
Figure 4-1	FDL for VTA Kinkisharyo on Resilient Direct Fixation Fasteners with Dynamic Stiffness of 140,000 lb/in and Fastener Separation of 30in	4-7
Figure 4-2	Measured Force Density Levels for Various Transit Vehicles	4-10
Figure 4-3	Comparison of Mean FDL, and Mean FDL Plus One Standard Deviation for Test Vehicles Operated On Ballast-and-Concrete Tie Track with Continuous Welded Rail at 45mph	4-12
Figure 5-1	Time Domain Average of Response at NB-255 for 0.5-Second Window – 0.1 Second per Division.....	5-6
Figure 5-2	Time Domain Average of Response at NB-255 for 2-Second Window – 0.1 Second per Division.....	5-7
Figure 5-3	Effect of Transfer Function Component Averaging	5-14
Figure 5-4	Line Source Responses Estimated for Four Boreholes.....	5-15
Figure 5-5	Line Source Responses Calculated from Seismic Wave Velocity Profiles	5-18
Figure 5-6	Measured LSR relative to Theoretical LSR.....	5-19
Figure 6-1	Example of Long Range Ground Vibration Propagation at Toronto.....	6-6
Figure 7-1	Floating Slab Performance Data	7-8
Figure 7-2	Vibration Control Provisions	7-11

1 INTRODUCTION

This report concerns the Preliminary Engineering design for ground borne noise and vibration control for operation of Sound Transit's North Link Preferred Alternative alignment through the University of Washington campus in Seattle, Washington. The alignment and UW buildings are illustrated in Figure 1-1. The civil station limits of the study extend from 1200+00, at the southern boundary of the campus, to the Brooklyn Station at 1259+00. This study is limited to those buildings on the University of Washington campus that have been identified by the University of Washington as vibration sensitive, and to campus buildings along the alignment that might be impacted by ground-borne noise. The principal focus of the report is ground borne vibration control for sensitive basement level laboratory spaces.

The Preliminary Engineering work includes line source response tests, shear wave velocity surveys, theoretical modeling of vibration propagation and line source responses, measurement of the vibration force characteristics of a vehicle similar to the one Sound Transit is purchasing for the Initial Segment, extensive interaction with interested parties (stake holders) of the University of Washington campus, and use of archival data for vibration control provisions. The work was conducted by Wilson, Ihrig & Associates under subcontract to the joint venture of Puget Sound Transit Consultants. GeoRecon served as a subcontractor to Wilson, Ihrig & Associates for the collection of geophysical data at three boreholes on campus.

The remainder of the report is organized as follows.

Chapter 2 concerns design goals and performance standards that were arrived at through consultation with the University staff. Of paramount concern on the part of the University staff are impacts on the existing vibration environments of current and future research.

Chapter 3 outlines the prediction methodology, based on procedures described in the Federal Transit Administration (FTA) manual for rail transit noise and vibration impact

analysis,¹ with modifications as appropriate for this site. The concepts of Force Density Level and Line Source Response as defined in the FTA manual are the primary metrics used for prediction.

Chapter 4 describes the Force Density Levels (FDL) measured for the Kinki Sharyo vehicle at the Valley Transportation Authority (VTA) in San Jose, California. FDLs for train speeds of 20mph up to 55mph in 5mph increments were obtained.

Chapter 5 concerns the determination of Line Source Responses by borehole transfer mobility tests (propagation tests) at four locations within the study area, and by theoretical modeling based on shear wave velocity profiles measured by GeoRecon. The model results were adjusted to match measured Line Source Responses at short range and used to predict vibration at distances beyond the effective range of the borehole tests.

Chapter 6 concerns the predicted ground vibration at various buildings located near the alignment for standard resilient direct fixation track. These predictions form the baseline vibration estimates for the project.

Chapter 7 concerns mitigation strategies for vibration control, including floating slab track, reduced train speed, single train operation, rail straightness, rail grinding, wheel truing, moveable point frogs, and increased maintenance. Predicted ground vibration levels for floating slab track and high compliance fasteners are provided.

Chapter 8 briefly describes the potential for ground borne noise impacts, based on predicted one-third octave vibration velocity levels and conversions to one-third octave sound pressure levels. Noise levels are presented in terms of A-weighted levels.

Chapter 9 outlines a vibration monitoring plan and measurement protocol.

¹ **Transit Noise and Vibration Impact Assessment**, U.S. Department of Transportation, Federal Transit Administration, April 1995.

2 IMPACT CRITERIA

This section concerns UW vibration criteria and design goals for the North Link alignment through the UW campus. These criteria are based on ambient third octave vibration levels provided by the University of Washington.

The UW considers the current ambient vibration environment as a fundamental resource that must be preserved to protect current and future vibration sensitive research. Current research on the UW campus includes a variety of experiments in physics, chemistry, biology, engineering, and other major fields. Many of these experiments involve gravitation, molecular structures, and nanotechnology.² The state of the art in these latter areas involves geometries of the order of the hydrogen atom, and are therefore of particular concern with respect to laboratory vibration environments. Providing low vibration environments for laboratory research can be an important factor in attracting talent and funding, not just at the UW, but at virtually every institution involved in nano-scale research. The competition between research institutions and scientists in this area is intense. The sensitivity of laboratory research to vibration is likely to increase over time with decreasing geometric scales. Regardless of the actual sensitivity, even the perception of possible vibration due to rail operations can be a factor in funding requests and hiring with respect to nano-scale research. Thus, preserving a low vibration environment is in the interests of the University of Washington and the community as a whole.

Consistent with this perspective, the UW has defined impact criteria for all light rail alignments during operation as follows:

“In order to preserve the ambient condition for current and future research activities on the UW campus, the UW wishes Sound Transit to design a train that limits the ST Vibration to be equal to or less than the measured ambient vibration spectra at each building foundation as listed in the attached graph. For this purpose, ambient will be defined as the linear average (energy average) root mean square amplitudes at the

² The prefix “nano” refers to a factor of 10^{-9} . The term “nano-scale” refers to geometries of the order of 10^{-9} m, or one billionth of a meter. For example, the wavelength of light is of the order of 100nm, and the diameter of the hydrogen atom is of the order of 0.1nm, where the unit “nm” is an abbreviation for “nano-meter”.

building foundation as measured by the UW. The train generated vibration levels should be expressed in terms of maximum amplitude per each 1/3 octave band frequency determined at the distance of closest approach for each building under consideration. Using these definitions, the UW requests that the train vibration levels be less than or equal to the current ambient vibration levels. This criteria needs to be met using source mitigation only.”

The UW has provided background vibration spectra to further define the impact criteria for many of its buildings, based on narrow-band Fourier analyses of single twenty-second samples of vibration obtained at each building by the UW’s consultant. These Fourier spectra were converted to third octave band vibration velocities by the UW’s consultant, and are listed in Table 2-1. These data are one-third octave vibration levels in decibels relative to 1 $\mu\text{in/sec}$ (10^{-6}in/sec), variously abbreviated as “dB”, “VdB”, “dBV”, etc., and denoted here as L_V . The corresponding velocity, V in micro-in/sec, is given by:³

$$V(\mu\text{in/sec}) = 10^{(L_V(\text{dB})/20)}$$

Henceforth, these ambient levels will be referred to as the “UW Thresholds”, “UW Ambient Vibration Levels”, or, simply, the “UW Ambient Levels”.

Recognizing UW’s request to maintain low ambient vibration levels during train operations, the UW Thresholds are used as a design goal for the Link LRT to minimize potential vibration effects on future research activities. Sound Transit proposes to limit vibration on the UW campus as much as practicable with vibration control provisions that have demonstrated records of performance.

The uncertainty in measuring third-octave vibration consists of systematic errors and random errors. The systematic error is typically about 1dB or less, and includes errors in instrumentation

³ The English units of in/second and micro-inch/second are employed here for ground vibration. This is a matter of historical usage. Vibration may also be described with metric units, eg 1 micro-meter/second, or micron/second. There are 39.38 micro-inches per micro-meter, and thus 39.38 micro-inches/second per micro-meter/second. For practical conversions, one may assume that there are 40micro-in per micro-meter, and so on.

frequency response, attenuator errors, amplifier errors, and detector errors. Random error is related to the nature of the vibration being measured. Random vibration analog data filtered through third-octave filters fluctuate about some root-mean-square amplitude, and the fluctuation will decrease with increasing averaging time. For an averaging time of 1-second, the 80% confidence interval of the 10Hz one-third octave band filter is approximately +3 and -5dB. This increases to +6 and -10dB for 99% confidence. The interval decreases with increasing averaging time. For a 32-second averaging time, the 80% confidence interval is $\pm 0.75\text{dB}$.⁴ The maximum vibration level due to ST trains is defined here as the level of rms vibration occurring during the train passage time. The train passage time for a train consist of the four Kinkisharyo vehicles under procurement would be six seconds at forty-five miles per hour and nine seconds at thirty miles per hour. Averaging times of this order are usually adequate for quantifying ground vibration from trains. These averaging times are inherent in the ground vibration prediction procedure for rail transit trains.

⁴ Instruction Manual, Type 1921 Real-Time Analyzer, General Radio Company, 1969. Pg., 3-7

Table 2-1 UW Requested Thresholds: Vertical Root-Mean-Square Velocity Level - dB re 1 micro-in/sec

Building	1/3 Octave Band Center Frequency																	
	2	2.5	3.16	4	5	6.3	8	10	13	16	20	25	31.6	40	50	63	80	100
1) EE/CS	26	28	25	25	26	29	30	32	30	33	26	23	27	24	24	27	32	19
2) Johnson	34	35	34	32	33	31	31	32	36	37	35	35	44	43	44	39	38	39
3) Bagley	30	36	32	30	29	27	26	28	27	26	28	26	31	28	33	35	27	35
4) New Chemistry	28	31	29	28	26	25	26	26	24	24	25	21	28	25	28	30	19	18
5) Wilcox	25	26	27	27	27	29	31	32	30	30	30	20	23	22	27	25	25	27
6) Physics & Astronomy	34	34	36	32	30	27	28	30	30	26	23	21	26	22	22	30	22	---
7) Burke	29	30	32	33	33	32	33	36	35	35	36	34	33	33	35	32	29	27
8) Benson [2]	30	36	32	30	29	27	26	28	27	26	28	26	31	28	33	35	27	35
9) Roberts	24	26	26	28	27	26	31	30	30	30	24	25	26	25	30	29	27	27
10) Winkenwerder [1]	26	28	26	28	31	30	33	33	30	29	32	33	32	31	28	29	29	32
11) Henderson	33	40	37	36	35	32	35	35	32	29	27	24	25	27	21	18	21	14
12) Ocean. Res. II	27	28	29	28	28	27	29	31	28	28	31	32	32	33	24	26	23	16
13) UWMC NN Wing	31	38	35	34	35	34	31	32	31	29	26	21	23	17	15	19	13	8
14) Fisheries Sciences	31	37	34	35	33	32	30	30	42	31	30	30	33	30	30	32	26	21
15) Fisheries Tech Res	30	35	35	35	33	31	32	34	34	34	36	35	30	26	23	21	17	12
16) More	27	30	29	33	32	32	34	35	35	34	39	37	41	48	39	40	36	38
17) Marine Studies	27	29	28	29	29	27	28	29	30	33	30	31	38	38	42	33	30	26
18) Bioeng./Genomics [3]	27	28	29	28	28	27	29	31	28	28	31	32	32	33	24	26	23	16
19) Fluke	28	32	31	32	33	34	34	37	41	45	41	42	44	41	31	37	25	20
20a) Mech Eng	28	31	30	30	33	27	30	29	29	34	28	31	30	23	20	25	19	18
20b) Mech Eng-Annex	32	32	30	30	30	29	33	33	31	38	31	38	43	32	32	31	29	23
21) Ocean Sciences	27	31	29	29	31	36	32	30	46	37	36	33	46	35	37	46	36	33
22) CHDD	31	34	31	31	33	31	34	32	30	30	30	30	35	31	32	34	30	27
23) Fisheries Center	30	34	31	31	32	29	33	31	34	37	42	41	41	40	41	43	37	32

Notes: [1] No data were gathered at Winkenwerder Hall; data is from nearby Bloedel Hall.

[2] No data were gathered at Benson Hall; data is from nearby Bagley Hall.

[3] No data were gathered at the Bioengineering / Genomics Building site; data is from nearby Oceanography Research II Building.

3 PREDICTION METHODOLOGY

The prediction methodology is consistent with that described in the Federal Transit Administration (FTA) guidance manual, and employs numerical predictions based on shear and compression wave velocity vs. depth profiles to supplement test data and extrapolate to low frequencies and to large distances. The predicted quantities are identical to those used in the FTA guidance manual. The fundamental assumption is that the vibration velocity level at some distance from a rail transit track or structure is governed by the vehicle and track system force density level (FDL), and the Line Source Response (LSR) of the tunnel and soil or rock. Thus, the vibration velocity level is given by:

$$L_V (\text{dB re } 10^{-6} \text{ in/sec}) = \text{FDL}(\text{dB re } 1 \text{ lb/ft}^{1/2}) + \text{LSR}(\text{dB re } 1 \text{ ft}^{1/2} \mu\text{in/lb/sec})$$

Additional adjustments for track vibration isolation, suspension modifications, etc., are added to the above equation.

3.1 Force Density Level

The force density level is defined for the vehicle and track taken as a system. Thus, the force density level of a vehicle on one type of track may differ from the force density of the same vehicle on a different track. Differences in track may involve rail support stiffness and rail height variation, or roughness. The interaction between the vehicle suspension and track support may vary depending on track structure.

The forces produced by a vehicle and track system are assumed distributed uniformly and incoherently over the train length.⁵ Hence, the unit of the force density is $1 \text{ ft}^{1/2} \mu\text{in/sec/lb}$, and the level is given in decibels relative to $1 \text{ ft}^{1/2} \mu\text{in/sec/lb}$. These forces are produced by rail and wheel roughness, by track support in-homogeneities such as periodic supports of the rails, and by imbalanced rotating components in the transit vehicle truck. While the forces produced at the wheel/rail interface are concentrated in the region of the truck, the moving vehicle distributes the

⁵ The term “incoherent:” means that the forces applied at one point beneath the vehicle track system are unrelated to the forces applied at an immediately adjacent point.

forces over a length of track for a given finite time interval. The vibration criteria are given in terms of the root-mean-square vibration velocity, which necessarily involves an average of the square of the vibration velocity over some time interval, which has been assumed to be the train passage duration. The time interval necessary for passage of the train consist of four Kinkisharyo vehicles would range between five and nine seconds for trains speeds between thirty and fifty miles per hour. During this averaging time, the train typically moves 200 to 400 feet, so that the vibration forces are distributed over the track in a roughly uniform fashion, the effects of rail discontinuities notwithstanding.

The assumption of incoherence is debatable. A set of imbalanced wheels rotating in unison cannot be considered incoherent, though their relative phases would be incoherent from one train to the next. Vibration due to tie passage and periodic undulation of the rail may be coherent. However, the motion of the source produces Doppler frequency shifts that tend to reduce coherence, and reflections from soil in-homogeneities may contribute to the destruction of coherence.

The pass-by vibration is not necessarily incoherent with respect to time. The pass-by vibration signature of a single light rail vehicle truck (or possibly wheel set) due to a rail roughness profile is repeated with each truck (or wheel set) passage, provided that they are of identical design. The typical light rail vehicle has two motored trucks and a single center non-motored trailer truck. Four vehicles coupled together and with perfectly smooth wheels would produce four virtually identical vibration signatures for a given fixed rail profile. This feature may allow discrimination between vibration due to rail roughness and that due to wheel roughness, and is discussed further below.

The moving static loads imparted by the vehicle constitute another source of ground motion. These sources are non-radiating for uniform track and laterally homogeneous soil, because the train speed is less than the velocity of propagation of vibration in the soil.⁶ Unless one is very close to the track, within perhaps 10 to 20 feet, the static deflection due to quasi-periodic axle

⁶ This does not hold for high speed trains such as the TGV in France, where train speeds of the order of 180mph may exceed the shear wave velocity of marine sediments.

passage would not be discernable, as it would be buried in the overall static deflection signature of the train. The effect is well represented by Boussinesq's theory of elastic deformation of an elastic half-space under a vertical point load.⁷ Finally, the frequency spectrum of the moving static loads of the wheel sets and trucks is very low, typically below the range of concern. The spectrum shifts to lower frequencies as one moves away from the track.

Adjustments are applied to the estimates of force density level to account for floating slab insertion losses (or gains) and differences in track support stiffness relative to the stiffness of the track used for measurement of the FDL. A force density level is developed for each train speed.

3.2 Line Source Response

The Line Source Response (LSR) is the 1/3 octave band vibration velocity response to incoherent 1/3 octave band forces distributed over a specified length. The LSR is a function of train length and distance from the track or tunnel. Mathematically, the LSR is:

$$LSR = 10 \log_{10} \int_L |M(x) / M_0|^2 dx$$

Where $M(x)$ is the mobility amplitude, or velocity response to input force as a function of frequency, M_0 is a reference mobility, and the integral is over the train length, L . The LSR may be given in decibels relative to the "power" reference level of $10^{-12} (\text{in/sec/lb})^2 \text{ft}$. In linear units, the reference level would be $10^{-6} (\text{in/sec/lb}) \text{ft}^{1/2}$, as is used in the FTA guidance manual. The LSR is a function of frequency, and, for convenience, the LSR is usually defined at 1/3 octave band center frequencies. Where the mobility is provided as a narrow-band frequency response spectrum, the root-mean-square of the mobility over the 1/3 octave spectrum may be used in the above integral, as is the case here.

Adjustments to the LSR may be applied to account for unique propagation conditions such as tunnel/soil interaction, building foundation responses, and floor resonance amplification. For this

⁷ Fung, Y. C., **Foundations of Solid Mechanics**, Prentice Hall, Englewood Cliffs, New Jersey. 1965 pg. 200

report, predictions at the ground surface or basements are made without reference to upper floor levels.

No adjustments are currently included for tunnel/soil coupling loss. (Tunnel/soil coupling losses may be computed with finite element model or other tunnel/soil interaction model and incorporated for final design if appropriate). The tunnel soil coupling loss would likely be negligible below 50Hz for the tunnel wall thickness and soil stiffness involved. There may be some directivity associated with the tunnel diameter that would be most apparent at frequencies above that where the wavelength of shear waves in the surrounding soil becomes comparable with the tunnel diameter. This frequency would likely be in excess of 50Hz for the high shear wave velocity soils encountered at the site. For example, the shear wave velocity has been measured to be of the order of 1800ft/second. The tunnel diameter would likely be about 18ft. Thus, the shear wavelength would be equal to the tunnel diameter at a frequency of approximately $1800/18 = 100\text{Hz}$. The tunnel wall would be relatively thin, and its motion would be controlled by the surrounding soil, with the result that the wall would not provide much vibration reduction at the frequencies considered.

4 VEHICLE FORCE DENSITY LEVELS

A vehicle manufactured by Kinkisharyo has been selected by Sound Transit for North Link. The vehicle is very similar to the Kinkisharyo vehicle currently used at the Santa Clara Valley Transportation Authority (VTA) in San Jose, California, except that the Sound Transit version would be approximately five feet longer than the VTA vehicle, and slightly heavier by a commensurate amount (approximately 6,000 lbs, or 6 percent heavier). However, the dynamic forces would largely be determined by the trucks and track, because the secondary suspension system decouples the vehicle body from the truck at frequencies above the secondary suspension resonance frequency, which is usually about 2Hz. The trucks would be nearly identical. Thus, the force density level of the Sound Transit Kinkisharyo vehicle should be similar to that of the San Jose Kinkisharyo vehicle running on the same track. The force density might actually be slightly lower for the Sound Transit version than that for the VTA version, because the forces produced by the trucks of the Sound Transit vehicle would be spread out over a slightly longer length relative to that of the VTA vehicle, and the decibel difference would be of the order of $10\log_{10}(394/360) = 0.4$ dB. However, the slightly greater vehicle weight of the Sound Transit vehicle would compress the primary suspension springs slightly relative to those of the VTA vehicle, with the result that non-linearity in the primary suspension system might increase vibration forces slightly, thus canceling the slight reduction in force density level. Also, the primary suspension springs of the Sound Transit vehicle might be designed to be slightly stiffer than those of the VTA vehicle to support the slightly greater weight. The force density level for the Sound Transit vehicle is assumed to be the same as that of the VTA vehicle, the effects of track differences notwithstanding. The actual force density level for the Sound Transit vehicle on representative track will not be determined until it can be tested in 2006 or 2007.

The vibration forces are believed to be generated primarily by rail height undulation and roughness and by wheel run-out and tread roughness. Of these, rail undulation and excessive wheel radial run-out may be most important at low frequencies. Rail corrugation and wheel roughness due to flats may be most important at high frequencies. Excessively rough wheels or wheels with substantial wheel flats may dominate the force spectrum. Variations in rail support stiffness would also produce “parametric” excitation vibration forces. Poorly maintained switch frogs and rail joints can contribute markedly to vibration. Sound Transit would employ

continuous welded rail, so that rail joints will not be a factor, except perhaps at connections with special trackwork. The vehicle's primary suspension resonance frequency, un-sprung mass, various resonances of the truck components, track design, and rail vehicle interaction affect the spectrum and amplitude of the forces transmitted to the tunnel structure and ground.

4.1 Kinkisharyo Force Density Tests at VTA

The force density levels for a Kinkisharyo vehicle were measured at the VTA system in Santa Clara, California. The test procedures, data analysis, and results are described in Appendix C. The basic procedure included the following steps:

- 1) Measure the Line Source Response at three test sites for 4 to 6 measurement points at each test site
- 2) Record ground vibration at each measurement point for a passing VTA transit vehicle at speeds of 20mph to speeds as high as 55mph in 5mph increments.
- 3) Determine the vibration exposure level of each of the ground vibration signatures by analyzing the train passage vibration with a 1/3 octave band analyzer with an integration time of about ten seconds to fully bracket the passby signature
- 4) Normalize the measured 1/3 octave band spectrum to the train passby duration by adding a factor of $10\log_{10}(T_{\text{analysis}}/T_{\text{passage}})$ to the "raw" 1/3 octave band data
- 5) Subtract the measured LSR from the normalized passby 1/3 octave data
- 6) Energy average the results over each measurement point, train direction, and location for each speed

The normalization procedure essentially converts the measured passby levels to levels that would be obtained for a train of infinite length. The corresponding LSR used for determination of the FDL must be defined for an infinite source length. In practice, an LSR was determined over a finite length and extrapolated analytically to an infinite length where appropriate.

The Force Density Levels obtained for the VTA Kinkisharyo vehicle are plotted in Figure 4-1 for speeds of 20mph up to 55mph in 5mph increments. The force density levels exhibit low frequency peaks that vary directly with train speed, and are presumably due to wheel rotation or rail undulation, roughness, and axle/truck separation. The peaks reach a maximum at about 8 to 10Hz, consistent with a primary suspension resonance frequency of about 8 to 10Hz. A second broad peak occurs at about 63 to 80Hz, and is related to track resonance or resilient wheel resonance.⁸ The frequency of this peak does not vary much with train speed, consistent with a mechanical resonance as apposed to a geometric or parametric excitation effect. More interestingly, the FDL at high frequencies appears to be independent of train speed. This behavior is not well understood, but has been observed for other vehicles, such as the Portland Tri-Met vehicles. A minimum in the spectrum appears at about 16 to 20Hz. As indicated above, while the spectral characteristics may be largely due to resonances and geometric effects, the fundamental excitation would still be due to rail and wheel roughness, unbalanced rotating components, and variations in track support stiffness.⁹

The FDL estimates are for standard resilient direct fixation (STDF) fasteners of nominal dynamic stiffness of 140,000 lb/in. High compliance direct fixation (HCDF) fasteners may yield lower vibration levels at frequencies above about 30Hz, but could increase the FDL at low frequencies by a decibel or two. Conversely, increasing the dynamic stiffness of the fastener above 140,000 lb/in might reduce low frequency vibration at 8 to 10Hz by a decibel or two. However, there could be an increased risk of rail corrugation with very stiff rail fasteners, and rail corrugation would increase vibration at frequencies of the order of 500 to 1000Hz.

Examples of high compliance resilient fasteners include the “egg” type fastener produced by Advanced Track Products. This fastener is similar to the Cologne Egg originally manufactured by the German rubber manufacturer, Clouth, and employs elastomer-in-shear as the primary

⁸ The track resonance is the resonance of the wheel set mass and rails on the rail supports.

⁹ One way to think about low frequency vibration produced by a transit train is that the vehicle represents a filter. Discrete peaks due to axle set and truck passage, and waves in the rail, are filtered by the truck suspension, much as a radio is tuned to certain radio station frequencies. However, the frequencies associated with transit ground vibration vary in proportion to train speed, so that the frequencies “move” through the sensitive range of the suspension resonance, the frequency of which remains constant.

vibration isolating element. The standard resilient direct fixation fastener usually includes an elastomer pad bonded to a metal top and bottom plates, and usually exhibits higher ratio of static-to-dynamic stiffness relative to that of elastomer-in-shear fasteners such as Clouth's Cologne Egg.

4.2 Rail Undulation and Wheel Run-out

The vibration signatures of several passes of the VTA Kinkisharyo vehicle were Fourier analyzed with a single conversion of the time series and rectangular weighting in an attempt to discriminate between vibration due to wheel run-out and rail undulation. This analysis is described in detail in Appendix C. The results indicate that, as expected from theoretical considerations, wayside ground vibration produced by periodic or quasi-periodic passage of axle sets and trucks consists of a spectrum modulated by an envelope of discrete spectral peaks with frequencies related to axle and truck separation. This modulation envelope affects the spectrum of vibration that would be attributed to the rail alone, which spectrum may, in addition, contain discrete frequency peaks related to periodic undulation of the rail. The modulation peaks are most pronounced at the primary suspension resonance frequency of the truck. The wheel rotation frequency is also present, but the rotation frequency is coincident with one of the modulation peaks, obfuscating its differentiation. The conclusion of the analysis is that rail roughness or undulation may be more important than wheel eccentricity or run-out in producing ground vibration.

There is little information concerning rail undulation at U.S. transit systems. Rail undulation caused by roller straightening machines has been identified in the literature as a cause of wayside vibration.¹⁰ Rail undulation with magnitude of the order of 0.05in (0.1in peak-to-peak) produced substantial low frequency ground vibration in soft soils at 8 to 12Hz during passage of unit trains with 100-ton hopper cars at Canadian Northern Rail in Kamloops, British Columbia. The undulation wavelength was related directly to the circumference of the rollers

¹⁰ Dawn and Stanworth, JSV, 66(3), 1979, pp. 355-362

used to straighten the rail during manufacture.¹¹ The rail undulation could not be reliably ground out, and the rail was eventually replaced with rail straightened to British Steel¹² specifications of 0.015" deviation from straight in any ten-foot chord for rail. The vibration reduction thus obtained was of the order of 8 to 10 dB, or a factor of 2.5 to 3 in amplitude.¹³

The rail with excessive undulation in Kamloops was originally installed as part of a track upgrade, and the rail that it replaced was straightened by older, less sophisticated "gag press" techniques. Anecdotal information suggests that the specification for gag pressed rail was that the rail "shall be straight". In spite of this qualitative specification, the ground vibration with such rail was substantially lower than that produced by the roller straightened rail. Interestingly, the rail straightened to British Steel specifications was also straightened by the same manufacturer of the original rail with a roller straightener.

Rails were recently ground to remove the effects of roller straightener induced undulation at a section of mainline railroad in Texas, and, evidently, a reduction of rail undulation amplitude was obtained.¹⁴ The ability of a rail grinding train to grind out rail undulation depends on the design of the rail grinder.

There is no clear specification for rail undulation amplitude for rail manufactured in the United States. The AREMA standards contain a provision for upturn at the ends of the rails relative to welding. One may assume that rail undulation is thus uncontrolled, and that amplitudes could conceivably be of the order of 0.05in. Vibration at 8 and 10Hz observed at other systems by Wilson, Ihrig & Associates suggests that the problem may be more common than not. If undulation can be controlled, the FDL at 8 and 10Hz might be lowered substantially, though other factors may limit the reduction. These other factors include wheel run-out, parametric

¹¹ Nelson, James T., Wilson, Ihrig & Associates, Report to CN Rail concerning wayside ground vibration in Kamloops. (1980's)

¹² British Steel has been reorganized and is now renamed Corus

¹³ The rail installed at the Banfield corridor in Portland was supplied by British Steel, and the FDL for the Tri-Met vehicles are also relatively low.

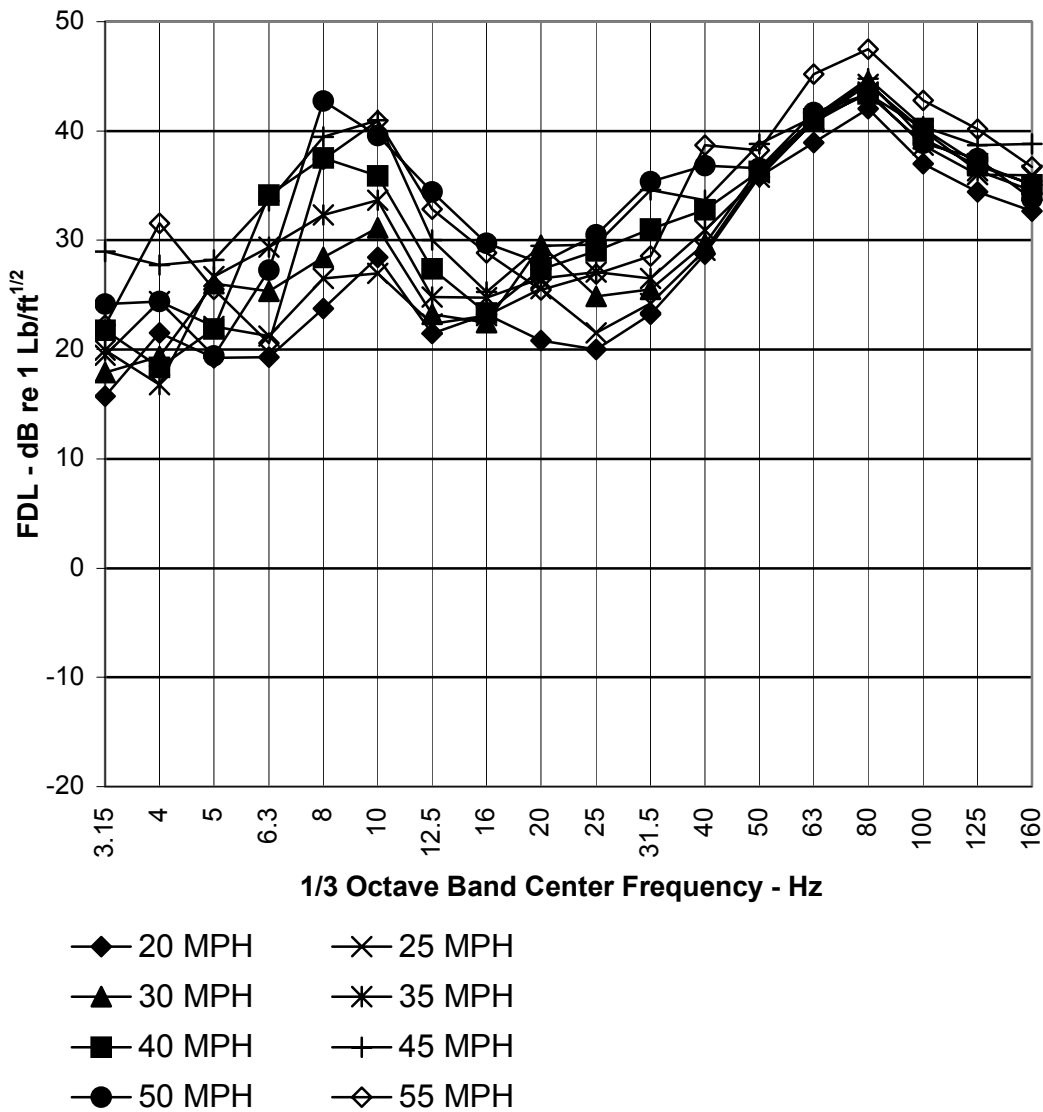
¹⁴ Discussion with a rail grinder manufacturer.

effects such as rail support in-homogeneity, rail head ball radius variation, and so on. Conversely, if rail undulation is not controlled, and the rail at VTA was exceptionally straight, the FDL could be higher than measured at the 8 and 10Hz third octaves.

Sound Transit is interested in obtaining more definitive rail straightness data during the Final Design of North Link. Rail straightness can be measured, but the process requires a very accurate laser metrology system to measure rail height variation over perhaps 100 feet to a resolution of a few thousandths of an inch.

Wheel run-out may also be a cause of substantial low frequency vibration at 8 and 10Hz. However, the truing tolerances of Bochum resilient wheels are of the order of 0.016 in, possibly less than rail undulation amplitudes.¹⁵ Sound Transit is interested in obtaining wheel run-out data during Final Design for both the VTA vehicle and the new ST Kinkisharyo vehicles for comparison and refinement of predictions.

¹⁵ Information provided by the manufacturer in response to questions concerning wheel truing tolerance.



Adjusted for Resilient Direct Fixation Fastener of 140,000 lb/in
 Averaged Channel, Direction, and Location
 Train Length=90 ft

Figure 4-1 FDL for VTA Kinkisharyo on Resilient Direct Fixation Fasteners with
 Dynamic Stiffness of 140,000 lb/in and Fastener Separation of 30in

4.3 Comparison with Other Vehicles

The FDL obtained for the VTA Kinkisharyo vehicle is compared with FDLs for other vehicles in Figure 4-2. These FDLs were measured at other systems under varying track conditions. The train speed represented in the figure is 55mph. There is considerable spread in the data due to variations in track conditions, rail straightness, wheel roughness, suspension design, and measurement procedures. The FDL reported here for the Kinkisharyo vehicle is near the middle of the range of the FDLs shown.

The highest FDL shown is that of the San Francisco MUNI LRV2 vehicle. The primary suspension resonance frequency of this vehicle is at about 12 to 16Hz. The primary suspension is an elastomer journal bearing bushing that is much stiffer than the chevron type suspension systems used by most light rail vehicles. The MUNI LRV2 was the subject of complaints and court action regarding vibration impact on residences in San Francisco. This was eventually controlled by aggressive rail grinding to remove rail imperfections and by wheel truing.

The second highest FDL is that of the SF MUNI SLRV. This vehicle has a softer suspension than that of the SF MUNI LRV2, but has a damped wheel rather than a resilient wheel, and stiff H-frame trucks. Both MUNI vehicles exhibit similar FDLs at frequencies above 50Hz, and also below 10Hz. The differences in primary suspension have a strong effect on the FDL at frequencies between 10 and 50Hz.

The FDL for the Los Angeles Blue Line is most similar to that measured for the Kinkisharyo vehicle. This FDL was measured on ballast-and-tie track with rail supported by Pandrol plates, rubber pads, Pandrol clips and concrete ties. The vehicle was manufactured by Nippon Sharyo, weighed 90,000 lb, and had an un-powered center trailer truck with conventional wheel sets with Bochum 54 resilient wheels.

The lowest FDL was measured for the Portland Type 1 vehicle manufactured by Bombardier, the Santa Clara VTA manufactured by UTDC, and the San Diego LRV manufactured by Siemens. These vehicles are standard floor height vehicles with freely rotating un-powered center trucks and conventional wheel sets.

The FDL measured for the Portland Type 2 Siemens vehicle is quite low, and may represent the lowest FDL that can be reasonably expected for a vehicle of its type. The Portland Type 2 vehicle consists of a three-piece body with the center body fixed to the center truck. The center truck has independently rotating un-powered Bochum 84 wheels on stub axles. Both the Portland Type 1 and Portland Type 2 vehicles exhibit low FDLs at the primary suspension resonance frequency, though the speed shown for the Portland Type 2 vehicle was 45mph while that of the Portland Type 1 vehicle was adjusted for 55mph relative to a lower speed, so the comparison is not direct. However, the FDL for the Portland Type 2 vehicle is consistent with FDLs observed for other vehicles, and specifically for the earlier Type 1 vehicle. Portland Tri-Met has a rigorous wheel-truing program, which may affect the FDL, especially at higher frequencies. However, as discussed above and in Appendix C, rail straightness may be the most important factor in wayside vibration at Portland. The FDL for the Portland Type 1 vehicle was measured on the Banfield corridor on ballasted track with rail supplied by British Steel, and the FDL for the Portland Type 2 vehicle was measured on ballasted track with rail supplied by Rocky Mountain Steel, formerly CF&I. Both of these rails were ground within several months prior to measuring the force density. This, combined with Tri-Met's effective wheel truing program, may have contributed to the low FDL measured for this vehicle.

If the MUNI vehicles were removed from comparison, the FDLs shown in Figure 4-2 would group more tightly, and the San Jose VTA Kinkisharyo vehicle would be at the upper end of the range of the remaining group. The VTA Kinkisharyo FDL is thus representative of FDLs for this type of vehicle.

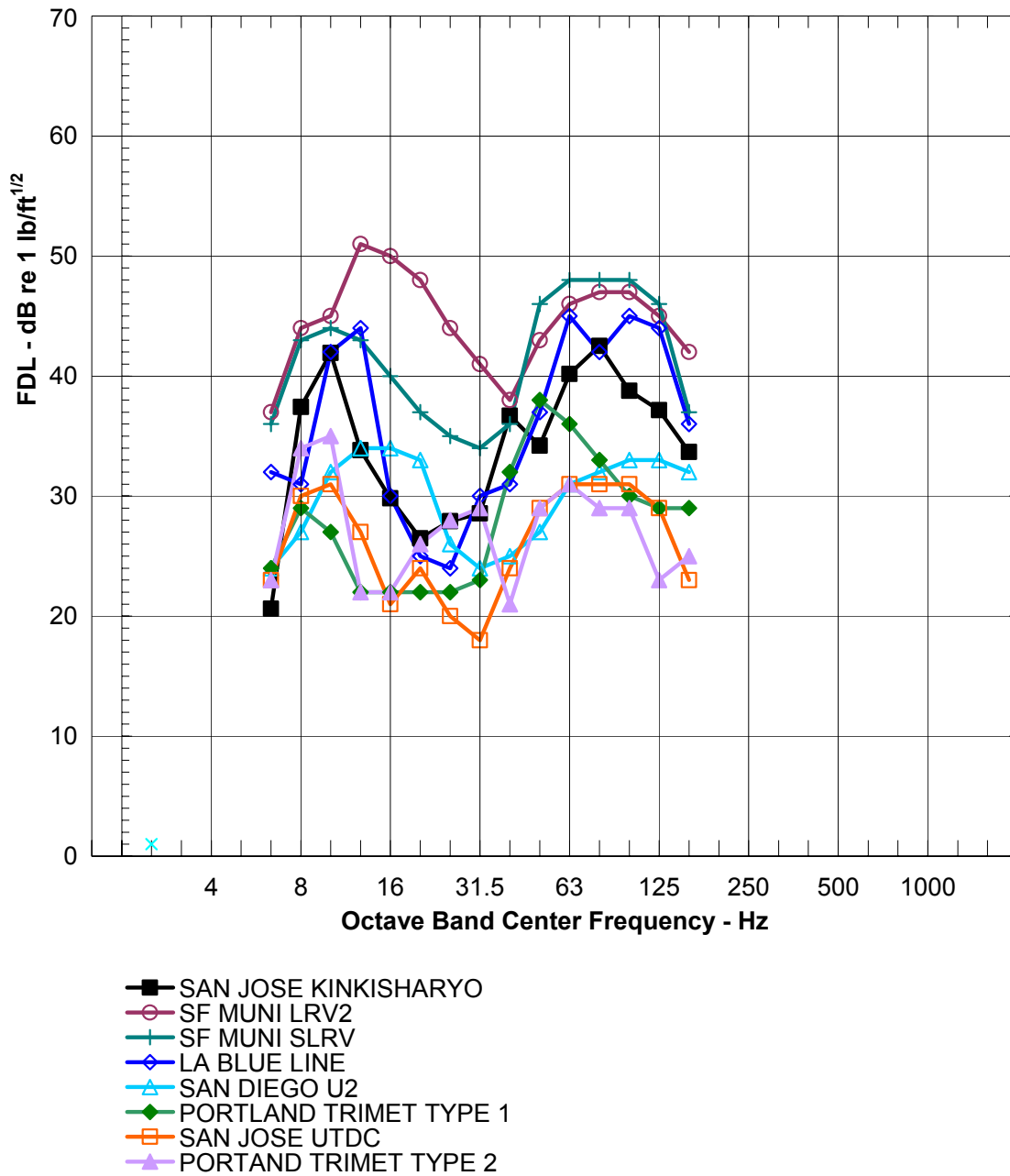


Figure 4-2 Measured Force Density Levels for Various Transit Vehicles

4.4 Uncertainty in FDL

Figure 4-3 shows a comparison of the measured 45mph Force Density Levels for the Kinkisharyo vehicle measured at each of the three measurement locations at the VTA. The purpose of the comparison is to provide an estimate of the uncertainty that might be associated with the FDL measurement. Only one test result was available for 55mph, two for 50mph train speeds, and three for the 45mph run. Each of these results was the energy average of several passes, transducer locations, and the two directions. The average shown is an energy average of the three results. The “mean plus one standard deviation” is ten times the logarithm of the sum of the mean energy and the standard deviation of the energy. The result indicates that the deviation is about 2 to 3 decibels. The spread in the measurement results is greater than the standard deviation. These results were obtained by energy averaging, and the higher FDLs tend to dominate the decibel range.

The individual uncertainties for each measurement include variations of results from one train sample to the next, and one position to the next. The variation from one train to the next may be as little as 2 dB at frequencies above 5Hz, provided that speed is well controlled. The variation is higher at 5Hz and lower bands, due to the short integration times used for analysis. The predicted levels at frequencies below 5Hz are not excessive. The variation from one train sample to the next is similar to, or less than the variation from one section of track to another, where the variation may be several decibels, as indicated by the low FDL at 80Hz observed at Moffett compared with the other two locations. Variations may occur between train directions, which is not understood, but may be related to variations of test speed.

The data shown in Figure 4-3 indicate the degree of uncertainty in the overall prediction procedure, given the same track and vehicle type. An uncertainty of ± 3 dB is assumed for the purpose of combining with the uncertainty of the UW Campus LSR to estimate the uncertainty of the overall prediction. This uncertainty is comparable with or may be greater than that implied by the difference between the mean energy FDL and the mean energy plus one standard deviation FDL shown in Figure 4-3. Note that ± 3 dB corresponds to a +100% and -50% variation of energy of the vibration.

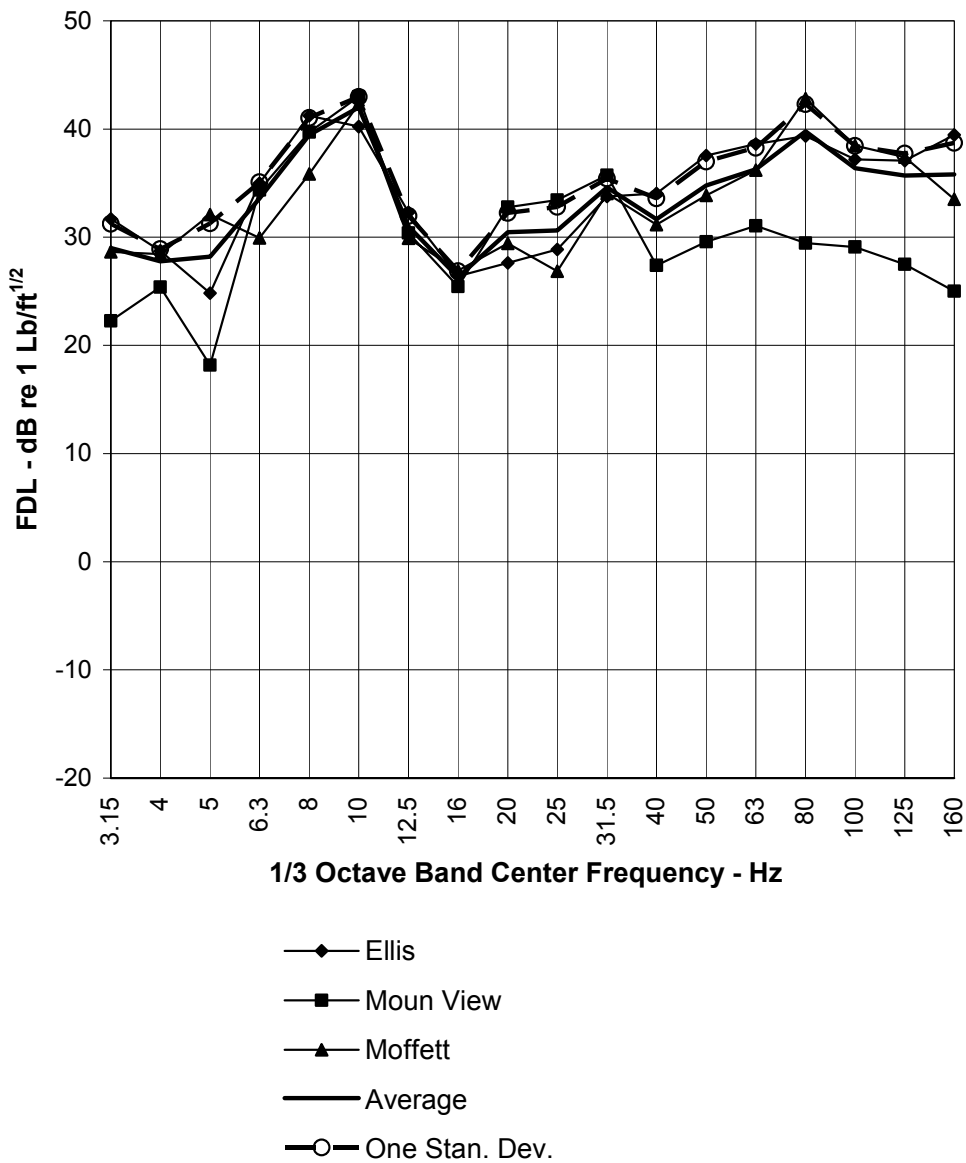


Figure 4-3 Comparison of Mean FDL, and Mean FDL Plus One Standard Deviation for Test Vehicles Operated On Ballast-and-Concrete Tie Track with Continuous Welded Rail at 45mph

5 LINE SOURCE RESPONSE DETERMINATION

This section describes the methods employed for estimating the LSRs used for prediction. Both empirical and numerical methods were employed to predict vibration at large distances and at low frequencies to overcome effects of background vibration and instrumentation noise.

5.1 Borehole LSR Tests

The LSR is determined by the following steps:

- 1) Measuring the transfer mobility as a function of frequency with resolution of 0.5Hz from the borehole to the ground surface at representative horizontal offsets
- 2) Averaging the square of the transfer mobility function over each 1/3 octave band of frequencies to obtain the 1/3 octave Point Source Response (PSR) at each representative distance
- 3) Least squares regression of 1/3 octave PSRs versus horizontal offset or slant distance
- 4) Integration of the regression curves representing the PSR over the train length to obtain the LSR

The ideal method for determining the LSR is by measuring the impulse velocity response, or transfer mobility, at a receiver in response to forces delivered at points along the track centerline at the top of rail. For tunnels, this is impossible without drilling numerous holes spaced at about 10 to 20 feet apart along the tunnel alignment. Hence, a compromise solution involves drilling a single borehole down to track depth and measuring the response at the ground surface at various distances from the borehole to forces delivered at the bottom of the hole. Regression or interpolation is then used to develop a curve of the square of the mobility magnitude as a function of distance between source and receiver. This regression curve is used to integrate the square of the mobility magnitude over the train length, assuming that the soil is laterally homogeneous. The train is assumed to be immediately opposite a particular receiver. Both interpolation and regression methods were employed in this study. Implicit in this approach is the assumption that the soil layer is uniform about the vertical axis of the borehole.

The prediction procedure ignores reflections of vibration energy from nearby building foundations, underground structures, and the like, which reflections may be substantial. The measured LSRs are necessarily affected by these reflections, increasing the scatter of measurement results about some mean. Avoiding reflections from buildings, underground structures, and the like, is almost impossible in urban settings, or where buildings are located in close proximity to the measurement. Under these circumstances, regression analysis of the measured data reduces these variations, providing a smooth regression curve. Regression, however, does not eliminate electrical noise or background vibration effects. The effects of electrical noise and background vibration are reduced by transfer function component averaging during the laboratory analysis of the recorded impulse response data.

Measurement Locations

Line Source Responses were estimated from measurements of the mobility at four boreholes during the course of the PE phase. An earlier borehole test at the center of the campus also provided another estimate of the LSR. Thus, five LSRs were determined at five locations, only four of which were close to the Modified Montlake Alignment. These four were employed for predictions.¹⁶ The fifth location appears to be non-representative, exhibiting a lower response than the others.

The measurement locations are identified in Table 5-1. These locations were selected to be representative of sensitive receivers.

¹⁶ At the recent IWRN-8 conference, comments were made that projections of vibration are best made for the soils present at the source. This has some validity, in that the stiffness of the soil in the vicinity of the source determines the amount of energy that can be imparted to the soil.

Table 5-1 Borehole Test Locations

Hole	Station	Nearest Building
NB-253	NB-1208+20	Husky Stadium
NB-254	SB-1214+70	Wilcox Hall
NB-255	SB-1223+00	Mechanical Engineering
NB-256	SB-1258+00	Kane Hall

Procedure

The procedure includes drilling a 6in diameter hole to test depths of nominally 90, 100, 110, and 120ft, spanning the tunnel depth. At each test depth, the drill string was retracted, the bit removed, a load cell attached to the end of the string, and the string reintroduced into the hole. Impact forces were generated with the driller's two sampling hammers. One of these hammers weighed 140lbs, and the other 300lbs. Approximately 100 samples were obtained at each depth with the 140lb hammer and 30 samples with the 300lb hammer. A greater number of samples were not obtained with the 300lb hammer due to rope burn and the desire to avoid possible drilling equipment malfunction. The peak impact forces are typically of the order of 3,000 to 10,000lb, depending on soil stiffness. However, these are spread over a much broader range of frequencies than those considered here.

During impact generation, surface vibration responses were measured at various distances ranging from about 25ft from the hole to as much as 400ft from the hole for a total of seven locations. The data obtained at these locations were subjected to regression analysis and/or interpolation of the response as a function of distance or the logarithm of distance.

Additional responses were obtained inside buildings both near the seismic line and as far as 1,000ft from the borehole. These latter measurements provide an estimate of the response inside sensitive buildings for comparison with exterior ground surface responses. The UW has required that the surface vibration predictions be used for comparison with UW Thresholds for determination of impact. Thus, these latter building responses were not used for analysis.

The force and vibration responses were recorded on magnetic digital audio tape (DAT) with a TEAC RD145 16-channel DAT recorder.

The data were analyzed in the laboratory with a multi-channel Fourier analysis system developed by WIA for this purpose. Details of the analysis are described in Appendix A.

The third octave Point Source Responses (PSR), in decibels relative to 10^{-6} in/sec/lb were obtained for each impact depth and horizontal offset. The third octave PSRs obtained at all four holes for depths of 110 to 120ft were combined and subjected to regression analysis to develop a “global” regression curve of third octave PSR versus horizontal offset. The global regression curve of PSR versus horizontal offset was integrated over the length of a four car train to estimate the LSR at offsets out to 300ft.

Two types of regression curves were employed. One was a standard quadratic regression curve of the level in decibels of the PSR versus the common logarithm of the horizontal offset. This is the main approach described in the FTA Guidance manual. The second type was a linear regression of the level in decibels of the PSR versus the slant distance and the common logarithm of the slant distance. The latter curve represents a “physical model regression”, where so-called “geometric attenuation” is represented by the coefficient of the logarithm of slant distance, and loss factor by the coefficient of the linear slant distance. The “physical model” is most appropriate for extrapolation of data to zero offset. That is, at zero horizontal offset, the logarithm of the horizontal offset is undefined, and unusable for prediction, while the “physical model” avoids this problem by regressing with respect to the logarithm of the slant distance. In retrospect, the physical model could have been employed throughout without reliance on quadratic polynomial regression, because the differences between the two regression approaches are small, of the order of a decibel in the final LSR calculation, for distances less than a few hundred feet.

The global regression curve of PSR versus horizontal offset was integrated over the train length of about 120 meters, or 394 feet, to estimate the LSR at offsets out to 300 feet.

Time domain averages of the impact test data collected at NB-255 are plotted in Figure 5-1 and Figure 5-2 for one- and two-second conversion times, respectively. The top trace of each of these figures illustrates the input force amplitude as a function of time. The remaining traces illustrate the arrivals at various measurement points, ranging from 25 to 800 feet from the source. The ninth and tenth traces represent arrivals at the Mechanical Engineering building, relatively close to the source, and at Bagley Hall, located some 1,000 feet from the source. These traces were obtained by averaging the time domain signals for the 300-pound sampling hammer, using

a custom proprietary software package. The force signal was used as a trigger. Approximately 25 samples of time data were averaged. The arrivals can be observed in the traces out to about 400 feet. However, at 800 feet, and at Bagley Hall, there is no clear evidence of the arrival in the background vibration and noise signal.

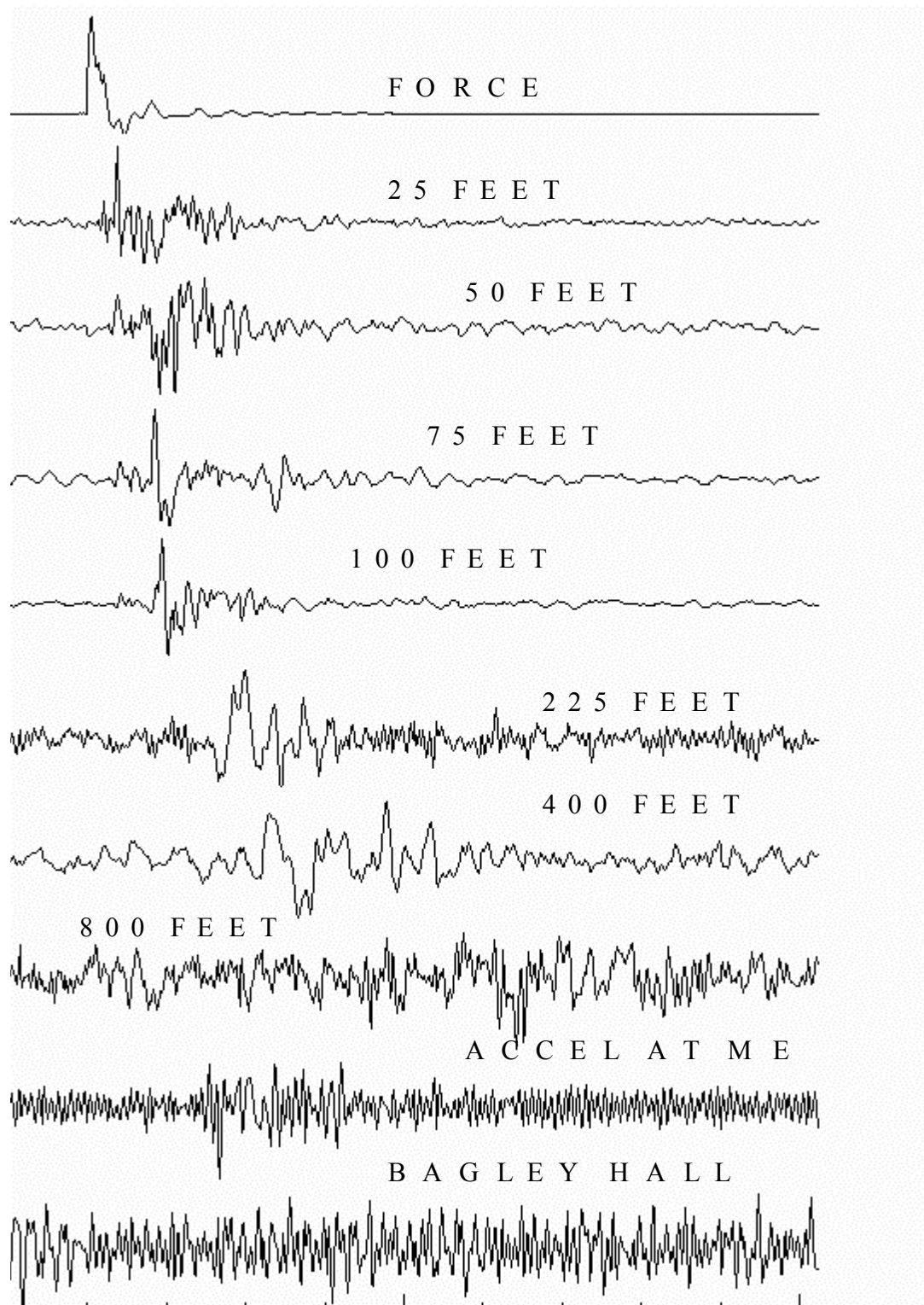


Figure 5-1 Time Domain Average of Response at NB-255 for 0.5-Second Window – 0.1 Second per Division

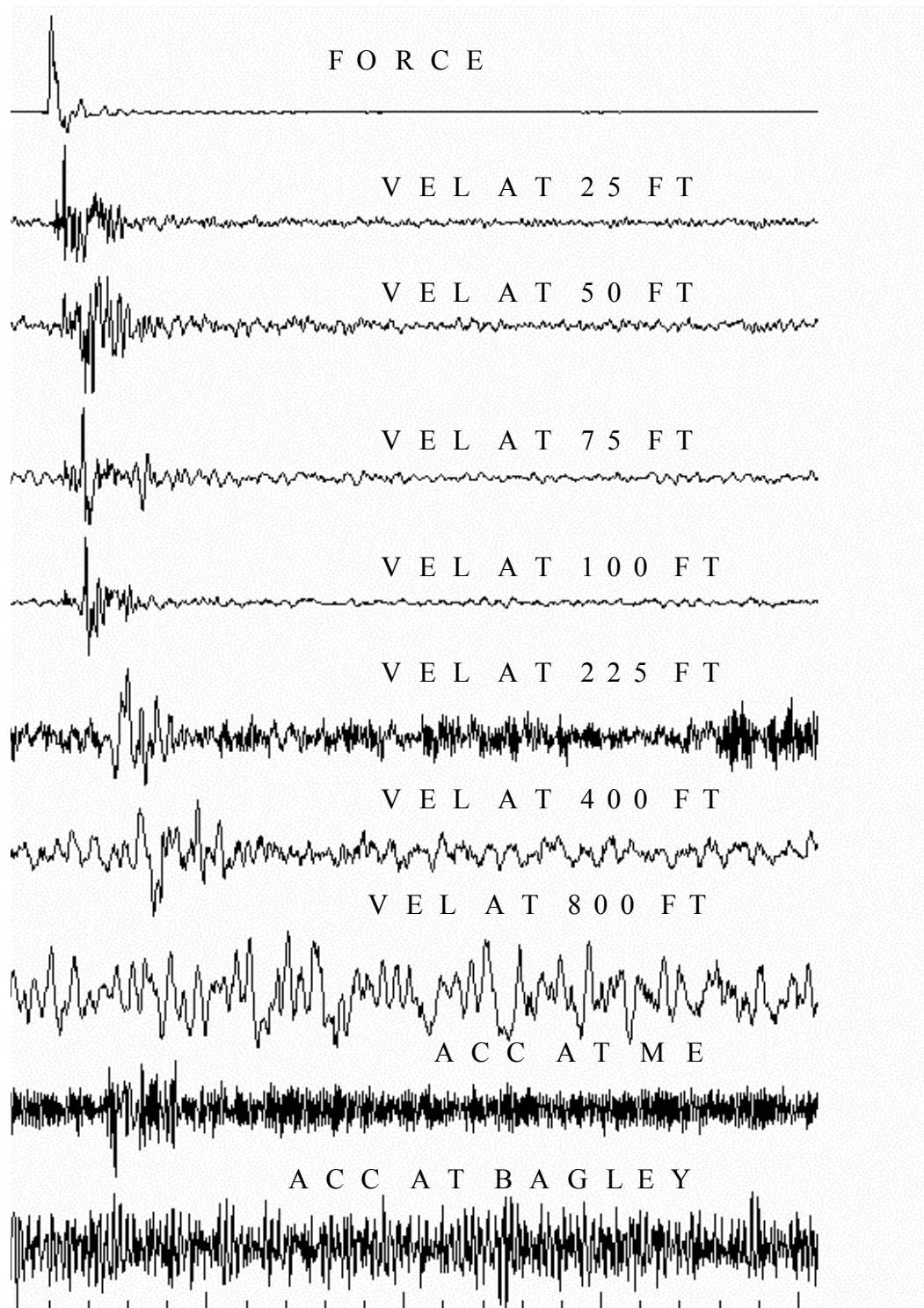


Figure 5-2 Time Domain Average of Response at NB-255 for 2-Second Window – 0.1 Second per Division

LSR Uncertainties

The measurement procedure employs cross-spectral averaging of transfer function components, using a dual channel Fourier analyzer. The complex transfer mobility functions were obtained from the average transfer function components by the following formula:

$$M = \langle G_{ab} \rangle / \langle G_{aa} \rangle$$

Where G_{ab} is the complex cross-spectrum between the force and velocity, and G_{aa} is the auto-spectrum of the force. The brackets, $\langle \rangle$, denote the average value, or expectation value. The cross- and auto-spectra are given by:

$$G_{ab} = f^*(\omega)v(\omega)$$

$$G_{aa} = f^*(\omega)f(\omega) = |f(\omega)|^2$$

$$G_{bb} = v^*(\omega)v(\omega) = |v(\omega)|^2$$

Here, $f^*(\omega)$ is the complex conjugate of the transformed force, and $v(\omega)$ is the transformed velocity, all functions of the radian frequency, ω .

The averaging process reduces the effect of instrumentation noise and background vibration that could otherwise obscure the transfer function. A measure of the background interference is the coherence function, γ^2 , which represents the ratio of the received signal energy to the total received signal energy. Thus, γ^2 , is given by:

$$\gamma^2 = |\langle G_{ab} \rangle|^2 / (\langle G_{aa} \rangle \langle G_{bb} \rangle)$$

The coherence is a function of frequency, and a single value is obtained for each frequency bin. The coherence does not improve with an increase in the number of samples, though the uncertainty in the coherence estimate improves.

The percent error of each transfer function component is a function of the coherence and number of impulses, N_d , given by:¹⁷

$$\text{Uncertainty (\%)} = (1 - \gamma^2)^{1/2} / (\gamma^2 2N_d)^{1/2}$$

Thus, if γ^2 is 0.1, and N_d is 30, the uncertainty in the estimate of M is 33%. In decibels, this is equivalent to $20\text{Log}_{10}(1.33) = 2.5\text{dB}$. If N_d is 100, the uncertainty would be 18%, equivalent to $20\text{Log}_{10}(1.18) = 1.4\text{dB}$.

Reasonable estimates of the transfer function are obtained with signal coherences as low as 10% and at least 30 samples. With low coherence, the transfer function is poorly defined unless the number of samples is increased substantially. In principal, the transfer function can be accurately measured if one is willing to sample “long enough”. In general, assuming a steady background “noise” environment, the transfer function’s “signal-to-noise” ratio would improve by three decibels per doubling of the number of samples, or “hammer hits”. That is, the estimate of the magnitude of the transfer function relative to the noise floor would improve by a factor of 1.4 for each doubling of the number of samples. The noise energy is averaged out at a rate of 50% per doubling of the number of samples, or hits. The average result is for the most part approached from above. That is, there is always some residual noise left in the result for a finite number of samples.

The narrow band transfer function thus obtained is called the Transfer Mobility. To simplify data manipulation and analysis, the square of the transfer mobilities were averaged over the bandwidth of each 1/3 octave band from 6.3Hz to 160Hz. The individual frequency bins of the narrowband mobilities were also weighted by the coherence function when mean-square-averaging over each one-third octave band to reduce the influence of components with poor coherence. The effect of coherence weighting is minimal, and usually results in less than one decibel difference between weighted and un-weighted coherence. The weighting is most useful for averaging out discrete frequency vibration due to rotating equipment or power line noise.

¹⁷ Bendat, J. S., Pierson, A. G., **Random Data Analysis and Measurement Procedures**, 2nd Ed., John Wiley & Sons, New York, pg. 314.

The real and imaginary parts of the cross-spectral components are squared and averaged during construction of the 1/3 octave band mobility, $M_{1/3}$, as follows:

$$M_{1/3}^2 = \frac{1}{\Gamma^2} \int_B |m|^2 \gamma^2 df = \frac{1}{\Gamma^2} \int \left[|m_S|^2 + |m_N|^2 + 2 \operatorname{Re}(\overline{m_S} m_N) \right] \gamma^2 df$$

where:

$B =$ 1/3 octave bandwidth

$m =$ mobility response + noise

$m_S =$ mobility response

$m_N =$ noise component of measured mobility

$\gamma^2 =$ coherence

$\Gamma^2 =$ integral of γ^2 over the bandwidth B

The integration is over the frequency, f .

The PSR is then obtained as $10 \log_{10}(M_{1/3}^2 / M_0^2)$, where M_0 is the reference mobility.

The integral of the real part of the cross product between the mobility response and the noise will tend to zero over a large bandwidth. At low frequencies a limited number of components are available to integrate, so that the term may contribute to the result. The magnitude of the noise component does not go away as a result of the integration. The only way to reduce the noise component further is by increasing the number of impacts used during testing. However, the coherence weighting reduces the influence of noise contributions.

The lowest third octave band that is usually employed in this procedure is the 6.3Hz band. The effective noise bandwidth of this third octave is about 23% of the nominal center frequency, or about 1.5Hz. The frequency resolution of each spectral component of the transfer mobility function obtained during data analysis is about 0.5Hz for a 200Hz analysis. Thus, only about 3 spectral components are available to define the 6.3Hz third octave band. This may be contrasted

with the 63Hz third octave bandwidth of about 15Hz, for which as many as 30 narrow band transfer function components can be averaged together to define the 63Hz third octave PSR. The analysis presented here includes estimates for the 3.15Hz third octave band. In this case, the bandwidth is about 1Hz or less, for which only 1 or maybe 2 spectral components can be averaged over the band. In this case, the scatter can be substantial if the coherence is particularly poor. If the coherence were high at 3.15Hz, the 1/3 octave PSR would be well defined. However, the response of the soil at the University of Washington is exceptionally low at 3.15Hz, with the result that instrumentation noise and surface background vibration tends to dominate the measurement, reducing coherence.

Averaging the real and imaginary parts of the mobility over the 1/3 octave band without squaring was considered for this project. If the phase of the mobility varies rapidly over the 1/3 octave band, as would be the case with distant receivers, the result would be partial cancellation of the integral of the mobility. Thus, an under-estimate would be obtained. Linear averaging of transfer function components across third octave bands was thus not employed. Reduction to minimum phase might allow this to be used, though this has not been investigated.

There may be some benefit in performing all computations with narrow band components, including force density estimates and line source response estimates, and summing the final results to obtain 1/3 octave vibration velocity levels. While the results and error analysis might be easier to understand, the approach would likely not change conclusions regarding vibration impacts. The FTA approach was chosen instead.

Figure 5-3 illustrates the benefits of averaging the complex transfer function components before calculating the third octave PSR. The third octave PSR determined from the averaged complex transfer function components (i.e., the cross-spectral average) is compared with the energy average of individual third octave PSRs obtained from corresponding individual impacts. Also shown is the energy average of the individual components plus and minus one standard deviation of the energy. The result obtained by averaging the complex transfer function components before calculating the third octave PSR is near the lower standard deviation curve, clearly illustrating the noise reduction feature of transfer function component averaging. Without it, the calculated LSR would be substantially higher, resulting in over-prediction.

At locations where good signal-to-noise ratios are available, the transfer functions may be defined with as few as two or three impacts at short range. In areas of poor response or high background vibration, or when instrumentation noise dominates the signal, one hundred samples may be required to obtain a reasonable estimate of the PSR. This was the case at the University of Washington, where the response of the soil was very low due to high soil stiffness. At large distances, even one hundred samples were not enough to adequately overcome the background noise levels.

At short ranges the uncertainty of the measured PSR or LSR is likely to be less than the uncertainty related to variations in soil stiffness, layer depths, damping properties, reflections from building foundations, and so forth. While we might be able to very accurately measure the transfer mobility at one particular location, the transfer mobility at another location may be considerably different. Cross-spectral component averaging allows us to reduce the uncertainty due to noise, but it does not reduce the uncertainty in the average over several spatially separated locations. The concept of confidence interval may not apply, because there is no single transfer mobility that would apply everywhere. (A “universal” transfer mobility would apply if the soils were identical at all locations.) Increasing the number of borehole tests would reduce the confidence interval from a statistical point of view, but it would not necessarily reduce the variance of the data. In this sense, a borehole test at a specific building would be more reliable than the average of ten borehole test results obtained over a geographic area with widely varying soil characteristics. However, the soil does not appear to vary greatly from one borehole to the next, judging from the shear wave velocity data obtained by GeoRecon. (See Appendix B) While there are differences, the deep layers appear to be similar, exhibiting high shear and compression wave velocities. For this reason, averaging several borehole test results obtained on the campus is a rational approach to characterizing the propagation conditions on the campus. This is the approach taken here. This approach would not have been followed if widely varying geologies were found along the proposed alignment.

Figure 5-4 illustrates the Line Source Responses estimated for each of the boreholes NB-253, NB-254, NB-255, and NB-256 at an offset of 200 feet, together with a mean and a mean plus one standard deviation of the mean. The spread in the estimated LSRs is of the order of 3 to 9dB over the spectrum. The standard deviation is roughly 1 to 3 dB, as illustrated by the mean plus

one standard deviation. Similar results were obtained at other distances, though the test results may be limited by noise at large distances or at low frequencies. The spread in the data and the standard deviation is greater than the uncertainty associated with the sampling as discussed above.

The LSR standard deviation would be combined with the uncertainty of the FDL and other uncertainties for computation of the overall uncertainty as discussed in section 6.5.

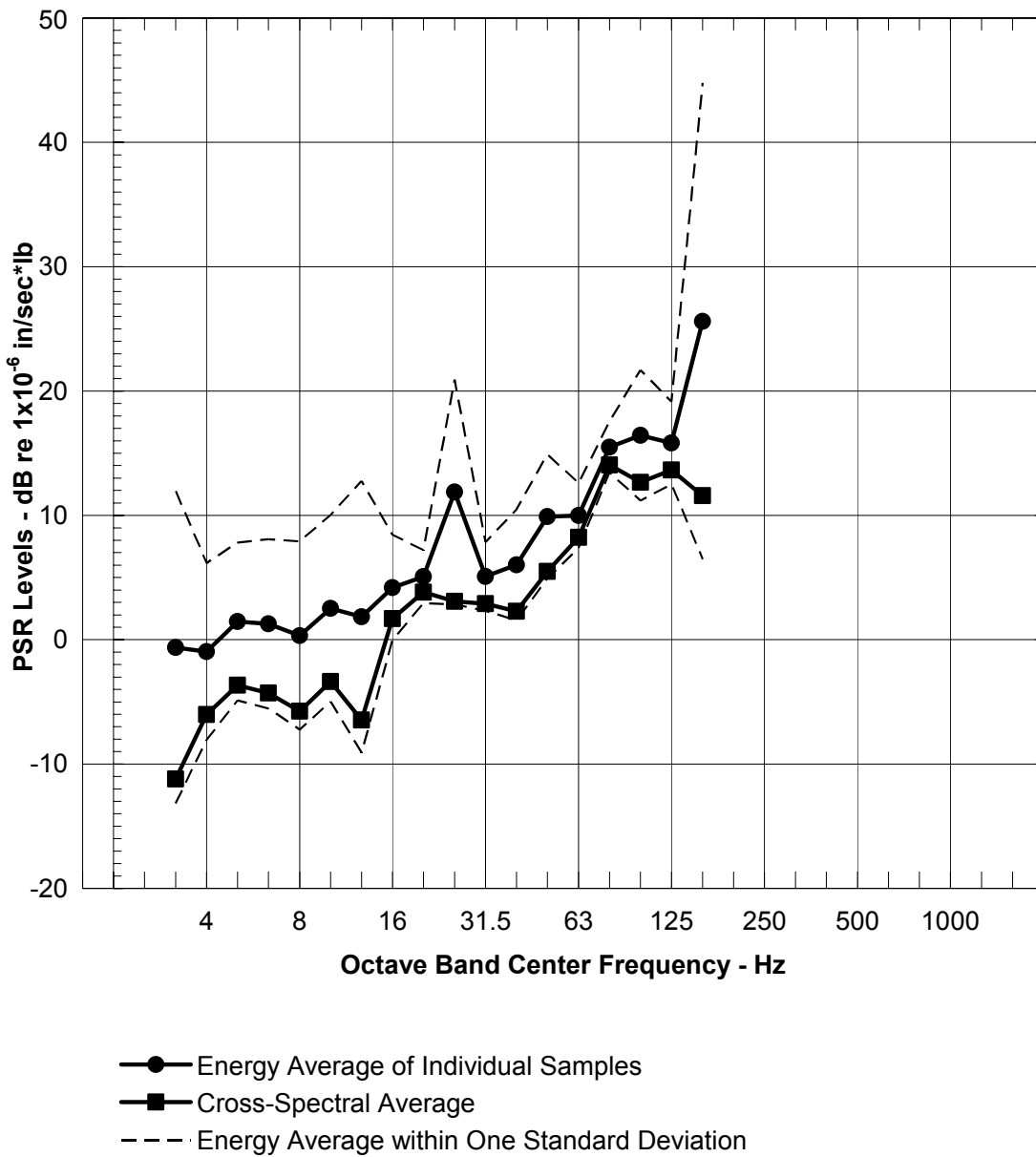
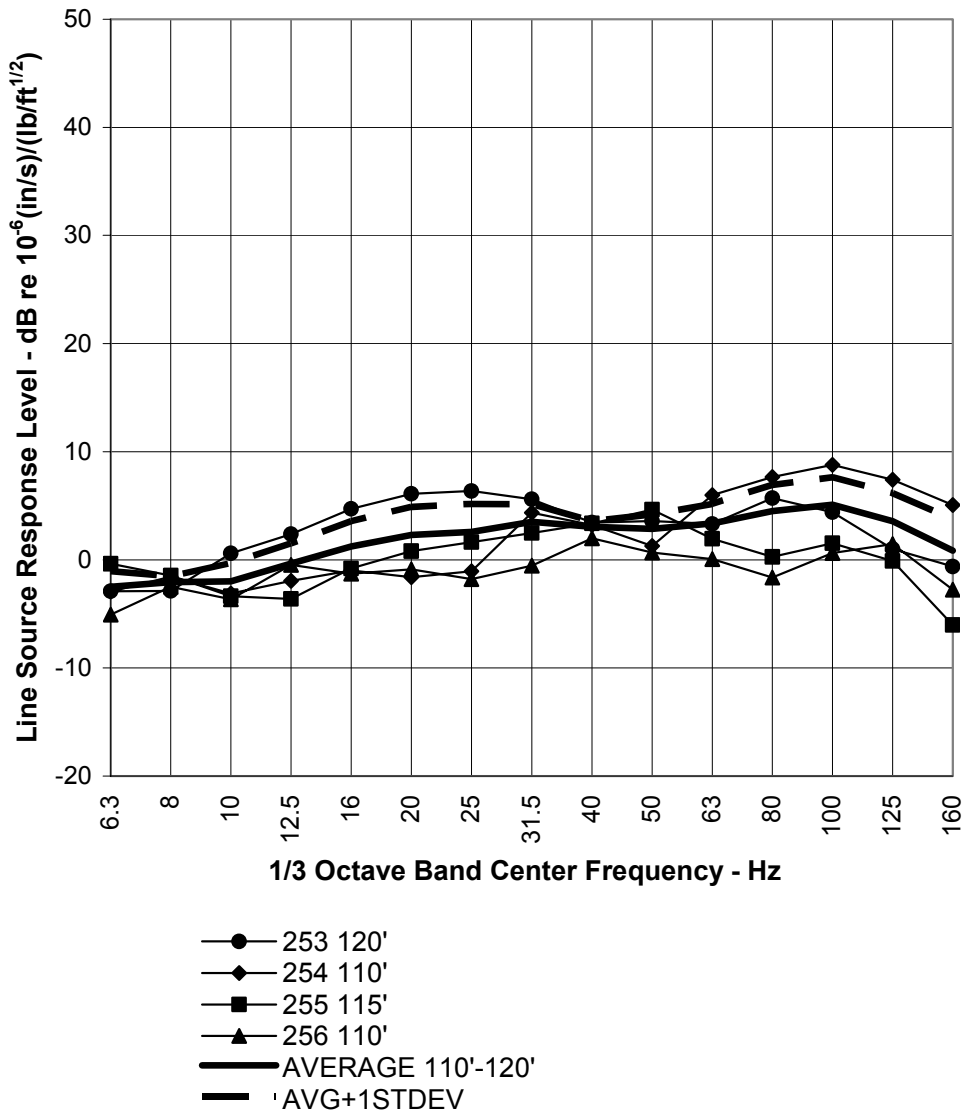


Figure 5-3 Effect of Transfer Function Component Averaging



Line Source Response at 200 Feet from Track Center Line
 Train Length=340 ft
 Source Depth=110-120ft

Figure 5-4 Line Source Responses Estimated for Four Boreholes

5.2 Numerically Calculated Line Source Responses

The original intent of the study was to employ regression curves for extrapolation to all distances. However, the background vibration degraded the data at larger distances, as evidenced by low coherence and inability to reliably detect the impulse response data. The low frequency and high frequency responses were also subject to instrumentation noise and background vibration. Theoretical models of the layered soil based on shear and compression wave velocities measured at boreholes NB-123, NB-253, and NB-255 were used to calculate the LSRs at distances greater than 300 feet. Each one-third octave LSR was “calibrated” by comparing the theoretical predictions with test results at 50, 100, and 200 feet for boreholes NB-253, NB-254, NB-255, and NB-256. The calibrated LSRs were then used for extrapolation to receivers beyond 300 feet. The process is briefly outlined below. A more detailed discussion is provided in Appendix B.

Numerical Procedure

Seismic wave velocity profiles were provided by Geo Recon at borings NB-253, NB-255, and NB-259 during the current PE phase, and at NB-123 during the alternatives analysis. Additional seismic wave velocity profiles were provided by Shannon and Wilson for borings NB-354 and NB-356. The wave velocity data for NB-123, NB-253, and NB-255 define shear and bulk moduli that were used for modeling vertical responses of the layered soil, using a proprietary seismic reflectivity model and computer code (LAYER) developed by the author of this report.¹⁸ The computer code has been validated against analytical calculations and borehole test data at other properties, and is compared with results measured at University of Washington campus as discussed below. The theoretical formulation of the model is similar to those described in the literature for forward modeling of earthquakes^{19, 20} and ground vibration.²¹

¹⁸ J. T. Nelson 2000, *Journal of Sound and Vibration* **231**, No. 3 727-737. Prediction of Ground Vibration from Trains using Seismic Reflectivity Methods for a Porous Soil.

¹⁹ B. L. N. Kennet 1983, *Seismic Wave Propagation in Stratified Media*, Cambridge University Press, Cambridge

²⁰ K. Aki and P. G. Richards 1980, *Quantitative Seismology, Theory and Methods, Volume I and II*, W. H. Freeman & Co., San Francisco

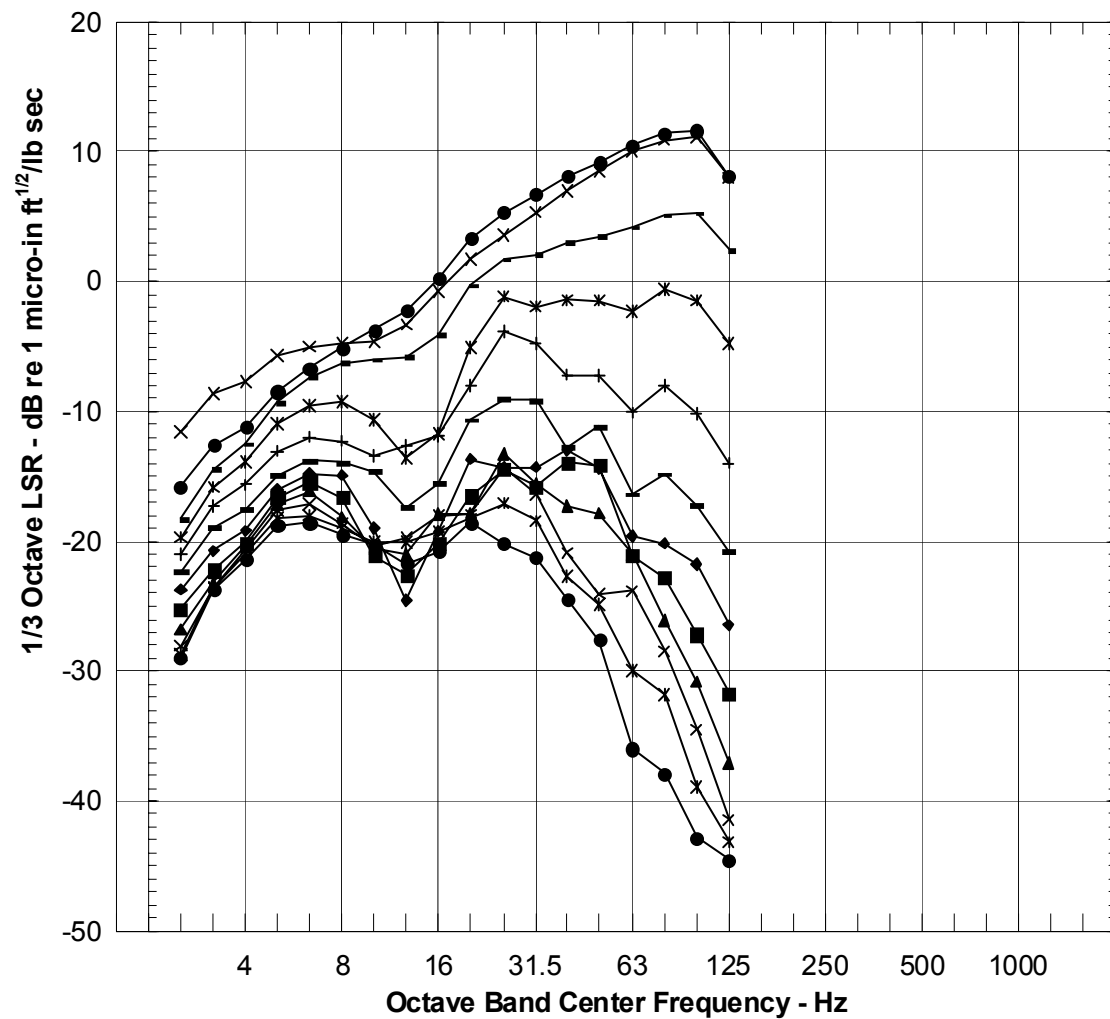
Quality factors of 20 and 40 were assumed for the upper layer and underlying layers, respectively. These quality factors describe the material damping, or loss factor, of the soil. The loss factor is inversely proportional to the quality factor. Typical soils have quality factors of the order of 10 to 20, while glacial tills are expected to have quality factors approaching those assumed here. The quality factors assumed for this study are believed to be similar to or higher than those existing at the site, and thus should give conservative predictions of attenuation versus distance. At 8 to 12Hz, the effect of quality factor is small over the distances assumed here.

Third octave transfer mobility functions were computed with the model for various source depths and offsets from 7.5m to 360m, or from 25 feet to 1180 feet. Cubic-spline interpolation was used to integrate the square of the magnitude of the transfer mobilities over the train length to obtain Line Source Responses. Examples of the calculated LSRs are plotted in Figure 5-5.

Calibration with Tests Results

The numerically calculated LSRs were compared with the LSRs obtained by integration of the global regression curve for Point Source Responses for offsets of 50, 100, and 200 feet. The differences are illustrated in Figure 5-6. The measured LSR and the calculated LSRs agree within roughly five decibels at ranges less than 200 feet. At frequencies below 20Hz, the measured LSRs are 2 to 6 dB above the theoretical LSRs. At frequencies above 20Hz, the measured LSRs are about 0 to 5 dB less than the theoretical LSRs. These differences are comparable with the standard deviation of the measured LSRs (See Appendix A), which validates the model over this range of offsets. The average differences shown in Figure 5-6 were added to the theoretical LSRs to extrapolate the test data to offsets greater than 300 feet.

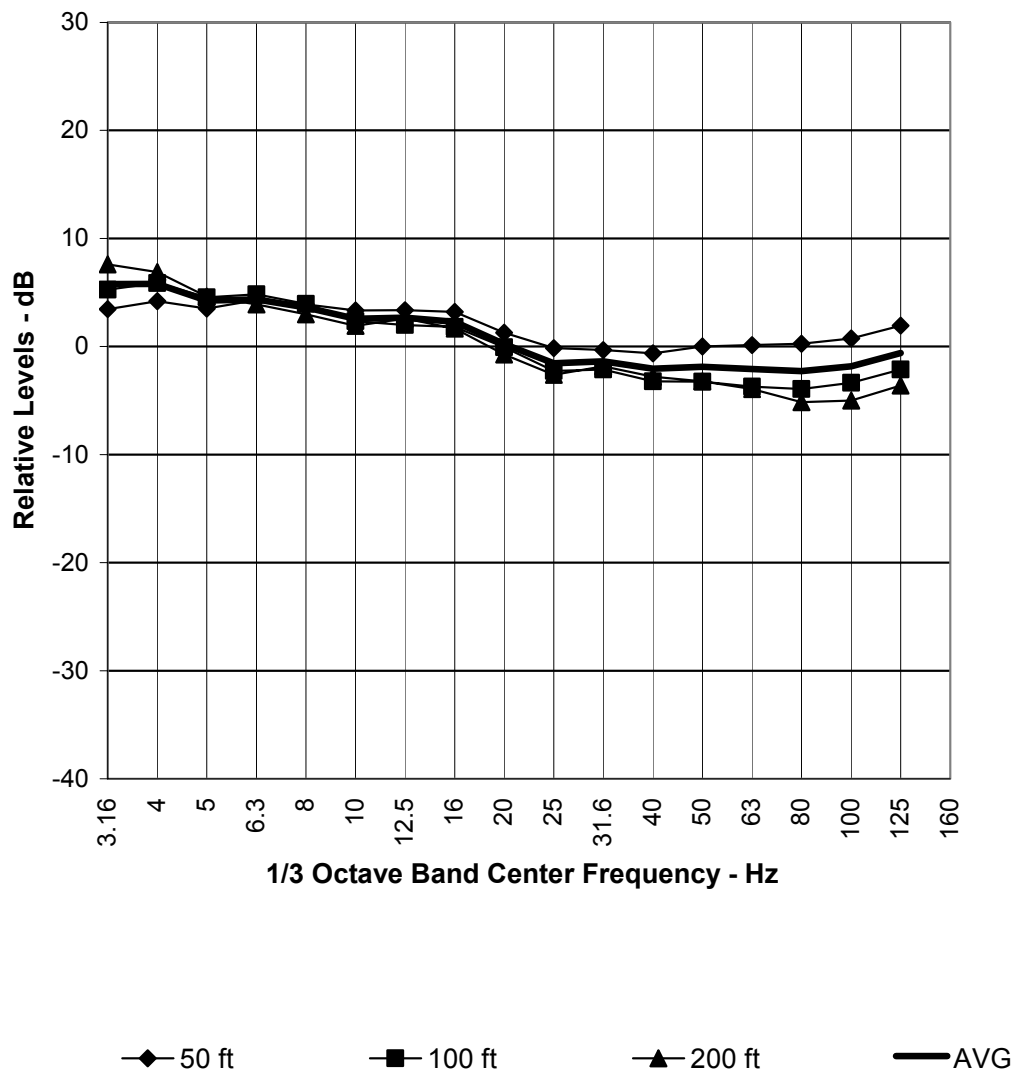
²¹ L. Auersch 1994 *Journal of Sound and Vibration* 173, 233-264. Wave Propagation in Layered Soils: Theoretical Solution in Wavenumber Domain and Experimental Results of Hammer and Railway Traffic Excitation.



Theoretical LSR Values Distance Comparison

—x— 15 M —●— 45 M —— 75 M —*— 105 M —+— 135 M —— 165 M
 —◆— 195 M —■— 215 M —▲— 245 M —x— 275 M —*— 305 M —●— 335 M

Figure 5-5 Line Source Responses Calculated from Seismic Wave Velocity Profiles



Calibration Factors

Figure 5-6 Measured LSR relative to Theoretical LSR

6 VIBRATION PREDICTIONS FOR STANDARD TRACK AND DESIGN SPEED

Estimates of vibration velocity level were made by combining the Line Source Response and Force Density Levels. The global regression results for the line source response were used for predictions at horizontal offsets less than 300 feet. At greater distances, the LSRs based on numerical estimates using the seismic wave velocities and adjustments to match the global regression result at short ranges were employed. Detailed estimates of vibration for standard direct fixation are given in Appendix D.

6.1 Assumptions

The predictions are based on the following assumptions:

Standard Resilient Direct Fixation Fasteners: Standard direct fixation fasteners are typified by natural rubber elastomer with bonded top and bottom plates, Pandrol clips, bottom plate anchorage, nominal static stiffness of 100,000 lb/in, and nominal dynamic stiffness of 140,000 lb/in.

Rail Condition: The condition and quality of the rails are assumed to be similar to those at the San Jose VTA where the Kinkisharyo vehicle FDL tests were conducted.

Vehicle: The vehicle is assumed to be 96ft long and of the same configuration and design as the Kinkisharyo vehicle of the San Jose VTA system, for which FDL data have been collected and used for prediction.

Slip-slide control: The vehicle for the Sound Transit system would include slip-slide control as a standard provision to control wheel flats and roughness, and thus control vibration and noise.

Two train consists of four vehicles each: Two four-car train consists are assumed to be operating simultaneously within the two tunnels. The vibration velocity level estimate for two trains is obtained by adding 3dB to the estimate for a single train operating in the nearest tunnel, which approach gives a slightly higher prediction than would otherwise be the case.

Train Speed: The design speed is assumed to be 30 to 55mph along the alignment throughout the campus, and 30 to 40mph on the horizontal curve between the campus boundary and the Brooklyn Station.

6.2 Predicted Ground Surface Vibration

Table 6-1 lists predicted ground surface vibration velocity levels and UW Thresholds by receiver. Values shown are the highest prediction for any train speed studied in each 1/3 octave band frequency. The tunnel depth and horizontal offset are included. The UW Thresholds are the same as those listed in Table 2-1. The levels that would exceed the UW Thresholds are shown in bold font.

The predicted ground surface vibration velocity levels are highest for Electrical Engineering (48dB at 80Hz), Wilcox Hall (60dB at 80Hz), Roberts Hall (51dB at 80Hz), More Hall (57dB at 80Hz), Fluke Hall (48dB at 80Hz), Mechanical Engineering (59dB at 80Hz), and Mechanical Engineering Annex (63dB at 80Hz).

The predicted levels exceed the UW Thresholds at the following buildings: 1) Electrical Engineering, 2) Johnson Hall, 3) Bagley Hall, 4) New Chemistry, 5) Wilcox Hall, 6) Physics & Astronomy, 7) Burke Museum, 8) Benson Hall, 9) Roberts Hall, 10) Winkenwerder Hall, 13) UW Medical Center, 16) More Hall, 19) Fluke Hall, 20a and 20b) Mechanical Engineering and Mechanical Engineering Annex, and 22) CHDD, a total of 15 of the 23 buildings considered (ME and ME Annex are counted as one building site).

The predicted levels shown in Appendix D for the core buildings consisting of Bagley Hall, New Chemistry, Physics & Astronomy, Benson Hall, and Johnson Hall, exceed the UW Threshold by a few decibels at 8Hz. The complete train speed results shown in Appendix D indicate that this would occur primarily for 50mph trains.

Table 6-1 Predicted Velocity Levels and UW Thresholds - Maximum over Train Operating Speed Range – Two Trains - Standard DF Fasteners on Rigid Invert

Building	Depth Offset		Frequency – Hz																
	Ft	Ft	3.15	4	5	6.3	8	10	12.5	16	20	25	31.5	40	50	63	80	100	
1) EE/CS	147	338	22	26	25	32	40	36	27	23	28	31	35	38	38	44	48	42	
UW Threshold			25	25	26	29	30	32	30	33	26	23	27	24	24	27	32	19	
2) Johnson Hall	132	677	16	21	19	26	34	26	17	15	18	17	22	26	26	25	27	19	
UW Threshold			34	32	33	31	31	32	36	37	35	35	44	43	44	39	38	39	
3) Bagley Hall	138	978	14	20	18	24	31	26	20	16	15	16	20	18	16	20	18	7	
UW Threshold			32	30	29	27	26	28	27	26	28	26	31	28	33	35	27	35	
4)Chemistry	125	1008	14	19	17	23	30	27	20	16	15	15	19	17	15	16	16	5	
UW Threshold			29	28	26	25	26	26	24	24	25	21	28	25	28	30	19	18	
5) Wilcox Hall	99	110	27	31	30	36	45	44	38	36	37	38	45	50	50	57	60	56	
UW Threshold			27	27	27	29	31	32	30	30	30	20	23	22	27	25	25	27	
6) Physics/Astronomy	121	1201	14	19	16	23	30	26	17	13	14	11	15	15	12	9	7	0	
UW Threshold			36	32	30	27	28	30	30	26	23	21	26	22	22	30	22		
7) Burke Museum	78	826	15	21	21	29	37	34	27	22	19	23	24	27	25	28	25	17	
UW Threshold			32	33	33	32	33	36	35	35	36	34	33	33	35	32	29	27	
8) Benson Hall *	134	1269	14	19	16	23	30	26	17	13	14	11	15	15	12	9	7	0	
UW Threshold			32	30	29	27	26	28	27	26	28	26	31	28	33	35	27	35	
9) Roberts Hall	113	255	25	29	27	34	43	41	36	32	33	34	40	43	42	49	51	47	
UW Threshold			26	28	27	26	31	30	30	30	24	25	26	25	30	29	27	27	
10) Winkenwerder Hall *	102	683	16	21	20	28	36	31	23	16	21	23	24	26	27	27	28	21	
UW Threshold			26	28	31	30	33	33	30	29	32	33	32	31	28	29	29	32	
11) Henderson Hall(30-40)	58	1208	7	7	17	26	29	26	16	13	16	13	13	10	14	7	7	-1	
UW Threshold			37	36	35	32	35	35	32	29	27	24	25	27	21	18	21	14	
12) Ocean. Research(30-40)	80	1833	4	5	14	22	25	21	11	7	8	6	3	-1	-3	-13	NA	NA	
UW Threshold			29	28	28	27	29	31	28	28	31	32	32	33	24	26	23	16	
13) UW Medical Center	108	910	14	20	19	26	33	28	22	18	16	20	22	22	21	20	18	12	
UW Threshold			35	34	35	34	31	32	31	29	26	21	23	17	15	19	13	8	
14) Fisheries Sciences(30-40)	68	1640	5	5	15	23	26	22	13	9	10	8	5	1	4	-3	NA	NA	
UW Threshold			34	35	33	32	30	30	42	31	30	30	33	30	30	32	26	21	
15) Fish. Teach & Res(30-40)	73	1858	4	4	13	22	24	21	11	6	9	6	2	-2	-3	-13	NA	NA	
UW Threshold			35	35	33	31	32	34	34	34	36	35	30	26	23	21	17	12	
16) More Hall	113	137	26	30	28	35	44	42	37	35	35	36	43	46	47	54	57	53	
UW Threshold			29	33	32	32	34	35	35	34	39	37	41	48	39	40	36	38	
17) Marine Studies(30-40)	70	1799	4	5	14	22	25	21	11	7	8	6	3	-1	-3	-13	NA	NA	
UW Threshold			28	29	29	27	28	29	30	33	30	31	38	38	42	33	30	26	
18) Bioeng./ Genomics *	100	1612	12	17	15	22	29	24	16	11	9	9	10	8	5	0	NA	NA	
UW Threshold			29	28	28	27	29	31	28	28	31	32	32	33	24	26	23	16	
19) Fluke Hall	140	333	22	26	25	32	40	36	27	23	28	31	35	38	38	44	48	42	
UW Threshold			31	32	33	34	34	37	41	45	41	42	44	41	31	37	25	20	
20a) Mech Engineering	124	105	26	31	28	36	45	42	38	35	36	37	43	47	48	56	59	55	
UW Threshold			30	30	33	27	30	29	29	34	28	31	30	23	20	25	19	18	
20b) Mech. Eng. Annex	124	9	27	31	30	38	46	44	38	35	36	38	44	49	51	59	63	59	
UW Threshold			30	30	30	29	33	33	31	38	31	38	43	32	32	31	29	23	
21) Ocean Sciences	104	2056	11	16	13	20	27	22	13	4	7	4	4	2	-6	-10	NA	NA	
UW Threshold			29	29	31	36	32	30	46	37	36	33	46	35	37	46	36	33	
22) CHDD	107	753	15	21	21	29	38	35	27	22	21	24	25	28	27	29	28	20	
UW Threshold			31	31	33	31	34	32	30	30	30	30	35	31	32	34	30	27	
23) Fisheries Center	100	1242	14	19	17	24	32	28	20	15	15	13	18	17	12	11	8	1	
UW Threshold			31	31	32	29	33	31	34	37	42	41	41	40	41	43	37	32	

- Background at Bagley Hall assumed for Benson Hall. Background at Bloedel Hall assumed for Winkenwerder Hall. Background at Oceanographic Research assumed for Bioengineering/Genomics
- NA Prediction not available, estimated to be less than 0dB (no impact)

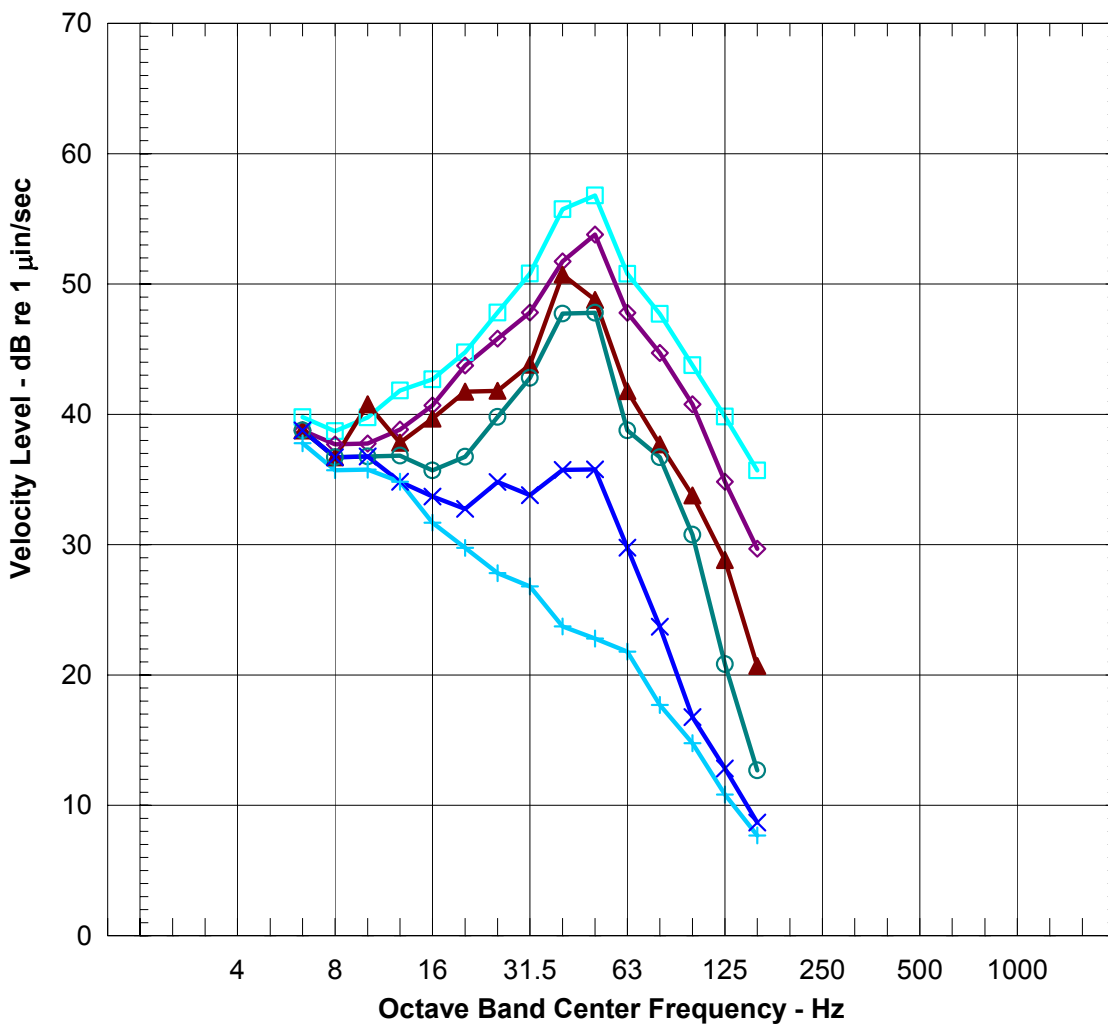
6.3 Basement Vibration Levels

The vibration predictions in Table 6-1 are made for the ground surface at the outside edge of the each building and as such do not take into account any effects from the foundation or other building vibration response (BVR). The influence of BVR was explored by conducting interior point source response measurements inside three buildings on the UW campus. The data collected at Savery Hall, Wilcox Hall and Mechanical Engineering Annex showed little difference between the ground surface and basement level responses at low frequencies. At high frequencies, the basement response was slightly lower than the surface responses. While a third octave BVR function was developed, it was not applied to the predicted levels for buildings on the campus other than those where it was measured. The basement predictions for ME Building, ME Annex, and Wilcox Hall are provided in Appendix D.

6.4 Example of Ground Vibration at Toronto

Ground vibration data measured in Toronto, Canada, are included here as a “reality check”. The soil in Toronto is a glacial till characterized by high shear and compression wave velocities, as is the soil at the University of Washington. Thus, ground vibration propagation at the University of Washington should be comparable with that at Toronto. Examples of ground vibration velocity levels obtained in the 1970’s at distances of 50, 100, 200, 400, and 800ft are provided in Figure 6-1. These data are for eight and ten-car heavy rail rapid transit trains running in the YSNE tunnels on stiff direct fixation fasteners (1 million pounds per inch) with solid steel wheels of generally revenue service condition. The depth of the tunnel was about 45 feet. The long range ground vibration propagation in Toronto was some of the most efficient that has been observed. The data shown are comparable with the levels predicted for the University of Washington campus with North Link Trains. At 50Hz, for example, the TTC ground vibration velocity level at 800ft was about 35dB re 1 micro-in/sec, or about 50µin/sec. The North Link trains running on continuous welded rail with resilient direct fixation fasteners should exhibit ground vibration levels considerably lower than those shown in Figure 6-1, simply because of lower rail support stiffness (140,000lb/in at North Link versus roughly 600,000lb/in at Toronto), use of modern wheel truing machines, rail grinding with modern vertical axis grinders, and greater tunnel depth (100ft at UW versus 45ft at Toronto).

The data shown in Figure 6-1 are affected by background vibration and instrumentation noise, an example of which is also plotted in the figure. This noise floor is due primarily to instrumentation noise, rather than background vibration. At 400 and 800 feet from the tunnel, the ground vibration produced by the trains is buried in the instrumentation noise floor at frequencies below 12Hz. If the noise energy were subtracted from the measured data at these low frequencies, the ground vibration produced by the trains would be less than 30 dB re 1 micro-in/second, or less than 30 micro-in/second.



Ground Surface Vibration Velocity Levels

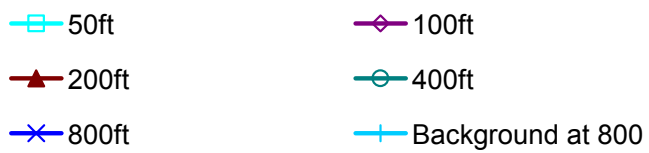


Figure 6-1 Example of Long Range Ground Vibration Propagation at Toronto

6.5 Two Trains versus One Train

The vibration predictions are for two trains running simultaneously past any particular point along the alignment. Ground vibration with a single train would produce lower ground vibration levels than predicted here by about 3dB. At locations close to the alignment, the near tunnel vibration usually dominates the spectrum. In this case, the differences between one train and two trains running simultaneously at the same speed and location may be little more than a decibel or two. At large distances, a three-decibel increase would be expected. The fraction of time during which vibration from two trains would be summing to the predicted levels would be small.

6.6 Uncertainty of the Predicted Levels

As discussed above, the uncertainty of the FDL test is about 3 decibels for the same vehicle and track condition. The uncertainty of the LSR tests would appear to be about 1 to 3 decibels. Assuming that the combined uncertainty is given by the root of the sum of the squares of the individual uncertainties (in decibels) would imply that the overall uncertainty of the prediction would be of the order of 4 to 5 decibels. Additional uncertainty in fastener corrections would increase the overall prediction uncertainty to perhaps 6 decibels.

The predicted vibration levels in Appendix D and Table 6-1 are the most likely that would occur for a single train with 3dB added to represent two trains. Thus, the probability that actual maximum vibration levels would be higher or lower than the predicted level is about 50%. The probability that the actual maximum vibration levels would be less than the predicted level plus a standard deviation of 6dB is 84%. Similarly, the probability that the actual vibration levels would be less than the predicted levels plus 10dB is about 95%. However, these probabilities apply at any single prediction point. When more than one receiver is considered, the probability that the actual vibration would be less than the predicted level at all buildings considered would be less than for a single receiver. That is, the risk of exceeding the predicted level at least at one building increases rapidly with an increase in the number of buildings considered.

7 IMPACT MITIGATION

7.1 Vibration Control Provisions

Vibration control provisions considered for this project include:

- 1) Reduction of speed to as low as 30mph.
- 2) Provision of a floating discontinuous “double-tie” slab track with standard resilient direct fixation fasteners and a nominal resonance frequency of about 12 to 16Hz for the tunnel segments on the UW Campus extending from the north end of the UW Station to 15th Avenue NE
- 3) High compliance direct fixation (HCDF) rail fasteners, such as the “Egg Type” fastener, with nominal dynamic stiffness of 80,000lb/in, for the tunnel segments on the UW campus from the southern boundary and extending through the UW Station. This would include the double crossover that would be located south of the UW Station. The tunnel sections extending from the northern boundary of the UW campus at 15th Avenue NE through the Brooklyn Station would also be treated with high compliance fasteners.
- 4) Rail grinding to control rail corrugation, remove defects, and possibly reduce rail undulation.
- 5) Wheel truing with a machine capable of truing resilient wheels to maximum run-out of 0.016 inch.
- 6) Moveable point frogs at the UW Station double crossover
- 7) Receiver based mitigation including relocation of some adversely affected UW research laboratories, or the provision of active or pneumatic (passive) vibration isolation systems for individual equipment.

Floating Slab Track

There are two floating slab track designs that have been considered. One of these is the discontinuous double-tie floating slab, consisting of pre-cast slabs supported on natural rubber springs, and the other is a continuous poured-in-place floating slab design offered by GERB, a manufacturer of steel coil springs. Each of these is discussed below.

GERB Floating Slab

A floating slab of 5Hz or lower resonance frequency would be required to control vibration at the primary suspension resonance frequency of 6.3 to 10Hz. Such a slab has been promoted by GERB, a European manufacturer of steel coil springs that has constructed a number of floating track slabs for rail systems in Europe, Asia, and the United States. The lowest design resonance frequency of installations provided thus far by GERB is about 5.4Hz.

Very little data exists concerning the insertion loss attributable to the GERB floating slab track under actual train operations, and none for slabs with design resonance less than 7Hz. GERB has conducted vibration insertion loss tests of a continuous floating slab with design resonance of 7Hz in Cologne, Germany, in 2005.²² The data is encouraging, and, based on that data, GERB has extrapolated insertion losses for a 4Hz slab, as shown in Table 7-1. The estimated insertion loss is 2 decibels at the 8Hz 1/3 octave band and 4 decibels at the 10Hz 1/3 octave band. The insertion loss at high frequencies is approximately 18 to 27 dB between 31.5 and 160Hz. These insertion losses are not particularly attractive considering the cost and uncertainties associated with the design.

²² **Report on Testing of the Cologne-Muhlheim Floating Track Slab and Extension to Seattle Sound Transit Line** (Proposal for a Low Frequency Floating Track Slab at the University of Washington Campus), Prepared by Scott Campbell and James Patterson, Kinetics/GERB Partnership, 7 June 2005

Table 7-1 Insertion Losses Estimated by GERB for a Continuous Poured-in-Place Floating Slab with Design Resonance 4Hz

Frequency – Hz	Insertion Loss – dB
5	-3.5
6.3	-0.9
8	2.1
10	4.2
12.5	6.0
16	8.6
20	12.9
25	14.9
31.5	18.6
40	22.6
50	26.8
63	26.2
80	20
100	17.9
125	20.6
160	19

There are a number of concerns with respect to low frequency floating slab track system with design resonance of 5Hz:

- 1) There is considerable uncertainty in predicted performance due to possible dynamic interaction of the slab with the vehicle suspension and lack of direct experimental data. Dynamic interaction could shift resonance frequencies without providing vibration reduction in the 6.3 to 12.5Hz bands, or, worse, amplify vibration. (Such an effect is believed by this author to be a cause of higher than expected resonance frequency at the Washington Metro C4 tunnel in Washington DC where continuous poured-in-place slabs with 16Hz design resonance were provided.)
- 2) There is some risk of amplification of vibration at the slab resonance frequency at low train speeds. At 30mph, for example, rail undulation with a 9ft wavelength would excite the slab at about 4.9Hz, and this excitation might be amplified by the resonance of the slab.
- 3) A high slab mass would be required to reduce the effects of coupling, but this would likely increase the tunnel diameter requirements. GERB has indicated that no such increase in tunnel diameter would be required beyond the 18ft-10in internal diameter

now anticipated for the North Link line. Additional mass can be provided with steel plates or high-density concrete.

- 4) The GERB floating slab is a continuous poured-in-place floating slab rather than a discontinuous double-tie system. A continuous floating slab would support bending waves and resonances that would degrade performance, limiting the insertion loss at frequencies above the design resonance. GERB has suggested that the GERB system could be adapted to a discontinuous double-tie system to avoid this problem. (A careful review of rail bending stresses would be required to determine if such an approach would be practical.)
- 5) The steel springs provided with the GERB slab system would be subject to corrosion, and might require more maintenance than natural rubber. Reliability of the springs over the lifetime of the system would be important. Experience has shown that corrosion of direct fixation fasteners and other metal components commonly occurs in tunnels where seepage occurs, and seepage in tunnels is quite common. GERB provides a high quality finish and rust inhibitor, and has indicated that no corrosion of steel springs has been observed with GERB floating slabs installed to date. The springs are normally installed in a removable configuration, and that they could be replaced easily in the event of damage to the springs due to fatigue or corrosion. However, if the inserts that hold the springs are damaged by corrosion, substantial cost for retrofit might be involved. Inserts made of stainless steel or a composite material might avoid this problem. Access to the springs could be an issue if the rail and fasteners are located over the springs, though this has not been an issue at other installations of continuous poured-in-place slabs.
- 6) Rail bending stresses are of concern with high compliance floating slab supports. However, GERB has installed low frequency floating slab track at a number of systems, and a record of performance and maintenance is being developed by the manufacturer. The continuous slab design is attractive for controlling rail stresses.
- 7) Fatigue of steel springs may occur due to repeated loading by the axles of the moving vehicles. GERB has indicated that the steel springs are designed conservatively, and

that fatigue has not occurred to date. Further, the GERB design with removable springs would allow replacement of fatigued springs should that occur. Corrosion notwithstanding, a properly designed steel spring system should not fatigue over the life of the track.

The 5Hz floating slab concept remains as an attractive vibration control provision, and further study of its performance would be conducted during final design. The continuous floating slab concept would also avoid parametric excitation of the track due to finite periodic supports. There are no 4 or 5Hz floating slabs in tunnels available for testing, so that experimental verification with an existing system is not presently possible, much less with one using light rail vehicles of the type planned for Sound Transit. Numerical finite difference or finite element models would be necessary to evaluate system performance. However, modeling is necessarily limited in the ability to accurately represent the moving load of the vehicle and vehicle/slab interaction. Thus, considerable care would be needed during final design to control uncertainty in predicted performance.

16Hz Double Tie Floating Slab

The discontinuous double-tie floating slab system that was developed at the Toronto Transit Commission and has since been employed in Atlanta (MARTA), San Francisco (BART), Los Angeles (LACMTA Red Line), Niagara Frontier (NFTA), Hong Kong, Athens, and the London Docklands is proposed for the tunnel sections extending from the northern end of the UW Station platform to the northern extent of the alignment on the UW campus. Each double-tie slab would be approximately 9 to 12 inches thick, would weigh about 5,000 to 7,000 lbs, and would be supported on resilient elastomer pads of nominal thickness of 3 to 4 inches. The design resonance would be approximately 12 to 16Hz. The rail would be fixed to the slabs with standard resilient direct fixation fasteners of a nominal static stiffness of 100,000lb/in and dynamic stiffness of 140,000lb/in. Fasteners with different stiffness may be considered for the floating slab if appropriate to control track resonance.

The above described discontinuous double-tie floating slab is recommended for the preferred alternative for the following reasons:

- 1) The Kinkisharyo vehicle's FDL is at a minimum at about 16Hz relative to other frequencies, so that the modest amplification of vibration at 16Hz by the floating slab system would be more tolerable than at the primary resonance frequency.
- 2) Natural rubber support pads and side pads would provide damping and limit amplification of vibration at the resonance frequency.
- 3) No modification of the tunnel diameter would be required.
- 4) The double-tie floating slab track has been installed successfully at many transit systems in North America for over twenty years, and maintenance data from these transit systems has proven its reliability. The NFTA system, in particular has a light rail vehicle running on a discontinuous double tie track of similar design to that proposed for the UW campus. The double tie system installed in Toronto has been in place for over 30 years with no apparent degradation.
- 5) Natural rubber support pads are expected to have a 100-year life, if not greater. They are not subject to corrosion, and, with proper formulation, are not subject to degradation by chemical attack or ozone.

Floating slab insertion losses estimated from measured tunnel invert or ground surface vibration data are compared in Figure 7-1. Three discontinuous double-tie designs are represented. Two of these are the Toronto Transit Commission Double Tie design, one with resilient direct fixation fasteners with a single un-bonded 45-durometer natural rubber pad²³, the other with two 45-durometer natural rubber pads. The stiffness of the latter fastener was one half that of the former. Both of these floating slabs were designed to exhibit a 16Hz natural frequency. The third double-tie floating slab is that of the Los Angeles Metro, which has a resonance frequency of between 12 and 16Hz²⁴. The rails were fixed to the double ties with bonded direct fixation

²³ S. T. Lawrence, **Toronto's Double Tie Trackbed System**, American Public Transit Association, Rapid Transit Conference, Chicago, 1978

²⁴ S. L. Wolfe, **Ground Vibration Measurements of Train Operations on Segment 2A of the Los Angeles Metro Red Line**, Draft Report, Wilson, Ihrig & Associates, for Parsons/Brinckerhoff/DMJM, November 1996

fasteners of nominal stiffness 150,000lb/in. Also shown is the vibration response of the San Francisco Municipal Railway continuous poured-in-place floating slab with embedded track²⁵. All of these data indicate a resonance peak, followed by a rapid decrease of response with increasing frequency. Considerable variation is observable in the performance due in part to uncertainties in the measurement results obtained at the ground surface.

The Los Angeles Metro floating slab response curve was used here for prediction of ground vibration for the North Link line through the University of Washington campus. The vibration reduction is listed in Table 7-2.

The floating slab response curve exhibits a loss of transmissibility at frequencies below 10Hz, implying that the slab would reduce vibration below 10Hz. Measurements at other systems also suggest such a favorable performance. From a theoretical point of view, the vibration isolation provided by a resiliently supported vibration isolator should be nil below the design resonance frequency. The apparent reduction is ignored for the purpose of prediction of vibration isolation on the UW campus.

Parametric excitation of the track and vehicle may occur due to the moving static load of the vehicles over the double-tie slabs. However, the double tie design with a 12 to 16Hz resonance frequency appears to perform at Toronto and Los Angeles as a single-degree of freedom isolator might be expected to perform, without evidence of parametric effects. This should be investigated further during final design.

²⁵ Steven L. Wolfe, **Floating Slab Design and Performance for Embedded In-Street Track – A Case Study at San Francisco Municipal Railway**, American Public Transit Association, Rapid Transit Conference, 1995

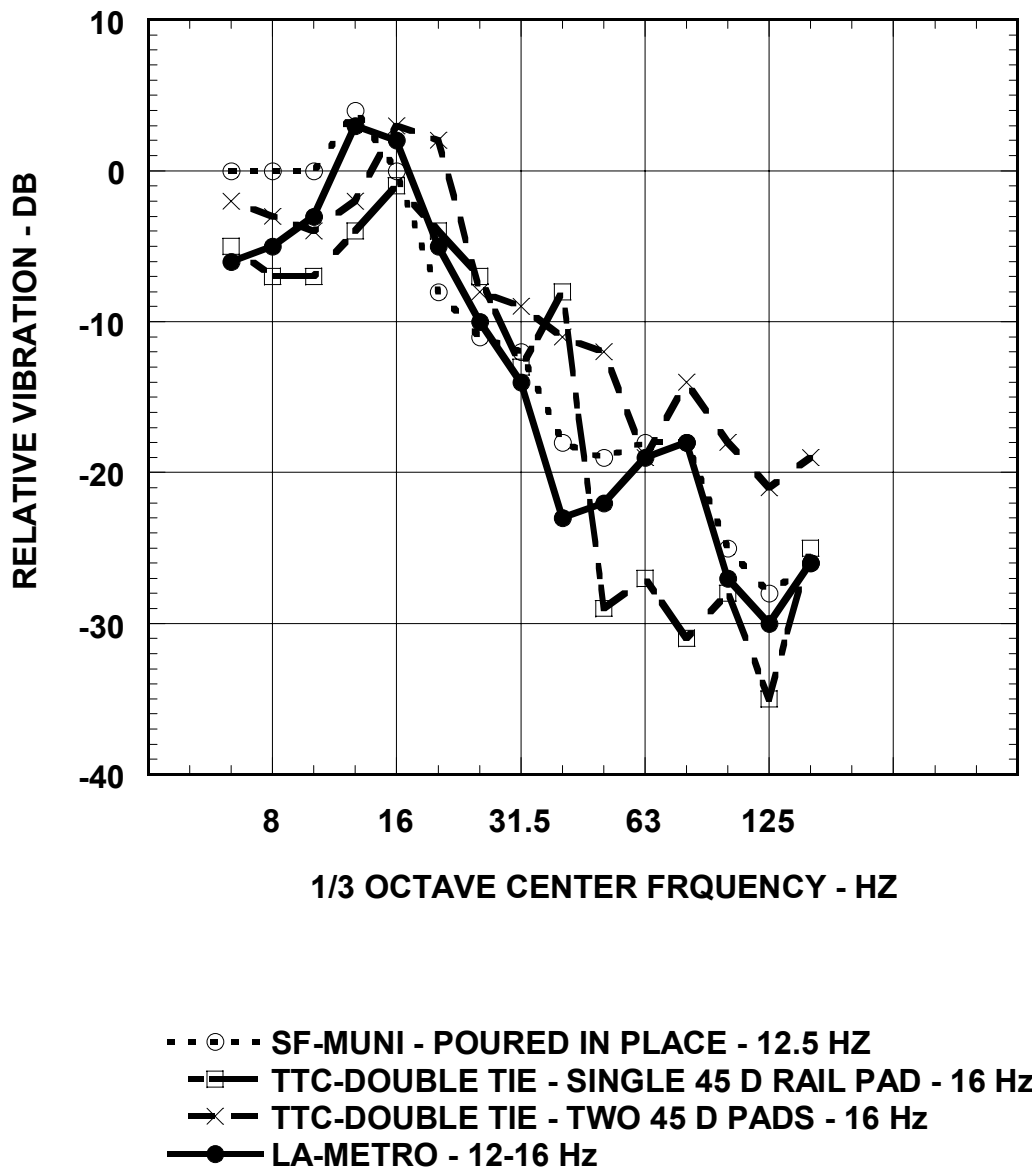


Figure 7-1 Floating Slab Performance Data

High Compliance Direct Fixation Fasteners

High compliance direct fixation fasteners are proposed for the tunnel alignment extending from the southern edge of the campus through the UW Station platform area. These fasteners would be provided at both tangent and special trackwork that would be located south of the stadium station. The section of the alignment extending from 15th Avenue NE north to Brooklyn Station would also be treated with HCDF. The vibration reduction associated with the high compliance fastener relative to the standard direct fixation fastener is given in Table 7-2.

Table 7-2 Vibration Transmission of Proposed Track Vibration Isolation Provisions Relative to Those of Standard DF Track

Frequency – Hz	HCDF	Double-Tie Floating Slab
3.15	0	0
4	0	0
5	0	0
6.3	0	0
8	0	0
10	1	0
12.5	2	3.5
16	2	3
20	1	-5
25	0	-10
31.5	-2	-14.5
40	-5	-23
50	-8	-22.5
63	-9	-18.5
80	-8	-17
100	-7	-27
125	-5	-30
160	-5	-26

Moveable Point Frog

A moveable point frog is proposed for the double crossover at the southern end of the UW Station near Station 1202+00 to control impact vibration as the vehicles traverse the frogs. For non-diverging trains, the moveable point frog is designed to eliminate the flange way gap normally associated with conventional rail bound manganese frogs, and should also be preferable to so-called flange bearing frogs or swing-nose frogs. The vibration generated by vehicles traversing the moveable point frog should be similar to that of the vehicle on continuous rail. No additional vibration increment is assumed for the frogs.

Vibration would be produced at the crossing diamond for diverging trains. An HCDF fastener may be needed for the double crossover diamond, though this should be carefully reviewed during final design. The need for vibration isolation would be dependant on the level of use and train speed, and the proximity of sensitive receivers that would benefit from such isolation. Train speed would likely be of the order of five to ten miles per hour. No predictions have been made for diverging trains.

Speed Reduction to 30mph

Sound Transit has proposed to reduce train speed as reasonable (no lower than 30mph) to achieve compliance with the UW Thresholds at key buildings, including Bagley Hall, New Chemistry, and Physics & Astronomy. The speed reduction may become an important component of the vibration reduction strategy, as it would substantially reduce low frequency vibration below 30Hz. Higher speeds may be achievable while meeting UW Thresholds at these core buildings, because there is considerable safety margin between predicted levels and the UW Thresholds. However, the consequences of train speed for other sensitive buildings on campus would also need to be taken into account.

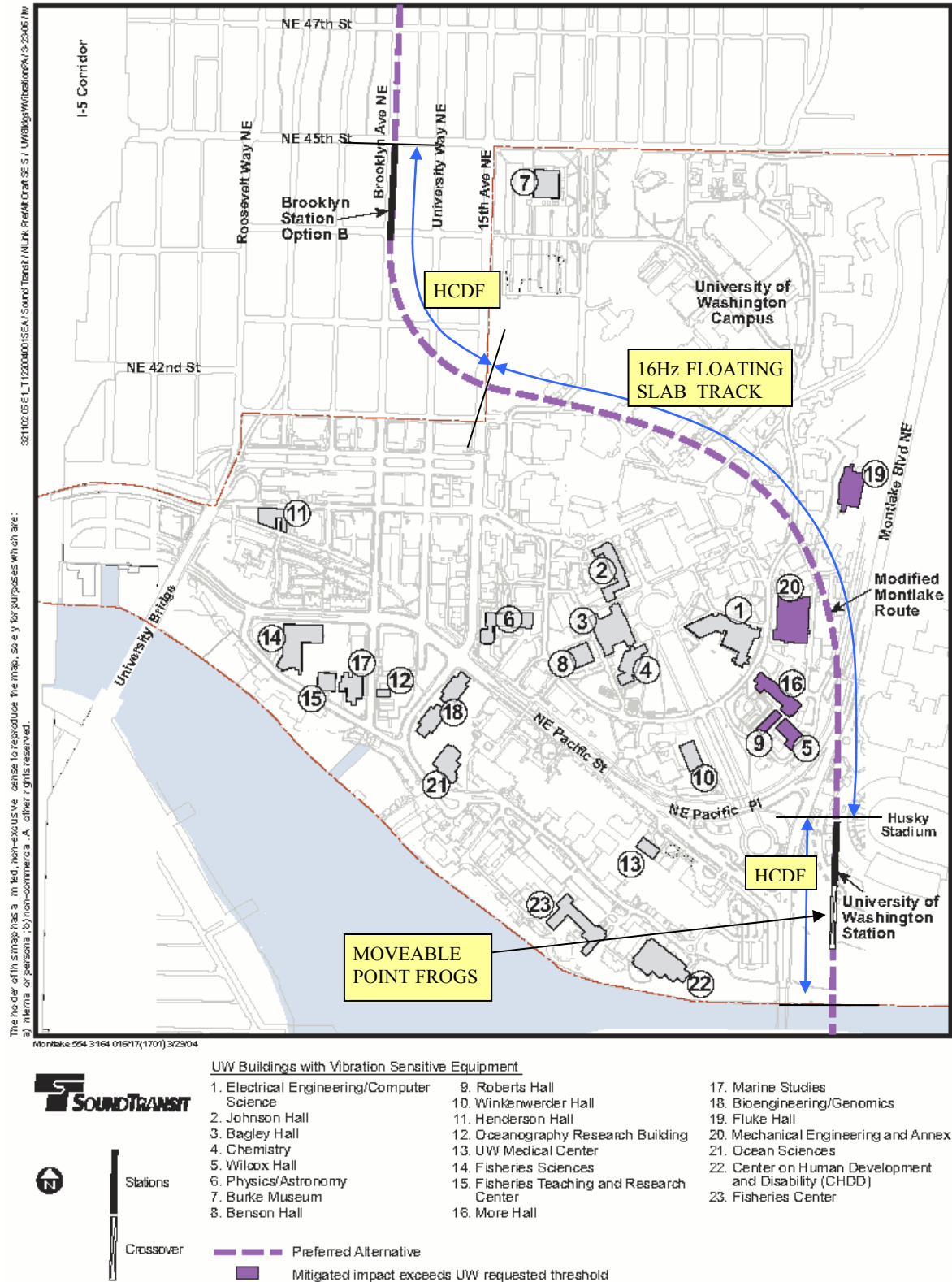


Figure 7-2 Vibration Control Provisions

Rail Grinding and Rail Corrugation Control

Rail corrugation is a constant maintenance issue at rail transit systems. The curved track proposed for the North Link Alignment through the University of Washington campus may require greater maintenance than tangent track to maintain smooth rail. The most effective control is rail grinding on a regular schedule determined by the rail corrugation rate. Maintaining rail and wheel profiles would be necessary to promote self-steering of the vehicle truck through the curve and thus reduce rail wear and corrugation. Grinding frequencies usually range between 3 to 6 years. One can show that for rail corrugation the minimum amount of metal removal can be obtained by grinding at an interval equal to the exponential growth time for corrugation formation. Thus, the optimal grinding interval may also promote rail life.

Other methods of rail corrugation control might include top-of-rail lubrication with a friction modifier, variation of train speed, or high compliance direct fixation fasteners. More research regarding fastener stiffness and rail corrugation is needed to understand rail corrugation.

There is some evidence that rail grinding using special techniques may help to reduce rail undulation caused by the steel mill's roller straightener. Per conversations with one rail grinder manufacturer, rail undulation at a railroad was reduced by grinding with a vertical axis grinder. However, the manufacturer also indicated that the best defense against rail undulation is selection of straight rail for installation, because there are limits as to how much undulation can be removed by grinding. This does suggest, though, that at least one rail grinder can reduce rail undulation. The system could be designed to admit such a rail grinder that has been shown to be effective. This would involve specification of clearance envelopes to allow use of grinders in tunnels, and to allow the grinders to get from the yard or other access point to the tunnels.

Wheel Truing Machines

Wheel truing machines are a standard provision at modern light rail systems. Although some existing systems may not have access to them, Sound Transit is already procuring them for the Initial Segment of light rail in Seattle. Wheel truing machines are listed here as a mitigation provision because they would be the principal defense against excessive ground vibration once

the system is in operation. Early detection of rough or out-of-round wheels and speedy truing would help to control ground vibration on campus and mitigate vibration impacts.

The specification for the Hegenscheidt wheel truing lathe being purchased by Sound Transit indicates that the maximum radial run-out of trued wheels would be 0.012in. Penn Machine has indicated that wheel run-out after truing is similar for either lathe or milling machine type wheel truing machines. A lathe would probably be the preferred choice. Ground vibration amplitudes can be expected to be directly proportional to wheel radial eccentricity and radial run-out, so selection of an optimum truing machine is important to control ground vibration at the University of Washington. The truing tolerance of the wheel lather is comparable to or less than British specification for rail straightness. Both of these parameters must be controlled.

Wheel profile will play an important role in controlling rail corrugation and roughness, especially at the curved section of track through the UW campus. The radius of curvature is sufficiently large to promote rolling radius differential and avoid lateral slip of the tire across the rail. The wheels must be trued sufficiently often to prevent formation of hollow tread profiles and false flanging. Rail cant and super-elevation must be designed to work with the wheel tread profile to achieve optimum curving performance. The rail gauge should be maintained at standard gauge for tangent track. Asymmetrical rail profiles can be employed to promote self-steering in lieu of gauge widening. Flange lubrication may be required to reduce gauge face wear and related gauge widening.

Rail Straightness Specification

Modern rail is normally straightened with a roller straightener. The diameters of the roller straightener rollers are roughly similar to the diameters of rail vehicle wheels, and can produce an undulation in the rail with wavelength comparable to the circumference of the vehicle's wheels. The rail procurement contract should include a specification for rail straightness to control rail undulation. Rail grinders are not designed to take out undulations of this type, though, as discussed above, one rail grinding machine manufacturer has indicated some success with reducing rail undulation at a mainline. Once installed, the direct fixation fastener elastomer would likely creep, allowing the rail to assume its undulated shape. In ballasted track, the ballast conforms to the rail undulation, so that the undulation would remain in place after running in.

As discussed above with respect to the force density levels of the Kinkisharyo vehicle, the San Jose VTA vibration data suggest that rail undulation and roughness may be the principal source of ground vibration at frequencies of the order of 8 to 10Hz. Assuming that conventional domestic rail undulation is of the order of 0.050in (as was observed at Kamloops), limiting rail undulation to perhaps 0.015in might reduce vibration at these frequencies. This amplitude is slightly greater than the truing tolerance of the wheel lathe for Bochum 54 and 84 wheels.

Conversely, if the amplitude of undulation of the rail supplied to the Sound Transit North Link line would exceed that of the rail at the San Jose VTA test sites, higher levels of low frequency vibration would probably occur than those predicted here. An appropriate specification would prevent this eventuality.

At this time, insufficient evidence exists to be certain of these likely improvements and further investigation during final design is recommended before including this measure in the mitigation package for the project. During Final Design additional data regarding conventional rail manufacturing specifications, installation, and rail grinding effectiveness would be gathered to help evaluate the effect of rail straightness control on low frequency vibration.

Receiver-based mitigation

The University has requested that mitigation be applied at the source only and not the receiver, however two types of receiver mitigation should be considered for buildings close to the light rail alignment where vibration levels from the trains are predicted to exceed the UW requested threshold. These are relocation of research facilities or provision of vibration isolation systems.

Relocation of laboratory activities to a new location farther away from the light rail vibration source would be an effective mitigation measure because vibration levels decrease as the distance increases between the receiver and the vibration. Relocating research facilities is an appropriate option when there are a few research facilities that are affected and they can be reasonably relocated to a new location. Relocation of laboratories would be, in general, expensive, requiring architectural and “tenant improvement” construction, in addition to moving the laboratory equipment. Commercial scanning electron microscopes, laser interferometers, micro-balances, and the like would probably not require relocation, because predicted vibration levels with

floating slab track at these buildings are comparable with or less than manufacturer's specifications for such equipment.

Active or pneumatic (passive) vibration isolation systems can also be used for individual equipment. These are benches, tables, or desks that are supported by air spring isolators. Pneumatic isolators are passive in design and their effectiveness is limited to the frequency range above their design natural frequency. Active isolators can vary their natural frequency in response to different vibration levels. These systems are very effective in isolating sensitive equipment from floor vibrations.

7.2 Predicted Ground Surface Vibration with Proposed Vibration Control Provisions

Estimates of the predicted ground surface vibration velocity levels with 16Hz floating slab track and high compliance direct fixation fasteners were developed for train speeds of 30mph. The predictions are described in detail in Appendix E to this report. All predictions are made with the assumption of two trains operating simultaneously, each train consisting of four cars. No margin of uncertainty has been applied.

Table 7-3 lists predicted mean vibration energy levels and the UW Threshold for the various buildings for two four-car trains operating at 30mph. The distance from the buildings to the alignment and the type of mitigation provision is indicated. Also indicated is the maximum excess of light rail vibration above the UW Threshold in parentheses.

The maximum predicted excesses for those buildings located close to the proposed alignment, such as Wilcox Hall (15dB) and Mechanical Engineering Annex (14dB), are due to the track resonance frequency of about 63 to 100Hz. The excess would be much higher without the floating slab track. The predictions at the core buildings are -10dB for Bagley Hall, -13dB for Physics & Astronomy, and -9dB for New Chemistry, indicating a substantial margin of safety between the UW threshold and predicted energy means at these buildings.

Table 7-3 Energy Mean and UW Threshold Velocity Levels for Two 30mph Trains

Building	Frequency	3.15	4	5	6.3	8	10	12.5	16	20	25	31.5	40	50	63	80	100
1) New Electrical Engineering 338ft	Light Rail / FS	11	14	22	23	26	26	19	19	23	15	11	6	14	21	28	12
	UW Threshold	25	25	26	29	30	32	30	33	26	23	27	24	24	27	32	19
	Excess (-3)	-14	-11	-4	-6	-4	-6	-11	-14	-3	-8	-16	-18	-10	-6	-4	-7
2) Johnson Hall 677ft	Light Rail / FS	5	8	17	18	19	16	9	10	13	1	-3	-6	1	3	7	-11
	UW Threshold	34	32	33	31	31	32	36	37	35	35	44	43	44	39	38	39
	Excess (-12)	-29	-24	-16	-13	-12	-16	-27	-27	-22	-34	-47	-49	-43	-36	-31	-50
3) Bagley 978ft	Light Rail / FS	3	7	15	15	16	16	13	12	10	1	-5	-14	-9	-3	-2	-23
	UW Threshold	32	30	29	27	26	28	27	26	28	26	31	28	33	35	27	35
	Excess (-10)	-29	-23	-14	-12	-10	-12	-14	-14	-18	-25	-36	-42	-42	-38	-29	-58
4) New Chemistry 1008ft	Light Rail / FS	3	7	15	15	16	17	12	12	10	-1	-6	-15	-10	-7	-4	-25
	UW Threshold	29	28	26	25	26	26	24	24	25	21	28	25	28	30	19	18
	Excess (-9)	-26	-21	-11	-10	-10	-9	-12	-12	-15	-22	-34	-40	-38	-37	-23	-43
5) Wilcox Hall 110ft	Light Rail / FS	16	19	27	28	31	34	31	31	32	22	20	18	25	35	40	25
	UW Threshold	27	27	27	29	31	32	30	30	30	20	23	22	27	25	25	27
	Excess (15)	-11	-8	0	-1	0	2	1	1	2	2	-3	-4	-2	10	15	-2
6) Physics & Astronomy 1201ft	Light Rail / FS	3	7	14	14	15	16	10	9	9	-5	-10	-17	-12	-13	-13	-31
	UW Threshold	36	32	30	27	28	30	30	26	23	21	26	22	21	30	22	
	Excess (-13)	-33	-25	-16	-13	-13	-14	-20	-17	-14	-26	-36	-39	-33	-43	-35	-31
7) Burke Museum 826ft	Light Rail / HCDF	4	9	19	20	23	25	18	17	20	17	12	13	15	15	14	6
	UW Threshold	32	33	33	32	33	36	35	35	36	34	33	33	35	32	29	27
	Excess (-10)	-28	-24	-14	-12	-10	-11	-17	-18	-16	-17	-21	-20	-20	-17	-15	-21
8) Benson Hall 1269ft	Light Rail / FS	3	7	14	14	15	16	10	9	9	-5	-10	-17	-12	-13	-13	-31
	UW Threshold	32	30	29	27	26	28	27	26	28	26	31	28	33	35	27	35
	Excess (-11)	-29	-24	-15	-14	-11	-13	-20	-21	-20	-32	-42	-46	-46	-52	-40	-66
9) Roberts Hall 255ft	Light Rail / FS	14	17	25	25	29	31	29	28	28	19	16	11	18	26	31	16
	UW Threshold	26	28	27	26	31	30	30	30	24	25	26	25	30	29	27	27
	Excess (4)	-12	-11	-2	-1	-2	1	-1	-2	4	-6	-10	-14	-12	-3	4	-11
10) Winkenwerder Hall 683ft	Light Rail / FS	5	9	18	19	22	21	15	12	16	8	-1	-6	2	5	8	-9
	UW Threshold	26	28	31	30	33	33	30	29	32	33	32	31	28	29	29	32
	Excess (-11)	-21	-19	-13	-11	-11	-12	-15	-17	-16	-25	-33	-37	-26	-24	-21	-41
11) Henderson Hall 1208ft	Light Rail / HCDF	4	7	16	17	20	22	14	12	17	9	5	2	6	-2	<0	<0
	UW Threshold	37	36	35	32	35	35	32	29	27	24	25	27	21	18	21	14
	Excess(-10)	-33	-29	-19	-15	-15	-13	-18	-17	-10	-15	-20	-25	-15	-20		
12) Ocean Research 1833ft	Light Rail / HCDF	0	5	13	13	16	17	9	7	9	2	-5	-9	-11	-22		
	UW Threshold	29	28	28	27	29	31	28	28	31	32	32	33	24	26	23	16
	Excess(-13)	-29	-23	-15	-14	-13	-14	-19	-21	-22	-30	-37	-42	-35	-48		
13) UW Medical Center 910ft	Light Rail / HCDF	3	8	16	17	18	19	12	13	17	14	10	8	10	7	7	1
	UW Threshold	35	34	35	34	31	32	31	29	26	21	23	17	15	19	13	8
	Excess (-5)	-32	-26	-19	-17	-13	-13	-19	-16	-9	-7	-13	-9	-5	-12	-6	-7
14) Fisheries Sciences 1640ft	Light Rail / HCDF	1	5	14	14	17	18	10	8	11	4	-3	-7	-4	-12		
	UW Threshold	34	35	33	32	30	30	42	31	30	30	33	30	30	32	26	21
	Excess(-12)	-33	-30	-19	-18	-13	-12	-32	-23	-19	-26	-36	-37	-34	-44		
15) Fisheries Teaching Center 1858ft	Light Rail / HCDF	0	4	13	13	15	17	9	6	10	1	-5	-10	-11	-23		
	UW Threshold	35	35	33	31	32	34	34	34	36	35	30	26	23	21	17	12
	Excess(-17)	-35	-31	-20	-18	-17	-17	-25	-28	-26	-34	-35	-36	-34	-44		
16) More Hall 137ft	Light Rail / FS	15	18	26	27	30	32	30	30	30	20	18	14	22	32	37	23
	UW Threshold	29	33	32	32	34	35	35	34	39	37	41	48	39	40	36	38
	Excess (1)	-14	-15	-6	-5	-4	-3	-5	-4	-9	-17	-23	-34	-17	-8	1	-15
17) Marine Studies 1799ft	Light Rail / HCDF	0	5	13	13	16	17	9	7	9	2	-5	-9	-11	-22		
	UW Threshold	28	29	29	27	28	29	30	33	30	31	38	38	42	33	30	26
	Excess (-12)	-28	-24	-16	-14	-12	-12	-21	-26	-21	-29	-43	-47	-53	-55		

Table 7-3 (Continued) Energy Mean and UW Threshold Velocity Levels for Two 30mph Trains

Building	Frequency	3.15	4	5	6.3	8	10	12.5	16	20	25	31.5	40	50	63	80	100
18) Bioengineering 1612ft	Light Rail / FS	1	5	13	13	15	14	8	7	4	-7	-14	-24	-19	-22		
	UW Threshold	29	28	28	27	29	31	28	28	31	32	32	33	24	26	23	16
	Excess (-14)	-28	-23	-15	-14	-14	-17	-20	-21	-27	-39	-46	-57	-43	-48		
19) Fluke Hall 333ft	Light Rail / FS	11	14	22	23	26	26	19	19	23	15	11	6	14	21	28	12
	UW Threshold	31	32	33	34	34	37	41	45	41	42	44	41	31	37	25	20
	Excess (3)	-20	-18	-11	-11	-8	-11	-22	-26	-18	-27	-33	-35	-17	-16	3	-8
20a) Mech Eng Building 105ft	Light Rail / FS	15	19	26	27	30	33	30	31	31	21	19	15	24	33	39	25
	UW Threshold	30	30	33	27	30	29	29	34	28	31	30	23	20	25	19	18
	Excess (20)	-15	-11	-7	0	0	4	1	-3	3	-10	-11	-9	4	8	20	7
20b) Mech Eng Annex 9ft	Light Rail / FS	16	19	28	29	32	34	31	31	31	22	19	17	27	37	43	28
	UW Threshold	30	30	30	29	33	33	31	38	31	38	43	32	32	31	29	23
	Excess (14)	-14	-11	-2	0	-1	1	0	-7	0	-16	-24	-15	-5	6	14	5
21) Ocean Sciences 2056	Light Rail / FS	0	4	11	11	12	12	5	0	2	-11	-21	-30	-30	-33		
	UW Threshold	29	29	31	36	32	30	46	37	36	33	46	35	37	46	36	33
	Excess(-18)	-29	-25	-20	-25	-20	-18	-41	-37	-34	-44	-66	-65	-67	-79		
22) CHDD 753ft	Light Rail / HCDF	4	9	19	20	23	26	18	16	22	19	13	14	16	16	17	9
	UW Threshold	31	31	33	31	34	32	30	30	30	30	35	31	32	34	30	27
	Excess (-6)	-27	-22	-14	-11	-11	-6	-12	-14	-8	-11	-22	-17	-16	-18	-13	-18
23) Fisheries Center 1242ft	Light Rail / HCDF	3	7	15	16	18	20	11	10	16	7	6	3	2	-2	-2	-10
	UW Threshold	31	31	32	29	33	31	34	37	42	41	41	40	41	43	37	32
	Excess (-11)	-28	-24	-17	-13	-15	-11	-23	-27	-26	-34	-35	-37	-39	-45	-39	-42

8 GROUND BORNE NOISE IN BUILDINGS

Ground borne noise is unwanted sound introduced into buildings by vibration propagated through the ground and into the building structure. Ground borne noise from rapid transit systems has been a serious problem in Toronto, causing substantial community reaction. The soil in Toronto is described as glacial till of relatively high shear and compression wave velocity and high quality factor (low damping) which is evidently similar to that found in Seattle. The floating slab system proposed for the UW campus alignment is very effective for controlling ground borne noise.

8.1 Criteria for Ground-Borne Noise

Appropriate levels for ground borne noise in libraries and classrooms would be a maximum of 35 and 40dBA, respectively, determined as the energy average of ground borne noise over the train passage duration. A level of 25 dBA would be appropriate for recording studios, TV studios, and concert halls. The American Public Transit Association (APTA) suggests that 40 dBA would be acceptable for schools and libraries.²⁶ The FTA impact criterion for “institutional land uses with primarily daytime use” is 40dBA.²⁷ The FTA further defines ground borne noise impact criteria for “Special Buildings”. These are listed below in Table 8-1.

Table 8-1 FTA Ground-Borne Noise Impact Criteria

Type of Building or Room	A-Weighted Noise Level – dBA
Category 2: Buildings: Residences and sleeping quarters	35
Category 3: Buildings: Institutional land use with primarily daytime use	40
Concert Halls, TV Studios, Recording Studios	25
Auditoriums	30
Theaters	35

8.2 Estimated A-Weighted Noise Levels

Ground-borne A-weighted noise levels in buildings on the University of Washington campus were estimated by adding adjustments to predicted ground surface vibration to account for

²⁶ American Public Transit Association, Guidelines, 1980.

²⁷ **Handbook of Urban Rail Noise and Vibration Control**, U. S. Department of Transportation, Urban Mass Transportation Administration, UMTA-MA-06-0099-82-1, February 1982, Pg B-20

foundation coupling loss, floor-to-floor attenuation, floor resonance amplification, noise radiation in rooms, and A-Weighting. The adjustments are listed in Table 8-2. The results are presented in Table 8-3. These predictions are the maximum levels predicted for simultaneous passage of two trains of four vehicles each passing at any of the speeds of 30, 35, 40, 45, 50, and 55mph. These predicted levels are for rms sound pressure levels averaged over the train passage duration.

Table 8-2 Adjustment Factors in Decibels to be Added to Ground Surface Vibration Velocity Levels in dB re 1micro-in/sec to Obtain Ground Borne Noise Level Estimates

Frequency – Hz	16	20	25	31.5	40	50	63	80	100	125	160
Foundation Response	-3	-4	-5	-4	-7	-8	-7	-7	-6	-5	-3
Floor-to-floor Response	1	-1	-2	-2	-2	-3	-3	-3	-3	-3	-3
Floor Resonance Amplification	5	6	7	8	8	7	7	6	6	5	4
Ground Borne Noise Adjustment	2	2	2	2	2	2	2	2	2	2	2
A-Weighting Adjustment	-57	-51	-45	-39	-35	-30	-26	-23	-19	-16	-13

With standard direct fixation fasteners, ground borne noise levels at basement and upper floor levels would be about 41 and 43 dBA, respectively, at Kane Hall, Smith Hall, and the Engineering Library. Ground borne noise would likely be audible. Corrugated rail or wheel flats would raise ground borne noise levels by about five decibels above those predicted. Similar predictions are indicated for the Mechanical Engineering Annex, located very close to the proposed alignment, for standard direct fixation fasteners without floating slab track isolation.

The predicted ground borne noise levels at the upper level floors of Smith Hall, Kane Hall, and Engineering Library with HCDF fasteners are all 37dBA. The predicted levels are 34, 37, and 37dBA, respectively, at Wilcox Hall, Engineering Library, and Mechanical Engineering Annex. The predicted level of 37dBA for the Engineering Library would be 2dB in excess of the recommended limit of 35dBA.

The estimated ground-borne noise levels for the proposed mitigation design identified in Figure 7-2 are all within the criteria given above. The 16Hz floating slab track greatly attenuates vibration at frequencies above 20Hz, and thus greatly attenuates ground-borne noise at frequencies where ground-borne noise usually is most apparent. No ground-borne noise impact is expected on the UW campus with the vibration control provisions recommended to mitigate ground vibration impacts on campus.

Table 8-3 Maximum Ground Borne A-Weighted Noise Levels for Various Buildings for 4-Car Trains at 30 to 55mph – dBA re 20 Micro-Pascal

Building	Standard DF		Cologne Egg		16-Hz Floating Slab	
	Basement	First Floor	Basement	First Floor	Basement	First Floor
New Electrical Engineering	25	27	18	21	4	8
Johnson Hall	3	6	-4	-1	-16	-13
Bagley Hall	-6	-3	-14	-10	-24	-21
New Chemistry	-8	-5	-16	-12	-26	-23
Wilcox Hall	38	40	31	34	17	20
Burke Museum	3	6	-5	-1	-17	-13
Roberts Hall	29	32	22	25	8	11
Winkenwerder Hall	4	7	-3	0	-15	-12
Medical Center	-5	-1	-12	-8	-24	-20
More Hall	35	38	28	31	14	17
Fluke Hall	25	27	18	21	4	8
Mechanical Engineering Annex	40	43	34	37	20	23
CHDD	4	8	-3	0	-15	-11
Smith Hall	41	43	34	37	20	23
Engineering Library	41	43	34	37	20	23
Suzzallo Library	35	38	28	31	14	17
Kane Hall	41	43	34	37	20	23
William H. Gates	6	9	-2	2	-13	-9
Meany Performance Hall	17	20	11	13	-2	1
Oedegaard Undergraduate Library	35	38	28	31	14	17
Buildings 1200 feet or more From the tunnel	-15	-11	-21	-18	-34	-30

Note: The negative numbers denote a negative decibel level, which represents a magnitude of sound pressure less than 20 Micro-Pascal.

If lower train speeds are used to control ground vibration, the ground borne noise levels would also be lowered relative to those that would occur with higher speed operation. However, ground borne noise levels would occur primarily near the track resonance frequency of 63 to 80Hz, which is not strongly affected by train speed. Thus, the predicted ground borne noise levels shown above for the highest level found between 30 and 55mph would not change very much with a reduction of train speed.

9 MONITORING

Comprehensive monitoring of ground vibration on the UW campus during pre-revenue and long term operation of Sound Transit light rail service can be conducted to verify conformance with design goals, detect degradation of vibration over time, and provide data for diagnostic and remedial action. Ground vibration monitoring of the sort contemplated for the UW campus would likely represent the state-of-the-art in verifying and controlling vibration impacts of a rail transit system on a research environment. Thus, there is little precedence for design and development of an appropriate system, though much of the instrumentation and computer based data analysis and storage used for noise monitoring at airports, for example, would be applicable. The techniques and software available for machinery health monitoring may also apply. Suppliers for both of these types of monitoring systems exist.

Pre-revenue vibration monitoring would be used to determine operational vibration levels at various buildings along the alignment, check performance relative to the UW Thresholds, and guide final design requirements for a long-term or permanent monitoring system. The second phase of the monitoring program would be long-term or permanent monitoring at monitoring stations that would be representative of the campus wide effects of Sound Transit operations. The long term monitoring would include in-tunnel as well as UW surface or building basement locations, and could include real-time detection. The design of any long-term monitoring system should be done with attention to need as well as practicality.

All of the predictions provided here are in terms of energy-mean or root-mean-square third octave vibration velocity levels. The terms energy-mean level and root-mean-square level are synonymous. Third octave vibration analyses should be done with continuous infinite-impulse-response filters of order 6 or higher. The data fed to the filters should be applied at least ten seconds prior to the beginning of integration, so that “turn-on transients” that would “kick” the filters would be avoided. Most real time analyzers available today are capable of this operation. Third octave vibration levels should not be synthesized from constant bandwidth Fourier spectra or auto-spectra, as these may yield uncertain results at low frequencies where the bandwidth of the third octave band filter may be comparable with the bin bandwidth of the analysis.

The integration time, or averaging time, is an important parameter for determining the energy mean level. In all cases, vibration monitoring should provide information on energy-mean vibration velocity levels over the time during which the train would pass the point of closest approach to the receiver. For example, the length over coupler faces of the Kinkisharyo light rail vehicle would be 28.926m, 94.88ft. A train consisting of four Kinkisharyo vehicles would have a length of 115.7m, or 379.5ft. A speed of 30mph is equivalent to 44ft/s. Thus, the time required for the train to pass a given point would be $379.5\text{ft}/44\text{ft/s} = 8.63\text{s}$, or about 9s. This would be the minimum integration time for a 30mph 4-car train, and would be most applicable at short range receivers. At long range, the actual signature of vibration would be much broader, especially at a receiver at the center of the curve, so that an integration time of perhaps 9 to 16 second would be appropriate. Shorter integration times would increase the uncertainty of the measurement unless successive integrations were energy averaged. The maximum level determined over a short integration time of one second would be higher than the energy-mean level, and thus would not be consistent with the prediction assumptions.

Ground vibration due to Sound Transit trains at long range would be very difficult to discriminate from background vibration. If cumulative vibration levels are in excess of criteria, then the ambient vibration energy would have to be subtracted from the measured vibration energy to determine the vibration energy level due just to the train. This also introduces uncertainties, and further underlines the need to use long integration times for these types of measurements. At short range receivers such as Wilcox Hall and Mechanical Engineering, the vibration levels in the 6.3Hz through 12.5Hz third octaves and in the 40Hz through 80Hz third octaves are predicted to be above the ambient levels and easily measured, at least in quiet basement environments. However, even in this case, the ambient may contribute to the measurement, and should be subtracted from the measured level if the measured level is no more than 10dB above the ambient level. This may lead to some difficulty with both measurement and interpretation of the data.

The predictions of ground vibration are for the ground surface, without adjustment for building responses. However, the lowest background vibration would likely be in basement areas where the UW thresholds were also measured, so that the best place to measure vibration would be at the basement floor where the floor is supported by undisturbed soil or rock. The measurements

should not be conducted “in structure” where floor resonances may amplify vibration relative to the foundation levels.

Only vertical vibration should be measured and compared with predictions and criteria, because the predicted levels and criteria are for vertical vibration. Experience has shown that the vertical vibration at the ground surface is representative of vibration in the other axes, and usually exceeds the vibration in the horizontal plane on concrete grade slab and structural floors. This is due to the in-plane stiffness of the concrete floor which is usually much higher than the vertical stiffness.

9.1 Pre-Revenue Service Monitoring

Prior to startup of revenue service, third octave ground borne vibration from Kinkisharyo vehicles should be measured at each of the sensitive buildings. The measurements should be conducted with a test train with trued wheels, and with a test train with wheels that have not been trued after brake testing to determine the range of vibration between trains with trued and untrued wheels. The rails should be ground prior to measurements with a vertical axis grinder to both smooth the rail and provide a profile consistent with design. A run-in time is probably not necessary prior to rail grinding, and may be detrimental to the rail if longitudinal periodic work hardening occurs prior to grinding.

The measured raw vibration levels should be adjusted as necessary for background vibration and then compared with the UW Thresholds. Background levels of vibration need not be the same as the UW Thresholds, and they should be determined before and after each train measurement.

The levels need not be done simultaneously at all locations, but coordinated tests with multiple receivers would reduce test and track time. The analog data should be recorded on digital tape for later analysis and for archival purposes. The recordings would allow identification of train passby vibration signatures by inspection of the level of vibration versus time. Time codes should be preserved to unambiguously identify train samples and discriminate them from other events.

Vibration should be measured at selected surface locations at various horizontal offsets from the tunnels to determine attenuation versus distance and perhaps identify suitable permanent monitoring locations.

The analog data should also be analyzed with a Fourier analyzer to obtain a detailed narrow-band constant bandwidth spectrum that can be compared with the modulation envelopes discussed above to determine if rail undulation is contributing to low frequency vibration. If so, recommendations concerning additional rail grinding should be developed.

After completion of the rail grinding and acquisition of the fleet, vibration produced by the entire fleet of trains should be measured. Wheels should be trued as necessary to maintain a reasonable maximum noise level, consistent with “normal” operation. The results of individual trains and the energy average for each direction should be obtained. The energy mean level and standard deviation for each direction should be determined, and an account should be made for the number of cars in the train consist.

These data will serve as a baseline for operations against which degradation of ground vibration can be assessed. After conducting these measurements, the UW and ST may agree to refine the design of the permanent monitoring system.

9.2 Permanent Monitoring

Permanent monitoring of ground borne vibration would provide real-time data that would document operational changes in ground vibration characteristics over time, provide a means of real-time identification of problem vehicles prior to passage through the campus, and provide warning signals to researchers of vibration impending events. The extent of the real time monitoring would depend on the actual vibration levels that would occur. That is, monitoring vibration at laboratories where the vibration would be consistently below the UW Threshold would be of little value. Even if the vibration data were detectable above the ambient, but less than perhaps ten decibels above the ambient, the practicality of subtraction of the ambient and unambiguous identification of samples would be questionable.

Long term or permanent monitoring would detect elevated vibration due to rail corrugation and wear. Rail corrugation would likely show up at frequencies above 30Hz, and so the detection of

rail corrugation would be most beneficial for short to intermediate offsets. Excessive vehicle hunting due to rail and/or wheel profile wear may contribute to low frequency vibration at long range, but this should be detectable at short ranges as well.

The most attractive locations for monitoring would be those where the ground borne vibration would be clearly above the ambient level, such as at the Mechanical Engineering Building, the Mechanical Engineering Annex, and Wilcox Hall. The HUB and Smith Halls would also be excellent monitoring locations due to their locations above the alignment (assuming that their ambient vibration levels are low enough), even though they are not on the list of sensitive buildings identified by the UW. The basement floors of these buildings would serve as proxies for the entire campus.

The UW has suggested monitoring locations that would be roughly similar to the above locations, but included instrumented boreholes at various time intervals. Boreholes would be attractive for monitoring because of the low ambient levels likely to be encountered at the bottom of the holes at perhaps 120ft depth. However, the holes may fill with water, and tube waves (acoustic waves in the fluid) may complicate the measurement, unless the transducers are grouted in. However, grouted transducers would not be removable for calibration and/or repair, while basement locations would admit at least yearly inspection, calibration, and possible upgrade.

Transducers used for monitoring should have very low noise characteristics. Examples of low noise seismic accelerometers include the Wilcoxon Research Model 731, which produces a buffered electrical signal voltage with nominal sensitivity of 10v/g, low end roll off frequency of 0.1Hz, and high end mounted resonance frequency of 800Hz. This transducer combined with an analog integrator would provide excellent response over the frequency range of 1Hz to 500Hz. A 2-Hz seismometer would provide excellent low frequency noise characteristics, perhaps preferable to that of a seismic accelerometer. The principal limitation of the seismometer would be the high-end spurious resonances that may occur at frequencies of the order of 50Hz or higher. The manufacturer should be consulted concerning noise characteristics and frequency range. The output signal of the seismometer could be transmitted over large distances on campus with balanced lines with matched impedance, though the practicality of this has not been determined

with respect to electrical interference. Electrical interference could be circumvented by transmitting vibration data digitally or by frequency modulated carrier.

Permanent monitoring station signals could be analyzed with computer systems or analyzers located at each monitoring station, with the analysis data being transmitted over the campus computer network. Alternatively, the analog data output from the transducer and/or preamp could be transmitted by low impedance cable to a central processing computer. Modern desk top computers with dual processing capabilities, 2GHz CPU's, and SCSI disk drives should be able to process vibration data at one 1000Hz sampling rate from five locations, giving a real-time bandwidth of 500Hz, nominal. This computer could be interfaced to the campus network for real time querying of data and also for archiving data and backup. The computer can send warnings by electronic mail to interested researchers or issue an alert concerning ground vibration events. The data base could be queried by researchers to determine if a vibration event occurred coincident with an anomalous experimental observation.

The value of in-tunnel monitoring has not been determined, as vibration at the tunnel wall would be controlled by relatively short sections of track. The surface locations provide a broader picture of the vibration, because the vibration is produced over larger sections of track.

Transducers could also be located north and south of the campus to detect vibration from vehicles with excessive wheel flats prior to passing under campus. This would allow a slow order or other practical measures to minimize anomalous excessive vibration from vehicles. While a vehicle with rough wheels may elevate ground vibration, the effect is most notable at high frequencies of the order of 30Hz and above, but is relatively small at low frequencies. Thus, distal locations where only low frequency vibration survives the propagation, such as at New Chemistry, would likely not be affected by trains with rough wheels. Short offset receivers, such as Wilcox and Mechanical Engineering, may well benefit from real-time detection of excessive vibration from a vehicle. However, vibration at these receivers would already be controlled to a large extent by floating slab track (which would benefit the entire campus), and thus may not be impacted by vehicles with rough wheels either.

10 CONCLUSION

The preliminary engineering and design recommendations described in this report are intended to provide a practical design for the Sound Transit North Link preferred alternative, and, at the same time, preserve an environment that is acceptable to the UW for research. With the proposed vibration isolation provisions, the vibration environment on the UW campus is predicted to be acceptable for most research activities, including those involving the highest resolution commercial scanning electron microscopes at even the closest buildings such as Wilcox Hall and Mechanical Engineering. However, some research in the closest buildings may be affected, and, as pointed out by the UW research community, the type of research or its sensitivity to vibration one hundred or even ten years from now is unknown.

10.1 Ground Surface Vibration

A summary of the predicted ground surface vibration levels during train passage at twenty-three buildings identified by the UW as vibration sensitive are compared with the UW Threshold basement floor vibration levels in Table 10-1. The maximum levels over the range of train speeds of 30 to 55mph were used to summarize the predictions for the unmitigated condition. The train speed must necessarily pass through 30mph on its way to or from 55mph from station stops. At a presumed acceleration of 3mph/sec, the train would be in the neighborhood of each of the model speeds for a few seconds or more. Acceleration rates will vary depending on grade and load. Estimates of vibration at constant speeds of 30 to 55mph are provided in Appendix D.

Without mitigation, vibration levels at fifteen of the twenty-three buildings are expected to exceed the UW Threshold levels (Mechanical Engineering and Mechanical Engineering Annex are counted as one building.) These buildings are located within about 1,200 feet of the proposed alignment.

With a 30mph speed restriction and 16Hz floating slab as mitigation, predicted energy mean ground surface vibration levels exceed the UW basement floor threshold levels at five buildings, including Wilcox Hall (110 feet from the alignment), Roberts Hall (255ft from the alignment), More Hall (137ft from the alignment), Fluke Hall (333ft from the alignment), and Mechanical Engineering (105ft from the alignment) and Mechanical Engineering Annex (9ft from the

alignment). The excess at Fluke Hall occurs at the 80Hz third octave, where the level at the track resonance frequency protrudes above a steeply declining UW Threshold, and thus might be considered trivial. The largest excesses are expected to occur at Wilcox and Mechanical Engineering Annex and to a lesser extent at Roberts Hall. At More Hall, the excess is 1 dB at 80Hz.

The 16Hz floating slab would not reduce ground vibration at frequencies below 12Hz; the main benefit of the floating slab installation would be the control of ground vibration and ground borne noise at frequencies above 20Hz. Some amplification of vibration at 12 and 16Hz would occur, but this would be at a minimum in the FDL third octave spectrum. The selection of design resonance would depend on measurements of the FDL for the Sound Transit Vehicle. The deep tunnel alignment and relatively stiff soils encountered at this site will help to control ground vibration at frequencies below the resonance frequency of the floating slab. This would appear to be an optimum solution. (This solution would likely not be attractive for sites with soft soils.)

The standard deviation of the measured LSR and FDL for trains on rigid invert is estimated to be six decibels. The probability of exceeding the predicted vibration plus one standard deviation would be roughly 16% at any particular receiver. That is, there would be an 84% probability that the actual levels at any one receiver would be less than the predicted level plus one standard deviation. The confidence level would rise to 95% if 1.7 standard deviations (about 10dB) were added to the predicted energy mean. When a group of receivers is considered, the risk of exceeding the predicted level at least at one of the receivers increases as the size of the group increases.

Long-range estimates of vibration are based on conservative assumptions of damping, so that attenuation rates should be higher than assumed. The effect of damping is small at low frequencies, but increases with increasing frequency and distance. Moreover, in-homogeneities in the soil, such as large rocks and boulders, or convoluted layering, may scatter vibration energy into deeper strata, thus providing some additional attenuation that is not included here.

Further testing of the Sound Transit vehicle is necessary to check the Kinkisharyo vehicle's FDL for final design. Sound Transit's first opportunity to test the vehicle will be in late 2006 or in 2007. The vibration level of the low frequency peak associated with the primary suspension will

also be controlled by rail roughness and undulation amplitude. Rail straightness will be investigated during final design. Low frequency ground vibration is variable. The spectral vibration peaks are modulated by the wheel and truck passage frequencies, and are likely to be affected by the number of vehicles in the train. This will be considered further during final design. An opportunity will exist to measure ground surface vibration produced by trains running in the Beacon Hill tunnel now under construction. The soils are believed to be similar to those found at the UW, though a comparison of soils data should be conducted. Such data should be incorporated into the final design.

10.2 Ground-Borne Noise

A substantial ancillary benefit of implementing mitigation to control ground vibration would be very effective control of ground-borne noise in campus buildings. The floating slab would provide substantial ground borne noise reduction for the campus and the provision of high compliance fasteners through the UW Station to the southern boundary of the campus would also provide protection for buildings along the alignment in this area.

Table 10-1 Comparison of Predicted Exterior Ground Surface Vibration Velocity Levels with UW Threshold for Two Trains

<u>Building</u>	Tunnel Depth	Horizontal Distance	Exceed UW Threshold Without Mitigation	Exceed UW Threshold With Mitigation
	(Ft)	(Ft)		
1) New Electrical Engineering	147	338	Yes	No
2) Johnson Hall	132	677	Yes	No
3) Bagley Hall	138	978	Yes	No
4) New Chemistry	125	1,008	Yes	No
5) Wilcox Hall	99	110	Yes	Yes
6) Physics/Astronomy	121	1,201	Yes	No
7) Burke Museum	78	826	Yes	No
8) Benson Hall	134	1,269	Yes	No
9) Roberts Hall	113	255	Yes	Yes
10) Winkenwerder Hall	102	683	Yes	No
11) Henderson Hall	58	1,208	No	No
12) Oceanographic Research	80	1,833	No	No
13) UW Medical Center	108	910	Yes	No
14) Fisheries Sciences	68	1,640	No	No
15) Fisheries Teaching Center	73	1,858	No	No
16) More Hall	113	137	Yes	Yes
17) Marine Studies	70	1,799	No	No
18) Bioengineering/ Genomics	100	1,612	No	No
19) Fluke Hall	140	333	Yes	Yes
20) Mechanical Engineering and Annex	124	9	Yes	Yes
21) Ocean Sciences*	104	2056	No	No
22) CHDD	107	753	Yes	No
23) Fisheries Center*	100	1242	No	No

* Background not available, but based on background at other buildings

** Mechanical Engineering Receivers Considered as Single Receiver

APPENDIX A LINE SOURCE RESPONSE TESTS

CONTENTS

A-1	INTRODUCTION	1
A-2	MEASUREMENT LOCATIONS	1
A-3	FIELD PROCEDURE	3
A-4	LABORATORY DATA ANALYSIS	3
A-5	ANALYSIS.....	4
	Point Source Responses versus Offset.....	5
	Individual LSRs Calculated for Each Borehole from Individual PSRs Determined by Regression of Mobility Level Data vs Log Offset.....	25
	Global LSRs Calculated from PSRs Determined by Regression of Mobility Level Test Data vs Log Offset for All Boreholes	31
	Individual LSRs Calculated from PSRs Determined by Regression of Absolute Value of Magnitude of Mobility Data vs. Offset	37
	LSRs Computed by Interpolation of Mobility Data vs. Horizontal Offset.....	43
	Comparisons of Global and Energy Averaged LSR's	54
A-7	CONCLUSION.....	65

FIGURES

Figure A-1	Borehole Test Locations	2
Figure A-2	Point Source Responses at 3.15 Hz.....	7
Figure A-3	Point Source Responses at 4 Hz.....	8
Figure A-4	Point Source Responses at 5Hz.....	9
Figure A-5	Point Source Responses at 6.3 Hz.....	10
Figure A-6	Point Source Responses at 8Hz.....	11
Figure A-7	Point Source Responses at 10 Hz.....	12
Figure A-8	Point Source Responses at 12.5 Hz.....	13
Figure A-9	Point Source Responses at 16 Hz.....	14
Figure A-10	Point Source Responses at 20 Hz.....	15
Figure A-11	Point Source Responses at 25 Hz.....	16
Figure A-12	Point Source Responses at 31.5Hz.....	17
Figure A-13	Point Source Responses at 40Hz.....	18
Figure A-14	Point Source Responses at 50 Hz.....	19
Figure A-15	Point Source Responses at 63 Hz.....	20

Figure A-16	Point Source Responses at 80 Hz.....	21
Figure A-17	Point Source Responses at 100 Hz.....	22
Figure A-18	Point Source Responses at 125 Hz.....	23
Figure A-19	Point Source Responses at 160 Hz.....	24
Figure A-20	Line Source Responses for Each Borehole at 25 Foot Offset from Track Center	26
Figure A-21	Line Source Responses for Each Borehole at 50 Foot Offset from Track Center	27
Figure A-22	Line Source Responses for Each Borehole at 100 Foot Offset from Track Center.....	28
Figure A-23	Line Source Responses for Each Borehole at 200 Foot Offset from Track Center.....	29
Figure A-24	Line Source Responses for Each Borehole at 400 Foot Offset From Track Center.....	30
Figure A-25	Comparison of Line Source Responses with LSR Based on Global Regression of PSR for 25 Ft Offset – Regression of Decibel Level vs. Log Offset.	32
Figure A-26	Comparison of Line Source Responses with LSR Based on Global Regression of PSR for 50 Ft Offset – Regression of Decibel Level vs. Log Offset.	33
Figure A-27	Comparison of Line Source Responses with LSR Based on Global Regression of PSR for 100 Ft Offset – Regression of Decibel Level vs. Log Offset	34
Figure A-28	Comparison of Line Source Responses with LSR Based on Global Regression of PSR for 200 Ft Offset – Regression of Decibel Level vs. Log Offset	35
Figure A-29	Comparison of Line Source Responses with LSR Based on Global Regression of PSR for 400 Ft Offset – Regression of Decibel Level vs. Log Offset	36
Figure A-30	LSR Based on Regression of Magnitude of Mobility vs. Horizontal Distance at Horizontal Offset of 25 Feet	38
Figure A-31	LSR Based on Regression of Magnitude of Mobility vs. Horizontal Distance at Horizontal Offset of 50 Feet	39
Figure A-32	LSR Based on Regression of Magnitude of Mobility vs. Horizontal Distance at Horizontal Offset of 100 Feet	40
Figure A-33	LSR Based on Regression of Magnitude of Mobility vs. Horizontal Distance at Horizontal Offset of 200 Feet	41
Figure A-34	LSR Based on Regression of Magnitude of Mobility vs. Horizontal Distance at Horizontal Offset of 400 Feet	42
Figure A-35	LSR Based on Linear Interpolation of Magnitude of Mobility vs. Horizontal Distance for 140lb Hammer – Horizontal Offset of 25 Feet	44
Figure A-36	LSR Based on Linear Interpolation of Magnitude of Mobility vs. Horizontal Distance for 140lb Hammer – Horizontal Offset of 50 Feet	45

Figure A-37	LSR Based on Linear Interpolation of Magnitude of Mobility vs. Horizontal Distance for 140lb Hammer – Horizontal Offset of 100 Feet	46
Figure A-38	LSR Based on Linear Interpolation of Magnitude of Mobility vs. Horizontal Distance for 140lb Hammer – Horizontal Offset of 200 Feet	47
Figure A-39	LSR Based on Linear Interpolation of Magnitude of Mobility vs. Horizontal Distance for 140lb Hammer – Horizontal Offset of 400 Feet	48
Figure A-40	LSR Based on Linear Interpolation of Magnitude of Mobility vs. Horizontal Distance for 300lb Hammer – Horizontal Offset of 25 Feet	49
Figure A-41	LSR Based on Linear Interpolation of Magnitude of Mobility vs. Horizontal Distance for 300lb Hammer – Horizontal Offset of 50 Feet	50
Figure A-42	LSR Based on Linear Interpolation of Magnitude of Mobility vs. Horizontal Distance for 300lb Hammer – Horizontal Offset of 100 Feet	51
Figure A-43	LSR Based on Linear Interpolation of Magnitude of Mobility vs. Horizontal Distance for 300lb Hammer – Horizontal Offset of 200 Feet	52
Figure A-44	LSR Based on Linear Interpolation of Magnitude of Mobility vs. Horizontal Distance for 300lb Hammer – Horizontal Offset of 400 Feet	53
Figure A-45	Comparison of Energy Averaged LSR (140lb Hammer Data Used for Interpolation) – Horizontal Offset of 25 Feet	55
Figure A-46	Comparison of Energy Averaged LSR's (300lb Hammer Data Used for Interpolation) – Horizontal Offset of 25 Feet	56
Figure A-47	Comparison of Energy Averaged LSR (140lb Hammer Data Used for Interpolation) – Horizontal Offset of 50 Feet	57
Figure A-48	Comparison of Energy Averaged LSR's (300lb Hammer Data Used for Interpolation) – Horizontal Offset of 50 Feet	58
Figure A-49	Comparison of Energy Averaged LSR (140lb Hammer Data Used for Interpolation) – Horizontal Offset of 100 Feet	59
Figure A-50	Comparison of Energy Averaged LSR's (300lb Hammer Data Used for Interpolation) – Horizontal Offset of 100 Feet	60
Figure A-51	Comparison of Energy Averaged LSR (140lb Hammer Data Used for Interpolation) – Horizontal Offset of 200 Feet	61
Figure A-52	Comparison of Energy Averaged LSR's (300lb Hammer Data Used for Interpolation) – Horizontal Offset of 200 Feet	62
Figure A-53	Comparison of Energy Averaged LSR (140lb Hammer Data Used for Interpolation) – Horizontal Offset of 400 Feet	63
Figure A-54	Comparison of Energy Averaged LSR's (300lb Hammer Data Used for Interpolation) – Horizontal Offset of 400 Feet	64

A-1 INTRODUCTION

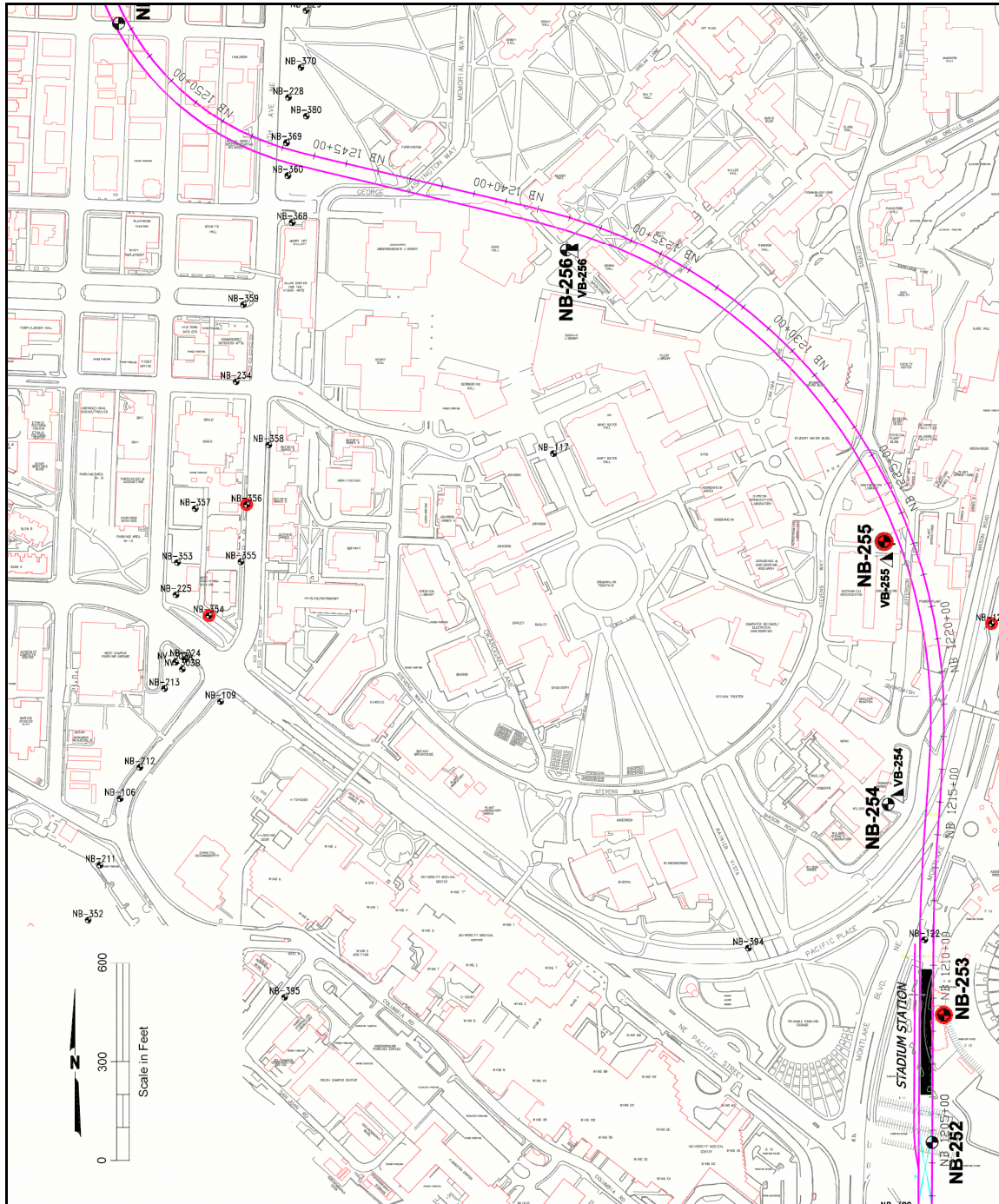
Line source responses were measured at the University of Washington campus as part of Preliminary Engineering. The results were analyzed in a variety of ways to determine the most representative method for calculating vibration levels that might be produced by the North Link tunnel. This report summarizes the results of the vibration propagation tests. Predictions of vibration velocity levels due to trains, or the effects of mitigation options, are not considered here. Line Source Responses based on shear wave velocity data are described in Appendix B.

A-2 MEASUREMENT LOCATIONS

Test were conducted at four measurement locations, identified by boring numbers as:

NB-253/VB-253	Approx. Station 1209+00	(Stadium parking lot)
NB-254/VB-254	Approx. Station 1215+50	Materials Science
NB-255/VB-255	Approx. Station 1224+00	Mechanical Engineering
NB-256/VB-256	Approx. Station 1238+00	Over SB Tunnel

The boreholes were drilled in holes with prefix “VB” immediately adjacent to the corresponding holes labeled with prefix “NB”. The measurement locations are identified Figure A-1. The drilling sites are referred to with the prefix “NB” throughout this report.



From Shannon & Wilson, Inc.

Figure A-1 Borehole Test Locations

A-3 FIELD PROCEDURE

The responses at the ground surface to impulses delivered to the bottom of the boreholes were measured for various impact depths approximating the range of depths of the proposed tunnel. The surface responses were detected with geophones spaced over distances ranging from about 25 feet to 600 feet from the source. Additional seismic accelerometers were positioned inside adjacent buildings at up to two representative positions.

The drilling rig used for drilling the holes also produced the dynamic forces. Analog dynamic force signals were generated with a load cell attached to the end of the drill string. The impact forces were produced with the drilling rig's sampling hammers. One of these weighed 140lb and the other 300lb. Approximately 100 or more individual impulse response samples were obtained with the 140lb hammer, and about 40 samples with the 300lb hammer, at each test hole and depth. (More samples would have been taken with the 300lb hammer, but some damage to the lifting might have occurred.)

The velocity response and force signal were recorded simultaneously on a 16-channel TEAC RD145 digital recorder on DAT tape.

A-4 LABORATORY DATA ANALYSIS

The recorded data were analyzed with a multi-channel data analysis system and custom software. The analysis included measurement of the transfer functions between the force signal and response velocity for each depth, hammer weight, and vibration velocity measurement point. This was done by Fourier transforming the force and velocity signals, using a 1024-point transform, and averaging the auto- and cross-spectral components over the 40 or 100 impacts.

The transfer function was obtained by the following formula:

$$M = \langle G_{ab} \rangle / \langle G_{aa} \rangle$$

Where G_{ab} is the cross-spectrum between the force and velocity, and G_{aa} is the auto-spectrum of the force. The brackets, $\langle \rangle$, denote the average value, or expectation value. The cross- and auto-spectra are given by:

$$G_{ab} = f^*(\omega)v(\omega)$$

$$G_{aa} = f^*(\omega)f(\omega) = |f(\omega)|^2$$

$$G_{bb} = v^*(\omega)v(\omega) = |v(\omega)|^2$$

Here, $f^*(\omega)$ is the complex conjugate of the transformed force, and $v(\omega)$ is the transformed velocity, all functions of the radian frequency, ω .

The coherence, γ^2 , represents the ratio of the received signal energy to the total received signal energy. Thus, γ^2 , is given by:

$$\gamma^2 = |\langle G_{ab} \rangle|^2 / (\langle G_{aa} \rangle \langle G_{bb} \rangle)$$

Thus, the coherence is a function of frequency, and a single value is obtained for each frequency bin.

The percent error of the mobility estimate as a function of coherence and number of impulses is given by:¹

$$\text{Uncertainty (\%)} = (1 - \gamma^2)^{1/2} / (\gamma^2 2N_d)^{1/2}$$

Thus, if γ^2 is 0.1, and N_d is 30, the uncertainty in the estimate of M is 33%. In decibels, this is equivalent to $20\text{Log}_{10}(1.33) = 2.5 \text{ dB}$. If N_d is 100, the uncertainty would be 18%, or 1.4dB.

Reasonable estimates of the transfer function are obtained with signal coherences as low as 10% and at least 30 samples. At lower coherence, the transfer function is poorly defined unless the number of samples is increased substantially. In principal, the transfer function can be accurately defined if one is willing to sample “long enough”. In general, assuming a steady background “noise” environment, the transfer function’s “signal-to-noise” ratio would improve by three decibels per doubling of the number of samples, or “hammer hits”. That is, the estimate of the magnitude of the transfer function relative to the noise floor would improve by a factor of 1.4 for each doubling of the number of samples.

The narrow band transfer function thus obtained is also called the Transfer Mobility, which is the vibration velocity spectrum relative to the input force spectrum. To simplify data manipulation and analysis, the Transfer Mobilities are energy averaged over the bandwidth of each 1/3 octave band from 6.3Hz to 160Hz. The individual frequency bins of the narrowband mobilities were also weighted by the coherence function when mean-square-averaging over each one-third octave band to reduce the influence of bins of poor coherence. The effect of coherence weighting is minimal, and usually results in less than one decibel difference between weighted and un-weighted coherence.

The Transfer Mobility Level in decibels relative to one micro-inch per second per pound is equal to $20\text{Log}_{10}|M/M_0|$, or $10\text{Log}_{10}(|M/M_0|^2)$. The reference magnitude, M_0 , is equal to 10^{-6}in/lb-sec . The Transfer Mobility Level in dB is referred to as the Point Source Response, or PSR.

A-5 ANALYSIS

Following the procedures outlined by the FTA,² the LSR was computed by least-squares-regression of the PSR in decibels as a function of the logarithm of horizontal offset from a borehole source, and integrating the square of the mobility magnitude over the train

¹ Bendat, J. S., Pierson, A. G., **Random Data Analysis and Measurement Procedures**, 2nd Ed., John Wiley & Sons, New York, pg. 314.

² Gutowski, T. G., and Dym, C. L., Propagation of Ground Vibration, **Journal of Sound and Vibration**, Vol. 49, No. 2, pp179-193 (1976).

length. The unit of the integrated square of the mobility is L^3/FS^2 , or, in English units, $(\text{in}/\text{lb-s})^2\text{ft}$. The LSR is equal to ten times the logarithm of this integral. Mathematically:

$$\text{LSR dB re } 10^{-6}(\text{in-ft}^{1/2}/\text{lb-s}) = 10\text{Log}_{10}(\int |M/M_0|^2 dx)$$

Where M_0 is the reference mobility of $10^{-6}\text{in}/\text{lb-s}$ and the integration is over the train length in feet. (The choice of units is made to be consistent with the Federal Transit Administration usage.³ A non-mixed choice of units (eg $\text{in}^3/\text{lb}^2\text{-s}^2$), or metric units, would be more attractive.) LSRs were computed with the integration procedure for a number of horizontal offsets, and a second regression was then used to obtain a simple polynomial representation of LSR as a function offset for convenient prediction.

Alternative methods for regression analysis were investigated for the preliminary engineering phase. The PSR was determined as above, but LSR's were computed for each offset by numerical integration, without using a second regression to develop simple regression curves.

Another method included regression of the experimental third octave band mobility amplitudes (not the levels in decibels, but the magnitudes in inches per second per pound) with respect to a polynomial function of the offset. This approach suffers from regression over an extreme numerical range, and leads to a poorly controlled regression curve.

Another approach, was interpolation (rather than regression) of the third octave mobility level in decibels between each vibration measurement offset. No assumptions regarding the nature of the mobility as a function of distance from the source is made when using an interpolated mobility in calculating the LSR, other than linear interpolation, and the assumption of azimuthal symmetry.

As discussed below, all of these approaches yielded essentially the same result within a few decibels where the data are well defined with reasonably high coherence between source and receiver. The regression of amplitude versus distance yielded the poorest result at large offsets, where negative amplitudes were obtained. Regardless, the greatest variation of LSR occurred between holes, rather than between methods.

Point Source Responses versus Offset

Figure A-2 through Figure A-19 are plots of measured third octave band PSRs. These data are compared with global regression curves obtained by two methods:

- 1) Global regression of third octave band mobility levels in decibels versus the logarithm of the horizontal offset

³ **Transit Noise and Vibration Impact Assessment**, Federal Transit Administration, U.S. Department of Transportation, April 1995

2) Global regression of third octave band mobility magnitudes in absolute units versus the horizontal offset

The term “global regression” means that the regression curves for each third octave band frequency were determined over data collected at all four holes tested during the Preliminary Engineering phase, as apposed to regression of data obtained at individual holes.

Additionally, curves representing the regression curve plus one standard deviation are shown. The standard deviation of the level in decibels was calculated by averaging the squares of all of the deviations of the measured data in decibels from the regression and taking the square root. The result, in decibels, was then added to the regression curve, also in decibels. Hence, the best-fit curve plus one standard deviation has a constant offset above the regression curve.

The normalized standard deviation of the fit of the absolute amplitude of the mobility was computed by averaging the squares of the deviations of the magnitudes from the absolute mobility regression, taking the square root, and dividing the result by the estimated mobility magnitude. The level in decibels was then obtained by adding ten times the logarithm of one plus the normalized deviation to the absolute magnitude regression curve.

The two regression curves are in reasonable agreement for most of the third octave bands. However, at 60 Hz and higher frequencies, the regression curve for the absolute value of the mobility becomes negative at large offsets, a physical impossibility. The result is a poor fit, even at intermediate distances of the order of 100 feet. The poor behavior of the regression of the absolute mobility versus distances suggests that the mobility amplitude is not suitable for regression. Regressions with constraints were not attempted to fix this problem.

Some of the individually measured Point Source Responses at specific frequencies deviate considerably from the regression curves. A number of reasons for this behavior exist. One is the variation in local surface geology, another is the mounting condition of the transducer, and still another is the response of the sidewalk or road surface pavement on which the transducer was mounted. Regression fits tend to smooth out these local effects, and provide a representative curve for prediction.

The results at 5Hz and lower bands are probably unreliable and are not included in the calculations of LSR's below.

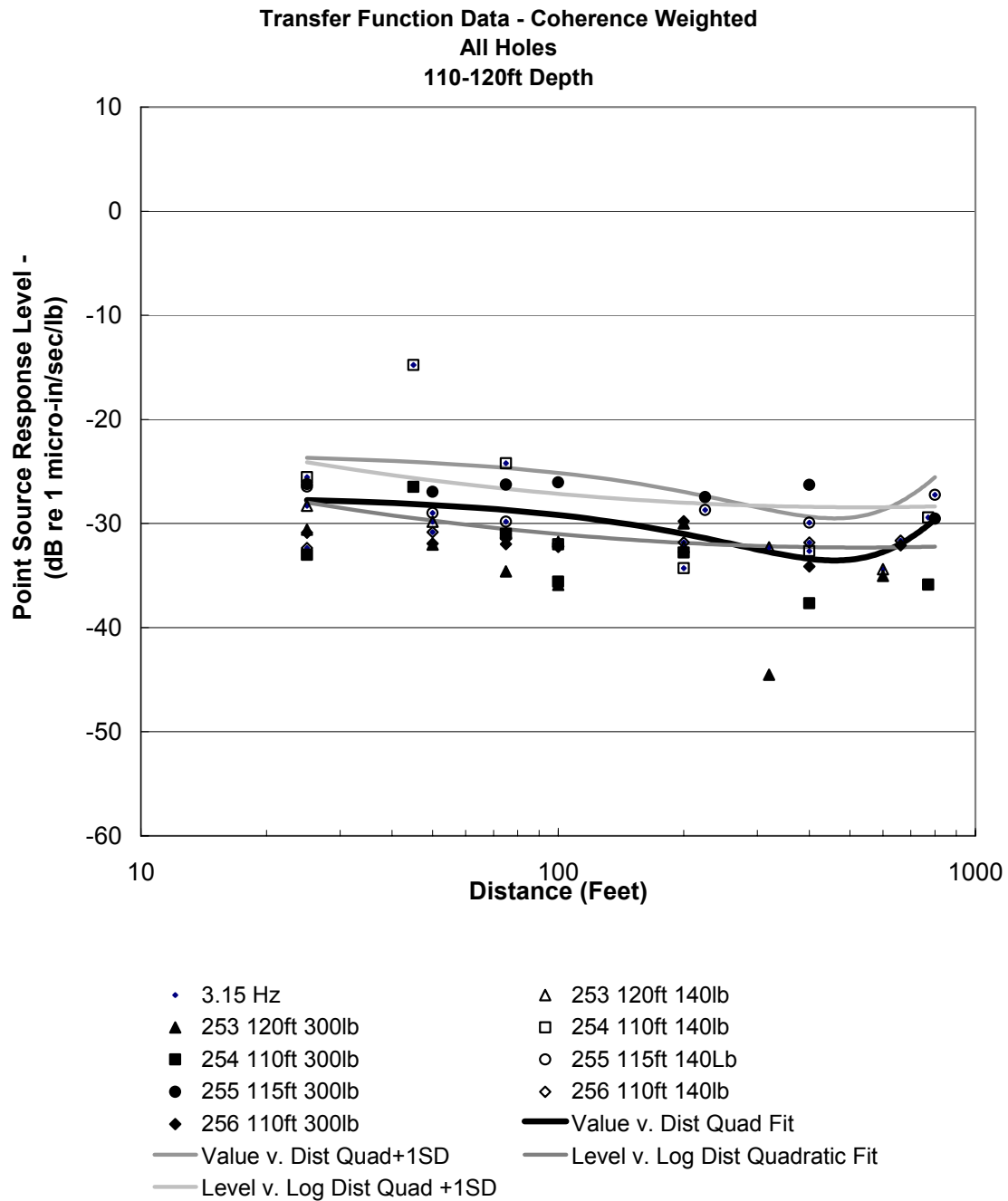


Figure A-2 Point Source Responses at 3.15 Hz

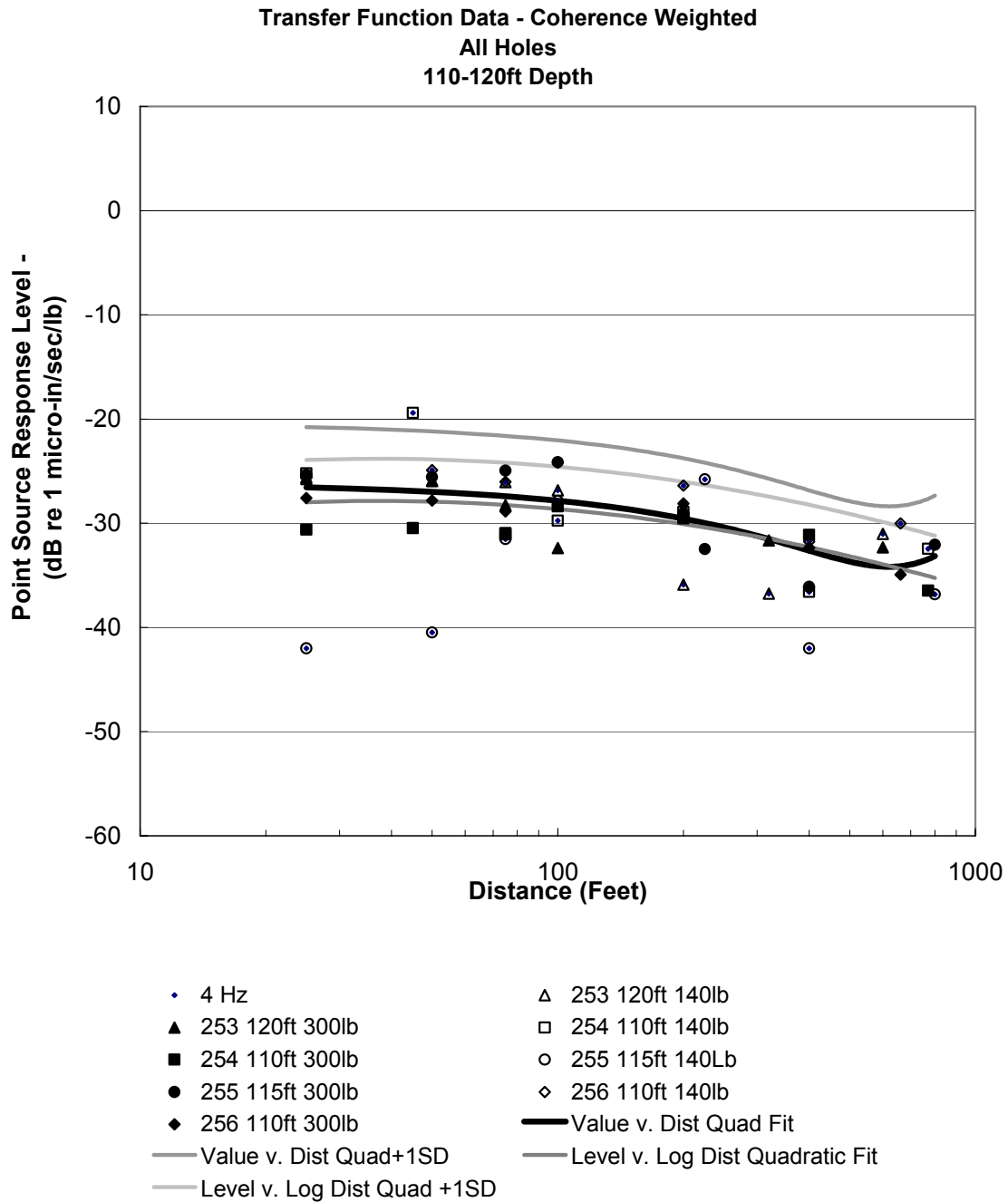


Figure A-3 Point Source Responses at 4 Hz

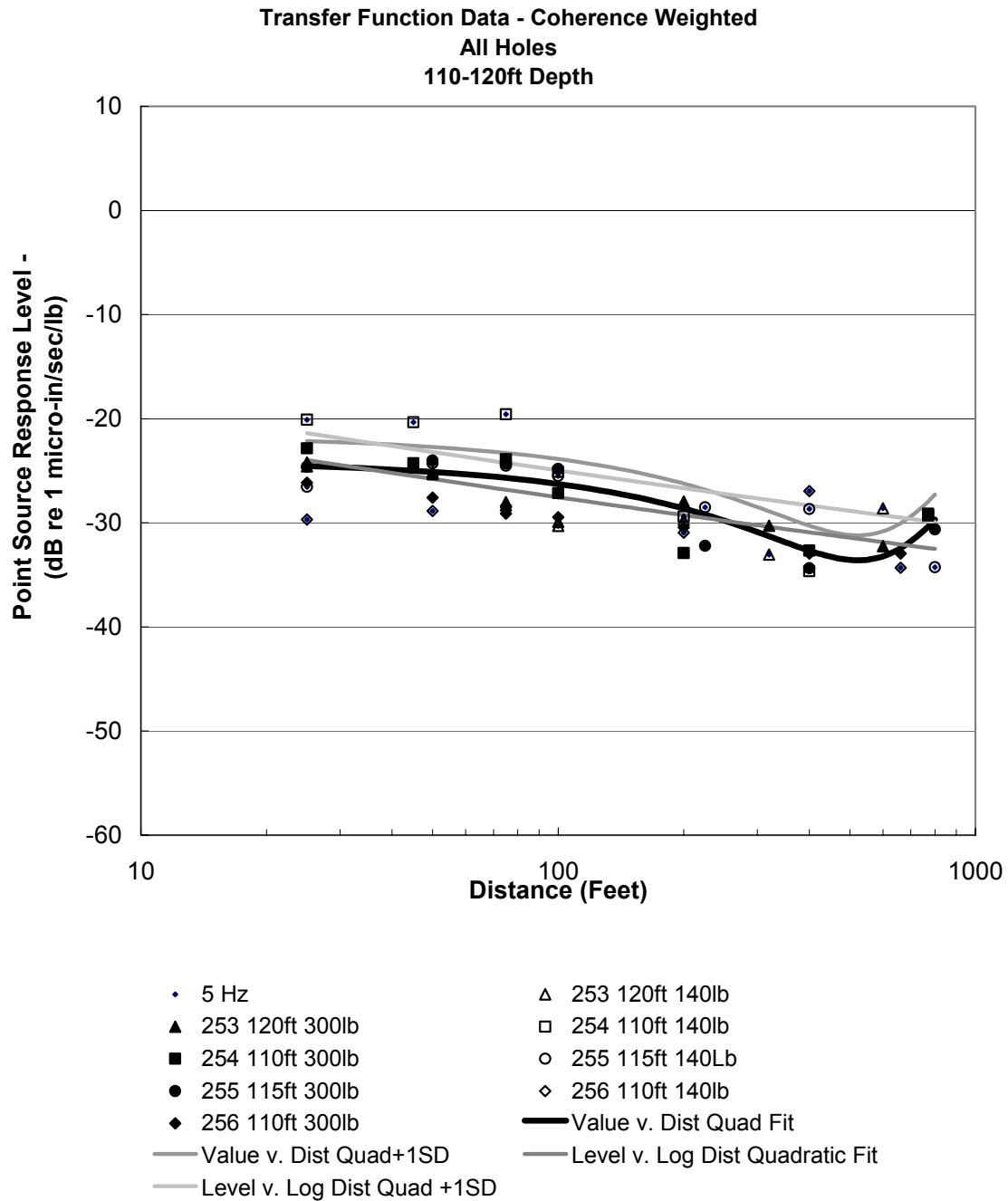


Figure A-4 Point Source Responses at 5Hz

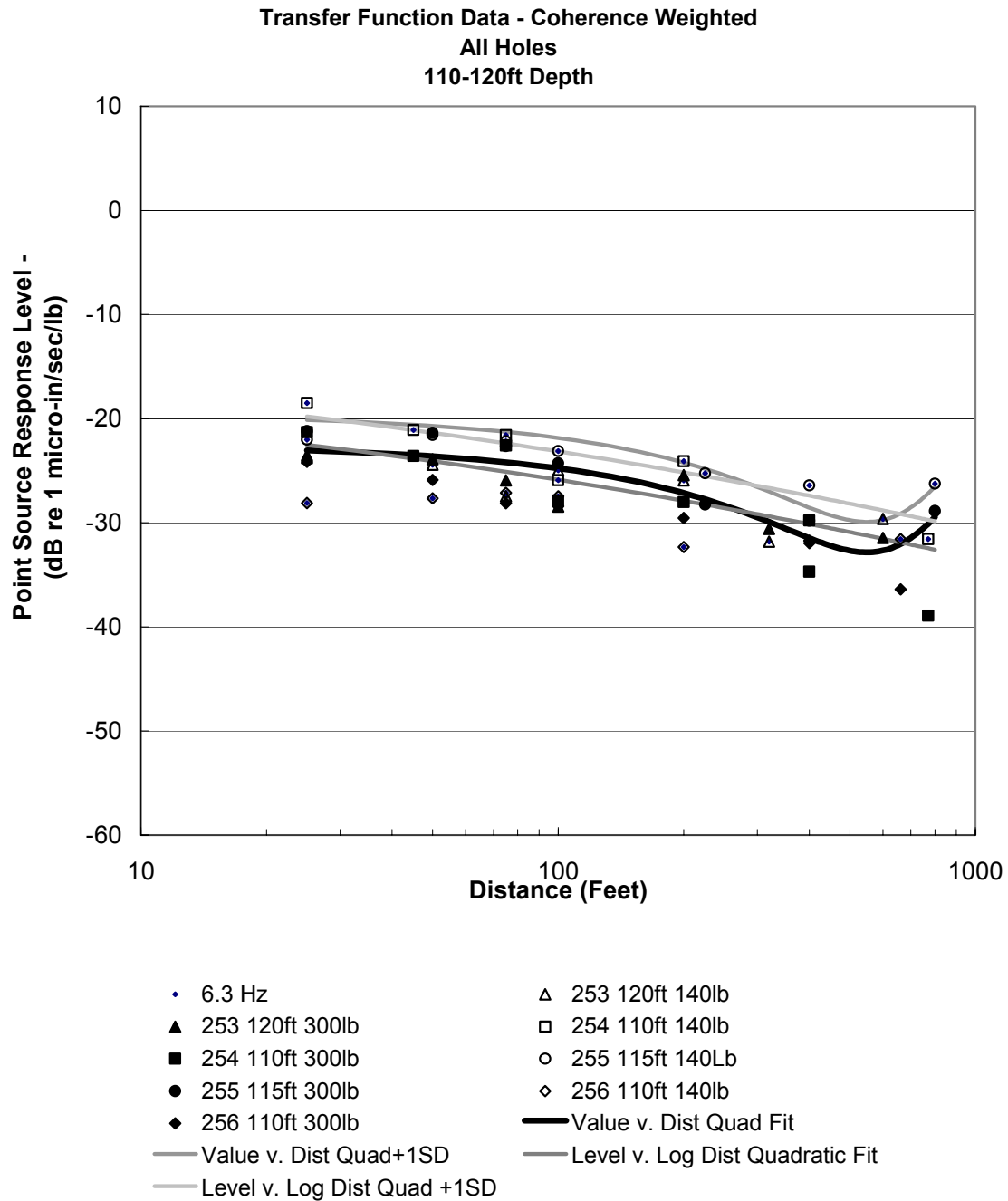


Figure A-5 Point Source Responses at 6.3 Hz

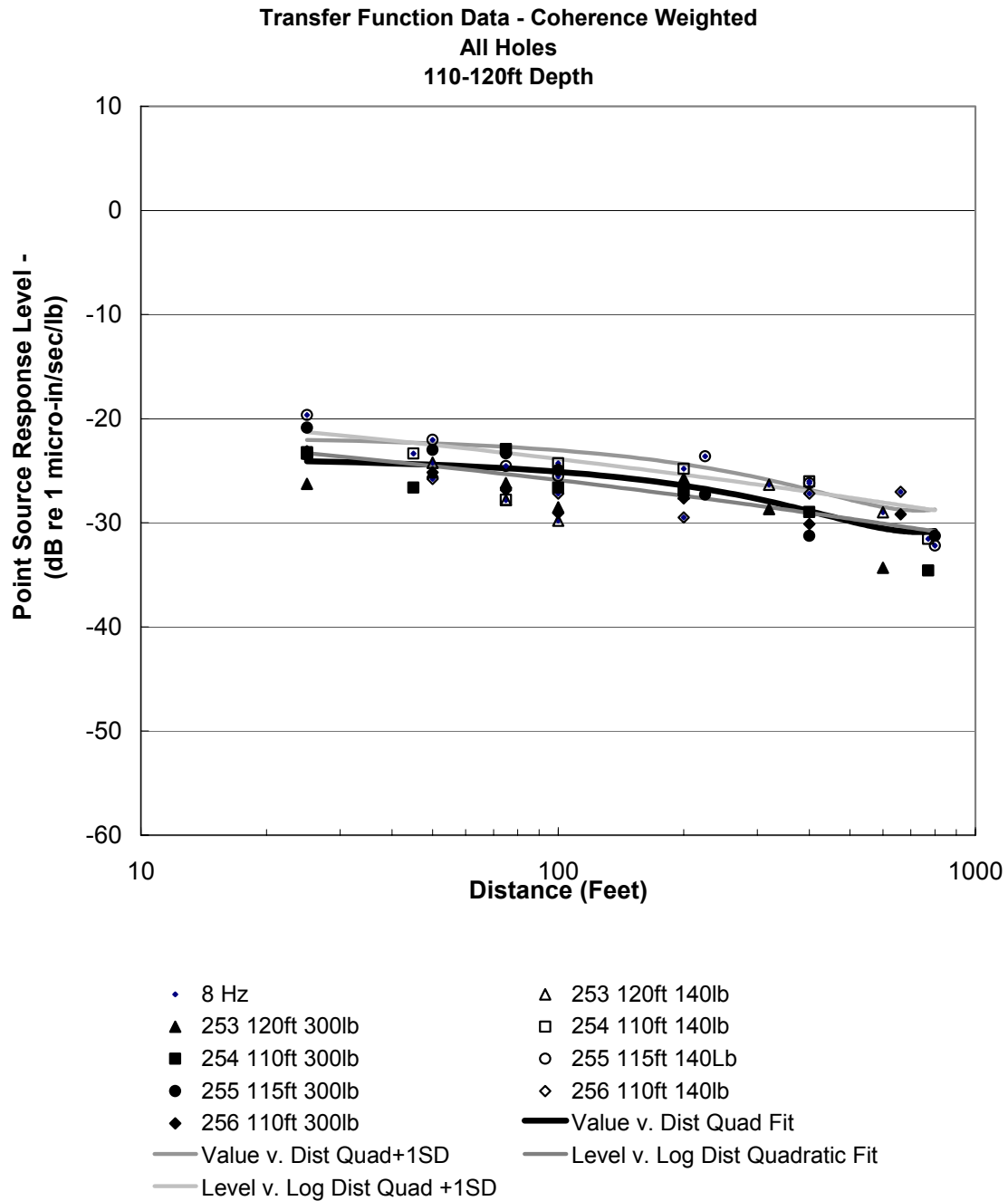


Figure A-6 Point Source Responses at 8Hz

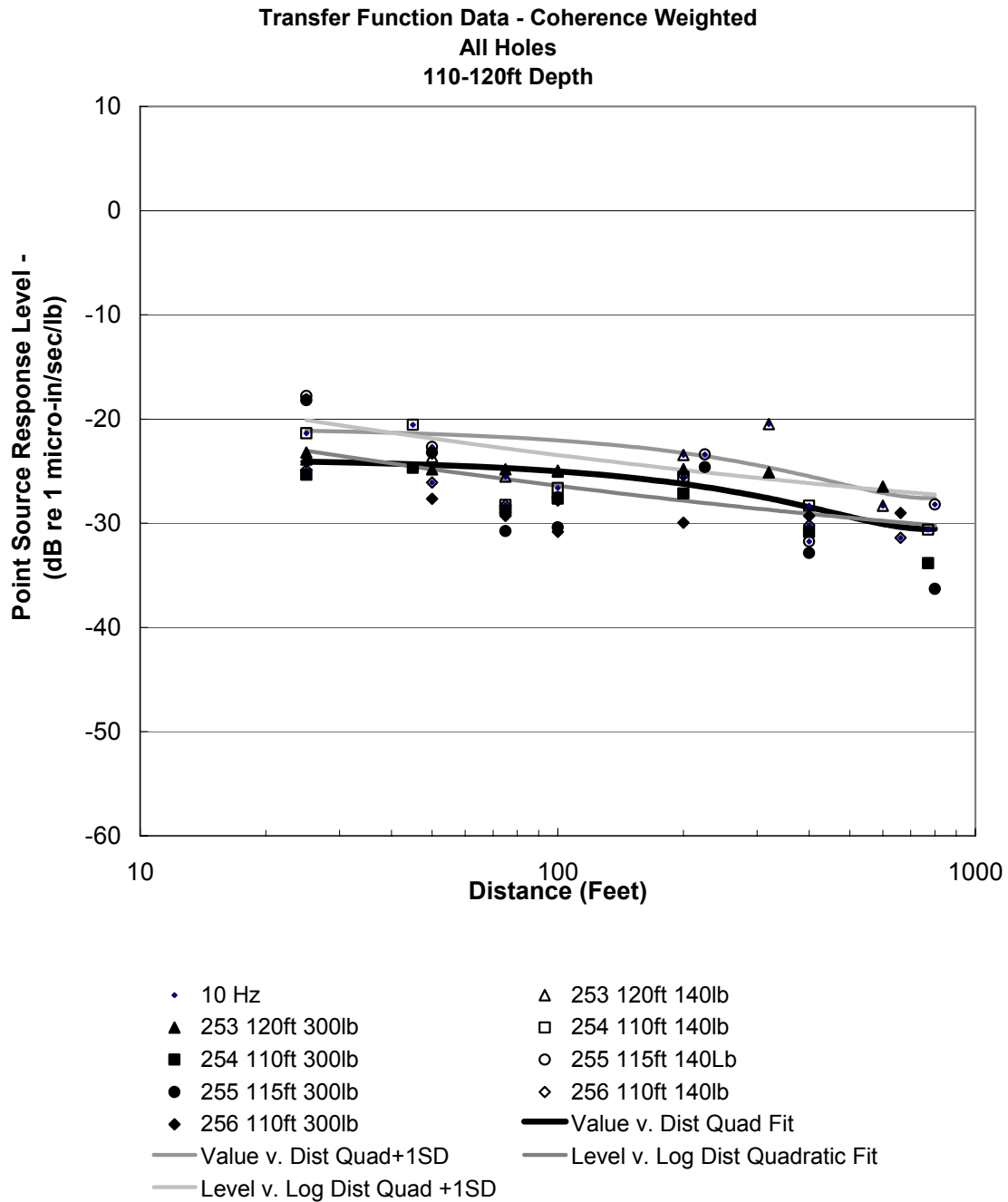


Figure A-7 Point Source Responses at 10 Hz

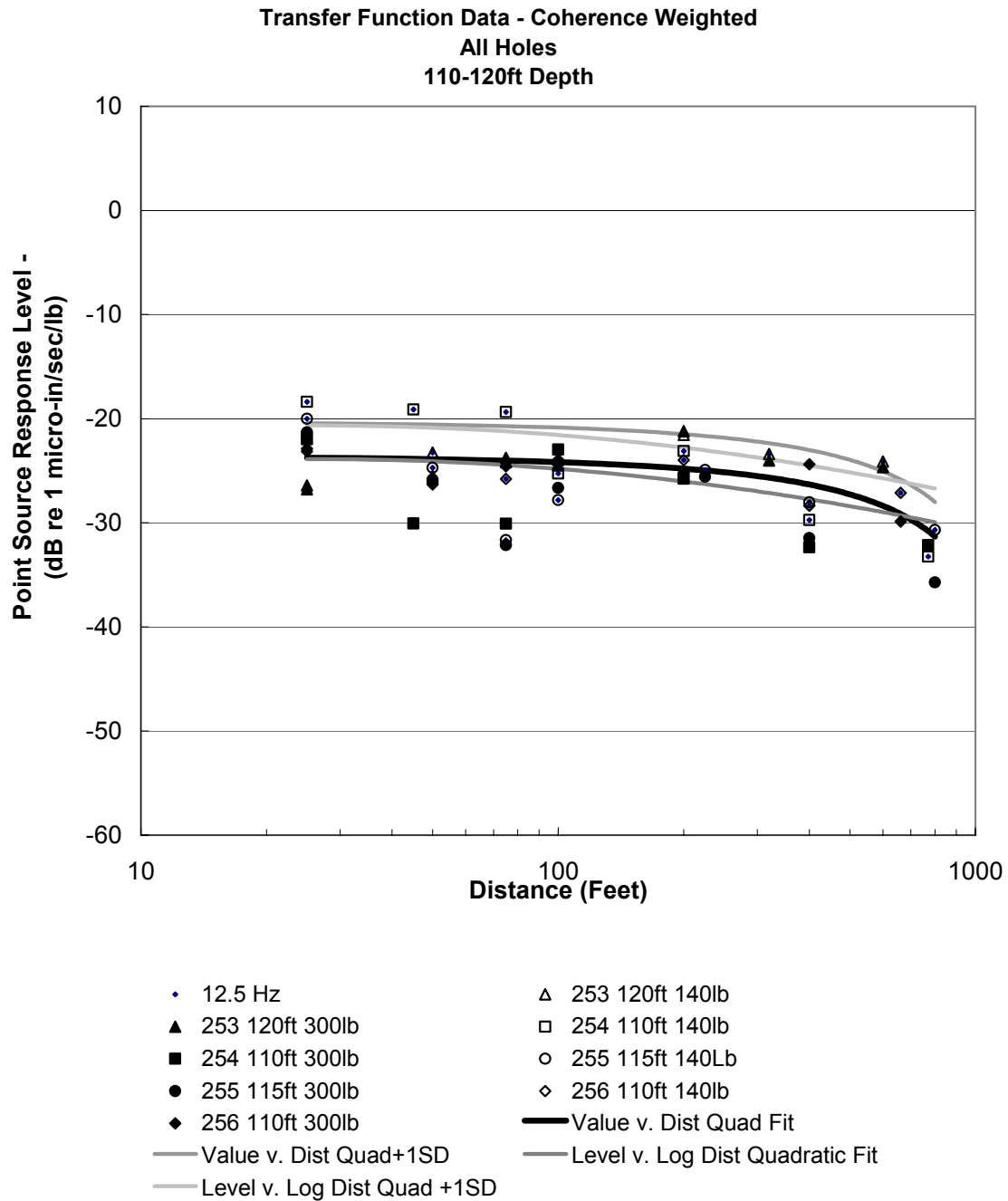


Figure A-8 Point Source Responses at 12.5 Hz

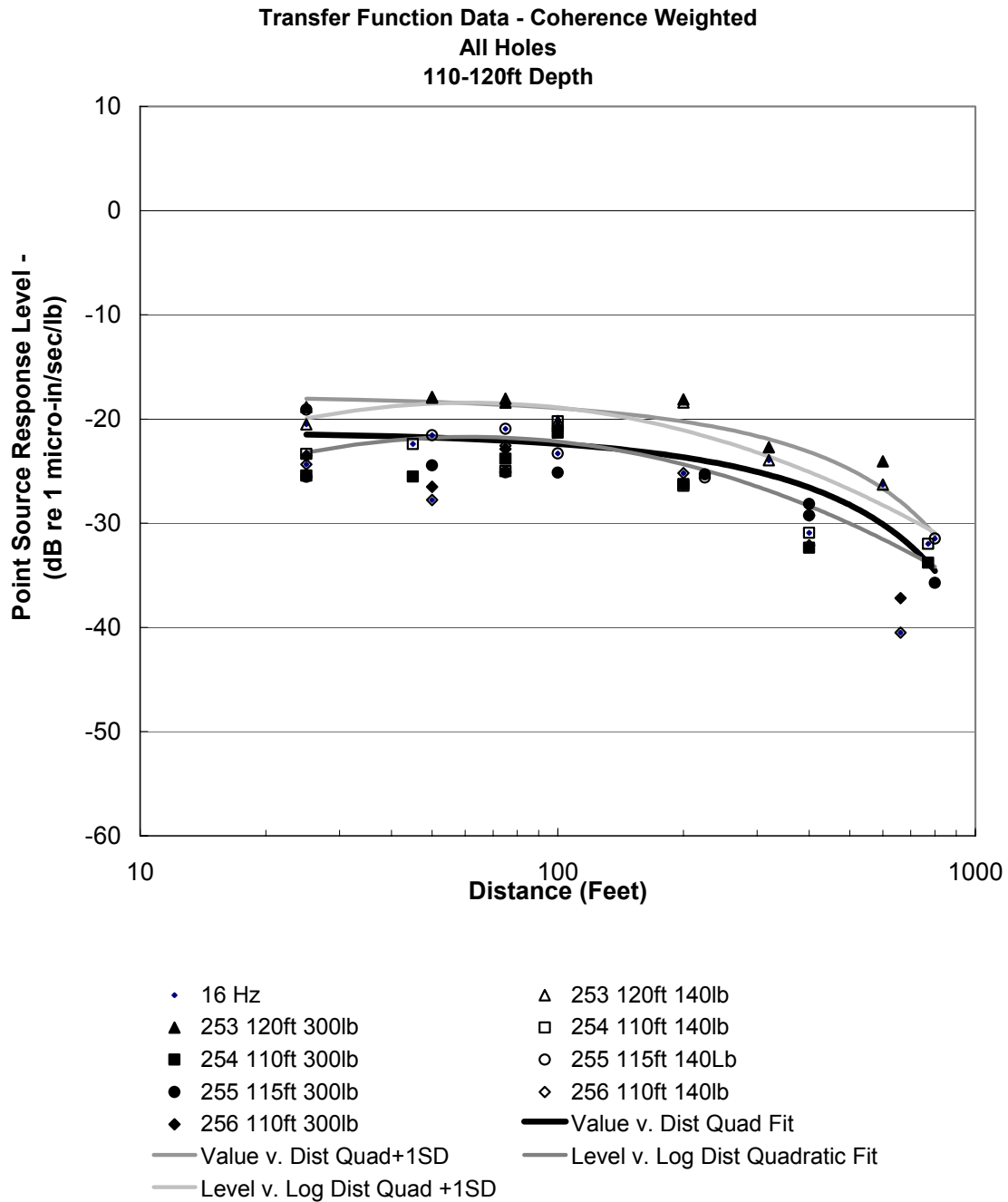


Figure A-9 Point Source Responses at 16 Hz

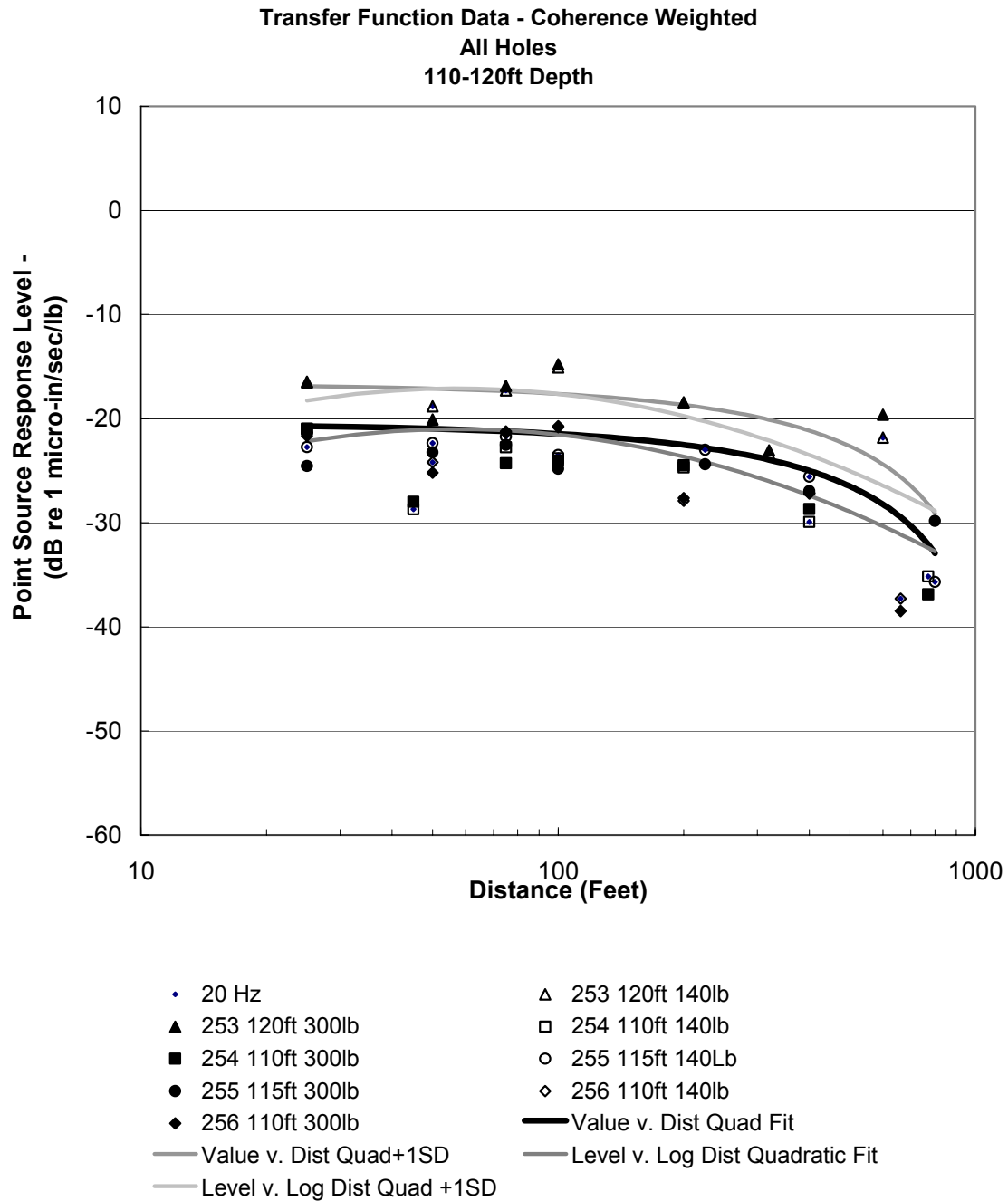


Figure A-10 Point Source Responses at 20 Hz

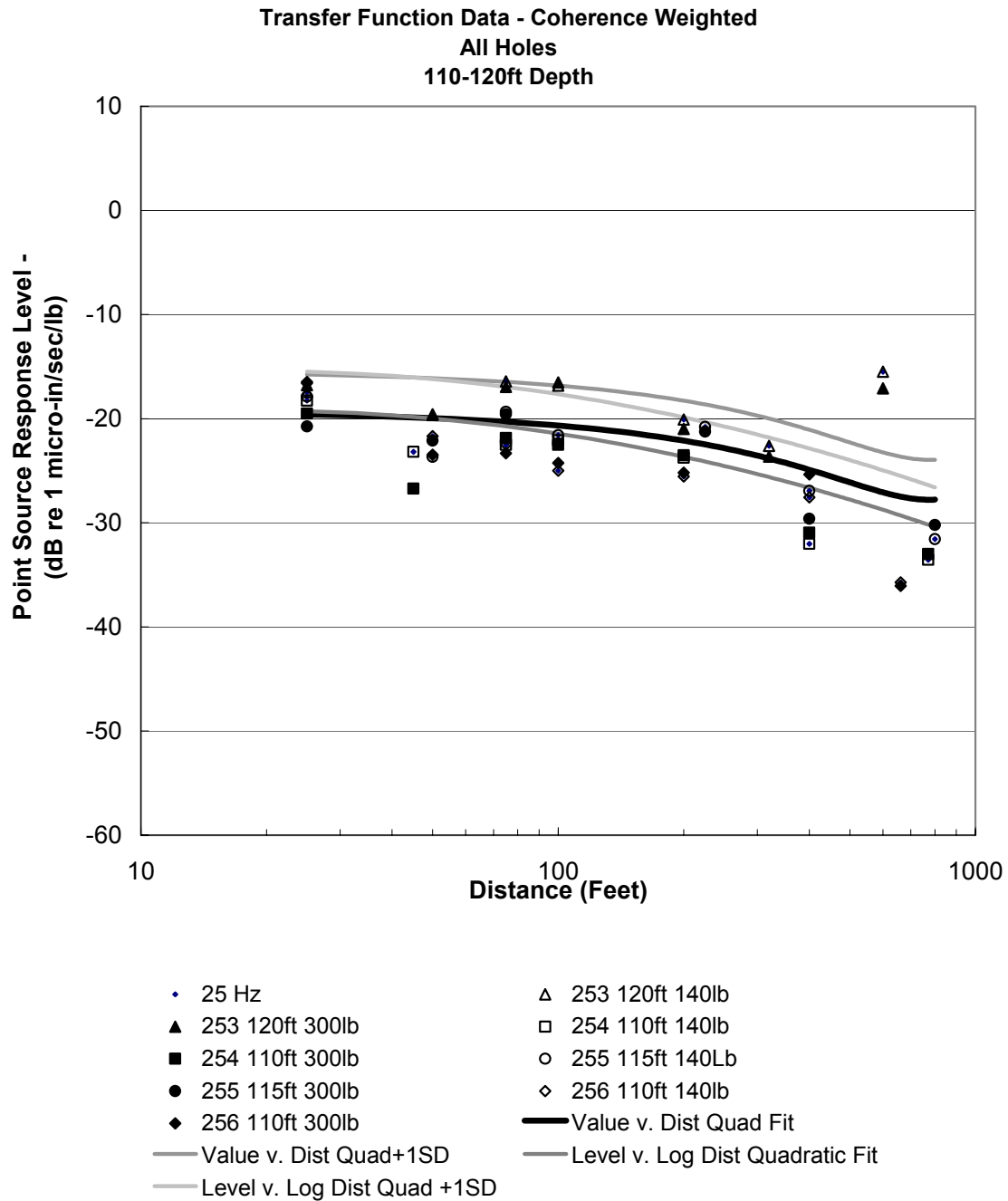


Figure A-11 Point Source Responses at 25 Hz

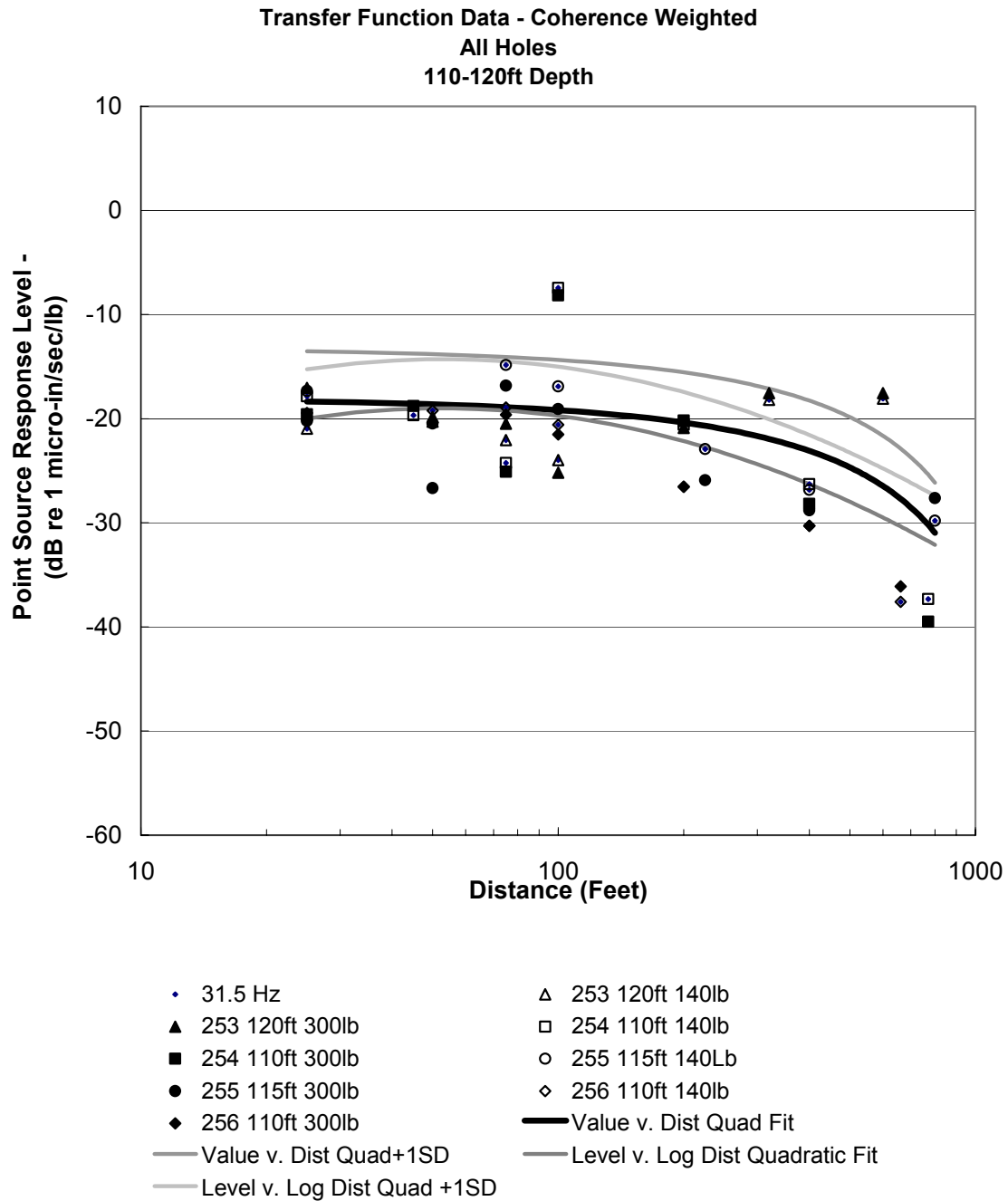


Figure A-12 Point Source Responses at 31.5Hz

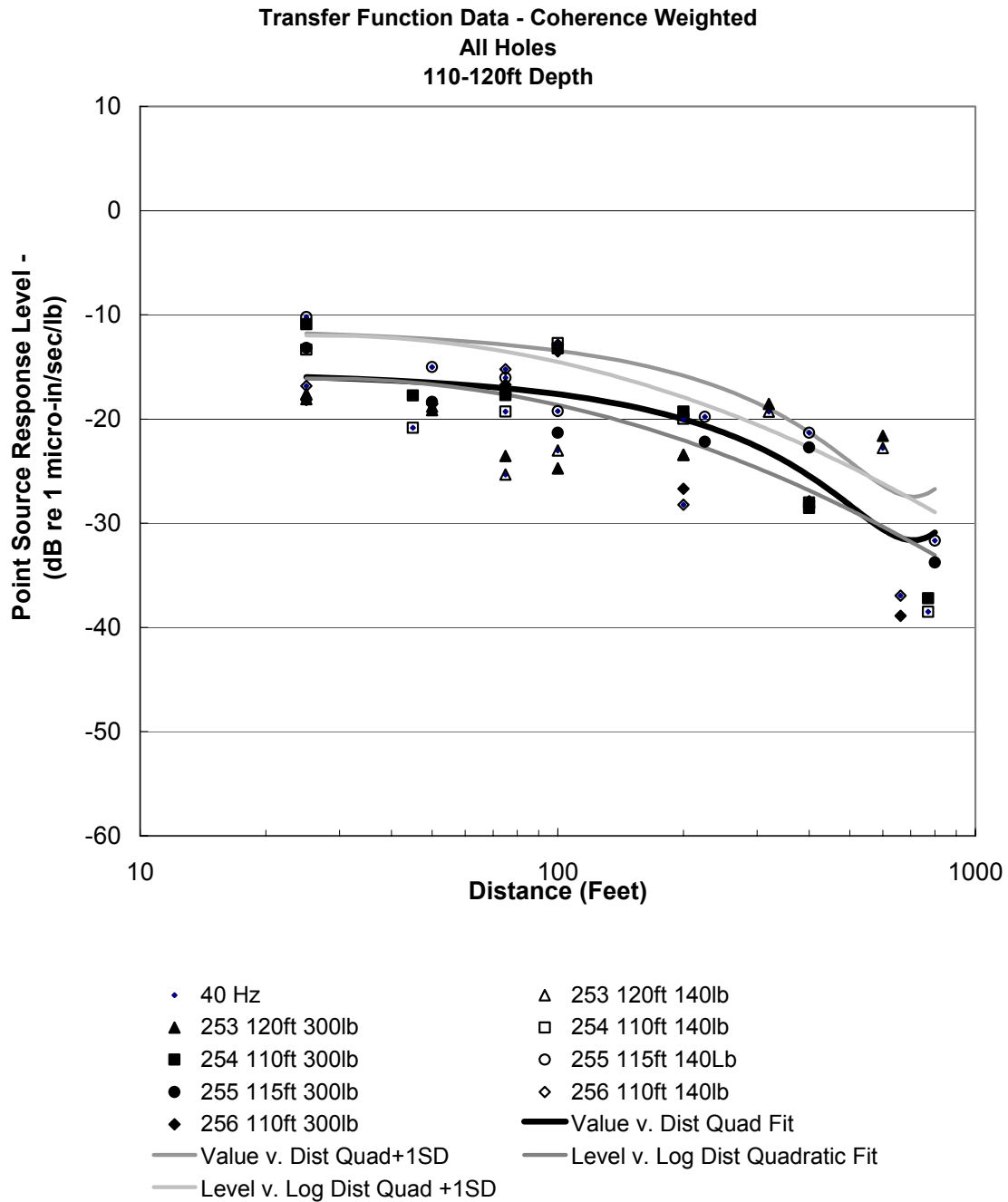


Figure A-13 Point Source Responses at 40Hz

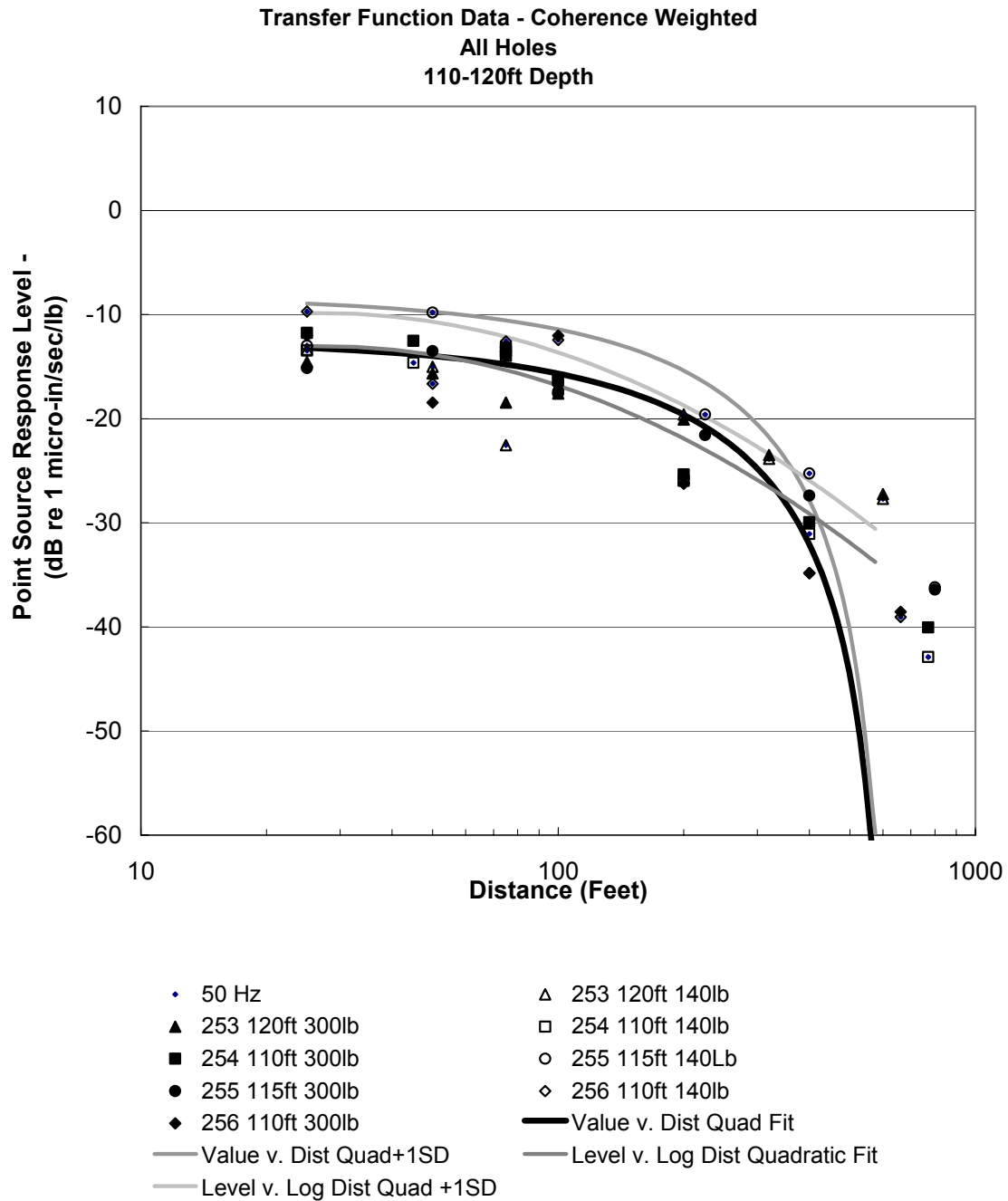


Figure A-14 Point Source Responses at 50 Hz

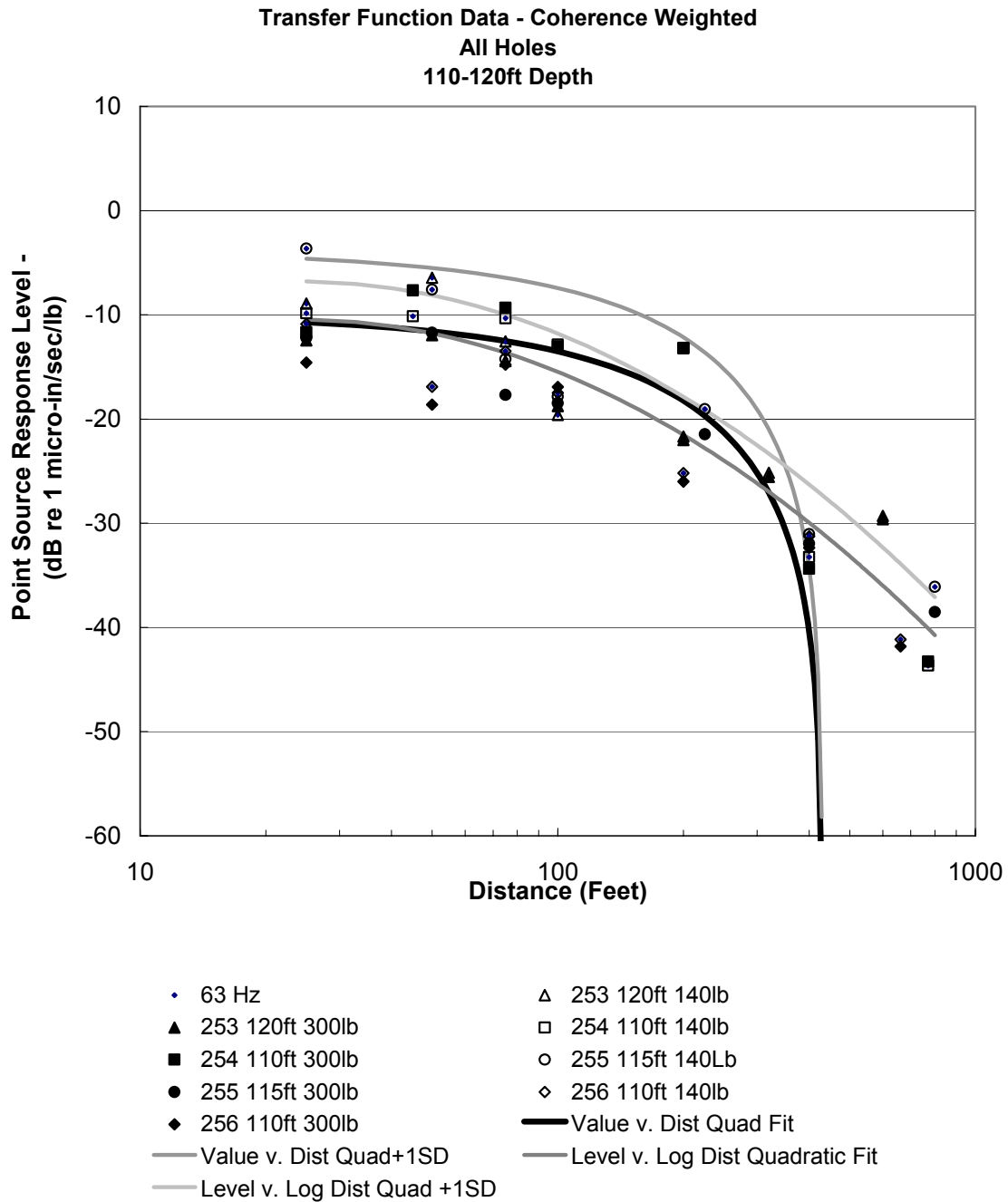


Figure A-15 Point Source Responses at 63 Hz

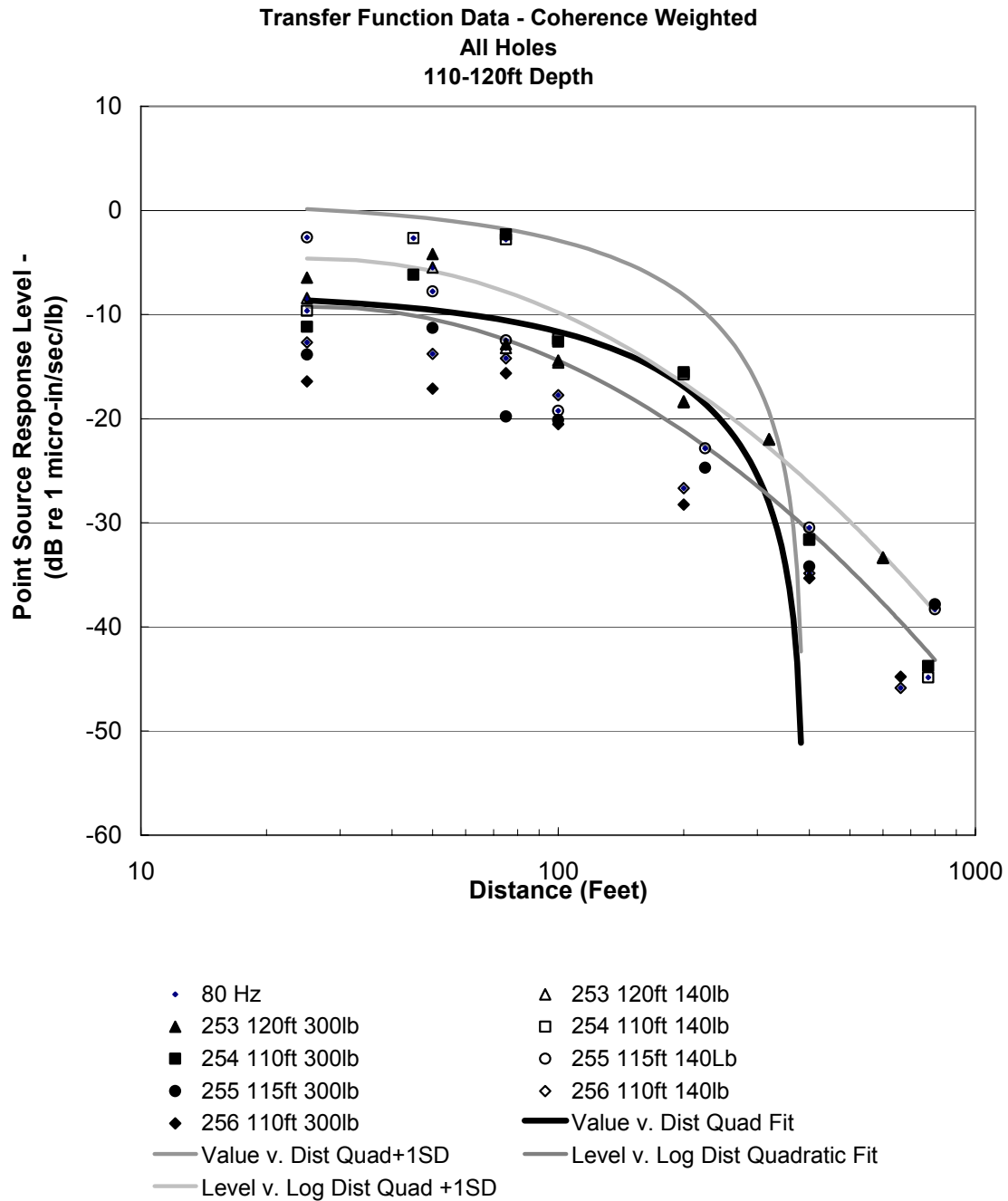


Figure A-16 Point Source Responses at 80 Hz

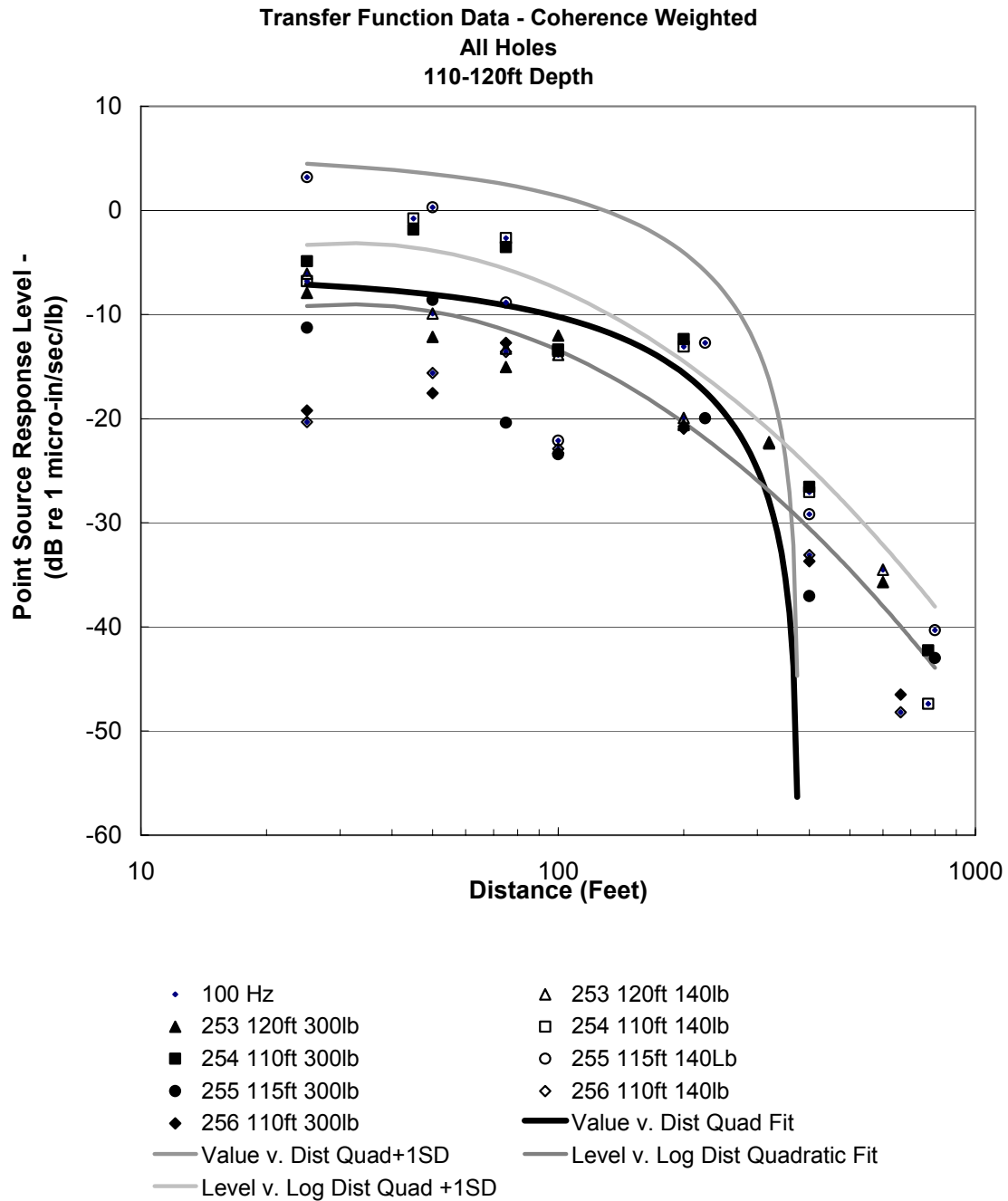


Figure A-17 Point Source Responses at 100 Hz

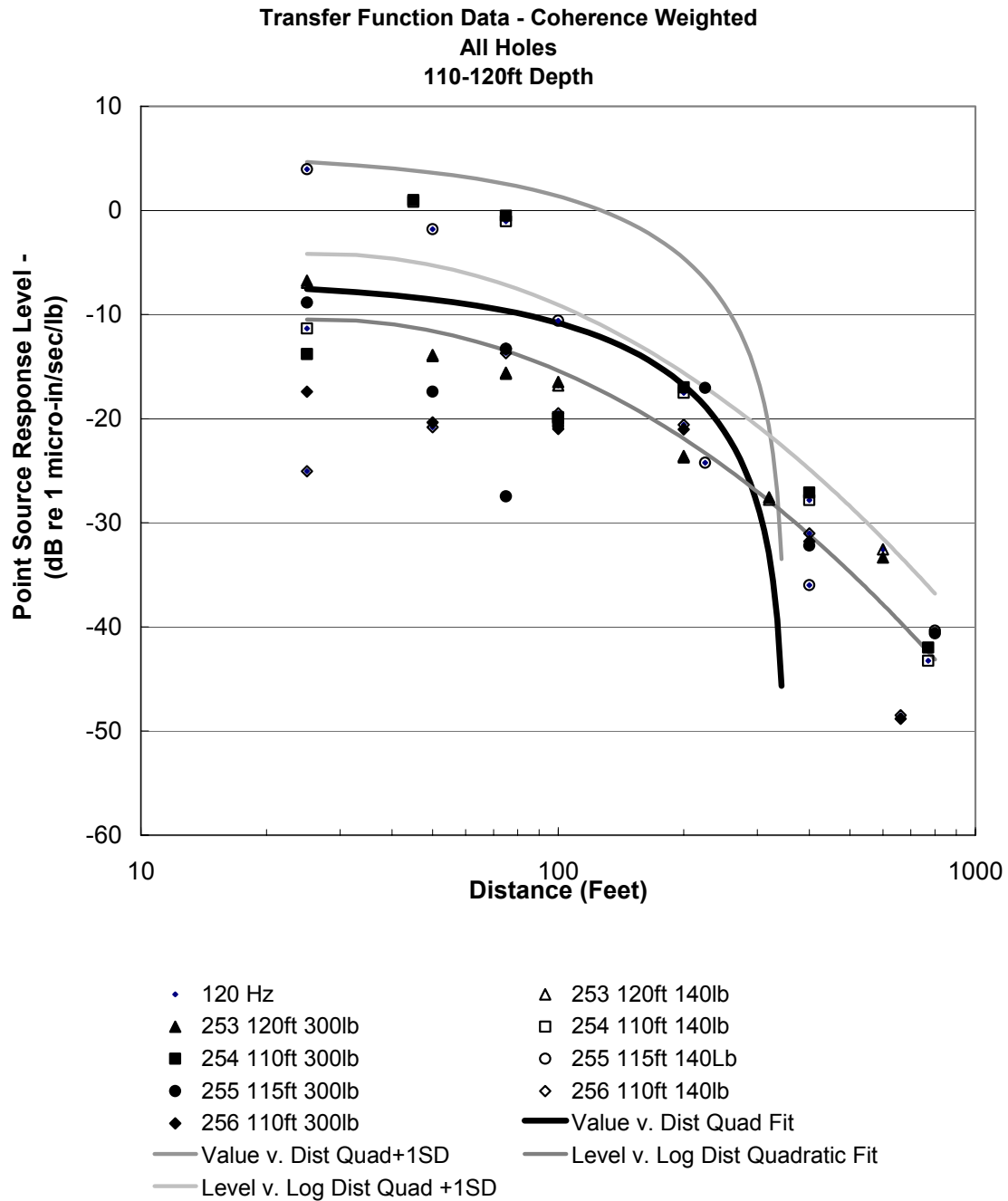


Figure A-18 Point Source Responses at 125 Hz

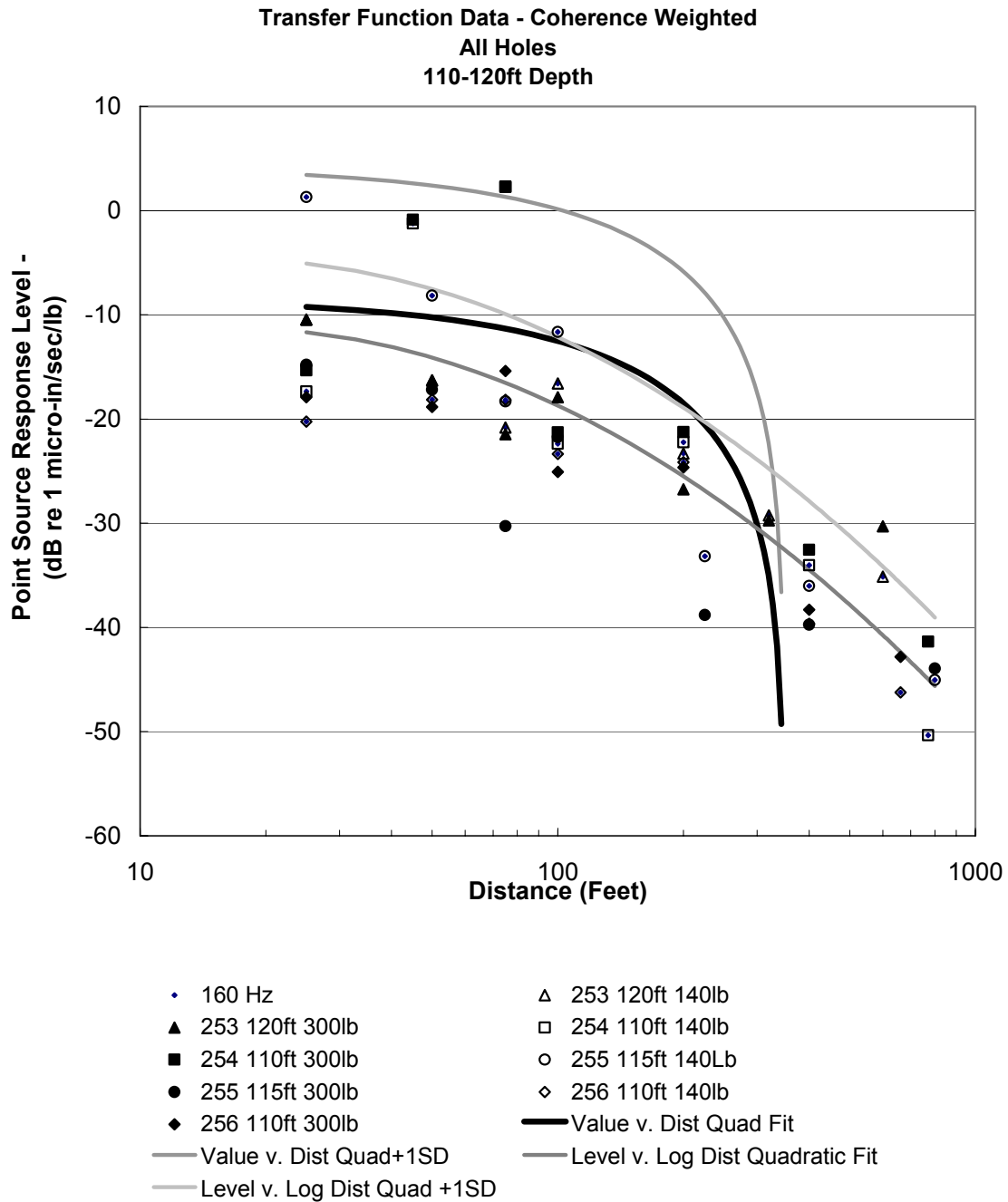


Figure A-19 Point Source Responses at 160 Hz

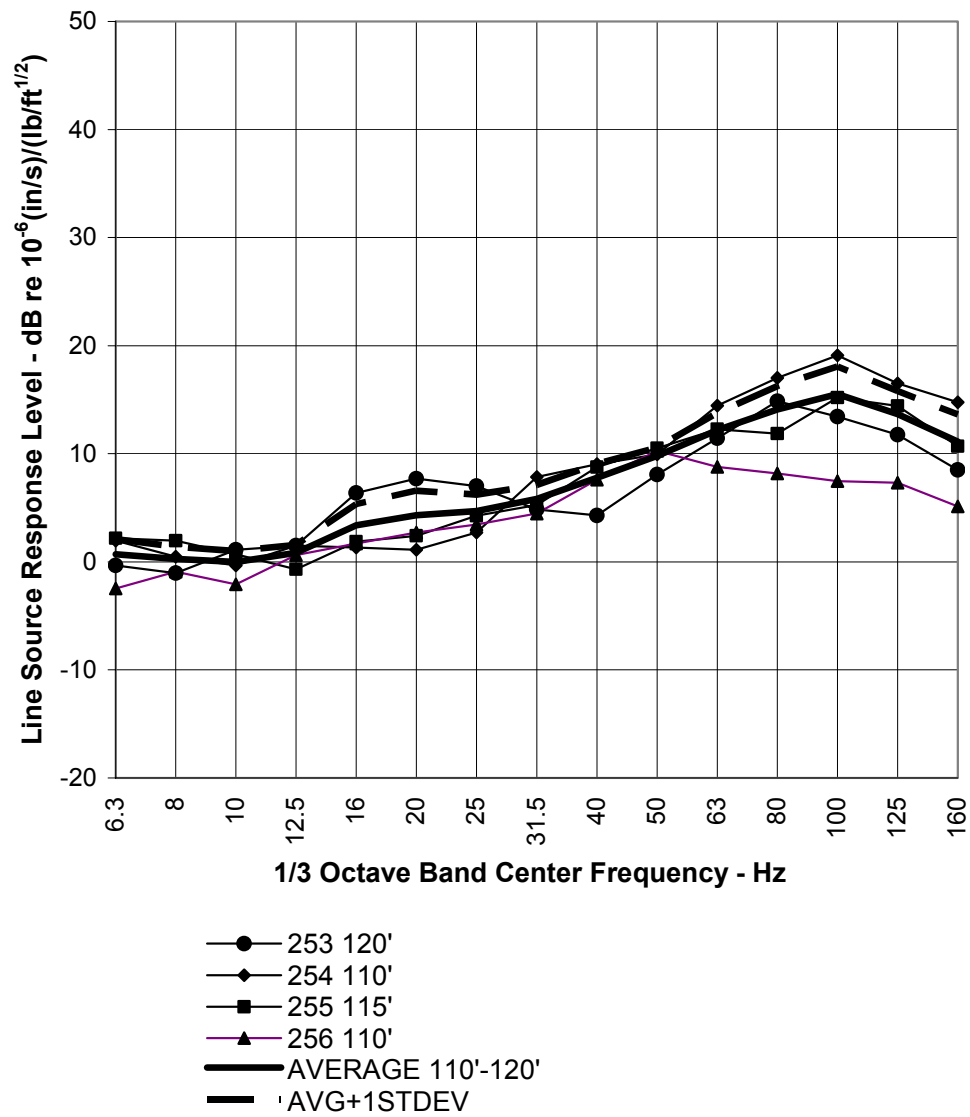
Individual LSRs Calculated for Each Borehole from Individual PSRs Determined by Regression of Mobility Level Data vs Log Offset

Line Source Responses were computed by:

- 1) Polynomial regression of the third octave band mobility level vs. log distance for each hole, using data for both the 140lb and 300lb hammer
- 2) Energy averaging of the computed LSR at representative distances of 25, 50, 100, 200, and 400 feet offset
- 3) Energy average plus one standard deviation of the mean at above distances

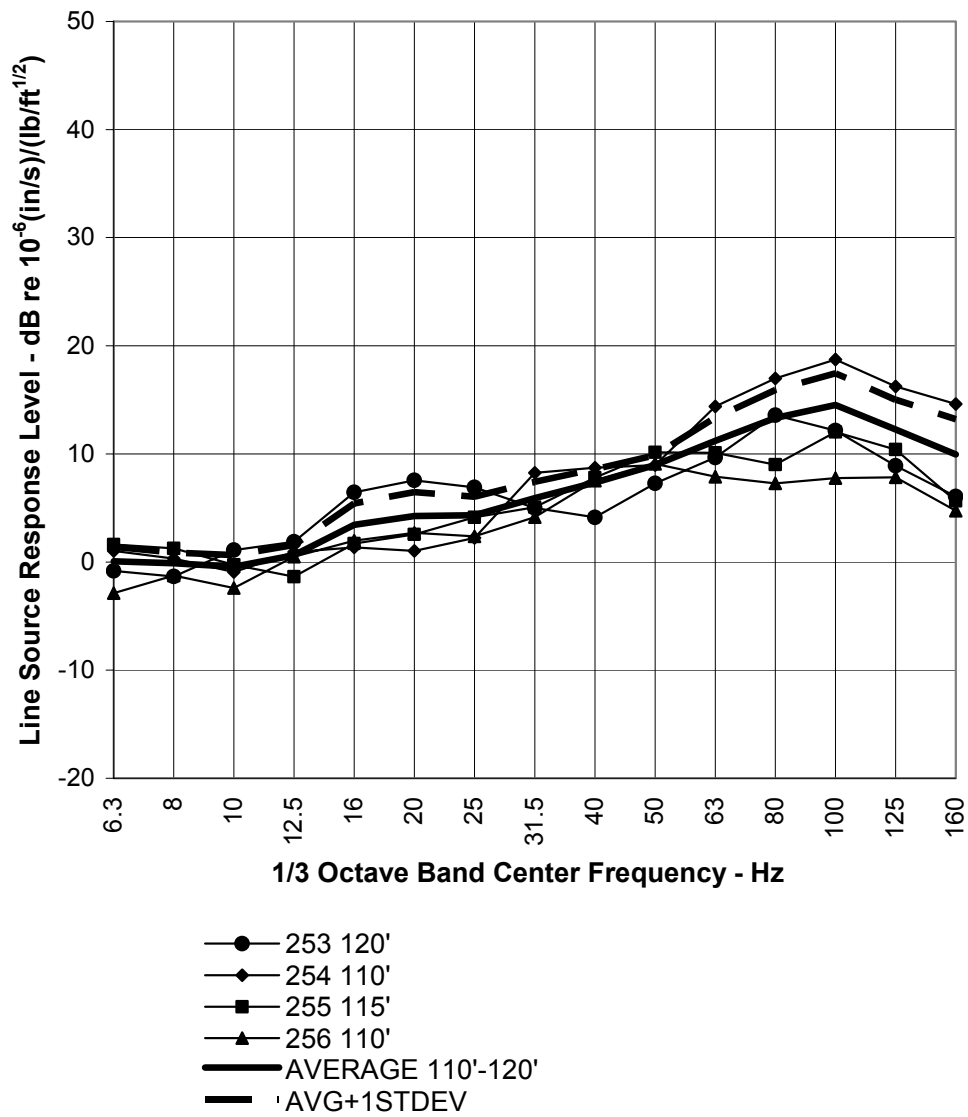
The results for each hole and the energy average and energy average plus one standard deviation are presented in Figure A-20 through Figure A-24 for offset distances of 25, 50, 100, 200, and 400 feet. Each Line Source Response was obtained by integrating the Point Source Response regression curves calculated for each hole over the train length, using the square of the magnitude obtained from the PSR regression curve.

The Line Source Responses based on regression curves are reasonably well grouped. The response for NB-253 appears to be the highest of the four. The corresponding mean deviations are of the order of a few decibels.



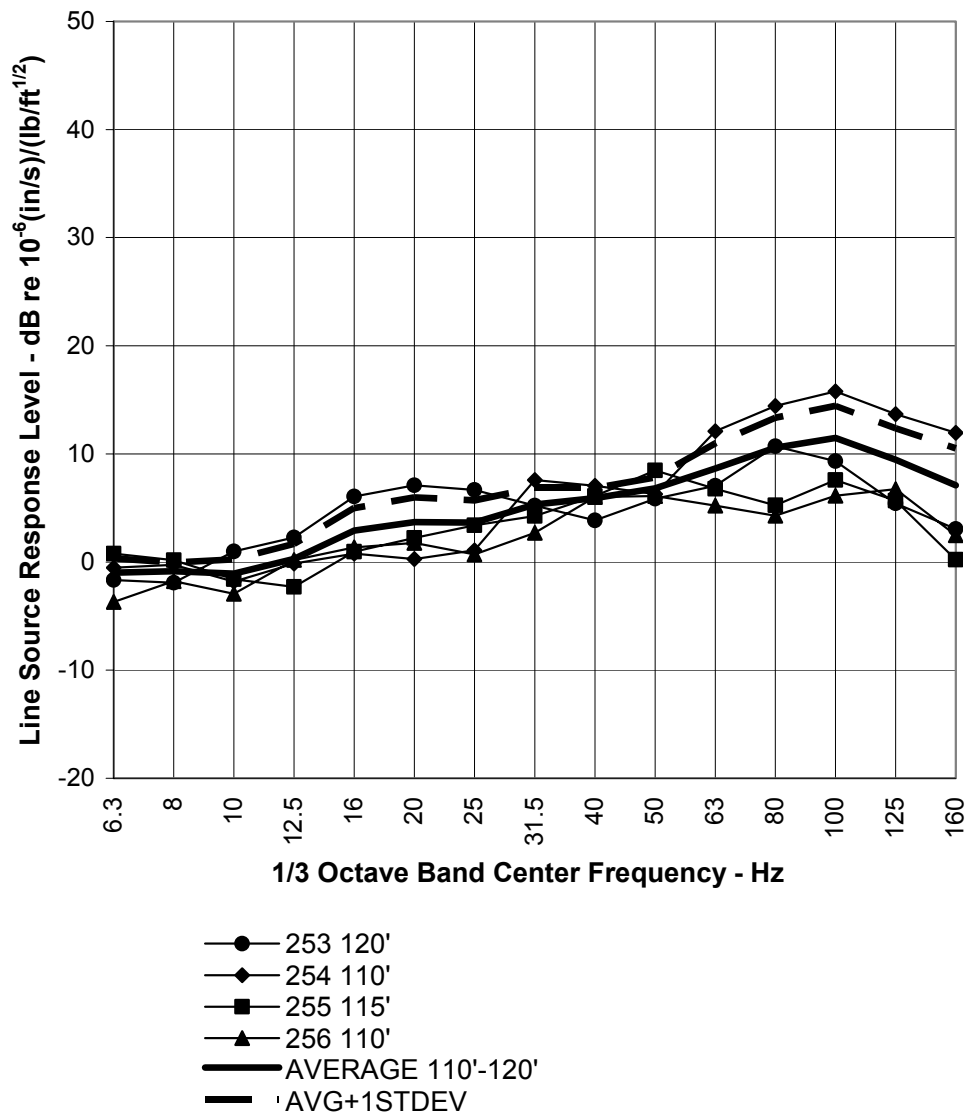
Line Source Response at 25 Feet from Track Center Line
 Train Length=340 ft
 Source Depth=110-120ft

Figure A-20 Line Source Responses for Each Borehole at 25 Foot Offset from Track Center



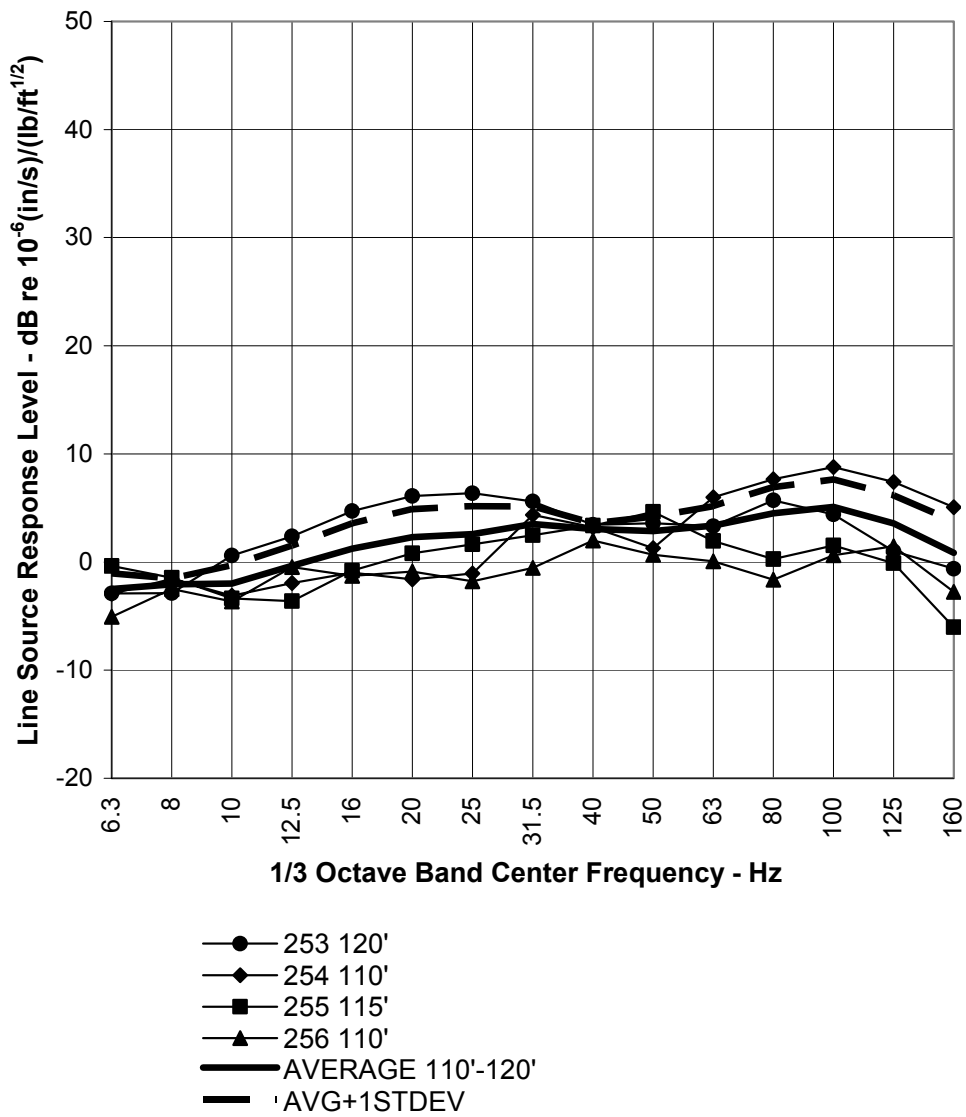
Line Source Response at 50 Feet from Track Center Line
 Train Length=340 ft
 Source Depth=110-120ft

Figure A-21 Line Source Responses for Each Borehole at 50 Foot Offset from Track Center



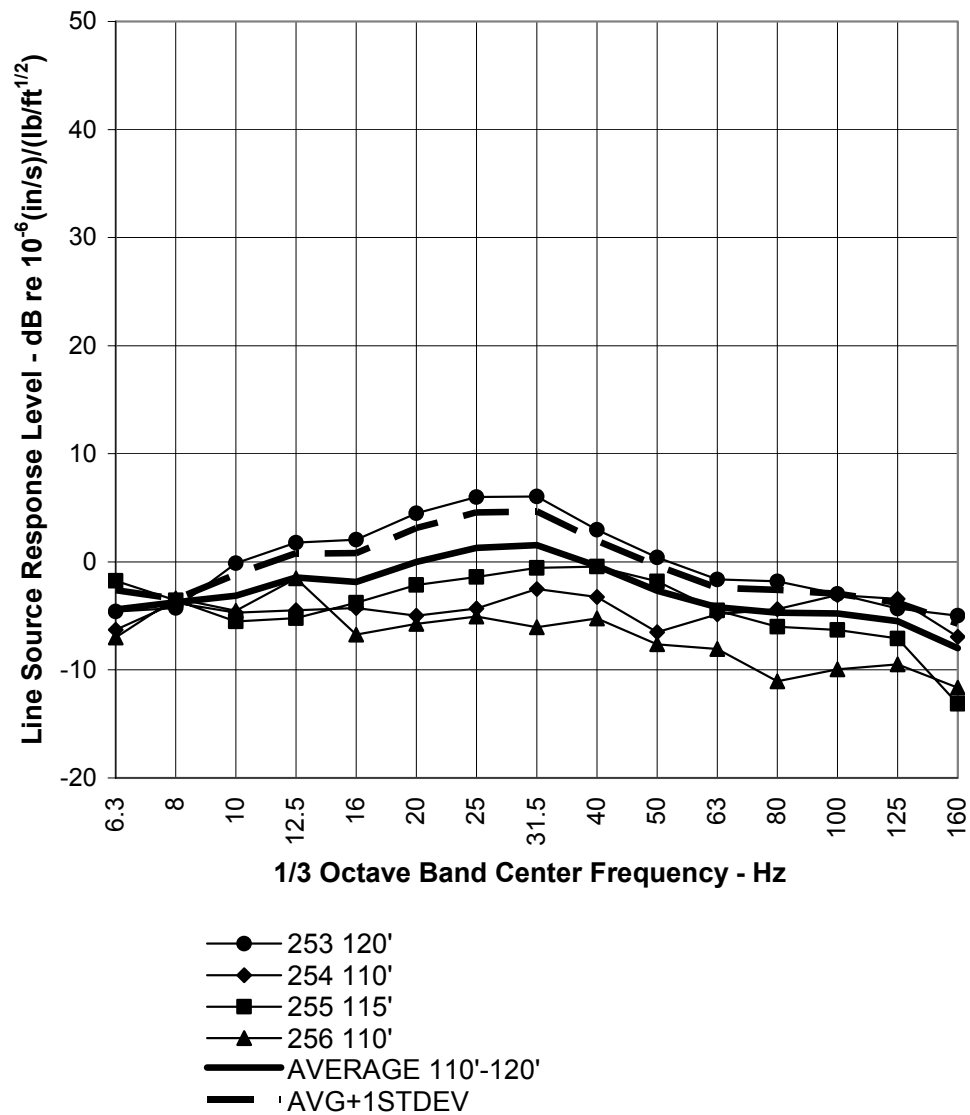
Line Source Response at 100 Feet from Track Center Line
 Train Length=340 ft
 Source Depth=110-120ft

Figure A-22 Line Source Responses for Each Borehole at 100 Foot Offset from Track Center



Line Source Response at 200 Feet from Track Center Line
 Train Length=340 ft
 Source Depth=110-120ft

Figure A-23 Line Source Responses for Each Borehole at 200 Foot Offset from Track Center



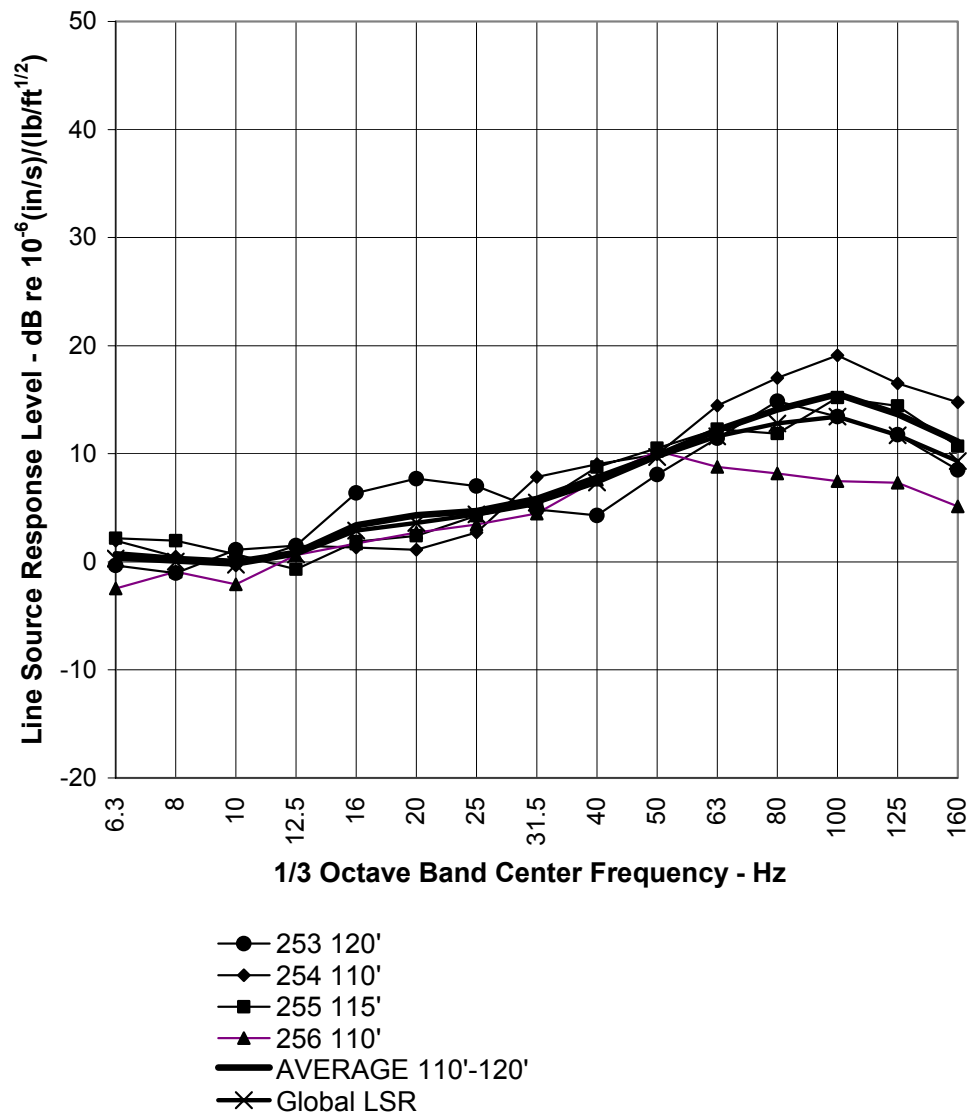
Line Source Response at 400 Feet from Track Center Line
 Train Length=340 ft
 Source Depth=110-120ft

Figure A-24 Line Source Responses for Each Borehole at 400 Foot Offset From Track Center

Global LSRs Calculated from PSRs Determined by Regression of Mobility Level Test Data vs Log Offset for All Boreholes

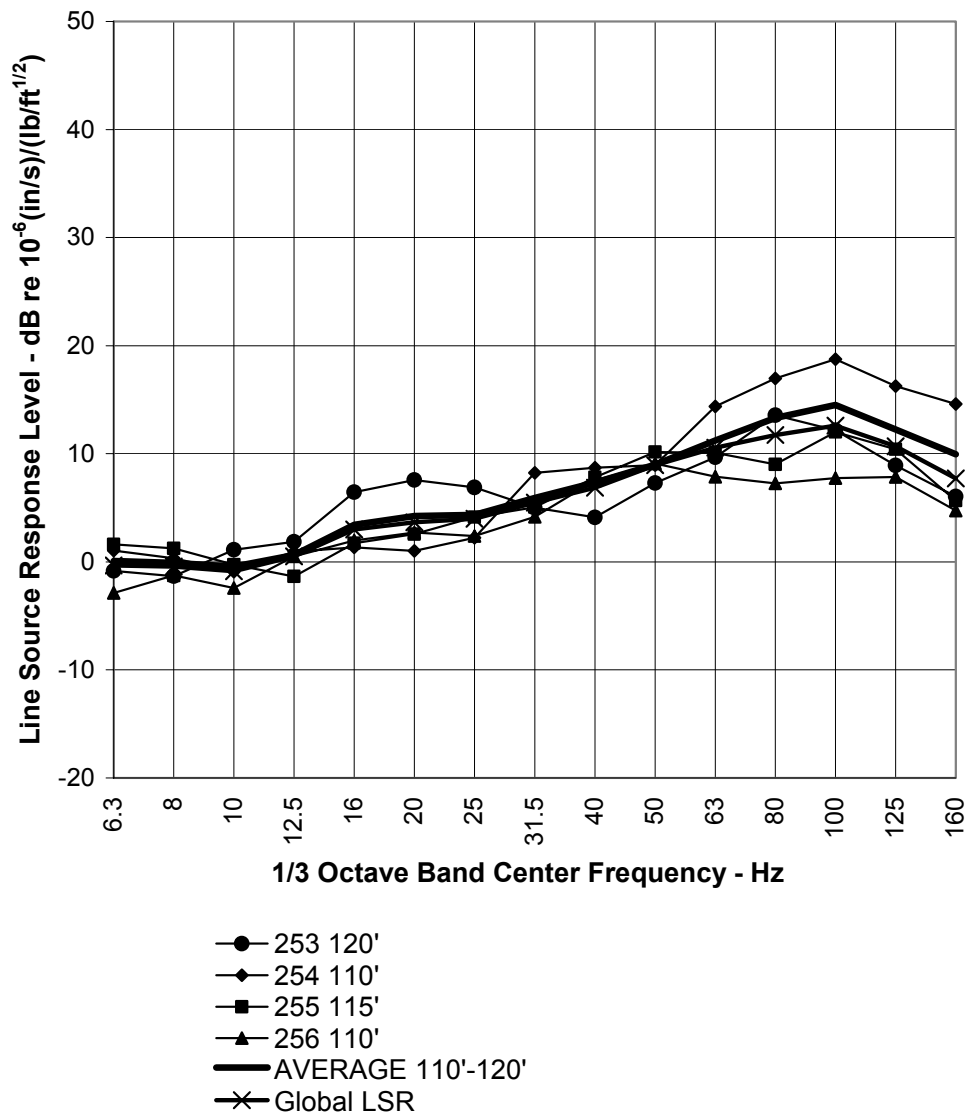
LSRs were computed by global polynomial regression of the third octave PSRs in decibels versus logarithm of offset for all holes, using data for both the 140lb and 300lb hammer. Thus, all available data were used for a given third octave band.

The globally determined LSRs are compared with the individual LSRs computed for each borehole and the energy average of these individual LSRs in Figure A-25 through Figure A-29 for the respective distances of 25, 50, 100, 200, and 400 feet. The global PSRs are plotted in Figure A-2 through Figure A-19. The global LSR agrees well with the energy averaged result.



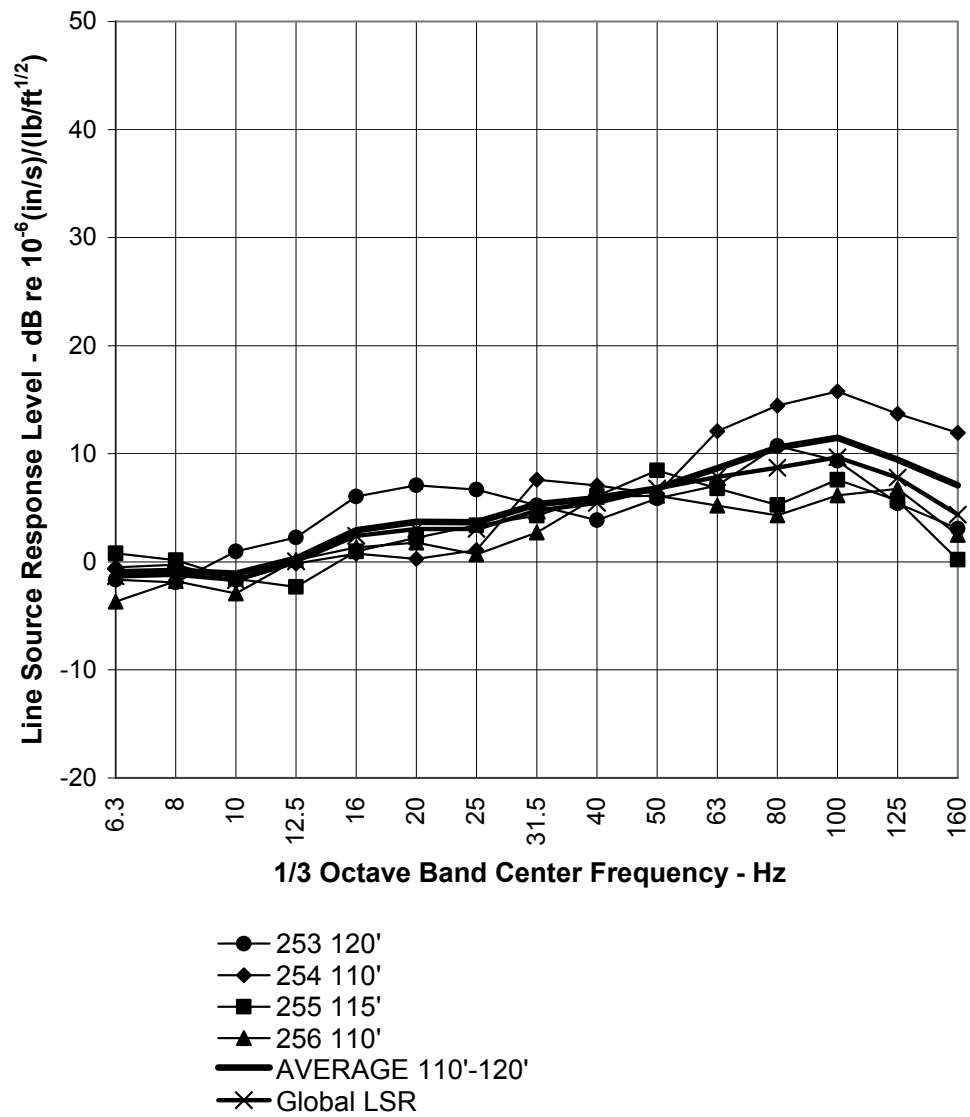
Line Source Response at 25 Feet from Track Center Line
 Train Length=340 ft
 Source Depth=110-120ft

Figure A-25 Comparison of Line Source Responses with LSR Based on Global Regression of PSR for 25 Ft Offset – Regression of Decibel Level vs. Log Offset



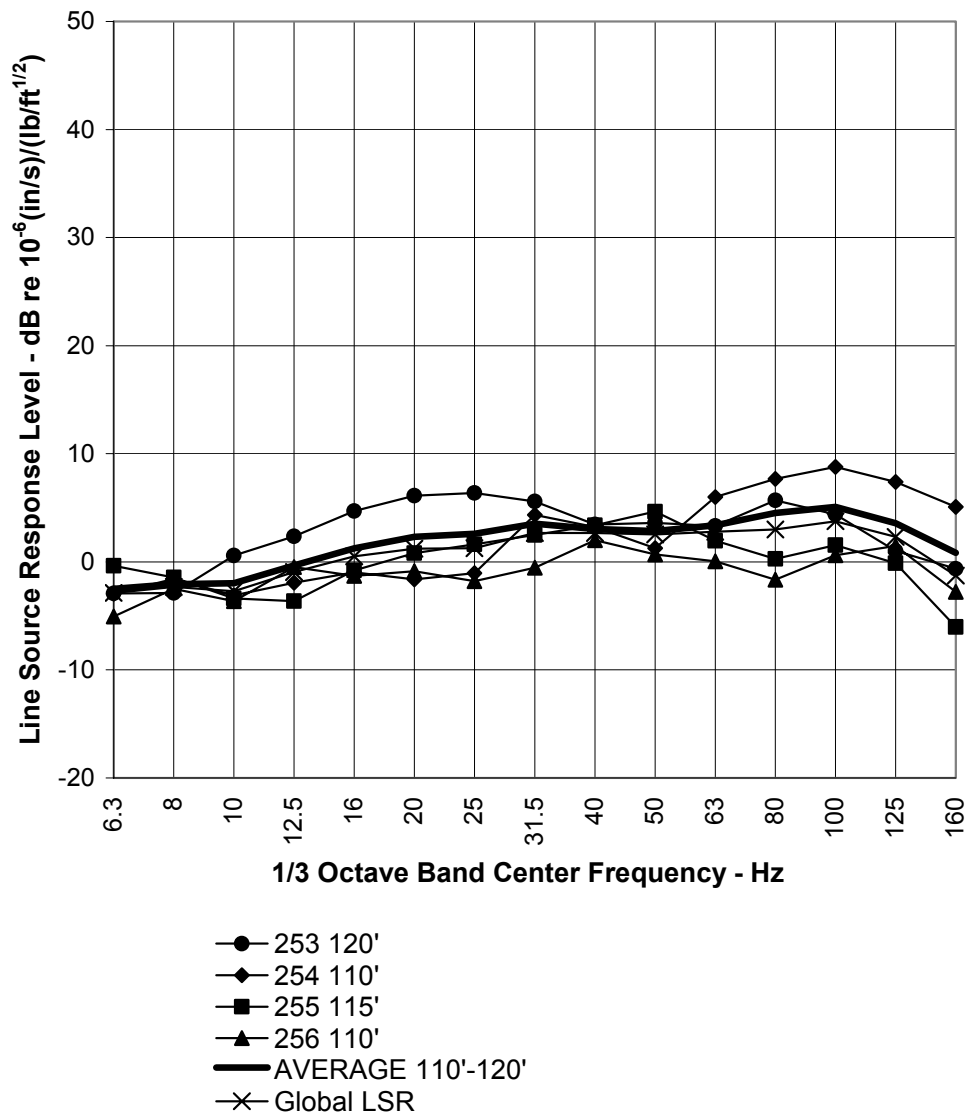
Line Source Response at 50 Feet from Track Center Line
 Train Length=340 ft
 Source Depth=110-120ft

Figure A-26 Comparison of Line Source Responses with LSR Based on Global Regression of PSR for 50 Ft Offset – Regression of Decibel Level vs. Log Offset



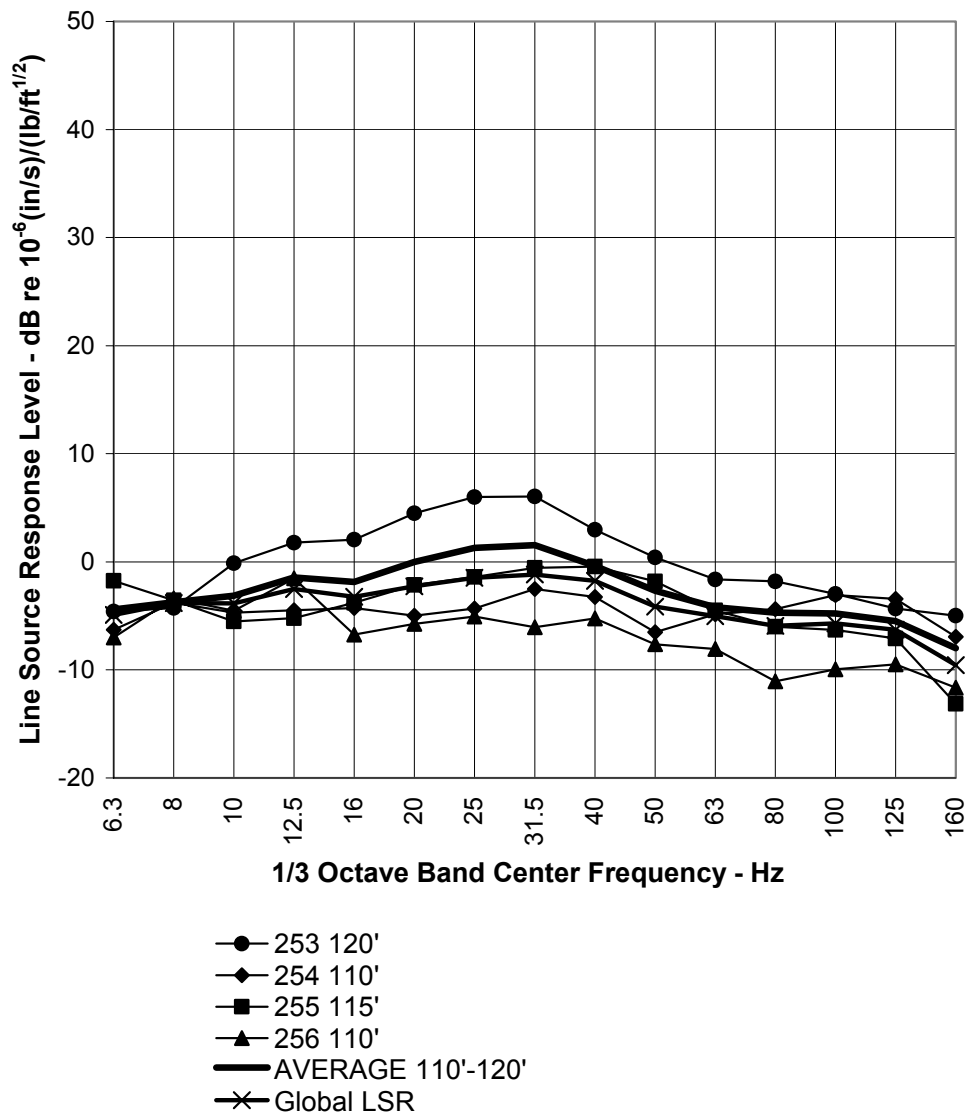
Line Source Response at 100 Feet from Track Center Line
 Train Length=340 ft
 Source Depth=110-120ft

Figure A-27 Comparison of Line Source Responses with LSR Based on Global Regression of PSR for 100 Ft Offset – Regression of Decibel Level vs. Log Offset



Line Source Response at 200 Feet from Track Center Line
 Train Length=340 ft
 Source Depth=110-120ft

Figure A-28 Comparison of Line Source Responses with LSR Based on Global Regression of PSR for 200 Ft Offset – Regression of Decibel Level vs. Log Offset

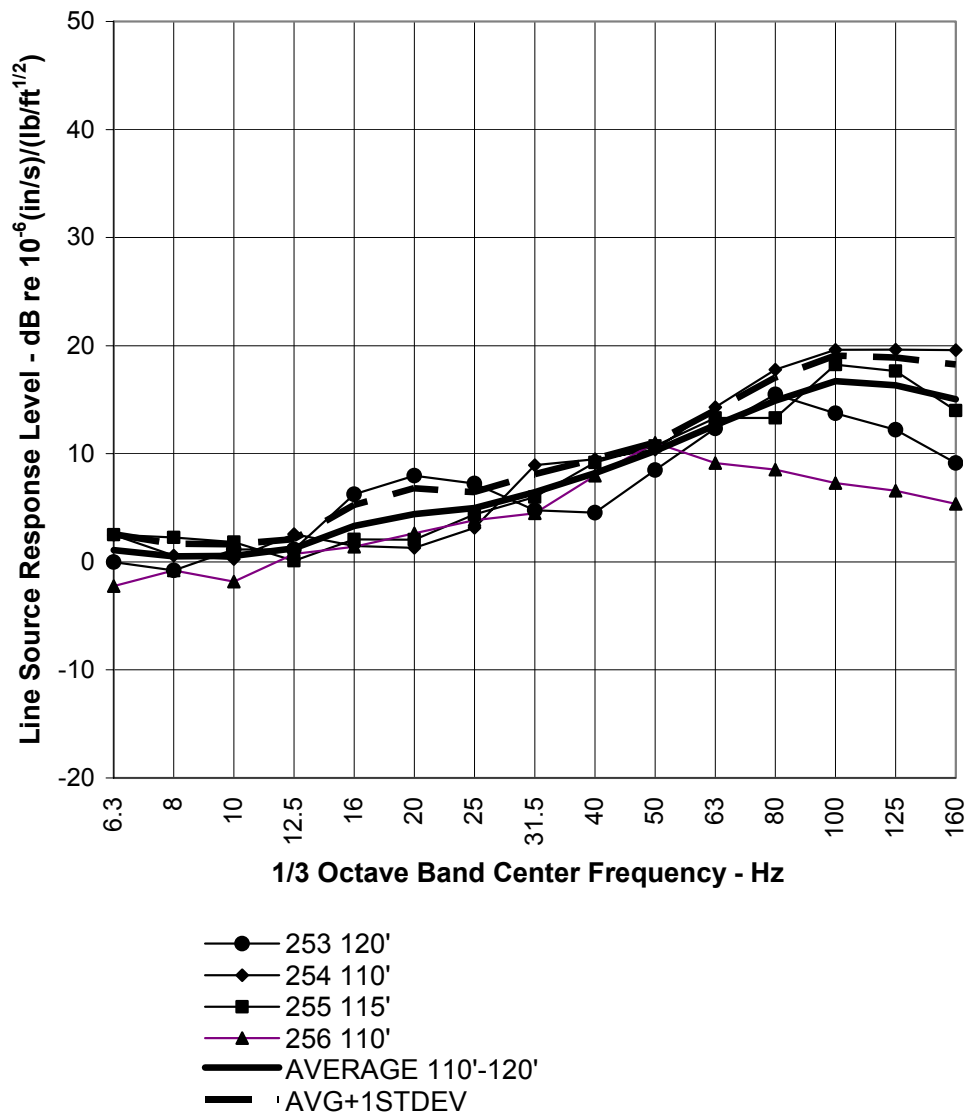


Line Source Response at 400 Feet from Track Center Line
 Train Length=340 ft
 Source Depth=110-120ft

Figure A-29 Comparison of Line Source Responses with LSR Based on Global Regression of PSR for 400 Ft Offset – Regression of Decibel Level vs. Log Offset

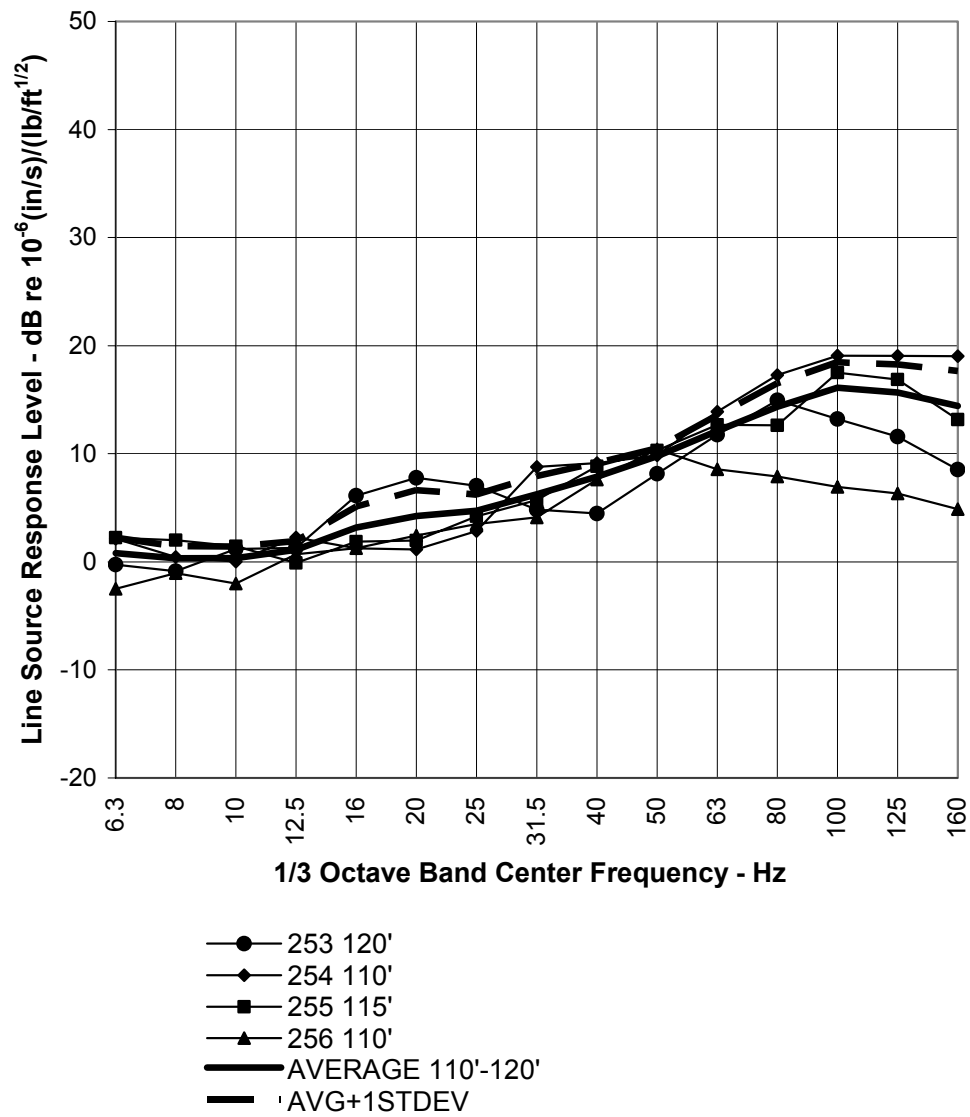
Individual LSRs Calculated from PSRs Determined by Regression of Absolute Value of Magnitude of Mobility Data vs. Offset

Line Source Responses were computed by integrating PSRs determined by regression of third octave band magnitudes of the mobility versus horizontal offset. The results are plotted for horizontal offsets of 25, 50, 100, 200, and 400 feet in Figure A-30 through Figure A-34, respectively. The results are reasonable for distances out to 200 feet. However, at greater distances, some of the mobility regression curves become negative, with the result that the integration became undefined, as discussed above.



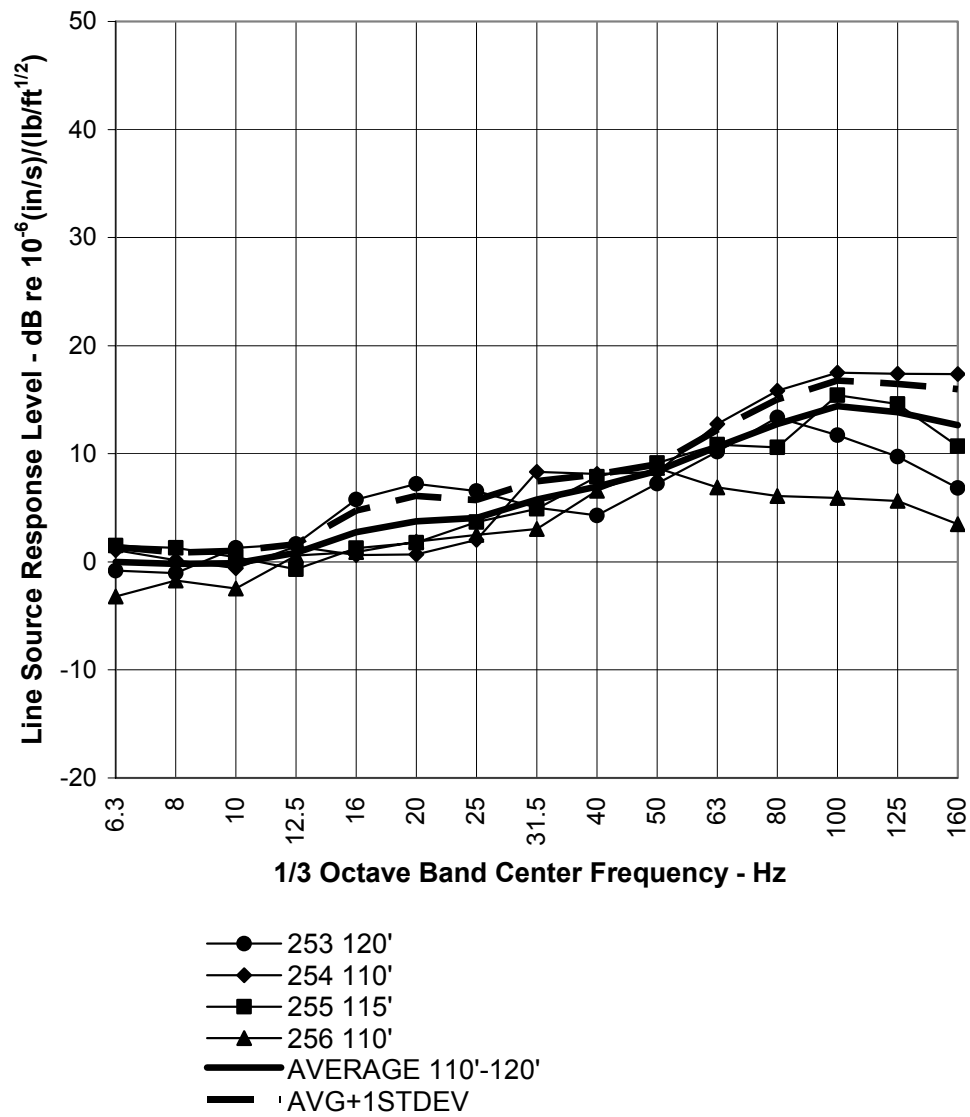
Line Source Response at 25 Feet from Track Center Line
 Train Length=340 ft
 Source Depth=110-120ft

Figure A-30 LSR Based on Regression of Magnitude of Mobility vs. Horizontal Distance at Horizontal Offset of 25 Feet



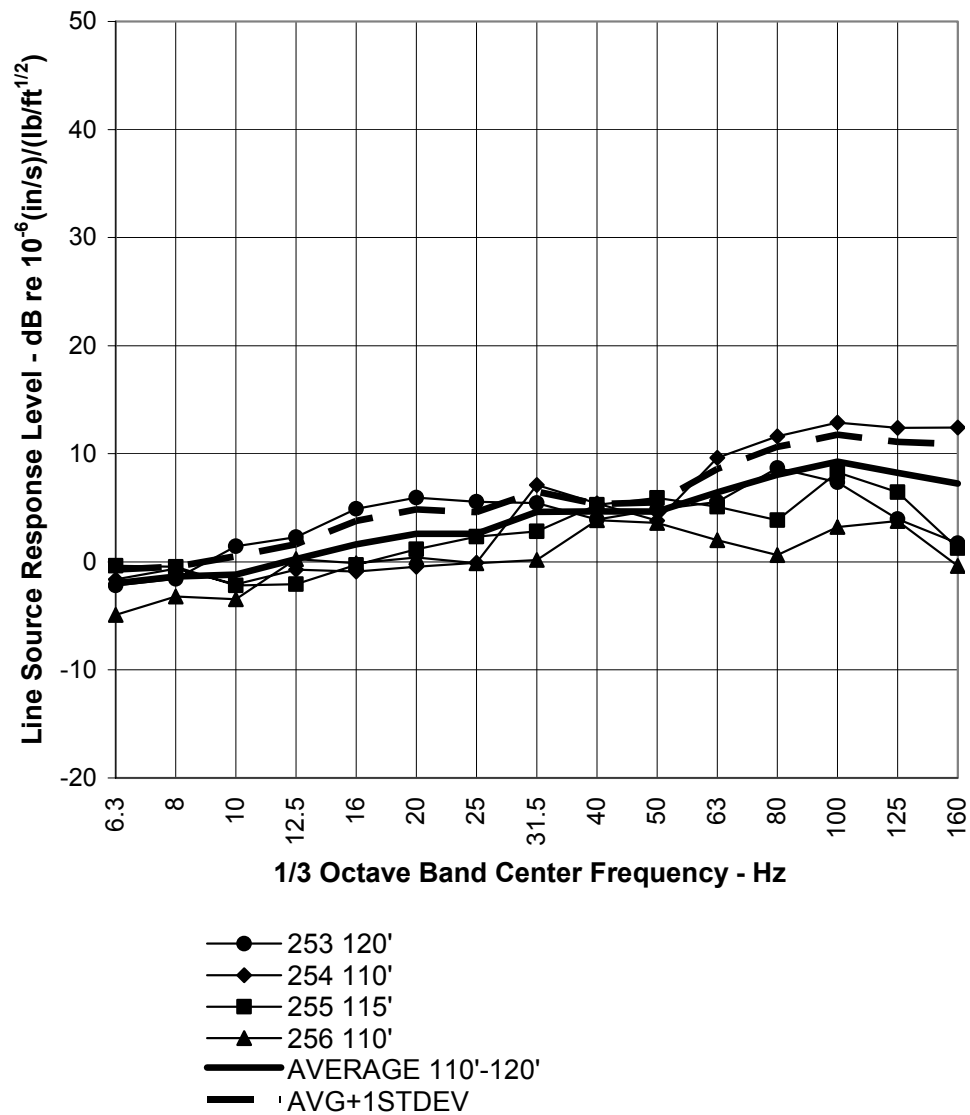
Line Source Response at 50 Feet from Track Center Line
 Train Length=340 ft
 Source Depth=110-120ft

Figure A-31 LSR Based on Regression of Magnitude of Mobility vs. Horizontal Distance at Horizontal Offset of 50 Feet



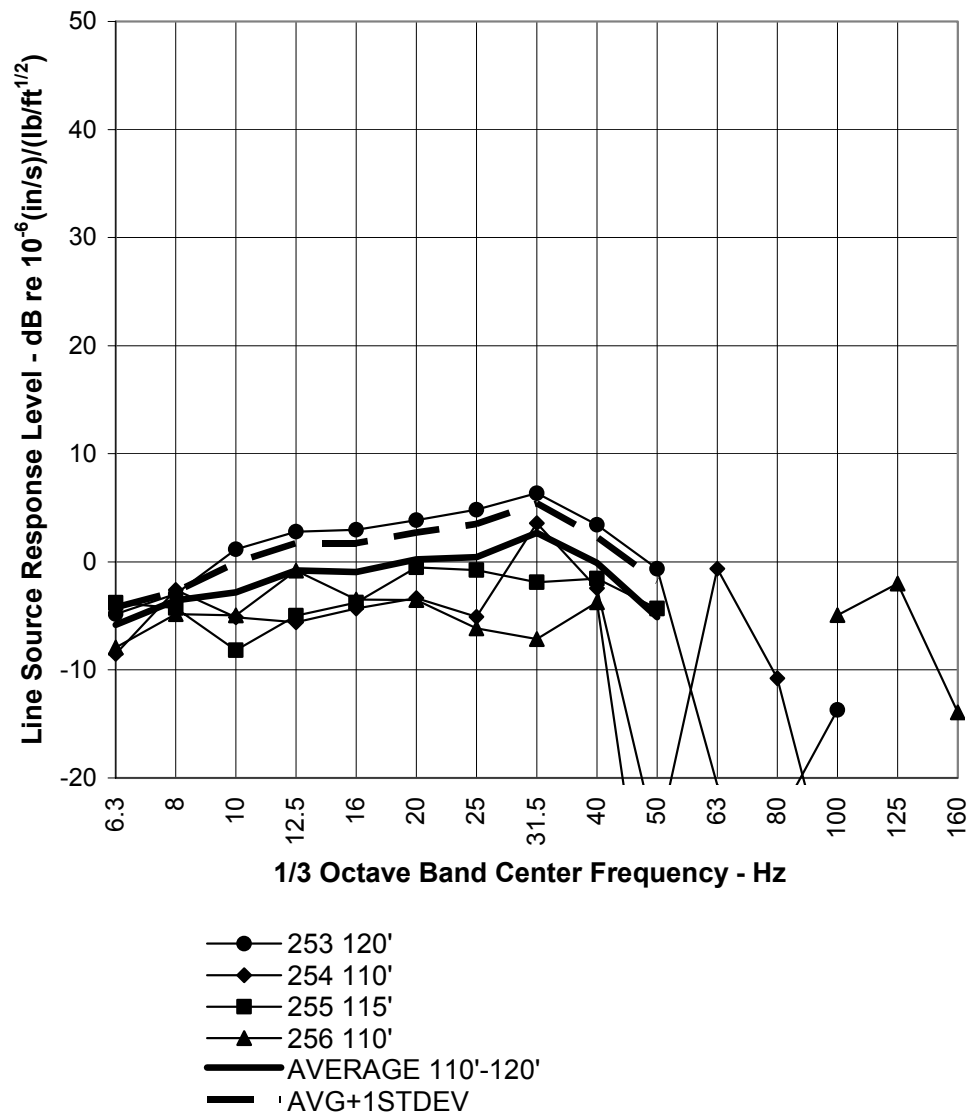
Line Source Response at 100 Feet from Track Center Line
 Train Length=340 ft
 Source Depth=110-120ft

Figure A-32 LSR Based on Regression of Magnitude of Mobility vs. Horizontal Distance at Horizontal Offset of 100 Feet



Line Source Response at 200 Feet from Track Center Line
 Train Length=340 ft
 Source Depth=110-120ft

Figure A-33 LSR Based on Regression of Magnitude of Mobility vs. Horizontal Distance at Horizontal Offset of 200 Feet



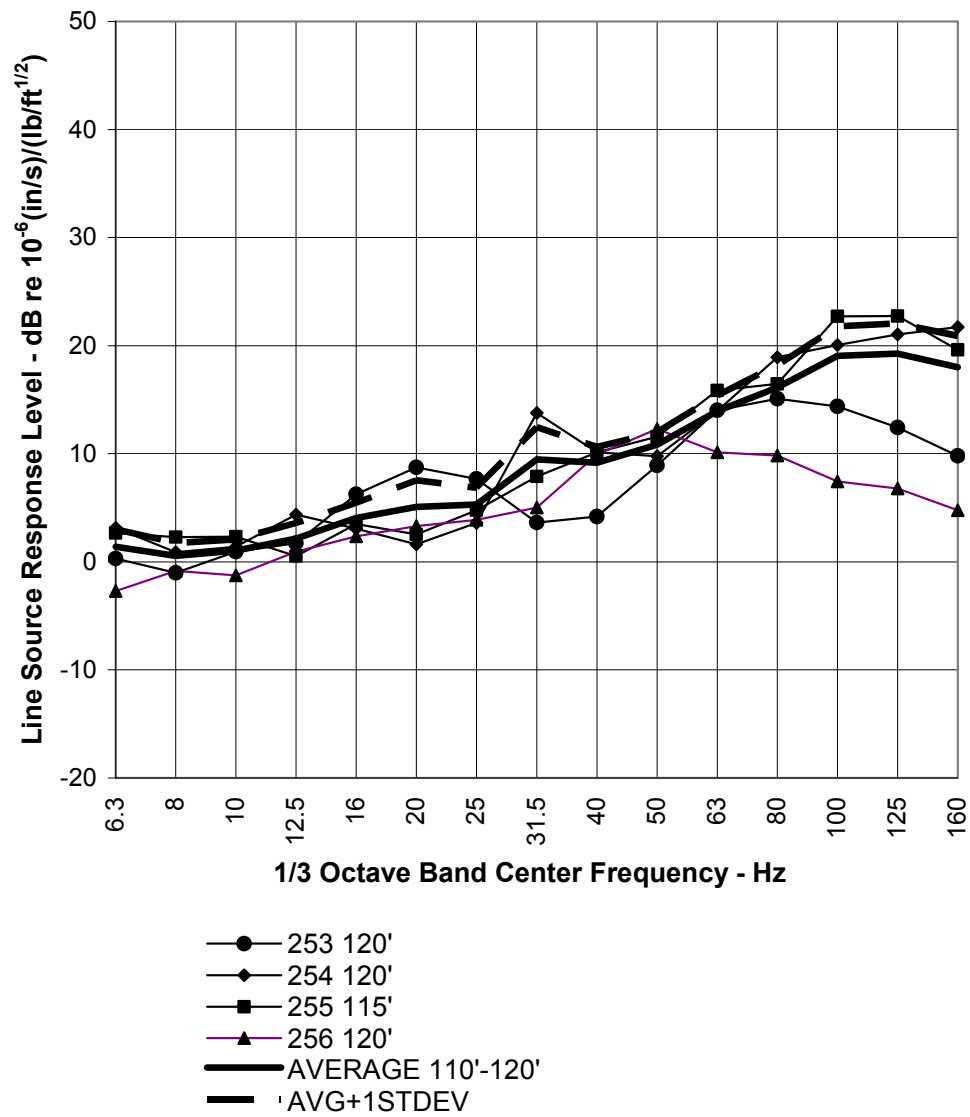
Line Source Response at 400 Feet from Track Center Line
 Train Length=340 ft
 Source Depth=110-120ft

Figure A-34 LSR Based on Regression of Magnitude of Mobility vs. Horizontal Distance at Horizontal Offset of 400 Feet

LSRs Computed by Interpolation of Mobility Data vs. Horizontal Offset

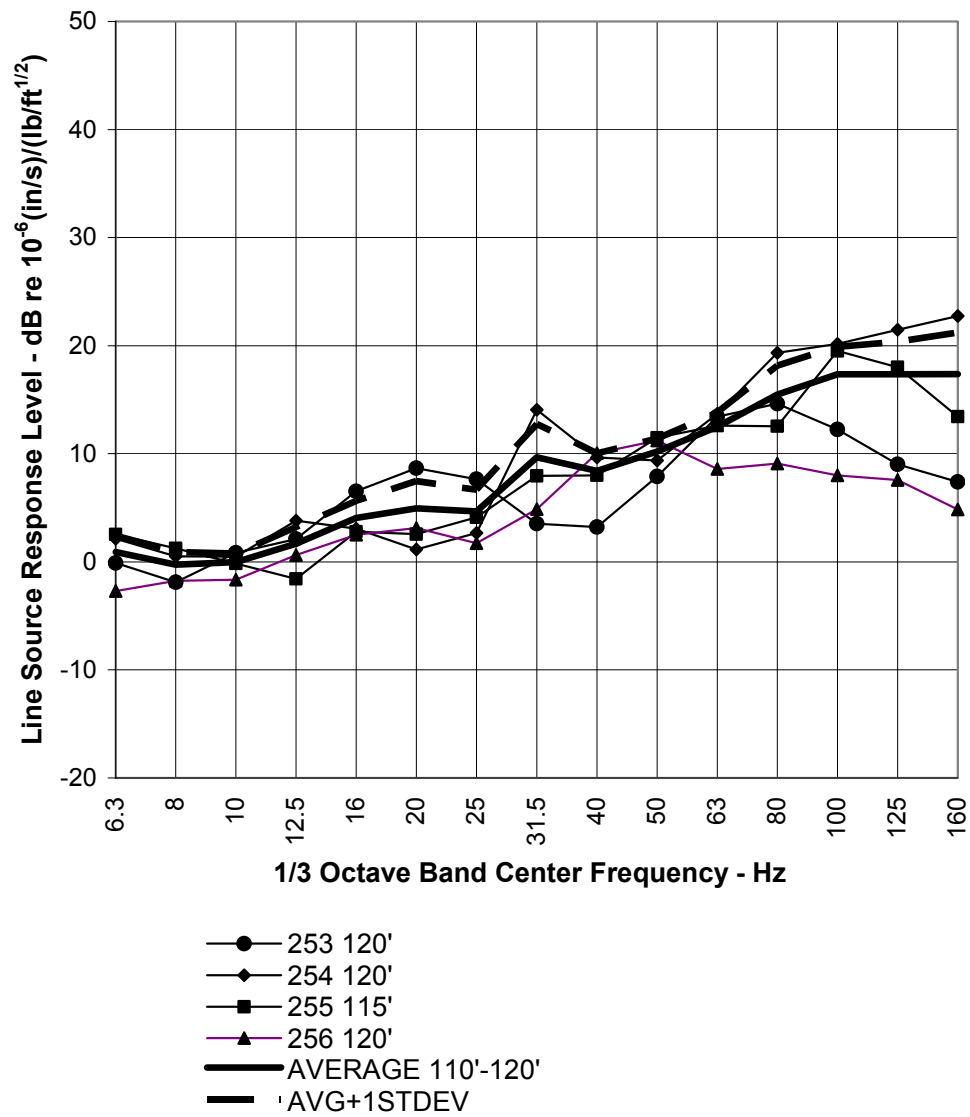
Mobilities were interpolated between measured mobilities at each horizontal offset measurement distance. The interpolation functions were then used to integrate the square of the mobility over the train length for offsets of 25, 50, 100, 200, and 400 feet. The results are presented in Figure A-35 through Figure A-39, respectively, for data collected with the 140lb hammer. The results are presented in Figure A-40 through Figure A-44, respectively, for data collected with the 300lb hammer.

The individual borehole LSR's are more spread out with interpolation than with regression of mobility data. However, The energy average of the individual borehole LSRs conforms roughly with the energy average of the individual borehole LSRs based on the regression approaches discussed above and with the globally determined LSR.



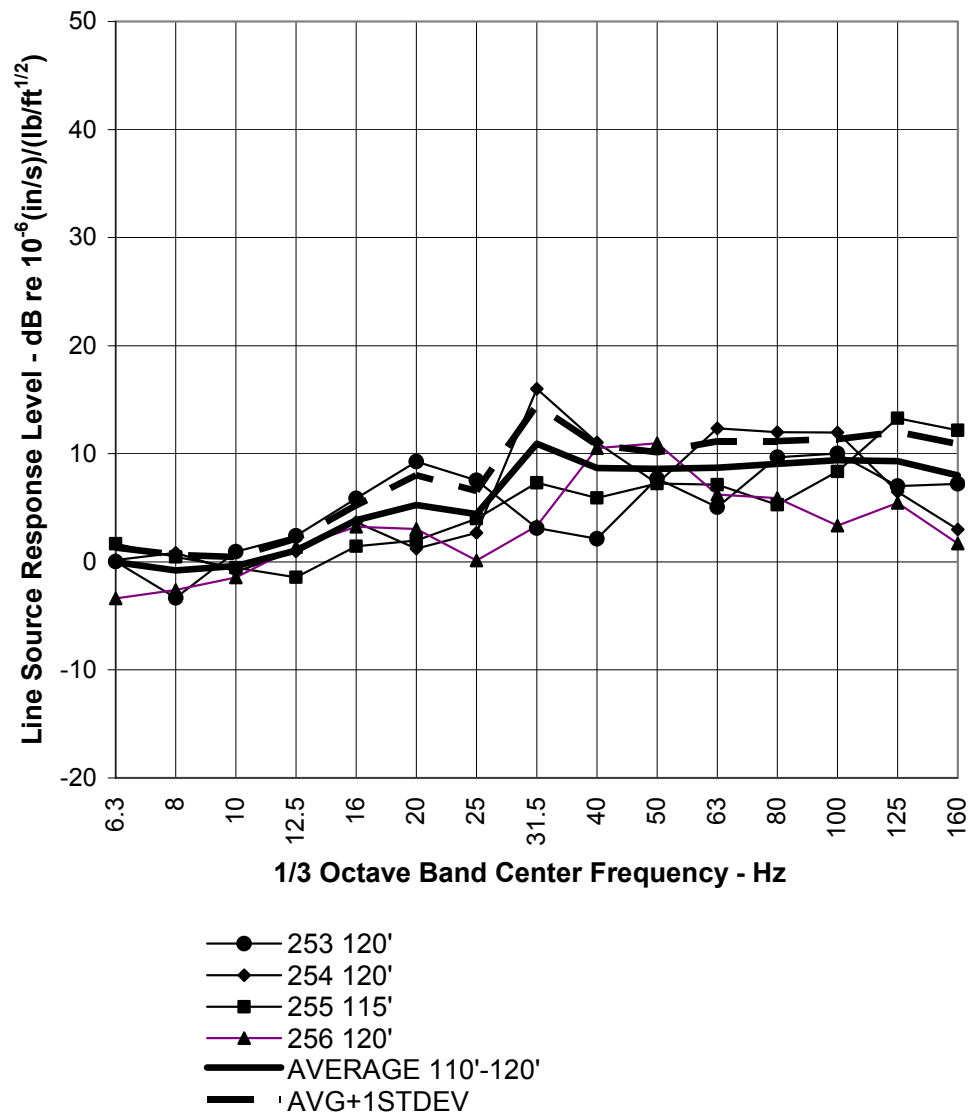
Line Source Response at 25 Feet from Track Center Line
 Train Length=340 ft
 Source Depth=110-120ft

Figure A-35 LSR Based on Linear Interpolation of Magnitude of Mobility vs. Horizontal Distance for 140lb Hammer – Horizontal Offset of 25 Feet



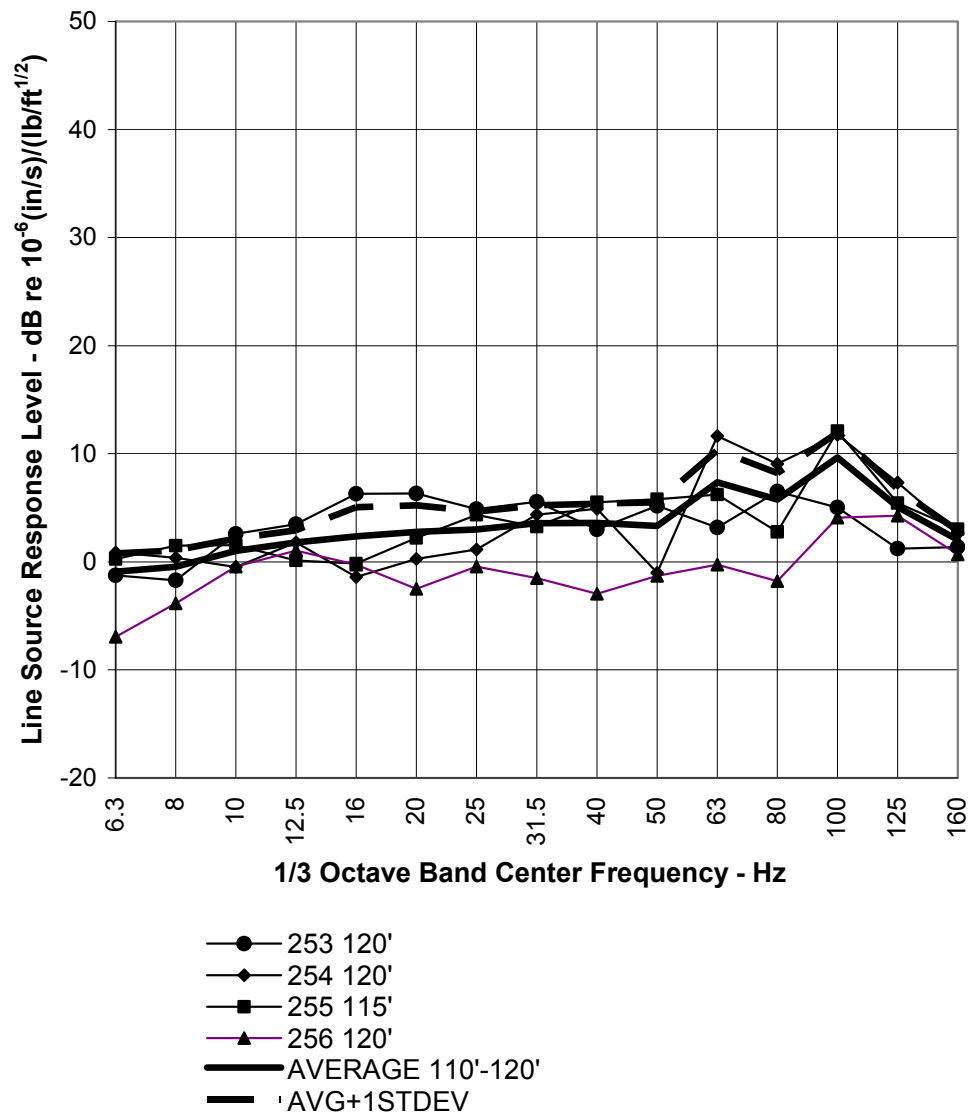
Line Source Response at 50 Feet from Track Center Line
 Train Length=340 ft
 Source Depth=110-120ft

Figure A-36 LSR Based on Linear Interpolation of Magnitude of Mobility vs. Horizontal Distance for 140lb Hammer – Horizontal Offset of 50 Feet



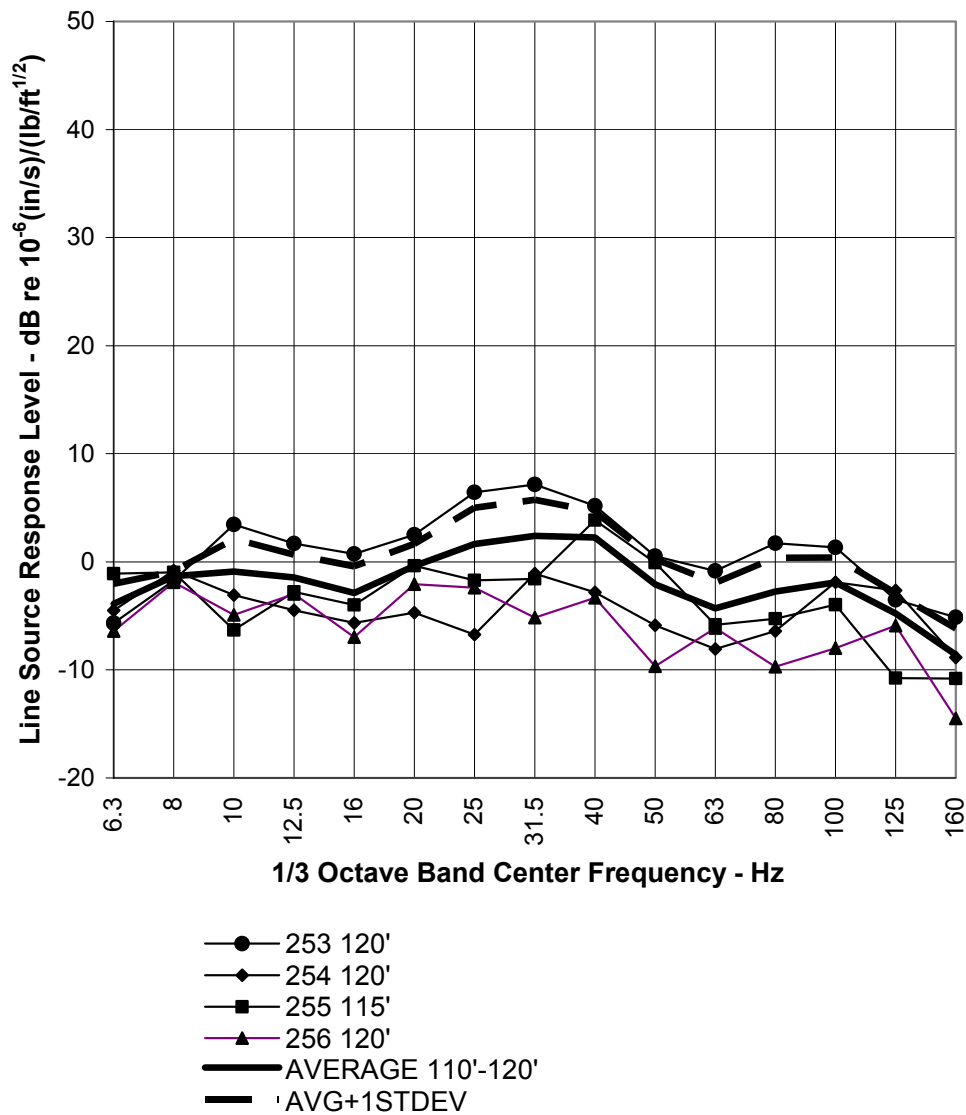
Line Source Response at 100 Feet from Track Center Line
 Train Length=340 ft
 Source Depth=110-120ft

Figure A-37 LSR Based on Linear Interpolation of Magnitude of Mobility vs. Horizontal Distance for 140lb Hammer – Horizontal Offset of 100 Feet



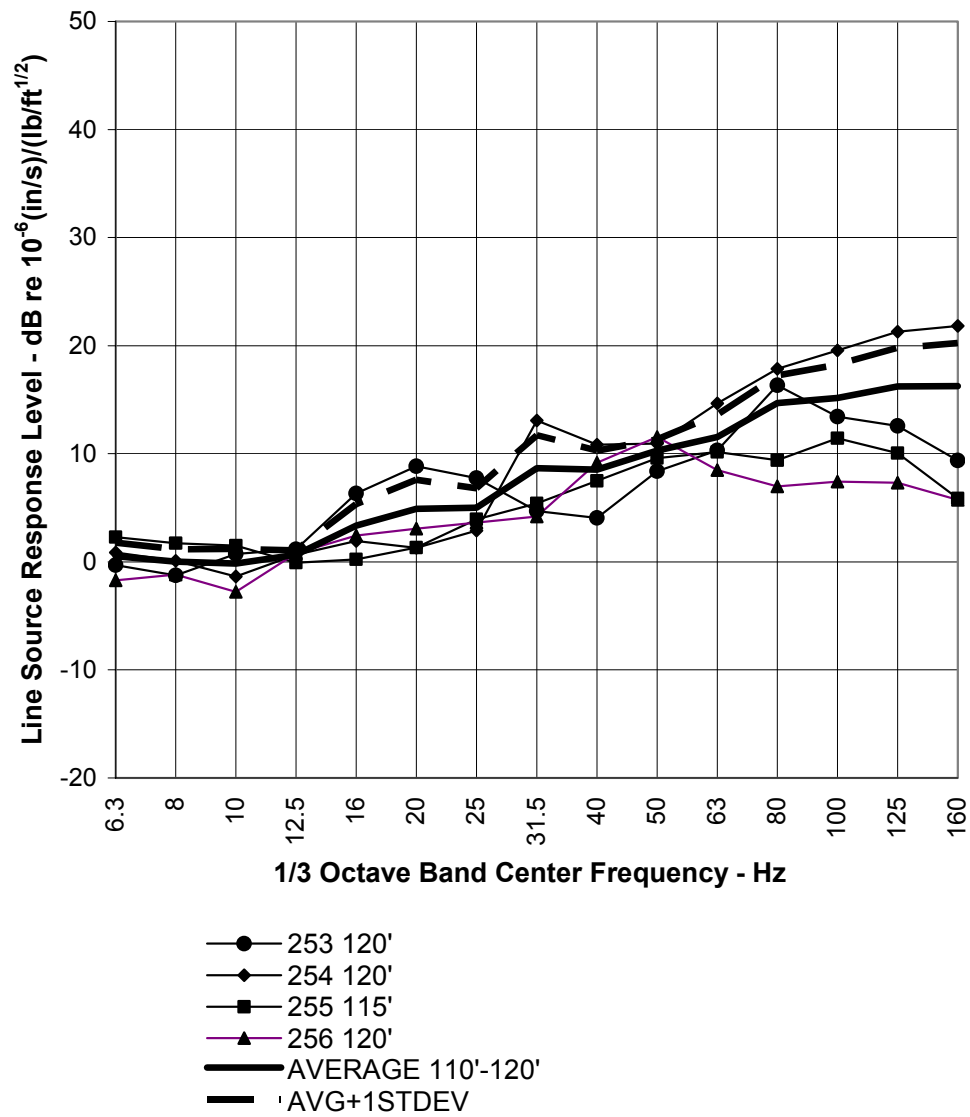
Line Source Response at 200 Feet from Track Center Line
 Train Length=340 ft
 Source Depth=110-120ft

Figure A-38 LSR Based on Linear Interpolation of Magnitude of Mobility vs. Horizontal Distance for 140lb Hammer – Horizontal Offset of 200 Feet



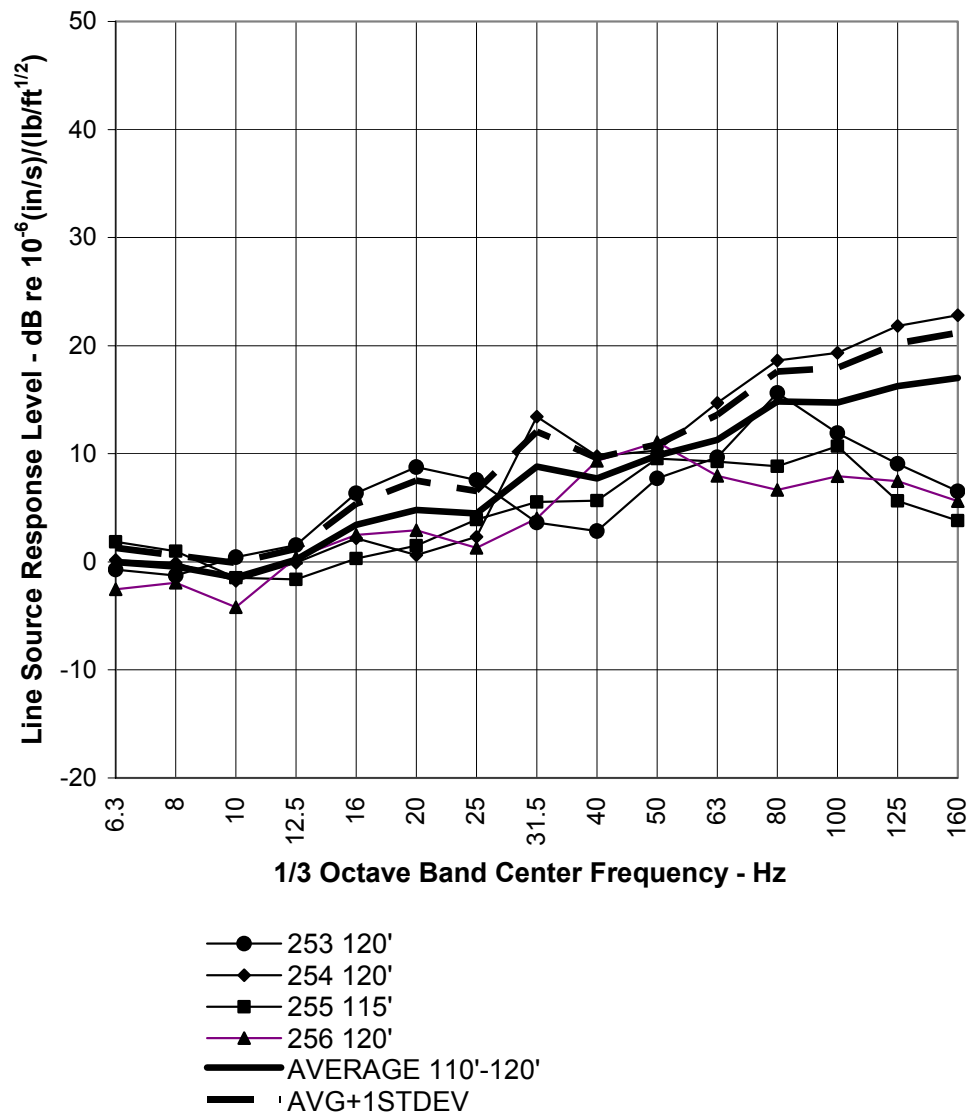
Line Source Response at 400 Feet from Track Center Line
 Train Length=340 ft
 Source Depth=110-120ft

Figure A-39 LSR Based on Linear Interpolation of Magnitude of Mobility vs. Horizontal Distance for 140lb Hammer – Horizontal Offset of 400 Feet



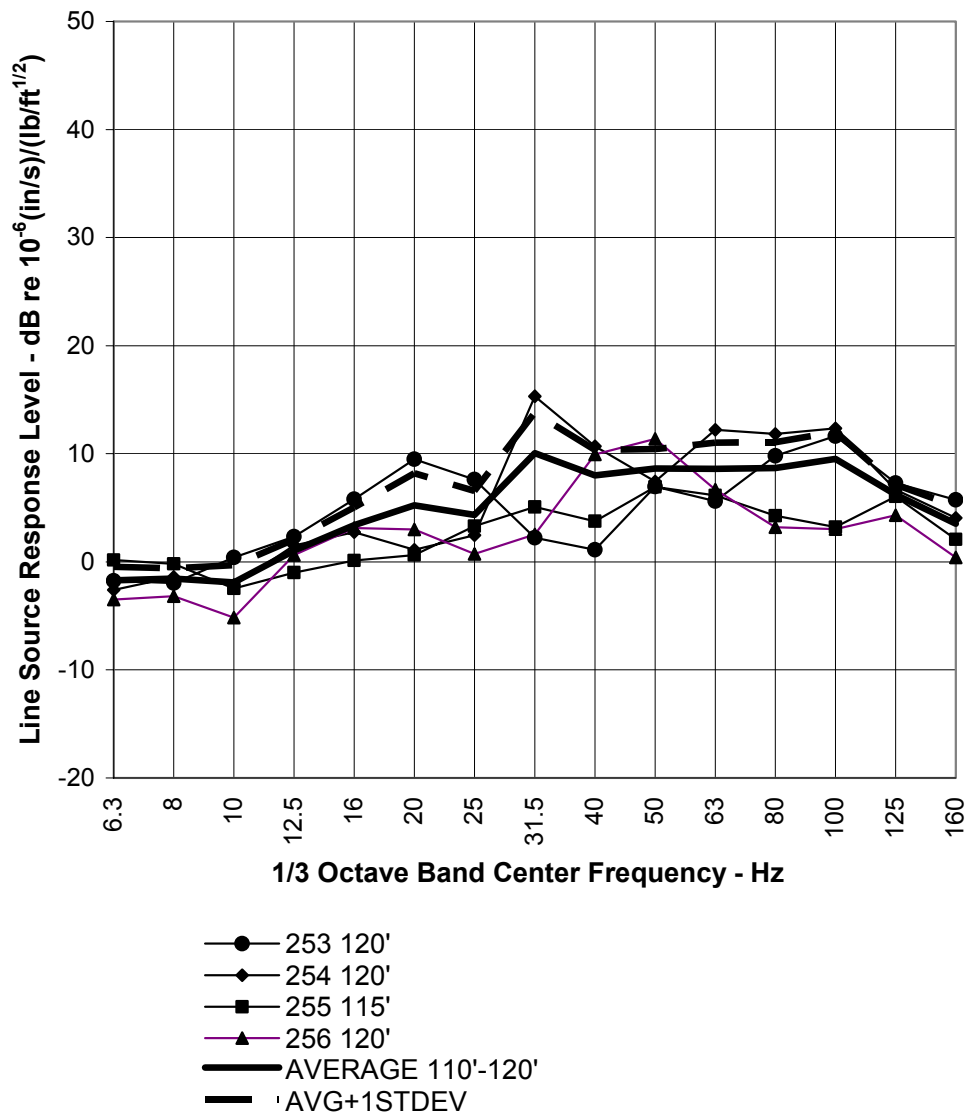
Line Source Response at 25 Feet from Track Center Line
 Train Length=340 ft
 Source Depth=110-120ft

Figure A-40 LSR Based on Linear Interpolation of Magnitude of Mobility vs. Horizontal Distance for 300lb Hammer – Horizontal Offset of 25 Feet



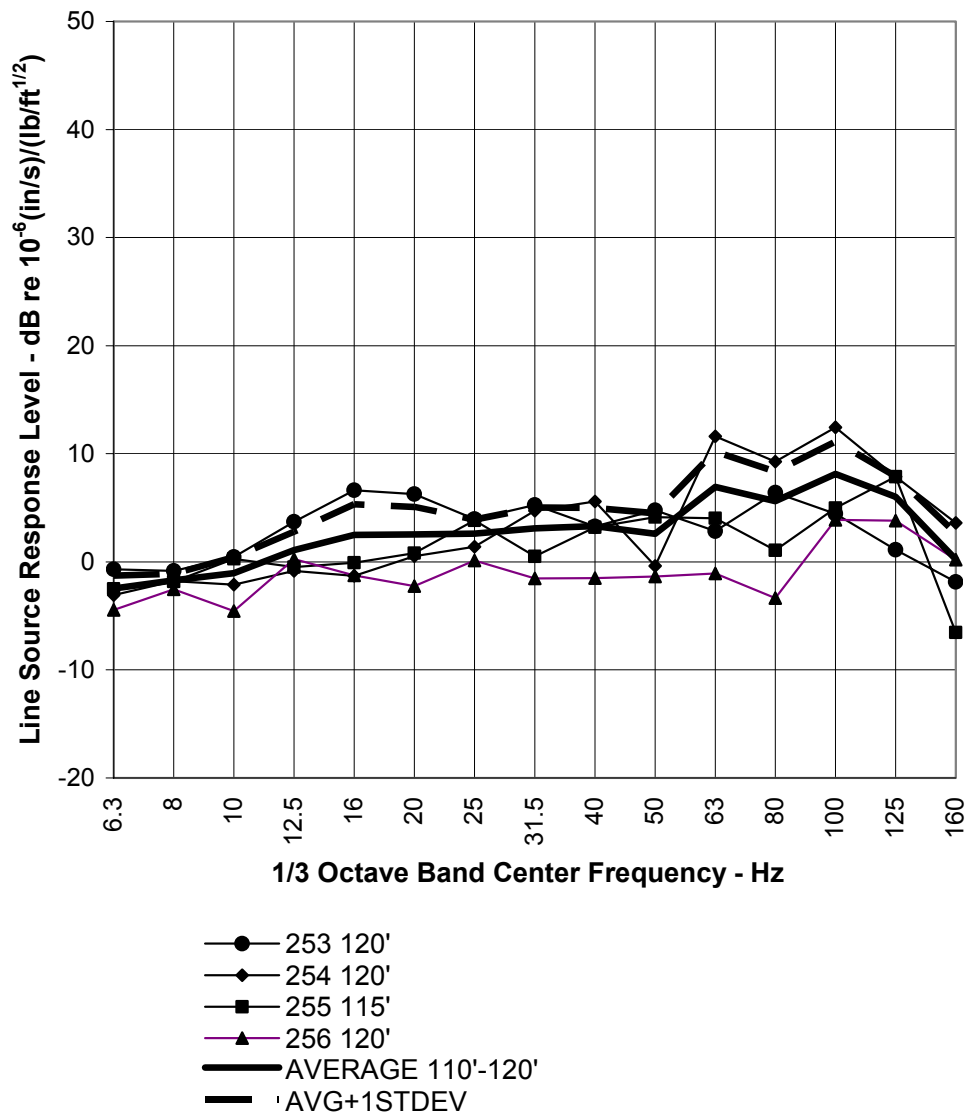
Line Source Response at 50 Feet from Track Center Line
 Train Length=340 ft
 Source Depth=110-120ft

Figure A-41 LSR Based on Linear Interpolation of Magnitude of Mobility vs. Horizontal Distance for 300lb Hammer – Horizontal Offset of 50 Feet



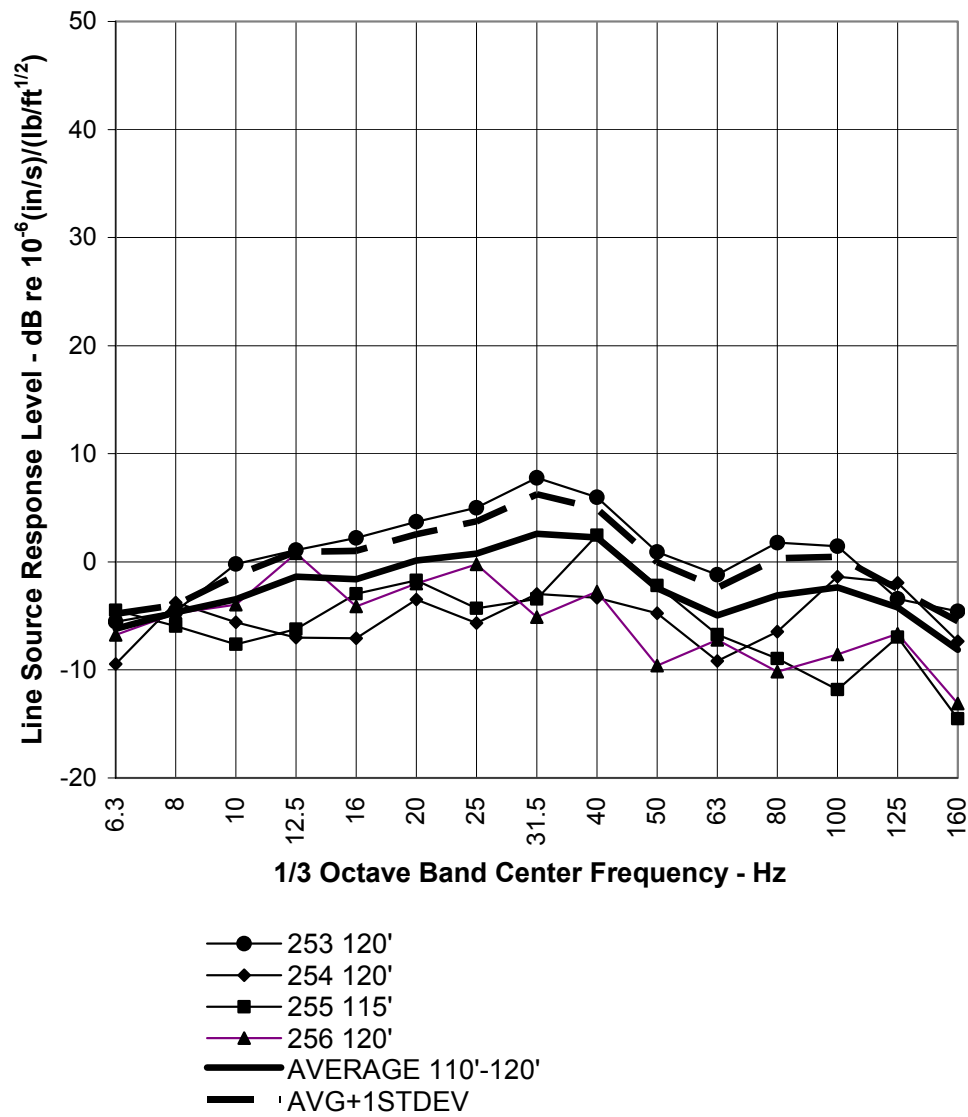
Line Source Response at 100 Feet from Track Center Line
 Train Length=340 ft
 Source Depth=110-120ft

Figure A-42 LSR Based on Linear Interpolation of Magnitude of Mobility vs. Horizontal Distance for 300lb Hammer – Horizontal Offset of 100 Feet



Line Source Response at 200 Feet from Track Center Line
 Train Length=340 ft
 Source Depth=110-120ft

Figure A-43 LSR Based on Linear Interpolation of Magnitude of Mobility vs. Horizontal Distance for 300lb Hammer – Horizontal Offset of 200 Feet



Line Source Response at 400 Feet from Track Center Line
 Train Length=340 ft
 Source Depth=110-120ft

Figure A-44 LSR Based on Linear Interpolation of Magnitude of Mobility vs. Horizontal Distance for 300lb Hammer – Horizontal Offset of 400 Feet

Comparisons of Global and Energy Averaged LSR's

The following charts, Figure A-45 through Figure A-54, are comparisons of LSR's based on global regression, energy averaged regressions for individual boreholes, and the energy averaged LSR's based on linear interpolation.

At 25 feet offset (Figure A-45 and Figure A-46), the LSR based on global quadratic regression of mobility level versus log offset is less than any of the other LSR's above 63 Hz.

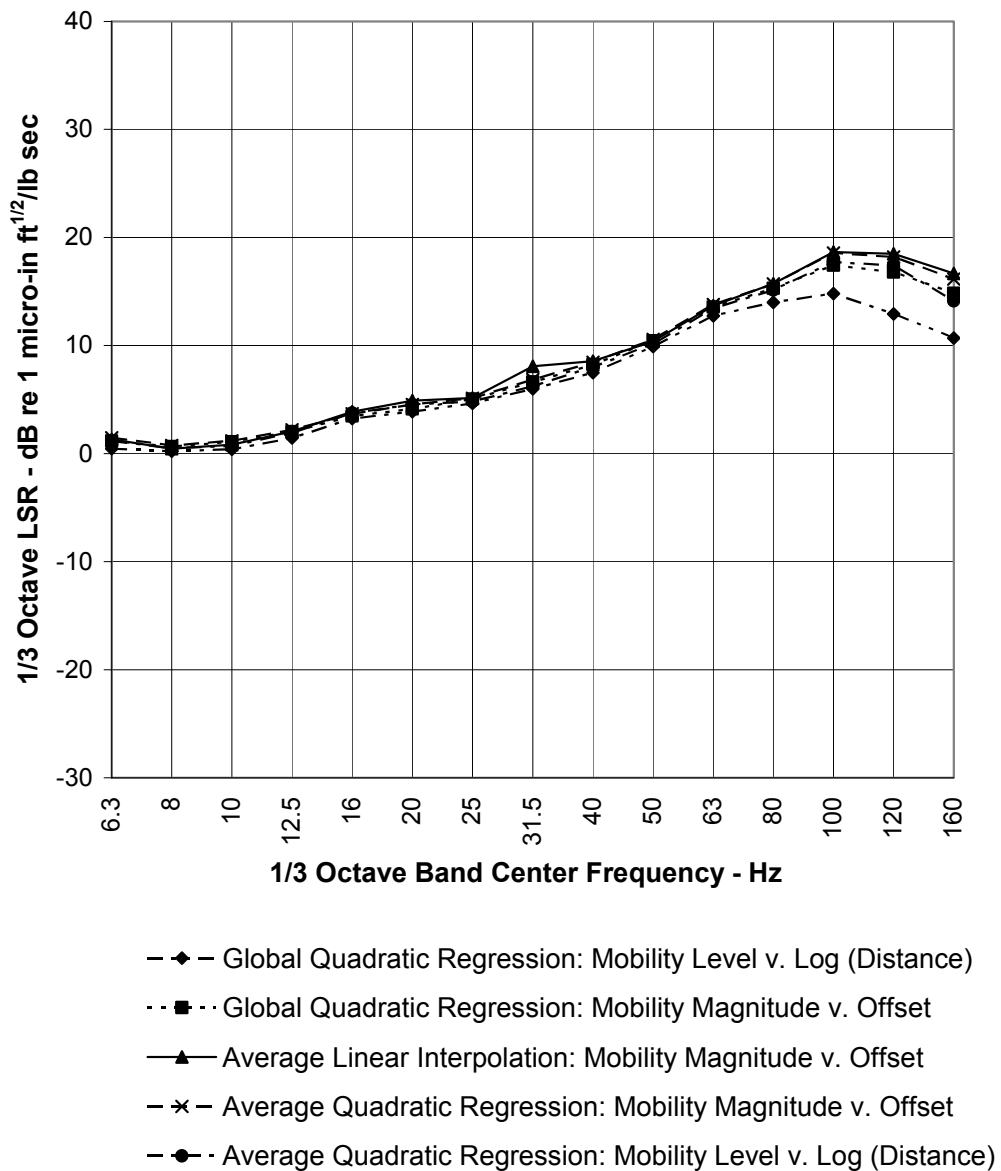
At 50 feet offset (Figure A-47 and Figure A-48), the energy averaged LSR based on regression of mobility level versus log offset also falls below the interpolated LSR above 63 Hz. The LSR based on linear interpolation begins to show a peak at 41.6 Hz that is not apparent in the other LSR's. The linear interpolation based LSR is at the high end of the range of estimates at frequencies above 63 Hz.

At 100 feet offset (Figure A-49 and Figure A-50), the LSR based on linear interpolation of individual borehole data is less than the other LSR estimates at frequencies above 63 Hz, opposite to the results for 25 and 50 feet offset. The LSR's based on regression of global and individual mobility magnitude versus offset dominate the spectrum above 50 Hz. The LSR based on interpolation contains a peak at 31.6 Hz. The results for the 140lb and 300lb tests are similar.

At 200 feet offset (Figure A-51 and Figure A-52), the LSR based on linear interpolation is in the middle of the range of LSR's above 50 Hz, but shows more irregularity than the others estimates. At low frequencies, the LSR based on linear interpolation is comparable with, though generally higher, than the other estimates.

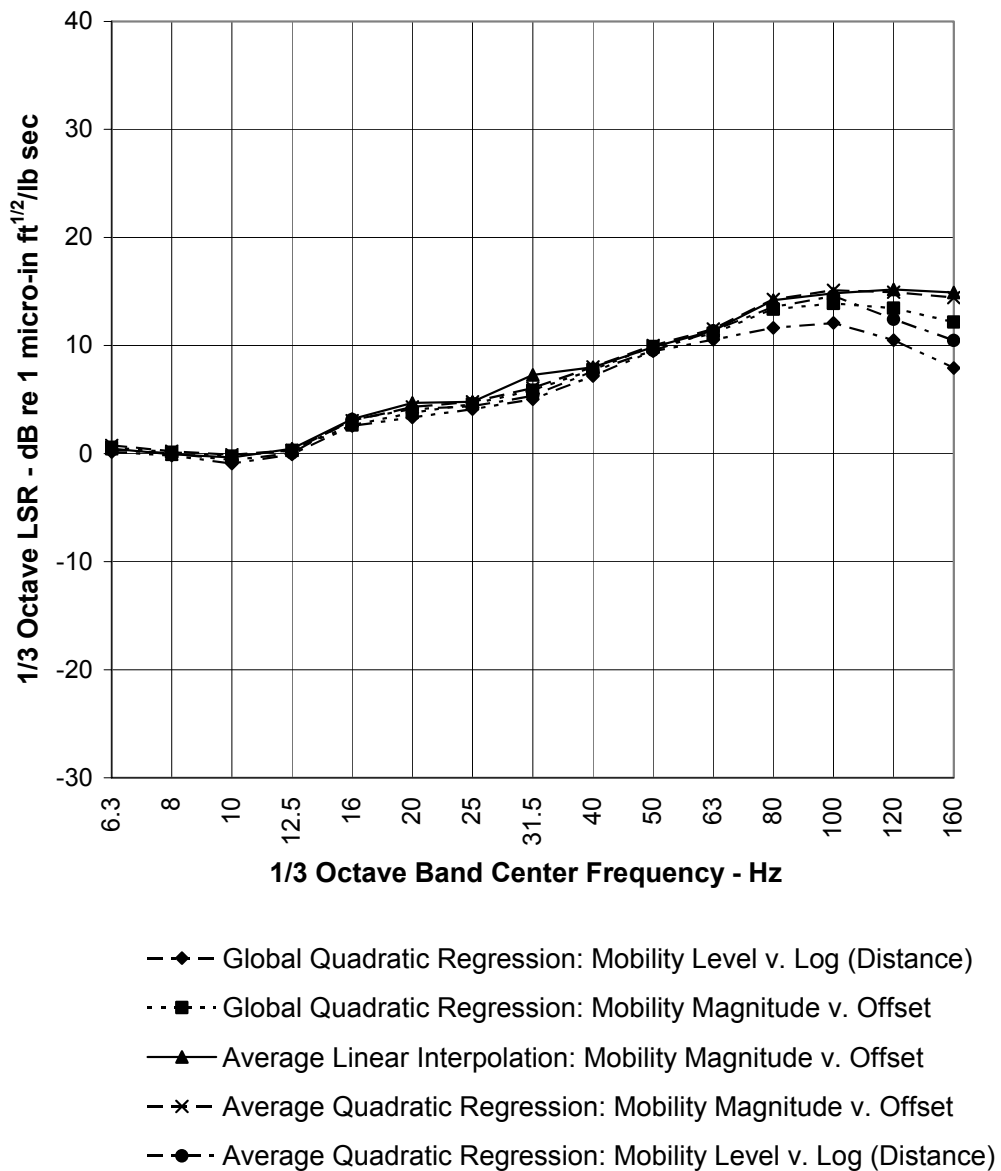
At 400 feet offset (Figure A-53 and Figure A-54) the LSR based on linear interpolation of individual borehole data follows the upper end of the range of estimates. The estimate based on a global regression of mobility magnitude versus horizontal offset fails above 50 Hz for the 140lb hammer test, due to a negative estimate of the absolute value of the mobility. This estimate does not fail with the 300lb hammer test data, but does show a rapid decline with distance above about 50 Hz, again due to the regression curve predicting unrealistically low, or non-physical, values of the mobility magnitude.

At frequencies below 50 Hz the results indicate very close agreement between the "Global" regression-based LSR's, the energy averaged regression-based LSR's, and the interpolation-based LSR's, except, perhaps, at 31.5Hz. At 100 feet offset, the energy averaged linear interpolation based LSR shows a peak at 31.6 Hz that is about 4 decibels higher than the rest of the LSR's.



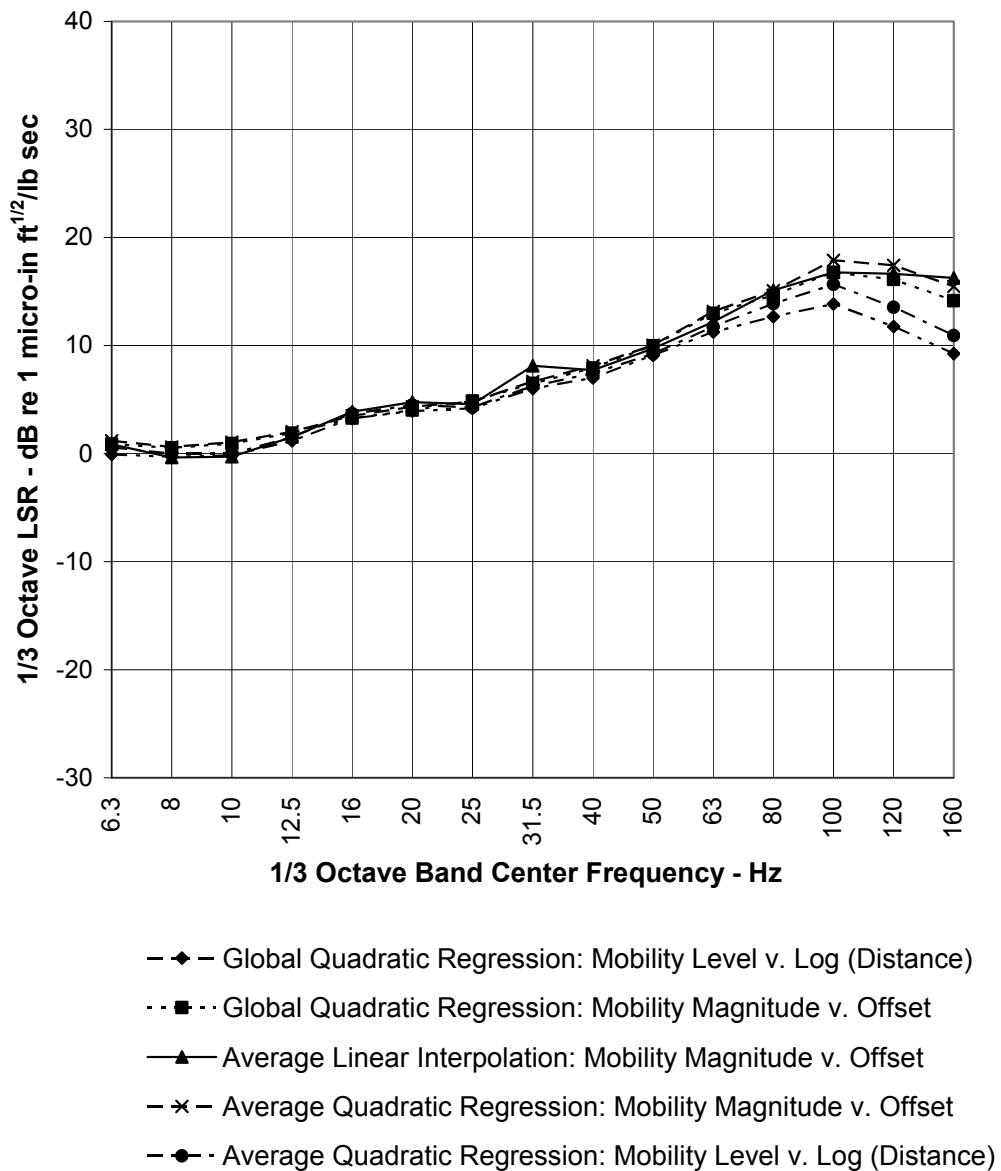
LSR Comparison 140lb Hammer
LSR at 25 Feet from Track Center Line
Train Length=340 ft
Source Depth=110-120ft

Figure A-45 Comparison of Energy Averaged LSR (140lb Hammer Data Used for Interpolation) – Horizontal Offset of 25 Feet



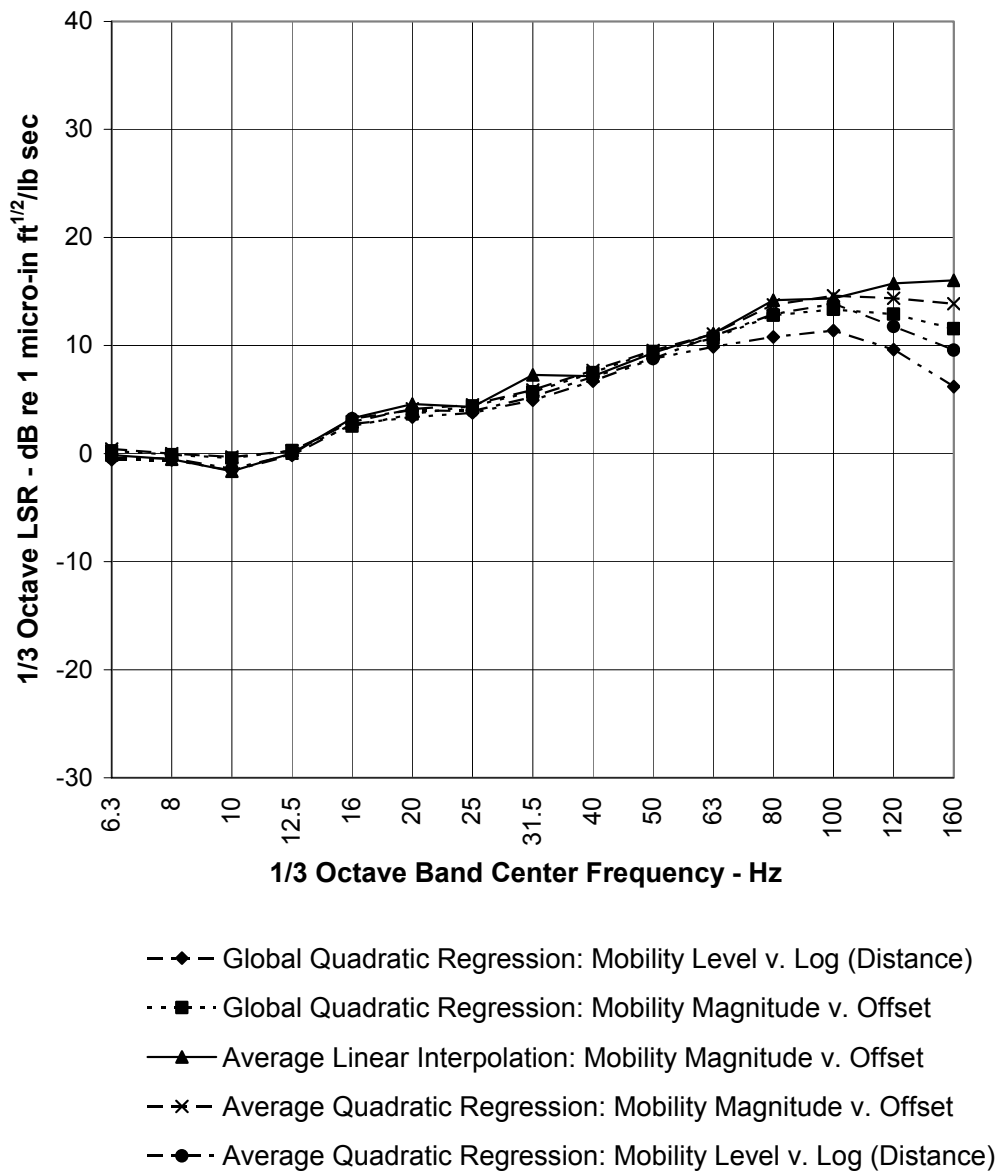
LSR Comparison 300lb Hammer
LSR at 25 Feet from Track Center Line
Train Length=340 ft
Source Depth=110-120ft

Figure A-46 Comparison of Energy Averaged LSR's (300lb Hammer Data Used for Interpolation) – Horizontal Offset of 25 Feet



LSR Comparison 140lb Hammer
LSR at 50 Feet from Track Center Line
Train Length=340 ft
Source Depth=110-120ft

Figure A-47 Comparison of Energy Averaged LSR (140lb Hammer Data Used for Interpolation) – Horizontal Offset of 50 Feet



LSR Comparison 300lb Hammer
LSR at 50 Feet from Track Center Line
Train Length=340 ft
Source Depth=110-120ft

Figure A-48 Comparison of Energy Averaged LSR's (300lb Hammer Data Used for Interpolation) – Horizontal Offset of 50 Feet

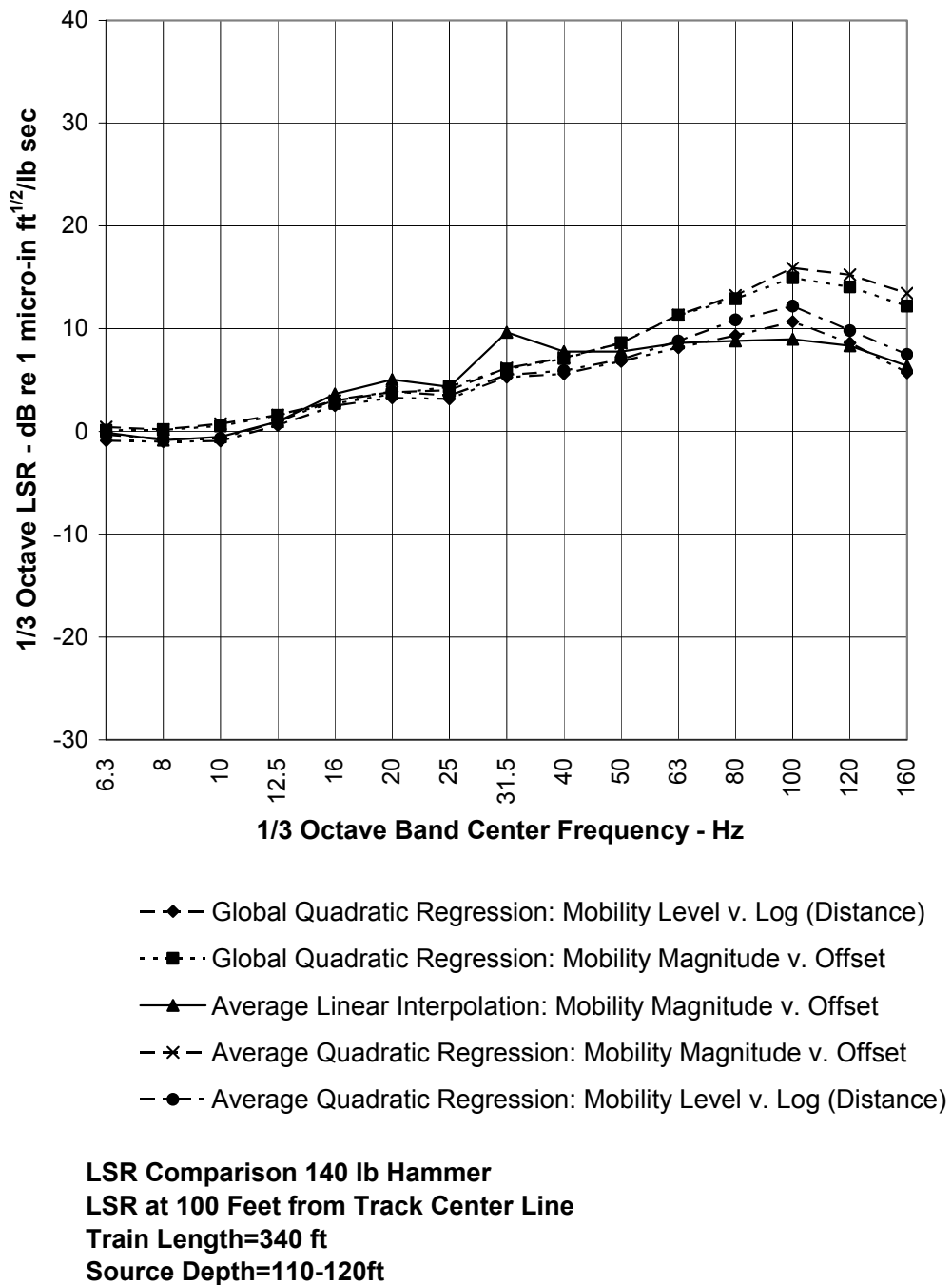
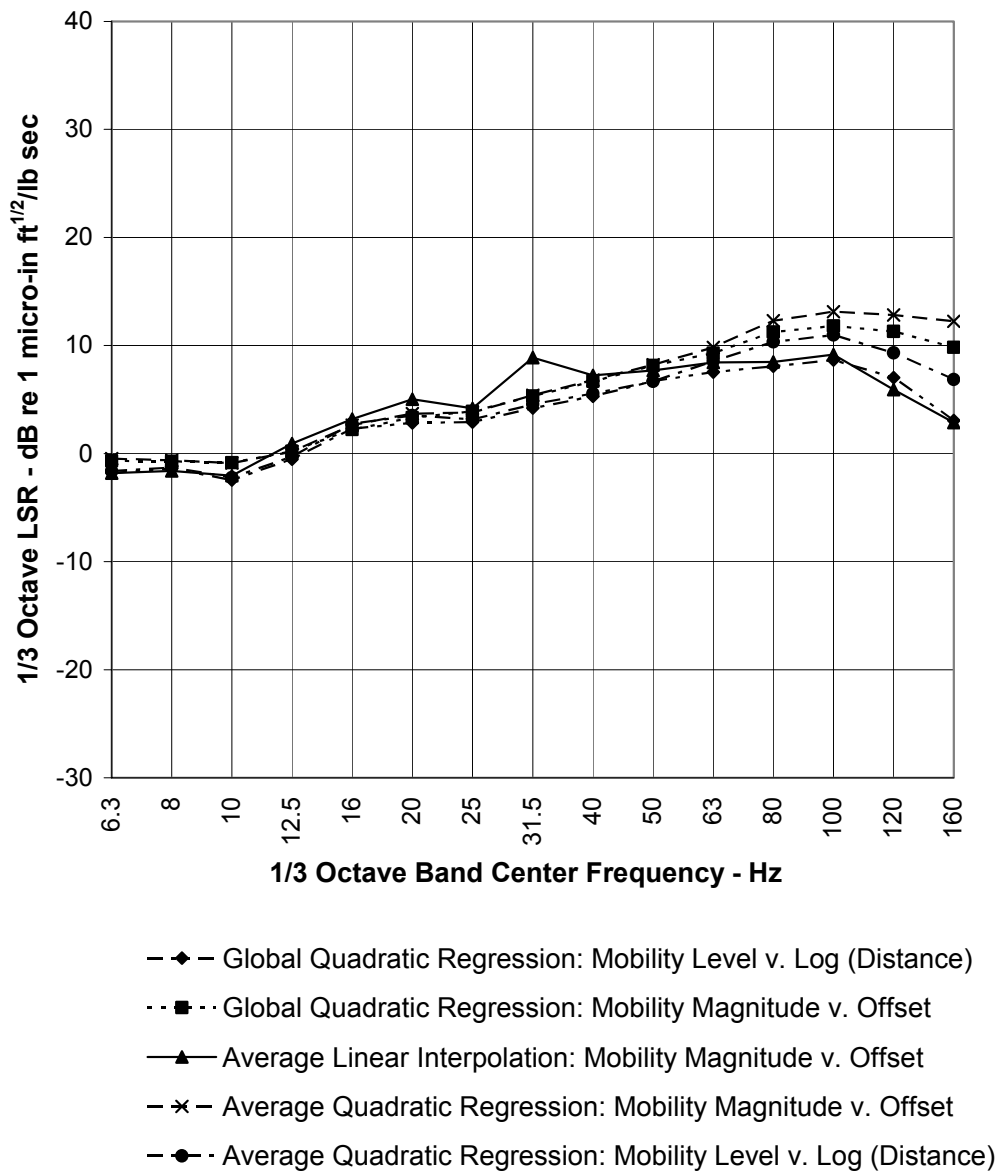
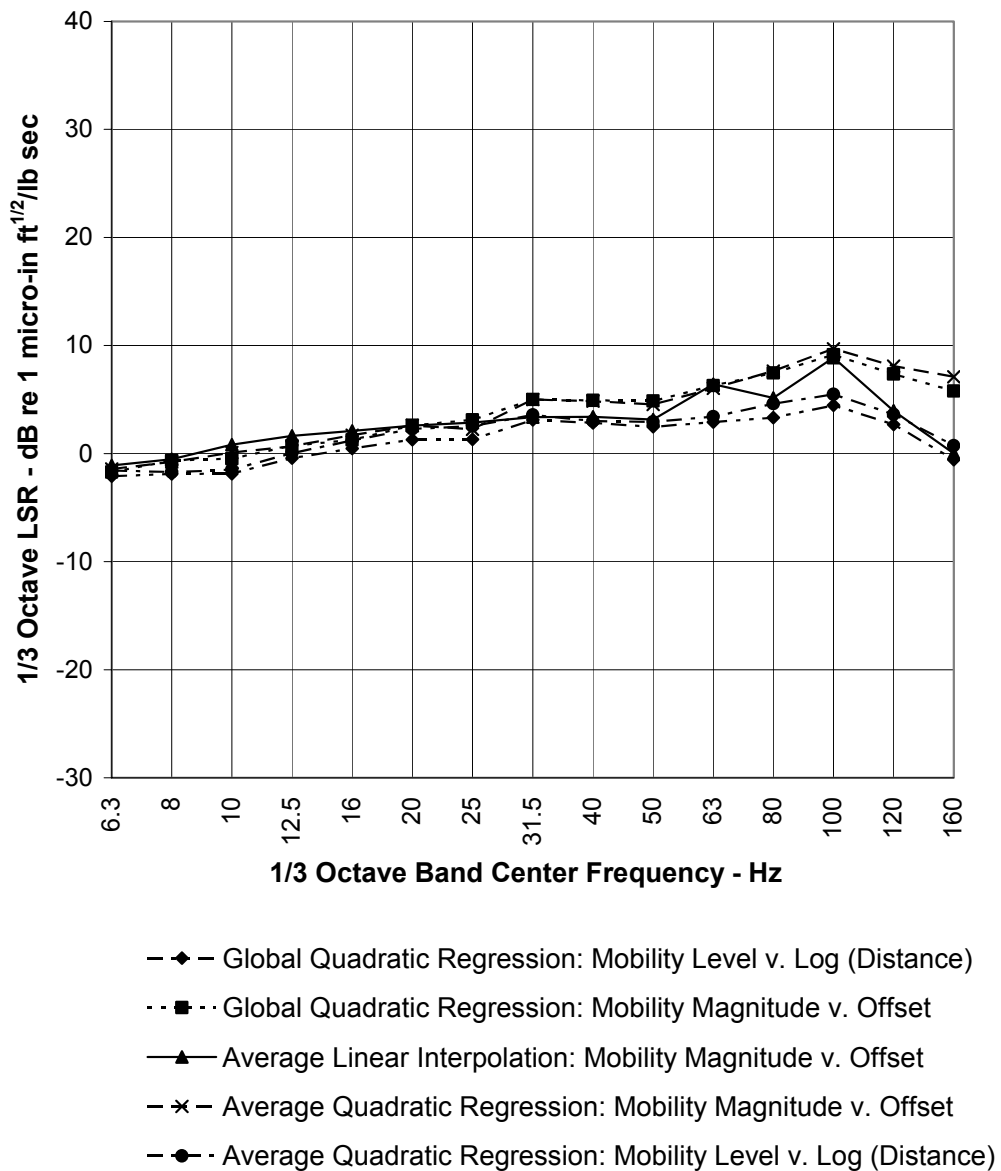


Figure A-49 Comparison of Energy Averaged LSR (140lb Hammer Data Used for Interpolation) – Horizontal Offset of 100 Feet



LSR Comparison 300 lb Hammer
 LSR at 100 Feet from Track Center Line
 Train Length=340 ft
 Source Depth=110-120ft

Figure A-50 Comparison of Energy Averaged LSR's (300lb Hammer Data Used for Interpolation) – Horizontal Offset of 100 Feet



LSR Comparison 140 lb Hammer
LSR at 200 Feet from Track Center Line
Train Length=340 ft
Source Depth=110-120ft

Figure A-51 Comparison of Energy Averaged LSR (140lb Hammer Data Used for Interpolation) – Horizontal Offset of 200 Feet

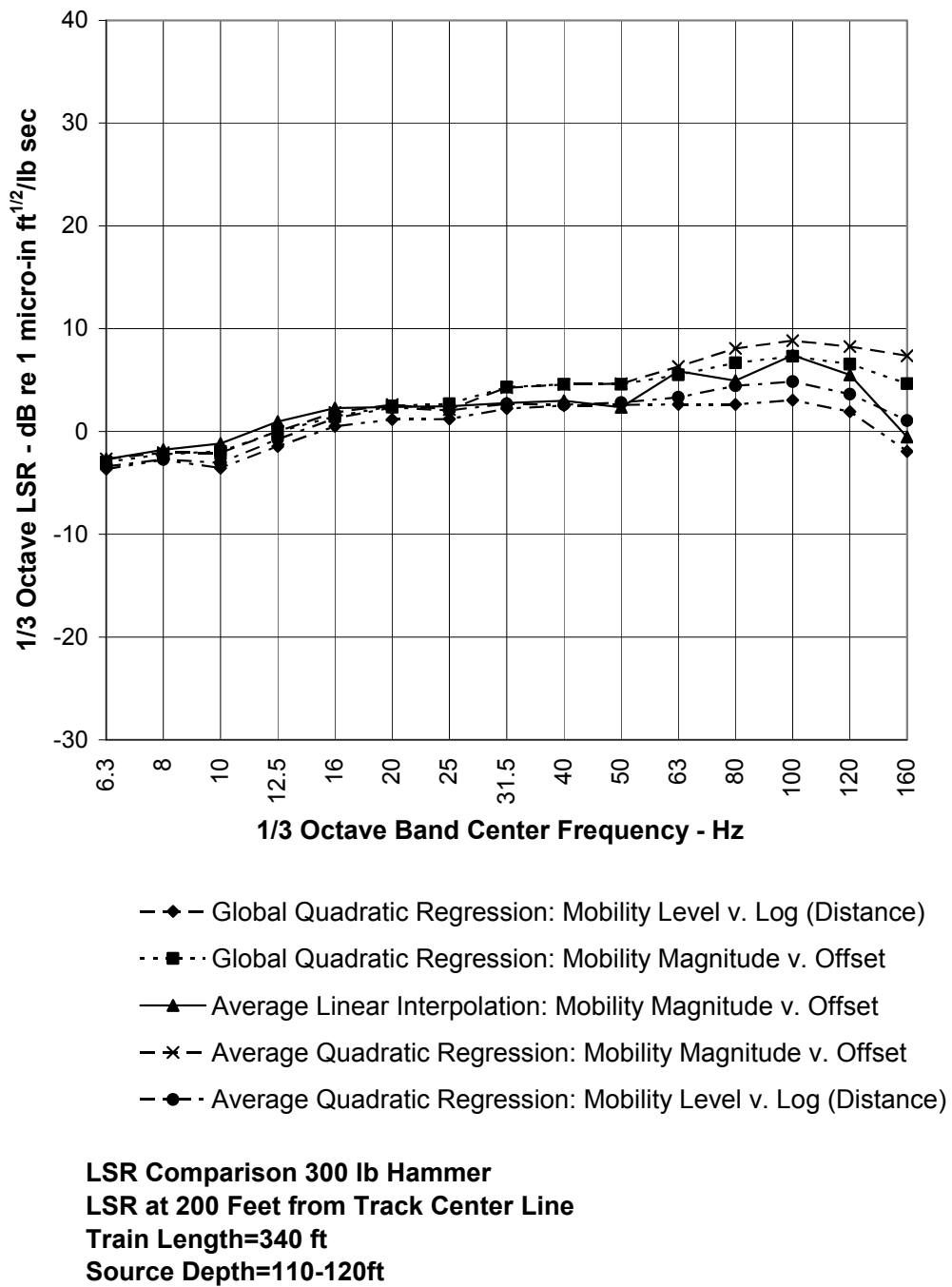
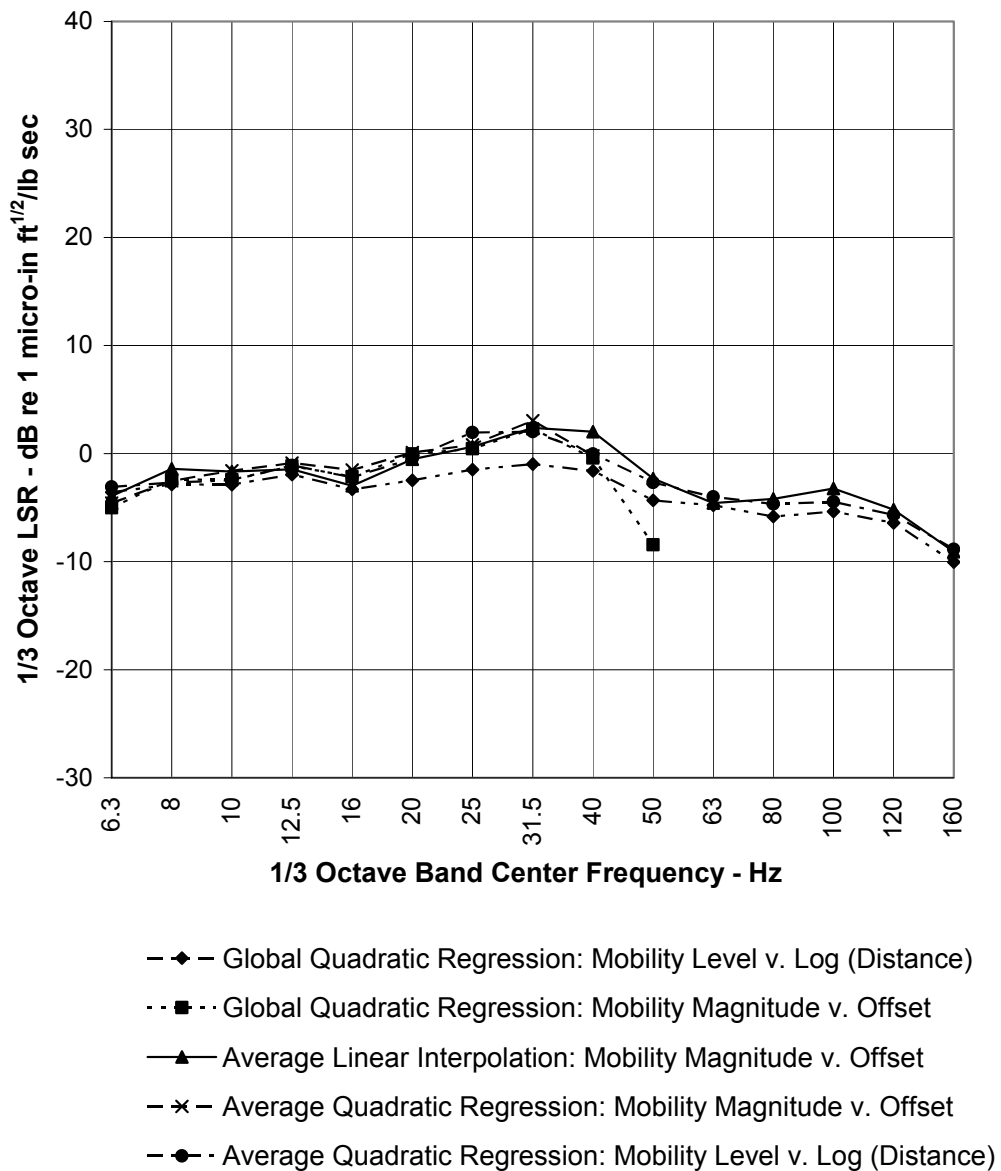


Figure A-52 Comparison of Energy Averaged LSR's (300lb Hammer Data Used for Interpolation) – Horizontal Offset of 200 Feet



LSR Comparison 140 lb Hammer
 LSR at 400 Feet from Track Center Line
 Train Length=340 ft
 Source Depth=110-120ft

Figure A-53 Comparison of Energy Averaged LSR (140lb Hammer Data Used for Interpolation) – Horizontal Offset of 400 Feet

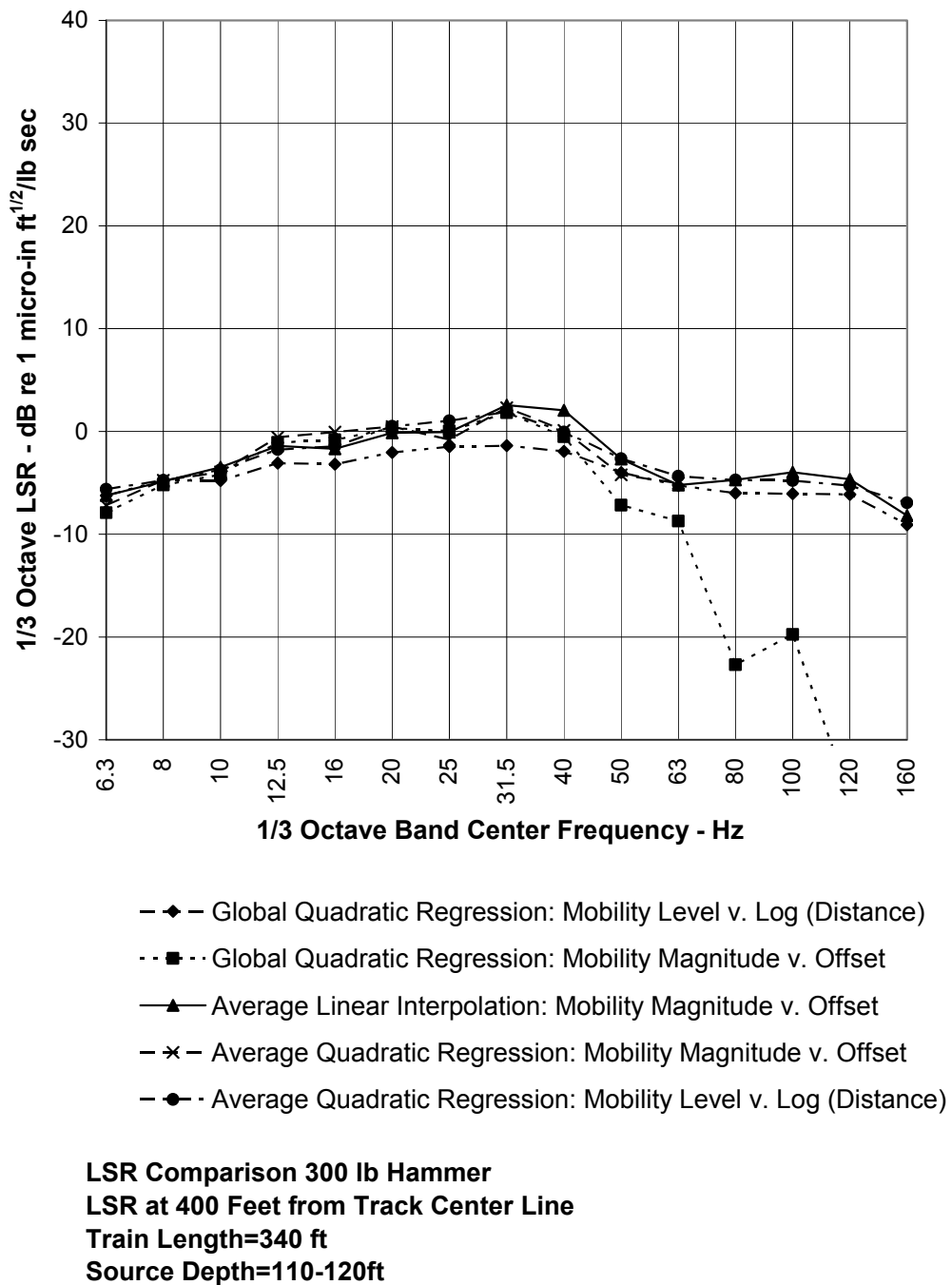


Figure A-54 Comparison of Energy Averaged LSR's (300lb Hammer Data Used for Interpolation) – Horizontal Offset of 400 Feet

A-7 CONCLUSION

The above results imply the following:

- 1) Regression of the third octave mobility versus level in decibels versus logarithm of horizontal offset provides a more uniform regression curve than interpolation.
- 2) Regression of the third octave mobility magnitude versus horizontal offset results in a poorly behaved regression curve at high frequencies and large offset, but is otherwise similar in result to regression of the third octave mobility versus logarithm of offset
- 3) Interpolation of individual borehole third octave band levels versus offset gives less smooth third octave LSR's than polynomial regression, though the energy average over all holes yields an interpolated LSR very similar to those obtained by energy averaging LSRs obtained by polynomial regression.
- 4) When results are energy averaged over all holes, the various methods yield very similar results.
- 5) The prediction curves at low frequencies and large distances appear to be dominated by background vibration and noise, as indicated by the up-turn of the quadratic with increasing distance, and by the "shelving" of the LSR with decreasing frequency below about 10 Hz. That is, background vibration and noise appear to be influencing the low frequency results, where coherence is generally poor.
- 6) The variation of LSR from hole to hole is generally greater than the variation in methods of regression analysis or interpolation, with the exception of regression of the amplitude of mobility versus logarithm of offset at large offsets. Thus, testing at multiple holes is of greater importance than the method of analysis with respect to reducing uncertainty.

Considering the foregoing, the approach based on least-squares regression of third octave mobility level versus some reasonable function of distance is most attractive at short ranges, as it gives well-behaved regression curves for each hole. (See Figure A-2 through Figure A-19.) Further, when averaged over all holes, the regression approach provides results that are in very good agreement with those obtained by linear interpolation. At large distances, the regression curves may over-predict the LSR, due to the influence of background vibration and/or instrumentation noise.

A regression of mobility level versus slant distance is attractive to avoid singularity of the regression at zero offset, which would occur for receivers located over the proposed tunnel alignment. Thus, some modification of the procedure in this direction should be employed to avoid singularity in regression versus log offset. These models do not solve the regression at large offsets of, perhaps 1000 feet, however, where noise dominates the measurement.

APPENDIX B LINE SOURCE MODEL CALCULATIONS AND COMPARISON WITH MEASUREMENTS

CONTENTS

B-1	INTRODUCTION	B-1
B-2	SHEAR WAVE VELOCITY MEASUREMENTS.....	B-1
B-4	COMPUTER MODEL.....	B-3
B-5	LSR COMPARISONS.....	B-4
B-6	CONCLUSION.....	B-4
B-7	PREDICTION.....	B-6

FIGURES

Figure B-1	Borehole Test Locations	B-2
Figure B-1	Vertical Seismic Velocity Profiles.....	B-7
Figure B-2	Computed LSRs At 50 Feet Horizontal Offset– Average for Tunnel Depths of 110 to 120 Feet	B-8
Figure B-3	Computed LSRs at 100 Feet Horizontal Offset– Average for Tunnel Depths of 110 to 120 Feet	B-9
Figure B-4	Computed LSRs at 200 Feet Horizontal Offset – Average for Tunnel Depths of 110 to 120 Feet	B-10
Figure B-5	Comparison of Energy Averaged LSR For NB123, NB253, and NB255 with Global Regression Result at 50 Feet Offset.....	B-11
Figure B-6	Comparison of Energy Averaged LSR For NB123, NB253, and NB255 with Global Regression Result at 100 Feet Offset.....	B-12
Figure B-7	Comparison of Energy Averaged LSR For NB123, NB253, and NB255 with Global Regression Result at 200 Feet Offset.....	B-13
Figure B-8	Comparison of Adjustment Factors to Reconcile Calculated LSR with Borehole LSR Test Results.....	B-14

B-1 INTRODUCTION

Line Source Responses (LSRs) were calculated with a seismic reflectivity model of layered soils, using shear wave velocity data collected by GeoRecon at boreholes NB-123, NB-253, NB-255, NB-354, and NB-356. The model results are summarized here, and energy averages of results obtained for NB-123, NB-253, and NB-255 are compared with LSRs obtained by global regression of borehole impulse response test data. The model results for NB-354 and NB-356, located at some distance from the North Link Alignment, predicted lower Line Source Responses than those predicted for the remaining boreholes, and were thus not used for comparison. The differences between measured and modeled Line Source Responses were used to develop a set of 1/3 octave band adjustments to the model results to “calibrate” the model results. The modeling effort was conducted under the Advanced Conceptual / Preliminary Engineering phase of the North Link tunnel alignment through the University of Washington campus.

B-2 SHEAR WAVE VELOCITY MEASUREMENTS

Vertical shear wave velocity profile tests were conducted at five locations. Three of these were along the North Link alignment at the following civil stations:

NB-123	Approx. Station NB 1220+00	
NB-253	Approx. Station NB 1208+30	(Stadium parking lot)
NB-255	Approx. Station SB 1223+00	(Mechanical Engineering)

The measurement locations for NB-123, NB-253 and NB-255 are identified in

Figure B-1. The map also shows the locations of borehole NB-254 and NB-256. LSR borehole tests were conducted at boreholes NB-253, NB-254, NB-255, and NB-256.

The borings at NB-354 and NB-356 were collected during an earlier phase of the study, are not on the campus, but are located along 15th Avenue at an earlier proposed alignment west of the campus.

Shear wave velocities were also measured at boring NB-259, north of the campus. These shear wave velocity test data were not considered in this analysis, because the depth of this boring was not as great as those of the above listed borings.

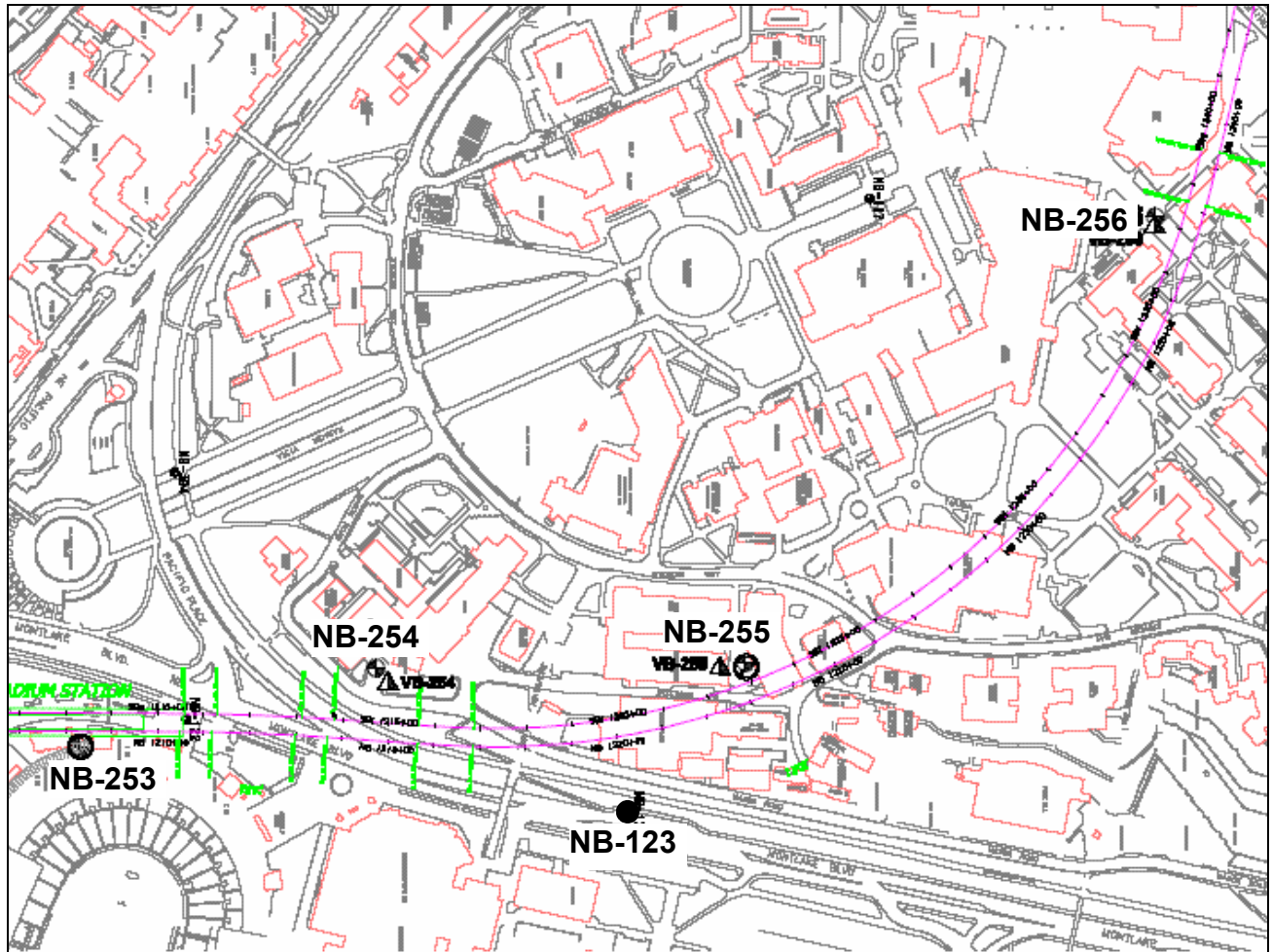


Figure B-1 Borehole Test Locations

The shear wave velocity data were collected with geophone arrays suspended in cased borings. Both P and S-wave velocities were measured. The procedure and results for borings NB-253, NB-255, and NB-259 are summarized in the report by prepared by GeoRecon.¹ The velocity data for NB-123 were provided by Geo Recon during the environmental analysis. The results for NB-354, and NB-356 were provided by the geotechnical consultant, Shannon & Wilson, during the environmental phase.

Figure B-1 illustrates the seismic velocity profiles that were measured at these boreholes. These data indicate some variation of seismic velocity from one hole to the next. The seismic velocities are high relative to those of typical alluvial soils, indicating that the shear modulus of the soil is high. The response of the soil is inversely proportional to the shear modulus. Thus, ground vibration from rail transit tunnels at the UW should be substantially less than from tunnels in soft alluvial soils.

B-4 COMPUTER MODEL

The computer model used for calculating impulse response functions was developed by Dr. James T. Nelson for modeling ground vibration in porous soils.² For this work, the model was restricted to analysis of viscoelastic wave propagation to shorten computation times. The model is exact within the limits of numerical precision, and provides a full set of impulse response functions for arbitrary force orientations and depths. The model uses Bessel-Hankel transforms in the wave-number domain for each frequency. Time domain responses can be obtained by Fourier inversion of the complex frequency response functions. Very similar methods of analysis are described by Auersch (1988) for layered elastic soils.³ The computer model thus provides an analytical approach to modeling experimental data collected from borehole LSR tests.

The impulse response functions obtained with the numerical model were convolved with 1/3 octave band response functions to obtain 1/3 octave band mobilities for each receiver point. These were integrated over the train length of about 120m with cubic spline interpolation of the 1/3 octave band mobilities. The procedure is analogous to the experimental determination of LSRs obtained by borehole impact tests conducted at NB-253, NB-254, NB-255, and NB-256, except that cubic spline interpolation rather than regression of the response as a function of source-receiver distance is used during calculation of the LSR. Also, a much larger number of offsets were employed for numerical modeling, spaced at 25- to 50-foot intervals. Responses out to as much as 200ft were computed for extra long range prediction.

¹ John Musser, Geo Recon International, Compression and Shear Wave Velocity Measurements, Borings NB-255, NB-253, NB-259, Puget Sound Transit Consultants, Seattle Washington, Report No. J04-764, September 13, 2004.

² J. T. Nelson 2000, *Journal of Sound and Vibration* **231**, No. 3 727-737. Prediction of Ground Vibration from Trains using Seismic Reflectivity Methods for a Porous Soil.

³ L. Auersch 1994 *Journal of Sound and Vibration* 173, 233-264. Wave Propagation in Layered Soils: Theoretical Solution in Wavenumber Domain and Experimental Results of Hammer and Railway Traffic Excitation.

The Line Source Response (LSR) is defined as the integral (sum) of the square of the mobility magnitude over the train length. The unit of the integrated square of the mobility is L^3/FS^2 , or in English units, $(\text{in/s/lb})^2\text{ft}$. The logarithm of the square root of this mean is then taken. Mathematically:

$$\text{LSR dB re } 10^{-6}(\text{in-ft}^{1/2}/\text{lb-s}) = 10\text{Log}_{10}(\int |M/M_0|^2 dx)$$

Where M_0 is the reference mobility of 10^{-6}in/s/lb and the integration is over the train length in feet. (The choice of units is made to be consistent with the Federal Transit Administration usage.⁴ A non-mixed choice of units (eg $\text{in}^3/\text{lb}^2\text{-s}^2$), or metric units, would be more attractive.)

B-5 LSR COMPARISONS

Figure B-2 through Figure B-4 illustrate the computed LSRs for each set of shear wave velocity data. Results for tunnel depths of 110 and 120ft were averaged to produce these estimates. The results for NB-123, NB-253, and NB-255 are in reasonable agreement. The results for NB-354 and NB-356 deviate from the former three at 200ft. These latter two holes were characterized by low shear wave velocities in the upper soil layers, in contrast to velocities at the other holes. (See Figure B-1.) In view of this, the energy average of the model results for NB-123, NB-253, and NB-255 were compared with experimental data and used to calibrate the model.

Figure B-5 through Figure B-7 compare the energy average of modeled LSRs for NB-123, NB-253, and NB-255 with the LSR obtained by global regression of test results obtained for NB-253, NB-254, NB-255, and NB-256. Data at impact source depths of 110 to 120ft were employed for the regression analysis. The modeled LSRs are the average of model results for source depths of 110 and 120 feet. Variation of calculated LSRs as a function of source depth between 110 and 120 feet are of the order of one decibel. The calculated LSRs are labeled as "Theoretical Values" in Figure B-5 through Figure B-7.

Figure B-8 illustrates the relative levels between calculated LSRs and those obtained by global regression of LSRs for each horizontal offset of 50, 100, and 200 feet. Also shown is the average of these difference curves. The average represents a calibration curve that is added to calculated LSRs for modeling long range vibration where regressed borehole test results are subject to background vibration and instrumentation noise.

B-6 CONCLUSION

The foregoing indicates good agreement between the calculated LSRs and LSRs obtained by global regression of borehole test data. The modeled LSRs are slightly less than the LSRs determined by

⁴ **Transit Noise and Vibration Impact Assessment**, Federal Transit Administration, U.S. Department of Transportation, April 1995

global regression at frequencies below about 20 Hz. The discrepancy between calculated and measured LSRs at 3.16 Hz, the bottom end of the spectrum, is least at 50 feet offset, and greatest at 200 feet, where the measured global LSR exceeds the calculated. At these frequencies, the measured LSRs are subject to poor coherence due to background vibration and instrumentation noise, so that one might expect the measured LSRs to exceed the modeled LSRs to some extent, though other uncertainties also influence the results. For example, these soils likely have variable layer thicknesses and elevations and other lateral in-homogeneities that are not reflected in a vertically heterogeneous viscoelastic solid. On the other hand, the ability to model vibration improves with decreasing frequency, due to large spatial averaging.

The ground vibration response at low frequencies of the order of 3.16 Hz necessarily involves wavelengths of the order of 400 feet, extending to substantial depth. Deep layers of soil that were below the seismic wave velocity survey depths may influence low frequency vibration, while leaving the high frequency response unchanged. Usually, soil stiffness increases with depth, due to increasing confining stress. The stiffness was assumed here to be constant below the maximum seismic velocity test depth, usually at 120 feet. Thus, the model predictions at 3.16 Hz are probably higher than would be the case if the stiffness was assumed to increase with depth. Thus, the calculated low frequency predictions are expected to be reasonably conservative, because at some depth the stiffness is likely to increase substantially with depth.

The modeled LSRs at offsets out to 200 feet exceed the measured LSRs by a few decibels at high frequencies. Part of this is due to the conservative assumptions regarding material damping of the soil. That is, a quality factor (Q) of 20 was assumed for the upper layer, and 40 for the subsurface layers, where Qs of 10 to 20 are more representative of soils. The damping, or loss factor, of soil is inversely proportional to the quality factor, Q. Thus, high-Q soils have very low damping, and low-Q soils have high damping. High Qs of 20 and 40 (low damping) were included in the model calculations to aid convergence, rather than to represent actual damping.

The agreement between calculated and measured LSRs at short range validates both approaches to the estimation of the LSR. During testing, reflections from building foundation and underground utilities may occur, and background vibration and instrumentation noise interfere with the measurement. Also, there may exist systematic errors in the measurement approach related to drilling rig vibration, drill string vibration, and tube waves. In spite of these potential measurement problems, the calculated results suggest that the borehole LSR test results are reasonably accurate over the frequency range of 6.3 to 125 Hz at distances out to at least 200 feet. Beyond 200 feet, the measured LSRs are higher than the modeled LSRs. At large offsets, especially beyond 400 feet, background vibration and instrumentation noise hide the impulse response, as indicated by the very poor coherence between source and receiver signals. Thus, the measured LSR would be higher than the actual LSR. The difference between the measured LSR and modeled LSR at these larger offsets indicates that the measured LSR is in excess of the actual LSR. Either much more sampling or a much larger vibration source would be needed to better define the actual LSR by testing.

The agreement between calculated and measured LSRs at short range also indicates that the modeled LSR is reasonably accurate at short range. The modeled LSR is used in this study to extrapolate vibration estimates to large offsets beyond 300ft, where unreliable test data are subject to noise and very low coherence. The differences indicated in Figure B-8 are added to the modeled LSR to

“calibrate” the model. This combined approach to vibration prediction incorporates both the borehole LSR test results and measured shear wave velocity profiles.

B-7 PREDICTION

Based on the above analysis, the approach used for vibration prediction at short range includes global regression of the Point Source Mobility level in decibels (PSR) versus the logarithm of horizontal offset for all borehole impact test data to calculate a global Line Source Response at all buildings located beyond 25 feet horizontally from the tunnel alignment out to perhaps the effective range of the measurements, here considered to be about 300ft. At shorter offsets, e.g. for buildings located over the alignment, regression of the slant distance and logarithm of slant distance (corresponding to a physical model based on a damped inverse-square-law), or quadratic regression of the logarithm of slant distance, are used to avoid singularity of the regression curve.

Extrapolations of borehole low frequency LSR test data using regression curves over offsets greater than 300ft overestimate the vibration response. The numerical estimates of the LSR based on seismic wave velocity profiles, conservative material damping assumptions, and calibration adjustments, are used for long range predictions at buildings such as Bagley Hall. Thus, the calculated LSRs provide a means of extrapolation of borehole test data to large offsets.

The modeled LSRs together with the adjustments indicated in Figure B-8 could also be used for short range predictions. The differences between the calibrated model LSRs and the LSRs based on global regression of impulse responses are of the order of a decibel or two at low offsets. However, the University of Washington and its consultant requested that the LSRs be determined by global regression of measured data, at least to the extent that the coherence is acceptable. Within 300 feet, the difference is negligible for practical purposes.

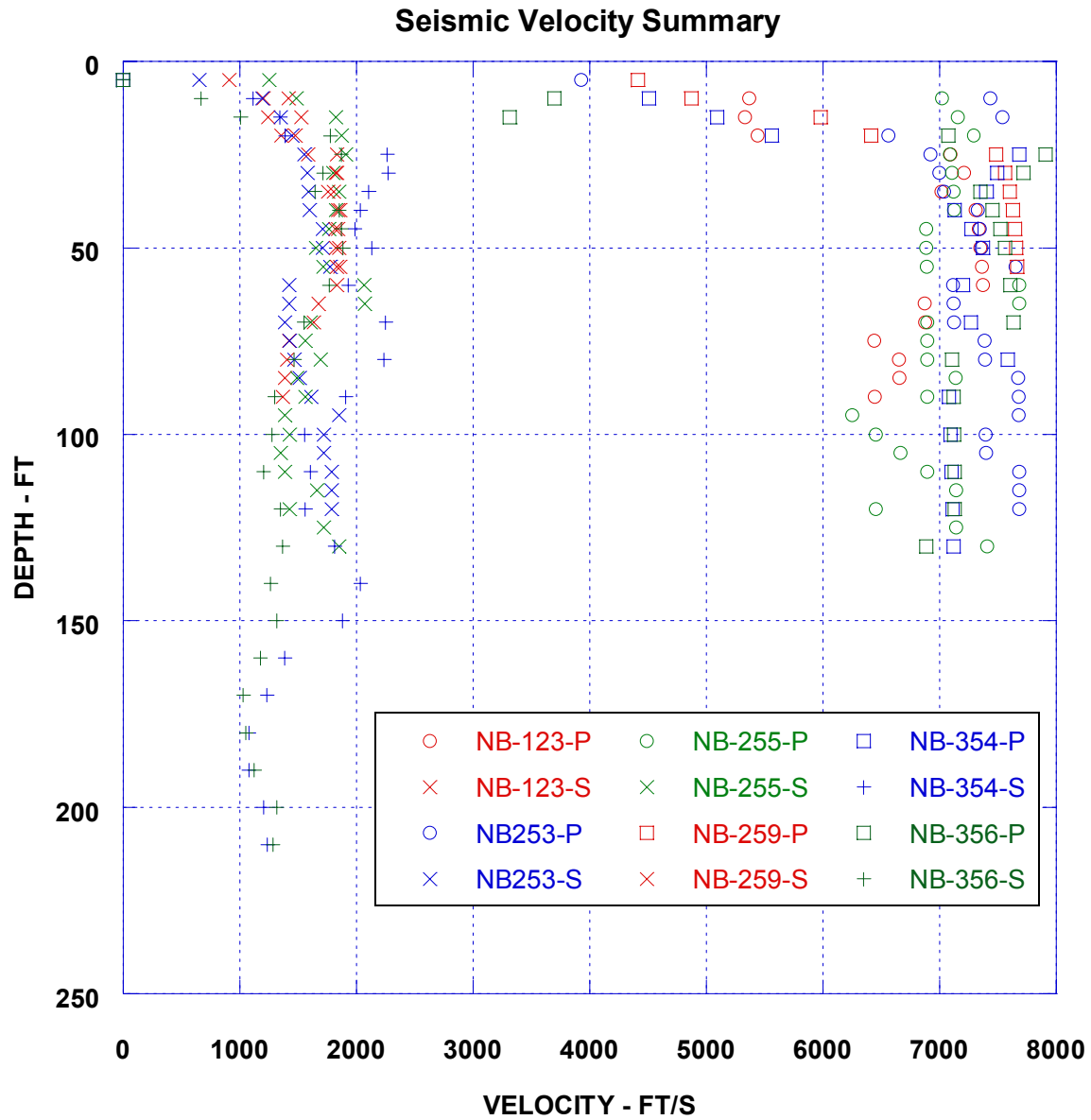


Figure B-1 Vertical Seismic Velocity Profiles

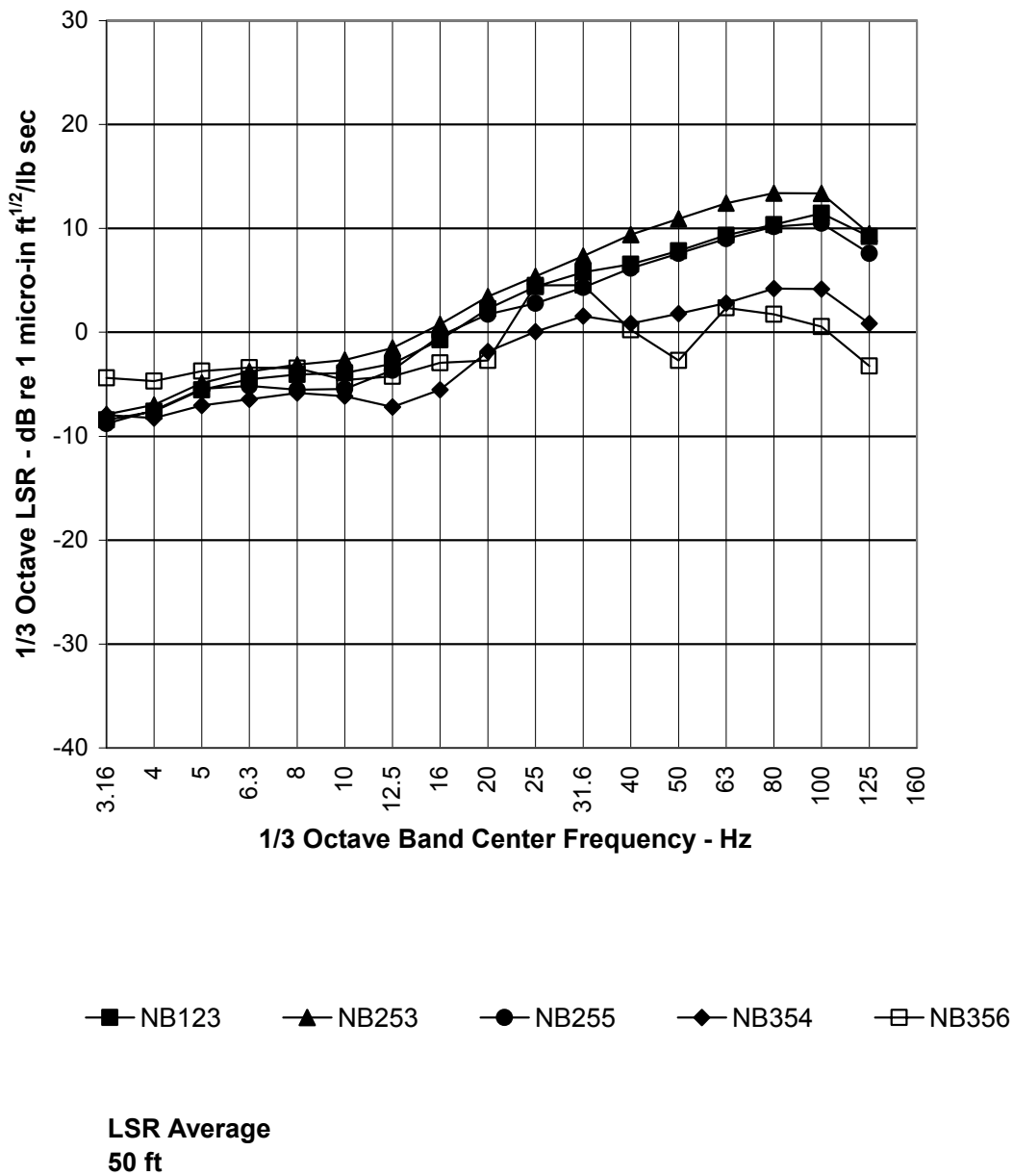


Figure B-2 Computed LSRs At 50 Feet Horizontal Offset– Average for Tunnel Depths of 110 to 120 Feet

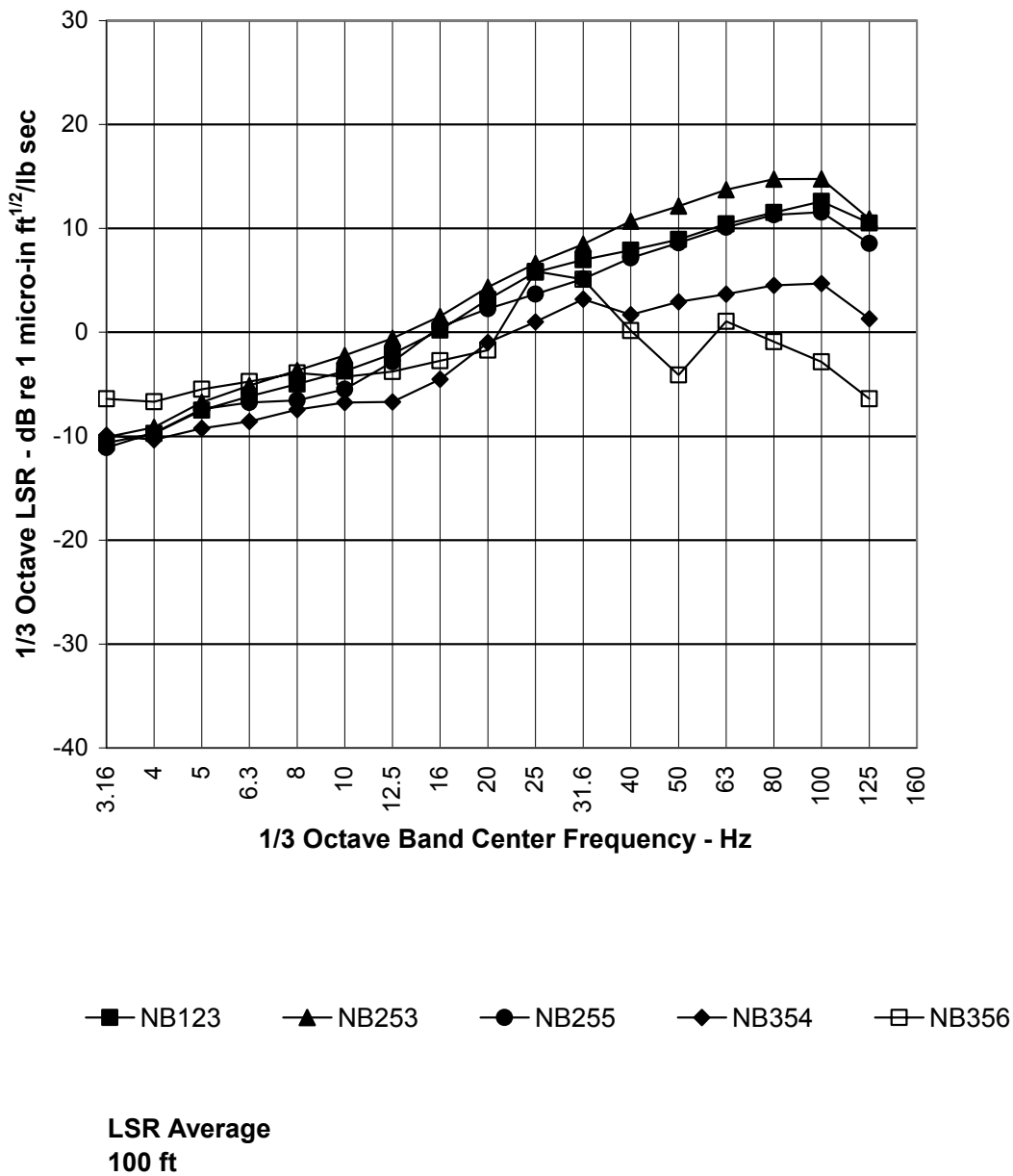


Figure B-3 Computed LSRs at 100 Feet Horizontal Offset– Average for Tunnel Depths of 110 to 120 Feet

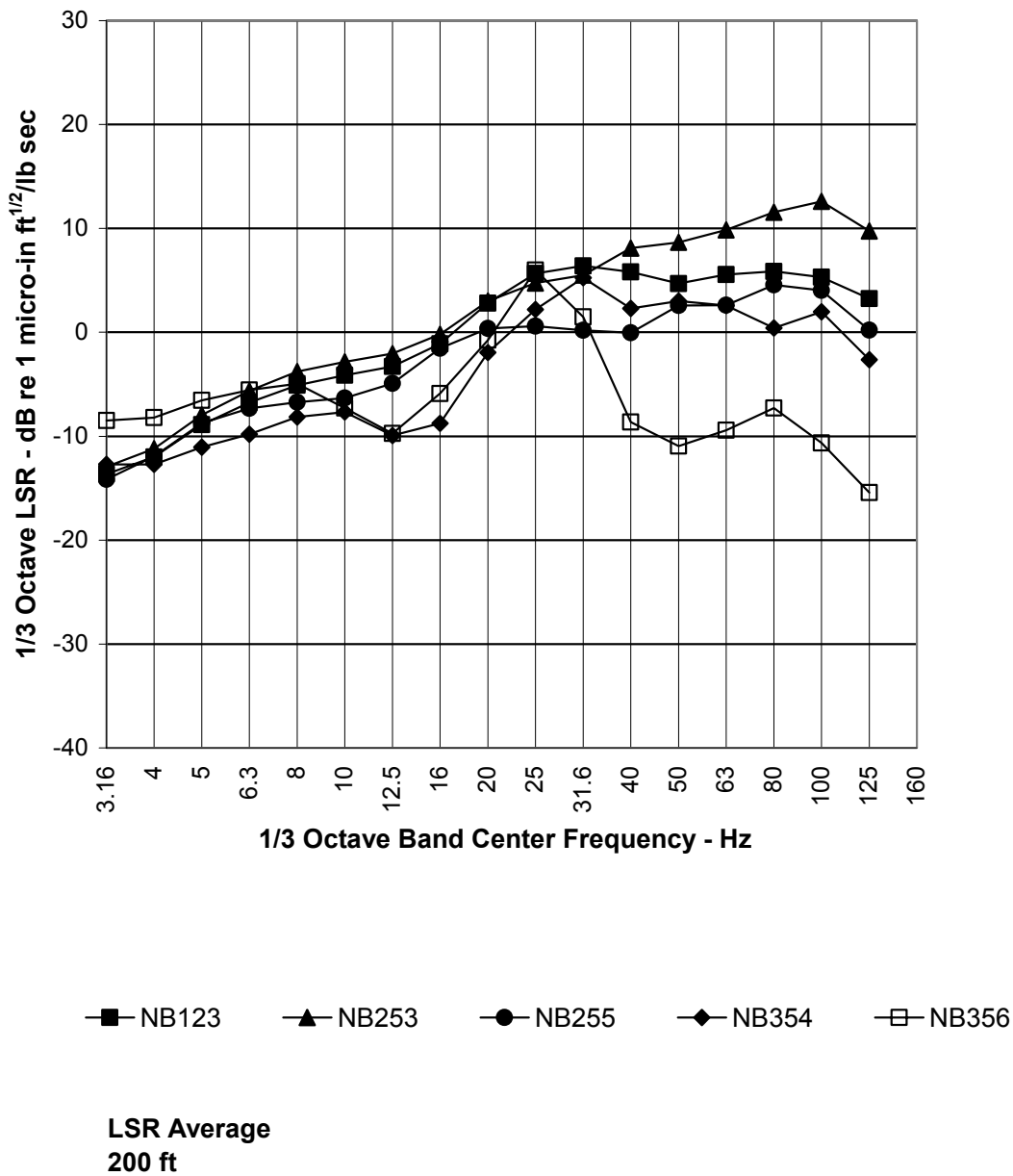
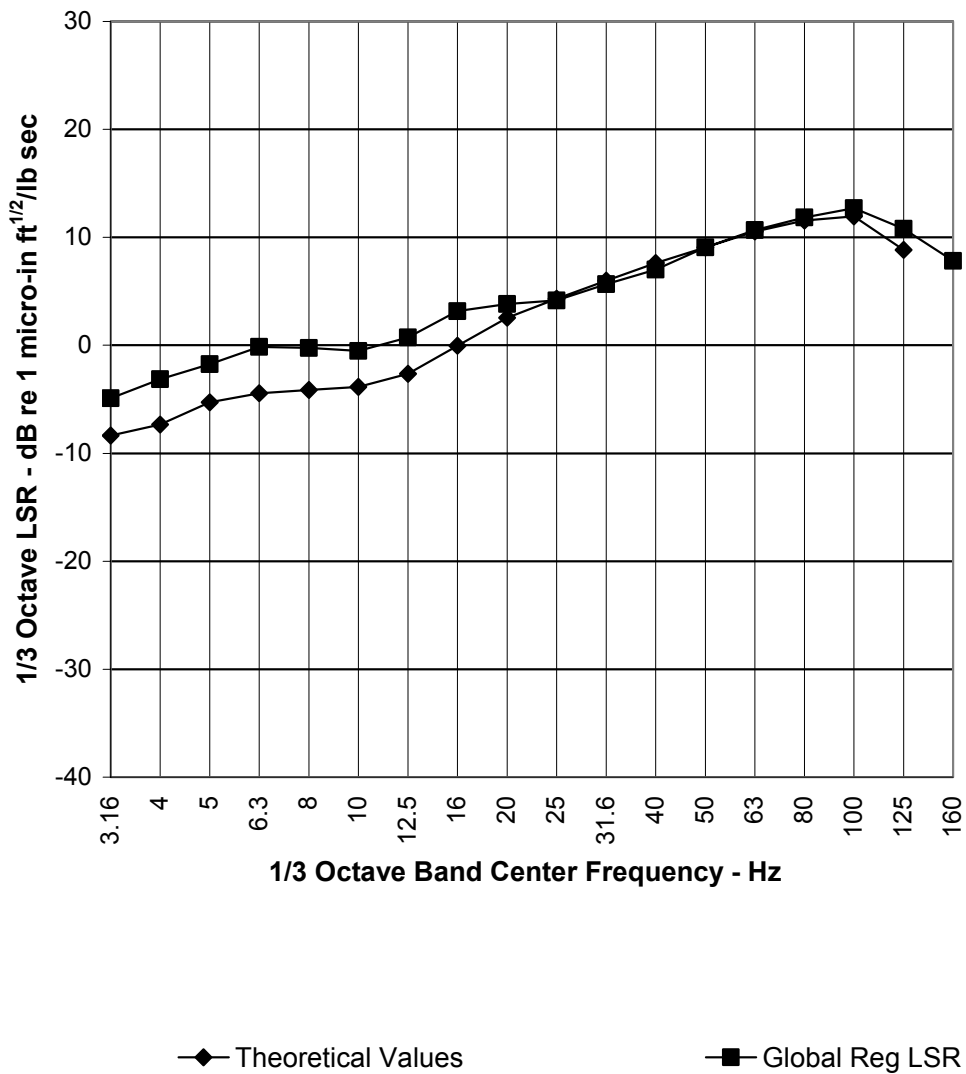
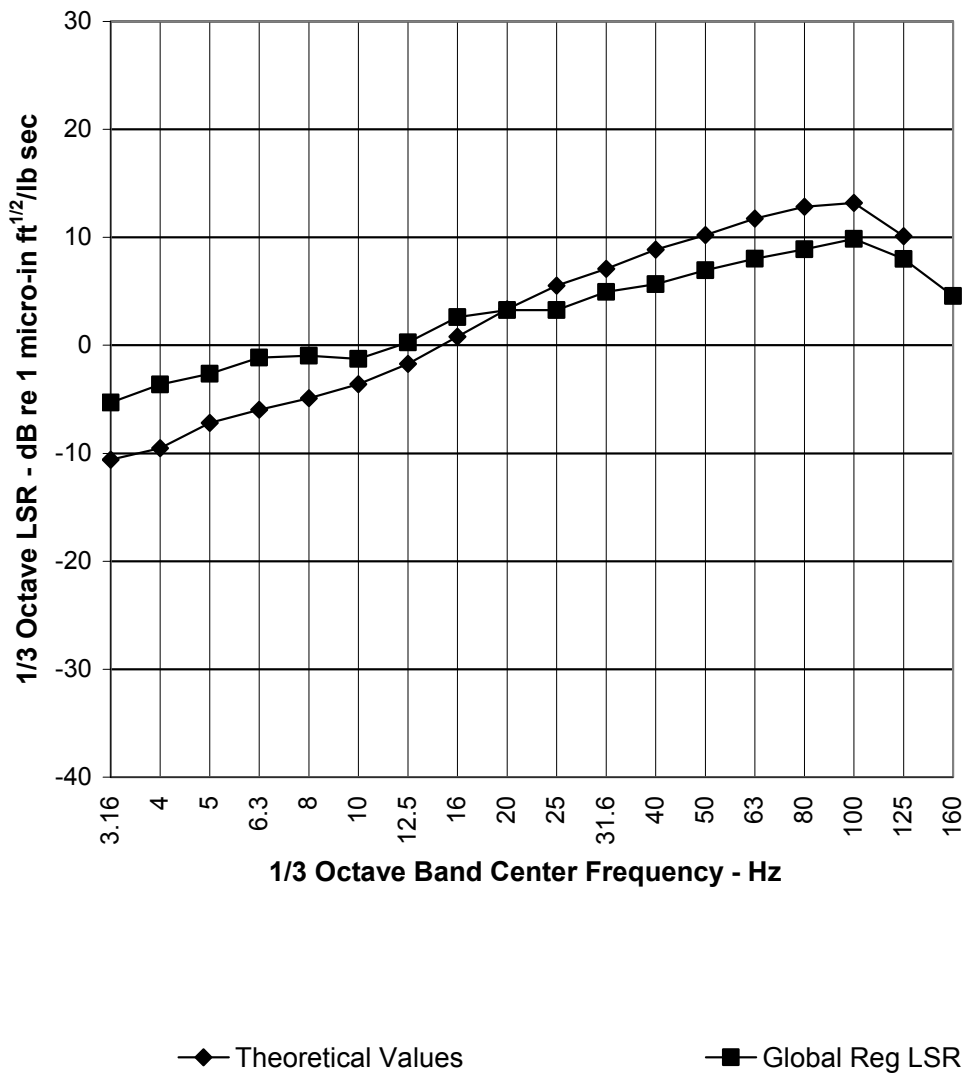


Figure B-4 Computed LSRs at 200 Feet Horizontal Offset – Average for Tunnel Depths of 110 to 120 Feet



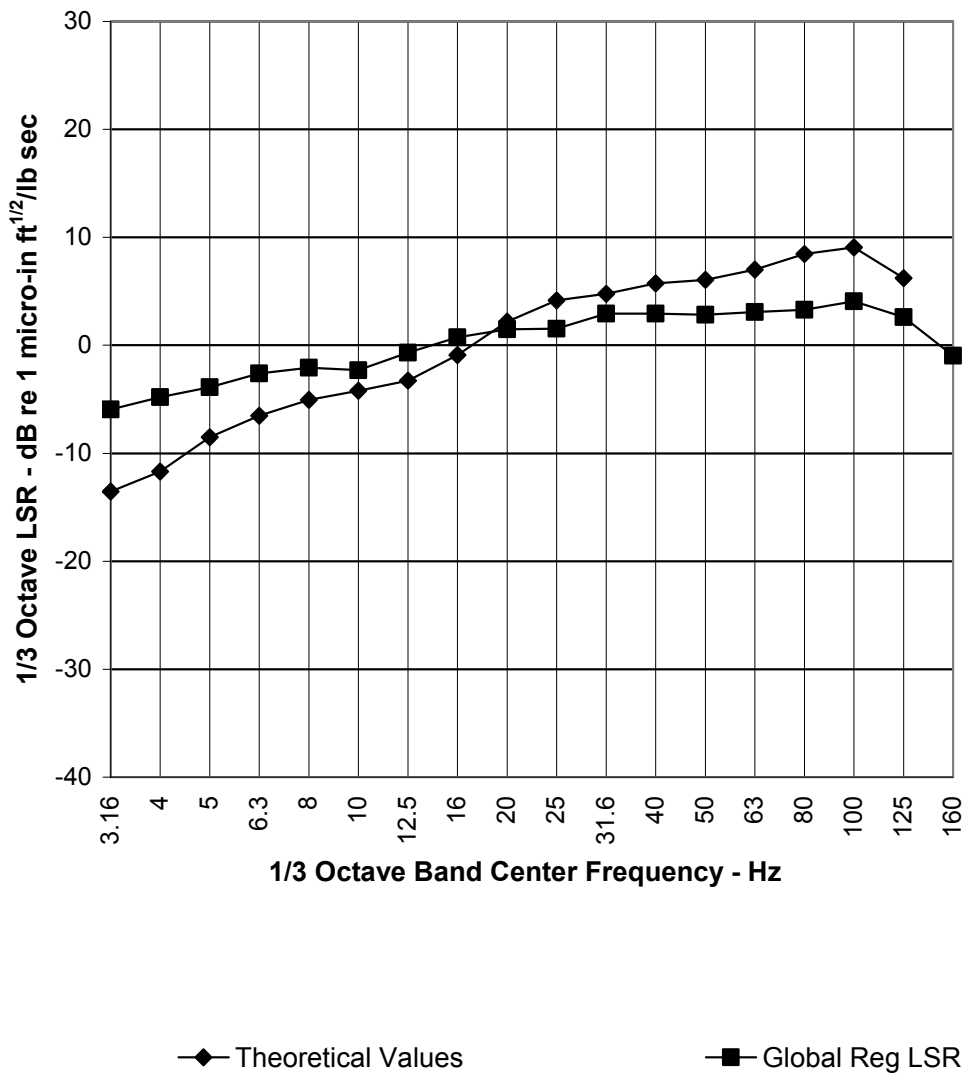
LSR Comparison
50 ft

Figure B-5 Comparison of Energy Averaged LSR For NB123, NB253, and NB255 with Global Regression Result at 50 Feet Offset



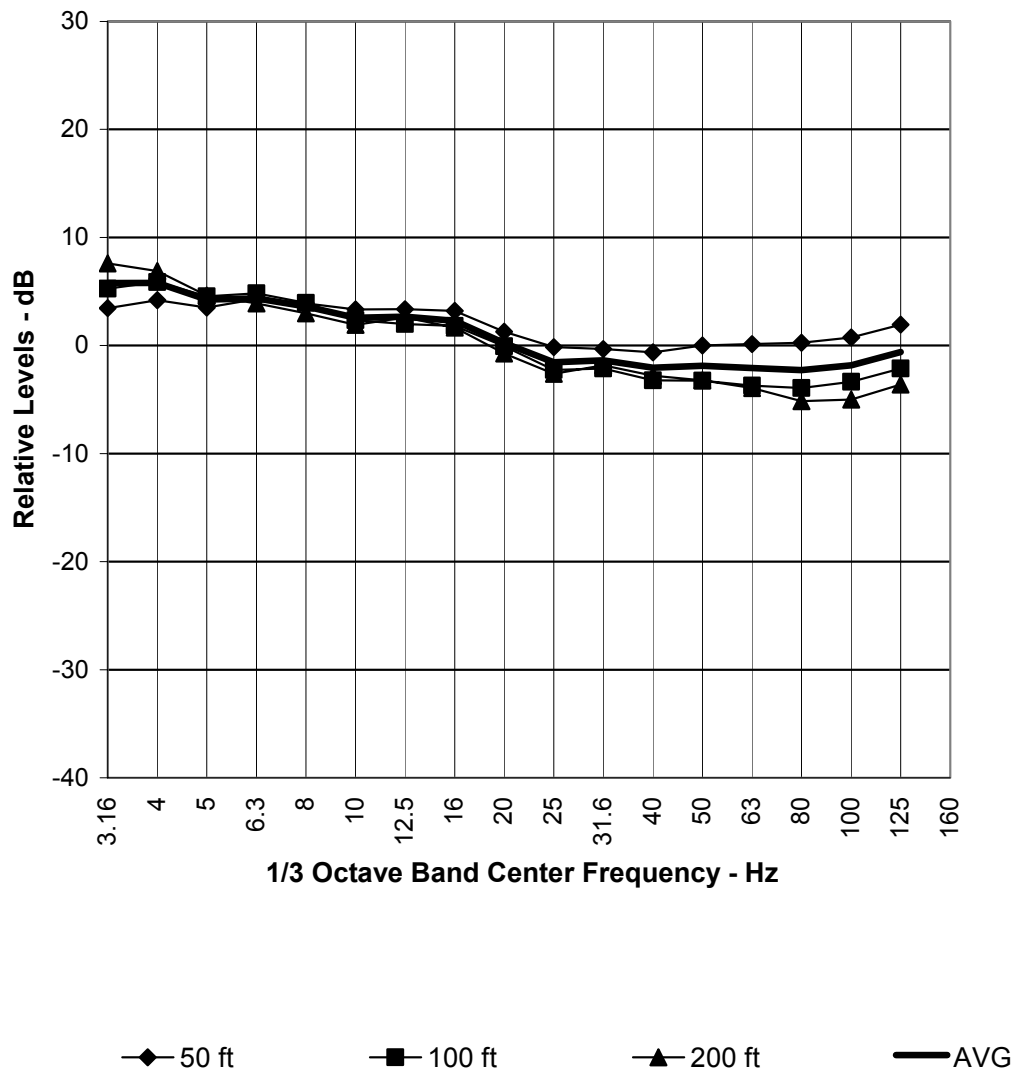
LSR Comparison
100 ft

Figure B-6 Comparison of Energy Averaged LSR For NB123, NB253, and NB255 with Global Regression Result at 100 Feet Offset



LSR Comparison
200 ft

Figure B-7 Comparison of Energy Averaged LSR For NB123, NB253, and NB255 with Global Regression Result at 200 Feet Offset



Calibration Factors

Figure B-8 Comparison of Adjustment Factors to Reconcile Calculated LSR with Borehole LSR Test Results

APPENDIX C: VTA KINKISHARYO FORCE DENSITY LEVEL TESTS

CONTENTS

C-1 INTRODUCTION	1
C-2 TEST SITES	1
C-3 TEST VEHICLES.....	2
C-4 INSTRUMENTATION	7
C-5 TEST PROCEDURE	7
C-6 DATA ANALYSIS.....	7
C-6.1 Train Vibration Analysis.....	7
C-6.2 Line Source Responses	8
C-6.3 FDL Calculation.....	8
C-7 TEST RESULTS.....	9
C-7.1 Vibration Levels.....	9
C-7.2 Line Source Responses	31
C-7.3 Force Density Levels	35
C-8 ADJUSTMENT FOR STANDARD DIRECT FIXATION FASTENERS	62
C-9 WHEEL RUNOUT AND RAIL UNDULATION	65
C-10 DISCUSSION	72

TABLES

Table C-1 Vehicle Data.....	2
Table C-2 Passage Times and Decibel Adjustments Added to Measured Velocity Levels.....	8
Table C-3 Adjustments Added to the FDL to Account for Finite Line Source Measurement ..	9
Table C-4 FDL for Resilient DF Fasteners of Stiffness 140,000 lb/in Relative to FDL for Ballast and Tie Track	63

FIGURES

Figure C-1 475 Ellis Street – Pole B1211 - 1216.....	3
Figure C-2 Central Expressway between Evelyn Street and Mountain View Station – Opposite Pole Number B1369	4
Figure C-3 Moffett Field Site – Between Poles B1130 and B1132	5
Figure C-4 VTA Kinkisharyo Vehicle	6

Figure C-5	20 MPH Train Vibration Velocity at 475 Ellis	10
Figure C-6	25 MPH Train Vibration Velocity at 475 Ellis	11
Figure C-7	30 MPH Train Vibration Velocity at 475 Ellis	12
Figure C-8	35 MPH Train Vibration Velocity at 475 Ellis	13
Figure C-9	40 MPH Train Vibration Velocity at 475 Ellis	14
Figure C-10	45 MPH Train Vibration Velocity at 475 Ellis	15
Figure C-11	20 MPH Train Vibration Velocity at Mountain View	16
Figure C-12	25 MPH Train Vibration Velocity at Mountain View	17
Figure C-13	30 MPH Train Vibration Velocity at Mountain View	18
Figure C-14	35 MPH Train Vibration Velocity at Mountain View	19
Figure C-15	40 MPH Train Vibration Velocity at Mountain View	20
Figure C-16	45 MPH Train Vibration Velocity at Mountain View	21
Figure C-17	50 MPH Train Vibration Velocity at Mountain View	22
Figure C-18	20 MPH Train Vibration Velocity at Moffett Field	23
Figure C-19	25 MPH Train Vibration Velocity at Moffett Field	24
Figure C-20	30 MPH Train Vibration Velocity at Moffett Field	25
Figure C-21	35 MPH Train Vibration Velocity at Moffett Field	26
Figure C-22	40 MPH Train Vibration Velocity at Moffett Field	27
Figure C-23	45 MPH Train Vibration Velocity at Moffett Field	28
Figure C-24	50 MPH Train Vibration Velocity at Moffett Field	29
Figure C-25	55 MPH Train Vibration Velocity at Moffett Field	30
Figure C-26	Line Source Responses at 475 Ellis	32
Figure C-27	Line Source Responses at Mountain View Site	33
Figure C-28	Line Source Responses at the Moffett Field Site	34
Figure C-29	FDL for Kinkisharyo Eastbound at 20 mph on Ballast and Concrete Tie Track 36	
Figure C-30	FDL for Kinkisharyo Westbound at 20 mph on Ballast and Concrete Tie Track 37	
Figure C-31	FDL for Kinkisharyo Vehicle at 20mph on Ballast & Concrete Tie Track - Energy Average of Eastbound and Westbound Result	38
Figure C-32	FDL of Kinkisharyo Vehicle Eastbound at 25mph on Ballast and Concrete Tie Track 39	
Figure C-33	FDL of Kinkisharyo Vehicle Westbound at 25mph on Ballast and Concrete Tie Track 40	
Figure C-34	FDL of Kinkisharyo Vehicle at 25mph on Ballast and Concrete Tie Track - Energy Average of Eastbound and Westbound Results	41
Figure C-35	FDL of Kinkisharyo Vehicle Eastbound at 30mph on Ballast and Concrete Tie Track 42	
Figure C-36	FDL of Kinkisharyo Vehicle Westbound at 30mph on Ballast and Concrete Tie Track 43	
Figure C-37	FDL of Kinkisharyo Vehicle at 30mph on Ballast and Concrete Tie Track - Energy Average of Eastbound and Westbound Results	44
Figure C-38	FDL of Kinkisharyo Vehicle Eastbound at 35mph on Ballast and Concrete Tie Track 45	
Figure C-39	FDL of Kinkisharyo Vehicle Westbound at 35mph on Ballast and Concrete Tie Track 46	

Figure C-40	FDL of Kinkisharyo Vehicle at 35mph on Ballast and Concrete Tie Track - Energy Average of Eastbound and Westbound Results	47
Figure C-41	FDL of Kinkisharyo Vehicle Eastbound at 40mph on Ballast and Concrete Tie Track	48
Figure C-42	FDL of Kinkisharyo Vehicle Westbound at 40mph on Ballast and Concrete Tie Track	49
Figure C-43	FDL of Kinkisharyo Vehicle at 40mph on Ballast and Concrete Tie Track - Energy Average of Eastbound and Westbound Results	50
Figure C-44	FDL of Kinkisharyo Vehicle Eastbound at 45mph on Ballast and Concrete Tie Track	51
Figure C-45	FDL of Kinkisharyo Vehicle Westbound at 45mph on Ballast and Concrete Tie Track	52
Figure C-46	FDL of Kinkisharyo Vehicle at 45mph on Ballast and Concrete Tie Track - Energy Average of Eastbound and Westbound Results	53
Figure C-47	FDL of Kinkisharyo Vehicle Eastbound at 50mph on Ballast and Concrete Tie Track	54
Figure C-48	FDL of Kinkisharyo Vehicle Westbound at 50mph on Ballast and Concrete Tie Track	55
Figure C-49	FDL of Kinkisharyo Vehicle at 50mph on Ballast and Concrete Tie Track - Energy Average of Eastbound and Westbound Results	56
Figure C-50	FDL of Kinkisharyo Vehicle Eastbound at 55mph on Ballast and Concrete Tie Track	57
Figure C-51	FDL of Kinkisharyo Vehicle Westbound at 55mph on Ballast and Concrete Tie Track	58
Figure C-52	FDL of Kinkisharyo Vehicle at 55mph on Ballast and Concrete Tie Track - Energy Average of Eastbound and Westbound Results	59
Figure C-53	FDL for Kinkisharyo Vehicle at Various Speeds - Energy Average Over All Data	60
Figure C-54	Energy Average of FDL for All Train Speeds - Illustration of Primary Suspension Stiffness	61
Figure C-55	FDL for VTA Kinkisharyo on Resilient Direct Fixation Fasteners with Stiffness of 140,000 lb/in and Separation of 30in.....	64
Figure C-56	Modulation Envelope of Ground Vibration due to Rail Roughness for a Single VTA Kinkisharyo Vehicle Traveling at 55 MPH	67
Figure C-57	Fourier Spectrum of 40mph Passby Signature.....	68
Figure C-58	Fourier Spectrum of 45 MPH Passby Signature	69
Figure C-59	Fourier Spectrum of 49 MPH Passby Signature	70
Figure C-60	Fourier Spectrum of 54 MPH Passby Signature	71

C-1 INTRODUCTION

Force Density Levels (FDL) for the Kinkisharyo light rail vehicle used at the Valley Transportation Authority (VTA) in San Jose, California were measured. These FDLs are combined as discussed in Appendix D with Line Source Responses (LSR) obtained on the UW campus to predict ground vibration at buildings along the Sound Transit North Link Line at the University of Washington (UW) campus in Seattle, Washington..

The tests in San Jose involved measurement of Line Source Responses from the ballasted track bed to wayside ground vibration measurement locations at three sites, measurement of ground vibration from passing test vehicles at various speeds, and normalization of the measured ground vibration velocity levels by the LSR. The result is the Force Density Level. The procedure is described in the FTA Guidance Manual.¹

C-2 TEST SITES

The FDL was measured at three sites on the VTA system, including:

- 1) 475 Ellis Street, Mountain View, between Poles B1211 and B1216 (Referred to as the 475 Ellis Site)
- 2) Central Expressway, between Evelyn Street and Mountain View Station, at Pole Number B1369 (Referred to as the Mountain View Site)
- 3) Moffett Field, Mountain View, Between Poles B1130 and B1132 (Referred to as the Moffett Field Site)

These sites are described in Figure C-1 through Figure C-3.

The site is characterized by level ground, with little background vibration. This site is perhaps the best site of the three, but the maximum train speed was limited to 45mph.

The Evelyn Street site in Mountain View also had level grade, but was adjacent to a boulevard, and thus was subject to some background vibration from traffic. However, little local traffic occurred late at night during the tests. The test train speed was limited to 50mph. Only four measurement points were employed at this site.

Train speeds up to 55 mph were used at the Moffett site. However, the track was depressed below grade in an open cut, and all measurements were at grade level behind the retaining wall of

¹ **Transit Noise and Vibration Impact Assessment**, Federal Transit Administration, April 1995.

the cut. Figure C-3 includes a cross-section illustrating the grade transition and location of retaining wall relative to the track.

C-3 TEST VEHICLES

A different test vehicle was employed for each test, thus providing some indication of variability between vehicles. The vehicle ID numbers and truing history are summarized below in Table C-1. The VTA vehicles accrue approximated 4,000 miles of service per month, and this rate was employed in developing the mileage estimates shown in Table C-1. A drawing of the test vehicle is provided in Figure C-4.

Table C-1 Vehicle Data

Test	Location	Vehicle	Truing History	Mileage After Truing
1	475 Ellis	952	6 May 2004	23,000
2	Mountain View	969	Original Cut	NA
3	Moffett	935	4 February 2004	35,000

NA: Not available

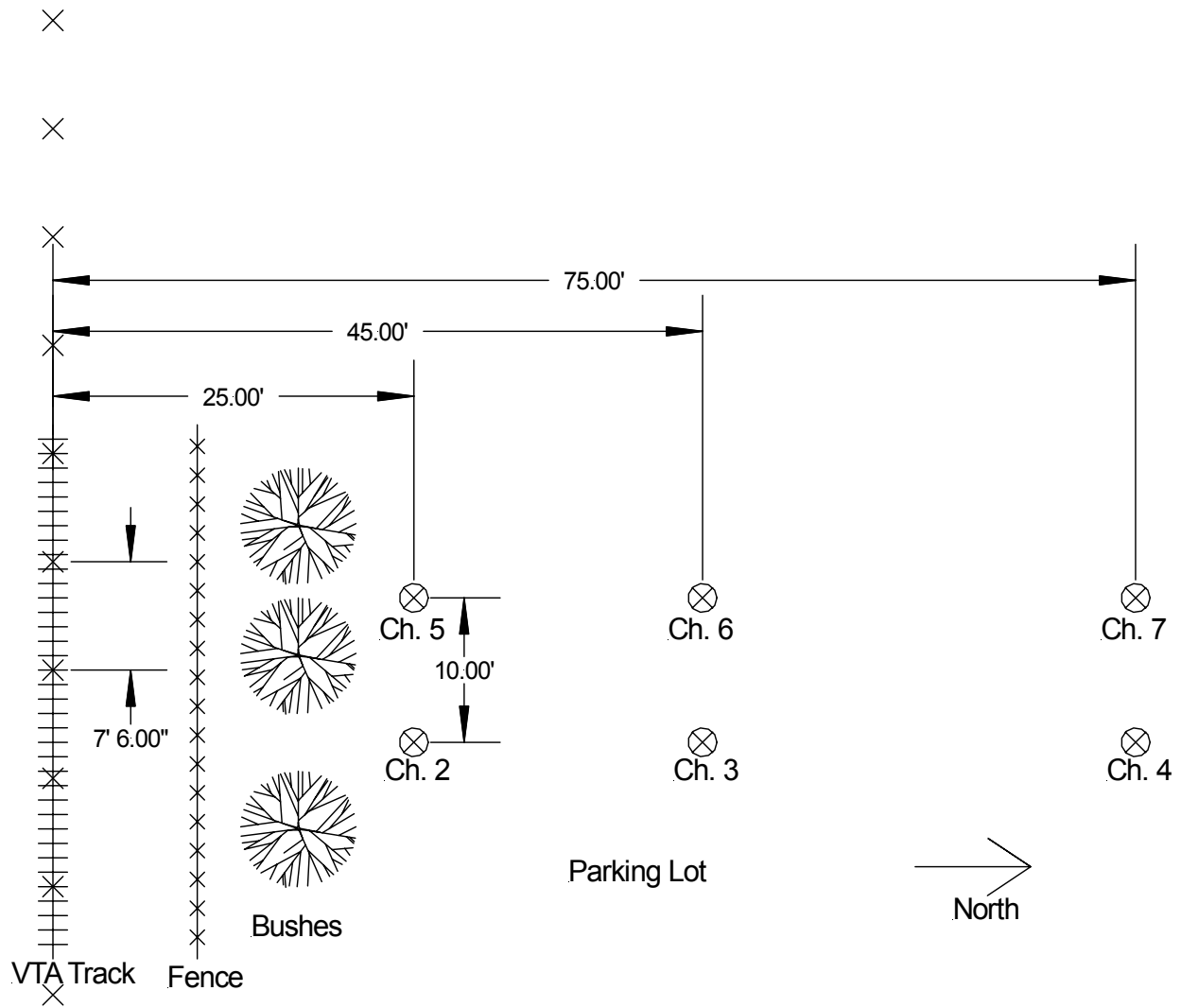


Figure C-1 475 Ellis Street – Pole B1211 - 1216

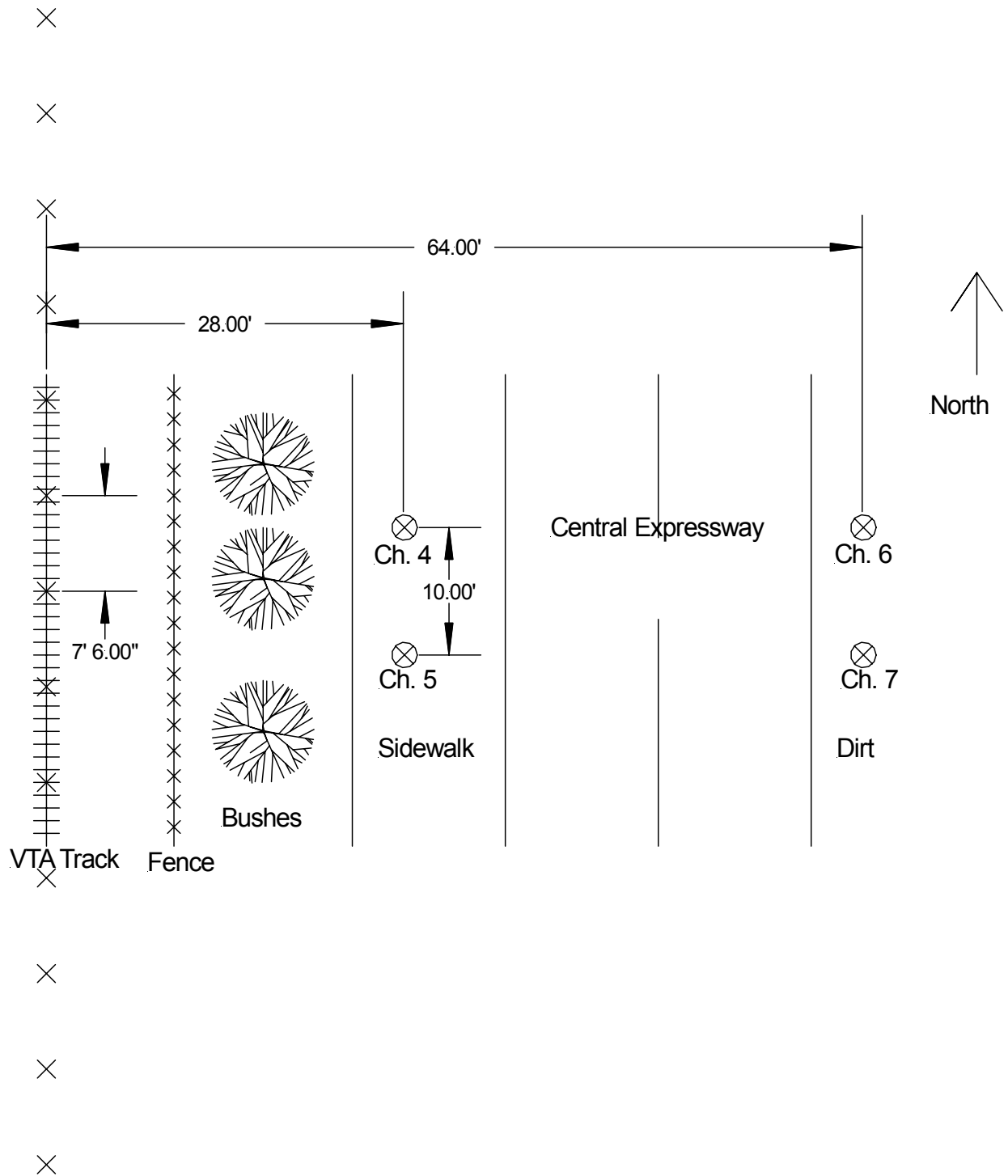


Figure C-2 Central Expressway between Evelyn Street and Mountain View Station – Opposite Pole Number B1369

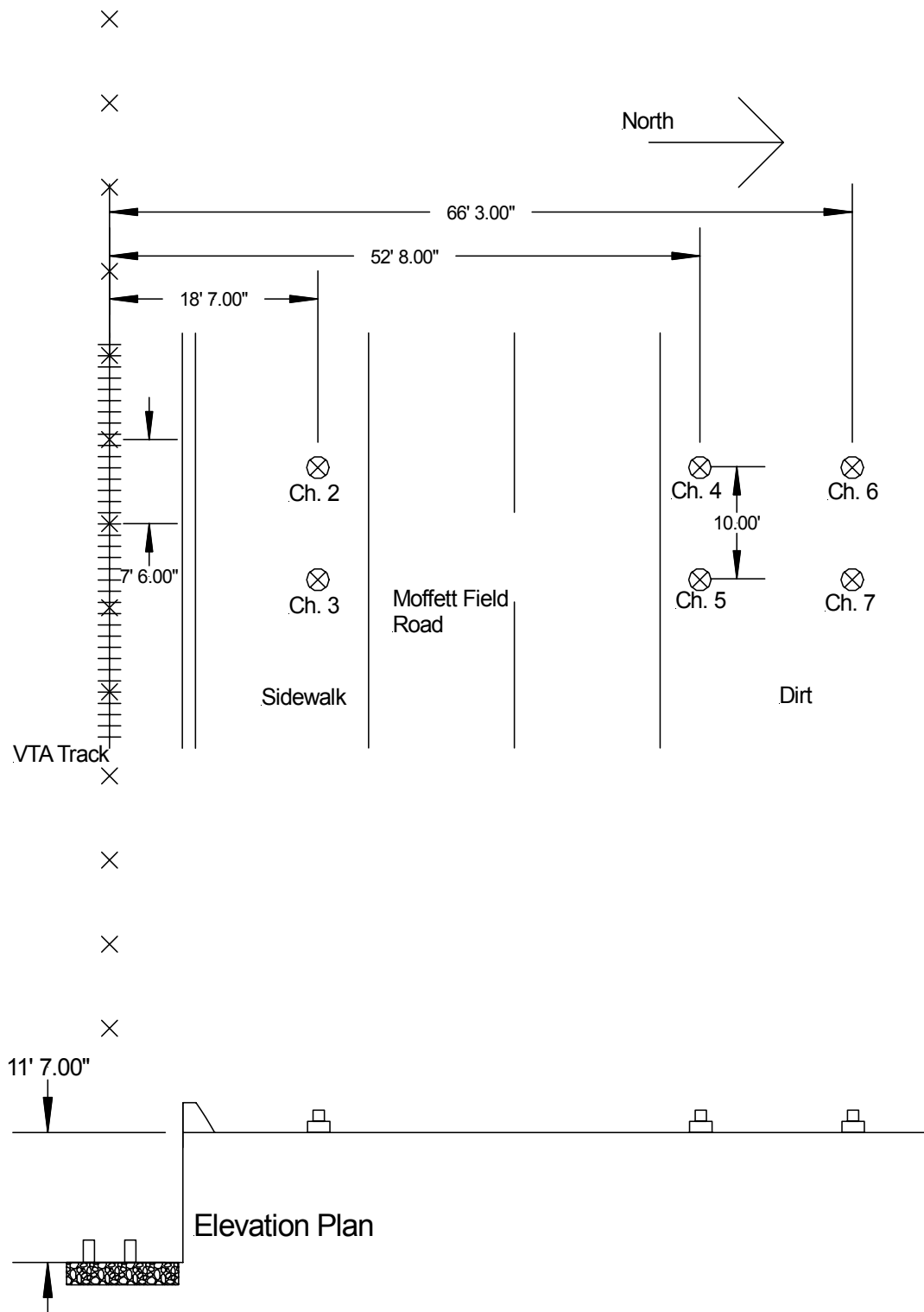


Figure C-3 Moffett Field Site – Between Poles B1130 and B1132

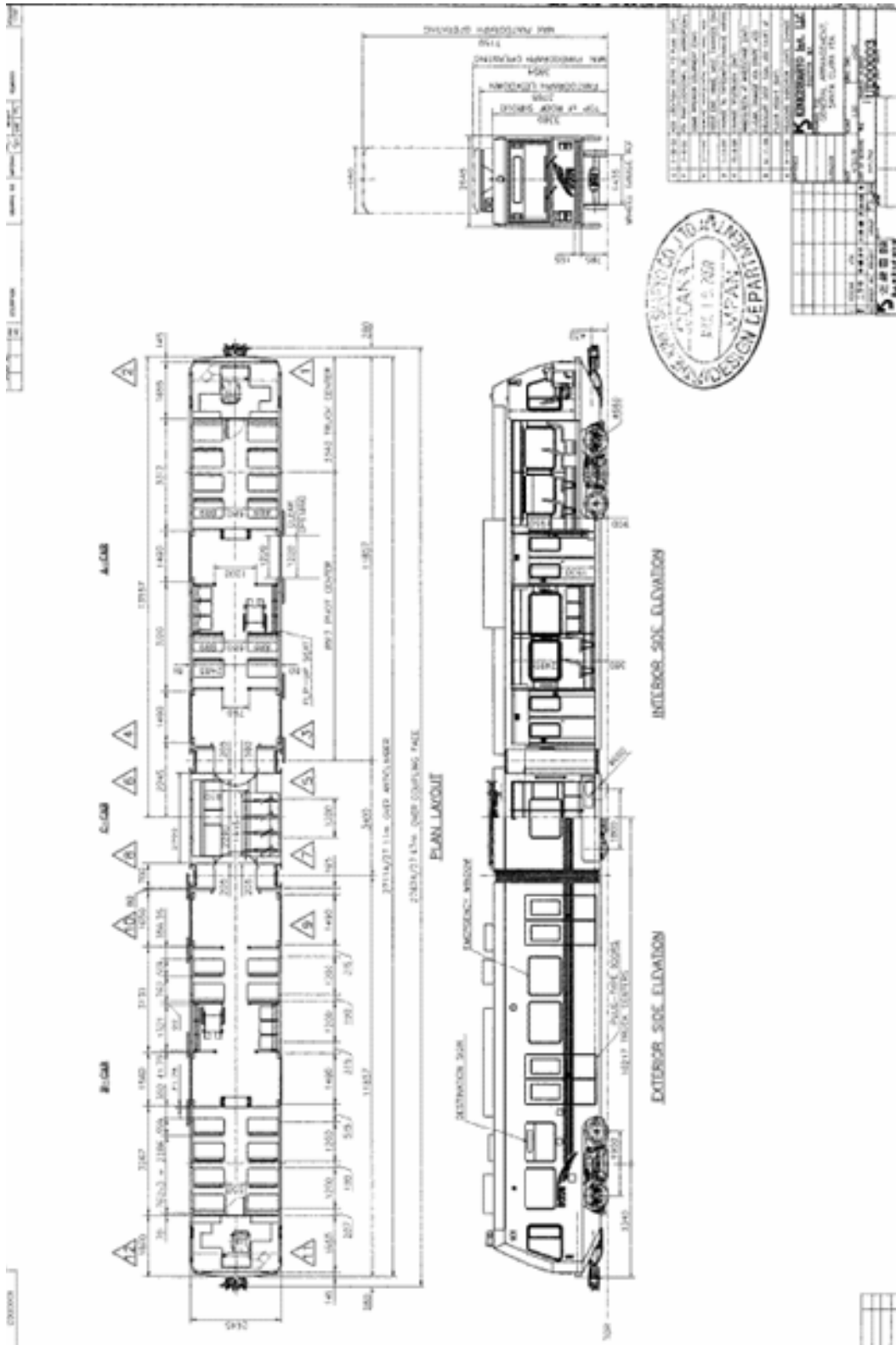


Figure C-4 VTA Kinkisharyo Vehicle

C-4 INSTRUMENTATION

The instrumentation employed included seven 8-Hz geophones, WIA geophone preamplifiers, a WIA Type 228 multi-channel amplifier, and a TEAC RD135 DAT PCM data recorder. The LSR's were measured with the same geophones, using impulses generated by a pneumatic hammer with 40-pound hammer weight. Thus, the variations of frequency responses of the geophones at low frequencies are cancelled out when computing the FDL by subtracting the LSR from the velocity levels.

C-5 TEST PROCEDURE

The field test procedure included travel to the site during the afternoon, installation of geophones, and recording passby vibration from revenue service trains. After cessation of revenue service, impulse responses were measured from equidistant impact points along the center of the track bed to up to six locations located at the wayside. The impacts were located between the ties, at the ballast surface, and the distance between impacts was 7.5 feet. Following the impacts, ground vibration data were recorded for the test vehicle at various speeds.

The speeds of the test train ranged from 20 to 45mph at Ellis Street site, 20 to 50mph at the Mt. View site, and 20 to 55mph at Moffett Field site, all in 5-mph increments. Information concerning train speed was relayed to the wayside test crew after each passage. Some variation in speed occurred. For example, the nominal speed of 50 mph involved speeds over a range of 48 to 52 mph.

Four samples of vibration were taken for each test train speed and direction. For the Moffett site, with six vibration pickups and a total of eight speeds, a total of 192 samples of vibration were obtained. At Mt. View, the number of train speeds was limited to 7, and the number of vibration pickups was four, so that 112 samples of vibration were obtained. Finally, at Ellis, only 6 train speeds were obtained, giving a total of 144 samples. The total number of train samples was 448.

C-6 DATA ANALYSIS

C-6.1 Train Vibration Analysis

The third octave analysis of the recorded ground vibration data included integration over the entire vibration signature of the passing train. Usually, this was about 9 or 10 seconds. The train passage duration, on the other hand, was about 1 to 2 seconds, depending on train speed. The force density level is referenced to the forces transmitted to the ground per root train length. Thus, the vibration data were normalized to the train passage duration by adding $10\log_{10}(T_{\text{measured}}/T_{\text{passage}})$ to the measured third octave vibration levels, where T_{measured} is the time duration used for integration of the train passby vibration data, and T_{passage} is the time period required for the 90ft long vehicle to pass the observation point. Integrating over the entire passby vibration signature of the single vehicle and normalizing to its passage time captures the entire vibration energy exposure, and gives the same result as that which would be obtained for an

infinitely long train, the effects of wheel spacing notwithstanding. The train passage durations and decibel adjustments for a 9 second integration time are listed below.

Table C-2 Passage Times and Decibel Adjustments Added to Measured Velocity Levels

Speed	Passing Time	Adjustment For 9 second Integration Time – Decibels
20	3.1	4.6
25	2.5	5.6
30	2.0	6.5
35	1.75	7.1
40	1.53	7.7
45	1.36	8.2
50	1.23	8.6
55	1.11	9.1

C-6.2 Line Source Responses

The impulse responses from each force input point on the ballasted embankment to each measurement point were obtained as a function of frequency, using a four hundred line Fourier transform algorithm implemented in a custom WIA instrumentation and software package. These narrow band transfer functions, or transfer mobilities, were converted to 1/3 octave point source responses. The Line Source Response at each measurement point was computed by summing the squares of the third octave Point Source Responses obtained for each track impact location, and multiplying the sum by the impact separation in feet, taking the logarithm of the result, and multiplying by ten. The source length was taken as equal to the vehicle length, following the procedures of the FTA Guidance Manual.

C-6.3 FDL Calculation

The finite length Line Source Responses for each measurement point were subtracted from the respective passby vibration levels to obtain the initial estimates of the FDL at each measurement point and for each train speed.

The 90-foot source LSR's used above are less than those that would have been obtained for an infinite line source. At distances close to the track, or at locations where there was a high degree of attenuation with distance, the difference is small and perhaps negligible. At 60 to 70 feet, the 90-foot train LSR is about 3 to 4 decibels less than the infinite train LSR. When averaged over all positions, the result is an upward bias in the initial estimate of the FDL by a few decibels. This has been compensated by adjusting the FDL data downward for the Evelyn and Moffett sites, where the attenuation versus distance was low, and much less than the rate found at 475 Ellis. The downward adjustments to the FDL are as shown in Table C-3. These adjustments were obtained by theoretical calculations of the Line Source Response for simple point source distributions, assuming 6dB per doubling of distance attenuation rule.

The low attenuation rate at the Moffett site may also be related to the retaining wall. Without the adjustments to the FDL shown in Table C-3, the FDL at Moffett would be excessively high.

Table C-3 Adjustments Added to the FDL to Account for Finite Line Source Measurement

Location	Distance	Adjustment – dB
Evelyn	28 ft	-2
	64	-4
Moffett	18.6	-1
	52	-3
	66	-4

The samples were further energy averaged over the measurement points, for each speed and direction, giving a total of 16 spectra. Finally, an energy average of the data was obtained for each test location and speed.

C-7 TEST RESULTS

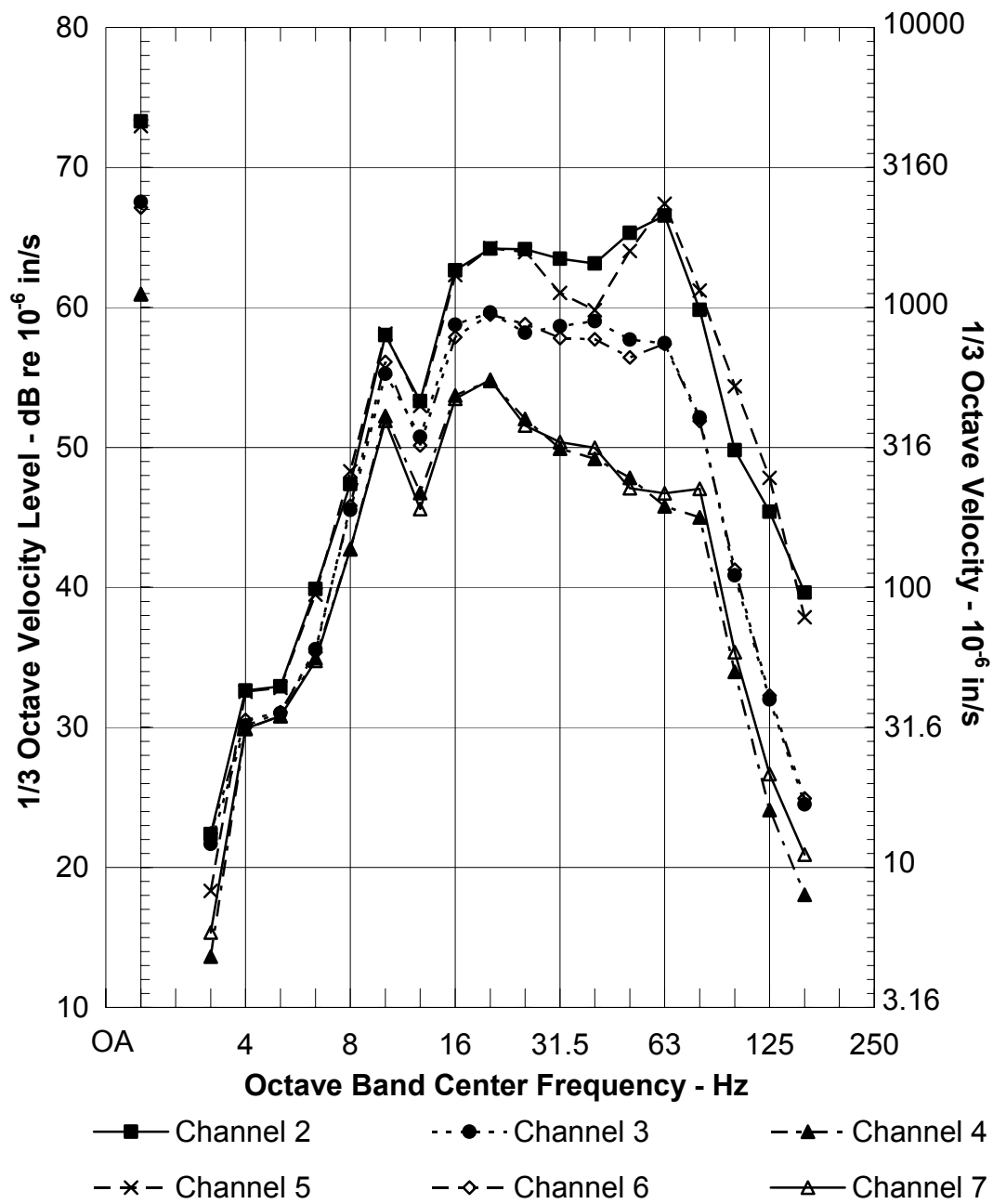
C-7.1 Vibration Levels

Third octave vibration velocity levels energy averaged over multiple eastbound and westbound vehicle passes are shown in Figure C-5 through Figure C-25. Speeds of 20 to 45 mph are represented for all locations, while speeds of 50 mph are represented at Mountain View and Moffett and speeds of 55 were only obtained at Moffett. The data in each of these figures includes the roll off of the 8-Hz geophone below 8Hz.

The scale shown at the left of each plot is the root-mean-square vibration velocity level in decibels relative to one micro-inch per second. The scale at the right hand side is the one-third octave root-mean-square velocity amplitude in units of one micro-inch per second. Thus, 1000micro-in/s is equivalent to 60dB velocity level, while 10micro-in/s is equivalent to 20dB velocity level.

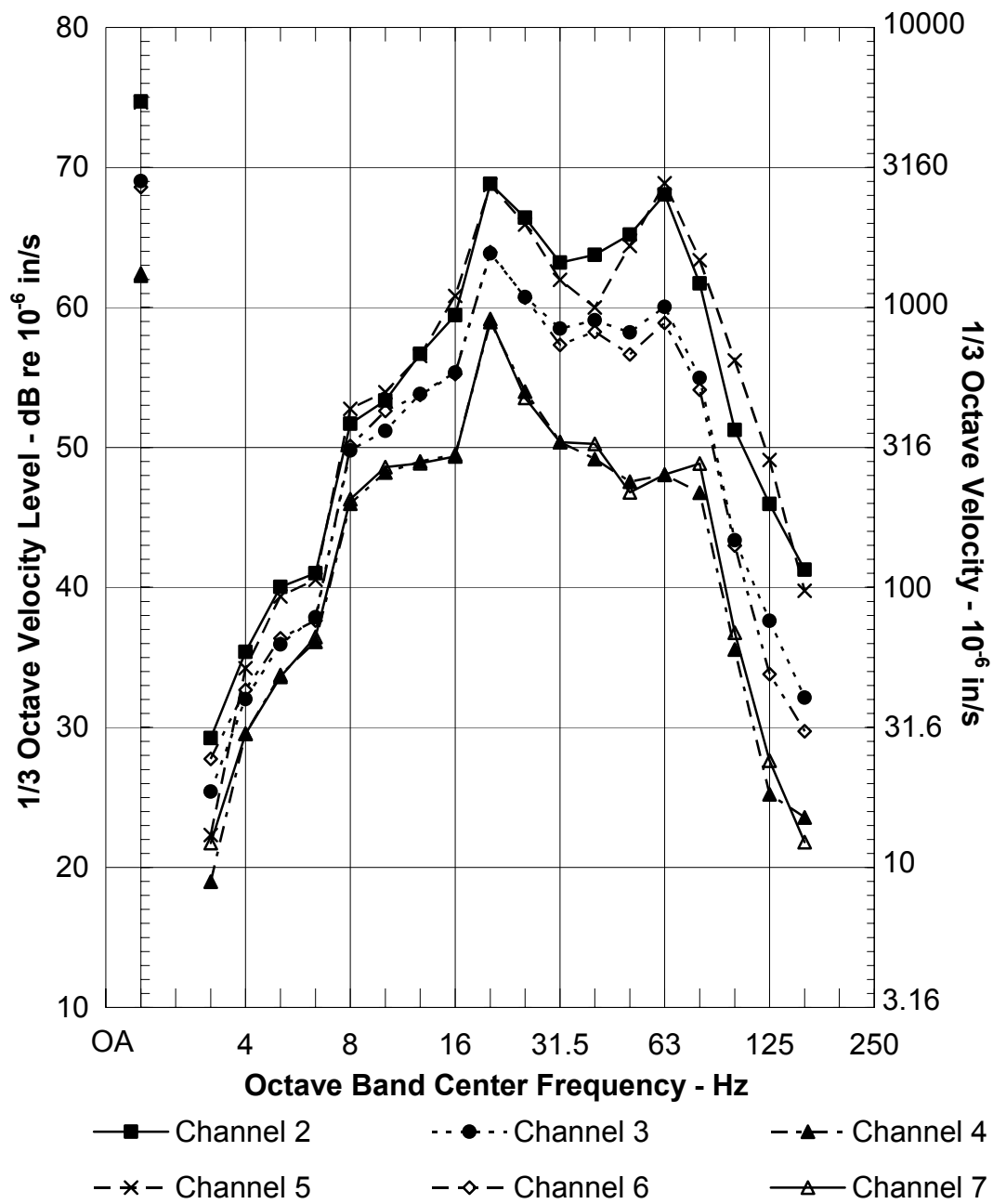
The attenuation of vibration with horizontal distance at the Ellis Street test site is clearly illustrated in the data shown in Figure C-5 through Figure C-10. In spite of this, the levels observed at the same distance from the track (Channels 2 and 5, for example) are virtually identical up to perhaps 25Hz. At higher frequencies, vibration levels measured at the same distance begin to diverge slightly. The velocity levels obtained at Mountain View site were all very consistent, regardless of distance. The LSRs obtained at this location, shown below, are also very consistent, regardless of position. Finally, at Moffett Field test site, the levels are reasonably consistent up to 63Hz, above which the retaining wall may have had a strong effect on vibration propagation. This too, is indicated in the LSRs discussed below.

The differences between velocity levels measured at various distances are essentially normalized away when the respective LSRs are subtracted to obtain the FDL. The results for the LSRs are discussed in the following section.



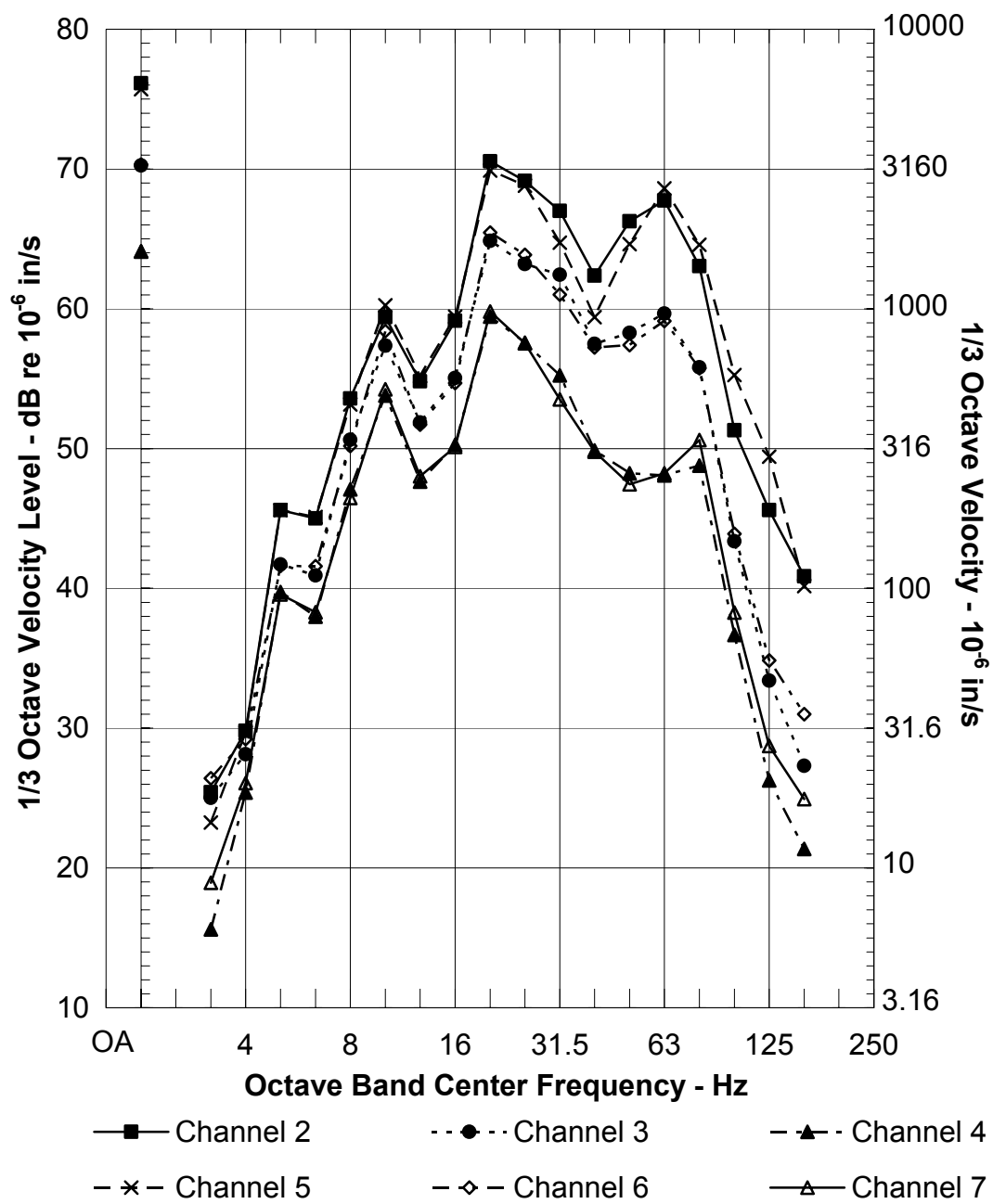
475 Ellis Vibration Velocity Levels
Kinkisharyo Train, 20 MPH

Figure C-5 20 MPH Train Vibration Velocity at 475 Ellis



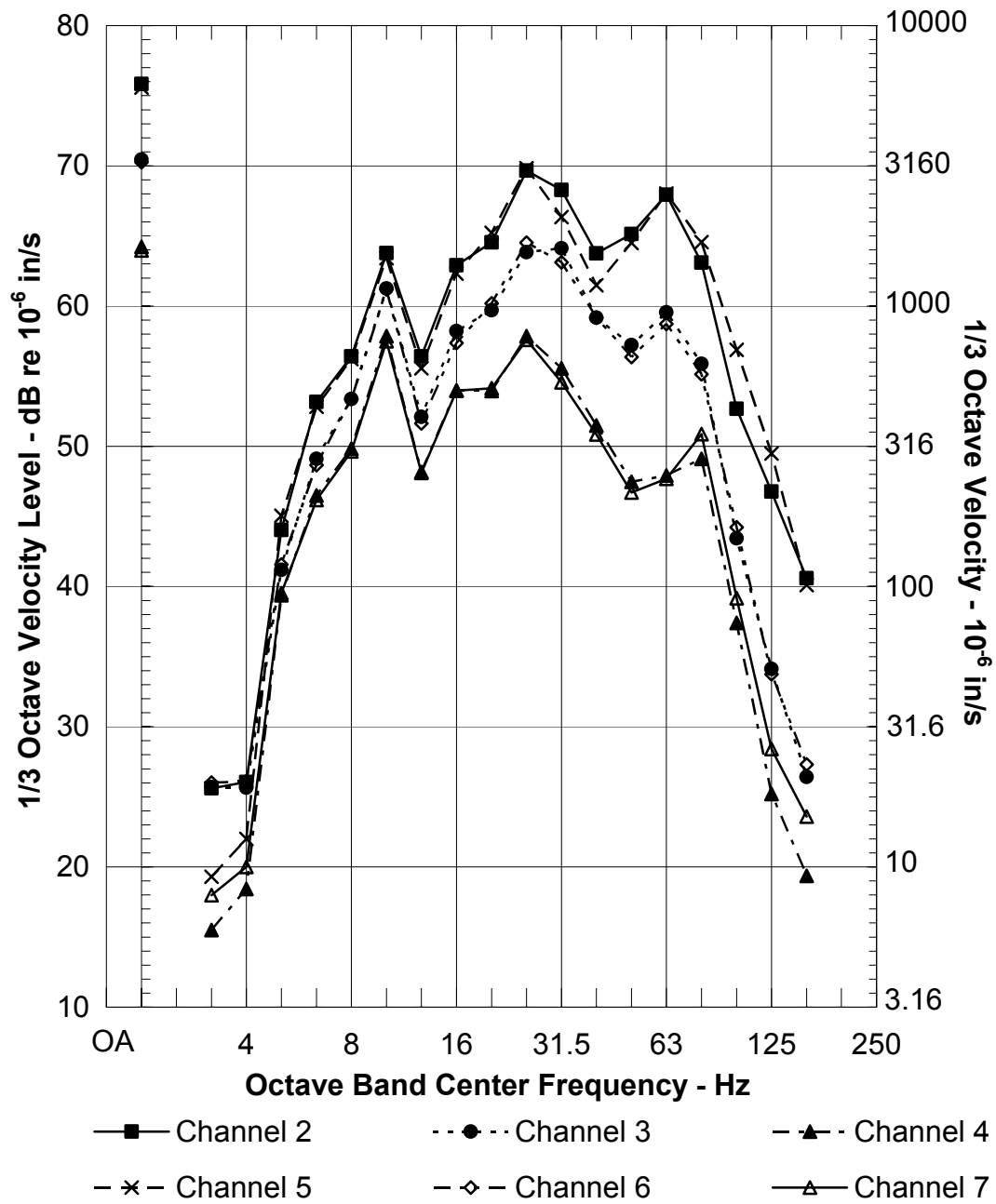
475 Ellis Vibration Velocity Levels
Kinkisharyo Train, 25 MPH

Figure C-6 25 MPH Train Vibration Velocity at 475 Ellis



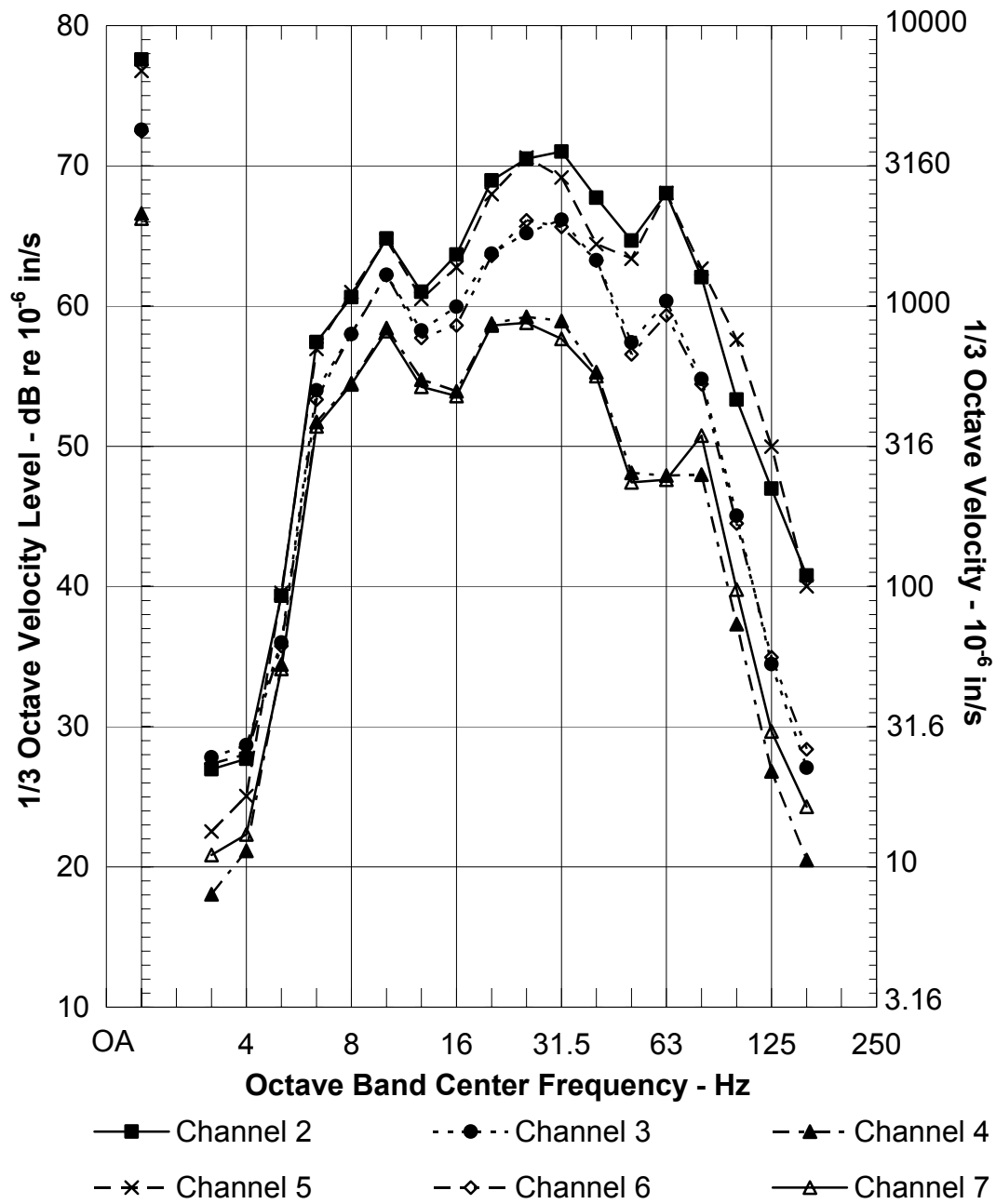
475 Ellis Vibration Velocity Levels
Kinkisharyo Train, 30 MPH

Figure C-7 30 MPH Train Vibration Velocity at 475 Ellis



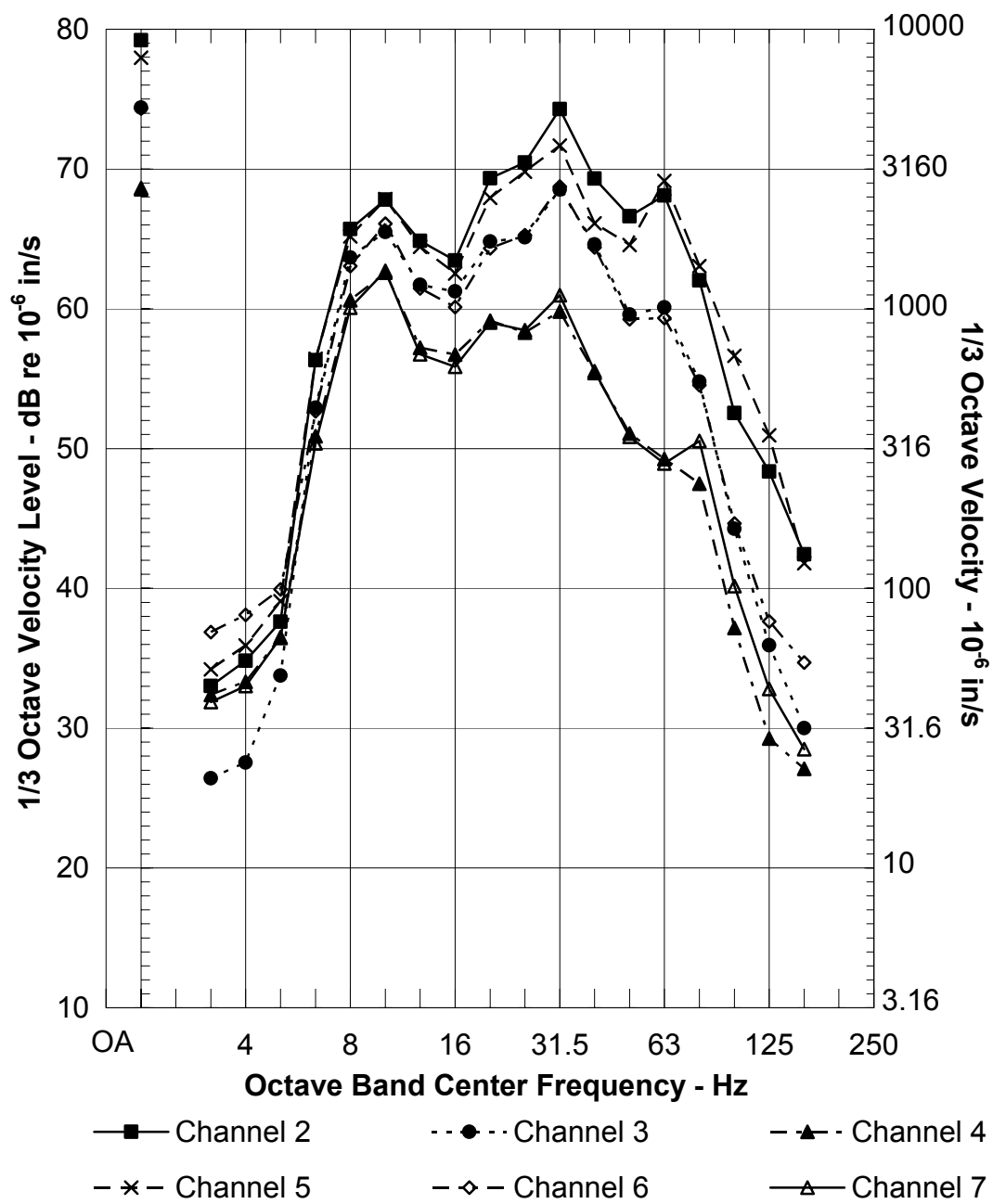
475 Ellis Vibration Velocity Levels
Kinkisharyo Train, 35 MPH

Figure C-8 35 MPH Train Vibration Velocity at 475 Ellis



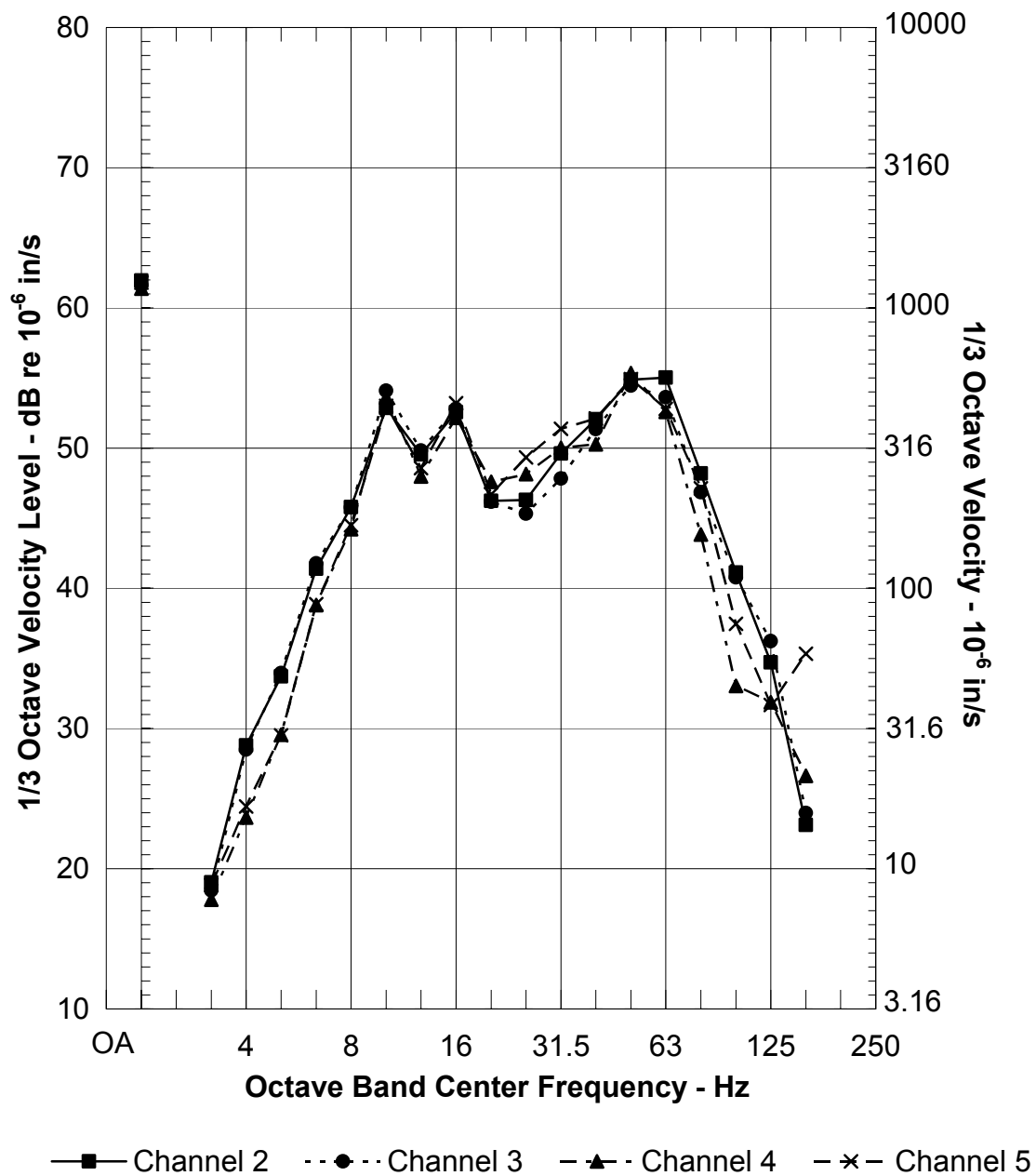
475 Ellis Vibration Velocity Levels
Kinkisharyo Train, 40 MPH

Figure C-9 40 MPH Train Vibration Velocity at 475 Ellis



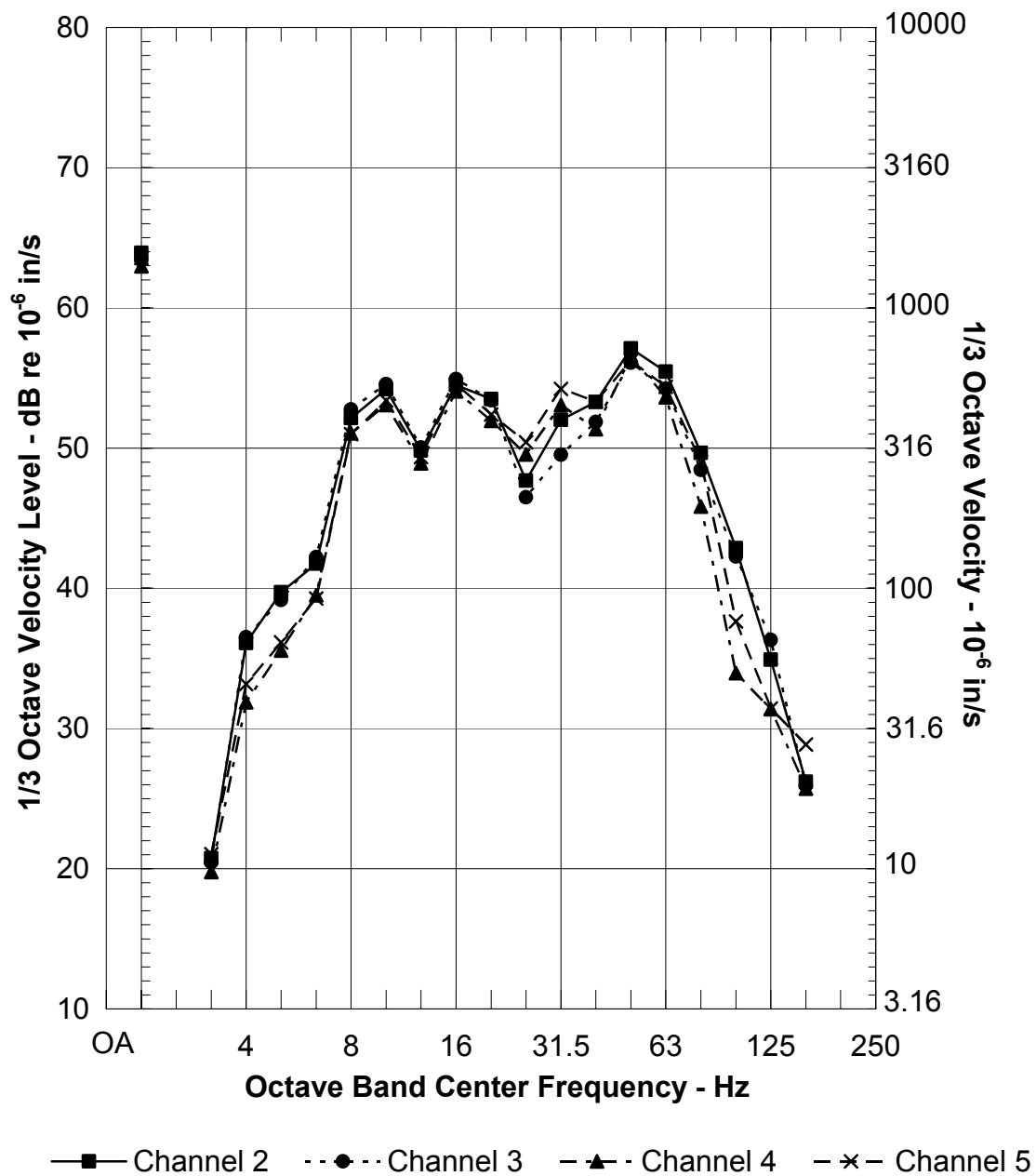
475 Ellis Vibration Velocity Levels
Kinkisharyo Train, 45 MPH

Figure C-10 45 MPH Train Vibration Velocity at 475 Ellis



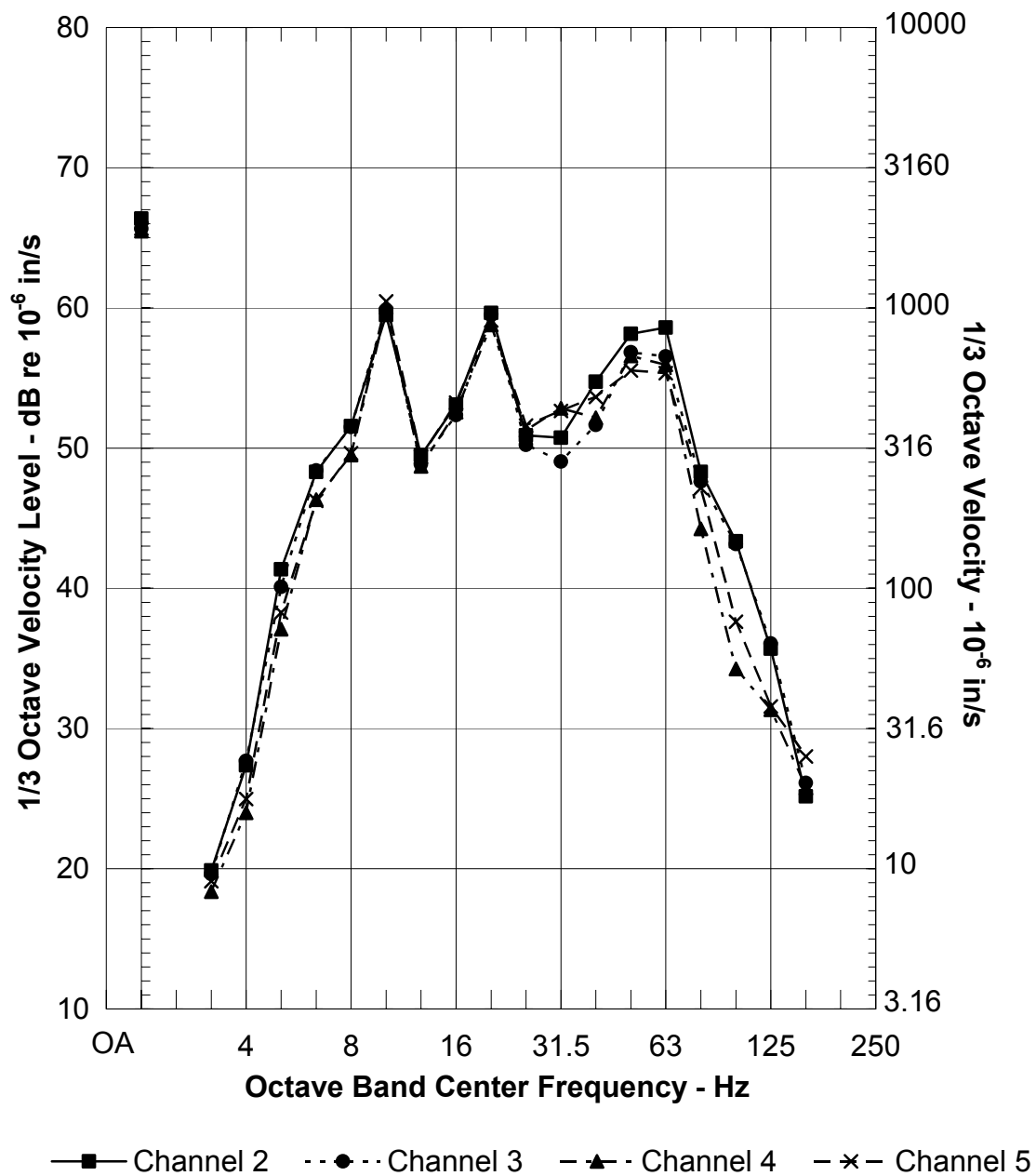
Mountain View Vibration Velocity Levels
Kinkisharyo Train, 20 MPH

Figure C-11 20 MPH Train Vibration Velocity at Mountain View



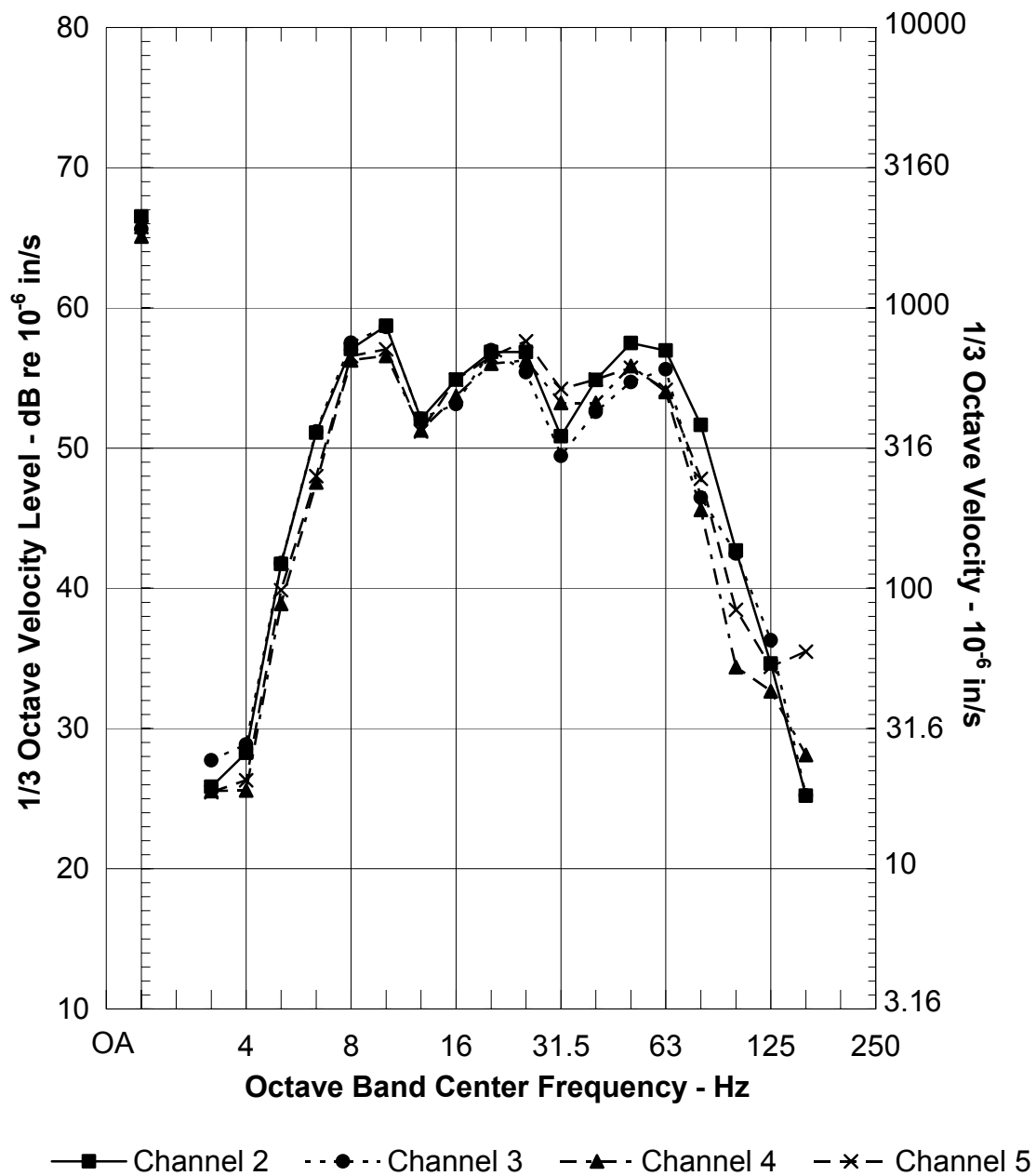
Mountain View Velocity Levels
Kinkisharyo Train, 25 MPH

Figure C-12 25 MPH Train Vibration Velocity at Mountain View



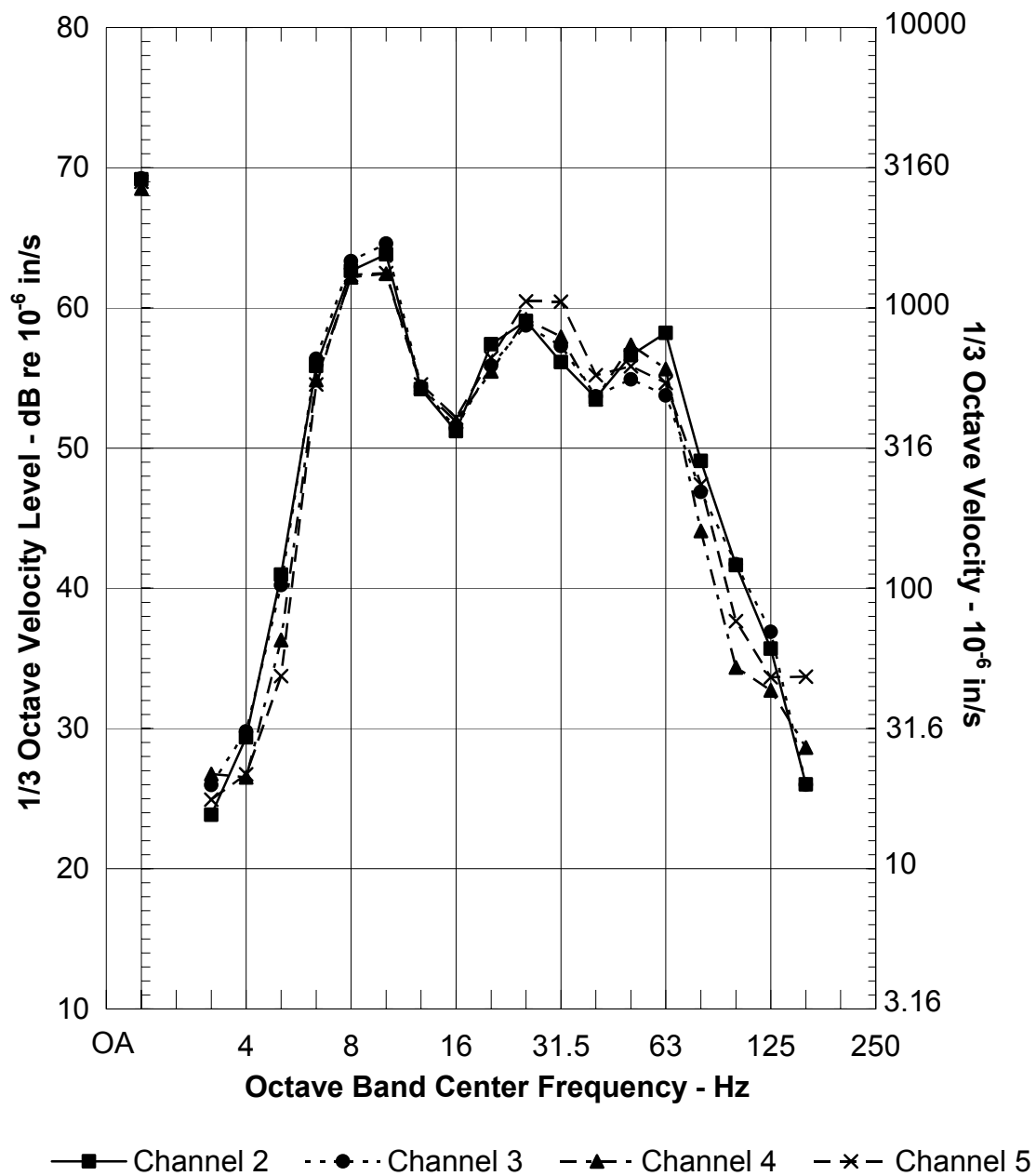
Mountain View Velocity Levels
Kinkisharyo Train, 30 MPH

Figure C-13 30 MPH Train Vibration Velocity at Mountain View



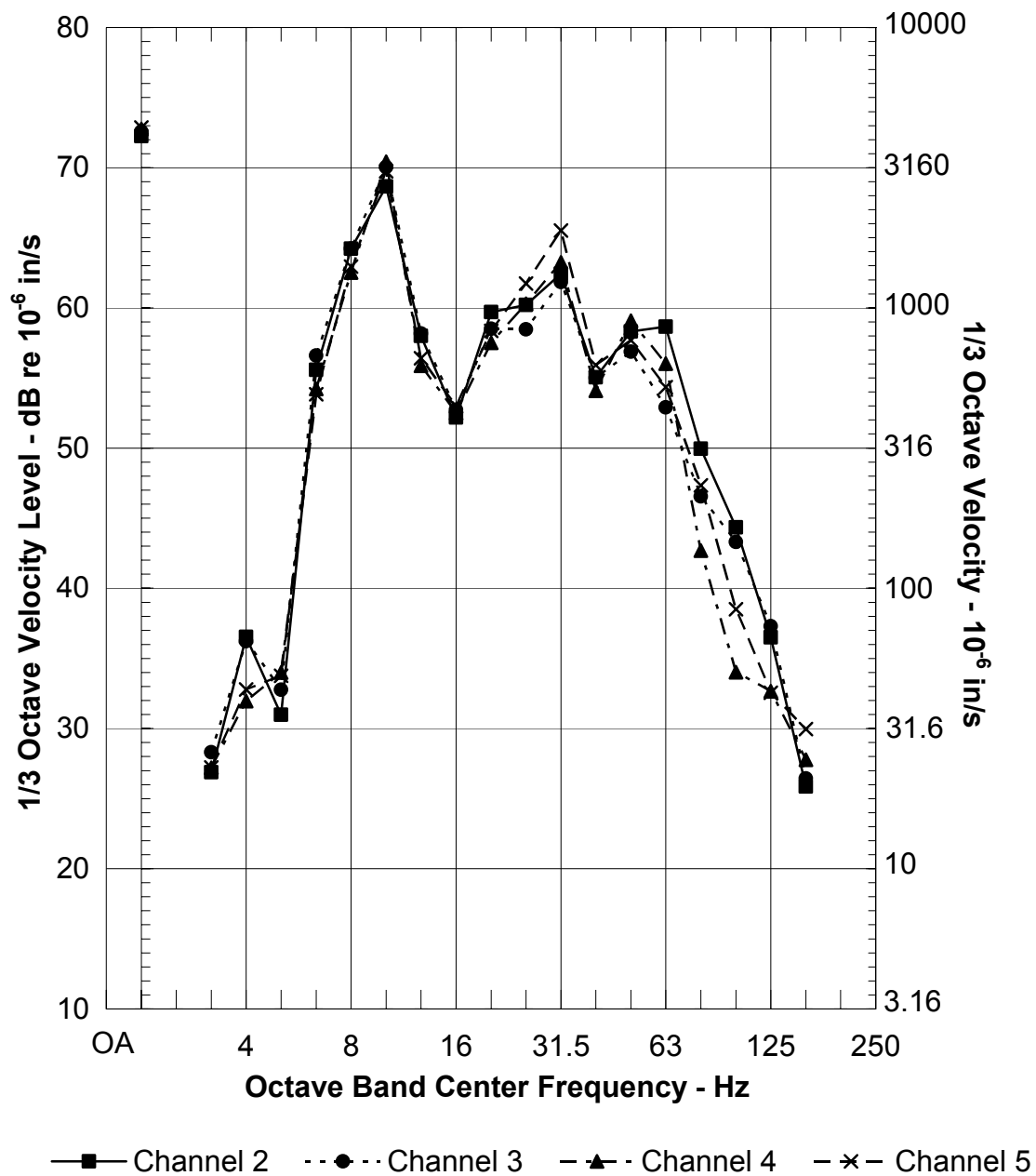
Mountain View Velocity Levels
Kinkisharyo Train, 35 MPH

Figure C-14 35 MPH Train Vibration Velocity at Mountain View



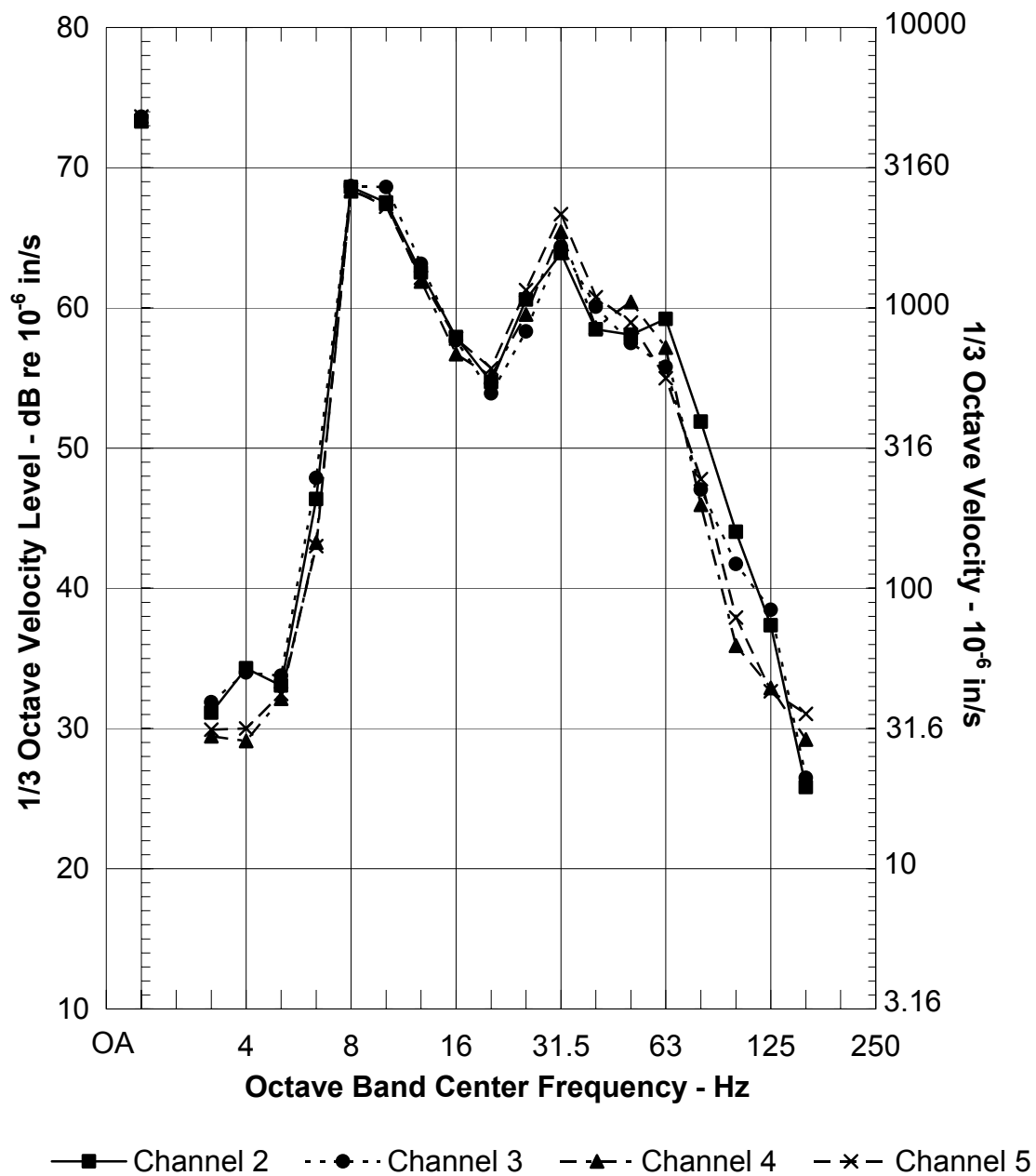
Mountain View Velocity Levels
Kinkisharyo Train, 40 MPH

Figure C-15 40 MPH Train Vibration Velocity at Mountain View



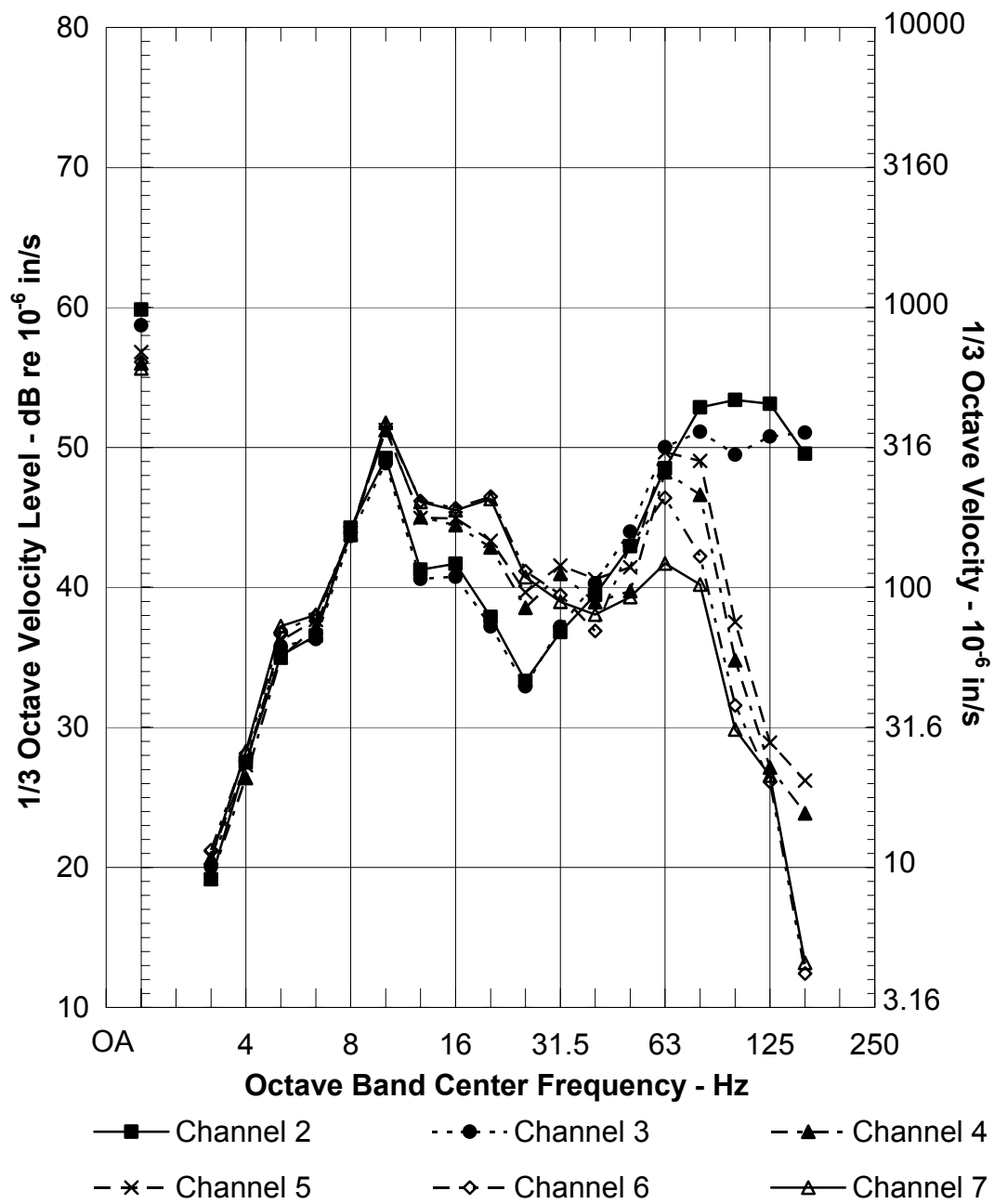
Mountain View Velocity Levels
Kinkisharyo Train, 45 MPH

Figure C-16 45 MPH Train Vibration Velocity at Mountain View



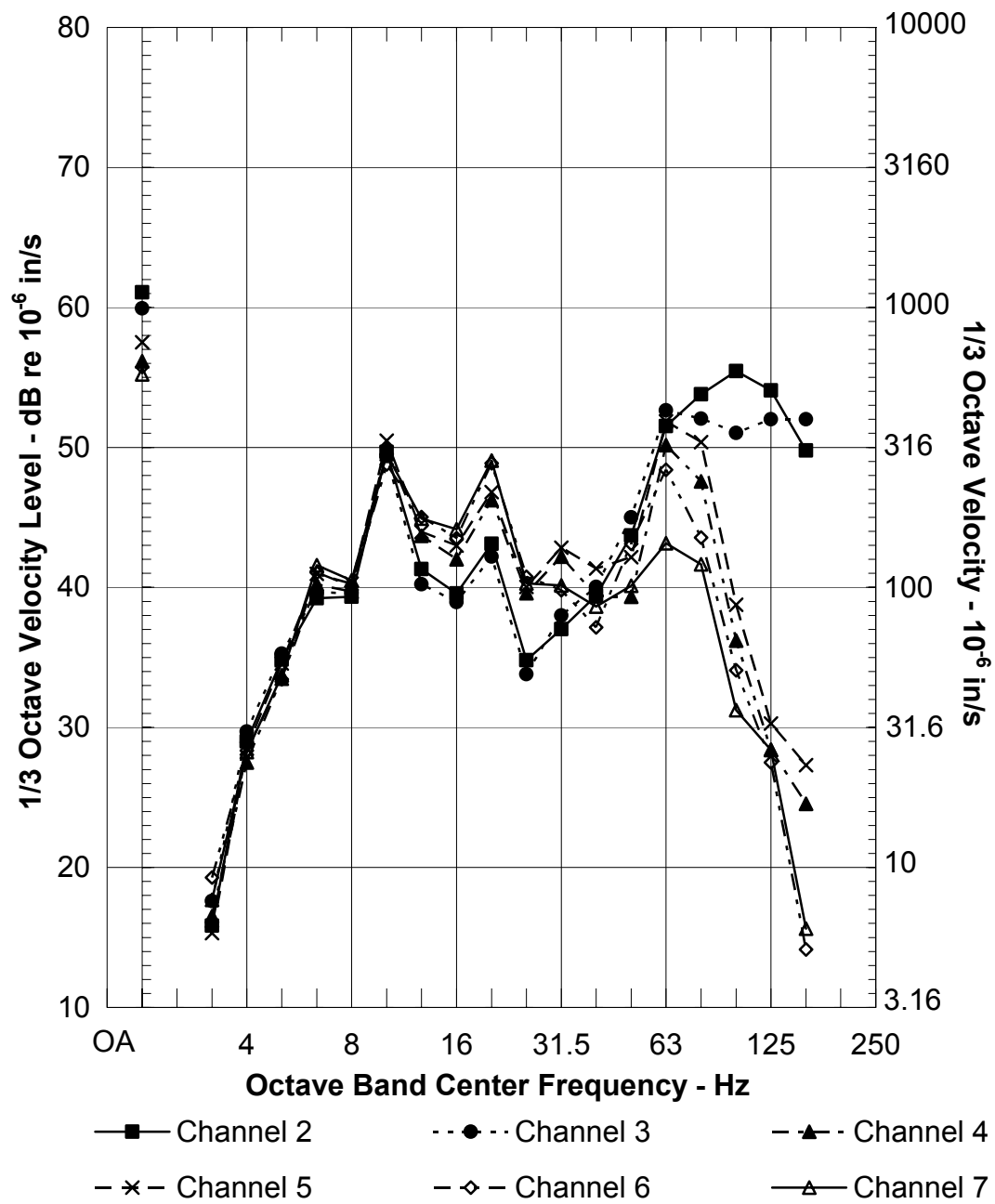
Mountain View Velocity Levels
Kinkisharyo Train, 50 MPH

Figure C-17 50 MPH Train Vibration Velocity at Mountain View



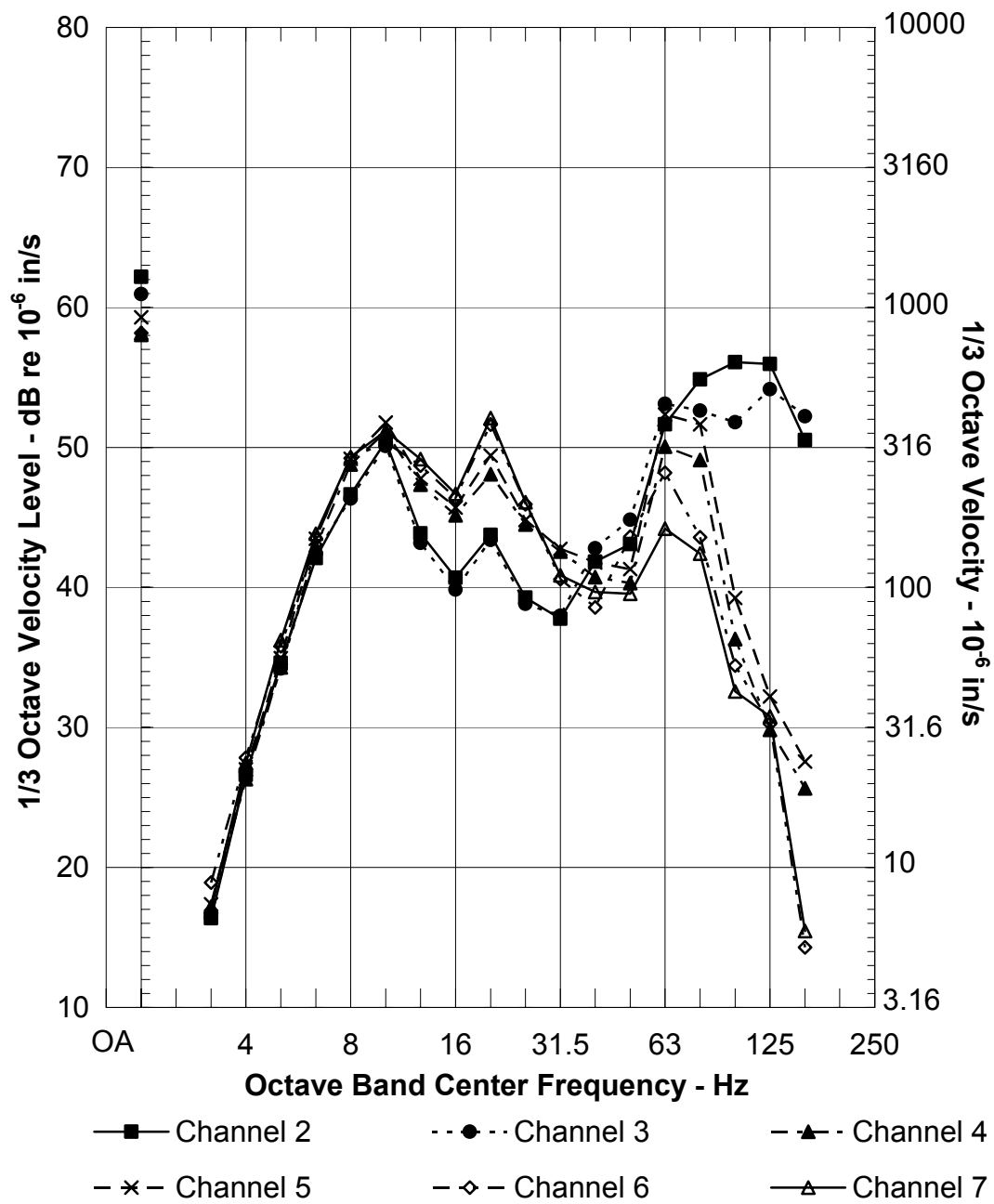
Moffett Field Vibration Velocity Levels
Kinkisharyo Train, 20 MPH

Figure C-18 20 MPH Train Vibration Velocity at Moffett Field



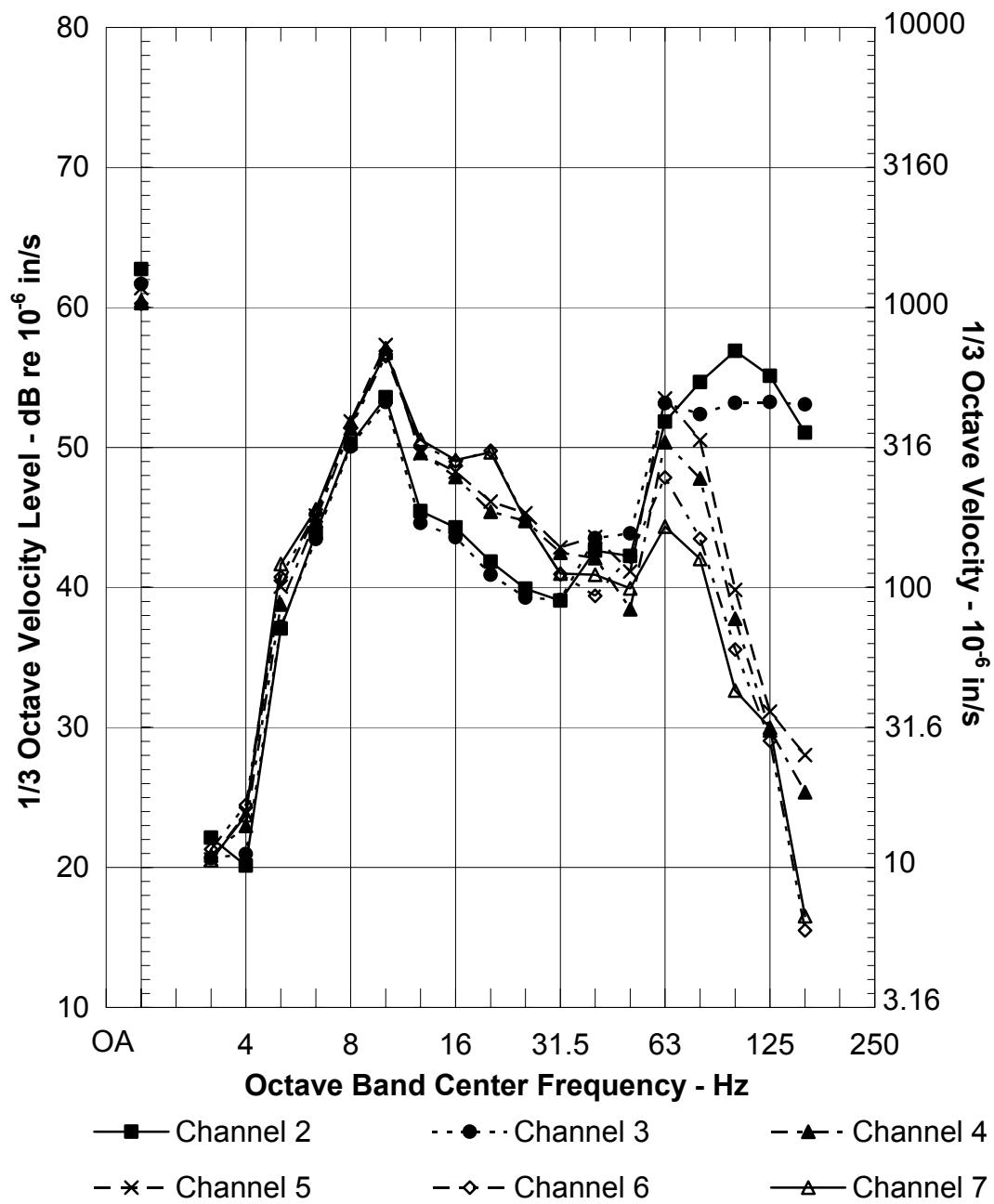
Moffett Field Vibration Velocity Levels
Kinkisharyo Train, 25 MPH

Figure C-19 25 MPH Train Vibration Velocity at Moffett Field



Moffett Field Vibration Velocity Levels
Kinkisharyo Train, 30 MPH

Figure C-20 30 MPH Train Vibration Velocity at Moffett Field



Moffett Field Vibration Velocity Levels
Kinkisharyo Train, 35 MPH

Figure C-21 35 MPH Train Vibration Velocity at Moffett Field

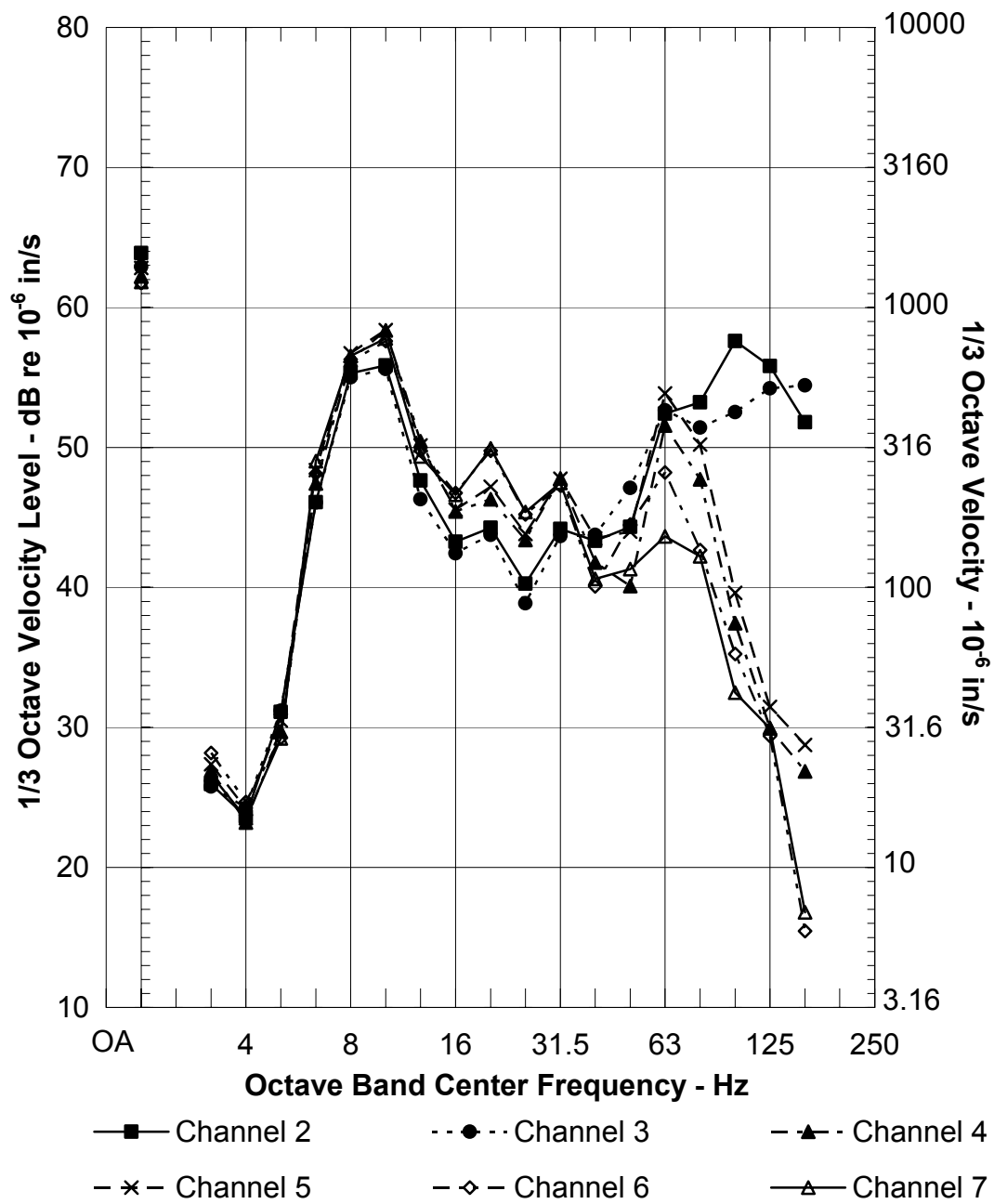
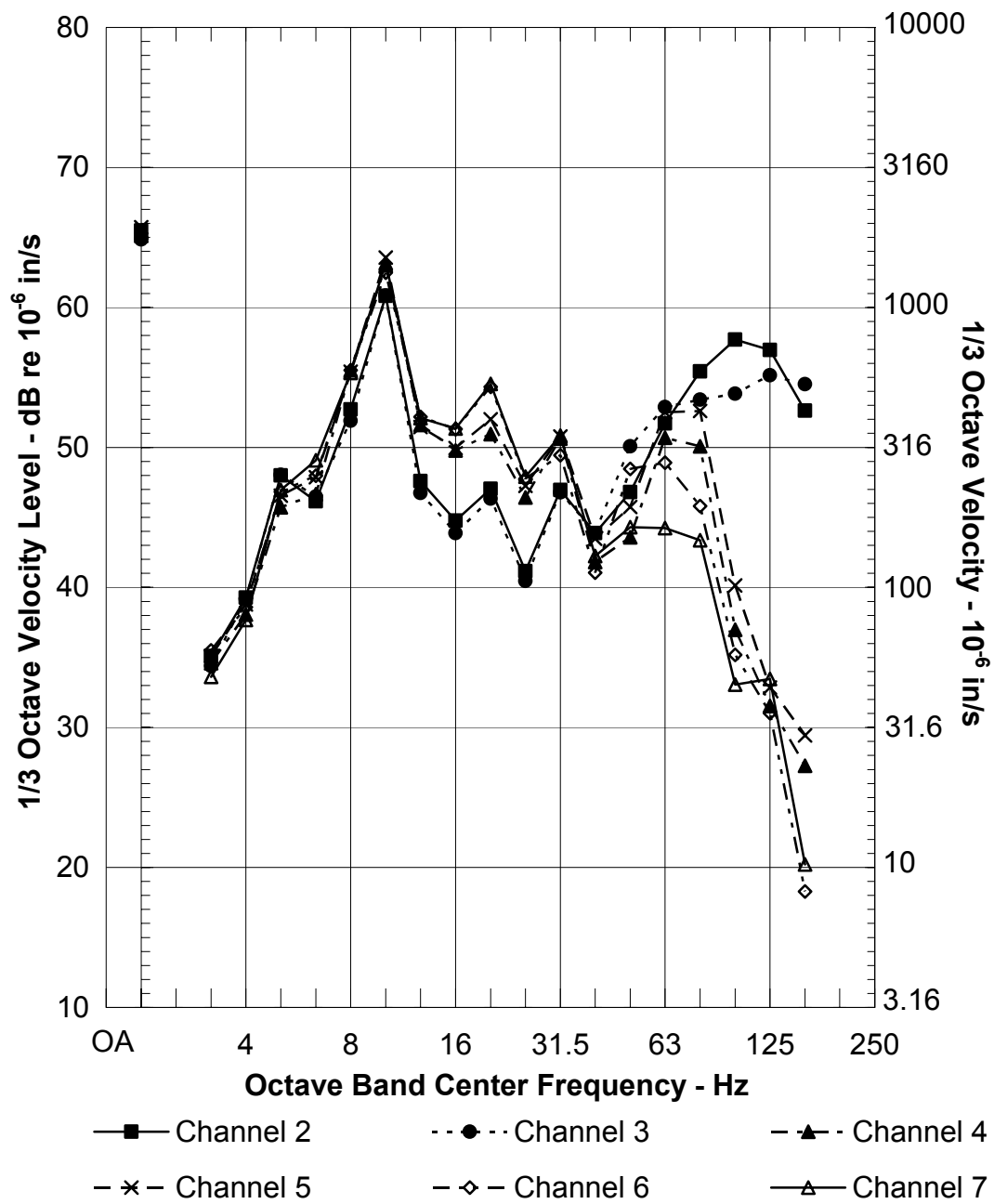
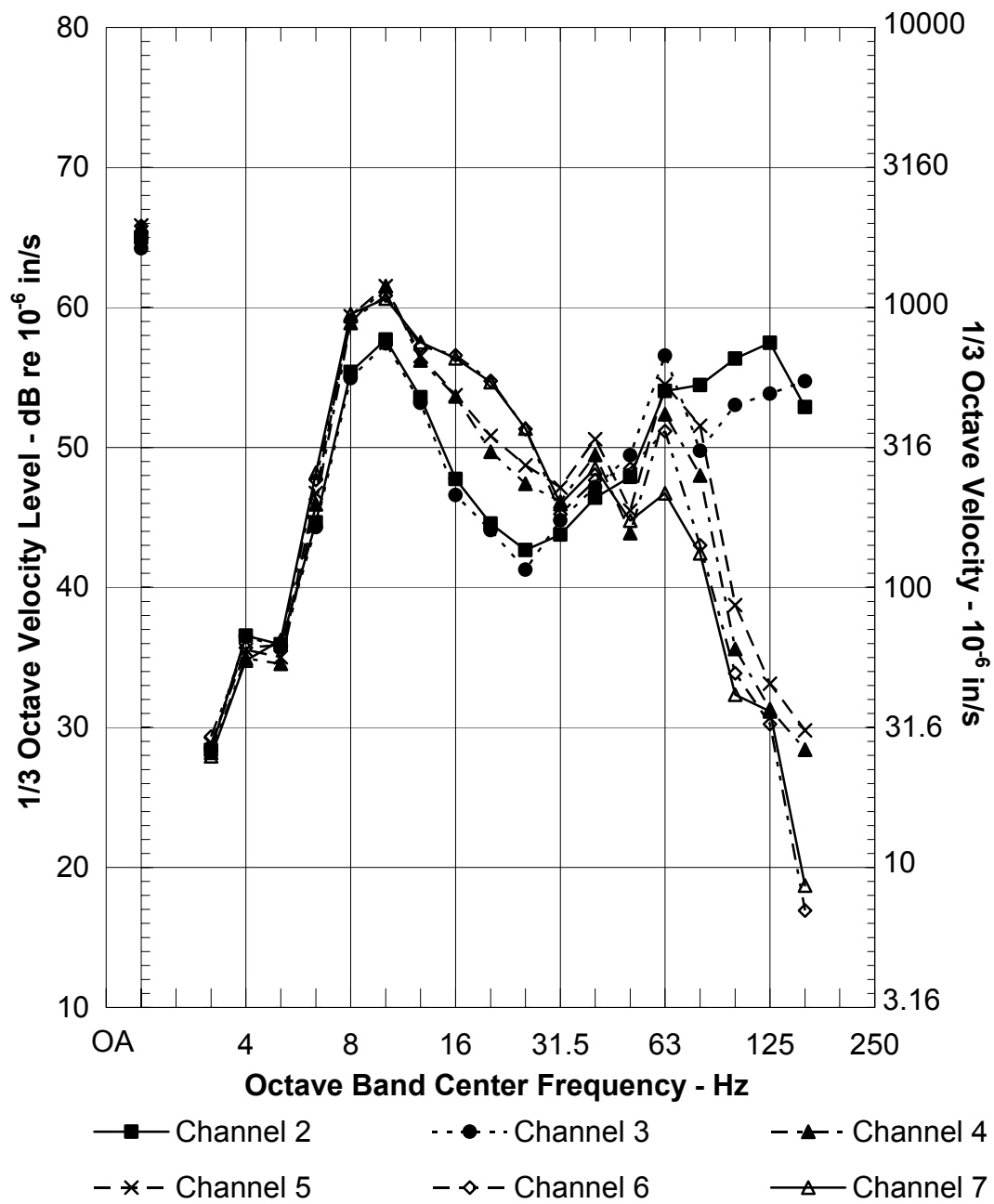


Figure C-22 40 MPH Train Vibration Velocity at Moffett Field



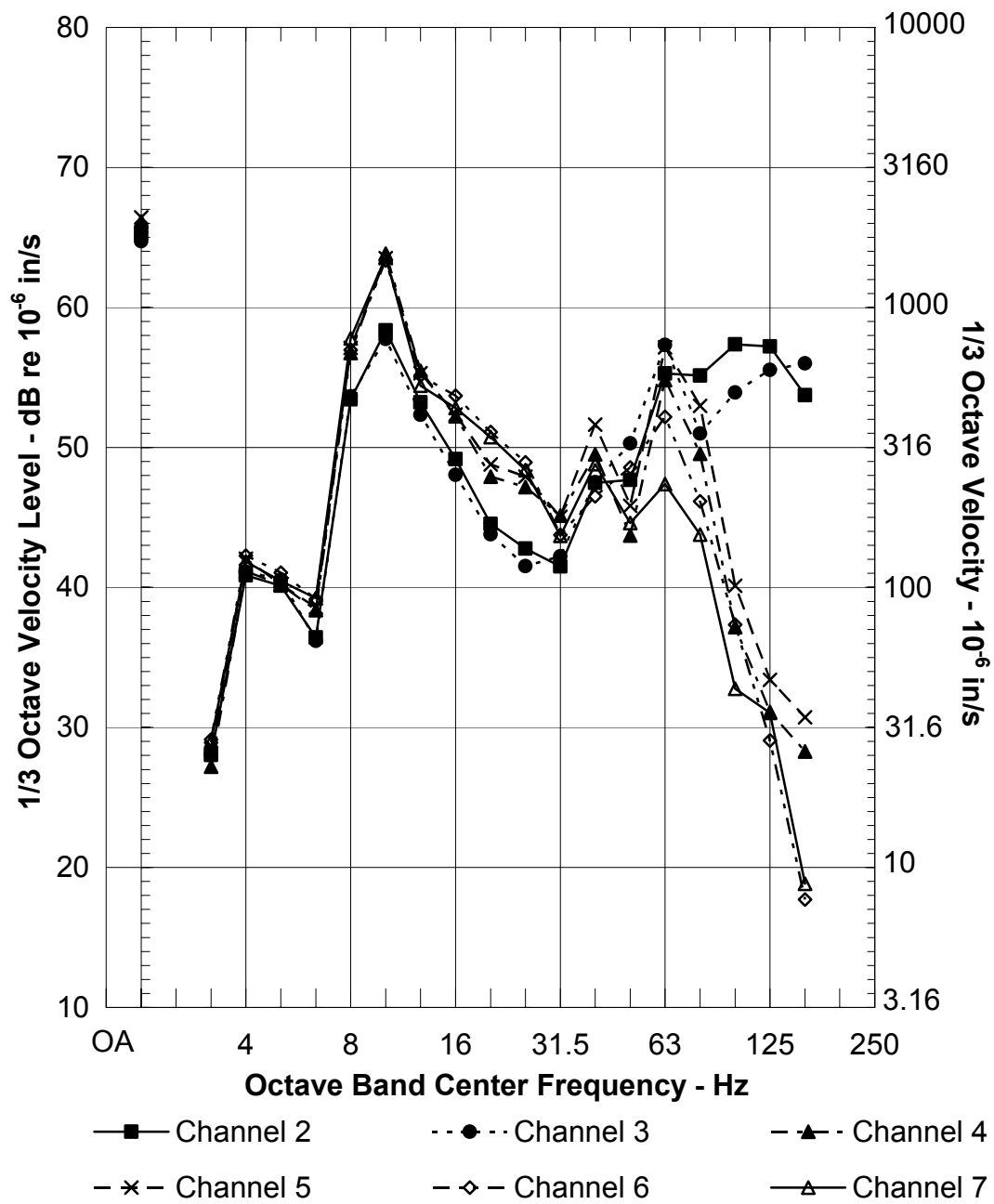
Moffett Field Vibration Velocity Levels
Kinkisharyo Train, 45 MPH

Figure C-23 45 MPH Train Vibration Velocity at Moffett Field



Moffett Field Vibration Velocity Levels
Kinkisharyo Train, 50 MPH

Figure C-24 50 MPH Train Vibration Velocity at Moffett Field



Moffett Field Vibration Velocity Levels
Kinkisharyo Train, 55 MPH

Figure C-25 55 MPH Train Vibration Velocity at Moffett Field

C-7.2 Line Source Responses

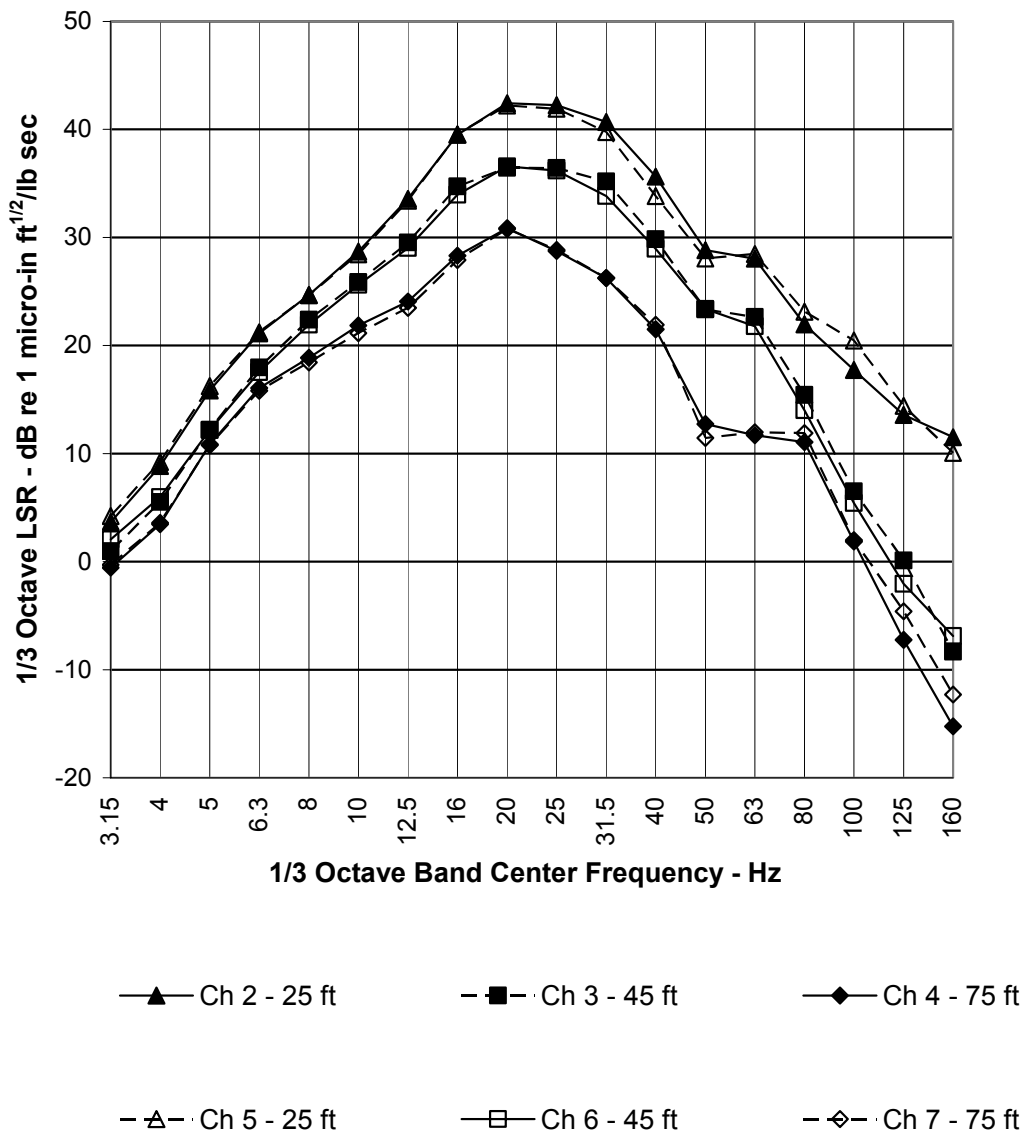
The line source responses measured at each location are illustrated in Figure C-26 through Figure C-28.

At 475 Ellis, considerable attenuation versus distance occurred, as is usual. The ground terrain was flat at this location, and shows a peak centered at about 20 to 25 Hz.

At the Mountain View site the attenuation between the 28- and 64-foot locations limited to a few decibels. Moreover, the LSR contains a very broad peak, with a uniform top between 10 and 60 Hz. At 64 feet, the LSR contains a node at about 20 Hz. The possibility exists of enhanced transmission between the two distances caused by the roads sub-grade compaction.

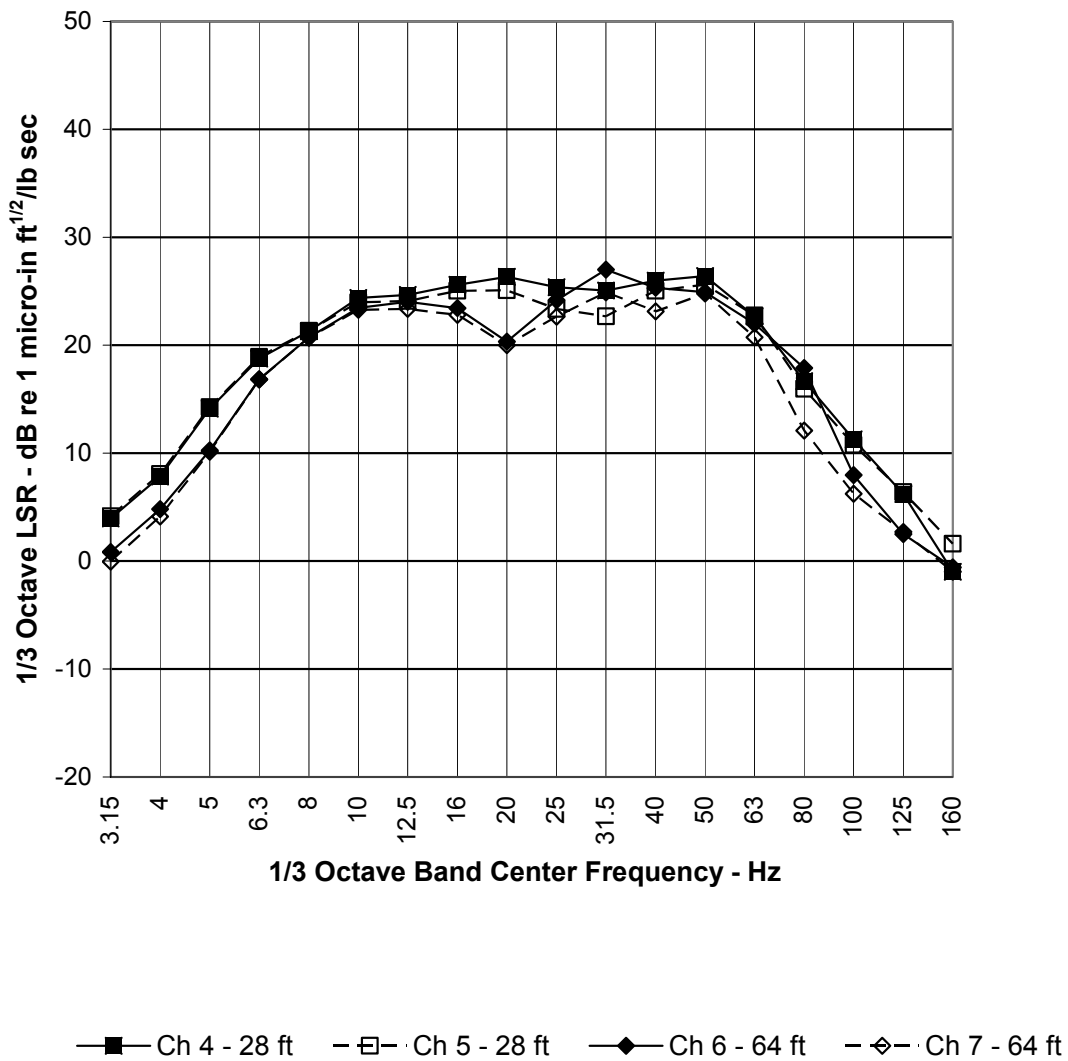
At Moffett, the LSR's exhibited an increase with increasing distance from the retaining wall at frequencies above about 10 Hz. The opposite behavior occurs at lower frequencies. This behavior is consistent with diffraction of vibration waves generated at the below-grade track position and propagating around the retaining wall to the distal receivers. The response at frequencies above 60 Hz at the 18.5-foot distance is consistent with propagation of vibration up the retaining wall.

The LSR's obtained at the same distance from the track at the same site are in good agreement, indicating that transducer mounting and data analyses were very consistent, and that the soil properties are reasonably uniform in the horizontal directions. If the transducers were separated by greater distances, such that large differences in soil layer depths, stiffness, and damping existed between the measurement points, less agreement would have been achieved between the LSR's at the same offset.



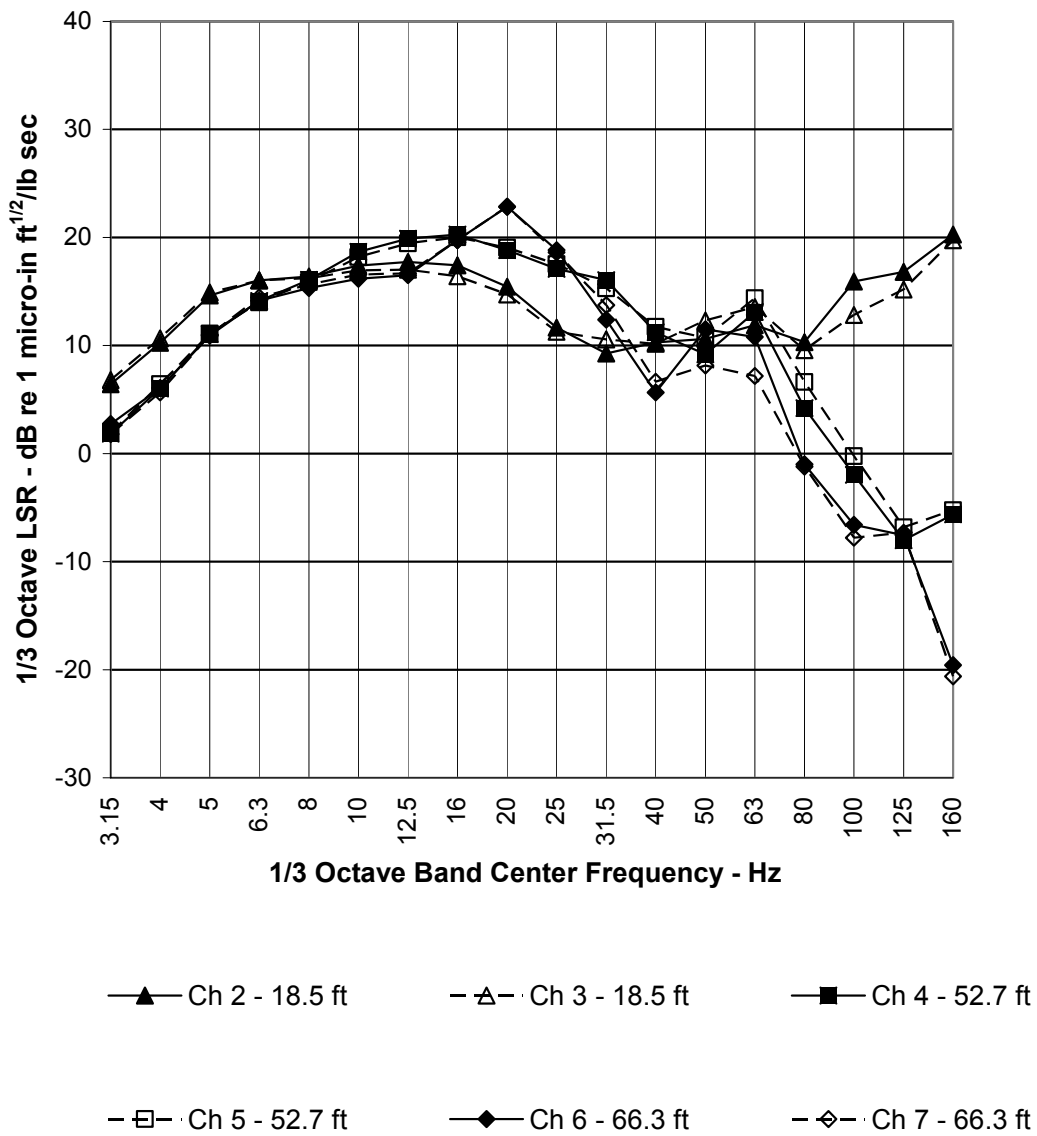
Soil LSR - 475 Ellis
 All Channels
 Train Length=90 ft

Figure C-26 Line Source Responses at 475 Ellis



Soil LSR - Mountain View
All Channels
Train Length=90 ft

Figure C-27 Line Source Responses at Mountain View Site



Soil LSR - Moffett Field
 All Channels
 Train Length=90 ft

Figure C-28 Line Source Responses at the Moffett Field Site

C-7.3 Force Density Levels

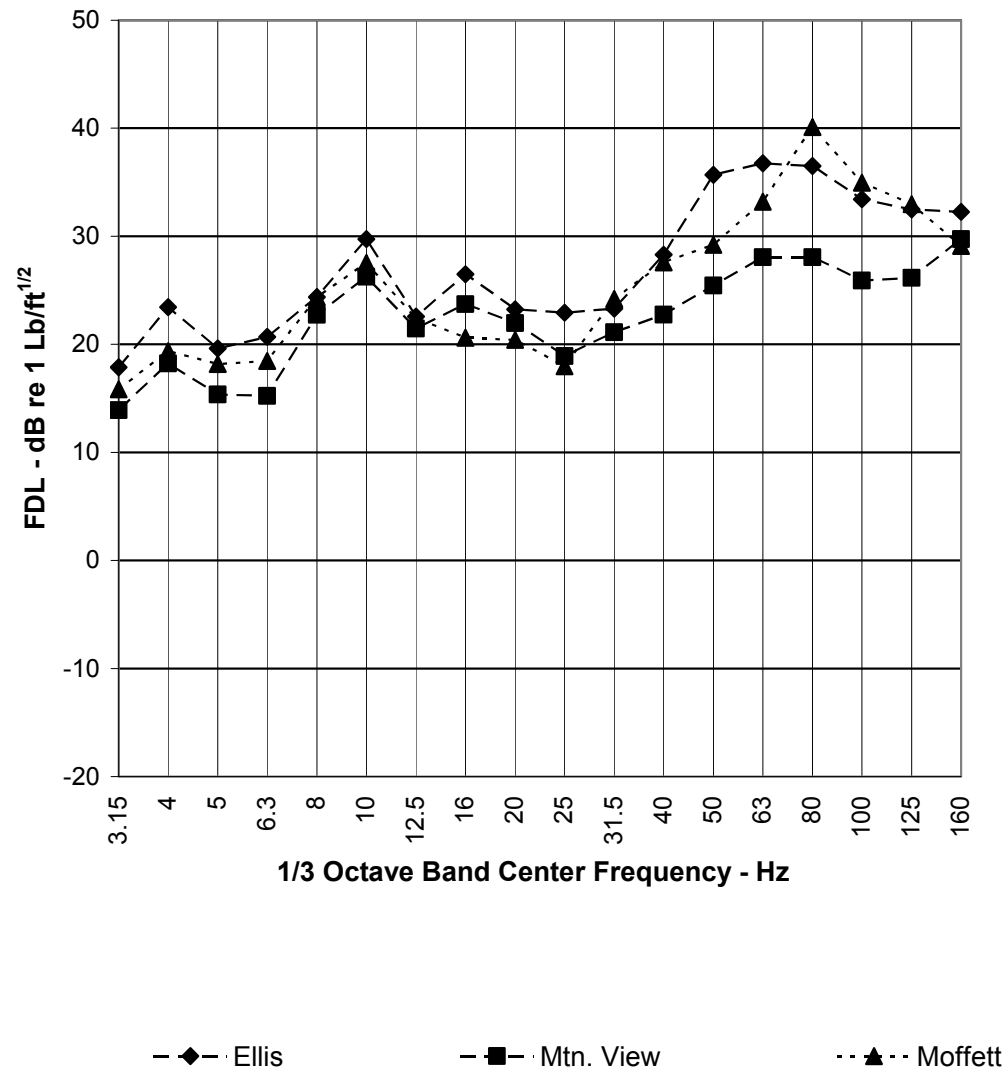
Third octave band Force Density Level spectra are presented below in Figure C-29 through Figure C-52. Speeds of 20 to 45 mph are represented in Figure C-29 through Figure C-46 for all three locations. Speeds of 50 and 55 mph could not be obtained at the Ellis site, and a speed of 55 mph could not be obtained at the Mountain View site. Thus, Figure C-47 through Figure C-49 do not have spectra for 50 mph runs at Ellis, and Figure C-50 through Figure C-52 show 55mph data for only the Moffett site.

Figure C-53 illustrates the energy-averaged FDL for each train speed. Each average includes each direction, measurement channel, and test site. These curves thus represent the FDL appropriate for design.

The frequency of the broad peak at about 80 Hz does not change with train speed. The peak is likely due to the track support resonance and the resonance of the resilient Bochum 54 and 84 wheels.

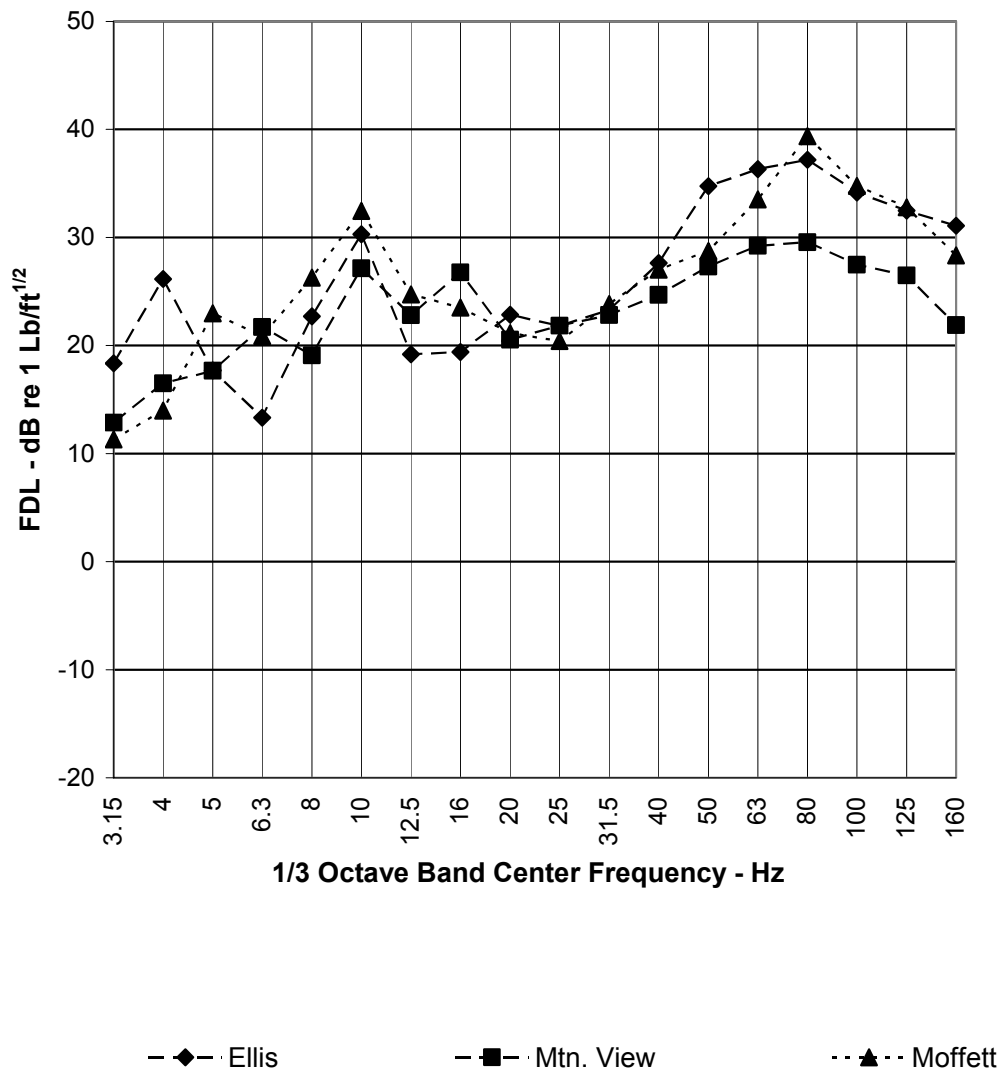
All of the data indicate the presence of a resonance in the primary suspension between 6.3 and 10 Hz. The frequency of wheel rotation and frequency of rail undulation increase linearly with train speed. The peak at 6.3 to 10 Hz appears to be very sensitive to train speed, suggesting a very lightly damped resonance of the primary suspension system. When the wheel rotation frequency and/or rail undulation frequency is coincident with the resonance frequency, the amplitude of vibration forces is limited only by damping in the suspension and radiation losses into the ground.

Figure C-54 illustrates the FDL averaged over all train speeds. This composite FDL should not necessarily be used for prediction purposes; its purpose is to illustrate the resonance of the primary suspension at about 8 to 10 Hz. There would appear to be a 12-decibel amplification of vibration forces at the primary suspension resonance, consistent with a damping ratio of about 12%.



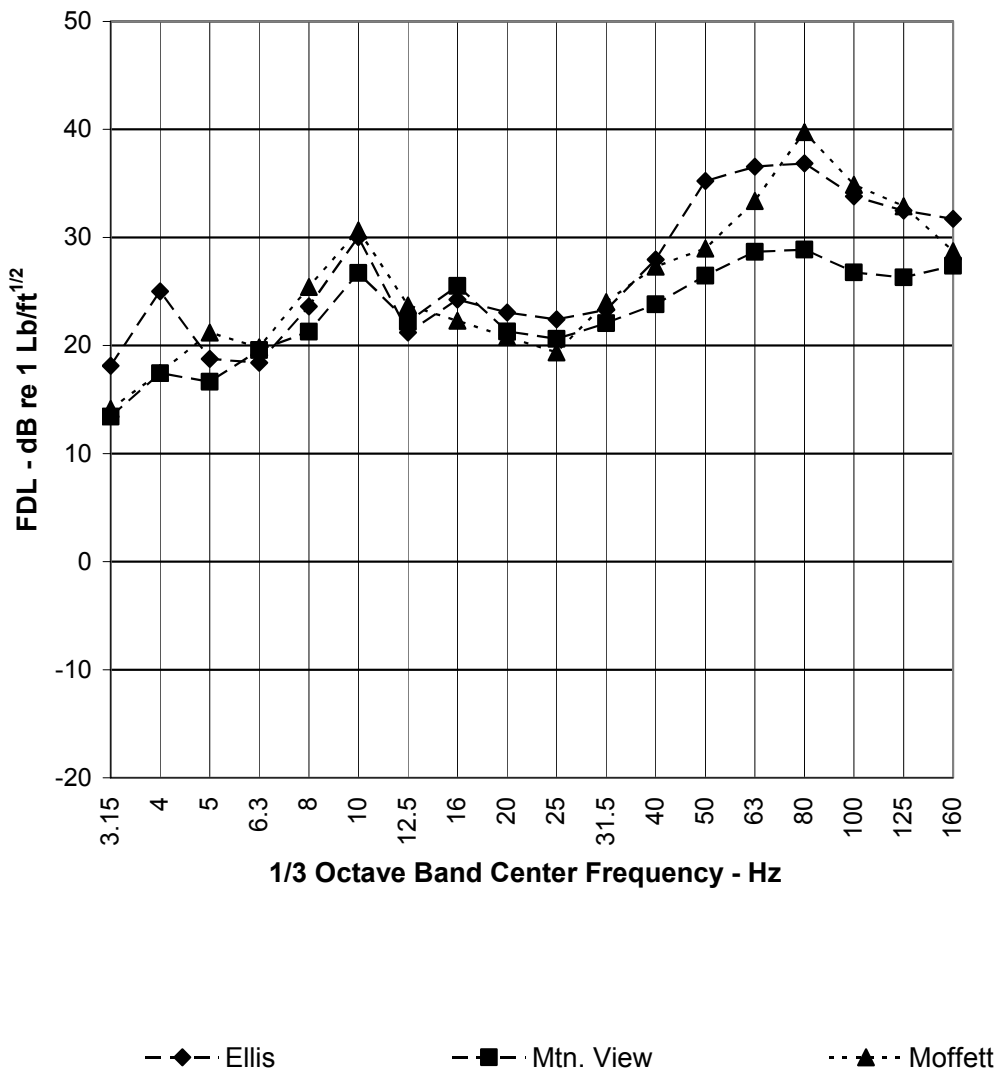
EB 20 MPH Test Train
All Locations, Averaged by Channel
Train Length=90 ft

Figure C-29 FDL for Kinkisharyo Eastbound at 20 mph on Ballast and Concrete Tie Track



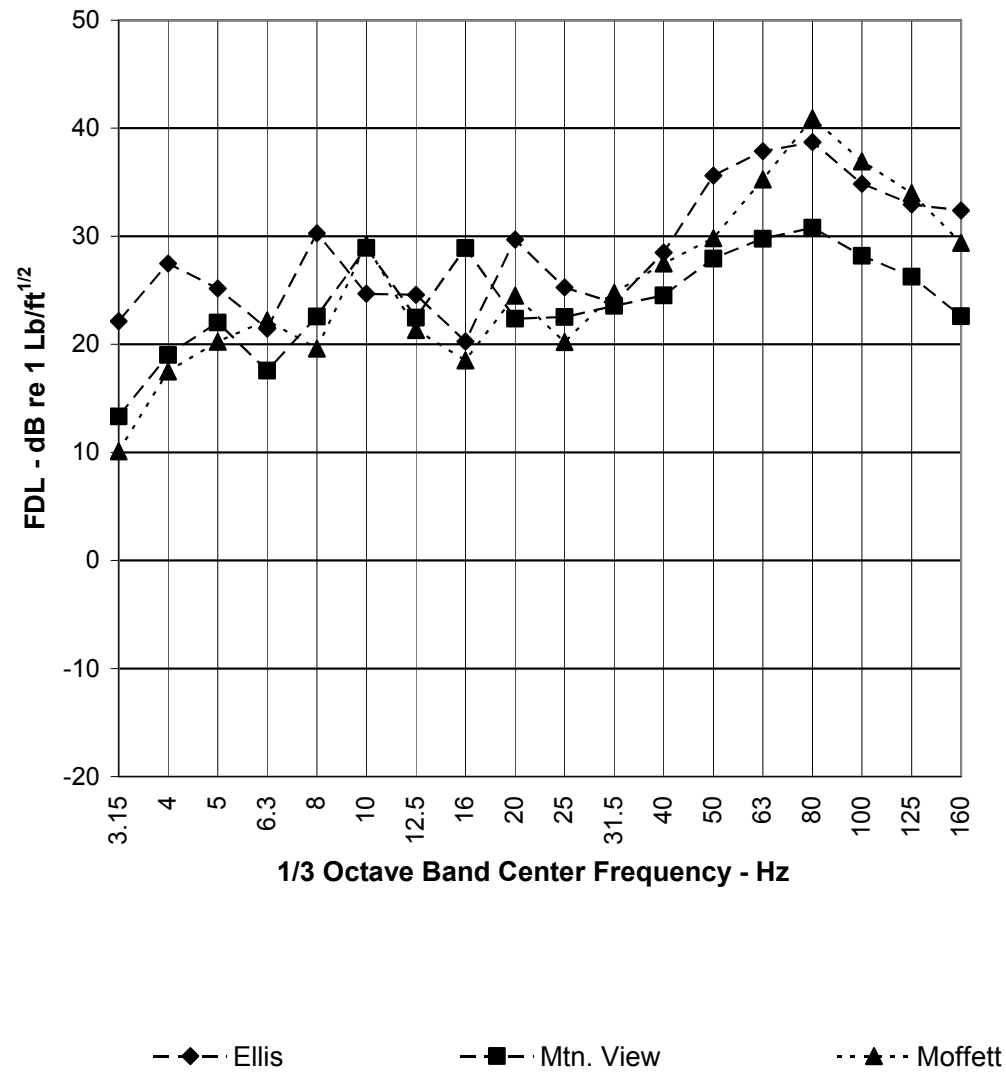
WB 20 MPH Test Train
All Locations, Averaged by Channel
Train Length=90 ft

Figure C-30 FDL for Kinkisharyo Westbound at 20 mph on Ballast and Concrete Tie Track



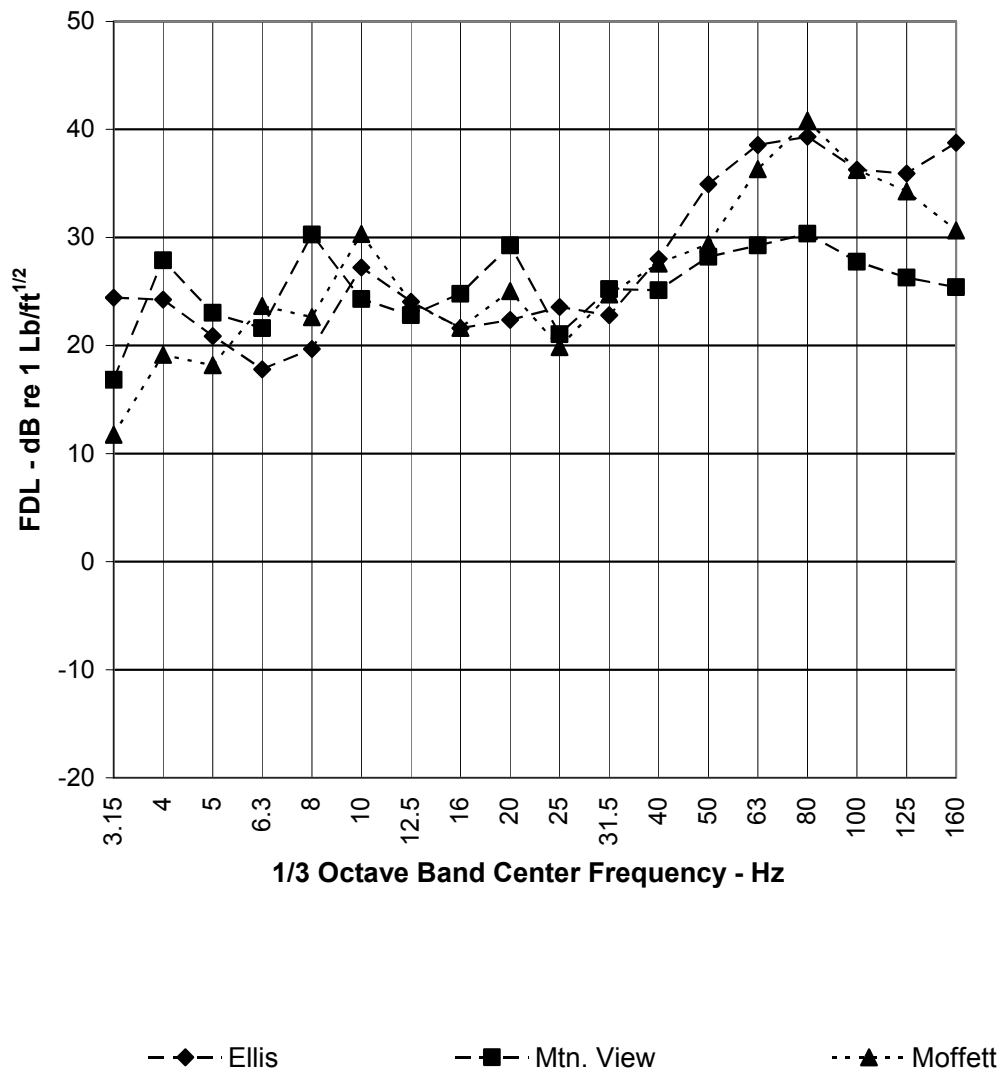
ALL 20 MPH Test Train
All Locations, Averaged by Channel
Train Length=90 ft

Figure C-31 FDL for Kinkisharyo Vehicle at 20mph on Ballast & Concrete Tie Track - Energy Average of Eastbound and Westbound Result



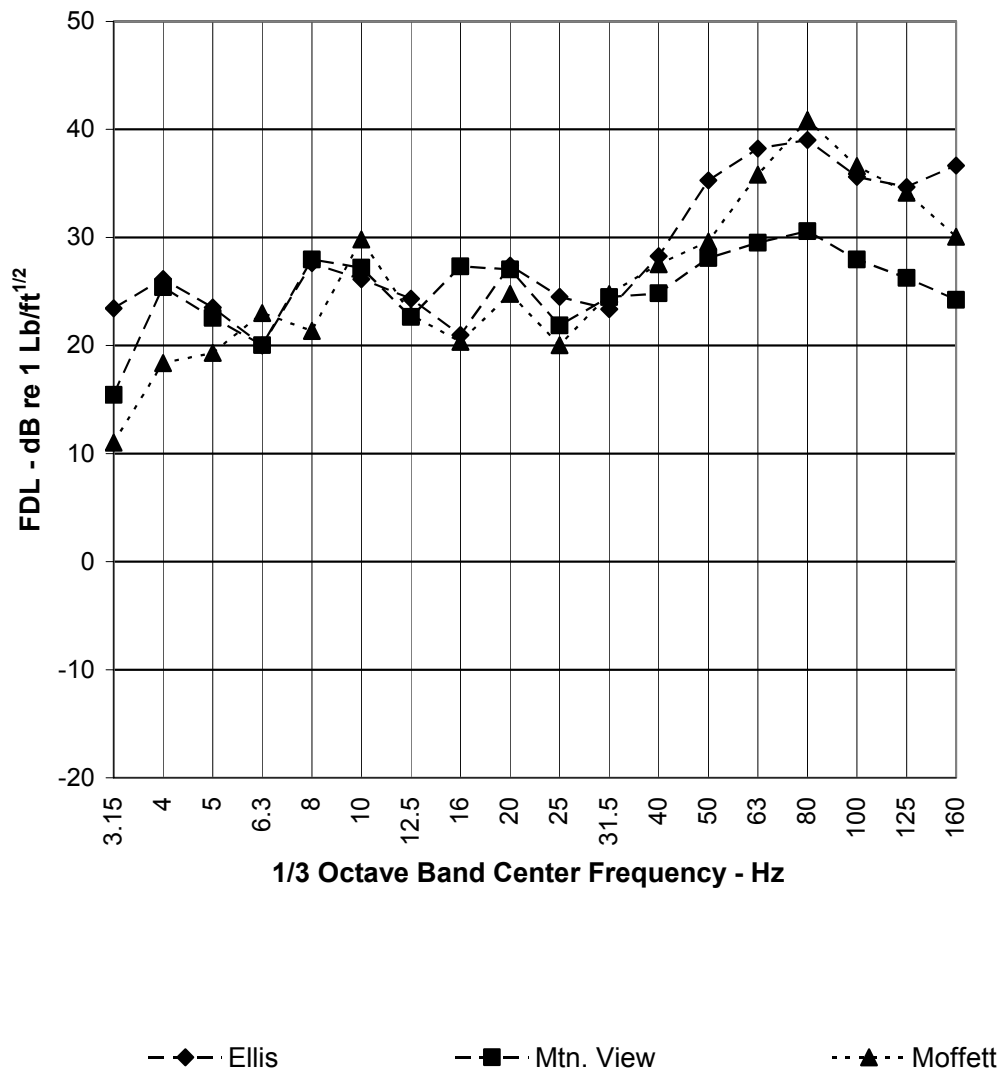
EB 25 MPH Test Train
All Locations, Averaged by Channel
Train Length=90 ft

Figure C-32 FDL of Kinkisharyo Vehicle Eastbound at 25mph on Ballast and Concrete Tie Track



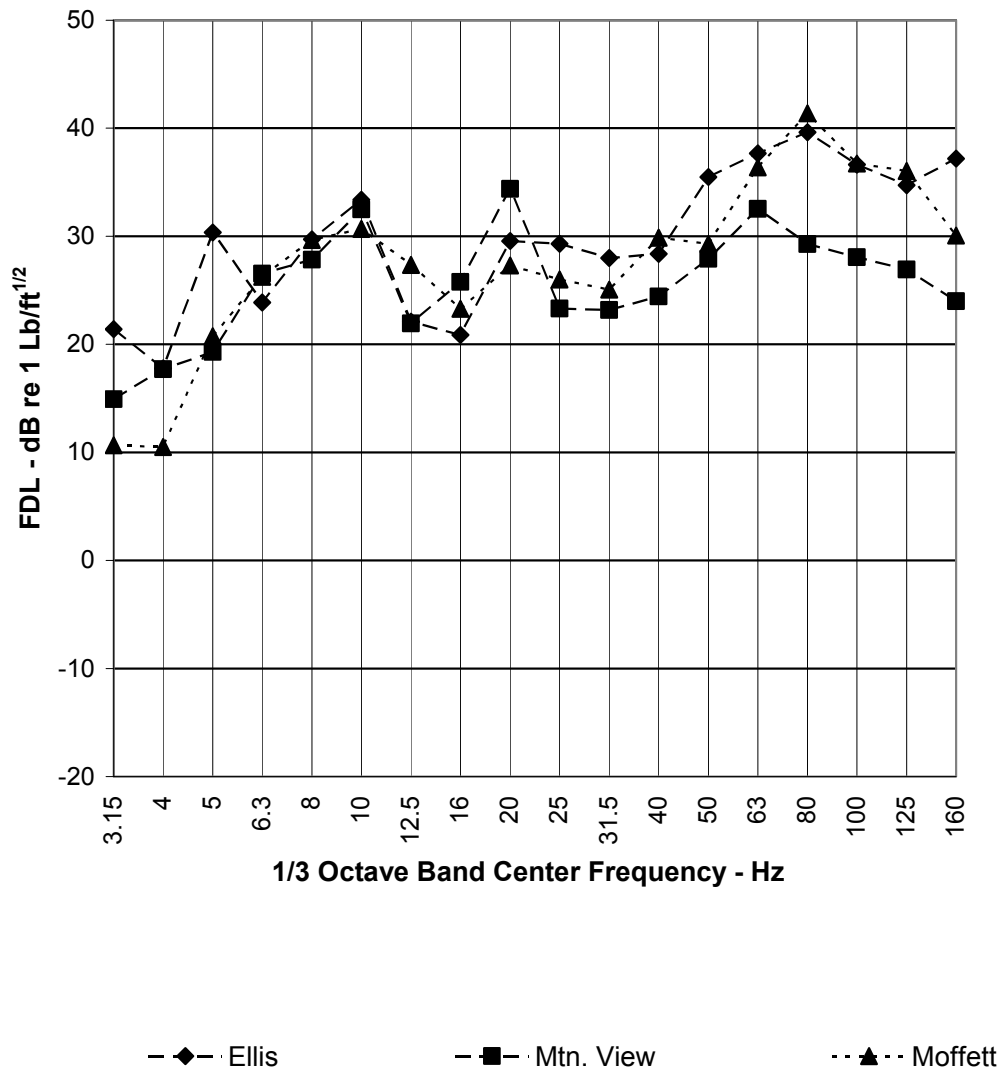
WB 25 MPH Test Train
All Locations, Averaged by Channel
Train Length=90 ft

Figure C-33 FDL of Kinkisharyo Vehicle Westbound at 25mph on Ballast and Concrete Tie Track



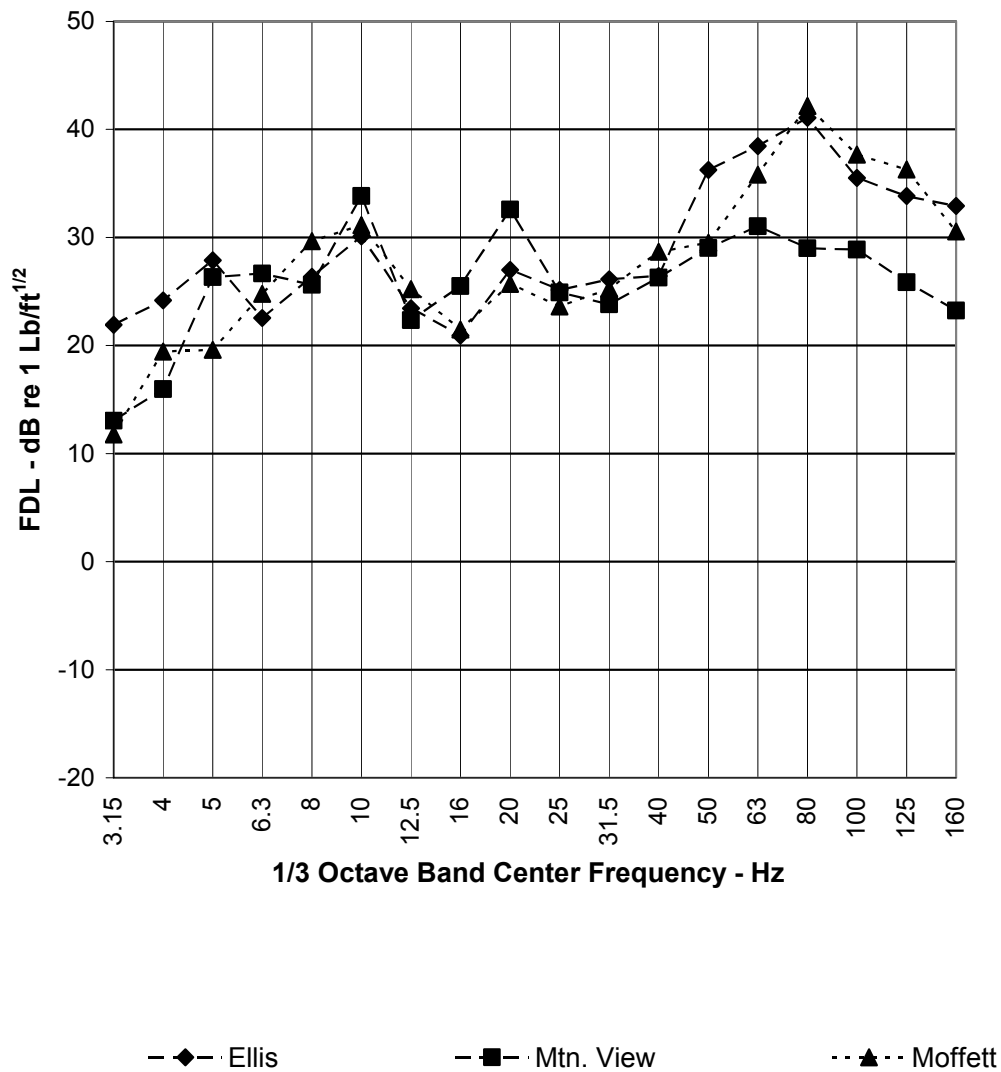
ALL 25 MPH Test Train
All Locations, Averaged by Channel
Train Length=90 ft

Figure C-34 FDL of Kinkisharyo Vehicle at 25mph on Ballast and Concrete Tie Track - Energy Average of Eastbound and Westbound Results



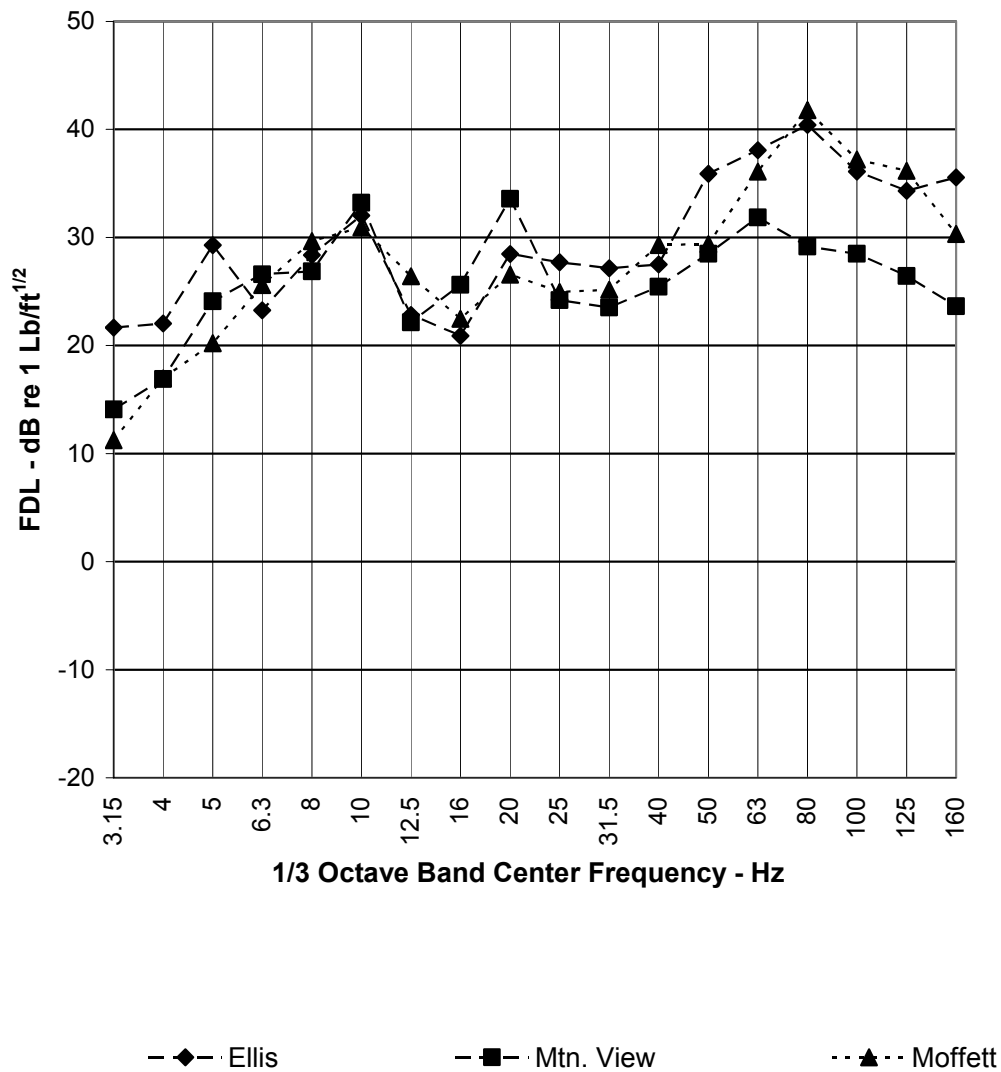
EB 30 MPH Test Train
All Locations, Averaged by Channel
Train Length=90 ft

Figure C-35 FDL of Kinkisharyo Vehicle Eastbound at 30mph on Ballast and Concrete Tie Track



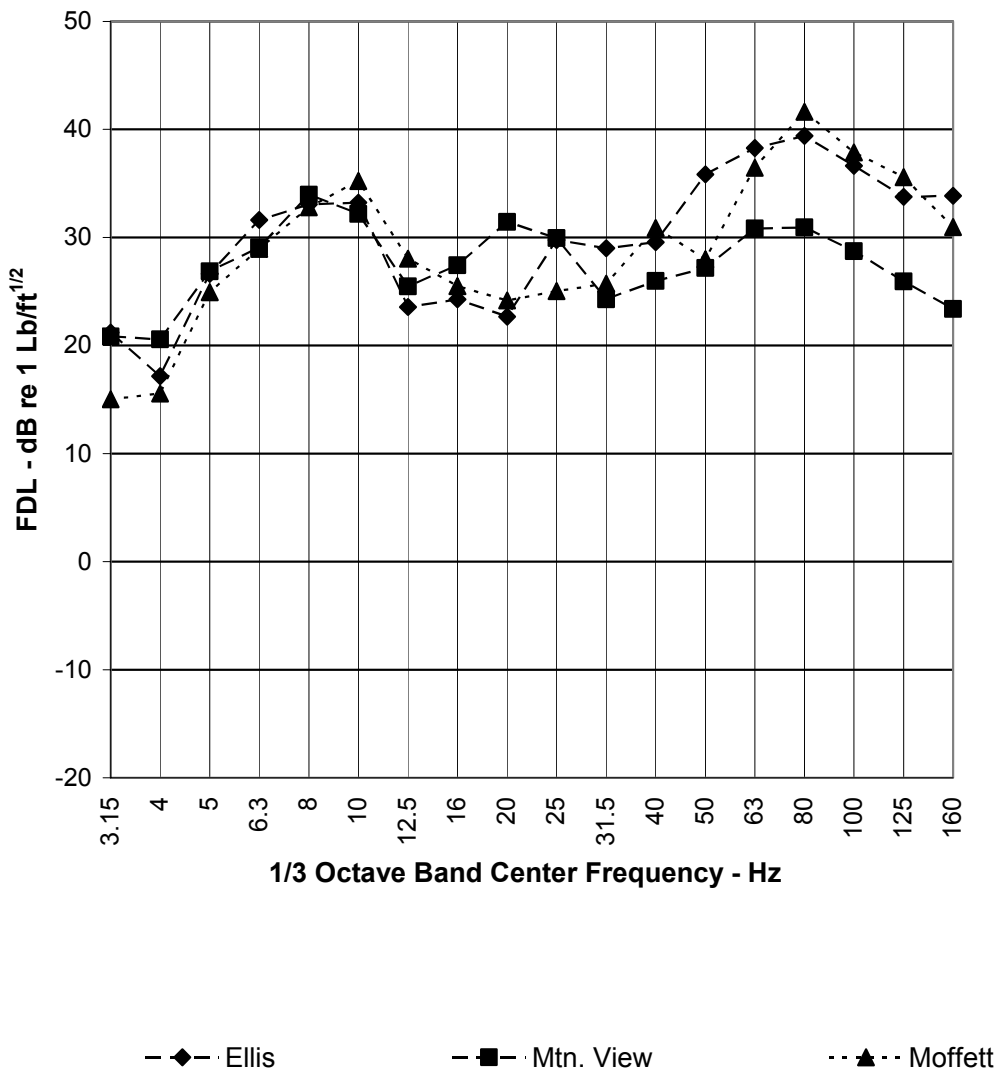
WB 30 MPH Test Train
All Locations, Averaged by Channel
Train Length=90 ft

Figure C-36 FDL of Kinkisharyo Vehicle Westbound at 30mph on Ballast and Concrete Tie Track



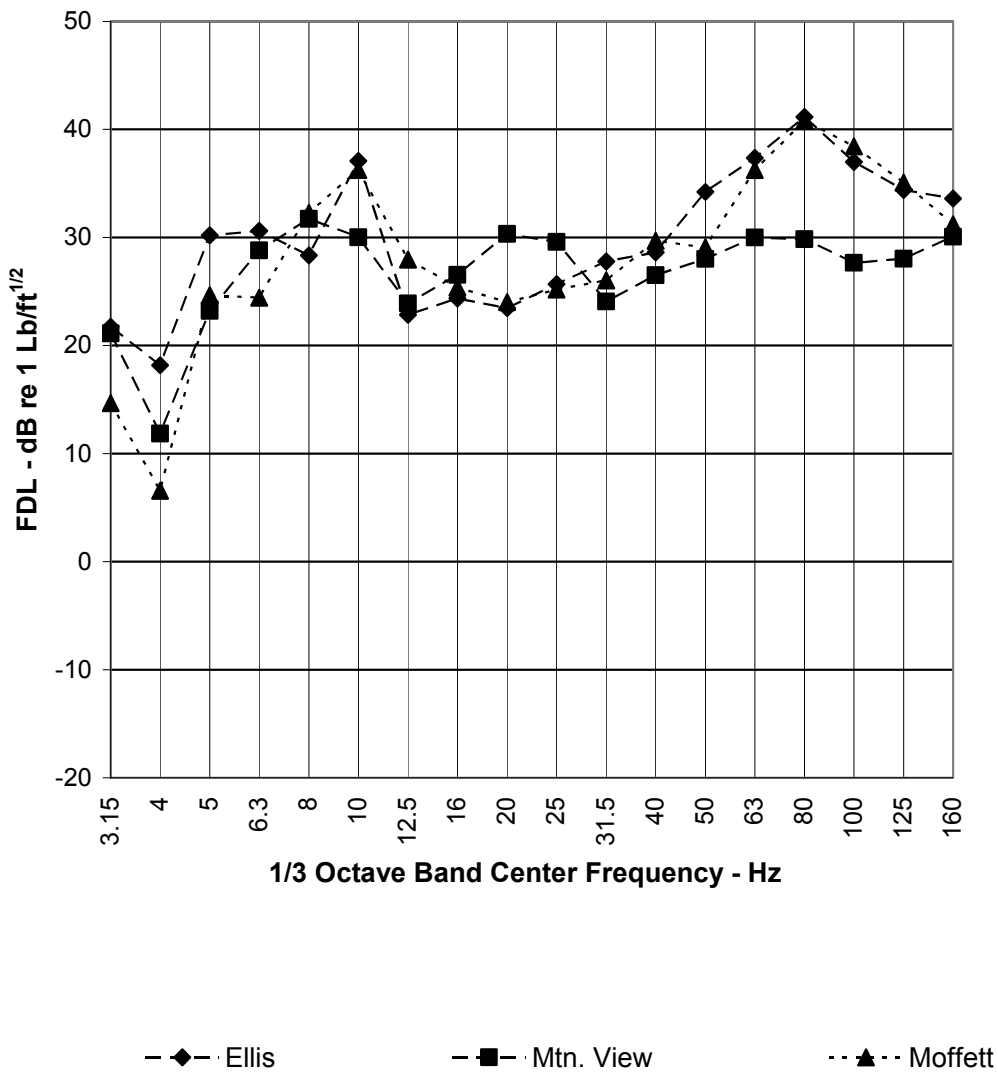
ALL 30 MPH Test Train
All Locations, Averaged by Channel
Train Length=90 ft

Figure C-37 FDL of Kinkisharyo Vehicle at 30mph on Ballast and Concrete Tie Track - Energy Average of Eastbound and Westbound Results



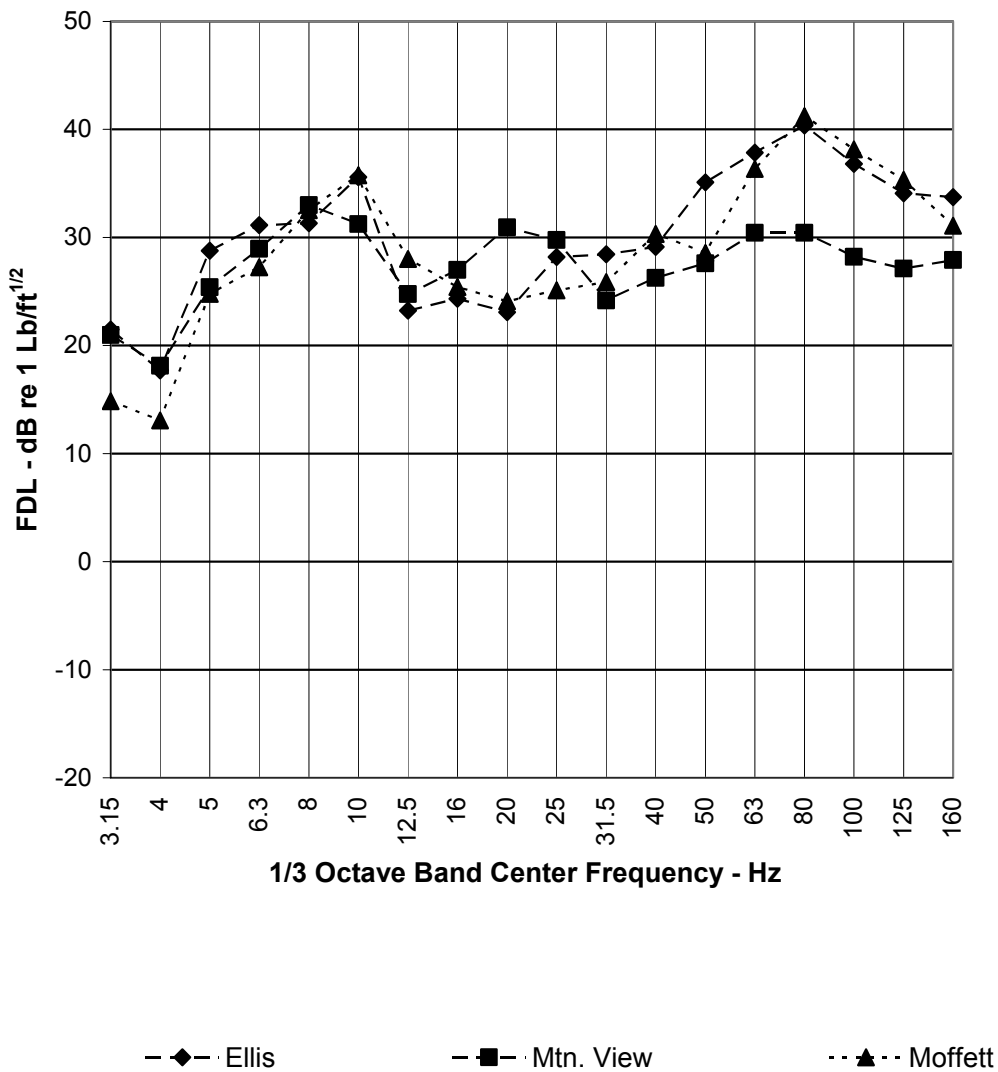
EB 35 MPH Test Train
All Locations, Averaged by Channel
Train Length=90 ft

Figure C-38 FDL of Kinkisharyo Vehicle Eastbound at 35mph on Ballast and Concrete Tie Track



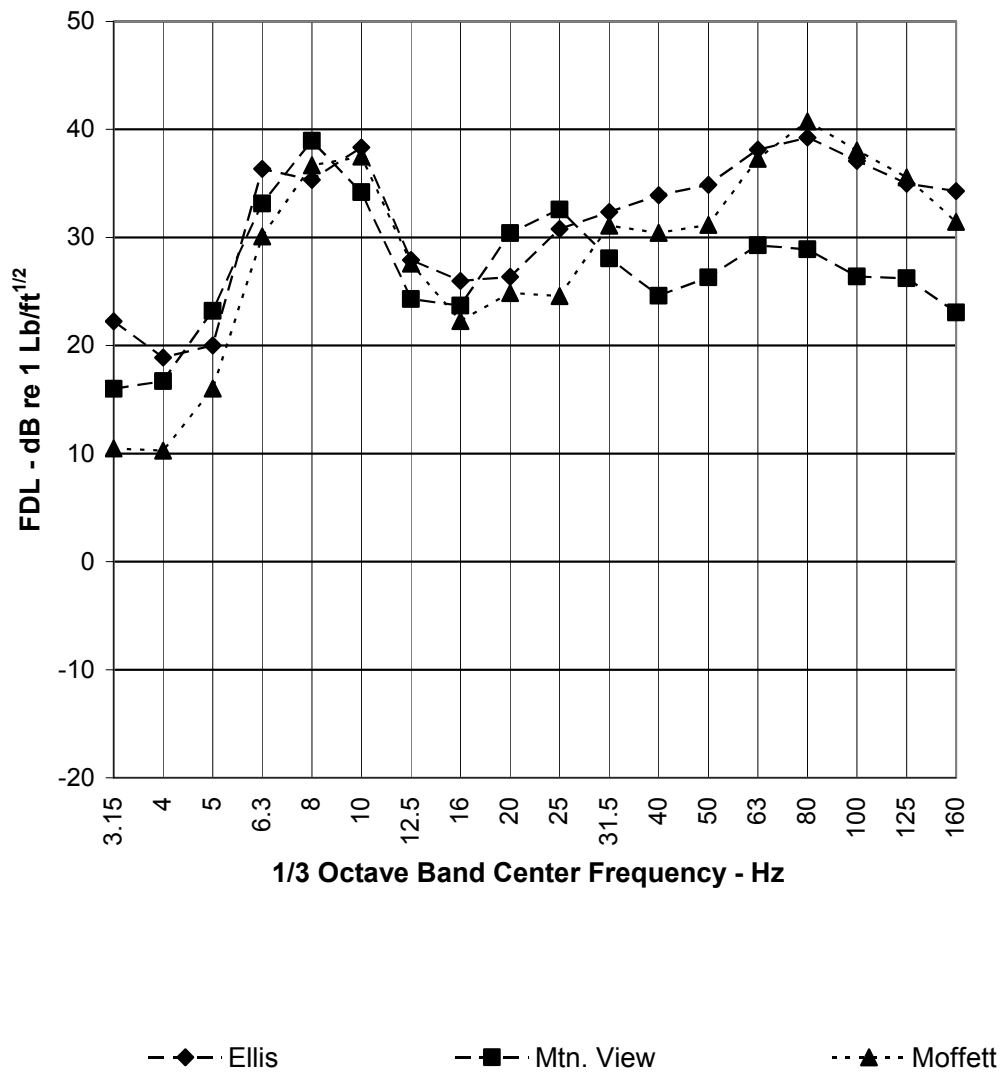
WB 35 MPH Test Train
All Locations, Averaged by Channel
Train Length=90 ft

Figure C-39 FDL of Kinkisharyo Vehicle Westbound at 35mph on Ballast and Concrete Tie Track



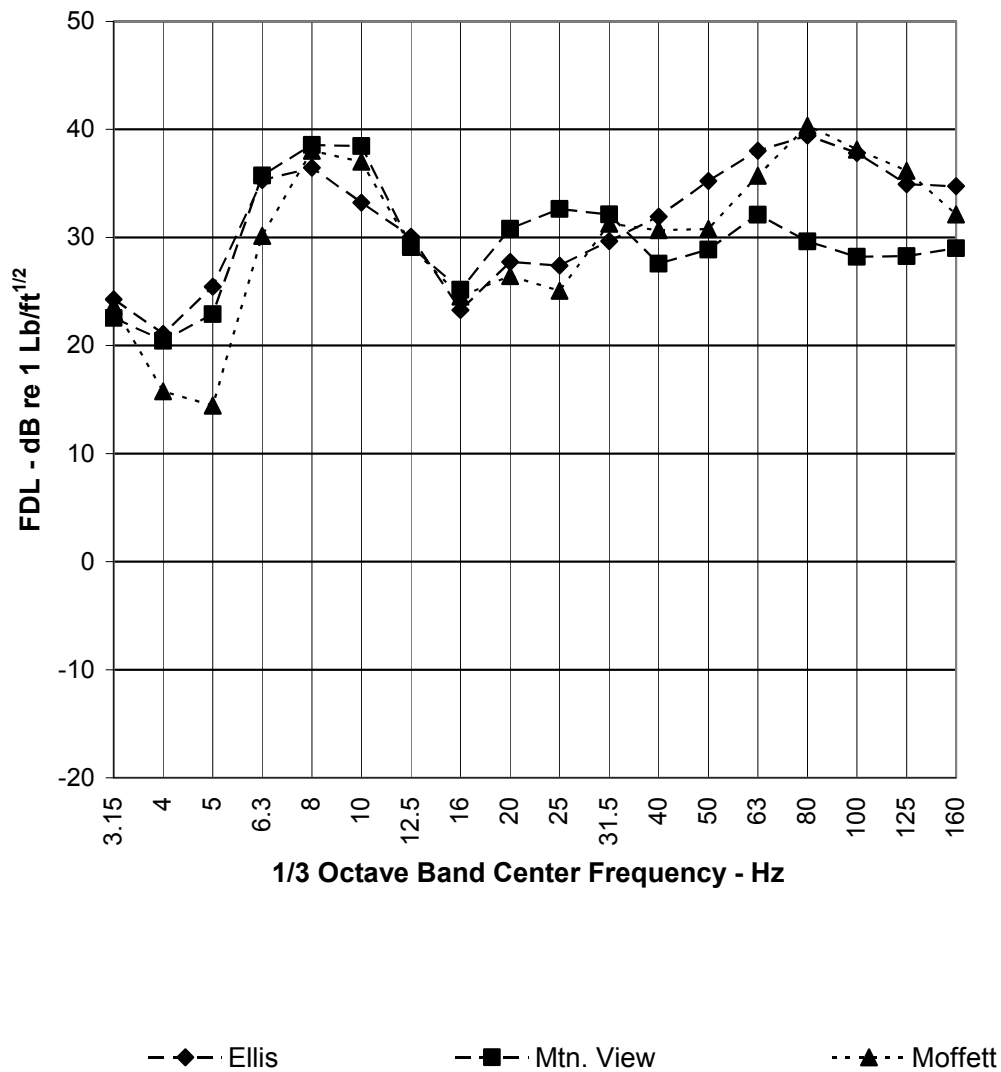
ALL 35 MPH Test Train
All Locations, Averaged by Channel
Train Length=90 ft

Figure C-40 FDL of Kinkisharyo Vehicle at 35mph on Ballast and Concrete Tie Track - Energy Average of Eastbound and Westbound Results



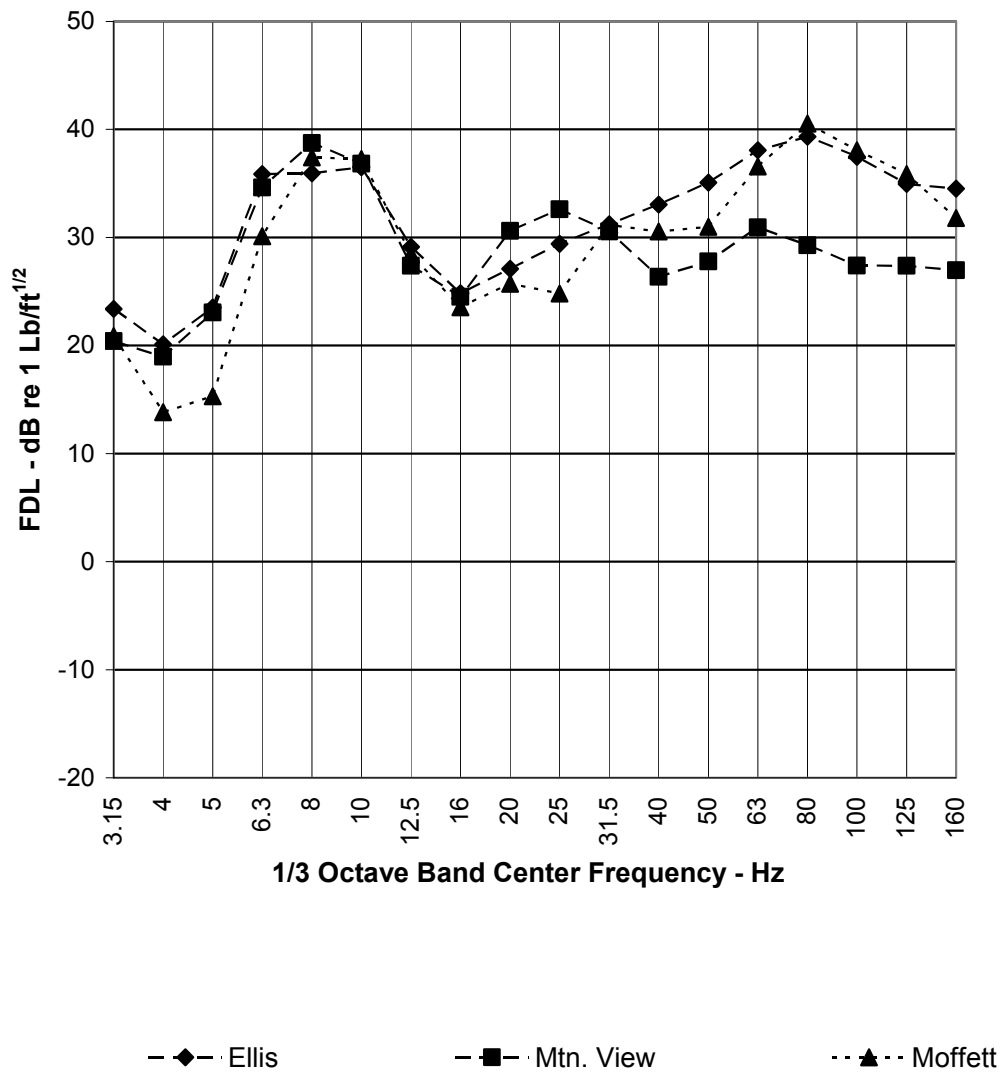
EB 40 MPH Test Train
All Locations, Averaged by Channel
Train Length=90 ft

Figure C-41 FDL of Kinkisharyo Vehicle Eastbound at 40mph on Ballast and Concrete Tie Track



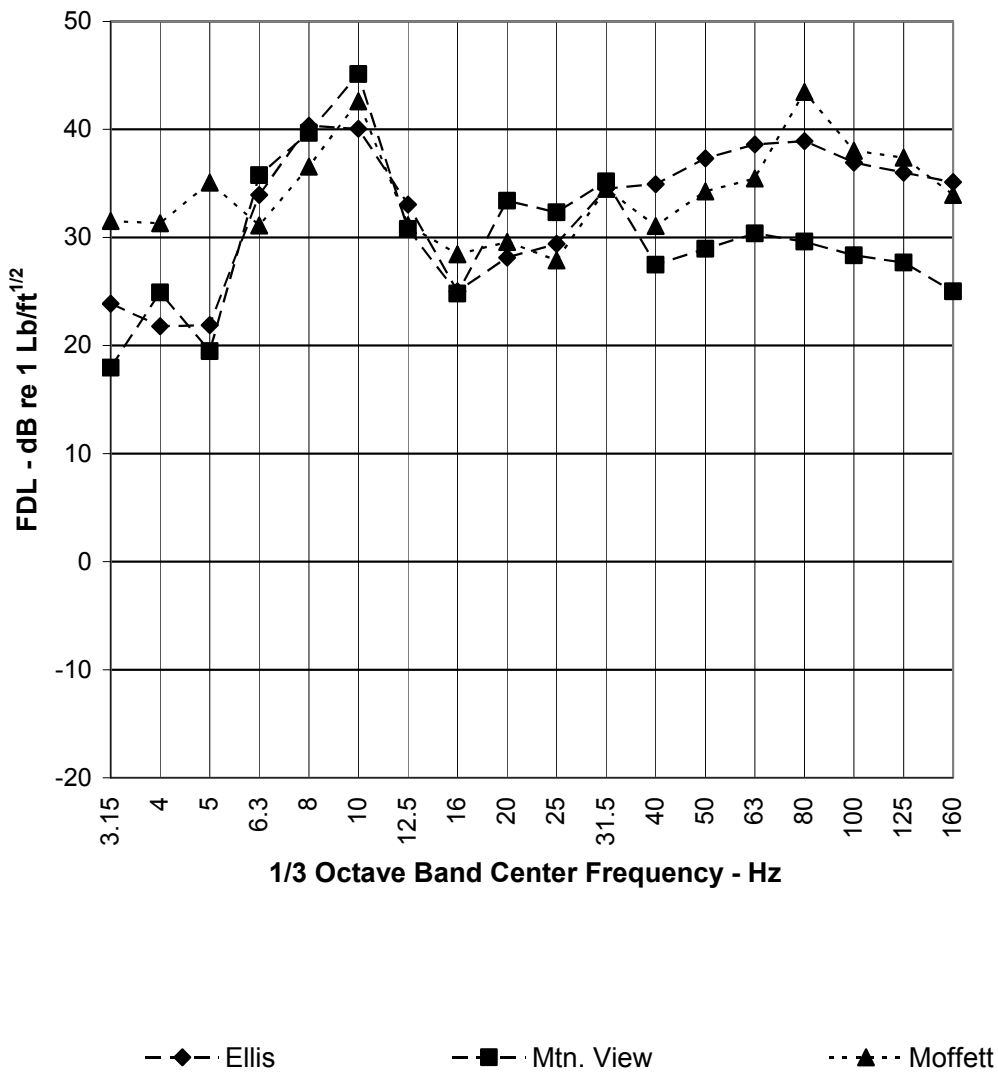
WB 40 MPH Test Train
All Locations, Averaged by Channel
Train Length=90 ft

Figure C-42 FDL of Kinkisharyo Vehicle Westbound at 40mph on Ballast and Concrete Tie Track



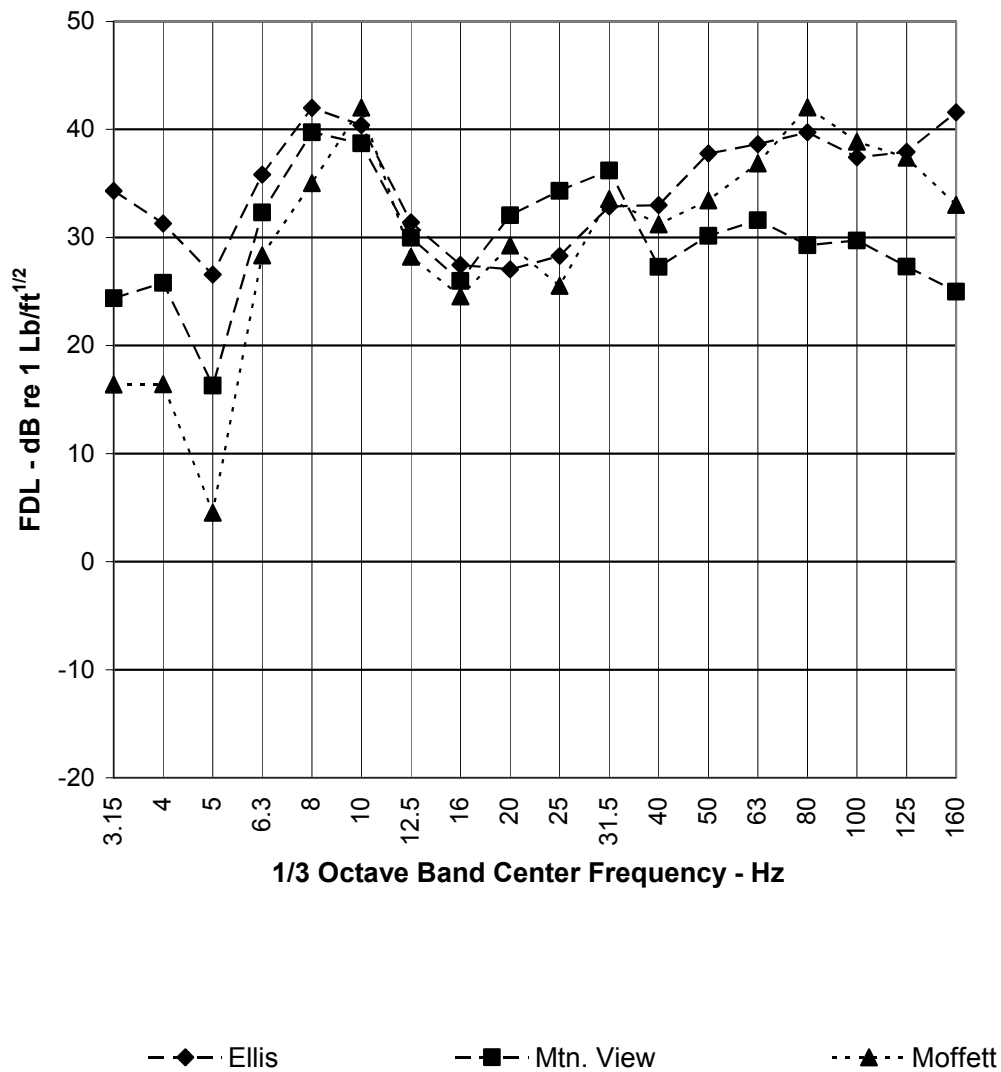
ALL 40 MPH Test Train
All Locations, Averaged by Channel
Train Length=90 ft

Figure C-43 FDL of Kinkisharyo Vehicle at 40mph on Ballast and Concrete Tie Track - Energy Average of Eastbound and Westbound Results



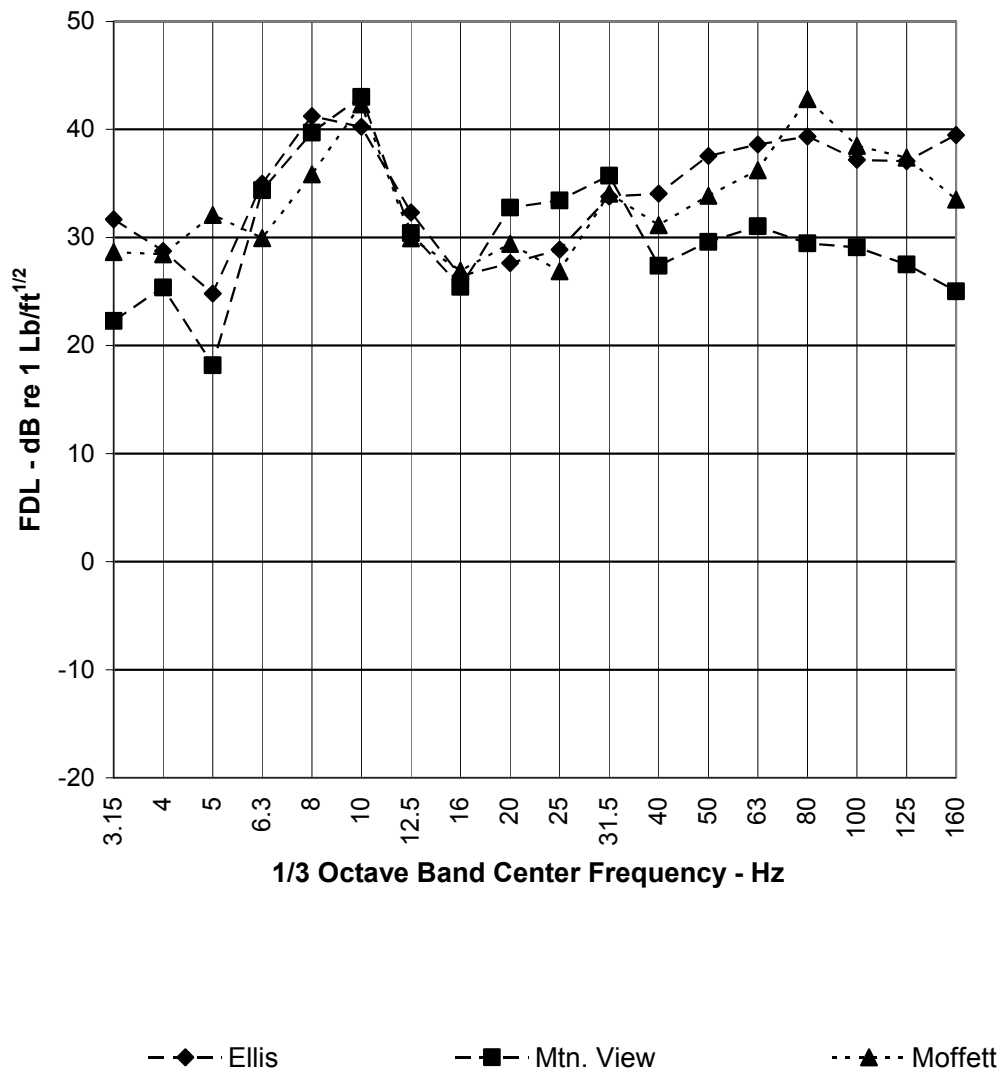
EB 45 MPH Test Train
All Locations, Averaged by Channel
Train Length=90 ft

Figure C-44 FDL of Kinkisharyo Vehicle Eastbound at 45mph on Ballast and Concrete Tie Track



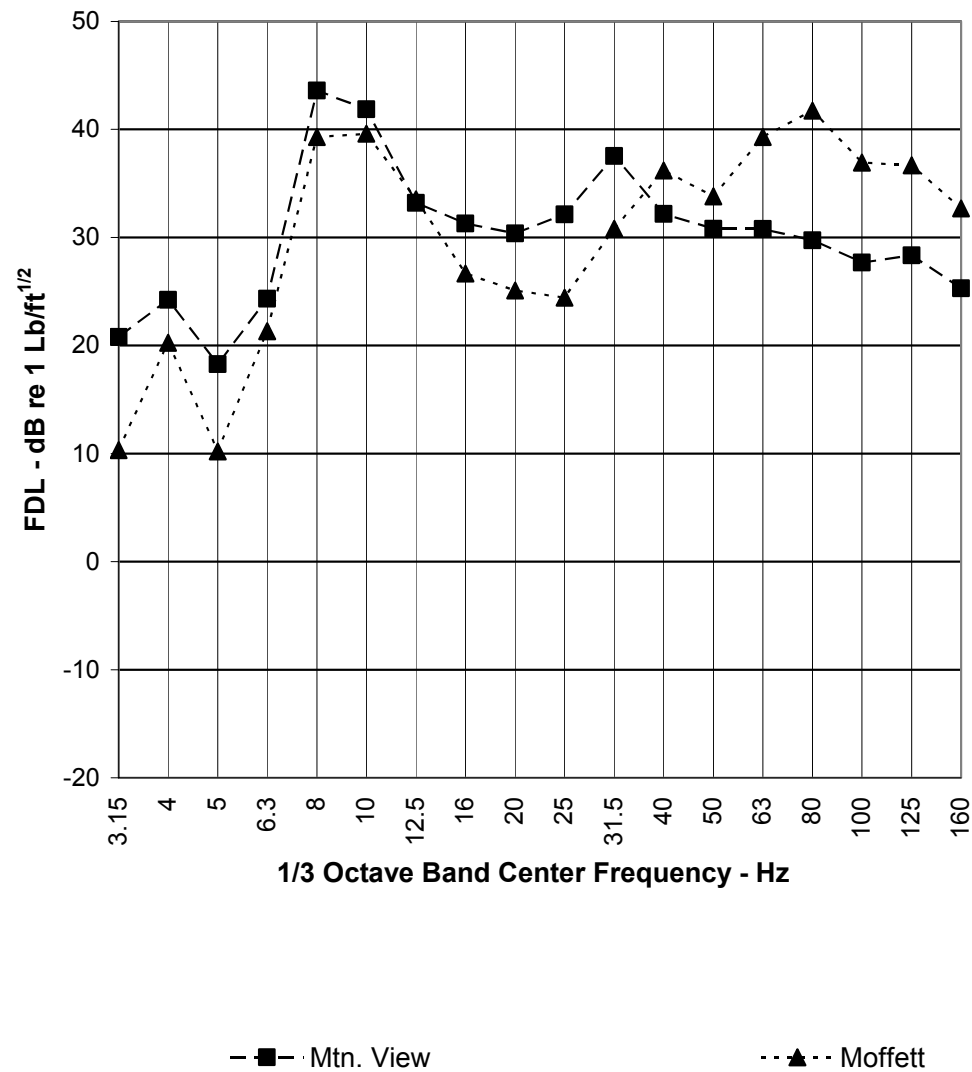
WB 45 MPH Test Train
All Locations, Averaged by Channel
Train Length=90 ft

Figure C-45 FDL of Kinkisharyo Vehicle Westbound at 45mph on Ballast and Concrete Tie Track



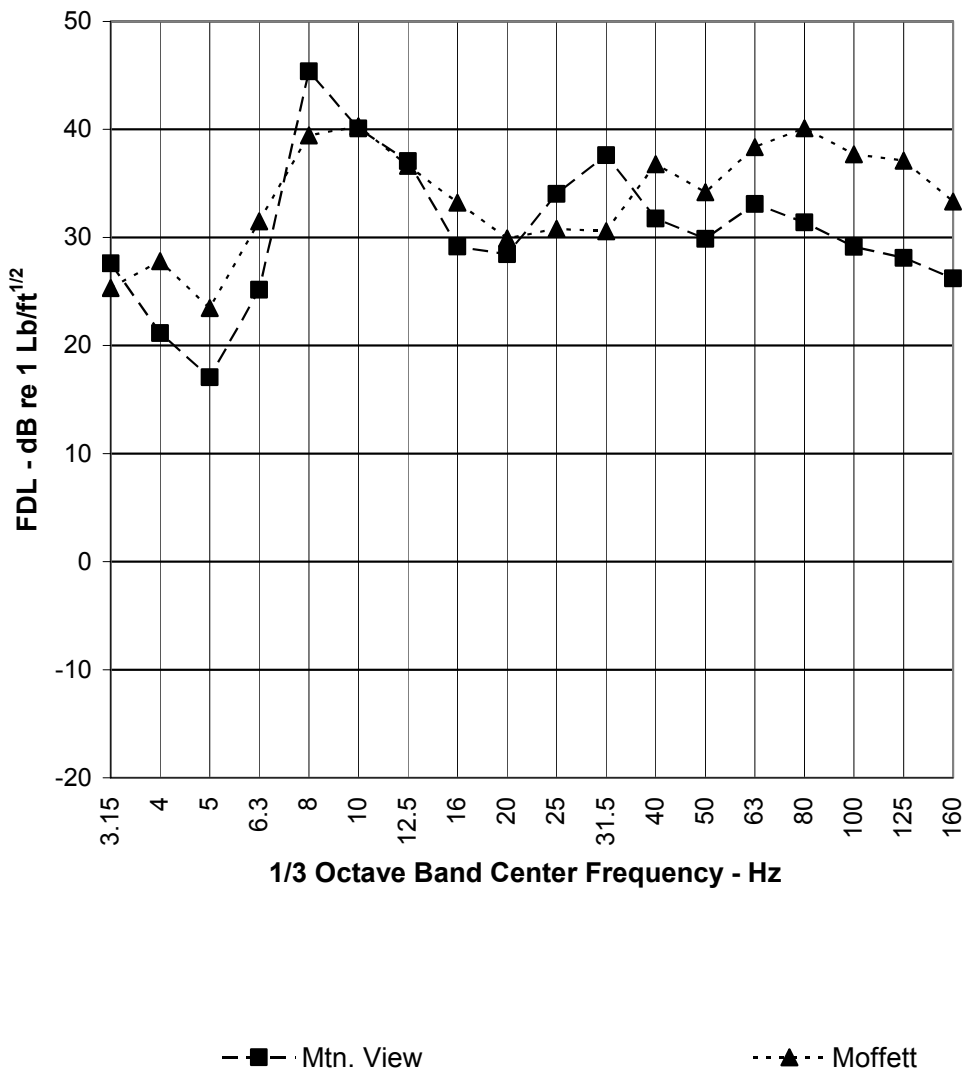
ALL 45 MPH Test Train
All Locations, Averaged by Channel
Train Length=90 ft

Figure C-46 FDL of Kinkisharyo Vehicle at 45mph on Ballast and Concrete Tie Track - Energy Average of Eastbound and Westbound Results



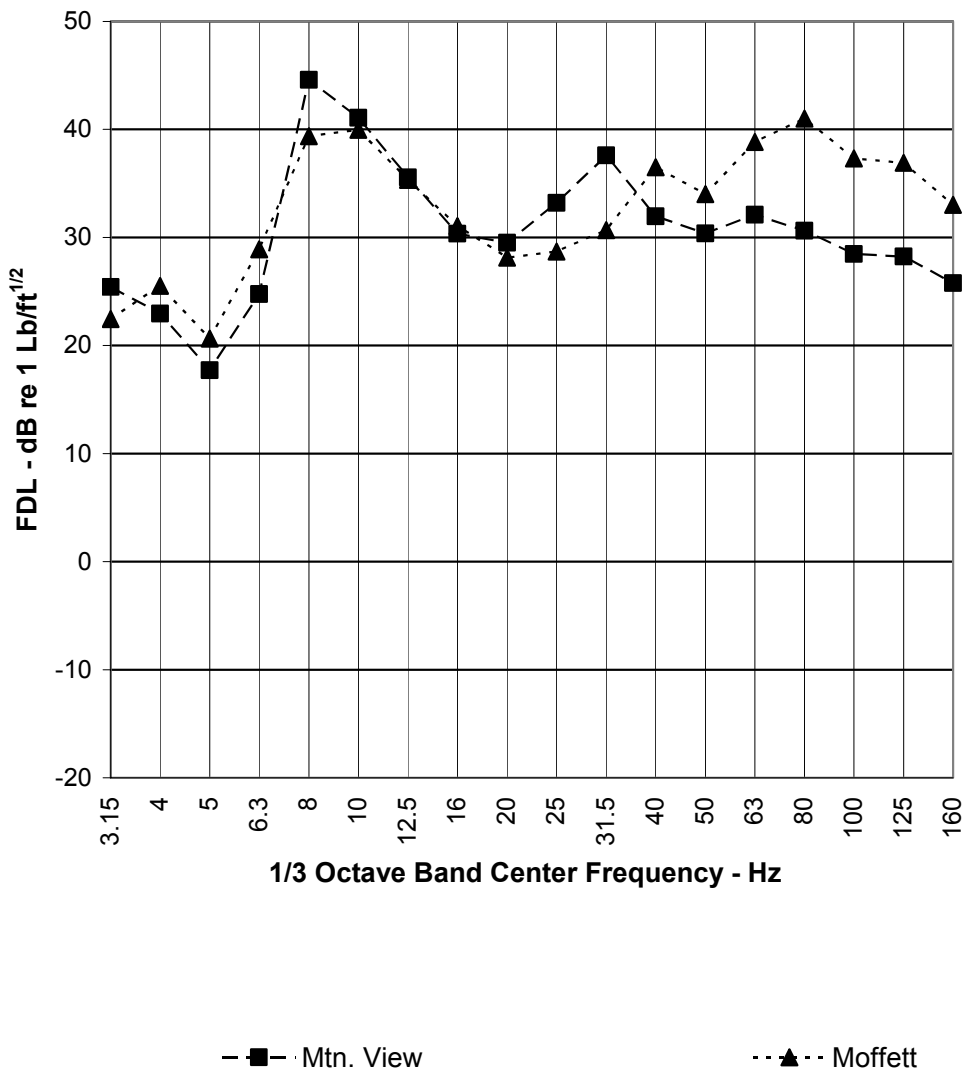
EB 50 MPH Test Train
All Locations, Averaged by Channel
Train Length=90 ft

Figure C-47 FDL of Kinkisharyo Vehicle Eastbound at 50mph on Ballast and Concrete Tie Track



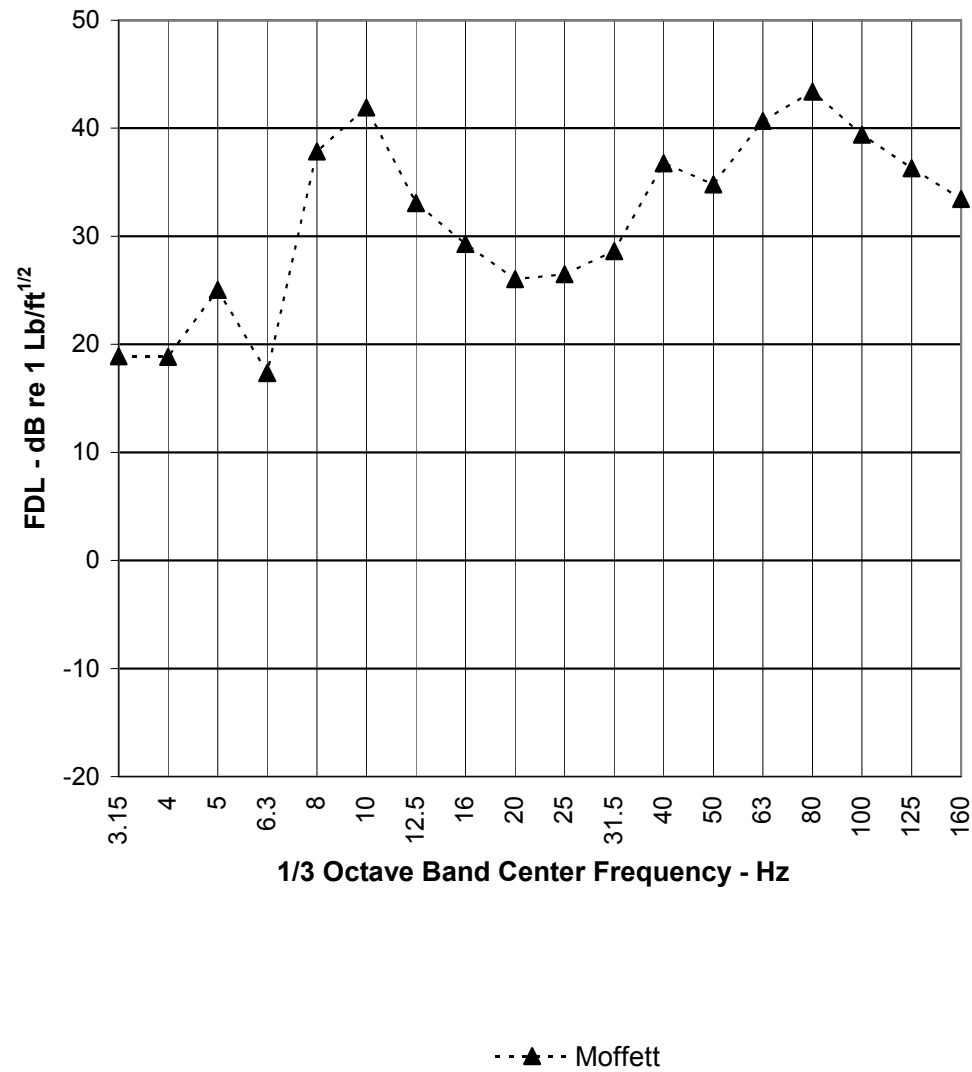
WB 50 MPH Test Train
All Locations, Averaged by Channel
Train Length=90 ft

Figure C-48 FDL of Kinkisharyo Vehicle Westbound at 50mph on Ballast and Concrete Tie Track



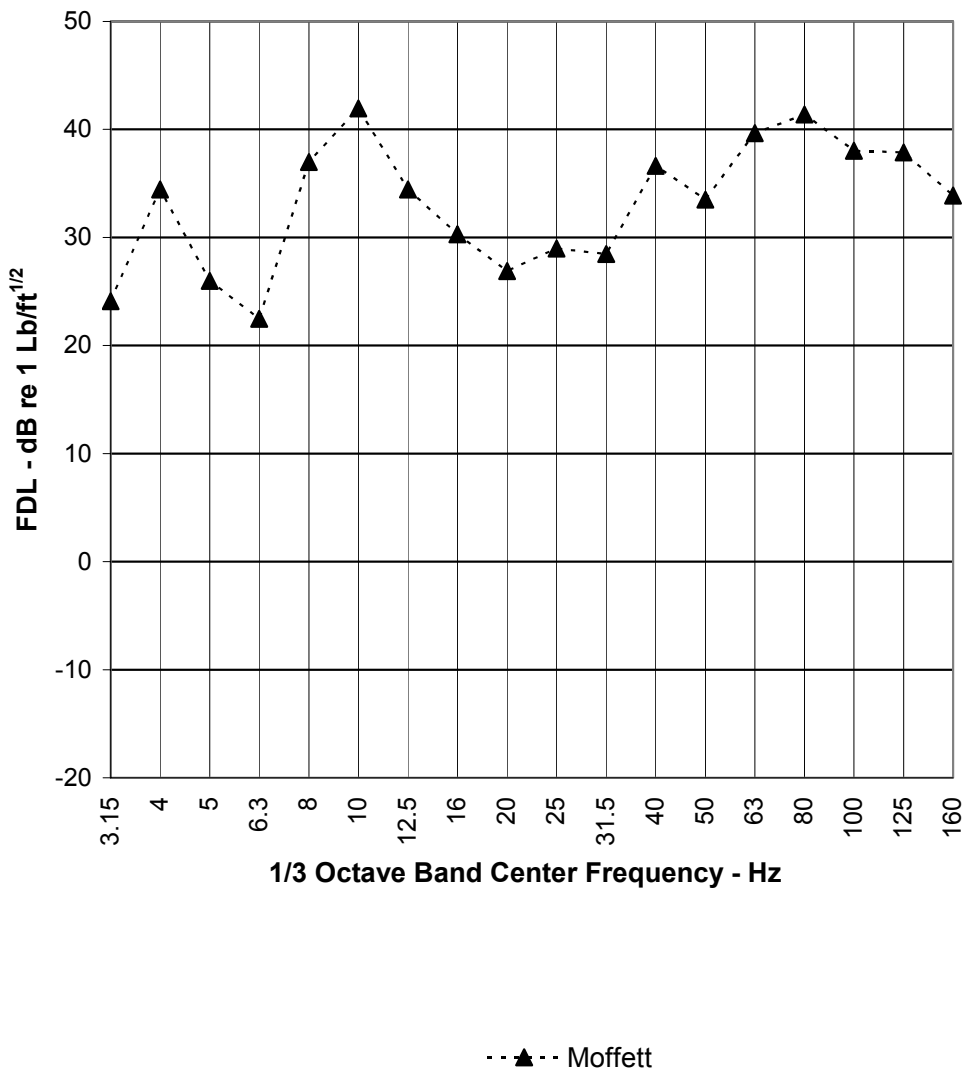
ALL 50 MPH Test Train
All Locations, Averaged by Channel
Train Length=90 ft

Figure C-49 FDL of Kinkisharyo Vehicle at 50mph on Ballast and Concrete Tie Track - Energy Average of Eastbound and Westbound Results



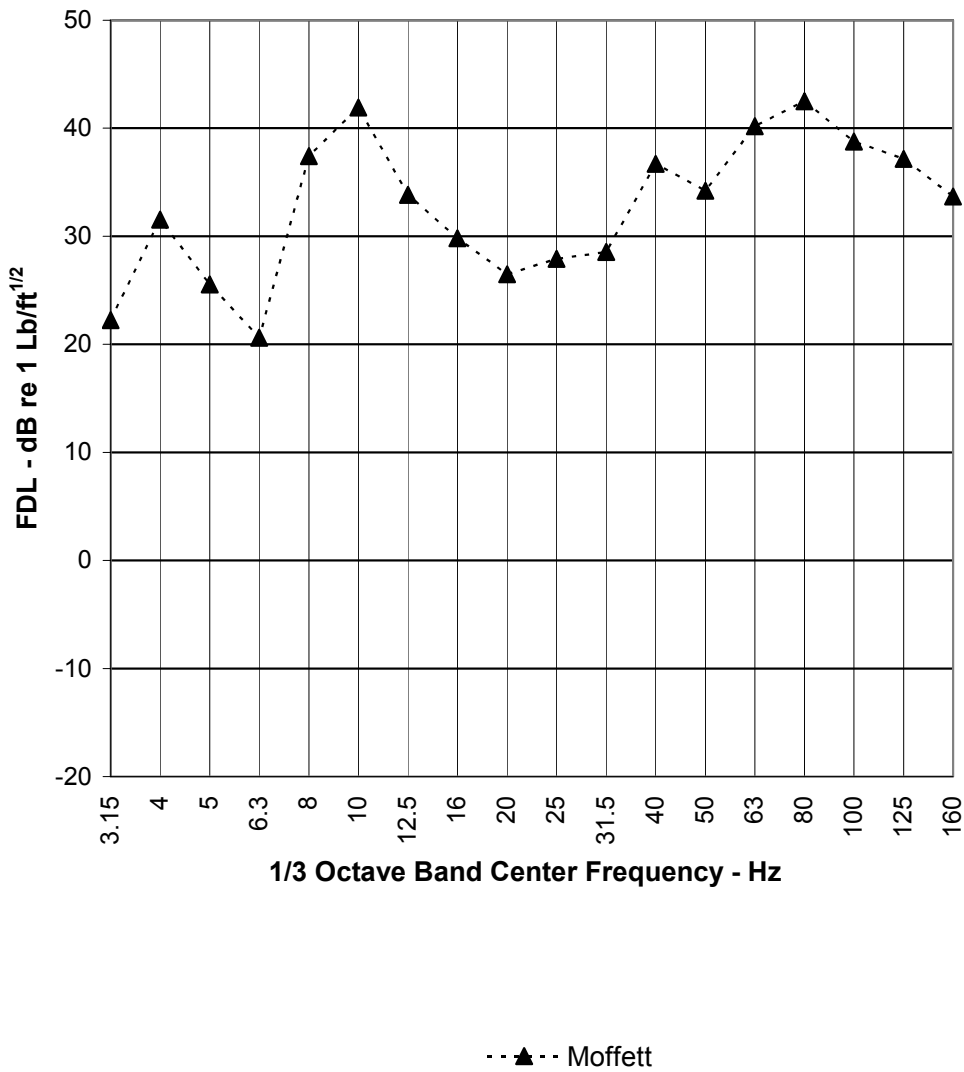
EB 55 MPH Test Train
All Locations, Averaged by Channel
Train Length=90 ft

Figure C-50 FDL of Kinkisharyo Vehicle Eastbound at 55mph on Ballast and Concrete Tie Track



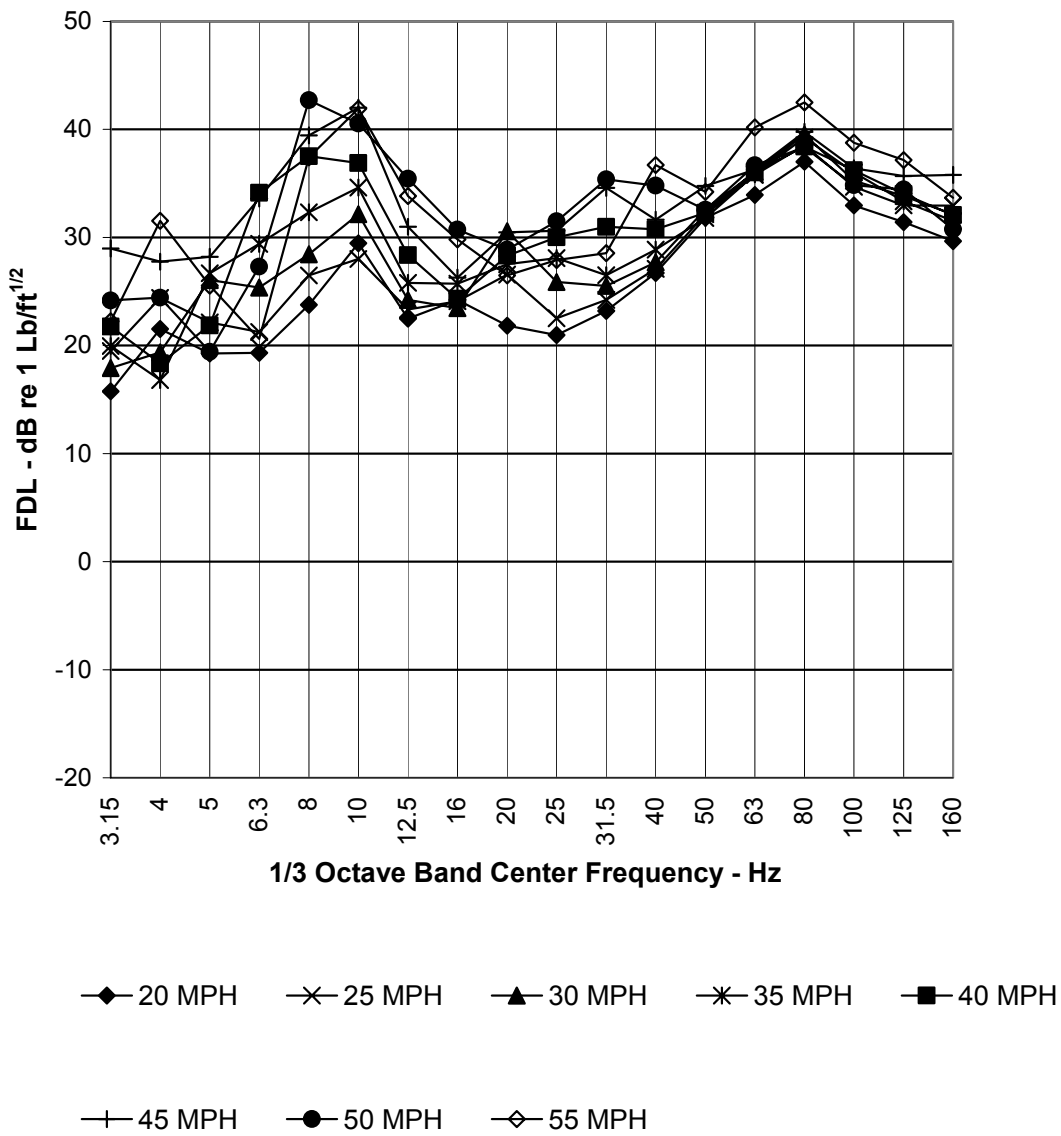
WB 55 MPH Test Train
All Locations, Averaged by Channel
Train Length=90 ft

Figure C-51 FDL of Kinkisharyo Vehicle Westbound at 55mph on Ballast and Concrete Tie Track



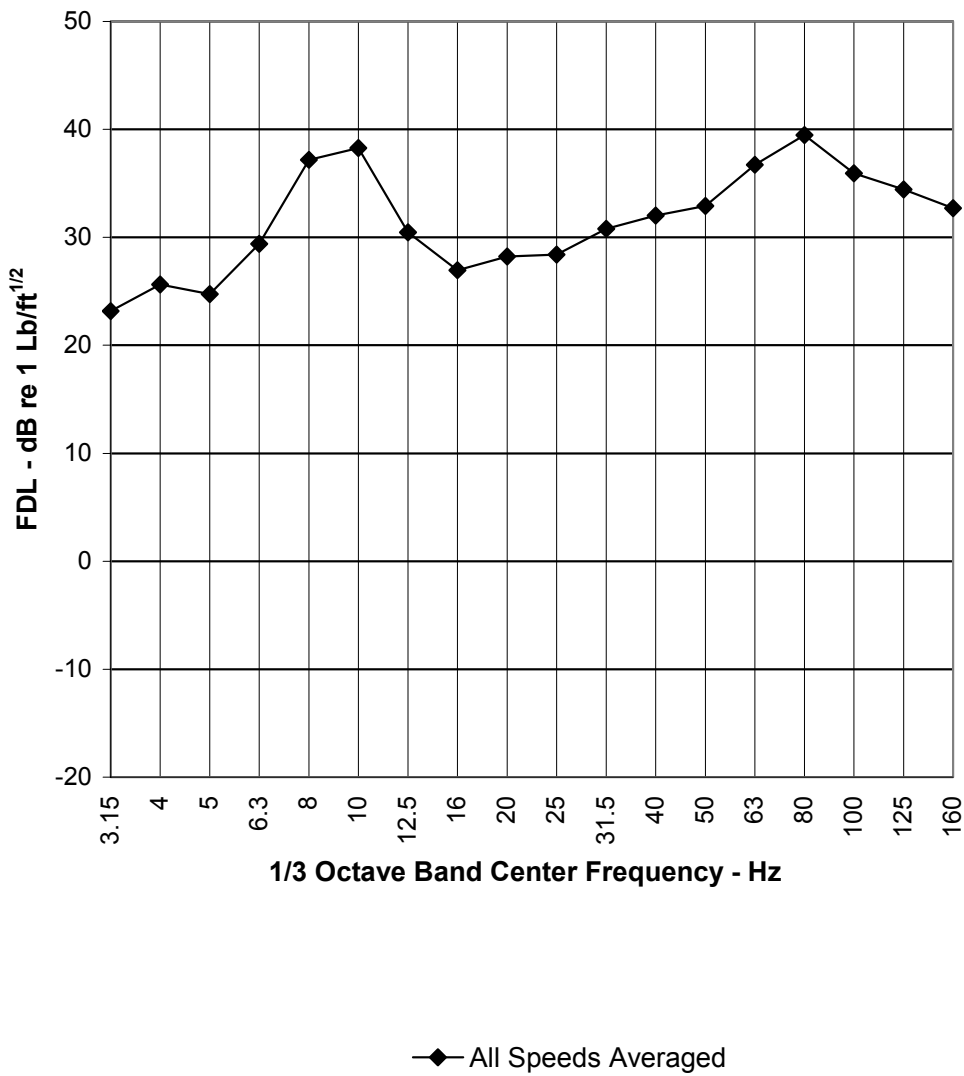
ALL 55 MPH Test Train
All Locations, Averaged by Channel
Train Length=90 ft

Figure C-52 FDL of Kinkisharyo Vehicle at 55mph on Ballast and Concrete Tie Track - Energy Average of Eastbound and Westbound Results



All Speeds
Averaged Channel, Direction, and Location
Train Length=90 ft

Figure C-53 FDL for Kinkisharyo Vehicle at Various Speeds - Energy Average Over All Data



Averaged Channel, Direction, and Location, and Speed
Train Length=90 ft

Figure C-54 Energy Average of FDL for All Train Speeds - Illustration of Primary Suspension Stiffness

C-8 ADJUSTMENT FOR STANDARD DIRECT FIXATION FASTENERS

The foregoing FDL estimates were based on measurements at ballasted track. The tunnel design would include resilient direct fixation fasteners of static stiffness about 100,000 lb/in, with a ratio of dynamic-to-static stiffness of about 1.4. The dynamic stiffness under axle load would be about 140,000lb/in. With a fastener pitch of 30in, the rail support modulus would be 4,660 lb/in/in. The rail support modulus of ballasted track is usually assumed to be about 3,000 lb/in/in of rail, though this may vary, depending on the system and ground stiffness. An adjustment was applied to the above FDLs to translate the them to direct fixation track. The adjustment factors are summarized in Table C-4.

The adjustments given in Table C-4 are based on theoretical calculations of a wheel set and resiliently supported rail with a velocity generator between the wheel and rail. The wheel and rail model is based on a so-call parallel impedance model that is used extensively for wheel/rail noise and vibration prediction. The model was described by Bender² for resilient rail fastener analysis and more recently by the author of this report³. The results of Bender's analysis were incorporated into prediction procedures developed under the auspices of the U. S. Department of Transportation.⁴

The resulting FDL's for each train speed are plotted in Figure C-55. Pending further analysis, these Force Density Levels represent the source vibration for prediction of ground vibration from the Sound Transit Tunnels.

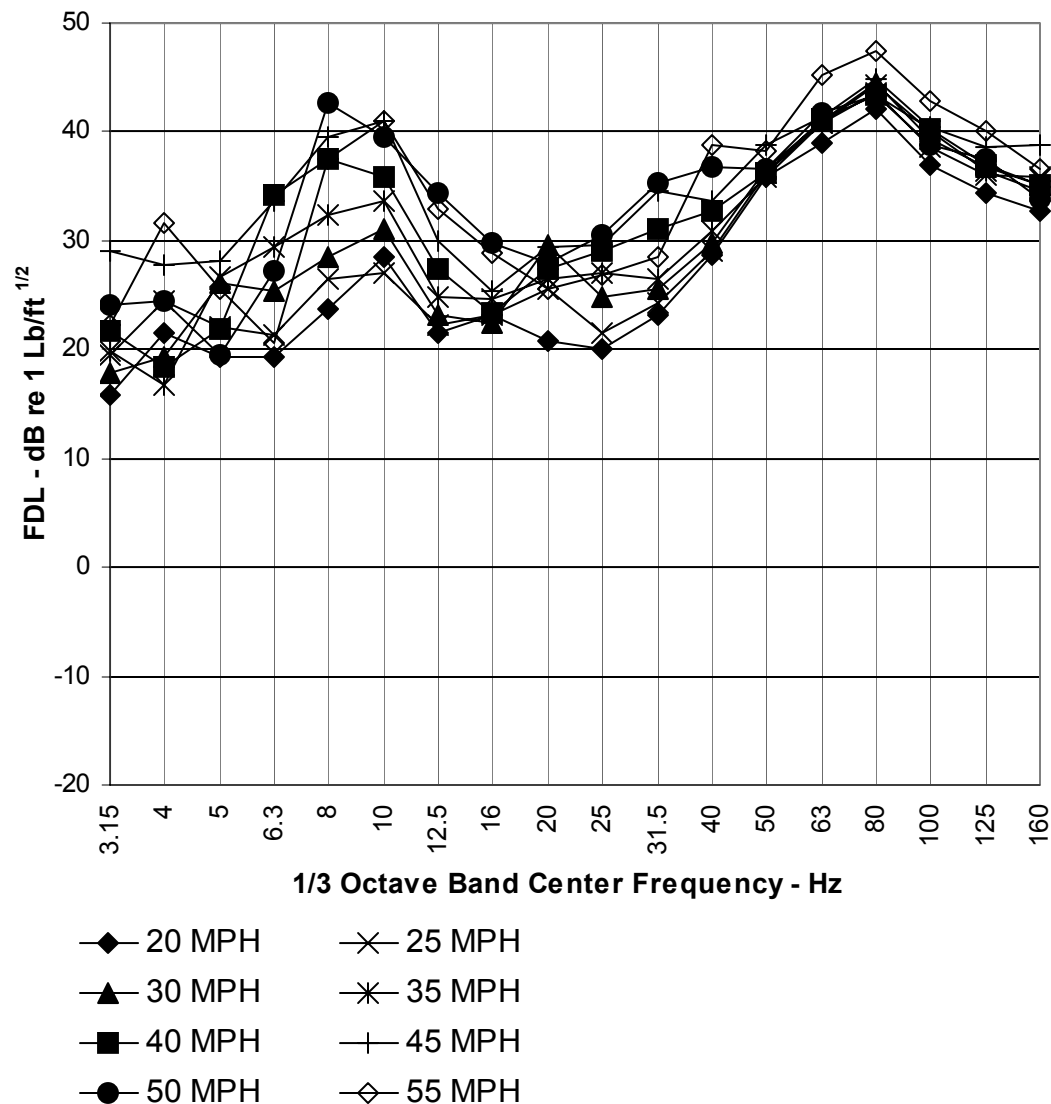
² Bender, E. K., Kurze, U. J., Nayak, P. R., Ungar, E. E., **Effects of Rail Fastener Stiffness on Vibration Transmitted to Buildings Adjacent to Subways**, BBN Report 1832 to Washington Metropolitan Area Transportation Authority (1969).

³ Nelson, J. T., **Wheel/Rail Noise Control Manual**, TCRP Report 23, Transit Cooperative Research Program, Transportation Research Board, 1997, pg. 38.

⁴ Nelson, J. T., Saurenman, H. J., **State of the Art Review: Prediction and Control of Groundborne Noise and Vibration from Rail Transit Systems, Interim Report**, Urban Mass Transit Administration, U.S. Department of Transportation, (1983) Report No. UMTA-MA-06-0049-83-4, pg. 5-18.

Table C-4 FDL for Resilient DF Fasteners of Stiffness 140,000 lb/in Relative to FDL for Ballast and Tie Track

Frequency – Hz	Adjustment
6.3	0
8	0
10	-1
12.5	-1
16	-1
20	-1
25	-1
31.5	0
40	2
50	4
63	5
80	5
100	4
125	3
160	3



Adjusted for Resilient Direct Fixation Fastener of 140,000 lb/in
Averaged Channel, Direction, and Location
Train Length=90 ft

Figure C-55 FDL for VTA Kinkisharyo on Resilient Direct Fixation Fasteners with Stiffness of 140,000 lb/in and Separation of 30in

C-9 WHEEL RUNOUT AND RAIL UNDULATION

The vibration produced by a single wheel set traversing a section of track is duplicated by each of the other wheel sets. As a result, the passby ground vibration signature due to rail roughness consists of a set of identical superposed vibration signatures, each delayed in time by an amount equal to the distances between the axles divided by the train speed. As a result, the vibration spectrum due to rail roughness is modulated by the spectrum of the axle passage. An example of the modulation envelope is shown in Figure C-56. The modulation envelope consists of a series of peaks. The separation between successive large peaks is about 2.5 Hz, and is due to the distance between trucks. These successive peaks are further modulated by envelopes separated by about 15 to 16 Hz, which is related to the axle separation on each truck. The axle separation of the powered trucks is 1,900 mm, while that of the center truck is 1,800 mm.

The vibration due to wheel roughness is superposed on the rail vibration signature. The wheel vibration spectra for a single wheel should consist of a series spectral peaks beginning with the fundamental wheel rotation frequency and continuing with its upper harmonics. If each of the wheel vibration signatures were identical and phased identically, they would be subject to the same modulation envelope as shown for rail roughness vibration. However, each wheel is different, and while the vibration signature produced by each wheel is periodic, the signatures of each wheel are random in phase, so that the envelope shown in Figure C-56 would not apply. As a result, one may expect to see a wheel vibration component at the wheel rotation frequency and its harmonics, un-modulated by the envelope shown in Figure C-56.

The foregoing suggests that the vibration due to the rail roughness can be distinguished from that due to the wheel roughness by inspection of the spectrum obtained by Fourier transformation of an entire vehicle passby vibration signature. To test this, four vibration signatures were Fourier transformed, using a 10 second conversion window and rectangular weighting. The power spectra were obtained from the transform, and truncated to 400 lines. The 400-line power spectra are illustrated in Figure C-57 through Figure C-60 for speeds of 40, 45, 50, and 55mph respectively.

Also shown in each of these figures are vertical blue lines that identify the modulation peaks of rail-roughness-induced vibration. The red lines identify the wheel fundamental rotation frequency and harmonics thereof. The speed assumption was adjusted slightly to obtain agreement between spectral peaks. The wheel diameter was assumed to be 25.25inches, corresponding to a 26in wheel that had been trued once.

The fundamental wheel rotation frequency corresponds to one of the axle passage modulation peaks. This is a coincidence between wheel circumference and axle separations, and the importance of this coincidence has not been determined. However, one may conjecture that the coincidence might lead to higher levels of vibration than might otherwise occur. The coincidence persists regardless of train speed.

The axle passage modulation envelope peaks do appear to line up with spectral peaks. In Figure C-57, this agreement is apparent at about 1.7 Hz, 3.4 Hz, 7 Hz, 8.9 Hz, 10.4 Hz, and 12.1 Hz. At 8.9 Hz, the axle passage spectral peak also corresponds to the wheel rotation frequency, and it is the highest spectral peak. However, the 3rd harmonic of the wheel rotation frequency is not

apparent in the spectrum. The second harmonic and an axle passage peak appear together between two spectral peaks at about 17.5 Hz. A similar correspondence exists in Figure C-58 for the 45 mph run. Again, the spectral peak at wheel rotation frequency and axle passage peak is dominant. These peaks are also, apparently, coincident with the primary suspension resonance frequency that appears to be at about 10 Hz.

For the 49 mph sample shown in Figure C-59, the wheel rotation frequency component, while visible at 10.9 Hz, is no longer prominent. The most prominent peak appears at 8.7 Hz, which is coincident with a peak in the rail roughness induced vibration envelope. However, the spectral peaks at the other rail roughness envelope peaks are subdued, with the exception of a peak at 21.5 Hz that is also coincident with the wheel rotation frequency. In Figure C-60, the spectral peaks are coincident with roughness envelope peaks at about 2.2 Hz, 4.8 Hz, and 9.5 Hz. There is no apparent peak at the wheel rotation frequency of 11.9 Hz, though a strong peak appears at about 12 to 13 Hz. The most dominant peak occurs at 9.5 Hz, which is clearly related to the rail roughness spectral peak; not the wheel rotation frequency.

Other peaks exist in the spectra that do not coincide with the theoretical peaks discussed above. In Figure C-59, for example, two peaks are apparent, one at 7.5 Hz, and the other at about 10 Hz. The former of these is marked by a purple line in each of the figures. These peaks may be due to undulations of the rail. While a spectral peak due to rail undulation may occur at a frequency different from that associated with the axle passage envelope, it may nevertheless appear because the axle passage envelope has finite amplitude over most of the spectrum, reaching zero only at specific frequencies. At frequencies where the envelope does reach zero, the vibration due to rail undulation would be nil.

There may also be differences in the presentation of each of the trucks as they pass the measurement point, so that gauge face roughness may contribute to the passby spectrum in a way that is not repetitive. Vibration due to gauge face contact might thus not be modulated to the same degree as vibration due to rail height roughness.

In Figure C-60, a spectral peak occurs at about 31.8 Hz, which is the crosstie passage frequency, signified by a green line. This coincidence is also apparent in the 49 mph sample shown in Figure C-59. However, the cross-tie passage frequency is not strongly apparent in the lower speed samples.

The foregoing analysis suggests that rail roughness at the Moffett test location was the most important source of vibration at speeds of 50 and 55 mph. The appearance of a strong peak at the coincident wheel rotation frequency and envelope peak for the 40 and 45 mph runs could be due to wheel run-out, though run-out is not apparent at higher speed runs.

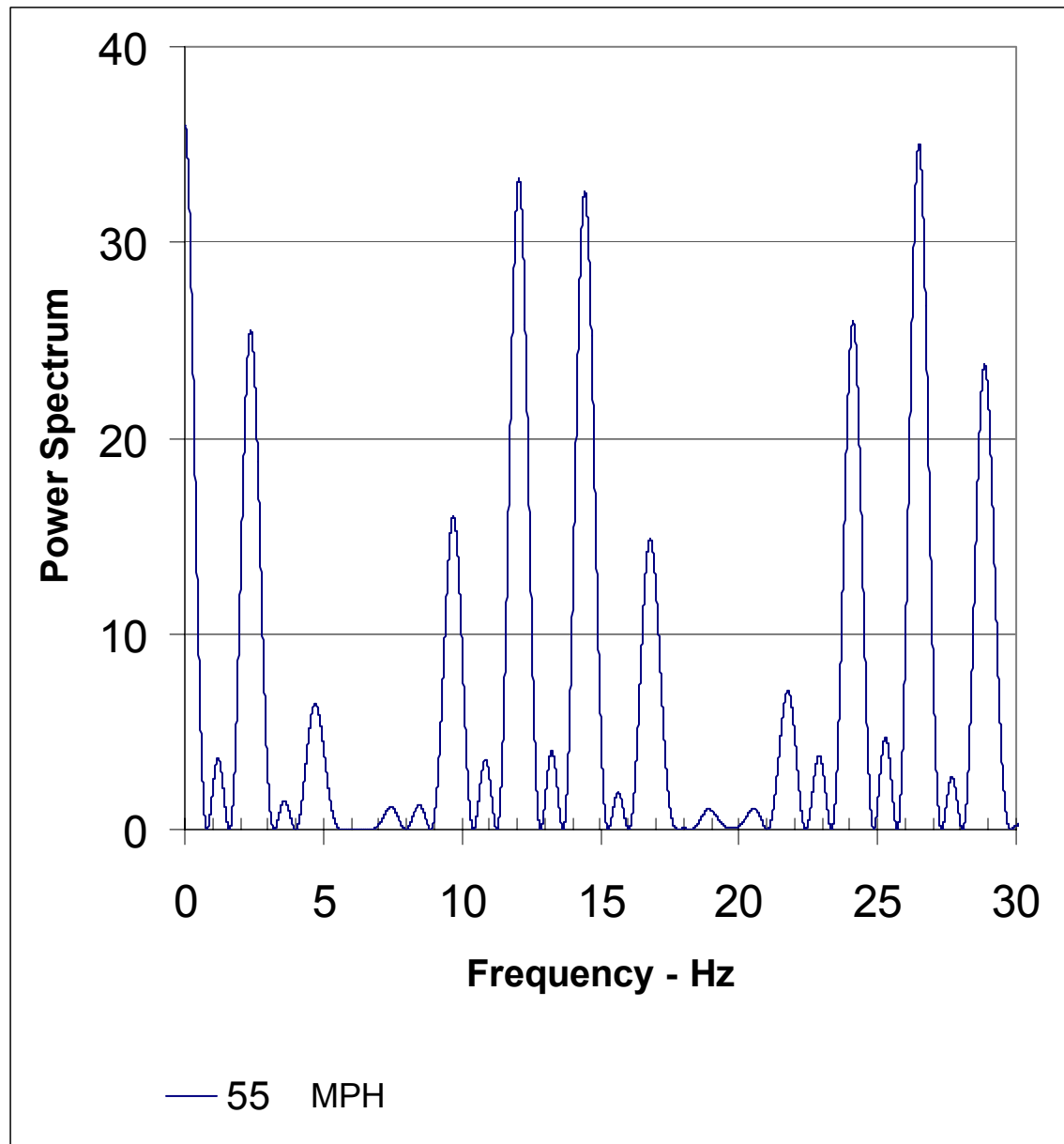


Figure C-56 Modulation Envelope of Ground Vibration due to Rail Roughness for a Single VTA Kinkisharyo Vehicle Traveling at 55 MPH

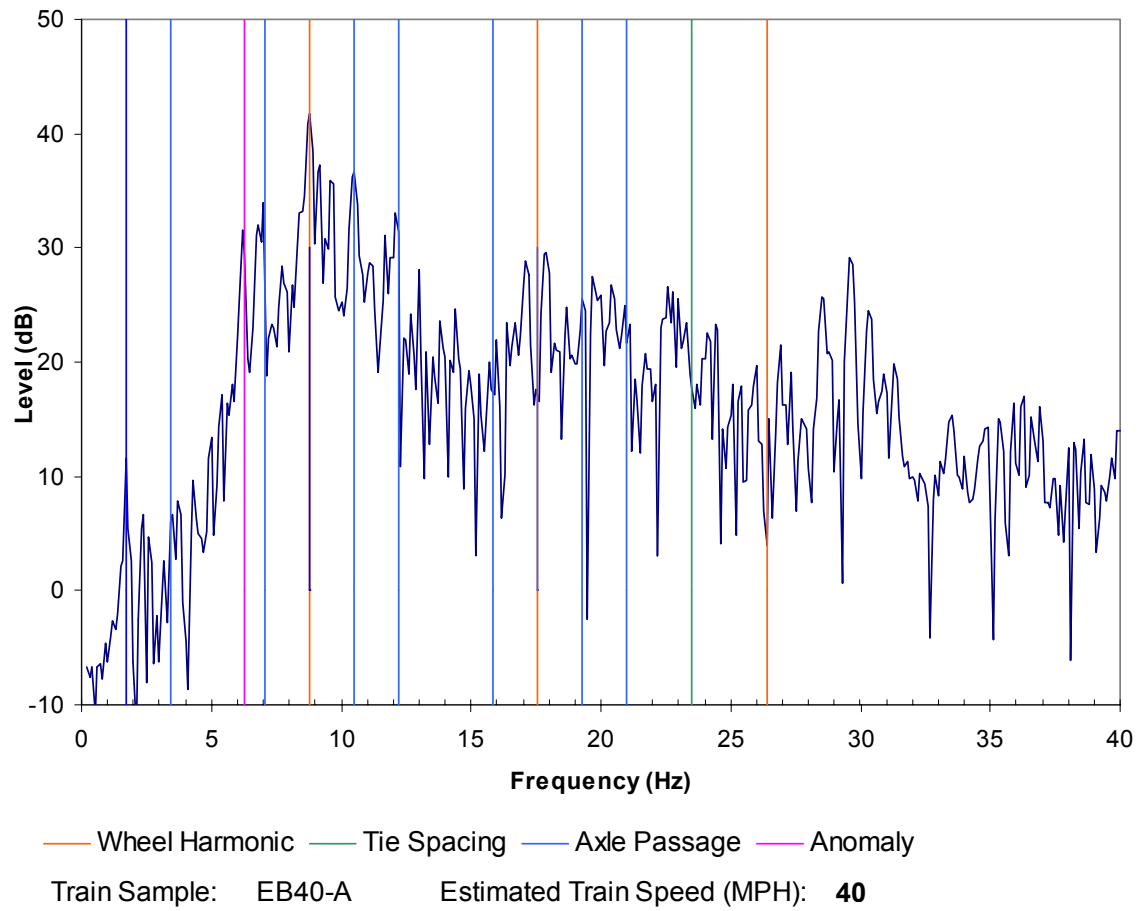


Figure C-57 Fourier Spectrum of 40mph Passby Signature

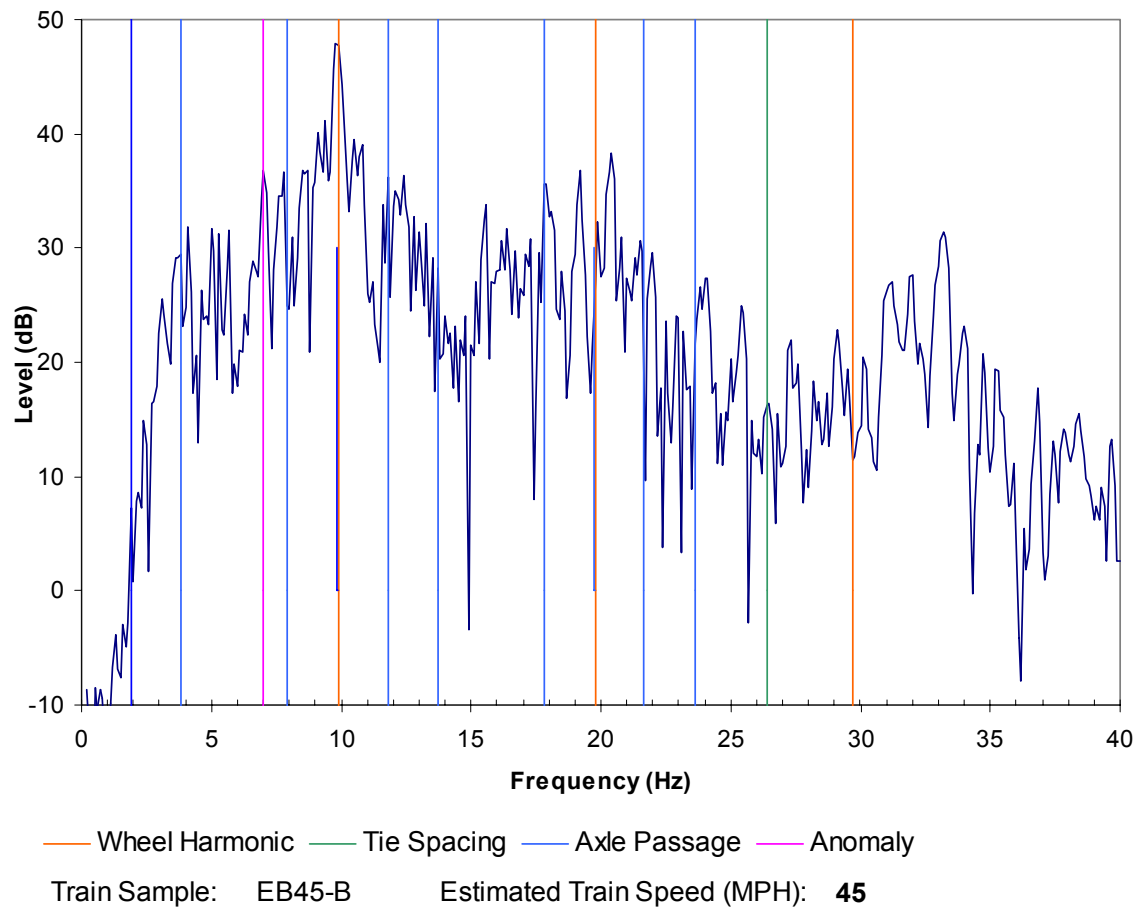


Figure C-58 Fourier Spectrum of 45 MPH Passby Signature

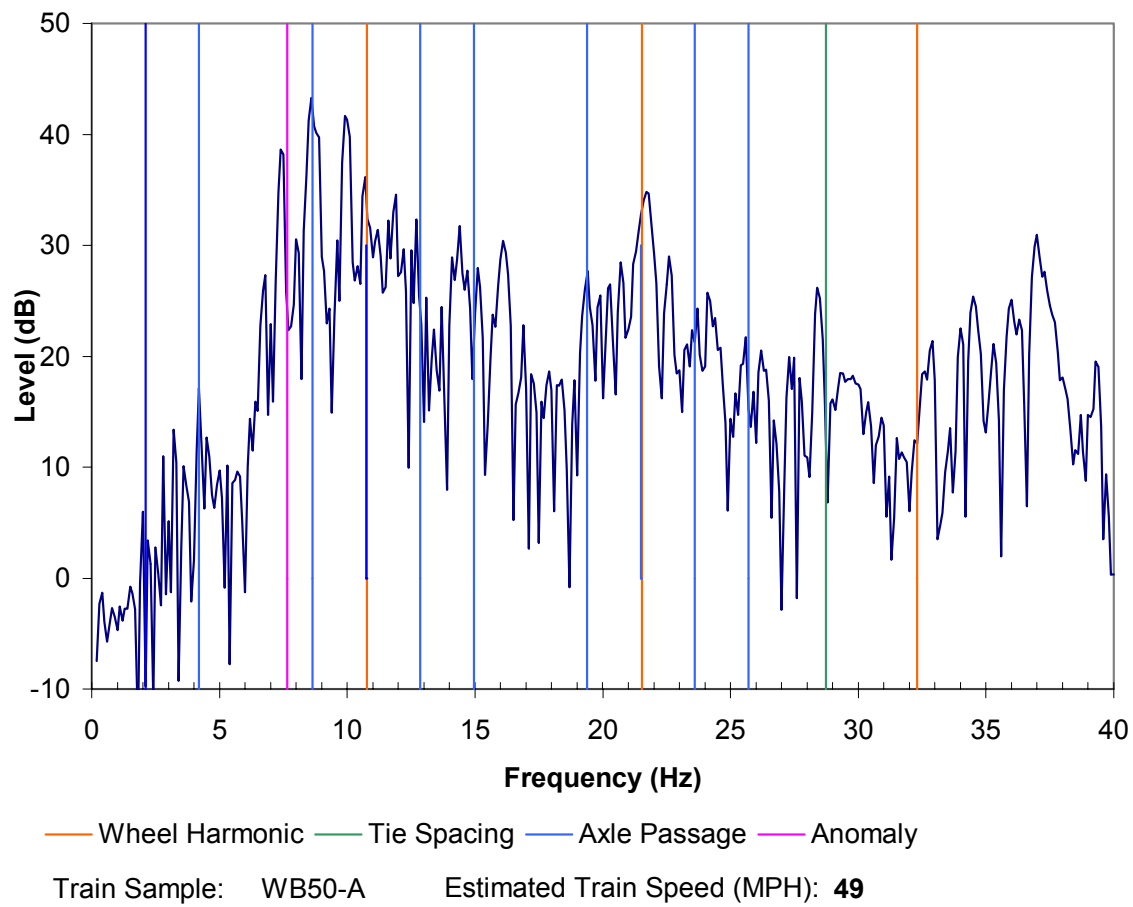


Figure C-59 Fourier Spectrum of 49 MPH Passby Signature

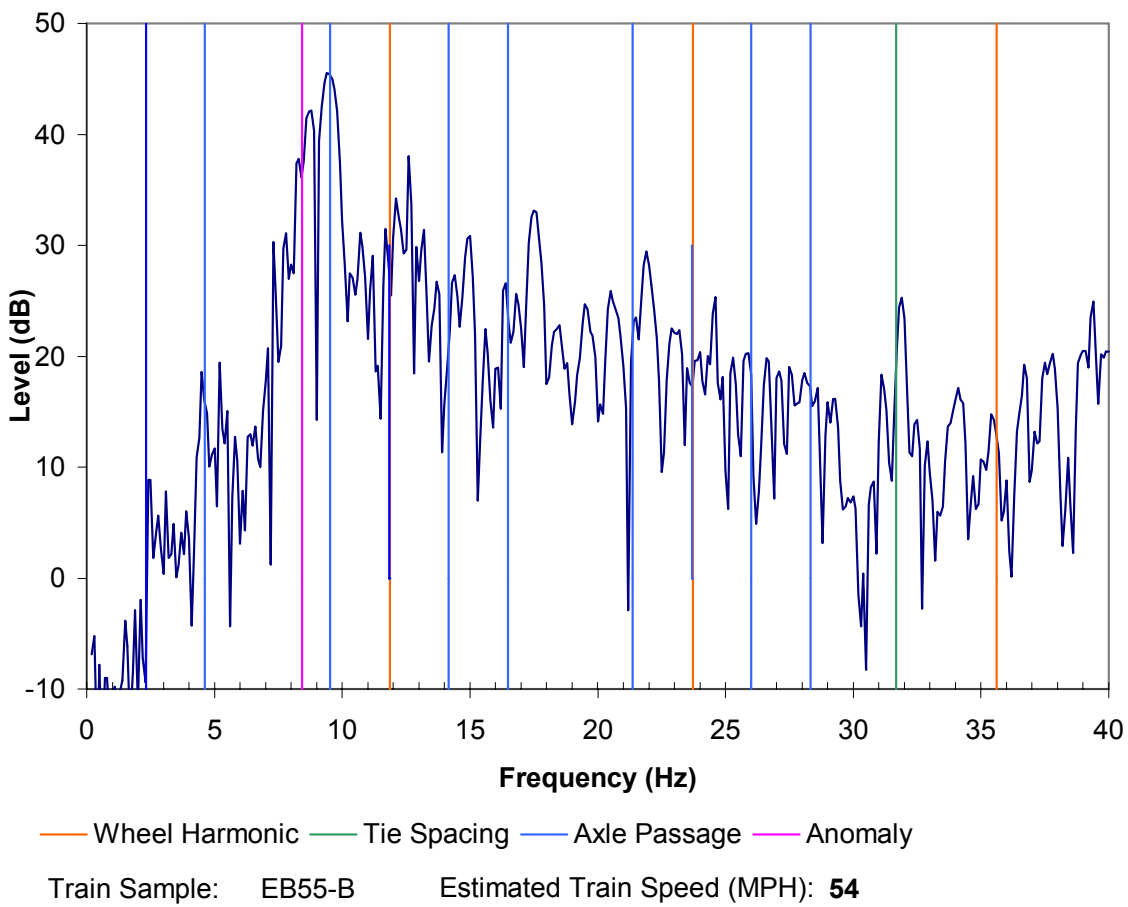


Figure C-60 Fourier Spectrum of 54 MPH Passby Signature

C-10 DISCUSSION

A strong vibration component exists at about 8 to 10 Hz, due to the primary suspension resonance of the vehicle and coincidence with wheel rotation and/or rail undulation frequencies. The suspension resonance appears to have a damping ratio of about 12%. The forces in this frequency range are strongly dependent on train speed, so that minor upward shifts in speed can produce substantial increases or reductions in the response of the primary suspension. This is a sign of a lightly damped system that could be controlled by increased damping if the existing damping of the primary suspension is low. Magnitude reductions of as much as 50% (6dB) might be reasonable to expect. However, increased damping also involves using elastomers of possibly higher creep rate, as apposed to natural rubber. Increasing the damping of the primary suspension stiffness or damping is not considered to be practical at this point in the project, though increasing damping of the floating slab side pad elastomer or direct fixation fastener elastomer might be explored.

Force density levels at wheel rotation frequencies depend strongly on the amplitude of wheel run-out and eccentricity. Wheel truing may introduce large run-out and eccentricity if not properly done. The radial run-out tolerance of a wheel-truing lathe is of the order of 0.012in for the Hegenscheidt wheel lathe considered for the North Link vehicle shop, and may be less than the rail undulation amplitude. The data reported here also indicate that wheel run-out may be less important than rail undulation in generation of ground vibration.

The analysis presented above indicates that rail undulation may be the most significant factor in producing ground vibration at low frequencies. Rail procurement specifications in the United States do not normally specify limits for undulation, but British Steel (now Corus) specifications for high-speed rail used to (and Corus may still) limit undulation over any 10-foot segment to 0.015 inch deviation from straightness. Data are not available for rail manufactured in the United States, but one may assume that rail undulation may exceed +/-0.015in, perhaps by a large amount. If wheel truing tolerances were kept to 0.012in, rail undulation would likely remain as the most important cause of low frequency ground vibration. This is supported by the narrowband spectra shown above

The amplitude of rail roughness has not been determined, but one may assume that it is of the order of several tens of thousandths of an inch. Undulation amplitudes of the order of 0.05inch have been observed in Kamloops at a section of continuous welded rail. Undulation amplitudes of rail rolled in the United States may be greater than those of European rail, and may be comparable with those found in Kamloops. The undulation amplitudes are controlled by the eccentricity or run-out of the rolls used by the roller-straightening machine. The rail manufacturer should be able to control these parameters by machining the rolls to less than a 0.005in radial run-out.

Rail grinding may reduce rail undulation, and some success with this has been reported to this author by a rail grinder manufacturer. The case in point involved main line railroad operations, where ride quality of the locomotive cab was affected by rail undulation caused by roller straightening. Grinding with a vertical axis grinding train apparently reduce cab vibration. This

result is encouraging, and suggests that rail grinding may offer a mitigation option that can be explored further.

Testing of the actual Kinkisharyo vehicle at Sound Transit may yield lower estimates of Force Density Level. Testing should be done at the earliest practical time to check the forcing characteristics of the vehicle. While the vehicle is ostensibly similar to the VTA vehicle, there might still be differences in truck design that would produce significantly different vibration characteristics. The wheel diameters of the Kinkisharyo vehicle may differ from the nominal 26-inch diameter of the VTA vehicle. Also, truck separations are probably different if the length of the vehicle is different. Thus, a different spectrum would be expected in the passby vibration signature.

**APPENDIX D: PREDICTED UNMITIGATED THIRD-OCTAVE VIBRATION
VELOCITY LEVELS**

TABLE OF CONTENTS

D-1	INTRODUCTION	1
D-2	CALCULATION METHODOLOGY	1
D-2.1	Force Density Level.....	1
D-2.2	Line Source Response.....	2
D-3	PREDICTED LEVELS.....	3
D-3.1	New Electrical Engineering (1)	5
D-3.2	Johnson Hall (2).....	5
D-3.3	Bagley Hall (3).....	5
D-3.4	New Chemistry (4).....	5
D-3.5	Wilcox Hall (5)	5
D-3.6	Physics and Astronomy (6).....	6
D-3.7	Burke Museum (7)	6
D-3.8	Benson Hall (8).....	6
D-3.9	Roberts Hall (9).....	6
D-3.10	Winkenwerder Hall (10)	6
D-3.11	Henderson Hall (11).....	7
D-3.12	Oceanographic Research Building (12).....	7
D-3.13	UW Medical Center (13)	7
D-3.14	Fisheries Sciences (14)	7
D-3.15	Fisheries Teaching and Research Center (15)	7
D-3.16	More Hall (16)	8
D-3.17	Marine Studies (17).....	8
D-3.18	Bioengineering/Genomics (18).....	8
D-3.19	Fluke Hall (19).....	8
D-3.20	Mechanical Engineering Building (20a).....	8
D-3.21	Mechanical Engineering Annex (20b).....	9
D-3.22	Ocean Sciences (21).....	9
D-3.23	Center on Human Development and Disability (22)	9
D-3.24	Fisheries Center (23).....	9
D-4	BUILDING VIBRATION RESPONSE	40
D-4.1	Procedure	40
D-4.2	Results.....	40
D-4.3	Predicted Basement Floor Vibration.....	40

TABLES

Table D-1	Assumed Parameters used for Predictions.....	4
Table D-2	Vibration Velocity Levels for All Buildings at 30-55 MPH.....	10

FIGURES

Figure D-1	FDLs for 30 to 55 MPH 4-Car Kinkysharyo train on Standard Direct Fixation Track	15
Figure D-2	Ground Surface Vibration Velocity Levels at Electrical Engineering for Two Simultaneous Train Passbys	16
Figure D-3	Ground Surface Vibration Velocity Levels at Johnson Hall for Two Simultaneous Train Passbys	17
Figure D-4	Ground Surface Vibration Velocity Levels at Bagley Hall for Two Simultaneous Train Passbys	18
Figure D-5	Ground Surface Vibration Velocity Levels at New Chemistry for Two Simultaneous Train Passbys	19
Figure D-6	Ground Surface Vibration Velocity Levels at Wilcox Hall for Two Simultaneous Train Passbys	20
Figure D-7	Ground Surface Vibration Velocity Levels at Physics and Astronomy for Two Simultaneous Train Passbys	21
Figure D-8	Ground Surface Vibration Velocity Levels at Burke Museum for Two Simultaneous Train Passbys	22
Figure D-9	Ground Surface Vibration Velocity Levels at Benson Hall for Two Simultaneous Train Passbys	23
Figure D-10	Ground Surface Vibration Velocity Levels at Roberts Hall for Two Simultaneous Train Passbys	24
Figure D-11	Ground Surface Vibration Velocity Levels at Winkenwerder Hall for Two Simultaneous Train Passbys	25
Figure D-12	Ground Surface Vibration Velocity Levels at Henderson Hall for Two Simultaneous Train Passbys	26
Figure D-13	Ground Surface Vibration Velocity Levels at Oceanography Research Building for Two Simultaneous Train Passbys	27
Figure D-14	Ground Surface Vibration Velocity Levels at Medical Center for Two Simultaneous Train Passbys	28
Figure D-15	Ground Surface Vibration Velocity Levels at Fisheries Sciences for Two Simultaneous Train Passbys	29
Figure D-16	Ground Surface Vibration Velocity Levels at Fisheries Teaching and Research Center for Two Simultaneous Train Passbys.....	30
Figure D-17	Ground Surface Vibration Velocity Levels at More Hall for Two Simultaneous Train Passbys	31
Figure D-18	Ground Surface Vibration Velocity Levels at Marine Studies for Two Simultaneous Train Passbys	32
Figure D-19	Ground Surface Vibration Velocity Levels at Bioengineering/Genomics for Two Simultaneous Train Passbys	33
Figure D-20	Ground Surface Vibration Velocity Levels at Fluke Hall for Two Simultaneous Train Passbys	34
Figure D-21	Ground Surface Vibration Velocity Levels at Mechanical Engineering Building for Two Simultaneous Train Passbys	35
Figure D-22	Ground Surface Vibration Velocity Levels at Mechanical Engineering Annex for Two Simultaneous Train Passbys	36
Figure D-23	Ground Surface Vibration Velocity Levels at Ocean Sciences for Two Simultaneous Train Passbys	37

Figure D-24	Ground Surface Vibration Velocity Levels at the Center on Human Development and Disability for Two Simultaneous Train Passbys	38
Figure D-25	Ground Surface Vibration Velocity Levels at Fisheries Center for Two Simultaneous Train Passbys	39
Figure D-26	Building Vibration Responses	41
Figure D-27	Predicted Basement Floor Vibration at Wilcox Hall	42
Figure D-28	Predicted Basement Floor Vibration at Mechanical Engineering Annex (20b)	43

D-1 INTRODUCTION

Detailed predictions of 1/3 octave vibration velocity levels for the University of Washington campus in Seattle, Washington were computed for two four-car light rail transit vehicles traveling simultaneously at speeds of 30 to 55mph, computed in 5 mph increments. Predictions are provided for a total of twenty-three buildings, including, among others, the core buildings of Bagley Hall, New Chemistry, Physics & Astronomy, and Johnson Hall, and the building closest to the alignment, Wilcox Hall, Roberts Hall, New Electrical Engineering, Mechanical Engineering Building, and Mechanical Engineering Annex.

D-2 CALCULATION METHODOLOGY

The exterior ground surface vibration level at each buildings was calculated with the following equation:

$$Lv \text{ (dB re 1 micro-in/sec)} = FDL + LSR$$

This relation represents the combination of track vibration forces and propagation to the affected receivers. No provision is made for tunnel/soil response, as analytical studies by this author indicate that tunnel/soil coupling losses would likely be small in relation to the losses related to propagation at frequencies below approximately 100Hz.

All calculations were done in terms of one third octave frequency bands, using Line Source Responses measured on the University of Washington campus in Seattle, theoretical calculations based on shear-wave velocity profiles measured on the campus, Force Density Levels for the Kinkisharyo vehicle measured at the Santa Clara Valley Transportation Authority in San Jose, California, and adjustments for standard direct fixation fasteners relative to ballast and tie track.

The calculations were made for horizontal offsets from the point of closest approach to the building. Tunnel depth and track configuration were taken at this point. Predictions were made for all train speeds from 30 to 55mph. The maximum train speed at the curve between the UW campus boundary and the Brooklyn Station would be 40mph due to geometric limitations. The maximum train speeds at all other sections of track were assumed to be 55mph. Actual train speeds on campus may be less for northbound trains, due to grade. Also, revenue trains entering and leaving the UW Station would likely be less than 55mph, though dead-heading trains could conceivably run at this speed.

The predictions are for two simultaneous trains, and were obtained made by adding three decibels to the predicted vibration levels for a single train. This approach does not allow for the likely condition of differing train speeds, so that the predictions are conservative. Simultaneous train passage at identical speeds would likely occur for a relatively small fraction of time, depending on headways.

D-2.1 Force Density Level

The Force Density Levels (FDL) were estimated by measuring ground vibration produced by a Valley Transportation Authority (VTA) Kinkisharyo vehicle traveling at controlled speeds of 30

to 55mph in 5mph increments. The FDL tests are discussed in Appendix C to this report. Adjustments for standard direct fixation (DF) track relative to ballasted track were added to the measured FDLs for the Kinkisharyo vehicle to represent the FDL for this vehicle operating on direct fixation track of nominal rail support dynamic modulus of 4,700lb/in/in. The adjustment included a modest increase in FDL above about 30Hz. Standard DF track is represented by resilient DF fasteners of 140,000lb/in dynamic stiffness placed at 30in pitch.

Figure D-1 shows the FDL's used for calculating vibration levels on campus. The FDL's exhibit two principal peaks, one related to the primary suspension resonance frequency, and the other related to the track/wheel-set resonance frequency, which may involve the axle, wheel center, resilient wheel elastomer spring, tire, rail, and track support stiffness.

No adjustment is included for the double crossover at the south end of the UW Station. This crossover would have moveable point frogs, and would thus not generate substantial transient vibration for non-diverging trains. Diverging trains would operate at very low speed, and the crossing diamond would likely be flange bearing to minimize transient vibration.

D-2.2 Line Source Response

Third octave Line Source Responses (LSRs) were calculated for offsets between 30 and 300 feet from the track centerline with a global regression curve of the Point Source Responses (PSR) measured at four boreholes (NB-253, NB-254, NB-255, and NB-256) on the UW campus. The global PSR was obtained by regression of all of the impulse response data obtained at these four holes, combined. The global regression included quadratic regression of measured third octave band point source responses versus the common logarithm of horizontal offset, x . Where quadratic fits with positive $\text{Log}(x)^2$ coefficient (implying a non-physical increase of vibration with increasing distance) would have been obtained for a particular third octave and, linear regression curves with respect to $\text{Log}(x)$ were used for integration of that particular third octave band LSR. For buildings located over the alignment, a linear regression of $\text{Log}(R)$ and R , where R is the slant distance, was used. This latter model more closely represents the combination of geometric spreading loss and material damping, or loss factor, for the soil.

The LSRs were computed by integrating the global regression curve for the PSR over the length of a hypothetical four-car LRV train, taking into account the offset of the location from the train track and proposed tunnel depth. The LSR's are based on measurements for source depths approximating the depth of the tunnel at the point of closest approach to the receiver.

For greater offsets than 300 feet, a numerical seismic reflectivity model of the layered soil was employed for prediction, using shear wave velocity profiles measured by Geo Recon. The numerical model predictions were adjusted to match the average of the measured LSR's at 50, 100, and 200 feet. The calibration adjustments increased numerical predictions at low frequencies by a few decibels and decreased the numerical predictions by a few decibels at high frequencies. The numerical model was employed rather than the regression curves representing experimental data at large offsets because of poor coherence between source and receiver test data. The time domain responses to arrivals at 400 feet were very difficult or impossible to detect in the presence of background vibration. At 800 feet, or at Bagley Hall, for example, there was no evidence of the arrival in the time domain data. Hence, extrapolation of borehole test data alone to distant receivers was considered to be inappropriate.

Predictions for tunnel depths greater than 120ft were made with an assumed depth of 120ft, the maximum depth for which LSR borehole test data were obtained. Similarly, predictions for tunnel depths less than 80ft were made with an assumed tunnel depth of 80ft, the minimum depth for which LSR borehole data were obtained.

D-3 PREDICTED LEVELS

The predicted levels of vibration velocity for each train speed are plotted below together with a background third-octave velocity spectrum provided by the University of Washington for each building under consideration.

The parameters employed for prediction are listed in Table D-1. The parameters include the civil station number at the point of closest approach to the building, horizontal offset, tunnel depth (overburden depth), and train speed range. The depth of the tunnel at the track centerline was employed for prediction because the amplitude response of the soil is roughly inversely related to the shear stiffness of the soil. The shear stiffness of the soil usually increases with confining stress, which is directly related to overburden depth. Hence, the overburden depth is most relevant to prediction.

All predictions are for root-mean-square vibration velocities in dB re 1 micro-in/second, determined over the duration of train passage, which may range from about 5 to 9 seconds for a four-car train.

Table D-1 Assumed Parameters used for Predictions

ID	Building	Speed	Nearest Station No.	Offset ft.	Depth ¹ Ft.
1	Electrical Engineering	30-55	1221+77	338	120
2	Johnson Hall	30-55	1237+26	677	120
3	Bagley Hall	30-55	1232+57	978	120
4	Chemistry	30-55	1222+99	1,008	120
5	Wilcox Hall	30-55	1214+29	110	100
6	Physics/Astronomy	30-55	1241+50	1,201	120
7	Burke Museum	30-55	1261+04	826	80 ²
8	Benson Hall	30-55	1233+56	1,269	120
9	Roberts Hall	30-55	1215+42	255	115
10	Winkenwerder Hall	30-55	1212+40	683	100
11	Henderson Hall	30-40	1250+75	1,208	80 ²
12	Oceanographic Research Building	30-40	1247+04	1,833	80 ²
13	UW Medical Center	30-55	1208+53	910	110
14	Fisheries Sciences	30-40	1248+74	1,640	80 ²
15	Fisheries Teaching & Research Center	30-40	1248+13	1,858	80 ²
16	More Hall	30-55	1216+21	137	115
17	Marine Studies	30-40	1247+68	1,799	80 ²
18	Bioengineering/ Genomics	30-55	1244+85	1,612	100
19	Fluke Hall	30-55	1226+35	333	120
20a	Mechanical Engineering Bldg	30-55	1223+23	105	115
20b	Mechanical Engineering Annex	30-55	1222+85	9	115
21	Ocean Sciences	30-55	1244+52	2,056	100
22	Center for Human Devel. and Disability	30-55	1200+52	753	100
23	Fisheries Center	30-55	1202+68	1,242	100

Note 1: Actual depth may be greater than assumed (conservative assumption)

Note 2: Actual depth may be as low as 60ft on the Brooklyn curve

The LSR and predicted levels for each train speed are listed in Table D-2 for each building.

D-3.1 New Electrical Engineering (1)

The New Electrical Engineering Building would be located at a horizontal offset of 338 feet from the nearest tunnel alignment at civil station 1221+77. The predictions were made with the adjusted numerical model. The predicted velocity levels are plotted in Figure D-2. The predicted ground surface velocity levels exceed the UW Threshold at frequencies above 20 Hz and at 6.3 to 10Hz. The maximum predicted velocity at 8Hz is 40dB for 50mph trains, exceeding the UW Threshold of 30dB by 10dB. The predicted maximum vibration velocity level at 80Hz is 47dB for 55mph.

D-3.2 Johnson Hall (2)

Johnson Hall would be located at a horizontal offset of 677 feet from the nearest tunnel alignment at civil station 1237+26. The predictions were made with the adjusted numerical model. The predicted third-octave velocity levels are plotted in Figure D-3. With the exception of a 3dB excess at 8 Hz for the 50mph train speed, all predicted levels are below the UW Threshold. The predicted level at 8Hz for 50mph trains is 34dB.

D-3.3 Bagley Hall (3)

Bagley Hall would be located at an offset of 978 feet from the alignment of the nearest tunnel at civil station 1232+57. The predictions were made with adjusted numerical model results. Figure D-4 illustrates predicted vibration velocity levels. The predicted levels at 50 and 45mph exceed the UW Threshold at 8Hz. The maximum predicted level is 31dB at 50mph, or 35micro-in/sec, at 8Hz. The maximum predicted level at 45mph is about 27dB, or 25micro-in/sec.

D-3.4 New Chemistry (4)

New Chemistry is located adjacent to Bagley Hall an offset of 1008 feet from the nearest tunnel alignment at civil station 1222+99. The predictions were made with the adjusted numerical model. The predicted levels for the ground surface are plotted in Figure D-5. The predicted ground surface vibration velocity level at 50mph is about 30 to 31dB at 8Hz, exceeding the UW Threshold of 26dB by about 5dB. The predicted velocity levels at 8 and 10Hz are about 0 to 1 dB above the UW threshold for the train speed of 45mph. At 55mph, the UW threshold of 26dB is exceeded by about 0 to 1dB at 10Hz.

D-3.5 Wilcox Hall (5)

Wilcox Hall would be at a horizontal offset of 110 feet from the nearest tunnel alignment at civil station 1214+29. The prediction was made with quadratic least squares regression of test data. The predicted ground surface vibration velocity levels are plotted in Figure D-6. The predicted vibration velocity levels exceed the UW Threshold at all train speeds. The velocity levels exceed the UW Threshold by 14dB at 8Hz at 50mph and by 35dB at 80Hz at 55mph.

D-3.6 Physics and Astronomy (6)

The Physics and Astronomy building would be located at an horizontal offset of 1,201 feet from the nearest tunnel at civil station 1241+50. The predictions were made with the adjusted numerical model. The predicted third-octave velocity levels are plotted in Figure D-7. With the exception of a 2dB excess above the UW Threshold of 28dB at 8 Hz for the 50mph train speed, all levels are below the UW Threshold. The predicted level at 8Hz for 50mph trains is 29 to 30dB.

D-3.7 Burke Museum (7)

The Burke Museum would be at a horizontal offset of 826 feet from the nearest track centerline of the Brooklyn Station. The predicted ground surface vibration velocity levels are plotted in Figure D-8 for trains on standard DF track. The maximum vibration velocity level is 37dB (63 micro-in/sec) at 8Hz for 50mph trains, exceeding the UW Threshold of 33dB by about 4dB. The tunnel depth is 80 feet. Train speed through the Brooklyn Station would likely be substantially less than 55mph, probably of the order of 30mph for trains stopping at the station. Predicted velocity levels at 45mph and lower speeds are all within the UW Thresholds.

D-3.8 Benson Hall (8)

Benson Hall would be located at a horizontal offset of 1,269 feet from the nearest tunnel alignment at civil station 1233+56. The predictions were made with the adjusted numerical model. The predicted ground surface vibration velocity levels are plotted in Figure D-9. The maximum vibration velocity level is 29 to 30dB (32 micro-in/sec) at 8Hz for 50mph trains, exceeding the UW Threshold of 26dB by about 3 to 4dB. Predicted velocity levels for all other train speeds are at or below the UW Threshold.

D-3.9 Roberts Hall (9)

Roberts Hall would be located at a horizontal offset of 255 feet from the nearest tunnel alignment at civil station 1215+42. The predictions were made with quadratic regression of borehole test data. The predicted ground surface vibration velocity levels are plotted in Figure D-10. The predicted ground surface levels exceed the UW Threshold at all train speeds. The excess is 12dB at 8Hz and by 24dB at 80Hz for 50 and 55mph trains, respectively. The maximum velocity levels are 43dB at 8Hz and 51dB at 80Hz for 50 and 55mph trains, respectively.

D-3.10 Winkenwerder Hall (10)

Winkenwerder Hall would be located at a horizontal offset of 683 feet from the nearest tunnel alignment at civil station 1212+40. The predictions were made with the adjusted numerical model. The predicted ground surface velocity levels for trains are plotted in Figure D-11. Except for the train speed of 50mph, the predicted levels are below the UW Threshold. At 50mph, the predicted velocity level at 8Hz is 36dB, 3dB above the UW Threshold of 33dB.

D-3.11 Henderson Hall (11)

Henderson Hall would be located at a horizontal offset of 1,208 feet from the nearest tunnel alignment at civil station 1250+75. The predictions were made with the adjusted numerical model. The predicted velocity levels are plotted in Figure D-12. The closest point of the tunnel to Henderson Hall would be at the curve between the UW campus boundary and the proposed Brooklyn Station. Train speeds at this section would be 40mph or less due to curving limits.

D-3.12 Oceanographic Research Building (12)

The Oceanographic Research Building would be located at a horizontal offset of 1833 feet from nearest tunnel alignment at civil station 1247+04. The predictions were made with the adjusted numerical model results. The predicted ground surface vibration velocity levels are plotted in Figure D-13. The predicted level for 50mph operation is 30dB at 8Hz, about 1dB above the UW threshold of 29dB. The predicted levels are less than the UW Threshold at all other train speeds. This portion of the alignment would be at the UW Campus boundary at the southern end of the curve leading into the Brooklyn Station, and train speeds would be 40mph or less, for which speed the predicted velocity levels are less than the UW Thresholds.

D-3.13 UW Medical Center (13)

The UW Medical Center would be located at a horizontal offset of 910 feet from the nearest tunnel alignment at civil station 1208+53. The predictions were made with the adjusted numerical model. The predicted ground surface vibration velocity levels are plotted in Figure D-14. The predicted level for 55mph is 33dB at 8Hz, exceeding the UW Threshold of 31dB by 2dB. The predicted vibration levels also exceed the UW Threshold at all train speeds at the 50Hz third octave.

D-3.14 Fisheries Sciences (14)

The Fisheries Sciences building would be located at a horizontal offset of 1,640 feet from the nearest tunnel alignment at civil station 1248+74. The predictions were made with the adjusted numerical model. The predicted ground surface vibration velocity levels are plotted in Figure D-15. The predicted level for 50mph is 31dB at 50mph train speed, in excess of the UW Threshold of 30dB by about 1dB. The predicted levels are less than the UW Threshold at all other train speeds. The point of closest approach of the tunnel would be on the curve between the UW campus boundary and Brooklyn Station. The maximum train speed would be 40mph, for which the predicted velocity levels are substantially less than the UW Threshold.

D-3.15 Fisheries Teaching and Research Center (15)

The Fisheries Teaching and Research Center would be located at a horizontal offset of 1,858 feet from the nearest tunnel alignment at civil station 1248+13. The predictions were made with the adjusted numerical model. The predicted ground surface vibration velocity levels for trains running on standard DF track are plotted in Figure D-16. The predicted levels are all below the UW threshold. The point of closest approach of the tunnel would be on the curve between the

UW campus boundary and Brooklyn Station. The maximum train speed would be 40mph, for which speed the predicted velocity levels are substantially less than the UW Threshold.

D-3.16 More Hall (16)

More Hall would be located at a horizontal offset of 137 feet from the nearest tunnel alignment at civil station 1216+21. The predictions were made with the quadratic regression of LSR test data. The predicted ground surface vibration velocity levels are plotted in Figure D-17. The maximum ground surface velocity level at 8Hz is 44dB, exceeding the UW Threshold of 34dB by 10dB, at a train speed of 50mph. The maximum predicted velocity level is 57dB (700micro-in/sec) at 80Hz for 55mph trains, exceeding the UW Threshold of 37dB by 20dB.

D-3.17 Marine Studies (17)

The Marine Studies building would be located at a horizontal offset of 1,799 feet from the nearest tunnel alignment at civil station 1247+68. The predictions were made with the adjusted numerical model. The predicted ground surface vibration velocity levels are plotted in Figure D-18. The predicted ground surface maximum level is 30dB at 8 Hz at 50mph, exceeding the UW Threshold of about 28dB by 2dB. Predicted vibration levels are less than the UW Threshold at all other speeds. The point of closest approach of the tunnel would be on the curve between the UW campus boundary and Brooklyn Station. The maximum train speed would be 40mph, for which speed the predicted velocity levels are substantially less than the UW Threshold.

D-3.18 Bioengineering/Genomics (18)

The Bioengineering/Genomics building would be located at a horizontal offset of 1,612 feet from the nearest tunnel alignment at civil station 1244+85. The predictions were made with the adjusted numerical model. The predicted ground surface vibration velocity levels are plotted in Figure D-19. The predicted maximum ground surface velocity level at 8Hz for 50mph trains is 29dB, equal to the UW Threshold of 29dB.

D-3.19 Fluke Hall (19)

Fluke Hall would be located at a horizontal offset of 333 feet from the nearest tunnel alignment at northbound civil station 1226+35. The predictions were made with the adjusted numerical model. The predicted ground surface vibration velocity levels are plotted in Figure D-20. The predicted level at 8Hz for 50mph train speed is 40dB, in excess of the UW Threshold of 34dB by 6dB. The predicted levels at remaining speeds down to 40mph also exceed the UW Threshold at 8Hz. The predicted ground surface levels exceed the UW Threshold at all train speeds at frequencies of 40Hz and above. The predicted maximum level at 55mph is 48dB at 80Hz, exceeding the UW Threshold of 44dB by 23dB.

D-3.20 Mechanical Engineering Building (20a)

The Mechanical Engineering Building would be located at a horizontal offset of 105 feet from the nearest tunnel alignment at civil station 1223+23. The LSR was computed by regression of global borehole test data. The predicted velocity levels are plotted in Figure D-21. The predicted

vibration levels exceed the UW threshold at all train speeds. The maximum level at 8Hz is about 45dB at 50mph, in excess of the UW Threshold of 30dB by 15dB. The maximum level at 80Hz is 59dB at 55mph, exceeding the UW Threshold of 9dB by 40dB.

D-3.21 Mechanical Engineering Annex (20b)

The Mechanical Engineering Annex would be located at a horizontal offset of 9 feet from the nearest tunnel alignment at civil station 1222+85. The predictions were made with the physical model involving regression of test data over slant distance and the logarithm of slant distance. The predicted ground surface vibration velocity levels are plotted in Figure D-22. The predicted ground vibration levels exceed the UW Threshold at all train speeds and over most of the frequency range considered. The maximum predicted level at 8Hz is 46dB for 50mph trains, exceeding the UW Threshold of 33dB by 13dB. The maximum predicted level at 80Hz is 63dB for 55mph, exceeding the UW Threshold of 29dB by 34dB.

D-3.22 Ocean Sciences (21)

The Ocean Sciences building would be located at a horizontal offset of 2,056 feet from nearest tunnel alignment at civil station 1244+52. The predictions were made with the adjusted numerical model. The predicted ground surface vibration velocity levels are plotted in Figure D-23. The predicted velocity levels are below the UW Threshold at all train speeds.

D-3.23 Center on Human Development and Disability (22)

The Center on Human Development and Disability would be located at a horizontal offset of 753 feet from the nearest tunnel alignment at civil station 1200+52. The predictions were made with the adjusted numerical model. The predicted ground surface vibration velocity levels are plotted in Figure D-24. The predicted ground surface vibration levels exceed the UW ambient at 8 and 10Hz. The maximum predicted level at 8Hz is 38dB for 50mph trains, exceeding the UW Threshold of 34dB by 4dB. The maximum predicted level at 10Hz is 35dB for 45 and 55mph trains, exceeding the UW Threshold of 33dB by 2dB.

D-3.24 Fisheries Center (23)

The Fisheries Center building would be located at a horizontal offset of 1,242 feet from the nearest tunnel alignment at civil station 1202+68. The predictions were made with the adjusted numerical model. The predicted ground surface vibration velocity levels are plotted in Figure D-25. The predicted ground surface vibration velocity levels are less than the UW Thresholds.

Table D-2 Vibration Velocity Levels for All Buildings at 30-55 MPH

Freq. (Hz)	3.15	4	5	6.3	8	10	12.5	16	20	25	31.5	40	50	63	80	100	125
1) Electrical Engineering - 338 ft Offset, 120 ft Predicted Depth																	
30 MPH	11	14	22	23	26	26	15	16	28	25	25	29	36	40	45	39	34
35 MPH	13	12	23	27	30	29	17	18	25	27	26	30	35	39	44	40	34
40 MPH	15	13	18	32	35	31	19	17	26	29	31	32	36	40	44	40	35
45 MPH	22	23	25	31	37	36	22	19	28	30	34	33	38	40	45	40	36
50 MPH	17	19	16	25	40	34	27	23	26	31	35	36	36	40	44	39	35
55 MPH	15	26	22	18	35	36	25	22	24	27	28	38	38	44	48	42	38
LSR	-10	-8	-7	-5	-6	-8	-11	-9	-5	-3	-3	-3	-3	-4	-3	-3	-5
2) Johnson Hall - 688 ft Offset, 120 ft Predicted Depth																	
30 MPH	5	8	17	18	19	16	5	7	18	11	12	17	24	21	24	16	10
35 MPH	7	6	18	22	23	18	7	10	15	13	13	19	23	21	23	17	10
40 MPH	9	7	13	26	28	21	9	8	15	15	17	21	23	21	23	17	10
45 MPH	16	17	19	26	30	26	12	10	18	16	21	21	26	22	24	17	12
50 MPH	11	13	10	20	34	24	17	15	16	17	22	25	24	22	23	15	11
55 MPH	9	21	16	13	28	26	15	14	14	13	15	26	25	25	27	19	13
LSR	-16	-14	-12	-11	-12	-18	-21	-18	-15	-17	-17	-15	-16	-23	-24	-26	-30
3) Bagley Hall - 978 ft Offset, 120 ft Predicted Depth																	
30 MPH	3	7	15	15	16	16	9	9	15	11	10	9	13	15	15	4	-3
35 MPH	5	5	16	19	20	19	11	11	12	13	11	10	13	15	15	4	-4
40 MPH	7	6	11	24	25	21	13	10	12	15	15	12	13	15	14	5	-3
45 MPH	14	16	18	23	27	26	16	12	15	16	19	13	16	16	16	5	-1
50 MPH	9	12	9	17	31	25	20	16	13	16	20	16	13	16	14	3	-3
55 MPH	7	20	15	10	25	26	19	16	11	13	13	18	15	20	18	7	0
LSR	-18	-15	-14	-13	-15	-18	-17	-16	-18	-17	-19	-24	-26	-29	-32	-39	-43
4) Chemistry - 1008 ft Offset, 120 ft Predicted Depth																	
30 MPH	3	7	15	15	16	17	9	9	15	9	9	8	13	12	13	2	-4
35 MPH	5	5	16	19	20	19	10	11	12	11	10	9	12	12	13	2	-4
40 MPH	7	6	11	23	25	21	13	9	12	13	14	11	13	12	12	2	-4
45 MPH	14	16	17	23	27	27	16	11	14	14	18	12	15	12	14	3	-2
50 MPH	9	12	8	17	30	25	20	16	13	15	19	15	13	13	12	1	-3
55 MPH	7	19	15	10	25	26	18	15	10	11	12	17	14	16	16	5	-1
LSR	-18	-15	-14	-14	-15	-17	-17	-17	-18	-19	-20	-25	-27	-32	-34	-41	-44
5) Wilcox Hall - 110 ft Offset, 100 ft Predicted Depth																	
30 MPH	16	19	27	28	31	34	27	28	37	32	35	41	48	53	57	52	48
35 MPH	18	17	28	32	35	36	29	31	34	34	36	42	47	53	57	53	48
40 MPH	20	18	23	36	40	39	31	29	34	36	40	44	48	53	56	53	48
45 MPH	27	28	30	36	42	44	34	31	37	37	44	45	50	53	57	53	50
50 MPH	23	24	21	30	45	42	38	36	35	38	45	48	48	54	56	52	49
55 MPH	21	31	27	23	40	44	37	35	33	34	38	50	49	57	60	56	52
LSR	-4	-3	-2	-1	0	0	1	3	4	4	6	8	8	9	9	10	8

Table D-2 (Continued) Vibration Velocity Levels for All Buildings at 30-55 MPH

Freq. (Hz)	3.15	4	5	6.3	8	10	12.5	16	20	25	31.5	40	50	63	80	100	125
6) Physics & Astronomy - 1200 ft Offset, 120 ft Predicted Depth																	
30 MPH	3	7	14	14	15	16	6	6	14	5	5	6	10	5	4	-4	-6
35 MPH	5	4	15	18	19	19	8	8	11	8	6	7	9	5	4	-3	-7
40 MPH	7	6	10	23	24	21	10	7	12	9	10	9	10	5	3	-3	-6
45 MPH	14	15	16	22	26	26	13	9	14	10	14	9	12	5	4	-3	-4
50 MPH	9	12	8	16	30	25	17	13	12	11	15	13	10	6	3	-4	-5
55 MPH	7	19	14	9	24	26	16	12	10	7	8	15	12	9	7	0	-3
LSR	-18	-16	-15	-14	-16	-18	-20	-20	-19	-23	-24	-27	-29	-39	-43	-46	-46
7) Burke Museum - 826 ft Offset, 80 ft Predicted Depth																	
30 MPH	4	9	19	20	23	24	16	15	19	17	14	18	23	24	22	13	7
35 MPH	6	6	19	24	27	27	17	17	16	19	15	19	22	24	22	14	6
40 MPH	7	8	14	29	32	29	20	15	17	21	20	21	23	24	21	14	7
45 MPH	15	17	21	28	34	34	23	17	19	22	23	22	25	24	23	15	9
50 MPH	10	14	12	22	37	33	27	22	17	23	24	25	23	25	21	13	7
55 MPH	8	21	18	15	32	34	25	21	15	19	17	27	25	28	25	17	10
LSR	-17	-14	-11	-8	-8	-10	-10	-11	-14	-11	-14	-15	-17	-20	-25	-29	-33
8) Benson Hall - 1269 ft Offset, 120 ft Predicted Depth																	
30 MPH	3	7	14	14	15	16	6	6	14	5	5	6	10	5	4	-4	-6
35 MPH	5	4	15	18	19	19	8	8	11	8	6	7	9	5	4	-3	-7
40 MPH	7	6	10	23	24	21	10	7	12	9	10	9	10	5	3	-3	-6
45 MPH	14	15	16	22	26	26	13	9	14	10	14	9	12	5	4	-3	-4
50 MPH	9	12	8	16	30	25	17	13	12	11	15	13	10	6	3	-4	-5
55 MPH	7	19	14	9	24	26	16	12	10	7	8	15	12	9	7	0	-3
LSR	-18	-16	-15	-14	-16	-18	-20	-20	-19	-23	-24	-27	-29	-39	-43	-46	-46
9) Roberts Hall - 255 ft Offset, 115 ft Predicted Depth																	
30 MPH	14	17	25	25	29	31	25	25	33	29	30	34	40	45	48	43	40
35 MPH	16	14	25	29	33	34	27	27	30	31	31	35	39	44	48	44	39
40 MPH	18	16	20	34	38	36	29	26	31	33	36	37	40	45	47	44	40
45 MPH	25	25	27	33	40	41	32	28	33	33	39	38	42	45	48	44	42
50 MPH	21	22	18	27	43	40	36	32	31	34	40	41	40	45	47	43	40
55 MPH	19	29	24	20	38	41	35	31	29	31	33	43	42	49	51	47	43
LSR	-7	-5	-4	-3	-3	-3	-1	0	0	1	2	2	1	1	0	1	0
10) Winkenwerder Hall - 683 ft Offset, 100 ft Predicted Depth																	
30 MPH	5	9	18	19	22	21	11	9	21	18	14	17	25	23	25	18	9
35 MPH	7	6	18	23	26	23	13	11	18	20	15	18	24	23	25	18	9
40 MPH	9	8	14	28	31	26	16	10	19	22	19	20	25	23	24	19	9
45 MPH	16	17	20	27	33	31	18	12	21	23	23	21	27	24	25	19	11
50 MPH	11	14	11	21	36	29	23	16	19	23	24	24	25	24	24	17	10
55 MPH	9	21	17	14	31	31	21	15	17	20	17	26	26	27	28	21	13
LSR	-16	-14	-11	-9	-10	-13	-15	-16	-12	-10	-15	-16	-15	-21	-23	-25	-31

Table D-2 (Continued) Vibration Velocity Levels for All Buildings at 30-55 MPH

Freq. (Hz)	3.15	4	5	6.3	8	10	12.5	16	20	25	31.5	40	50	63	80	100	125
11) Henderson Hall - 1208 ft Offset, 80 ft Predicted Depth																	
30 MPH	4	7	16	17	20	21	12	10	16	9	7	7	14	7	7	-2	-3
35 MPH	6	5	17	21	24	24	14	13	13	11	8	8	13	7	7	-1	-3
40 MPH	7	6	12	26	29	26	16	11	14	13	13	10	13	7	6	-1	-3
45 MPH	15	16	18	26	31	31	19	13	16	14	16	11	16	7	7	-1	-1
50 MPH	10	12	9	19	34	30	23	18	14	14	17	14	13	8	6	-2	-2
55 MPH	8	20	16	13	29	31	22	17	12	11	10	16	15	11	10	2	1
LSR	-17	-15	-13	-11	-11	-13	-14	-15	-17	-19	-21	-26	-26	-37	-40	-44	-43
12) Oceanography Research Building - 1833 ft Offset, 80 ft Predicted Depth																	
30 MPH	0	5	13	13	16	16	7	5	8	2	-3	-4	-3	-13	-	-	-
35 MPH	2	2	14	17	20	19	9	7	5	4	-2	-3	-3	-13	-	-	-
40 MPH	4	4	9	22	25	21	11	6	6	6	3	-1	-3	-13	-	-	-
45 MPH	12	13	15	22	27	26	14	8	8	6	6	0	0	-13	-	-	-
50 MPH	7	10	6	15	30	25	18	12	7	7	7	3	-3	-12	-	-	-
55 MPH	5	17	12	9	25	26	17	11	4	4	0	5	-1	-9	-	-	-
LSR	-20	-18	-16	-15	-16	-18	-19	-21	-24	-26	-31	-37	-42	-57	-	-	-
13) Medical Center - 910 ft Offset, 110 ft Predicted Depth																	
30 MPH	3	8	16	17	18	18	10	11	16	14	12	13	18	16	15	8	0
35 MPH	5	5	17	21	22	21	12	13	13	17	13	14	18	16	15	9	0
40 MPH	7	7	12	26	27	23	14	12	14	19	18	16	18	16	14	9	1
45 MPH	14	16	19	25	29	28	17	14	16	19	22	17	21	16	16	9	2
50 MPH	10	13	10	19	33	27	22	18	15	20	22	20	18	16	14	8	1
55 MPH	8	20	16	12	27	28	20	17	12	16	15	22	20	20	18	12	4
LSR	-18	-14	-13	-11	-13	-16	-16	-14	-16	-13	-16	-20	-21	-28	-32	-34	-39
14) Fisheries Sciences - 1640 ft Offset, 80 ft Predicted Depth																	
30 MPH	1	5	14	14	17	17	8	6	10	4	-1	-2	4	-3	-	-	-
35 MPH	3	3	15	19	21	20	10	9	7	6	0	-1	3	-3	-	-	-
40 MPH	5	4	10	23	26	22	13	7	8	8	5	1	4	-3	-	-	-
45 MPH	12	14	16	23	28	27	15	9	10	8	8	2	6	-2	-	-	-
50 MPH	8	10	7	16	31	26	20	14	8	9	9	5	4	-2	-	-	-
55 MPH	6	17	13	10	26	27	18	13	6	6	2	7	5	2	-	-	-
LSR	-20	-17	-15	-14	-15	-17	-18	-19	-23	-24	-29	-35	-36	-47	-	-	-
15) Fisheries Teaching & Research Center - 1858 ft Offset, 80 ft Predicted Depth																	
30 MPH	0	4	13	13	15	16	7	4	9	1	-3	-5	-3	-14	-	-	-
35 MPH	2	2	13	17	19	18	8	6	6	4	-2	-4	-4	-14	-	-	-
40 MPH	4	3	8	22	24	21	11	5	6	6	2	-2	-4	-13	-	-	-
45 MPH	11	13	15	21	26	26	13	7	9	6	6	-1	-1	-13	-	-	-
50 MPH	7	9	6	15	30	24	18	11	7	7	7	2	-3	-13	-	-	-
55 MPH	5	17	12	8	24	26	16	10	5	3	0	4	-2	-9	-	-	-
LSR	-21	-18	-16	-15	-16	-18	-20	-22	-24	-26	-32	-38	-43	-58	-	-	-

Table D-2 (Continued) Vibration Velocity Levels for All Buildings at 30-55 MPH

Freq. (Hz)	3.15	4	5	6.3	8	10	12.5	16	20	25	31.5	40	50	63	80	100	125
16) More Hall - 137 ft Offset, 115 ft Predicted Depth																	
30 MPH	15	18	26	27	30	32	26	27	35	30	33	37	45	50	54	50	46
35 MPH	17	16	26	31	34	35	28	30	32	33	34	38	44	50	54	51	45
40 MPH	19	17	22	35	39	37	30	28	33	35	38	40	45	50	53	51	46
45 MPH	26	27	28	35	41	42	33	30	35	35	42	41	47	50	54	51	47
50 MPH	21	23	19	29	44	41	37	35	33	36	43	44	45	51	53	49	46
55 MPH	19	30	25	22	39	42	36	34	31	32	36	46	46	54	57	53	49
LSR	-6	-4	-3	-2	-1	-2	0	2	3	3	4	5	5	6	7	8	6
17) Marine Studies - 1799 ft Offset, 80 ft Predicted Depth																	
30 MPH	0	5	13	13	16	16	7	5	8	2	-3	-4	-3	-13	-	-	-
35 MPH	2	2	14	17	20	19	9	7	5	4	-2	-3	-3	-13	-	-	-
40 MPH	4	4	9	22	25	21	11	6	6	6	3	-1	-3	-13	-	-	-
45 MPH	12	13	15	22	27	26	14	8	8	6	6	0	0	-13	-	-	-
50 MPH	7	10	6	15	30	25	18	12	7	7	7	3	-3	-12	-	-	-
55 MPH	5	17	12	9	25	26	17	11	4	4	0	5	-1	-9	-	-	-
LSR	-20	-18	-16	-15	-16	-18	-19	-21	-24	-26	-31	-37	-42	-57	-	-	-
18) Bioengineering/ Genomics - 1612 ft Offset, 100 ft Predicted Depth																	
30 MPH	1	5	13	13	15	14	5	4	9	3	0	-1	3	-4	-	-	-
35 MPH	3	2	14	17	19	16	6	6	6	6	1	0	2	-4	-	-	-
40 MPH	5	4	9	22	24	19	9	5	6	8	6	2	3	-4	-	-	-
45 MPH	12	13	15	21	26	24	12	7	8	8	9	3	5	-4	-	-	-
50 MPH	7	10	6	15	29	22	16	11	7	9	10	6	3	-3	-	-	-
55 MPH	6	17	12	8	24	24	14	11	4	6	3	8	5	0	-	-	-
LSR	-20	-18	-16	-15	-17	-20	-21	-21	-24	-24	-28	-34	-36	-48	-	-	-
19) Fluke Hall - 333 ft Offset, 120 ft Predicted Depth																	
30 MPH	11	14	22	23	26	26	15	16	28	25	25	29	36	40	45	39	34
35 MPH	13	12	23	27	30	29	17	18	25	27	26	30	35	39	44	40	34
40 MPH	15	13	18	32	35	31	19	17	26	29	31	32	36	40	44	40	35
45 MPH	22	23	25	31	37	36	22	19	28	30	34	33	38	40	45	40	36
50 MPH	17	19	16	25	40	34	27	23	26	31	35	36	36	40	44	39	35
55 MPH	15	26	22	18	35	36	25	22	24	27	28	38	38	44	48	42	38
LSR	-10	-8	-7	-5	-6	-8	-11	-9	-5	-3	-3	-3	-3	-4	-3	-3	-5
20a) ME Building - 105 ft Offset, 115 ft Predicted Depth																	
30 MPH	15	19	26	27	30	33	26	28	36	31	33	38	46	52	56	52	47
35 MPH	17	16	27	31	34	35	28	30	33	33	34	39	45	52	56	52	47
40 MPH	19	18	22	36	39	37	31	29	33	35	39	41	46	52	55	53	48
45 MPH	26	27	28	35	41	42	33	31	36	36	42	42	48	52	56	53	49
50 MPH	21	24	20	29	45	41	38	35	34	37	43	45	46	52	55	51	48
55 MPH	19	31	26	22	39	42	36	34	32	33	36	47	48	56	59	55	51
LSR	-6	-4	-3	-1	-1	-2	0	3	3	3	5	5	7	8	8	9	8

Table D-2 (Continued) Vibration Velocity Levels for All Buildings at 30-55 MPH

Freq. (Hz)	3.15	4	5	6.3	8	10	12.5	16	20	25	31.5	40	50	63	80	100	125
20b) ME Annex - 9 ft Offset, 115 ft Predicted Depth																	
30 MPH	16	19	28	29	32	34	27	28	36	32	34	40	49	55	60	55	51
35 MPH	18	17	29	33	36	37	29	30	33	35	35	41	48	55	60	56	51
40 MPH	20	18	24	38	41	39	31	29	34	36	39	43	49	55	59	56	51
45 MPH	27	28	30	37	43	44	34	31	36	37	43	44	51	55	60	56	53
50 MPH	23	24	21	31	46	43	38	35	34	38	44	47	49	56	59	55	52
55 MPH	21	31	27	24	41	44	37	35	32	34	37	49	51	59	63	59	54
LSR	-5	-3	-1	0	0	0	1	3	4	4	5	7	9	11	12	13	11
21) Ocean Sciences - 2056 ft Offset, 100 ft Predicted Depth																	
30 MPH	0	4	11	11	12	12	2	-3	7	-1	-6	-7	-8	-14	-	-	-
35 MPH	2	1	12	15	16	15	3	-1	3	1	-5	-6	-9	-15	-	-	-
40 MPH	4	3	7	20	21	17	6	-2	4	3	-1	-4	-8	-14	-	-	-
45 MPH	11	12	13	19	23	22	9	0	6	3	3	-3	-6	-14	-	-	-
50 MPH	6	9	5	13	27	21	13	4	5	4	4	0	-8	-14	-	-	-
55 MPH	4	16	11	6	21	22	11	3	2	1	-3	2	-6	-10	-	-	-
LSR	-21	-19	-18	-17	-19	-22	-24	-28	-26	-29	-35	-40	-48	-58	-	-	-
22) Center on Human Development and Disability - 753 ft Offset, 100 ft Predicted Depth																	
30 MPH	4	9	19	20	23	25	16	14	21	19	15	19	24	25	25	16	9
35 MPH	6	6	19	24	27	27	18	17	18	21	16	20	24	24	25	17	8
40 MPH	8	8	15	29	32	30	20	15	18	23	20	22	24	25	24	17	9
45 MPH	15	17	21	29	34	35	23	17	21	24	24	23	27	25	25	18	10
50 MPH	10	14	12	22	38	33	27	22	19	24	25	26	24	25	24	16	9
55 MPH	8	21	18	16	32	35	26	21	17	21	18	28	26	29	28	20	12
LSR	-17	-14	-10	-8	-8	-9	-10	-11	-12	-9	-14	-14	-15	-20	-22	-26	-31
23) Fisheries Center - 1242 ft Offset, 100 ft Predicted Depth																	
30 MPH	3	7	15	16	18	19	9	8	15	7	8	8	10	7	6	-3	-4
35 MPH	5	4	16	20	22	21	10	10	12	10	9	9	10	7	5	-2	-5
40 MPH	7	6	11	24	27	23	13	8	13	12	13	11	10	7	4	-2	-4
45 MPH	14	15	17	24	29	28	16	10	15	12	17	12	13	7	6	-1	-3
50 MPH	10	12	8	18	32	27	20	15	14	13	18	15	10	8	4	-3	-4
55 MPH	8	19	15	11	27	28	18	14	11	9	11	17	12	11	9	1	-1
LSR	-18	-15	-14	-13	-14	-16	-17	-18	-17	-20	-21	-25	-29	-37	-42	-45	-44

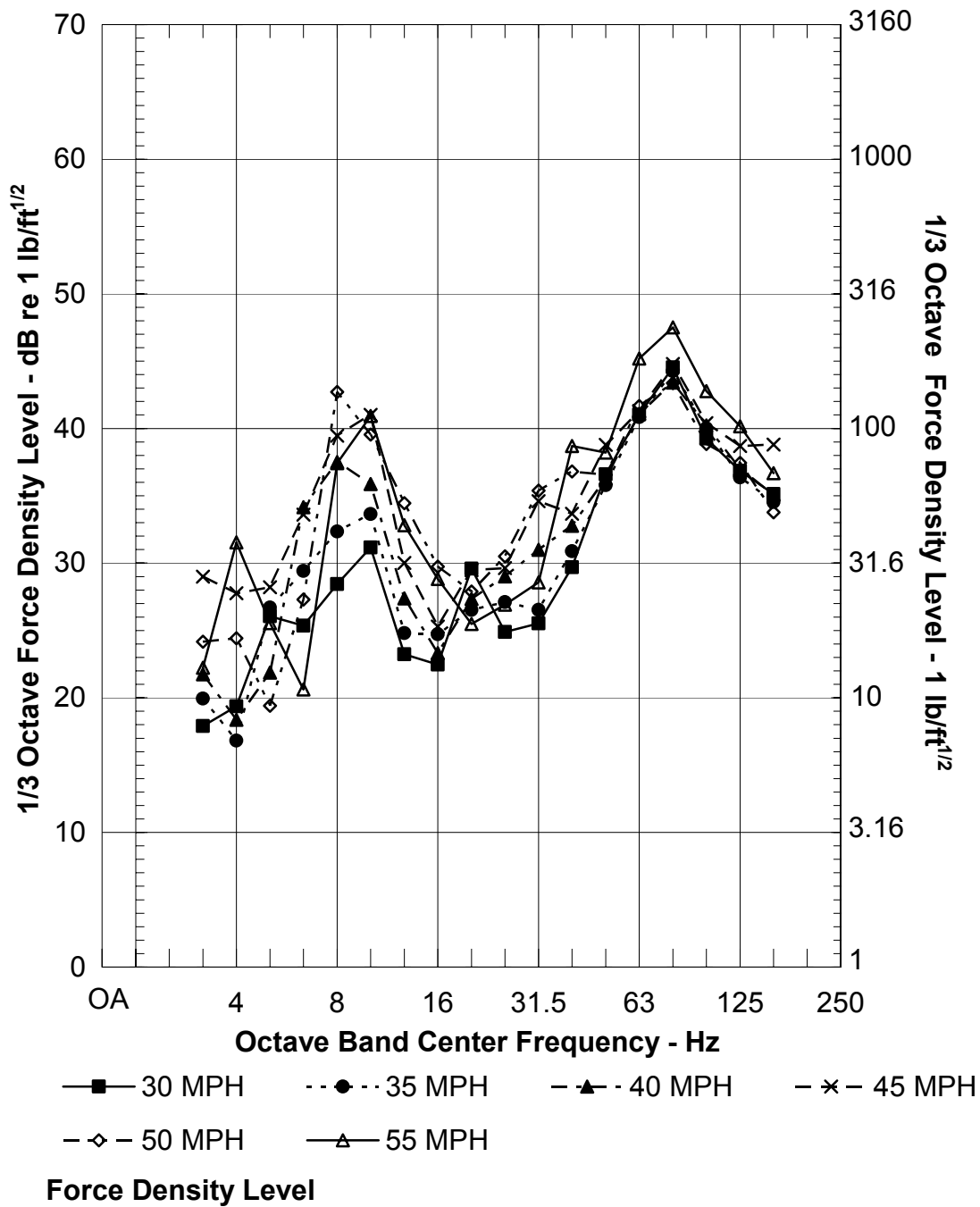
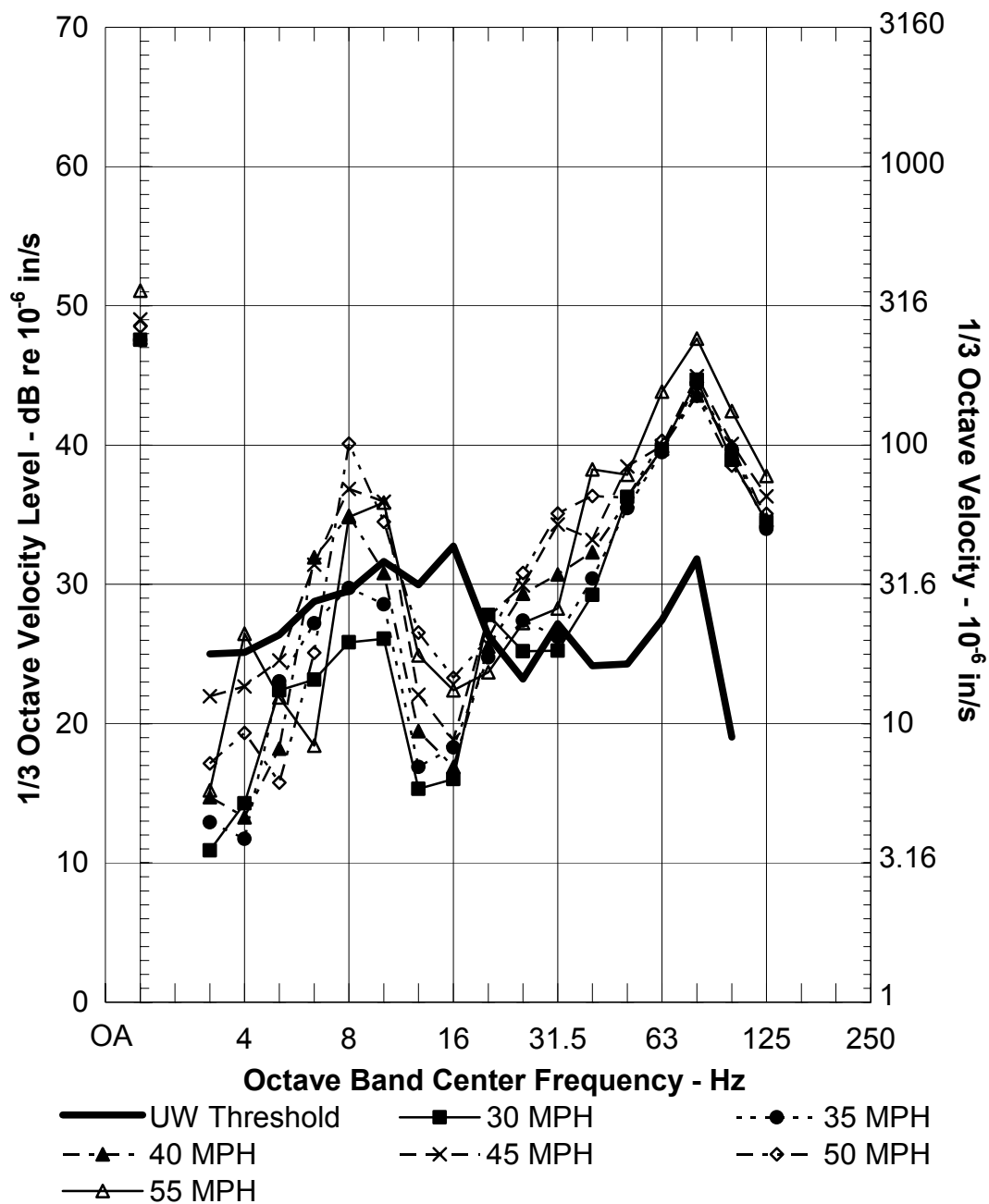
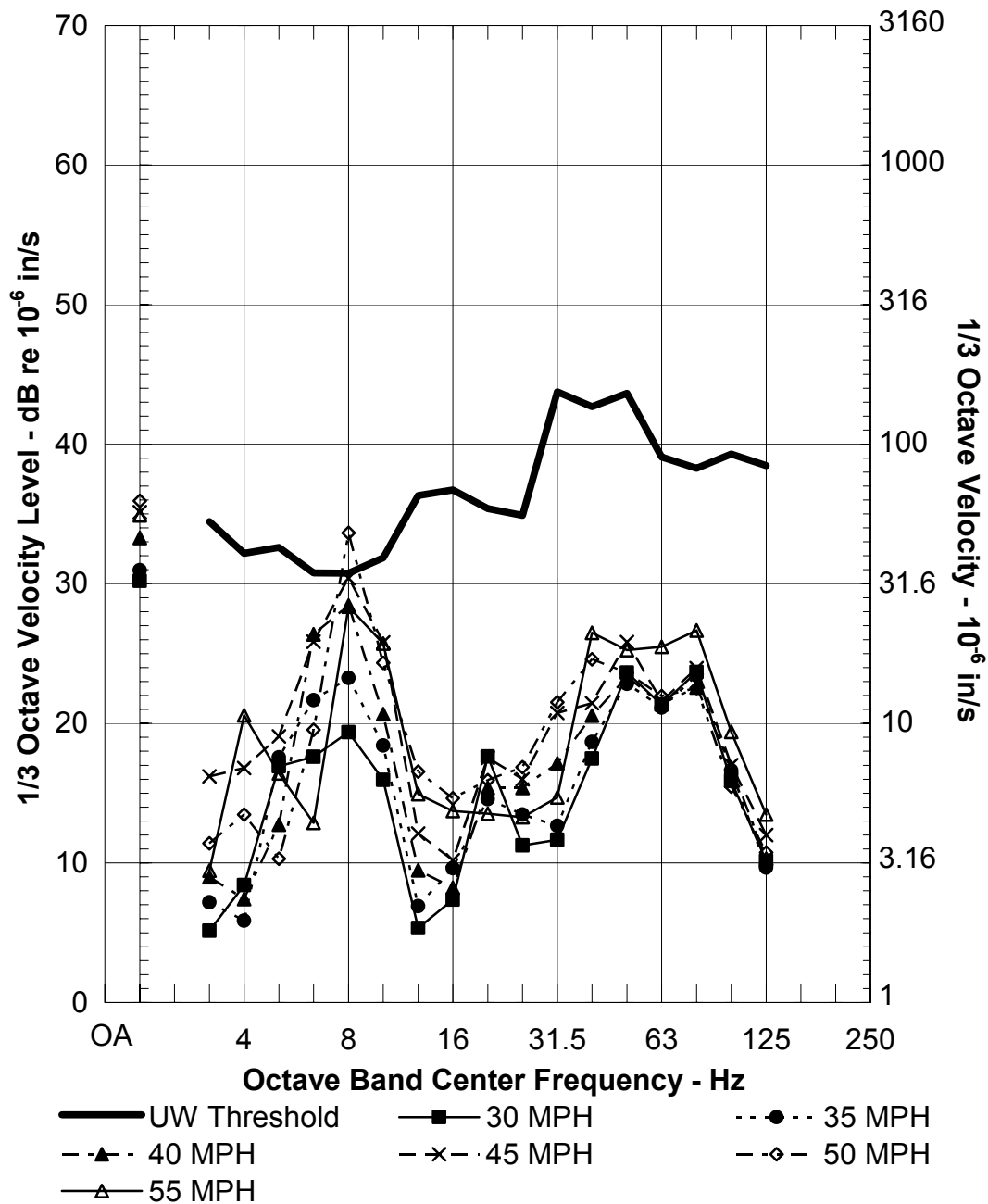


Figure D-1 FDLs for 30 to 55 MPH 4-Car Kinkysharyo train on Standard Direct Fixation Track



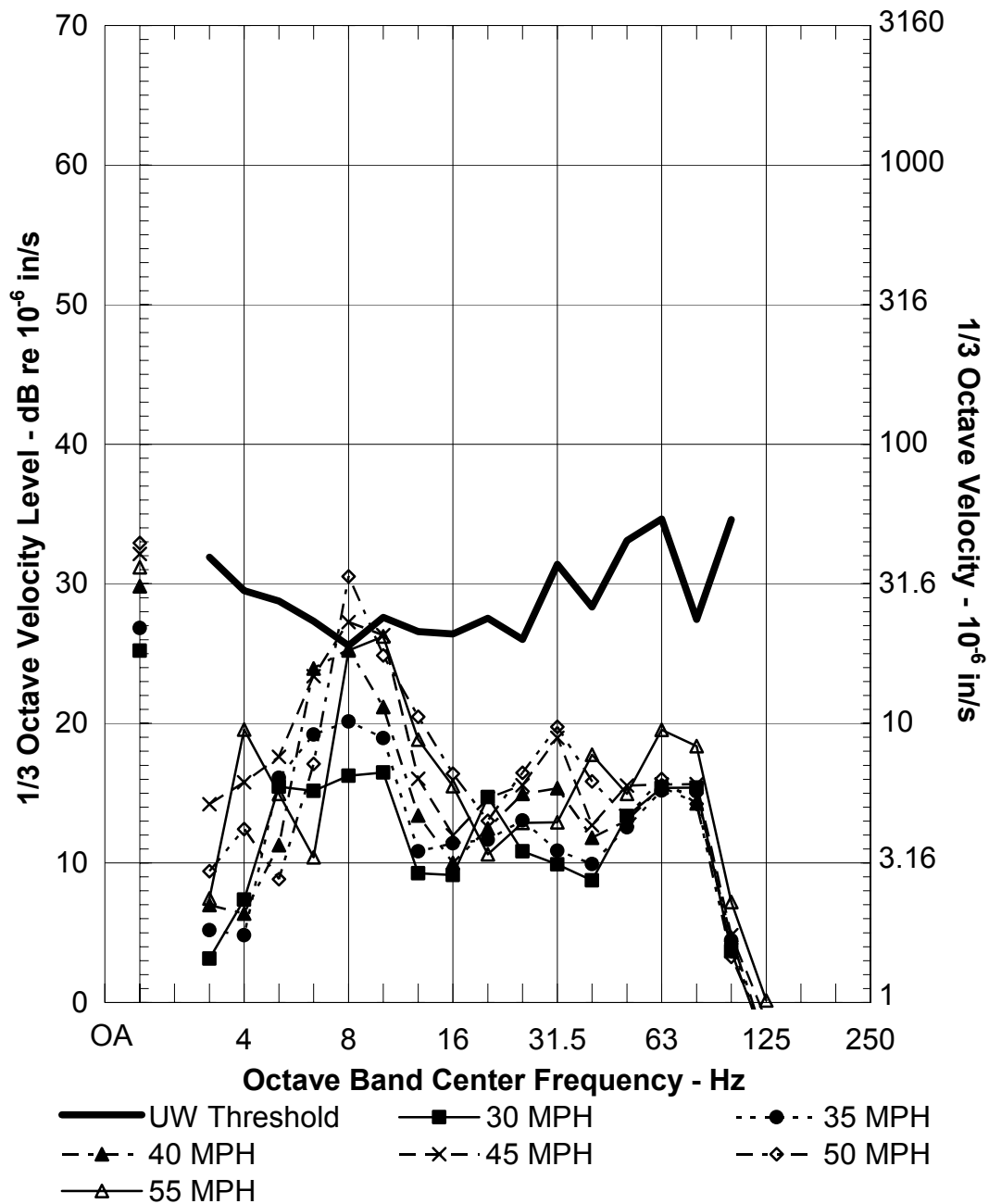
1) Elec. Engin. Vibration At Ground Surface
 Numerical Model Prediction
 VTA FDL, Two Simultaneous Trains, Standard DF
 338 ft Offset, 120 ft Predicted Depth

Figure D-2 Ground Surface Vibration Velocity Levels at Electrical Engineering for Two Simultaneous Train Passbys



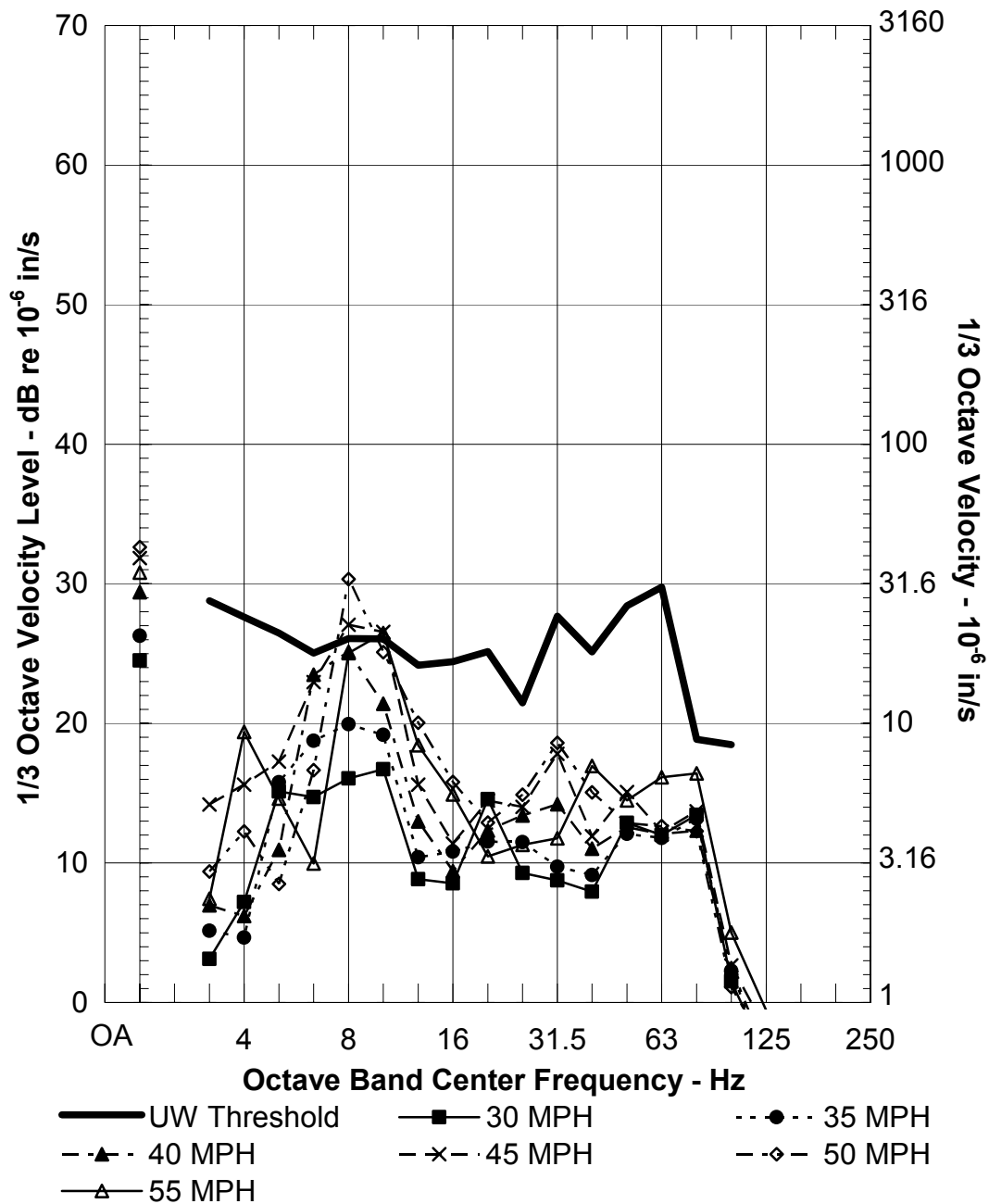
2) Johnson Hall Vibration At Ground Surface
 Numerical Model Prediction
 VTA FDL, Two Simultaneous Trains, Standard DF
 688 ft Offset, 120 ft Predicted Depth

Figure D-3 Ground Surface Vibration Velocity Levels at Johnson Hall for Two Simultaneous Train Passbys



3) Bagley Hall Vibration At Ground Surface
Numerical Model Prediction
VTA FDL, Two Simultaneous Trains, Standard DF
978 ft Offset, 120 ft Predicted Depth

Figure D-4 Ground Surface Vibration Velocity Levels at Bagley Hall for Two Simultaneous Train Passbys



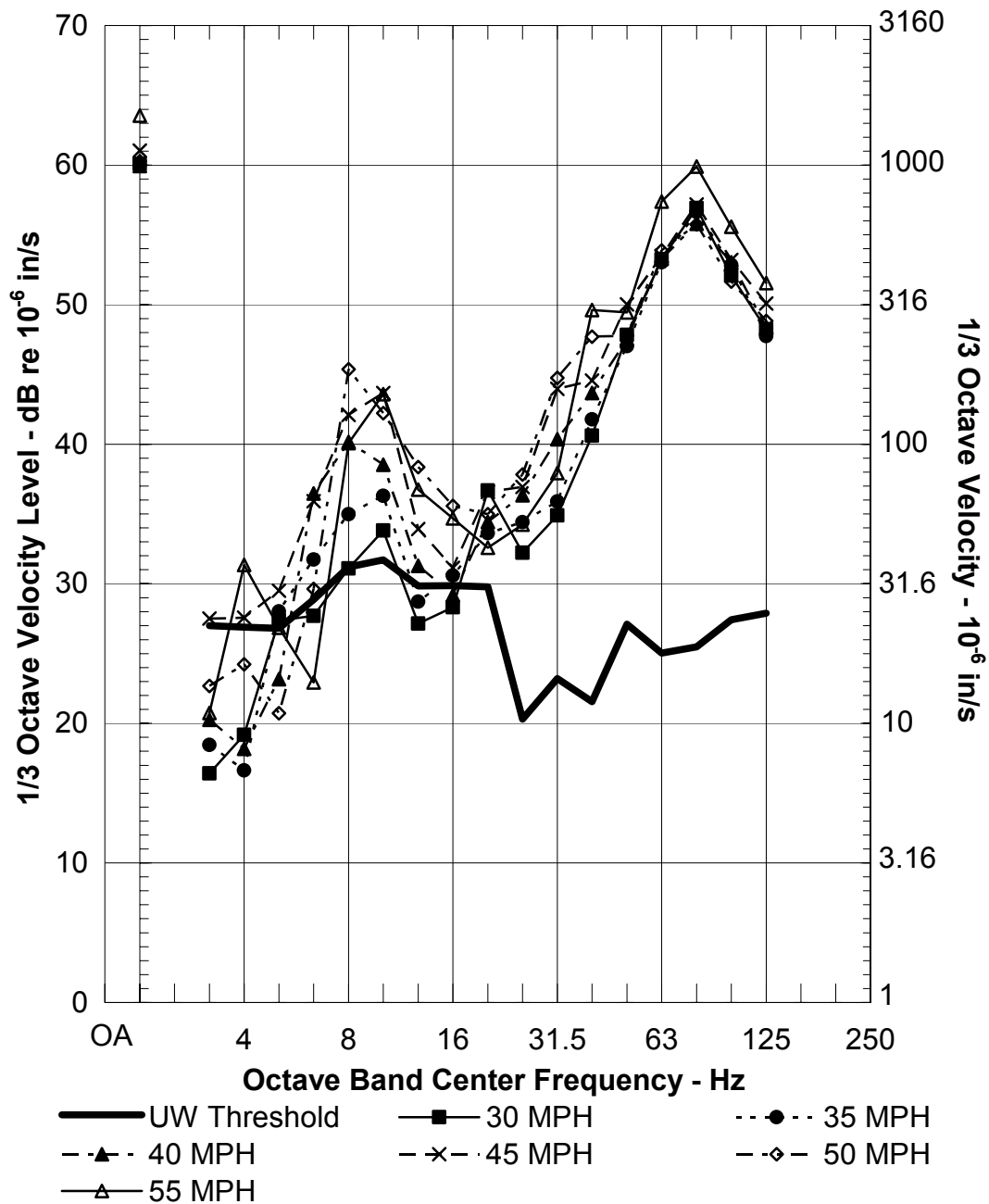
4) Chemistry Vibration At Ground Surface

Numerical Model Prediction

VTA FDL, Two Simultaneous Trains, Standard DF

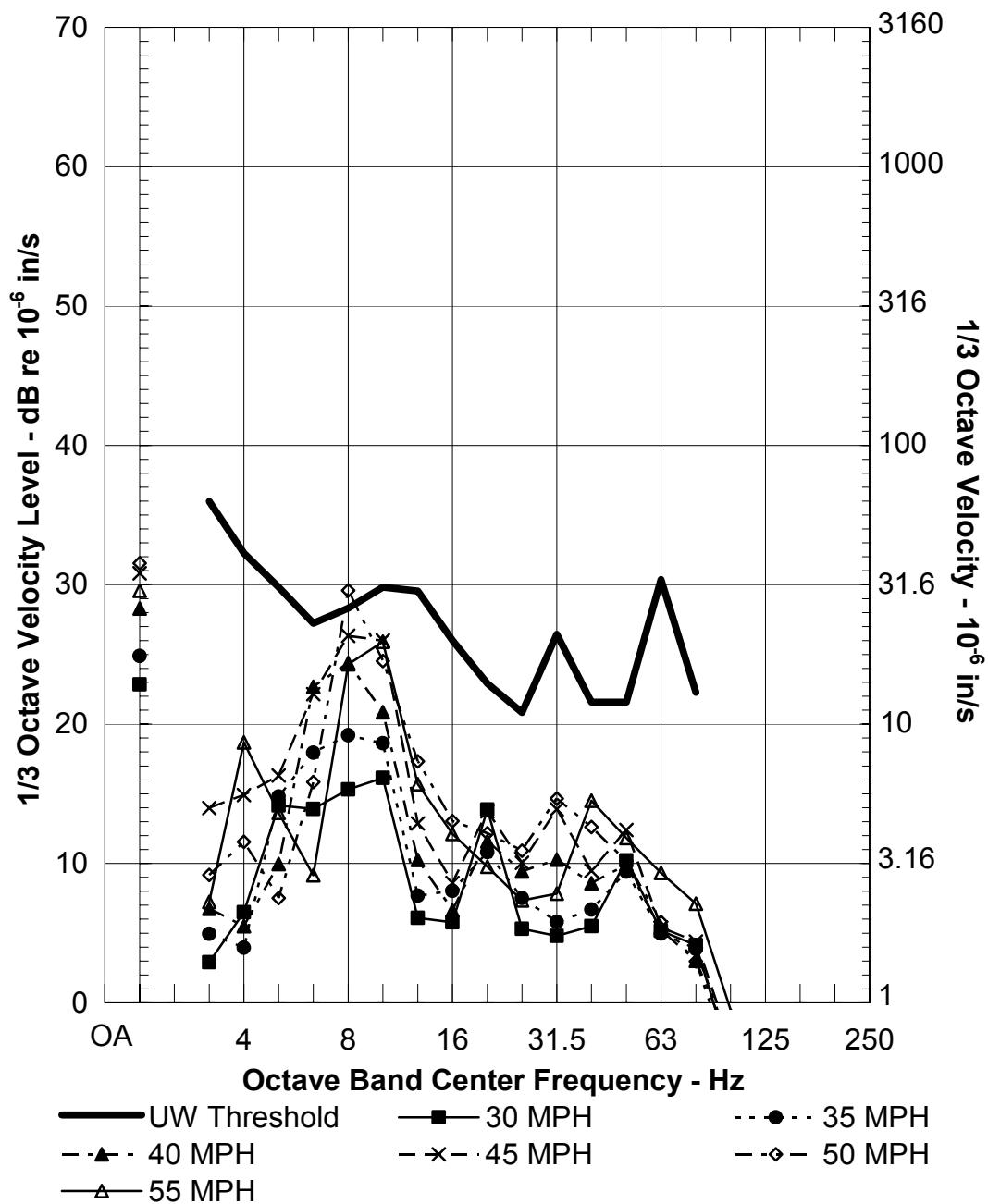
1008 ft Offset, 120 ft Predicted Depth

Figure D-5 Ground Surface Vibration Velocity Levels at New Chemistry for Two Simultaneous Train Passbys



5) Wilcox Hall Vibration At Ground Surface
 Global Quadratic LSR
 VTA FDL, Two Simultaneous Trains, Standard DF
 110 ft Offset, 100 ft Predicted Depth

Figure D-6 Ground Surface Vibration Velocity Levels at Wilcox Hall for Two Simultaneous Train Passbys



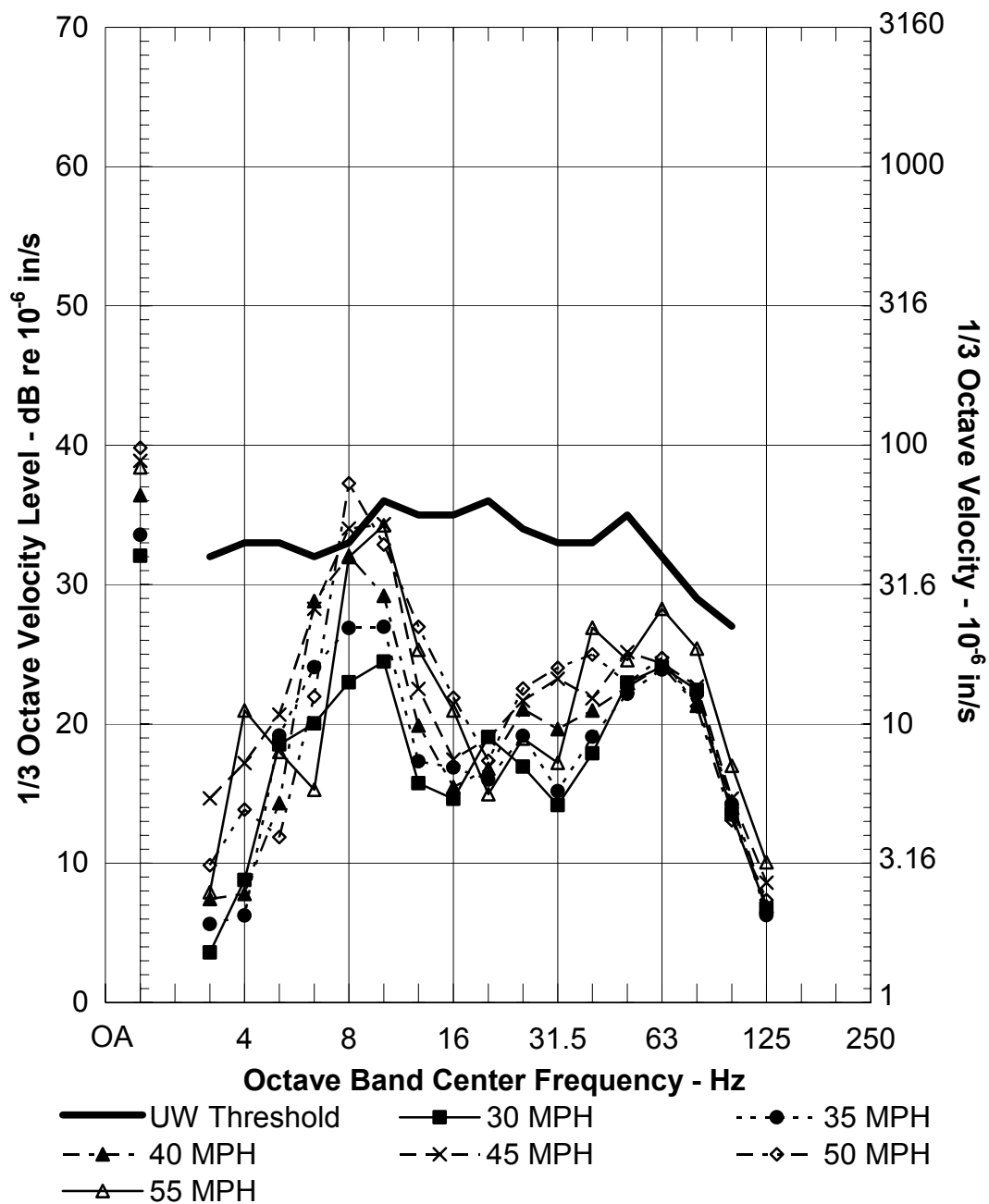
6) Physics & Astro. Vibration At Ground Surface

Numerical Model Prediction

VTA FDL, Two Simultaneous Trains, Standard DF

1200 ft Offset, 120 ft Predicted Depth

Figure D-7 Ground Surface Vibration Velocity Levels at Physics and Astronomy for Two Simultaneous Train Passbys



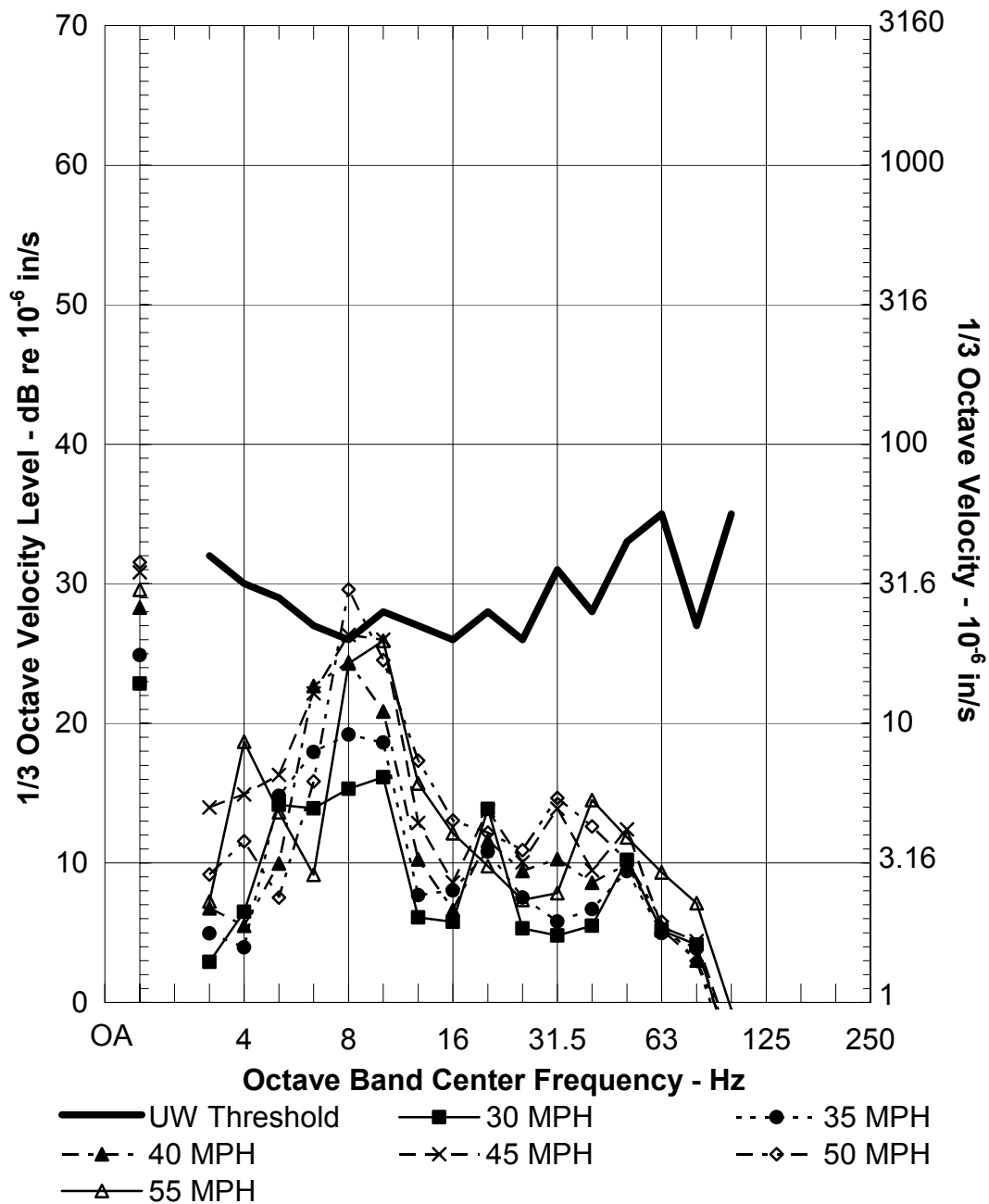
7) Burke Museum Vibration At Ground Surface

Numerical Model Prediction

VTA FDL, Two Simultaneous Trains, Standard DF

826 ft Offset, 80 ft Predicted Depth

Figure D-8 Ground Surface Vibration Velocity Levels at Burke Museum for Two Simultaneous Train Passbys



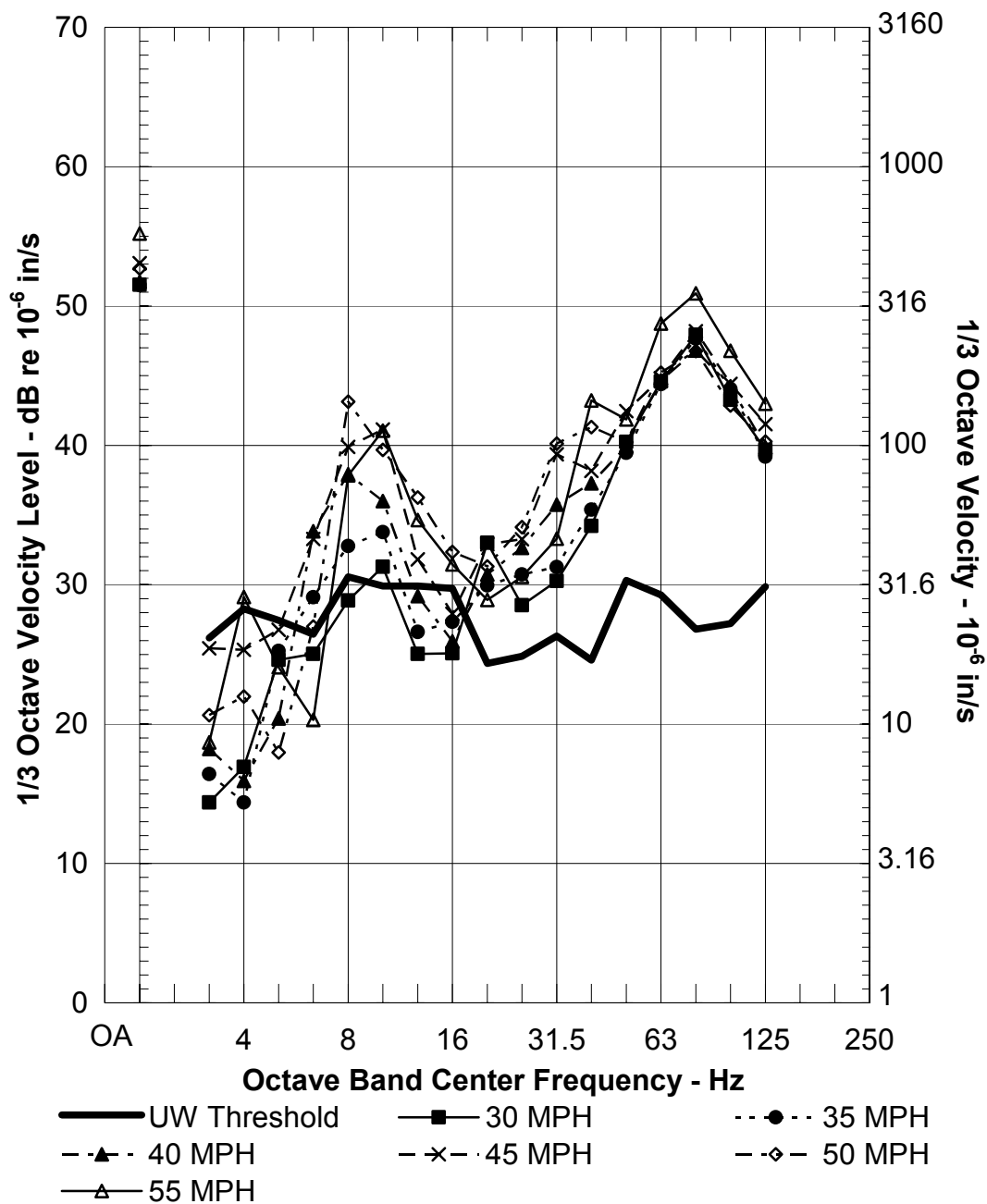
8) Benson Hall Vibration At Ground Surface

Numerical Model Prediction

VTA FDL, Two Simultaneous Trains, Standard DF

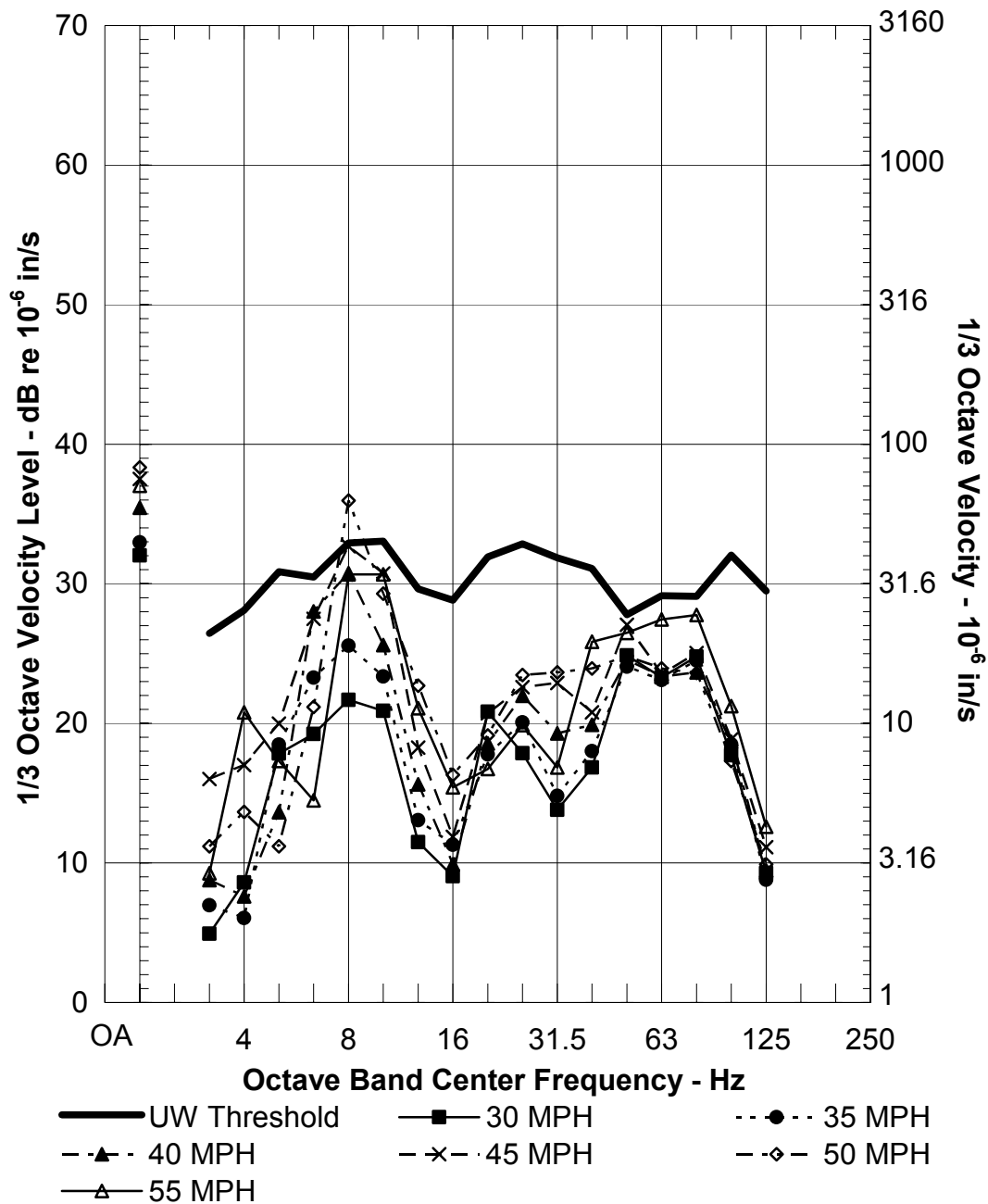
1269 ft Offset, 120 ft Predicted Depth

Figure D-9 Ground Surface Vibration Velocity Levels at Benson Hall for Two Simultaneous Train Passbys



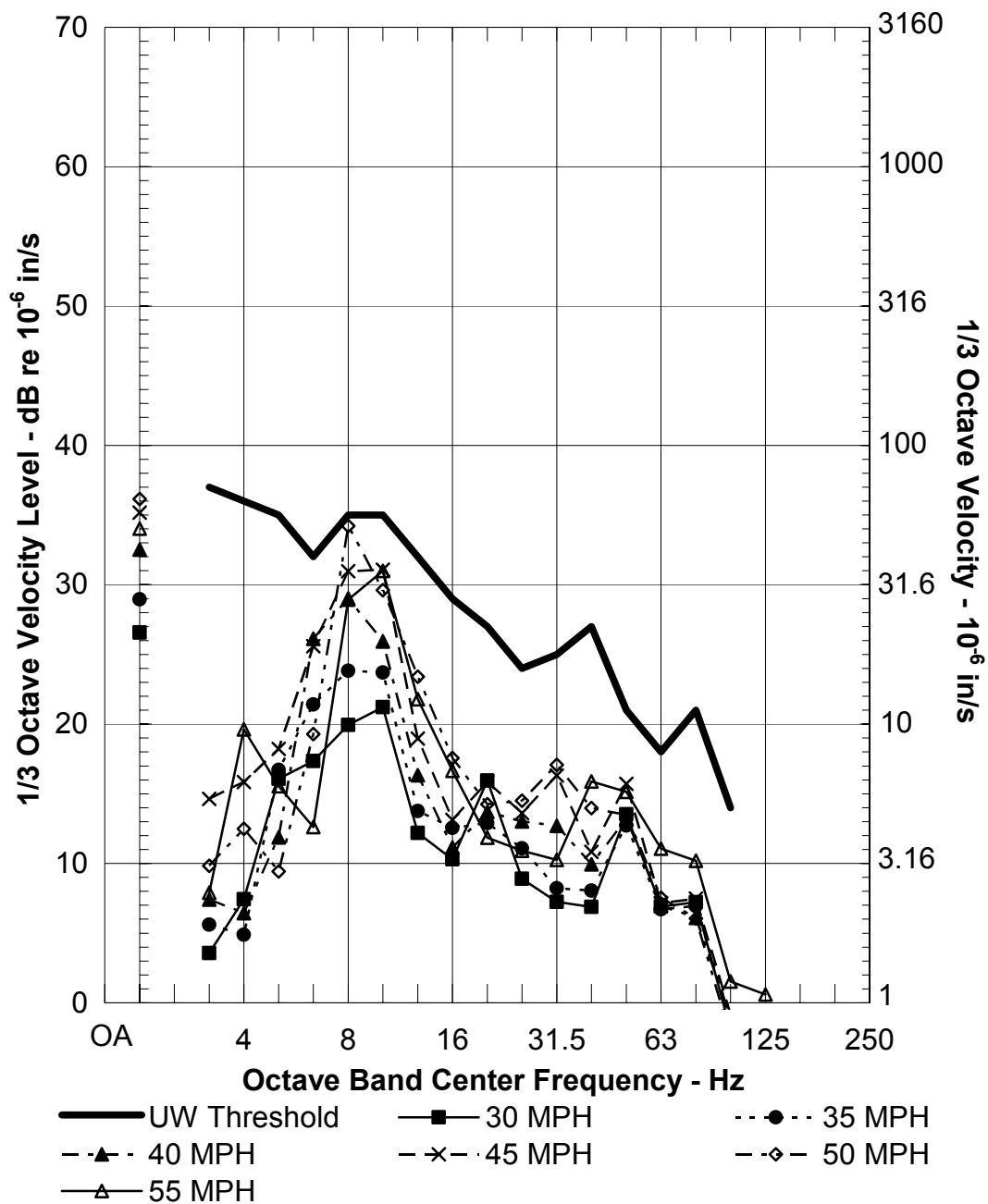
9) Roberts Hall Vibration At Ground Surface
Global Quadratic LSR
VTA FDL, Two Simultaneous Trains, Standard DF
225 ft Offset, 115 ft Predicted Depth

Figure D-10 Ground Surface Vibration Velocity Levels at Roberts Hall for Two Simultaneous Train Passbys



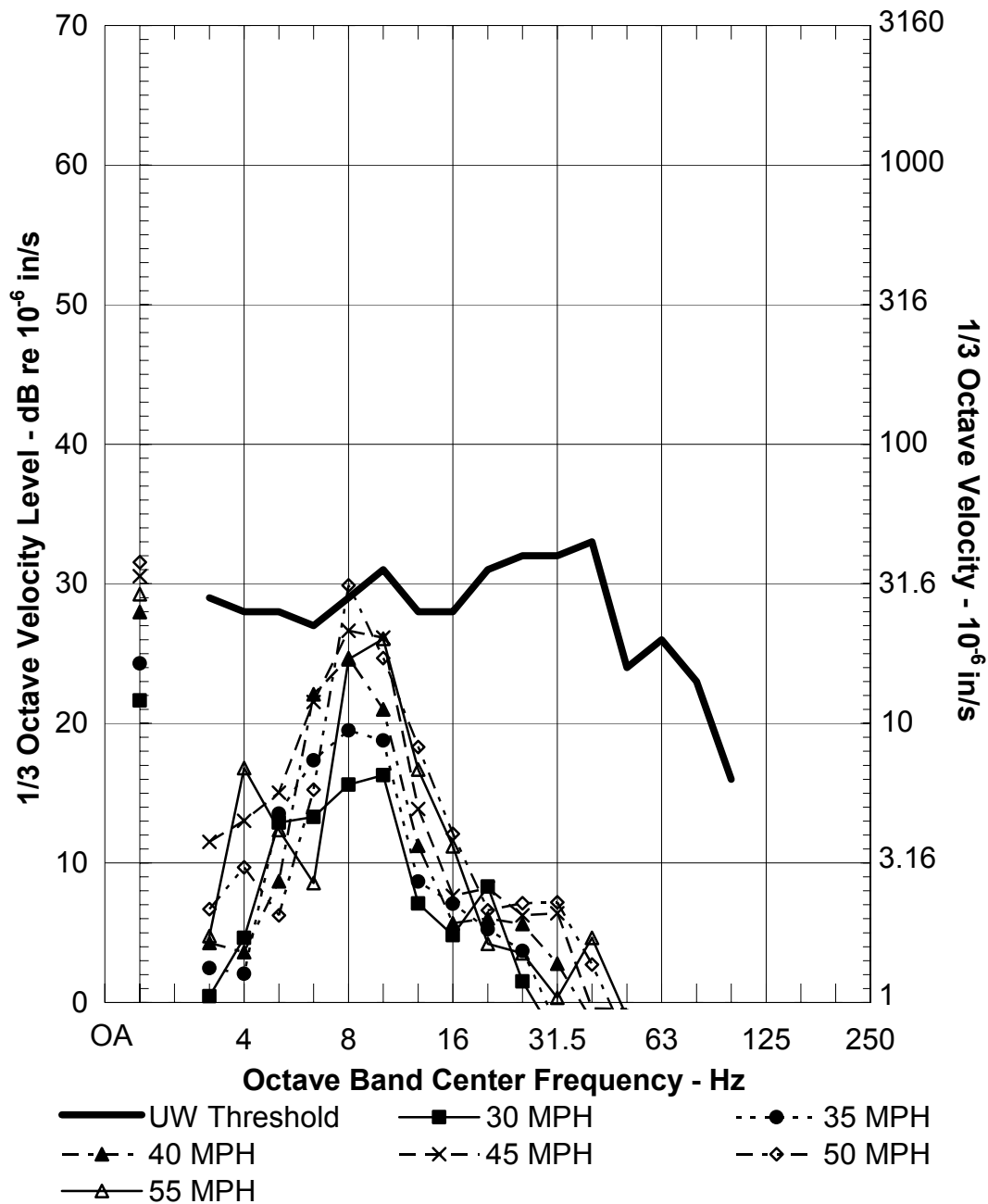
10) Winkenwerder Vibration At Ground Surface
Numerical Model Prediction
VTA FDL, Two Simultaneous Trains, Standard DF
683 ft Offset, 100 ft Predicted Depth

Figure D-11 Ground Surface Vibration Velocity Levels at Winkenwerder Hall for Two Simultaneous Train Passbys



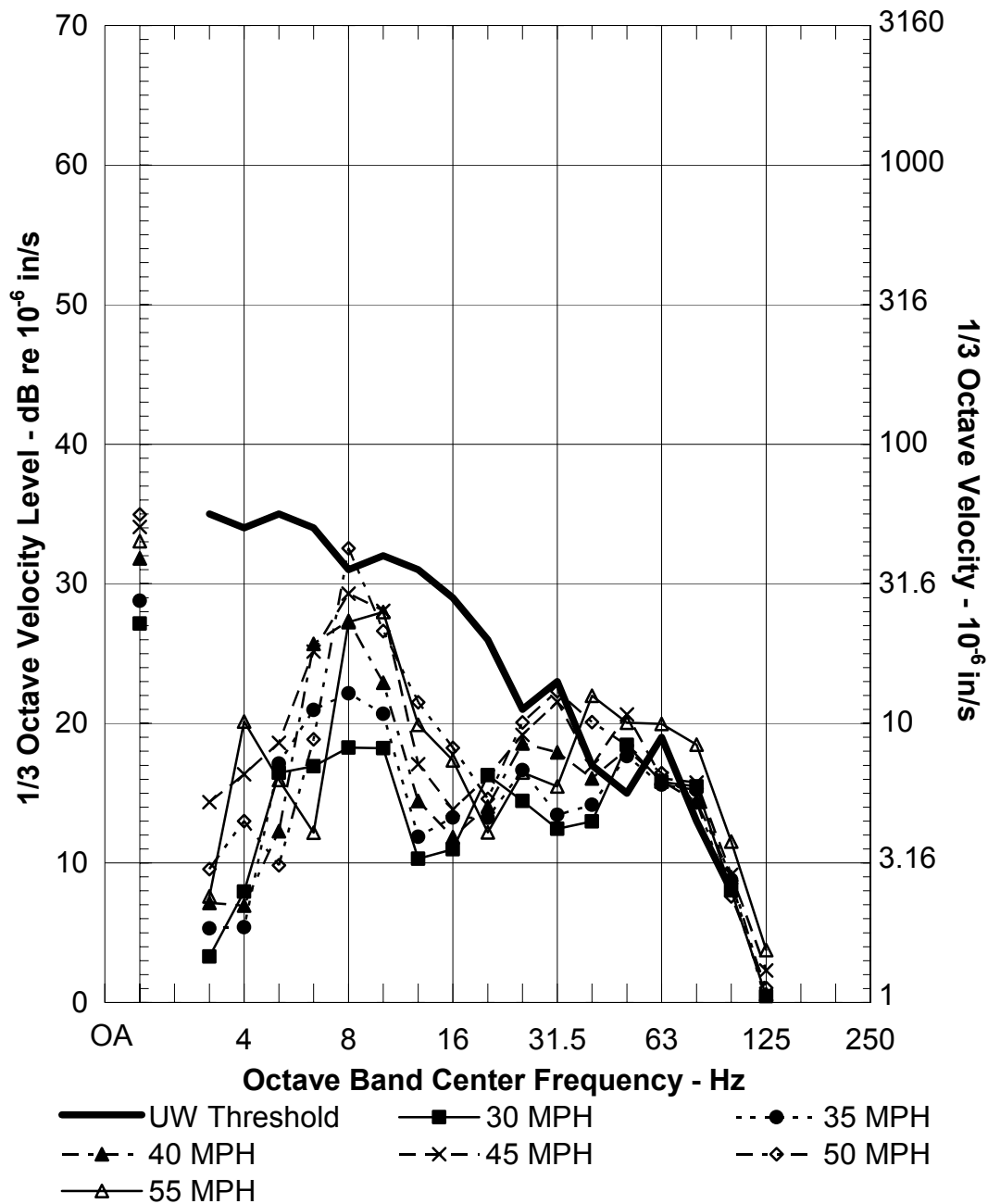
11) Henderson Hall Vibration At Ground Surface
 Numerical Model Prediction
 VTA FDL, Two Simultaneous Trains, Standard DF
 1208 ft Offset, 80 ft Predicted Depth

Figure D-12 Ground Surface Vibration Velocity Levels at Henderson Hall for Two Simultaneous Train Passbys



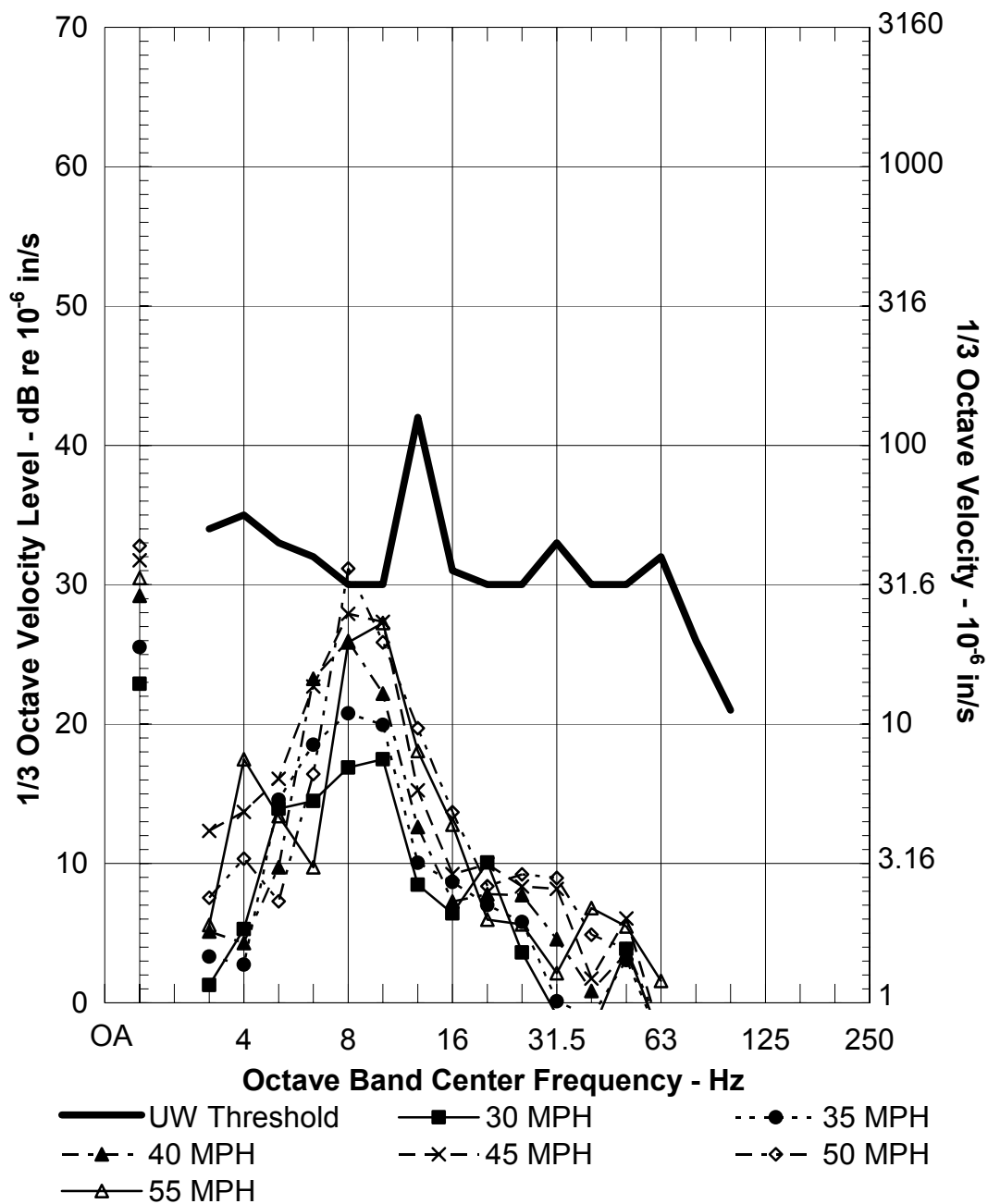
12) Oceanography Research Vibration At Ground Surface
Numerical Model Prediction
VTA FDL, Two Simultaneous Trains, Standard DF
1833 ft Offset, 80 ft Predicted Depth

Figure D-13 Ground Surface Vibration Velocity Levels at Oceanography Research Building for Two Simultaneous Train Passbys



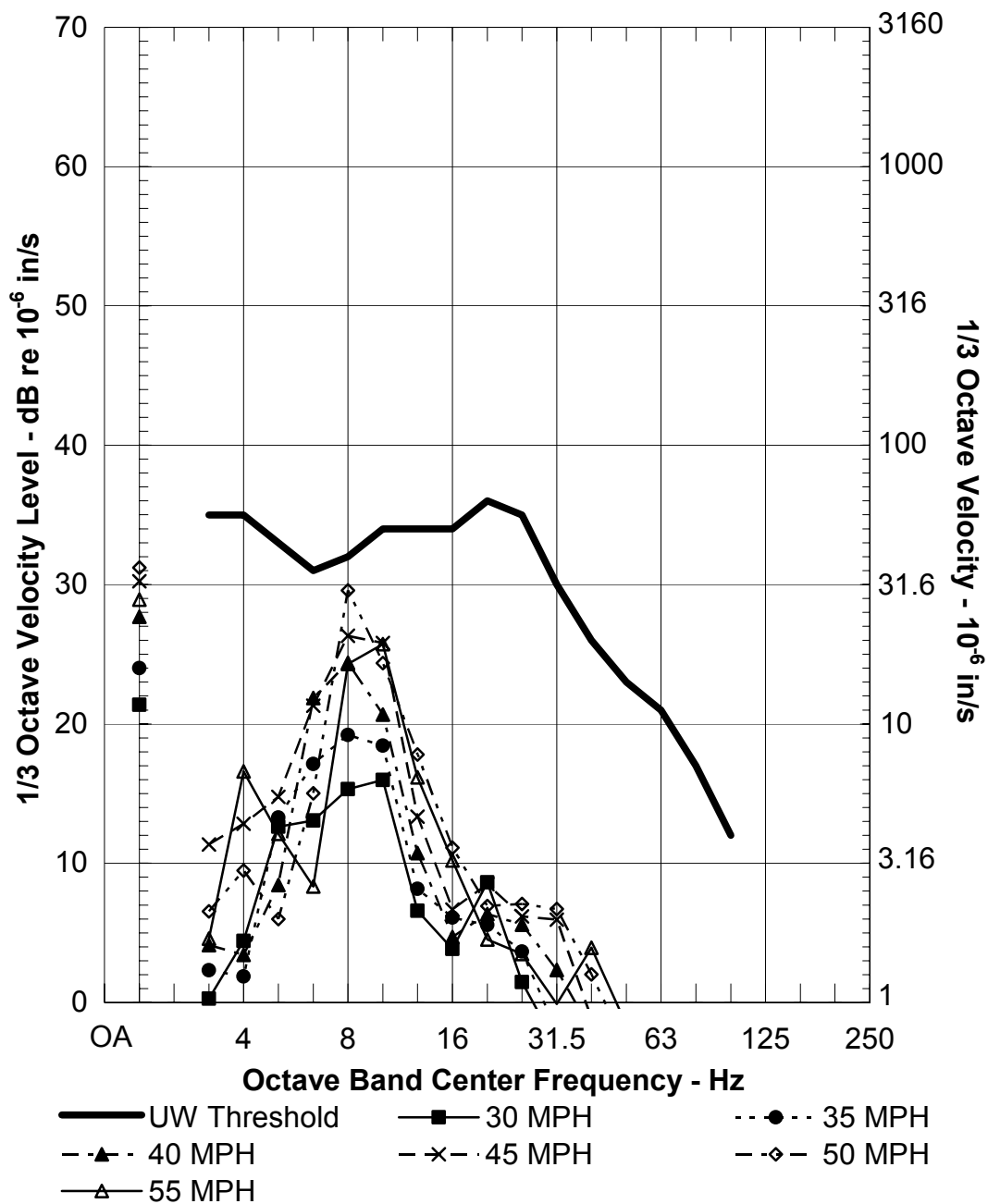
13) Medical Center Vibration At Ground Surface
Numerical Model Prediction
VTA FDL, Two Simultaneous Trains, Standard DF
910 ft Offset, 110 ft Predicted Depth

Figure D-14 Ground Surface Vibration Velocity Levels at Medical Center for Two Simultaneous Train Passbys



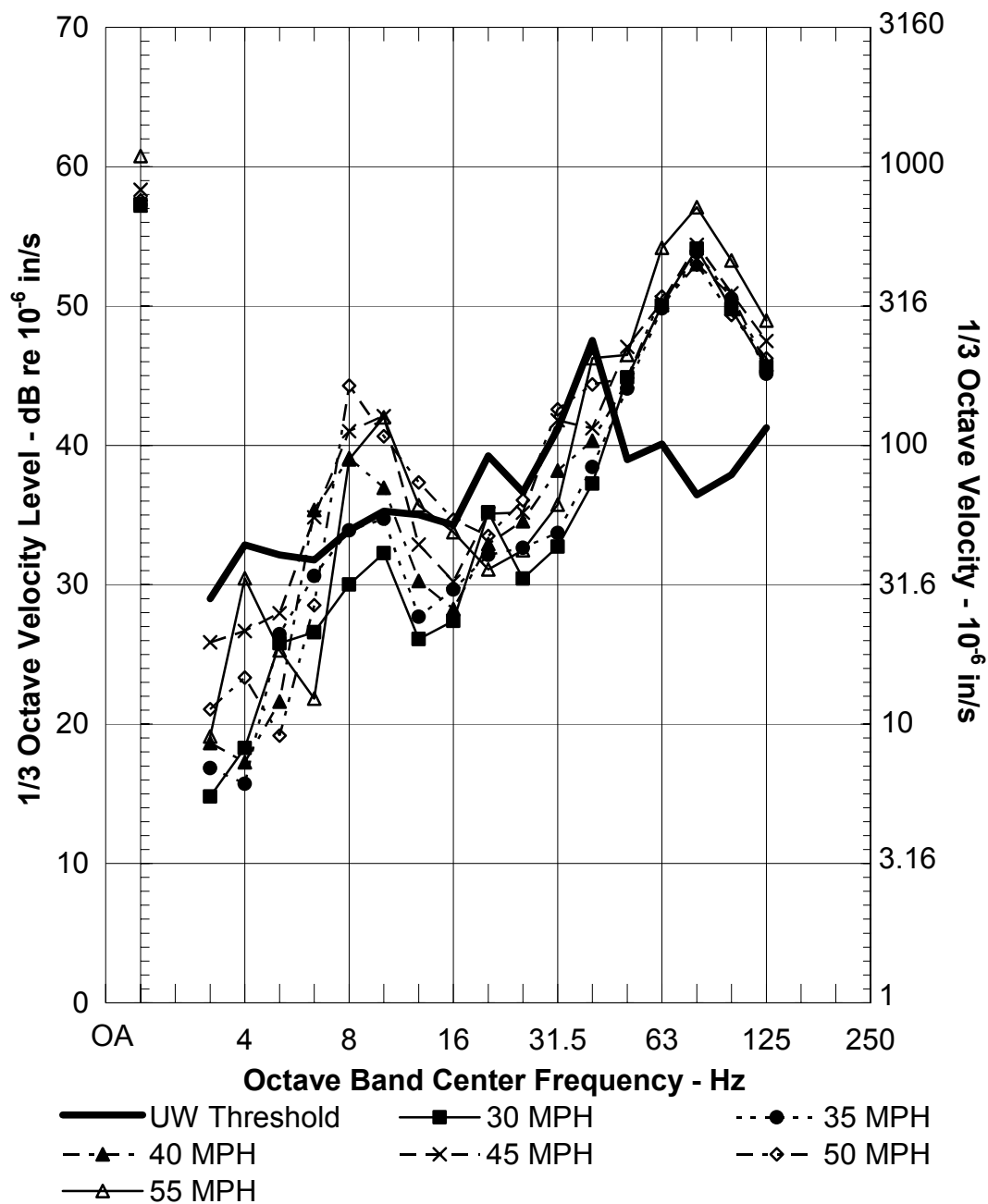
14) Fisheries Sciences Vibration At Ground Surface
Numerical Model Prediction
VTA FDL, Two Simultaneous Trains, Standard DF
1640 ft Offset, 80 ft Predicted Depth

Figure D-15 Ground Surface Vibration Velocity Levels at Fisheries Sciences for Two Simultaneous Train Passbys



15) Fisheries Teaching Vibration At Ground Surface
Numerical Model Prediction
VTA FDL, Two Simultaneous Trains, Standard DF
1858 ft Offset, 80 ft Predicted Depth

Figure D-16 Ground Surface Vibration Velocity Levels at Fisheries Teaching and Research Center for Two Simultaneous Train Passbys



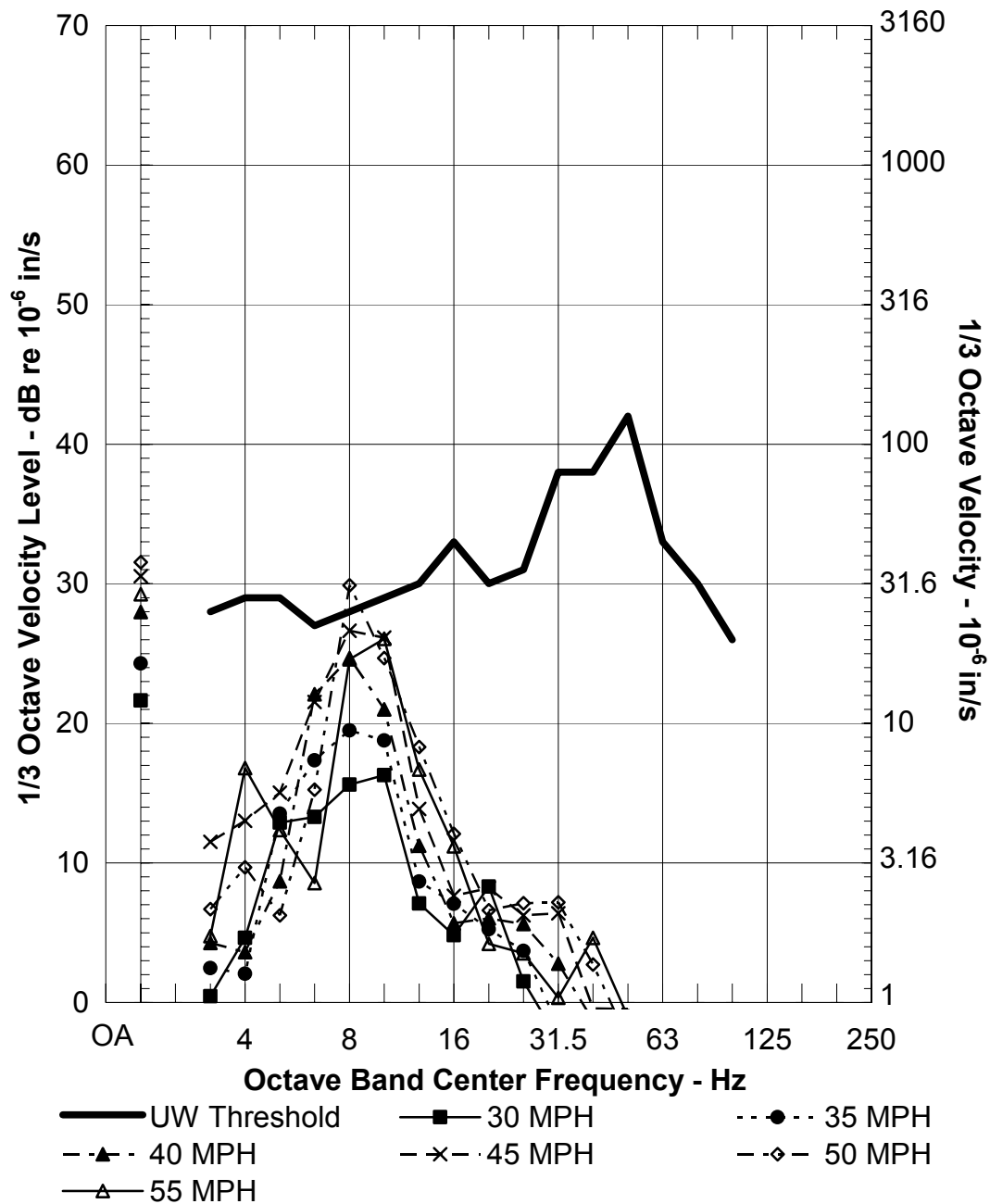
16) More Hall Vibration At Ground Surface

Global Quadratic LSR

VTA FDL, Two Simultaneous Trains, Standard DF

137 ft Offset, 115 ft Predicted Depth

Figure D-17 Ground Surface Vibration Velocity Levels at More Hall for Two Simultaneous Train Passbys



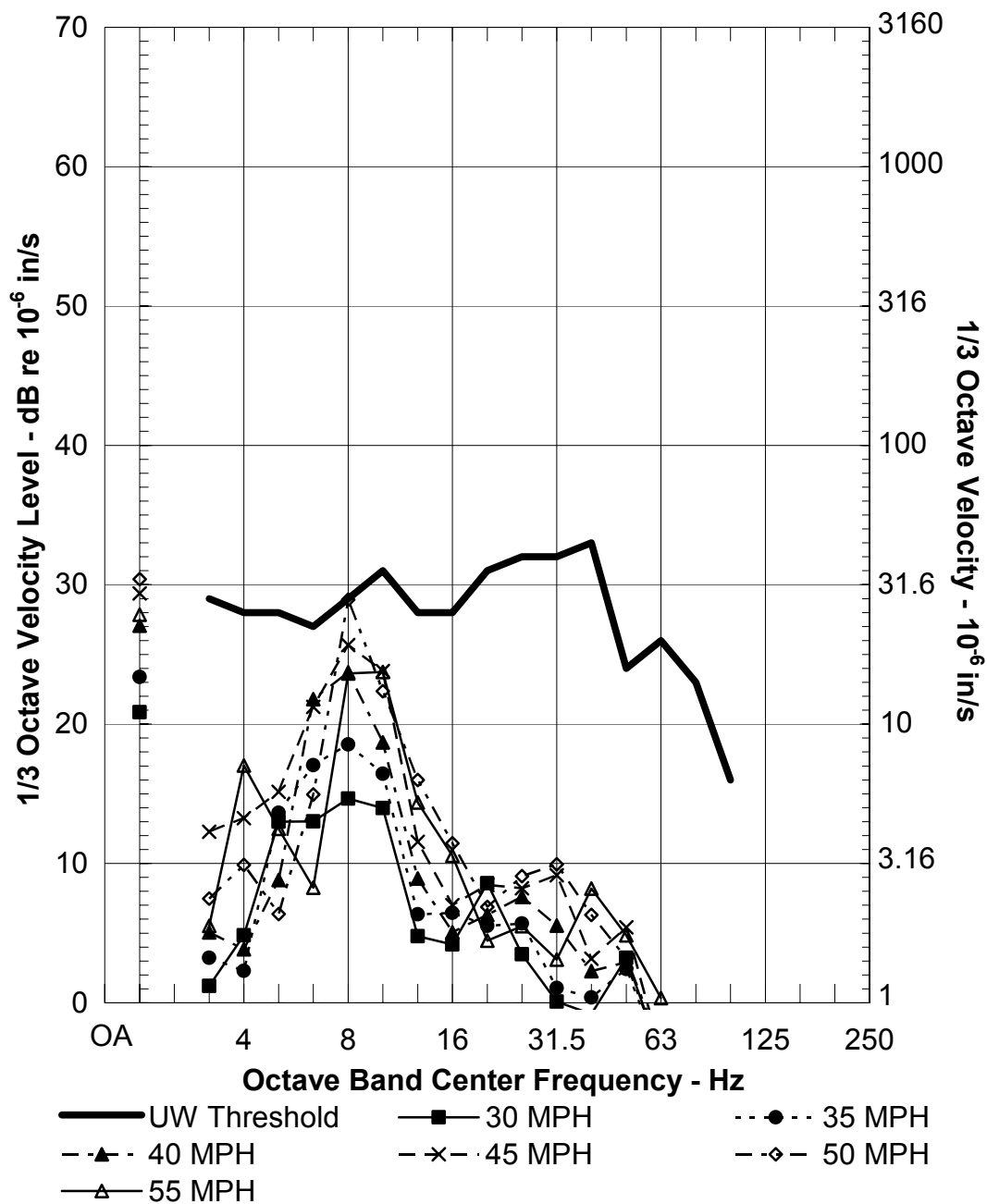
17) Marine Studies Vibration At Ground Surface

Numerical Model Prediction

VTA FDL, Two Simultaneous Trains, Standard DF

1799 ft Offset, 80 ft Predicted Depth

Figure D-18 Ground Surface Vibration Velocity Levels at Marine Studies for Two Simultaneous Train Passbys



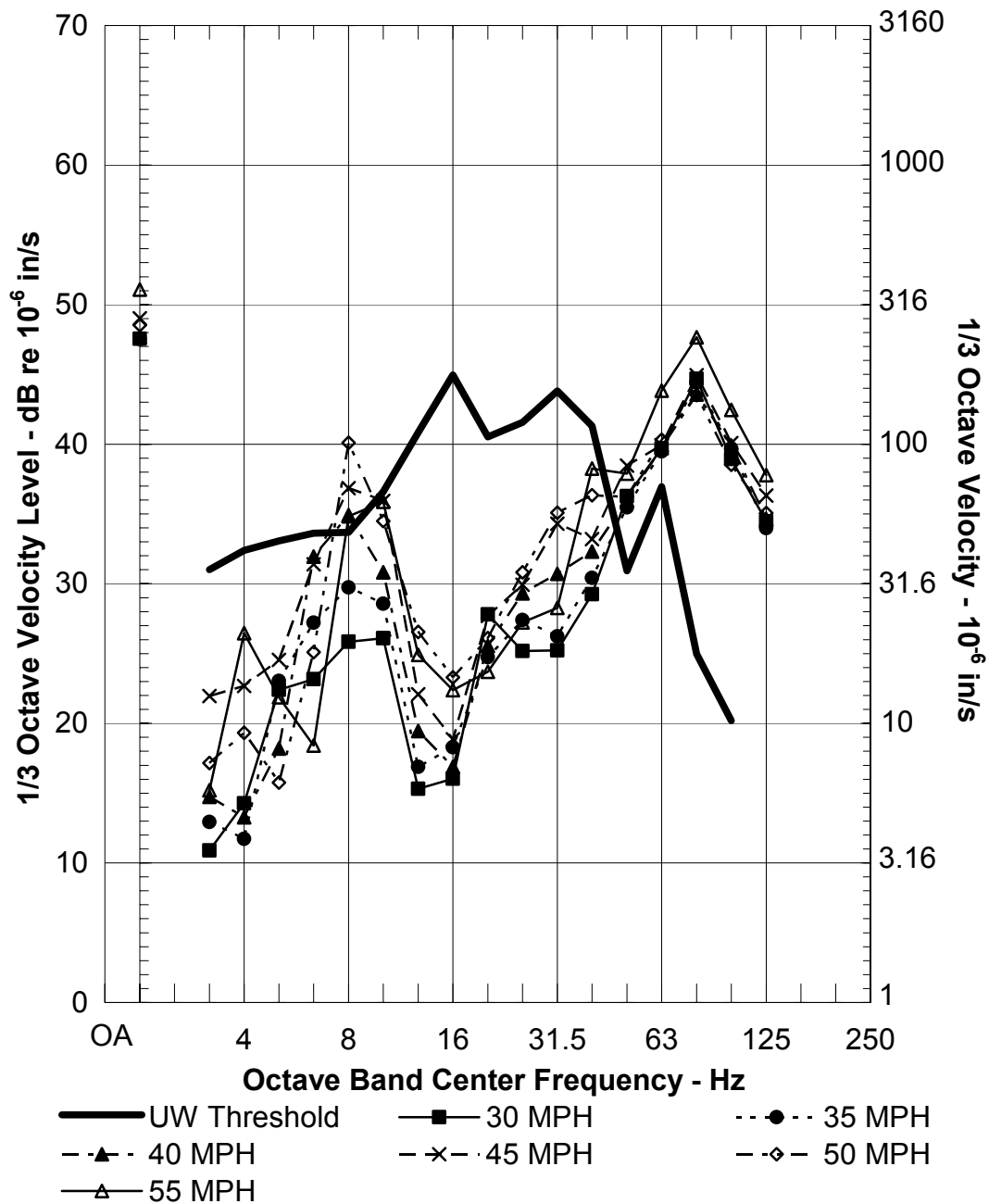
18) Bioengineering Vibration At Ground Surface

Global Quadratic LSR

VTA FDL, Two Simultaneous Trains, Standard DF

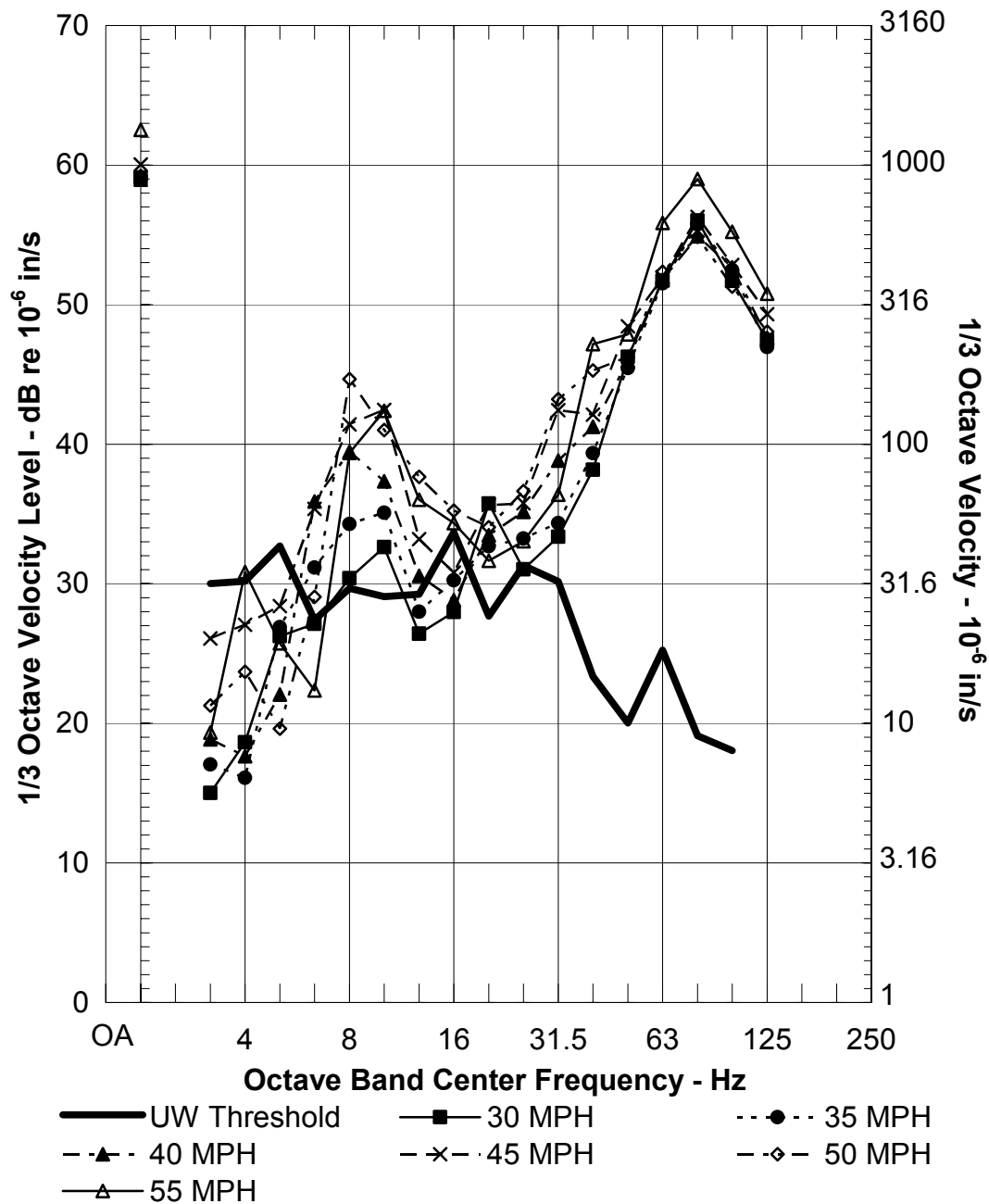
1612 ft Offset, 100 ft Predicted Depth

Figure D-19 Ground Surface Vibration Velocity Levels at Bioengineering/Genomics for Two Simultaneous Train Passbys



19) Fluke Hall Vibration At Ground Surface
Numerical Model Prediction
VTA FDL, Two Simultaneous Trains, Standard DF
333 ft Offset, 120 ft Predicted Depth

Figure D-20 Ground Surface Vibration Velocity Levels at Fluke Hall for Two Simultaneous Train Passbys



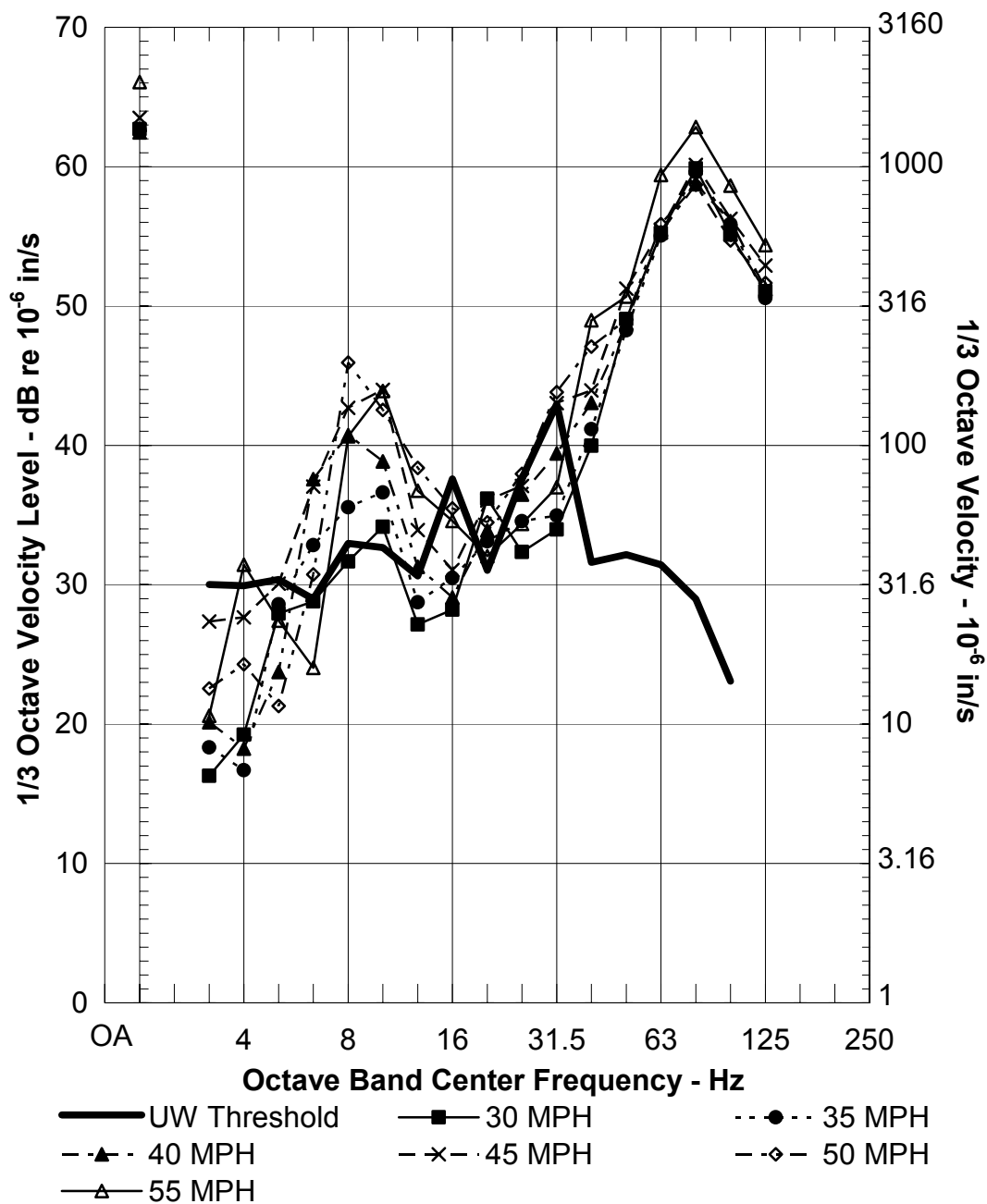
20a) ME Building Vibration At Ground Surface

Global Quadratic LSR

VTA FDL, Two Simultaneous Trains, Standard DF

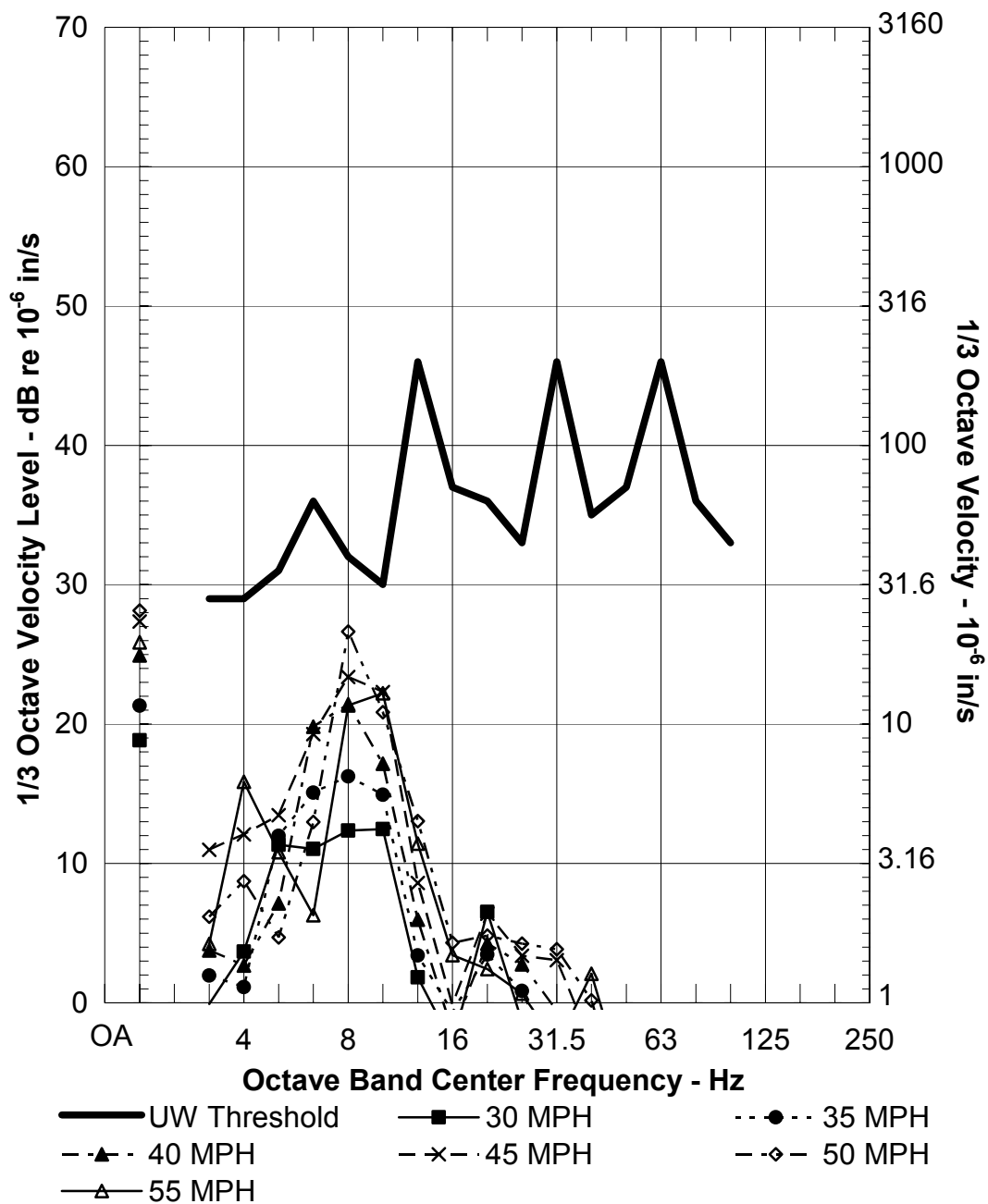
105 ft Offset, 115 ft Predicted Depth

Figure D-21 Ground Surface Vibration Velocity Levels at Mechanical Engineering Building for Two Simultaneous Train Passbys



20b) ME Annex Vibration At Ground Surface
Physical Model LSR
VTA FDL, Two Simultaneous Trains, Standard DF
9 ft Offset, 115 ft Predicted Depth

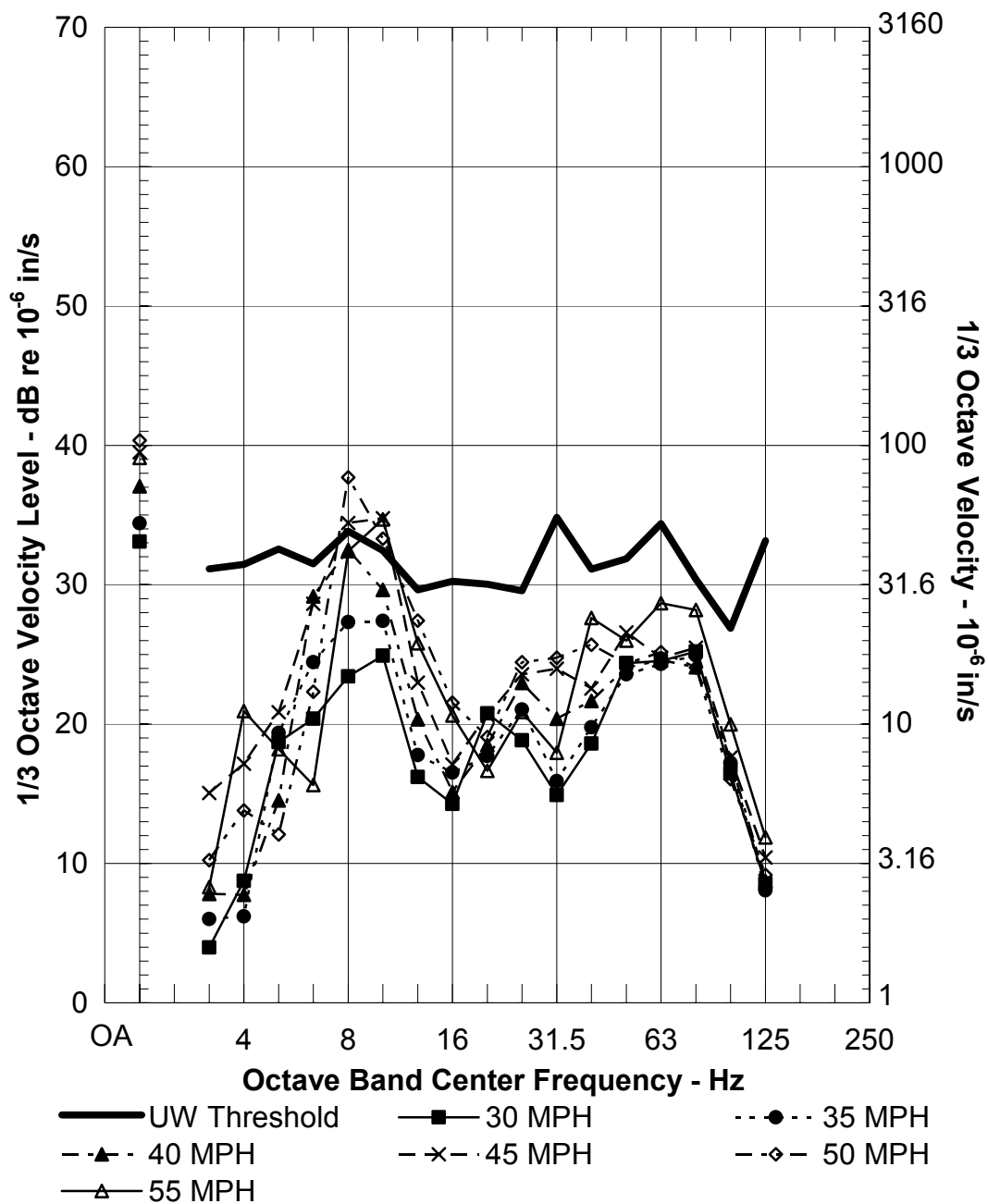
Figure D-22 Ground Surface Vibration Velocity Levels at Mechanical Engineering Annex for Two Simultaneous Train Passbys



**21) Ocean Sciences Vibration At Ground Surface
Numerical Model Prediction**

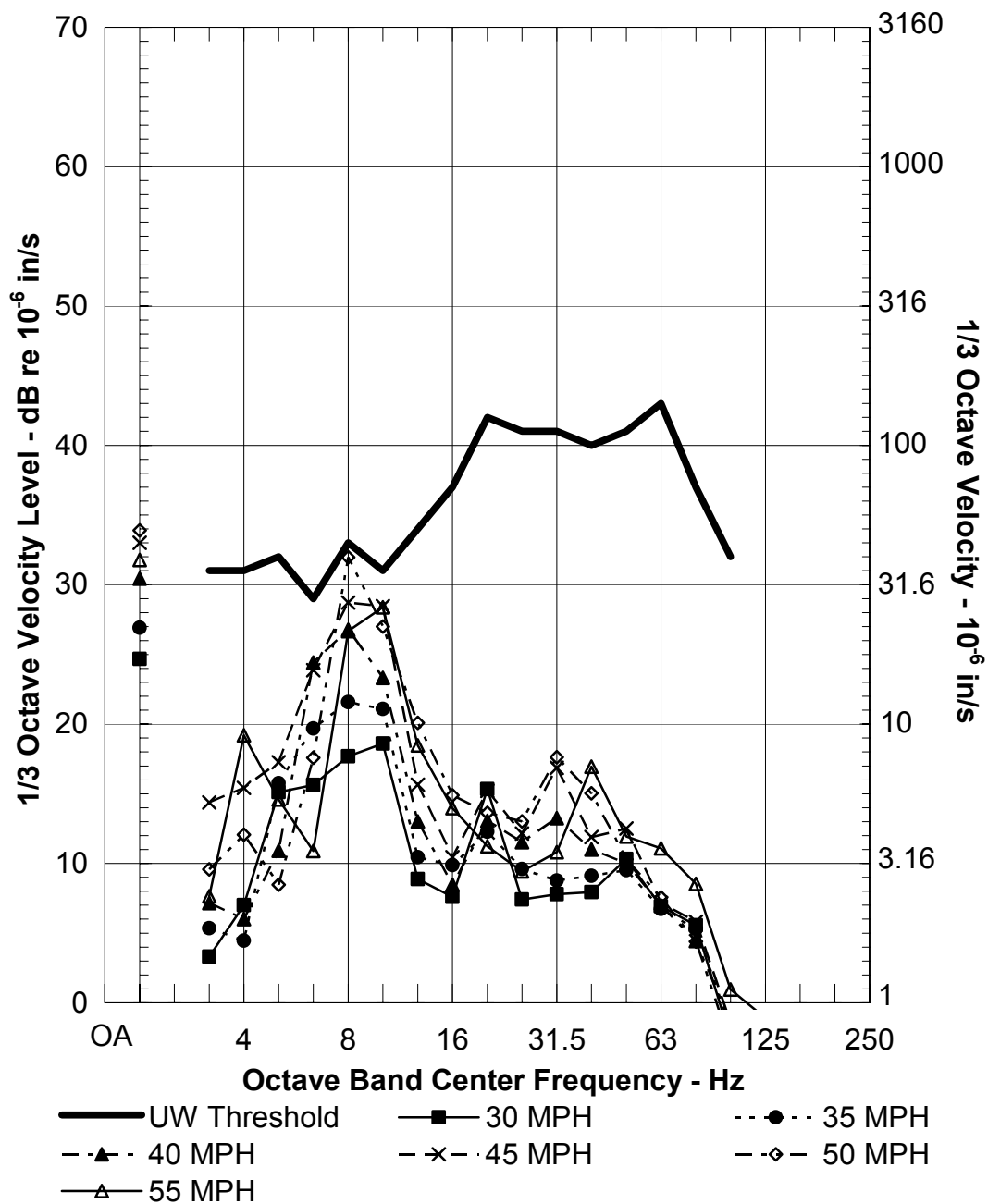
**VTA FDL, Two Simultaneous Trains, Standard DF
2056 ft Offset, 100 ft Predicted Depth**

Figure D-23 Ground Surface Vibration Velocity Levels at Ocean Sciences for Two Simultaneous Train Passbys



22) CHDD Vibration At Ground Surface
Numerical Model Prediction
VTA FDL, Two Simultaneous Trains, Standard DF
753 ft Offset, 100 ft Predicted Depth

Figure D-24 Ground Surface Vibration Velocity Levels at the Center on Human Development and Disability for Two Simultaneous Train Passbys



23) Fisheries Center Vibration At Ground Surface

Numerical Model Prediction

VTA FDL, Two Simultaneous Trains, Standard DF

1242 ft Offset, 100 ft Predicted Depth

Figure D-25 Ground Surface Vibration Velocity Levels at Fisheries Center for Two Simultaneous Train Passbys

D-4 BUILDING VIBRATION RESPONSE

Measurements of interior basement level floor vibration responses to borehole impact forces were made during the LSR tests to obtain a Building Vibration Response (BVR). The BVR is added to the predicted ground surface vibration to estimate the interior basement level vibration.

D-4.1 Procedure

Basement floor vibration responses to borehole impact forces were measured at Wilcox Hall, Mechanical Engineering, and Savory Hall. (Savory Hall was not identified as vibration sensitive by UW, but provided a convenient measurement location.) The PSR's were measured for each of these buildings, using the tests impacts from 140 and 300lb hammers in boreholes NB-254, NB-255, and NB-256, respectively. The results were then averaged to obtain a composite BVR.

D-4.2 Results

The measured BVRs and their linear average are plotted Figure D-26. The range of measured BVRs is relative small at frequencies below 12.5Hz, but increases at higher frequencies. The linear average of the BVRs is roughly -1dB, monotonous decreasing to -8dB at about 50Hz, thereafter increasing modestly. These data would suggest that there would be little difference between exterior ground surface vibration and interior basement floor vibration at frequencies below 12.5Hz.

D-4.3 Predicted Basement Floor Vibration

Basement floor vibration predictions for Wilcox Hall and Mechanical Engineering Annex are plotted in Figure D-27 and Figure D-28, respectively. Both of these predictions indicate two prominent peaks in the third octave spectrum, one at roughly the primary suspension frequency, and the other at the track/wheel-set resonance. The peak levels at the primary suspension resonance frequency are roughly comparable with shown in Figure D-6 and Figure D-22, respectively. However, the predicted basement floor vibration levels are less than those predicted for the ground surface at the track/wheel-set resonance at about 50 to 80Hz. The predicted basement floor vibration velocity levels exceed the UW Thresholds for both of these buildings.

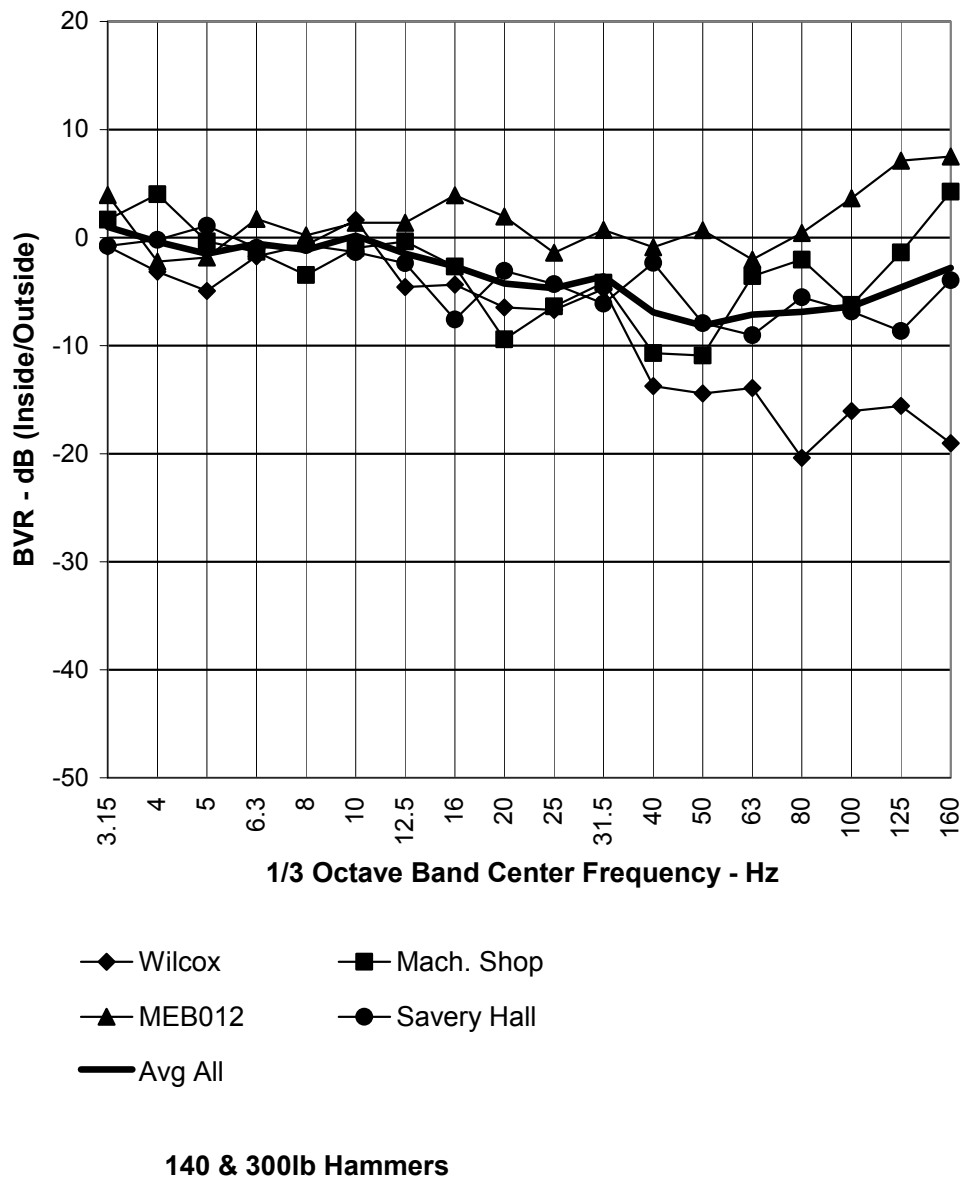
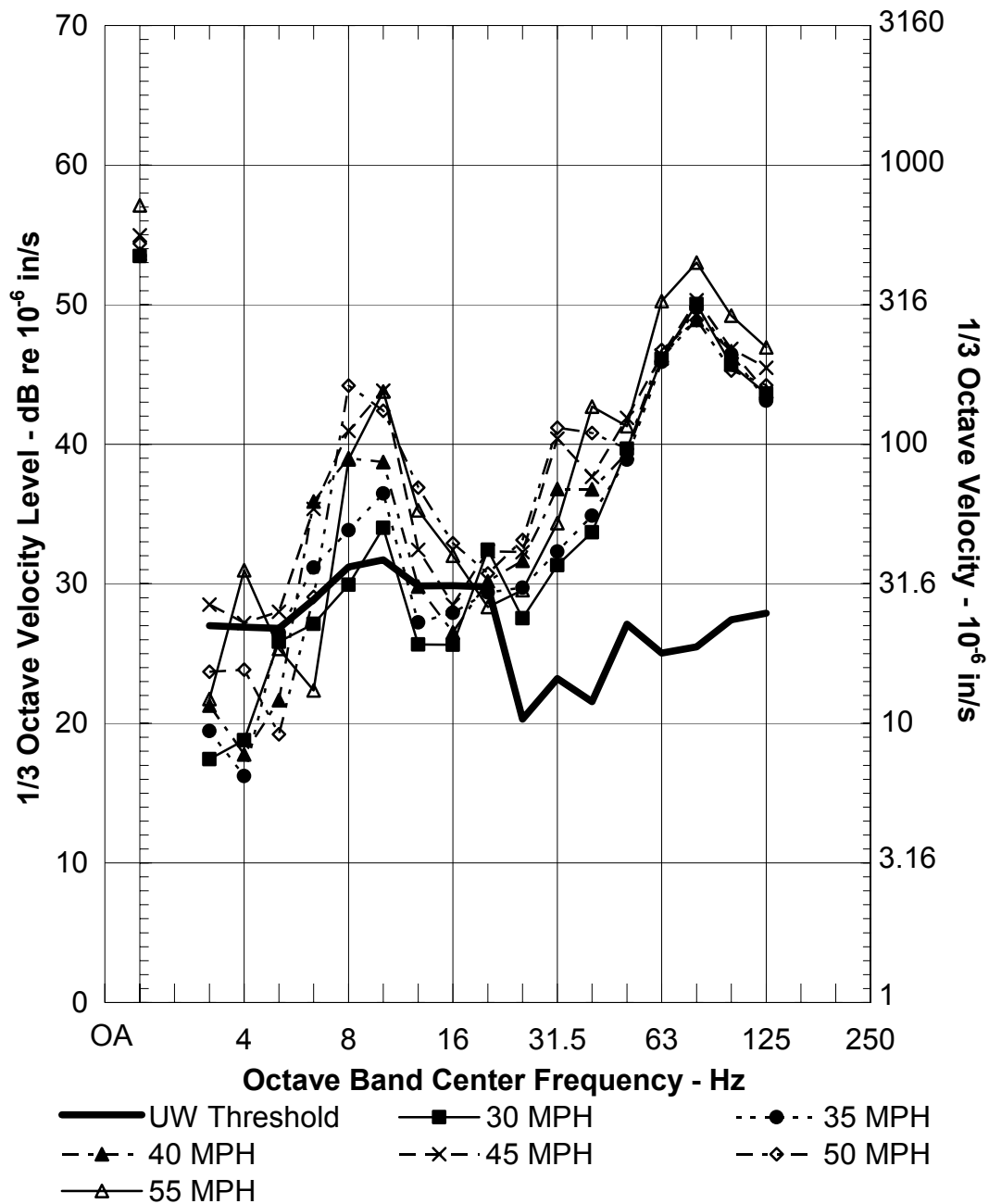
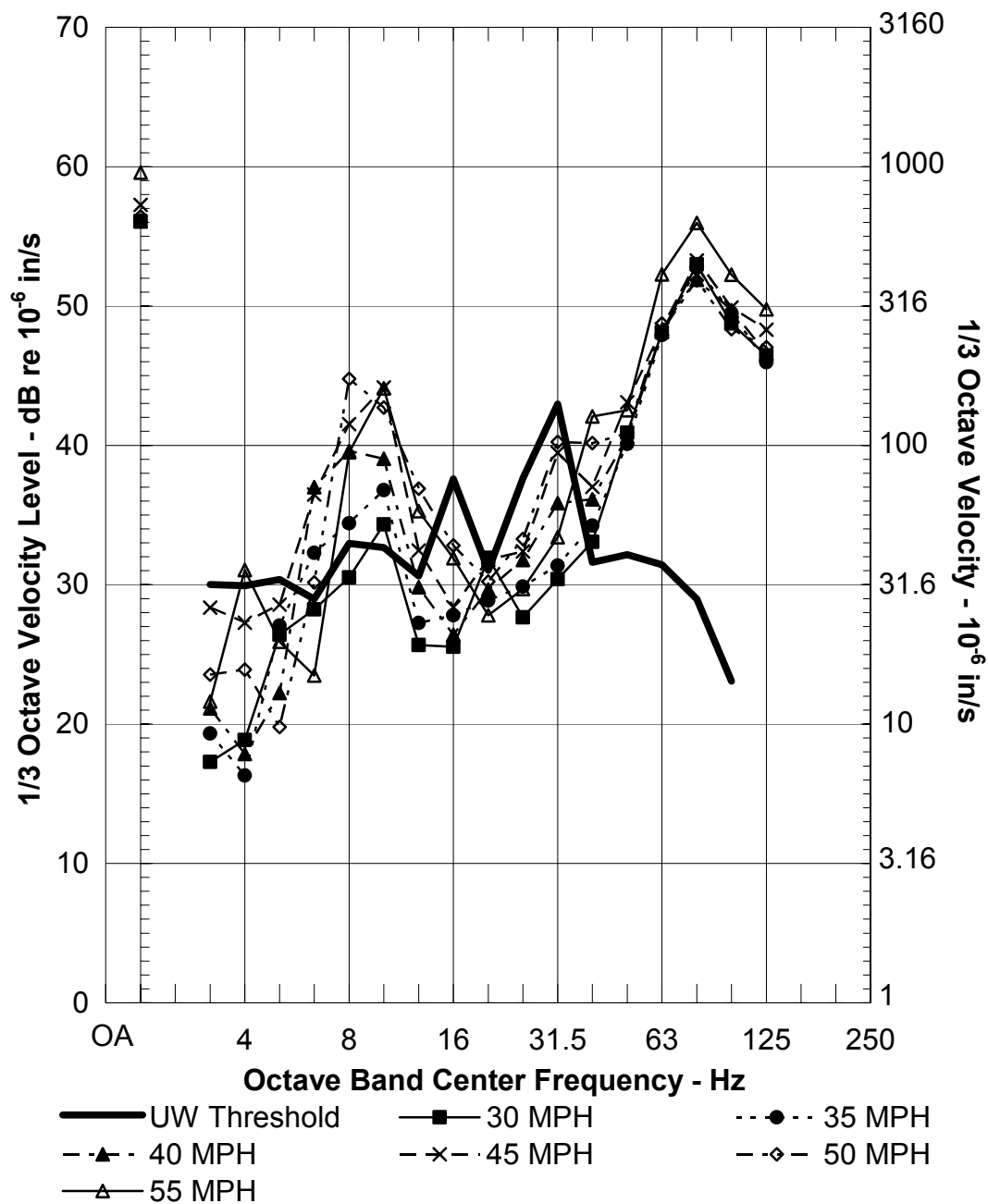


Figure D-26 Building Vibration Responses



5) Wilcox Hall Vibration At Basement
Global Quadratic LSR, Global Averaged BVR
VTA FDL, Two Simultaneous Trains, Standard DF
110 ft Offset, 100 ft Predicted Depth

Figure D-27 Predicted Basement Floor Vibration at Wilcox Hall



20b) ME Annex Vibration At Basement
Physical Model LSR, Global Averaged BVR
VTA FDL, Two Simultaneous Trains, Standard DF
9 ft Offset, 115 ft Predicted Depth

Figure D-28 Predicted Basement Floor Vibration at Mechanical Engineering Annex (20b)

**APPENDIX E: PREDICTED THIRD-OCTAVE VIBRATION VELOCITY LEVELS
FOR THE MITIGATED IMPACT DESIGN**

TABLE OF CONTENTS

E-1	INTRODUCTION	1
E-2	CALCULATION METHODOLOGY	1
E-2.1	Force Density Levels	1
E-2.2	Line Source Responses	2
E-2.3	Parameters	3
E-3	PREDICTED MITIGATED VIBRATION LEVELS	7
E-3.1	(1) Electrical Engineering/Computer Science	7
E-3.2	(2) Johnson Hall	7
E-3.3	(3) Bagley Hall	7
E-3.4	(4) Chemistry	7
E-3.5	(5) Wilcox Hall	7
E-3.6	(6) Physics and Astronomy	8
E-3.7	(7) Burke Museum	8
E-3.8	(8) Benson Hall	8
E-3.9	(9) Roberts Hall	8
E-3.10	(10) Winkenwerder Hall	8
E-3.11	(11) Henderson Hall	8
E-3.12	(12) Oceanography Research Building	9
E-3.13	(13) UW Medical Center	9
E-3.14	(14) Fisheries Sciences	9
E-3.15	(15) Fisheries Teaching and Research Center	9
E-3.16	(16) More Hall	9
E-3.17	(17) Marine Studies	9
E-3.18	(18) Bioengineering/Genomics	9
E-3.19	(19) Fluke Hall	10
E-3.20	(20a) Mechanical Engineering Building	10
E-3.21	(20b) Mechanical Engineering Annex	10
E-3.22	(21) Ocean Sciences	10
E-3.23	(22) Center on Human Development and Disability	10
E-3.24	(23) Fisheries Center	11

TABLES

Table E-1	FDL Used for Predictions	4
Table E-2	Prediction Parameters	4
Table E-3	Summary of Predicted Mitigated Vibration Levels at 30mph	12

FIGURES

Figure E-1	Adjustments Applied to FDL for VTA/Kinkysharyo Vehicle on Standard Direct Fixation Track to Obtain the FDL for the VTA/Kinkysharyo Vehicle on High Compliance Direct Fixation Track or Floating Slab Track.....	5
Figure E-2	Force Density Levels Assumed for Kinkysharyo Vehicle	6
Figure E-1	Electrical Engineering/Computer Science	15
Figure E-2	Johnson Hall	16
Figure E-3	Bagley Hall	17
Figure E-4	Chemistry Building.....	18
Figure E-5	Wilcox Hall.....	19
Figure E-6	Physics and Astronomy	20
Figure E-7	Burke Museum.....	21
Figure E-8	Benson Hall	22
Figure E-9	Roberts Hall.....	23
Figure E-10	Winkenwerder Hall.....	24
Figure E-11	Henderson Hall	25
Figure E-12	Oceanography Research Building	26
Figure E-13	UW Medical Center.....	27
Figure E-14	Fisheries Sciences	28
Figure E-15	Fisheries Teaching and Research Center.....	29
Figure E-16	More Hall.....	30
Figure E-17	Marine Studies	31
Figure E-18	Bioengineering/Genomics	32
Figure E-19	Fluke Hall	33
Figure E-20	Mechanical Engineering Building.....	34
Figure E-21	Mechanical Engineering Annex	35
Figure E-22	Ocean Sciences	36
Figure E-23	Center on Human Development and Disability.....	37
Figure E-24	Fisheries Center	38

E-1 INTRODUCTION

Detailed predictions of third-octave vibration velocity levels at the University of Washington campus in Seattle, Washington are provided in this appendix for the proposed mitigated impact design with two four-car trains operating simultaneously at 30 mph. The predicted levels are compared with the UW Thresholds of ambient vibration provided by the University of Washington as impact criteria.

The principal vibration control provisions consist of floating slab track extending from the north end of the Stadium Station platform to the northern extent of the alignment on the UW campus, and high compliance direct fixation (HCDF) fasteners extending from the southern end of the alignment at the campus boundary through the Stadium Station and from the northern end of the UW campus alignment through the Brooklyn Station. These fasteners necessarily include special trackwork high compliance fasteners at the moveable point frog crossover at the southern end of the station.

E-2 CALCULATION METHODOLOGY

The velocity level in decibels relative to 1 micro-in/sec is the sum of the Force Density Level (FDL), the Line Source Response (LSR) and adjustments for vibration control provisions. The ground surface vibration level at each buildings was calculated with the following equation:

$$Lv \text{ (dB re 1 micro-in/sec)} = FDL + LSR + \text{ADJUSTMENTS}$$

This relation represents the combination of track vibration forces, the effects of propagation to the affected receivers, and vibration reductions for floating slab track or high compliance direct fixation fasteners. No provision is made for tunnel/soil response, as analytical studies by this author indicate that tunnel/soil coupling losses would likely be small in relation to the losses related to propagation at frequencies below approximately 100Hz. Also, no adjustments are provided for building foundation response or floor resonance amplification.

All calculations incorporated LSR's measured on the University of Washington campus in Seattle as discussed in Appendix A or numerically determined LSR's based on shear-wave velocity profiles measured on the campus and adjusted to match short range LSR's measured at short range as discussed in Appendix B, and FDL's of the Kinki Sharyo vehicle measured at the Santa Clara Valley Transportation Authority in San Jose, California, as discussed in Appendix C.

E-2.1 Force Density Levels

Force Density Levels (FDLs) measured for VTA vehicles traveling at 30 mph on ballasted track with continuous welded rail were adjusted for standard direct fixation fasteners for the prediction of un-mitigated vibration levels, as discussed in Appendix D. Adjustments for train operation on a) high compliance direct fixation (HCDF) fasteners on rigid invert or b) floating slab track with a nominal resonance frequency of between 12.5 and 16Hz and standard direct fixation fasteners were added to the FDL shown in Appendix C and D for trains running at 30mph on rigid invert with standard direct fixation fasteners. Figure E-2 shows the FDL's used for calculating vibration levels for these two types of track.

The FDL for the Kinki Sharyo vehicle on floating slab track exhibits a strong peak at 80 Hz. This peak is due to the coincidence of a peak in the floating slab adjustment curve and a peak in the FDL measured for the Kinki Sharyo vehicle in San Jose. This is likely a worst case condition that may not be realized in practice, because the peaks are likely to spread apart, and better performance than assumed here is likely to be obtained for the floating slab at these high frequencies.

The standard direct fixation fasteners are assumed to have a dynamic stiffness of 140,000lb/in, giving a dynamic rail support modulus of 4,700lb/in/in for a 30in fastener pitch. The HCDF fasteners are assumed to have a dynamic stiffness of about 80,000lb/in, giving a rail support modulus of about 2,700 lb/in/in. The adjustment for HCDF track relative to Standard DF is illustrated in Figure E-1. This adjustment is based on theoretical calculations of wheelset/rail interaction.^{1,2} These adjustments are supported by measurements at the Toronto Transit Commission.³

The floating slab assumed for these calculations is similar to the Red Line floating slab design employed at the the Los Angeles County Metropolitan Transit Authority, consisting of a double-tie discontinuous floating slab with a nominal resonance frequency of between 12.5 to 16Hz and standard resilient DF fasteners of stiffness 140,000lb/in. The vibration transmissibility measured for this slab design is illustrated in Figure E-1.⁴

Three decibels were added to the predicted vibration levels for a single train to represent vibration for simultaneous passage of two trains. This approach is perhaps extreme because such a condition would occur for a fraction of time, depending on headways.

E-2.2 Line Source Responses

The Line Source Responses used for calculation are described in Appendix A and Appendix B. The same Line Source Responses used for predicting unmitigated vibration in Appendix D are employed here.

¹ Nelson, J. T., and Saurenman, H. J., **State-of-the-Art-Review: Prediction and Control of Groundborne Noise and Vibration from Rail Transit Trains**, Final Report, Wilson, Ihrig & Associates for US DOT/TSC, UMTA-MA-06-0049-83-4, Chapter 5.

² Bender, E. K., Kurze, U. J., Nayak, P. R., Ungar, E. E., **Effects of Rail Fastener Stiffness on Vibration Transmitted to Buildings Adjacent to Subways**, Report, Bolt Beranek and Newman, Inc., for Washington Metropolitan Area Transportation Authority (1969)

³ Wilson, Ihrig & Associates, "Measurement Program Results", **Yonge Subway Northern Extension Noise & Vibration Study, Report RD 115/3, Technical Reports – Consultants, Book 1 of 2**, Toronto Transit Commission, October 1976, .pp 59-65.

⁴ Wolfe, S. L., **Ground Vibration Measurements of Train Operations on Segment 2A of the Los Angeles Metro Red Line**, Wilson, Ihrig & Associates for Parsons Brinckerhoff, November 1996.

E-2.3 Parameters

The prediction parameters are listed in Table E-2. The predictions are based on the distance between the point of closest approach of nearest tunnel and the affected building. No provision was made for the additional distance between the building and the second train in the distal tunnel. The depths of the tunnels were taken approximately as the depths of the top-of-rail (TOR) below the ground surface above the tunnel at the point of closest approach to the receiver. The tunnel depths under the UW campus range from about 90 to 142 feet. A depth of 120 feet is employed for tunnel depths greater than 120 feet because that was the maximum depth of the boreholes used for measuring the Line Source Responses employed here. This approach gives a slightly conservative vibration estimate, because the Line Source Response tends to decrease with increasing depth. The tunnel depth along the curve between the campus boundary through to the Brooklyn Station decreases from about 90ft to 60ft. The assumed depths along this segment was 80feet, corresponding to the minimum depth for which LSR borehole test data were collected.

Table E-1 FDL Used for Predictions

Track Design	3.15	4	5	6.3	8	10	12.5	16	20	25	31.5	40	50	63	80	100	125	160
Standard Fastener	18	19	26	25	28	31	23	22	30	25	26	30	37	41	45	39	37	35
16 Hz Floating Slab	18	19	26	25	28	31	27	25	25	15	11	7	14	23	28	12	7	9
HCDF Fastener	18	19	26	25	28	32	25	24	31	25	24	25	29	32	37	32	32	30

Table E-2 Prediction Parameters

Identifier	Building	Vibration Control Provision	Nearest Station No.	Offset ft.	Depth ¹ ft.
1	Electrical Engineering	Floating Slab	1221+77	338	120 ¹
2	Johnson Hall	Floating Slab	1237+26	677	120 ¹
3	Bagley Hall	Floating Slab	1232+57	978	120 ¹
4	Chemistry	Floating Slab	1222+99	1,008	120 ¹
5	Wilcox Hall	Floating Slab	1214+29	110	100
6	Physics/Astronomy	Floating Slab	1241+50	1,201	120
7	Burke Museum	HCDF	1261+04	826	80
8	Benson Hall	Floating Slab	1233+56	1,269	120 ¹
9	Roberts Hall	Floating Slab	1215+42	255	115
10	Winkenwerder Hall	Floating Slab	1212+40	683	100
11	Henderson Hall	HCDF	1250+75	1,208	80 ²
12	Oceanographic Research Building	HCDF	1247+04	1,833	80 ²
13	UW Medical Center	HCDF	1208+53	910	110
14	Fisheries Sciences	HCDF	1248+74	1,640	80 ²
15	Fisheries Teaching & Research Center	HCDF	1248+13	1,858	80 ²
16	More Hall	Floating Slab	1216+21	137	115
17	Marine Studies	HCDF	1247+68	1,799	80 ²
18	Bioengineering/ Genomics	Floating Slab	1244+85	1,612	100
19	Fluke Hall	Floating Slab	1226+35	333	120 ¹
20a	Mechanical Engineering Bldg	Floating Slab	1223+23	105	115
20b	Mechanical Engineering Annex	Floating Slab	1222+85	9	115
21	Ocean Sciences	Floating Slab	1244+52	2,056	100
22	Center for Human Development and Disability	HCDF	1200+52	753	100
23	Fisheries Center	HCDF	1202+68	1,242	100

Note 1: Actual depth may be greater than assumed

Note 2: Actual depth is as low as 60ft.

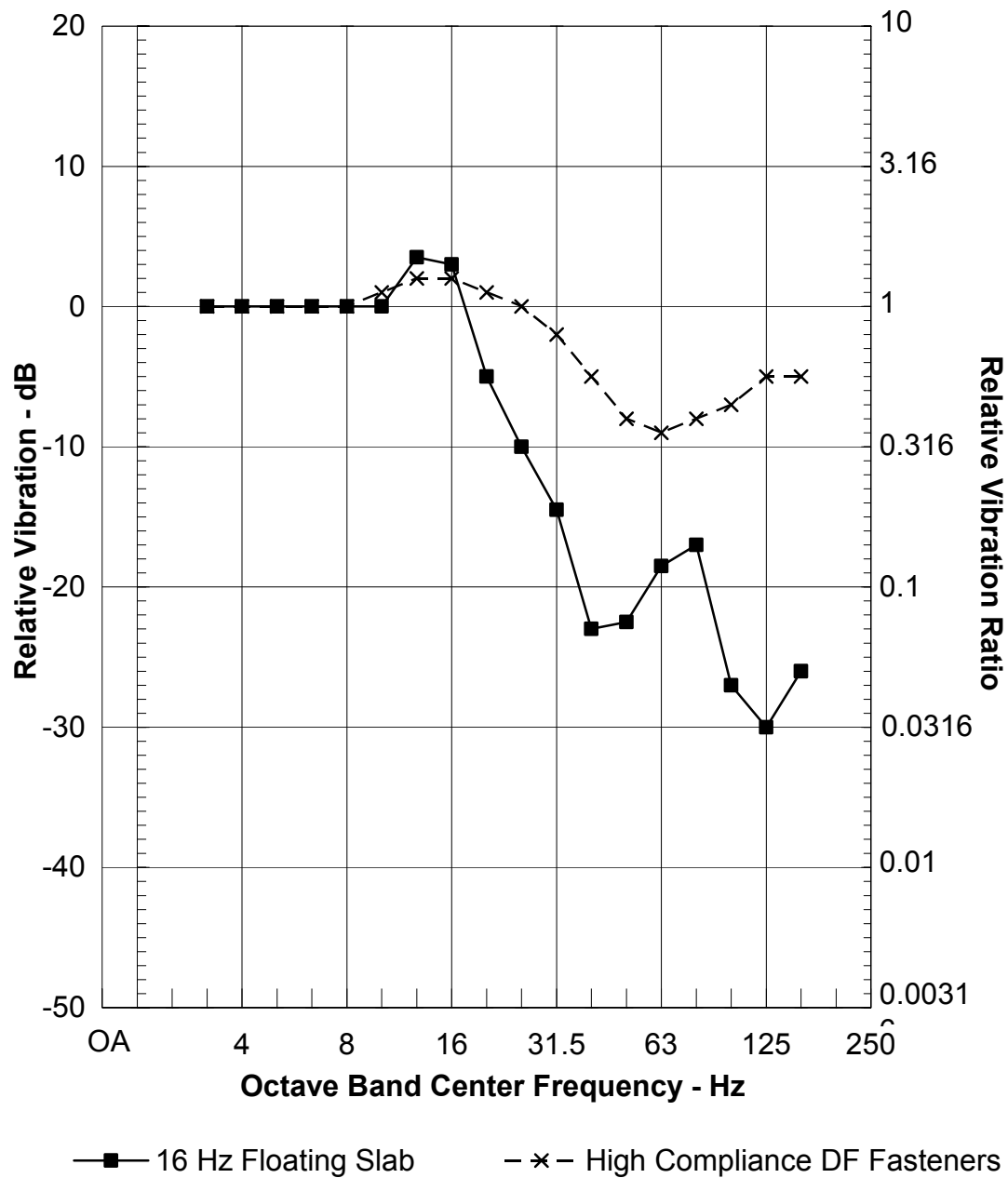
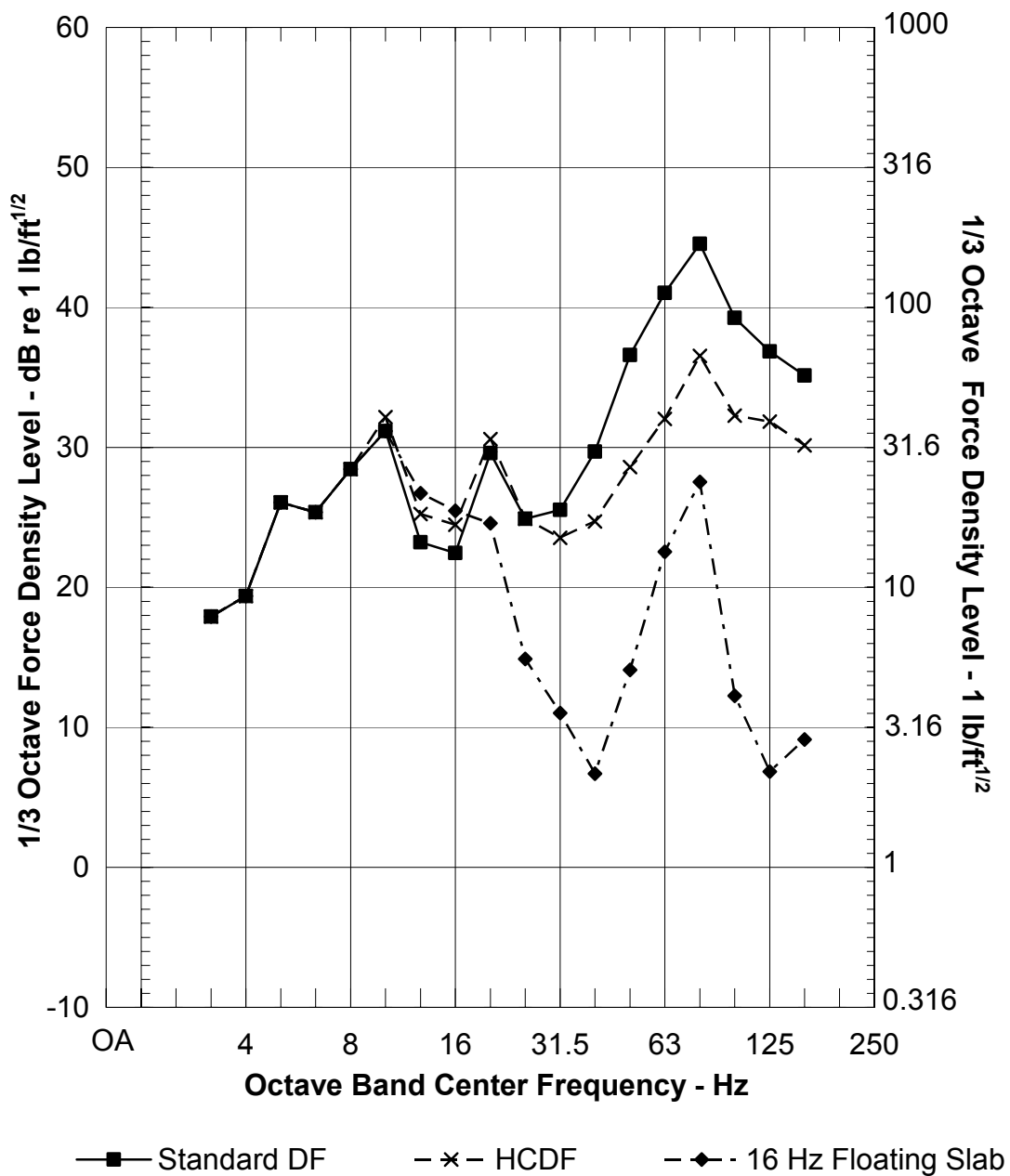


Figure E-1 Adjustments Applied to FDL for VTA/Kinkysharyo Vehicle on Standard Direct Fixation Track to Obtain the FDL for the VTA/Kinkysharyo Vehicle on High Compliance Direct Fixation Track or Floating Slab Track



**Force Density Levels
Single Two-Car Train**

Figure E-2 Force Density Levels Assumed for Kinkysharyo Vehicle

E-3 PREDICTED MITIGATED VIBRATION LEVELS

Predicted vibration levels for the buildings on the UW campus are plotted in Figure E-2 through Figure E-24. The left-hand scale is in velocity levels relative to one micro-inch per second. The right hand scale is in absolute units of micro-inches per second. Note that the right-hand tickmarks still conform to the decibel scale. The FDL's, LSR's, performance curves for HCDF and FS, 3dB adjustment for two trains, and predicted vibration levels are summarized in Table E-3. The predicted levels were computed with two or more digits of precision and rounded to the nearest decibel in Table E-3. In some cases, the sum of the various indicated elements deviate from the indicated total level by one decibel. The indicated total level is the correct level.

E-3.1 (1) Electrical Engineering/Computer Science

The New Electrical Engineering Building would be located at a horizontal offset of 338 feet from the nearest tunnel alignment at civil station 1221+77. The predictions were made with the adjusted numerical model. Predicted vibration velocity levels for four-car trains running on floating slab track are provided in Figure E-1. The predicted levels are below the UW Thresholds. No impact is predicted.

E-3.2 (2) Johnson Hall

Johnson Hall would be located at a horizontal offset of 677 feet from the nearest tunnel alignment at civil station 1237+26. The predictions were made with the adjusted numerical model. Predicted vibration velocity levels at Johnson Hall for floating slab track are provided in Figure E-2. The predicted levels are well below the UW Thresholds.

E-3.3 (3) Bagley Hall

Bagley Hall would be located at an offset of 978 feet from the alignment of the nearest tunnel at civil station 1232+57. The predictions were made with adjusted numerical model. The predicted velocity levels for Bagley Hall for floating slab track are in Figure E-3. The predicted vibration levels are below UW Thresholds.

E-3.4 (4) Chemistry

New Chemistry is located adjacent to Bagley Hall an offset of 1008 feet from the nearest tunnel alignment at civil station 1222+99. The predictions were made with the adjusted numerical model. The predicted levels for floating slab track are plotted in Figure E-4. All predicted vibration levels are less than the UW Thresholds.

E-3.5 (5) Wilcox Hall

Wilcox Hall would be at a horizontal offset of 110 feet from the nearest tunnel alignment at civil station 1214+29. The prediction was made with quadratic least squares regression of test data. Predicted vibration velocity levels for floating slab track are provided in Figure E-5. The

predicted levels are slightly above the UW threshold from 6.3 to 20 Hz and as high as 14 dB above the Threshold at 63 and 80 Hz.

E-3.6 (6) Physics and Astronomy

The Physics and Astronomy building would be located at an horizontal offset of 1,201 feet from the nearest tunnel at civil station 1241+50. The predictions were made with the adjusted numerical model. Predicted vibration velocity levels at Physics and Astronomy for floating slab track are provided in Figure E-6. The predicted levels are well below the UW Thresholds.

E-3.7 (7) Burke Museum

The Burke Museum would be at a horizontal offset of 826 feet from the nearest track centerline of the Brooklyn Station. The predictions were made with the adjusted numerical model. Predicted vibration velocity levels for high-compliance fasteners are provided in Figure E-7. The predicted levels are below the UW Thresholds.

E-3.8 (8) Benson Hall

Benson Hall would be located at a horizontal offset of 1,269 feet from the nearest tunnel alignment at civil station 1233+56. The predictions were made with the adjusted numerical model. Predicted vibration velocity levels at Benson Hall for floating slab track are provided in Figure E-8. The predicted levels are below the UW Thresholds.

E-3.9 (9) Roberts Hall

Roberts Hall would be located at a horizontal offset of 255 feet from the nearest tunnel alignment at civil station 1215+42. The predictions were made with quadratic regression of borehole test data. Predicted vibration velocity levels at Roberts Hall for trains running on floating slab track are provided in Figure E-9. The predicted level at 10Hz is 31dB, exceeding the UW Threshold of 30dB by about 1dB. The predicted level at 20Hz is 28dB, exceeding the UW Threshold of 24dB by 4 dB. The predicted level at 80Hz is 31dB, exceeding the UW Threshold of 27dB by 4dB. All other third-octave levels are below the UW Threshold.

E-3.10 (10) Winkenwerder Hall

Winkenwerder Hall would be located at a horizontal offset of 683 feet from the nearest tunnel alignment at civil station 1212+40. The predictions were made with the adjusted numerical model. Predicted vibration velocity levels for floating slab track are provided in Figure E-10. The predicted levels are below the UW Thresholds.

E-3.11 (11) Henderson Hall

Henderson Hall would be located at a horizontal offset of 1,208 feet from the nearest tunnel alignment at civil station 1250+75. The predictions were made with the adjusted numerical model. Predicted vibration velocity levels for high-compliance fasteners are provided in Figure E-11. The predicted levels are below the UW Thresholds.

E-3.12 (12) Oceanography Research Building

The Oceanographic Research Building would be located at a horizontal offset of 1833 feet from nearest tunnel alignment at civil station 1247+04. The predictions were made with the adjusted numerical model results. Predicted vibration velocity levels for high-compliance fasteners are provided in Figure E-12. The predicted levels are well below the UW Thresholds.

E-3.13 (13) UW Medical Center

The UW Medical Center would be located at a horizontal offset of 910 feet from the nearest tunnel alignment at civil station 1208+53. The predictions were made with the adjusted numerical model. Predicted vibration velocity levels for trains running on high-compliance fasteners are provided in Figure E-13. The predicted levels are below the UW Thresholds.

E-3.14 (14) Fisheries Sciences

The Fisheries Sciences building would be located at a horizontal offset of 1,640 feet from the nearest tunnel alignment at civil station 1248+74. The predictions were made with the adjusted numerical model. Predicted vibration velocity levels for high-compliance fasteners are provided in Figure E-14. The predicted levels are below the UW Thresholds.

E-3.15 (15) Fisheries Teaching and Research Center

The Fisheries Teaching and Research Center would be located at a horizontal offset of 1,858 feet from the nearest tunnel alignment at civil station 1248+13. The predictions were made with the adjusted numerical model. Predicted vibration velocity levels for high-compliance fasteners are provided in Figure E-15. The predicted levels are below the UW Thresholds.

E-3.16 (16) More Hall

More Hall would be located at a horizontal offset of 137 feet from the nearest tunnel alignment at civil station 1216+21. The predictions were made with the quadratic regression of LSR test data. Predicted vibration velocity levels for floating slab track are provided in Figure E-16. The predicted level at 80Hz is 37dB, 1 decibel in excess of the UW Threshold of 36dB. The remaining third-octave levels are below the UW Threshold.

E-3.17 (17) Marine Studies

The Marine Studies building would be located at a horizontal offset of 1,799 feet from the nearest tunnel alignment at civil station 1247+68. The predictions were made with the adjusted numerical model. Predicted vibration velocity levels for high-compliance fasteners are provided in Figure E-17. The predicted levels are below the UW Thresholds.

E-3.18 (18) Bioengineering/Genomics

The Bioengineering/Genomics building would be located at a horizontal offset of 1,612 feet from the nearest tunnel alignment at civil station 1244+85. The predictions were made with the

adjusted numerical model. Predicted vibration velocity levels for floating slab track are provided in Figure E-18. The predicted levels are below the UW Thresholds.

E-3.19 (19) Fluke Hall

Fluke Hall would be located at a horizontal offset of 333 feet from the nearest tunnel alignment at northbound civil station 1226+35. The predictions were made with the adjusted numerical model. Predicted vibration velocity levels at Fluke Hall for trains running on floating slab track are provided in Figure E-19. The predicted level at 80Hz is 28dB, in excess of the UW Threshold of 25dB by 3dB.

E-3.20 (20a) Mechanical Engineering Building

The Mechanical Engineering Building would be located at a horizontal offset of 105 feet from the nearest tunnel alignment at civil station 1223+23. The LSR was computed by regression of global borehole test data. Predicted vibration velocity levels for floating slab track are provided in Figure E-20. The predicted level at 8, 10 and 12Hz is 30 to 31, 33, and 30dB, in excess of the UW Thresholds of 30 and 29dB by perhaps 1, 4 and 1dB, respectively, subject to roundoff. The predicted level at 20Hz is 31dB, in excess of the UW Threshold of 28dB by 3dB. The predicted levels at 50 to 100Hz exceed the UW Threshold. The predicted level at 80Hz is 39dB, in excess of the UW Threshold of 19dB by 20dB.

E-3.21 (20b) Mechanical Engineering Annex

The Mechanical Engineering Annex would be located at a horizontal offset of 9 feet from the nearest tunnel alignment at civil station 1222+85. The predictions were made with the physical model involving regression of test data over slant distance and the logarithm of slant distance. The predicted vibration velocity levels for floating slab track are provided in Figure E-21. The predicted level at 10Hz is 34dB, in excess of the UW Threshold of 33dB by 1dB. The predicted levels between 63 and 100Hz are in excess of the UW Threshold. The level at 80Hz is 43dB, in excess of the UW Threshold of 29dB by 14dB.

E-3.22 (21) Ocean Sciences

The Ocean Sciences building would be located at a horizontal offset of 2,056 feet from nearest tunnel alignment at civil station 1244+52. The predictions were made with the adjusted numerical model. Predicted vibration velocity levels for floating slab track are provided in Figure E-22. The predicted levels are below the UW Thresholds.

E-3.23 (22) Center on Human Development and Disability

The Center on Human Development and Disability would be located at a horizontal offset of 753 feet from the nearest tunnel alignment at civil station 1200+52. The predictions were made with the adjusted numerical model. Predicted vibration velocity levels for high-compliance fasteners are provided in Figure E-23. The predicted levels are below the UW Thresholds.

E-3.24 (23) Fisheries Center

The Fisheries Center building would be located at a horizontal offset of 1,242 feet from the nearest tunnel alignment at civil station 1202+68. The predictions were made with the adjusted numerical model. Predicted vibration velocity levels at Fisheries Center for trains running on high-compliance fasteners are provided in Figure E-24. The predicted levels are below the UW Thresholds.

Table E-3 Summary of Predicted Mitigated Vibration Levels at 30mph

Freq. (Hz)	3.15	4	5	6.3	8	10	12.5	16	20	25	31.5	40	50	63	80	100	125
1) Electrical Engineering - 338 ft Offset, 120 ft Predicted Depth																	
LSR	-10	-8	-7	-5	-6	-8	-11	-9	-5	-3	-3	-3	-3	-4	-3	-3	-5
FDL (FS)	18	19	26	25	28	31	27	25	25	15	11	7	14	23	28	12	7
Two Trains	3	3	3	3	3	3	3	3	3	3	3	3	3	3	3	3	3
Total	11	14	22	23	26	26	19	19	23	15	11	6	14	21	28	12	4
2) Johnson Hall - 688 ft Offset, 120 ft Predicted Depth																	
LSR	-16	-14	-12	-11	-12	-18	-21	-18	-15	-17	-17	-15	-16	-23	-24	-26	-30
FDL (FS)	18	19	26	25	28	31	27	25	25	15	11	7	14	23	28	12	7
Two Trains	3	3	3	3	3	3	3	3	3	3	3	3	3	3	3	3	3
Total	5	8	17	18	19	16	9	10	13	1	-3	-6	1	3	7	-11	-20
3) Bagley Hall - 978 ft Offset, 120 ft Predicted Depth																	
LSR	-18	-15	-14	-13	-15	-18	-17	-16	-18	-17	-19	-24	-26	-29	-32	-39	-43
FDL (FS)	18	19	26	25	28	31	27	25	25	15	11	7	14	23	28	12	7
Two Trains	3	3	3	3	3	3	3	3	3	3	3	3	3	3	3	3	3
Total	3	7	15	15	16	16	13	12	10	1	-5	-14	-9	-3	-2	-23	-33
4) Chemistry - 1008 ft Offset, 120 ft Predicted Depth																	
LSR	-18	-15	-14	-14	-15	-17	-17	-17	-18	-19	-20	-25	-27	-32	-34	-41	-44
FDL (FS)	18	19	26	25	28	31	27	25	25	15	11	7	14	23	28	12	7
Two Trains	3	3	3	3	3	3	3	3	3	3	3	3	3	3	3	3	3
Total	3	7	15	15	16	17	12	12	10	-1	-6	-15	-10	-7	-4	-25	-34
5) Wilcox Hall - 110 ft Offset, 100 ft Predicted Depth																	
LSR	-4	-3	-2	-1	0	0	1	3	4	4	6	8	8	9	9	10	8
FDL (FS)	18	19	26	25	28	31	27	25	25	15	11	7	14	23	28	12	7
Two Trains	3	3	3	3	3	3	3	3	3	3	3	3	3	3	3	3	3
Total	16	19	27	28	31	34	31	31	32	22	20	18	25	35	40	25	18
6) Physics & Astronomy – 1200 ft Offset, 120 ft Predicted Depth																	
LSR	-18	-16	-15	-14	-16	-18	-20	-20	-19	-23	-24	-27	-29	-39	-43	-46	-46
FDL (FS)	18	19	26	25	28	31	27	25	25	15	11	7	14	23	28	12	7
Two Trains	3	3	3	3	3	3	3	3	3	3	3	3	3	3	3	3	3
Total	3	7	14	14	15	16	10	9	9	-5	-10	-17	-12	-13	-13	-31	-36
7) Burke Museum - 826 ft Offset, 80 ft Predicted Depth																	
LSR	-17	-14	-11	-8	-8	-10	-10	-11	-14	-11	-14	-15	-17	-20	-25	-29	-33
FDL (HCDF)	18	19	26	25	28	32	25	24	31	25	24	25	29	32	37	32	32
Two Trains	3	3	3	3	3	3	3	3	3	3	3	3	3	3	3	3	3
Total	4	9	19	20	23	25	18	17	20	17	12	13	15	15	14	6	2
8) Benson Hall - 1269 ft Offset, 120 ft Predicted Depth																	
LSR	-18	-16	-15	-14	-16	-18	-20	-20	-19	-23	-24	-27	-29	-39	-43	-46	-46
FDL (FS)	18	19	26	25	28	31	27	25	25	15	11	7	14	23	28	12	7
Two Trains	3	3	3	3	3	3	3	3	3	3	3	3	3	3	3	3	3
Total	3	7	14	14	15	16	10	9	9	-5	-10	-17	-12	-13	-13	-31	-36
9) Roberts Hall - 255 ft Offset, 115 ft Predicted Depth																	
LSR	-7	-5	-4	-3	-3	-3	-1	0	0	1	2	2	1	1	0	1	0
FDL (FS)	18	19	26	25	28	31	27	25	25	15	11	7	14	23	28	12	7
Two Trains	3	3	3	3	3	3	3	3	3	3	3	3	3	3	3	3	3
Total	14	17	25	25	29	31	29	28	28	19	16	11	18	26	31	16	10

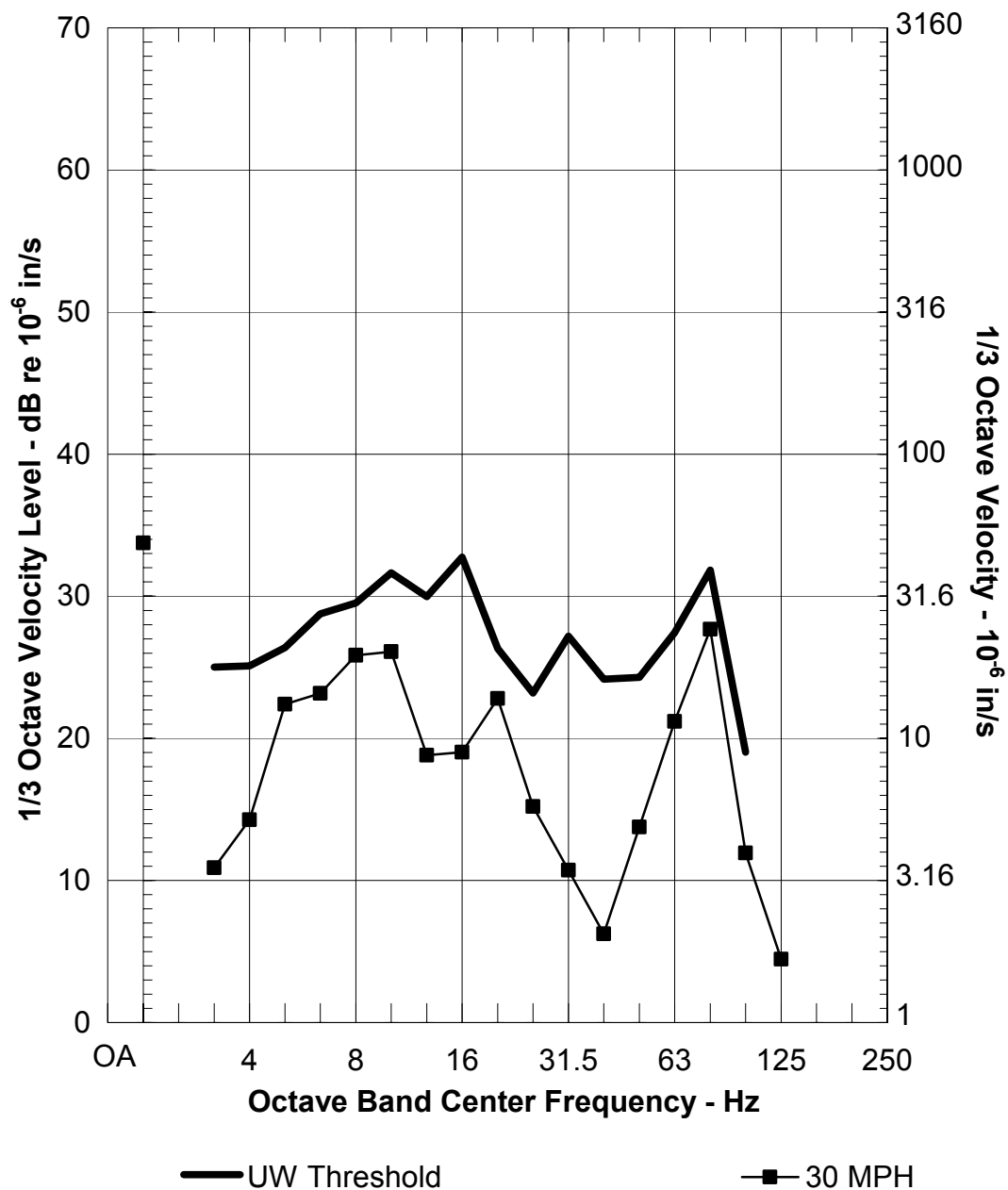
Table E-3 (Continued) Summary of Predicted Mitigated Vibration Levels at 30mph

Freq. (Hz)	3.15	4	5	6.3	8	10	12.5	16	20	25	31.5	40	50	63	80	100	125
10) Winkenwerder Hall - 683 ft Offset, 100 ft Predicted Depth																	
LSR	-16	-14	-11	-9	-10	-13	-15	-16	-12	-10	-15	-16	-15	-21	-23	-25	-31
FDL (FS)	18	19	26	25	28	31	27	25	25	15	11	7	14	23	28	12	7
Two Trains	3	3	3	3	3	3	3	3	3	3	3	3	3	3	3	3	3
Total	5	9	18	19	22	21	15	12	16	8	-1	-6	2	5	8	-9	-21
11) Henderson Hall - 1208 ft Offset, 80 ft Predicted Depth																	
LSR	-17	-15	-13	-11	-11	-13	-14	-15	-17	-19	-21	-26	-26	-37	-40	-44	-43
FDL (HCDF)	18	19	26	25	28	32	25	24	31	25	24	25	29	32	37	32	32
Two Trains	3	3	3	3	3	3	3	3	3	3	3	3	3	3	3	3	3
Total	4	7	16	17	20	22	14	12	17	9	5	2	6	-2	-1	-9	-8
12) Oceanography Research Building - 1833 ft Offset, 80 ft Predicted Depth																	
LSR	-20	-18	-16	-15	-16	-18	-19	-21	-24	-26	-31	-37	-42	-57	-79	-93	-101
FDL (HCDF)	18	19	26	25	28	32	25	24	31	25	24	25	29	32	37	32	32
Two Trains	3	3	3	3	3	3	3	3	3	3	3	3	3	3	3	3	3
Total	0	5	13	13	16	17	9	7	9	2	-5	-9	-11	-22			
13) Medical Center - 910 ft Offset, 110 ft Predicted Depth																	
LSR	-18	-14	-13	-11	-13	-16	-16	-14	-16	-13	-16	-20	-21	-28	-32	-34	-39
FDL (HCDF)	18	19	26	25	28	32	25	24	31	25	24	25	29	32	37	32	32
Two Trains	3	3	3	3	3	3	3	3	3	3	3	3	3	3	3	3	3
Total	3	8	16	17	18	19	12	13	17	14	10	8	10	7	7	1	-5
14) Fisheries Sciences - 1640 ft Offset, 80 ft Predicted Depth																	
LSR	-20	-17	-15	-14	-15	-17	-18	-19	-23	-24	-29	-35	-36	-47	-70	-86	-95
FDL (HCDF)	18	19	26	25	28	32	25	24	31	25	24	25	29	32	37	32	32
Two Trains	3	3	3	3	3	3	3	3	3	3	3	3	3	3	3	3	3
Total	1	5	14	14	17	18	10	8	11	4	-3	-7	-4	-12			
15) Fisheries Teaching & Research Center - 1858 ft Offset, 80 ft Predicted Depth																	
LSR	-21	-18	-16	-15	-16	-18	-20	-22	-24	-26	-32	-38	-43	-58	-80	-93	-101
FDL (HCDF)	18	19	26	25	28	32	25	24	31	25	24	25	29	32	37	32	32
Two Trains	3	3	3	3	3	3	3	3	3	3	3	3	3	3	3	3	3
Total	0	4	13	13	15	17	9	6	10	1	-5	-10	-11	-23			
16) More Hall - 137 ft Offset, 115 ft Predicted Depth																	
LSR	-6	-4	-3	-2	-1	-2	0	2	3	3	4	5	5	6	7	8	6
FDL (FS)	18	19	26	25	28	31	27	25	25	15	11	7	14	23	28	12	7
Two Trains	3	3	3	3	3	3	3	3	3	3	3	3	3	3	3	3	3
Total	15	18	26	27	30	32	30	30	30	20	18	14	22	32	37	23	16
17) Marine Studies - 1799 ft Offset, 80 ft Predicted Depth																	
LSR	-20	-18	-16	-15	-16	-18	-19	-21	-24	-26	-31	-37	-42	-57	-79	-93	-101
FDL (HCDF)	18	19	26	25	28	32	25	24	31	25	24	25	29	32	37	32	32
Two Trains	3	3	3	3	3	3	3	3	3	3	3	3	3	3	3	3	3
Total	0	5	13	13	16	17	9	7	9	2	-5	-9	-11	-22			
18) Bioengineering/ Genomics - 1612 ft Offset, 100 ft Predicted Depth																	
LSR	-20	-18	-16	-15	-17	-20	-21	-21	-24	-24	-28	-34	-36	-48	-72	-86	-95
FDL (FS)	18	19	26	25	28	31	27	25	25	15	11	7	14	23	28	12	7
Two Trains	3	3	3	3	3	3	3	3	3	3	3	3	3	3	3	3	3
Total	1	5	13	13	15	14	8	7	4	-7	-14	-24	-19	-22			

Table E-3 (Continued) Summary of Predicted Mitigated Vibration Levels at 30mph

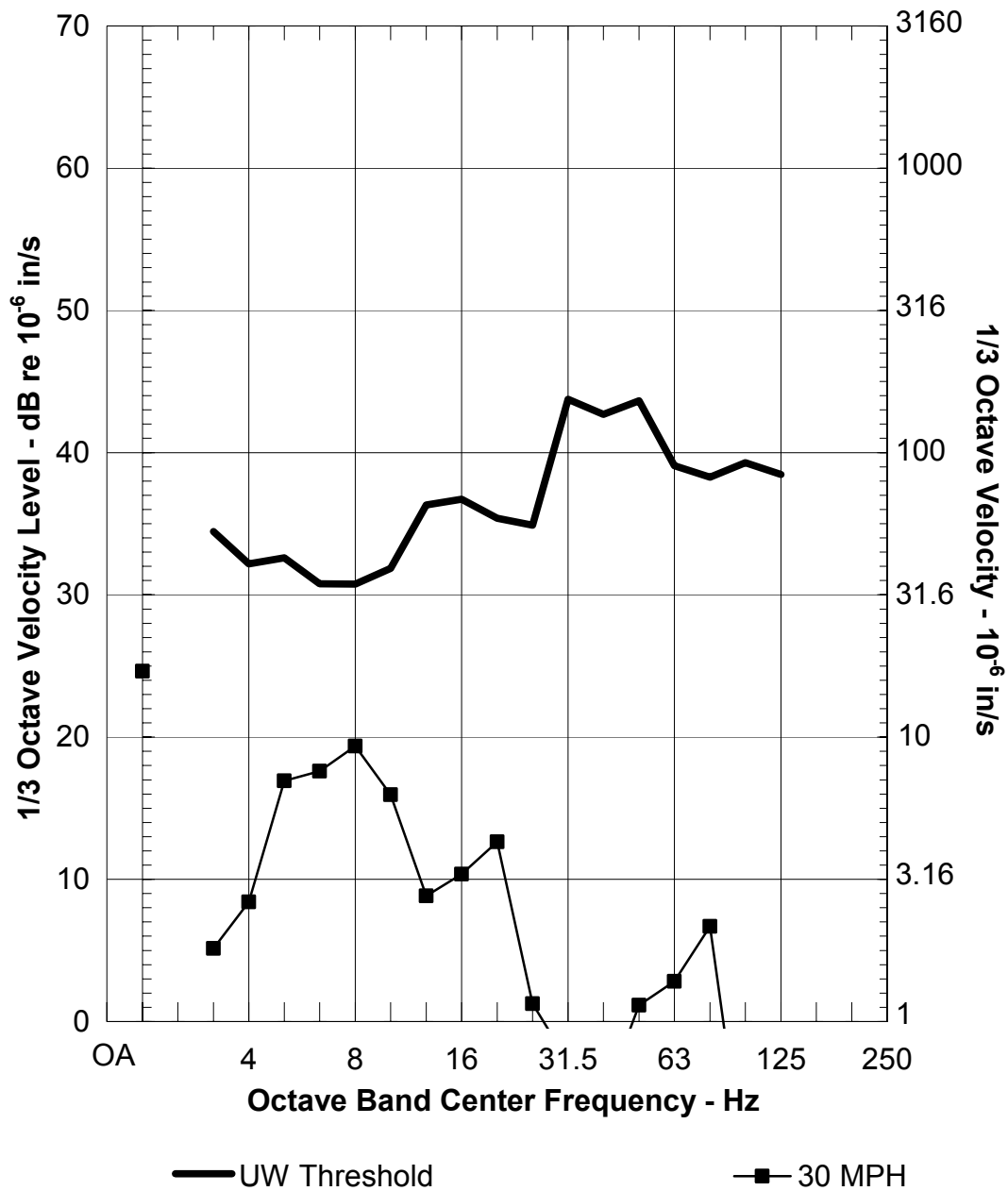
Freq. (Hz)	3.15	4	5	6.3	8	10	12.5	16	20	25	31.5	40	50	63	80	100	125
19) Fluke Hall - 333 ft Offset, 120 ft Predicted Depth																	
LSR	-10	-8	-7	-5	-6	-8	-11	-9	-5	-3	-3	-3	-3	-4	-3	-3	-5
FDL (FS)	18	19	26	25	28	31	27	25	25	15	11	7	14	23	28	12	7
Two Trains	3	3	3	3	3	3	3	3	3	3	3	3	3	3	3	3	3
Total	11	14	22	23	26	26	19	19	23	15	11	6	14	21	28	12	4
20a) ME Building – 105 ft Offset, 115 ft Predicted Depth																	
LSR	-6	-4	-3	-1	-1	-2	0	3	3	3	5	5	7	8	8	9	8
FDL (FS)	18	19	26	25	28	31	27	25	25	15	11	7	14	23	28	12	7
Two Trains	3	3	3	3	3	3	3	3	3	3	3	3	3	3	3	3	3
Total	15	19	26	27	30	33	30	31	31	21	19	15	24	33	39	25	17
20b) ME Annex - 9 ft Offset, 115 ft Predicted Depth																	
LSR	-5	-3	-1	0	0	0	1	3	4	4	5	7	9	11	12	13	11
FDL (FS)	18	19	26	25	28	31	27	25	25	15	11	7	14	23	28	12	7
Two Trains	3	3	3	3	3	3	3	3	3	3	3	3	3	3	3	3	3
Total	16	19	28	29	32	34	31	31	31	22	19	17	27	37	43	28	21
21) Ocean Sciences - 2056 ft Offset, 100 ft Predicted Depth																	
LSR	-21	-19	-18	-17	-19	-22	-24	-28	-26	-29	-35	-40	-48	-58	-82	-96	-104
FDL (FS)	18	19	26	25	28	31	27	25	25	15	11	7	14	23	28	12	7
Two Trains	3	3	3	3	3	3	3	3	3	3	3	3	3	3	3	3	3
Total	0	4	11	11	12	12	5	0	2	-11	-21	-30	-30	-33			
22) Center on Human Development and Disability - 753 ft Offset, 100 ft Predicted Depth																	
LSR	-17	-14	-10	-8	-8	-9	-10	-11	-12	-9	-14	-14	-15	-20	-22	-26	-31
FDL (HCDF)	18	19	26	25	28	32	25	24	31	25	24	25	29	32	37	32	32
Two Trains	3	3	3	3	3	3	3	3	3	3	3	3	3	3	3	3	3
Total	4	9	19	20	23	26	18	16	22	19	13	14	16	16	17	9	4
23) Fisheries Center - 1242 ft Offset, 100 ft Predicted Depth																	
LSR	-18	-15	-14	-13	-14	-16	-17	-18	-17	-20	-21	-25	-29	-37	-42	-45	-44
FDL (HCDF)	18	19	26	25	28	32	25	24	31	25	24	25	29	32	37	32	32
Two Trains	3	3	3	3	3	3	3	3	3	3	3	3	3	3	3	3	3
Total	3	7	15	16	18	20	11	10	16	7	6	3	2	-2	-2	-10	-9

Note: Rounding of numbers may yield sums that do not agree with the total level indicated. The total levels indicated were computed to two or more digits of precision and rounded to the nearest decibel.



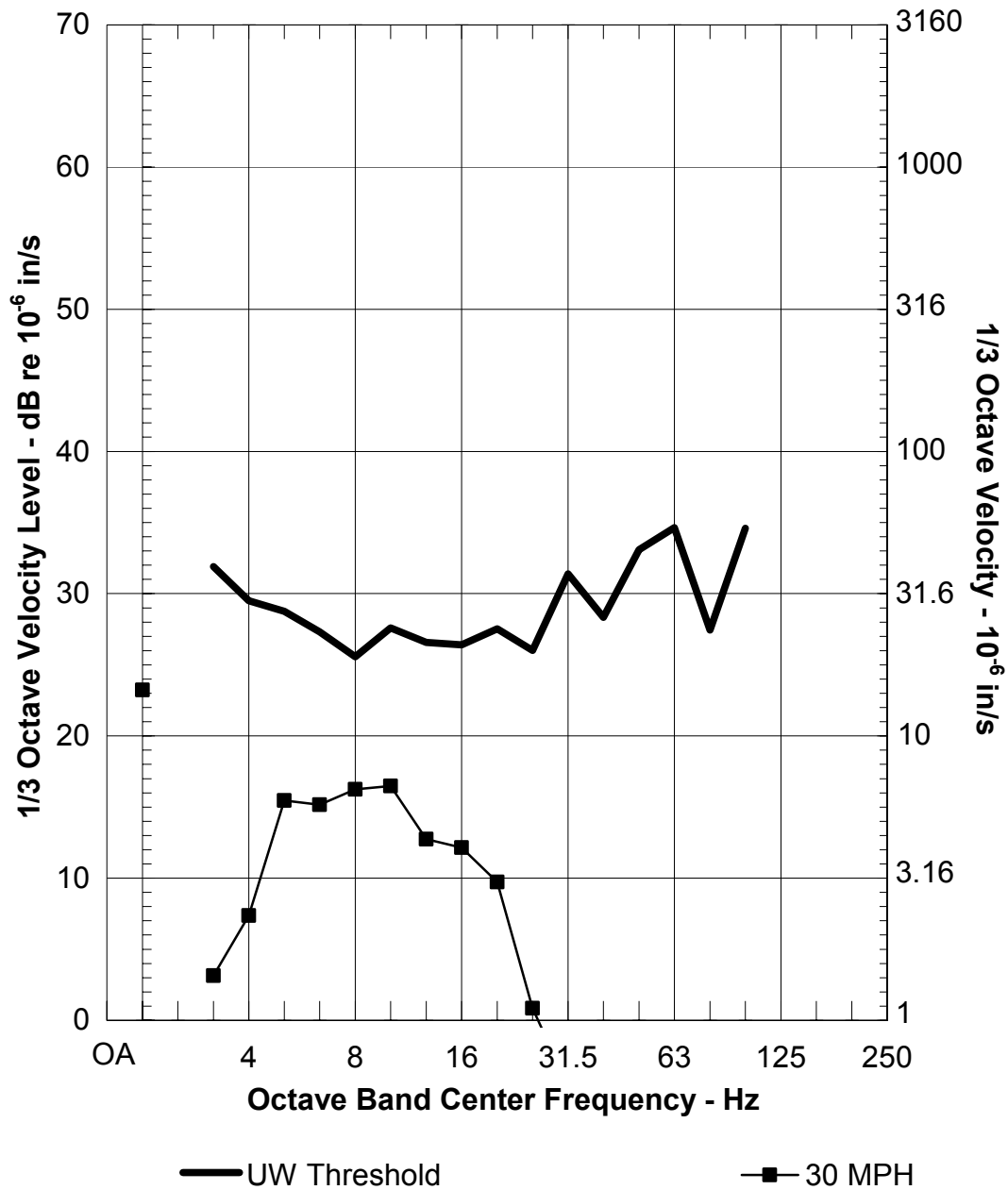
1) Elec. Engin. Vibration At Ground Surface
Numerical Model Prediction
VTA FDL, Two Simultaneous Trains, 16 Hz Floating Slab
338 ft Offset, 120 ft Predicted Depth

Figure E-1 Electrical Engineering/Computer Science



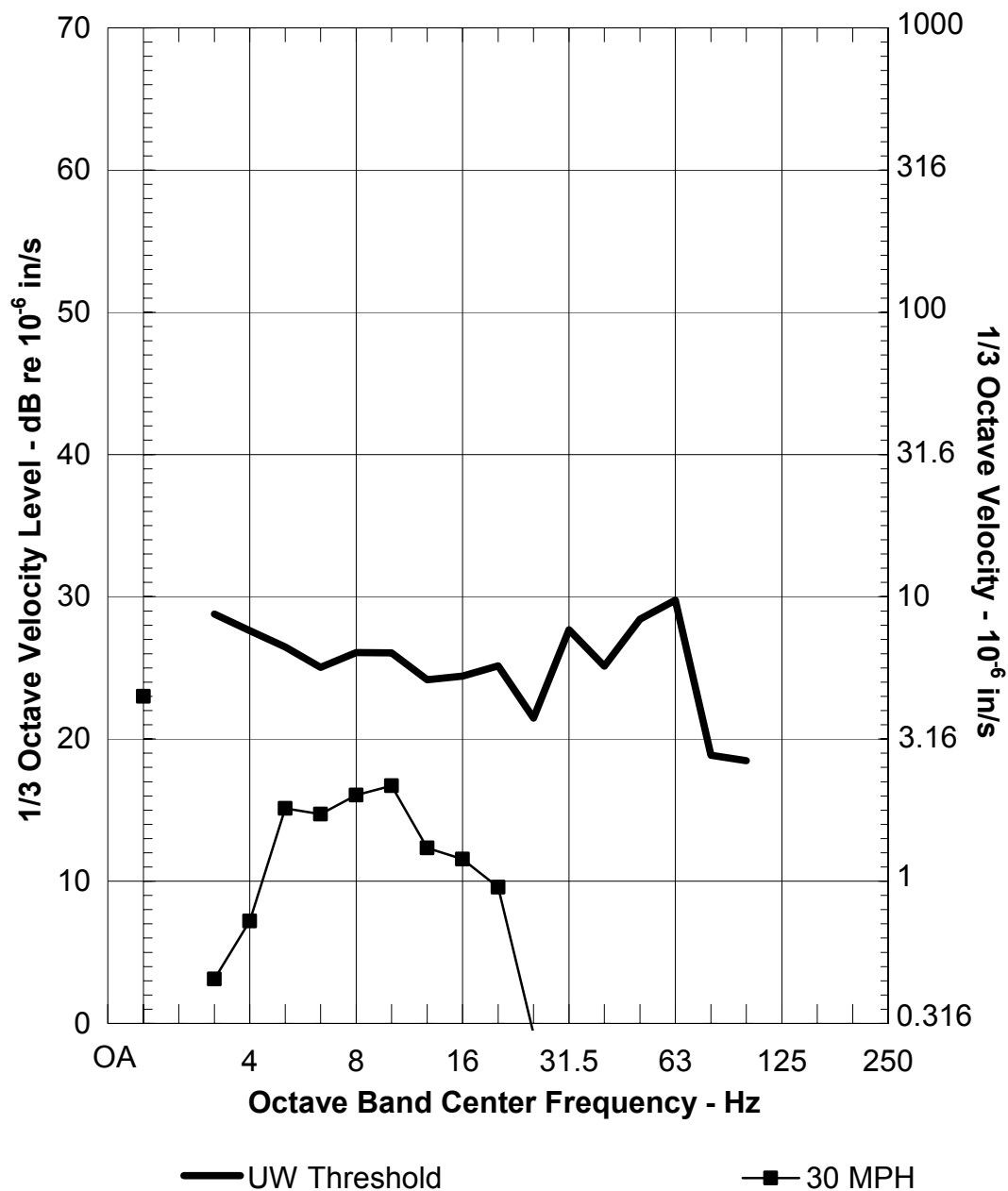
2) Johnson Hall Vibration At Ground Surface
Numerical Model Prediction
VTA FDL, Two Simultaneous Trains, 16 Hz Floating Slab
688 ft Offset, 120 ft Predicted Depth

Figure E-2 Johnson Hall



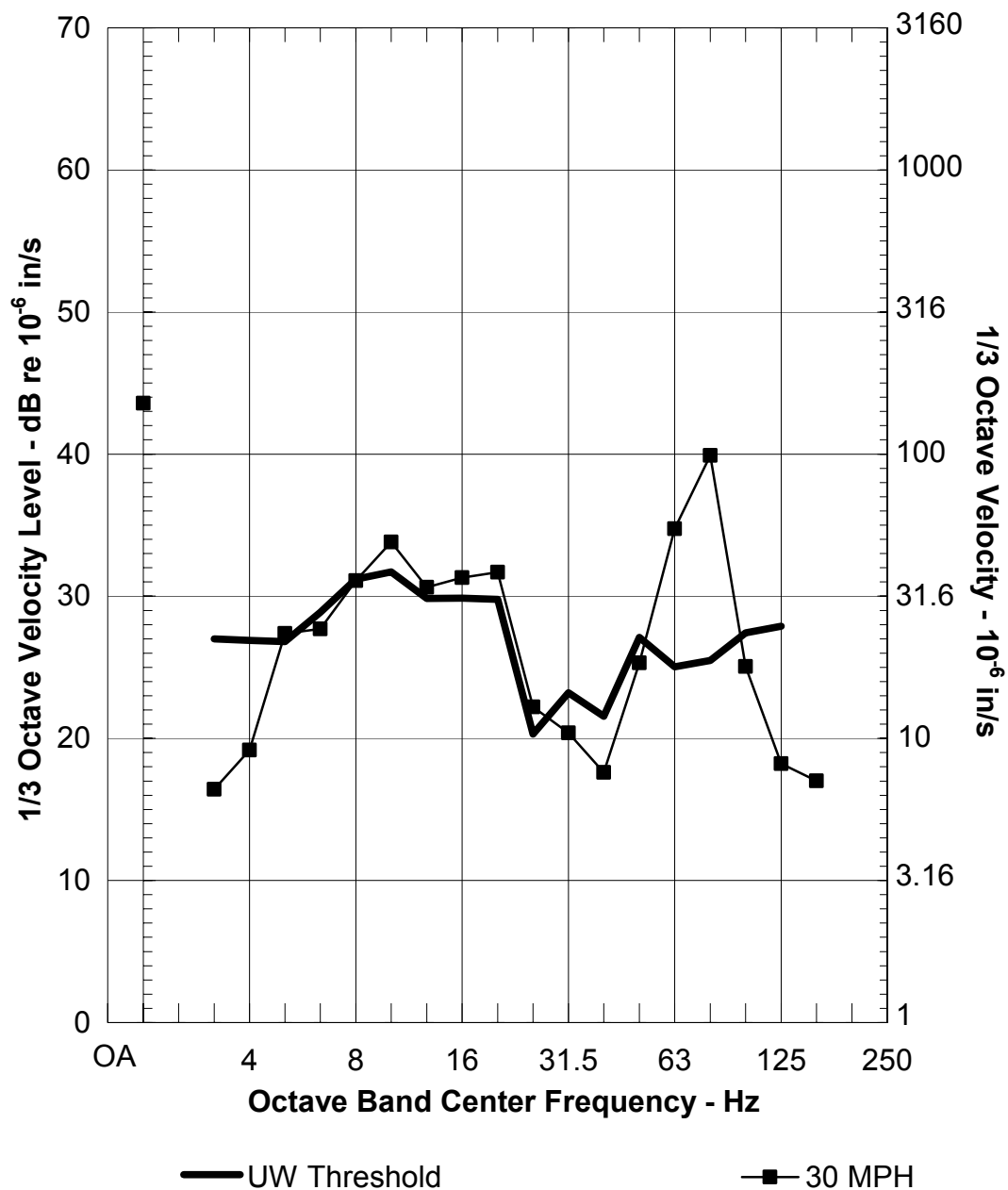
3) Bagley Hall Vibration At Ground Surface
Numerical Model Prediction
VTA FDL, Two Simultaneous Trains, 16 Hz Floating Slab
978 ft Offset, 120 ft Predicted Depth

Figure E-3 Bagley Hall



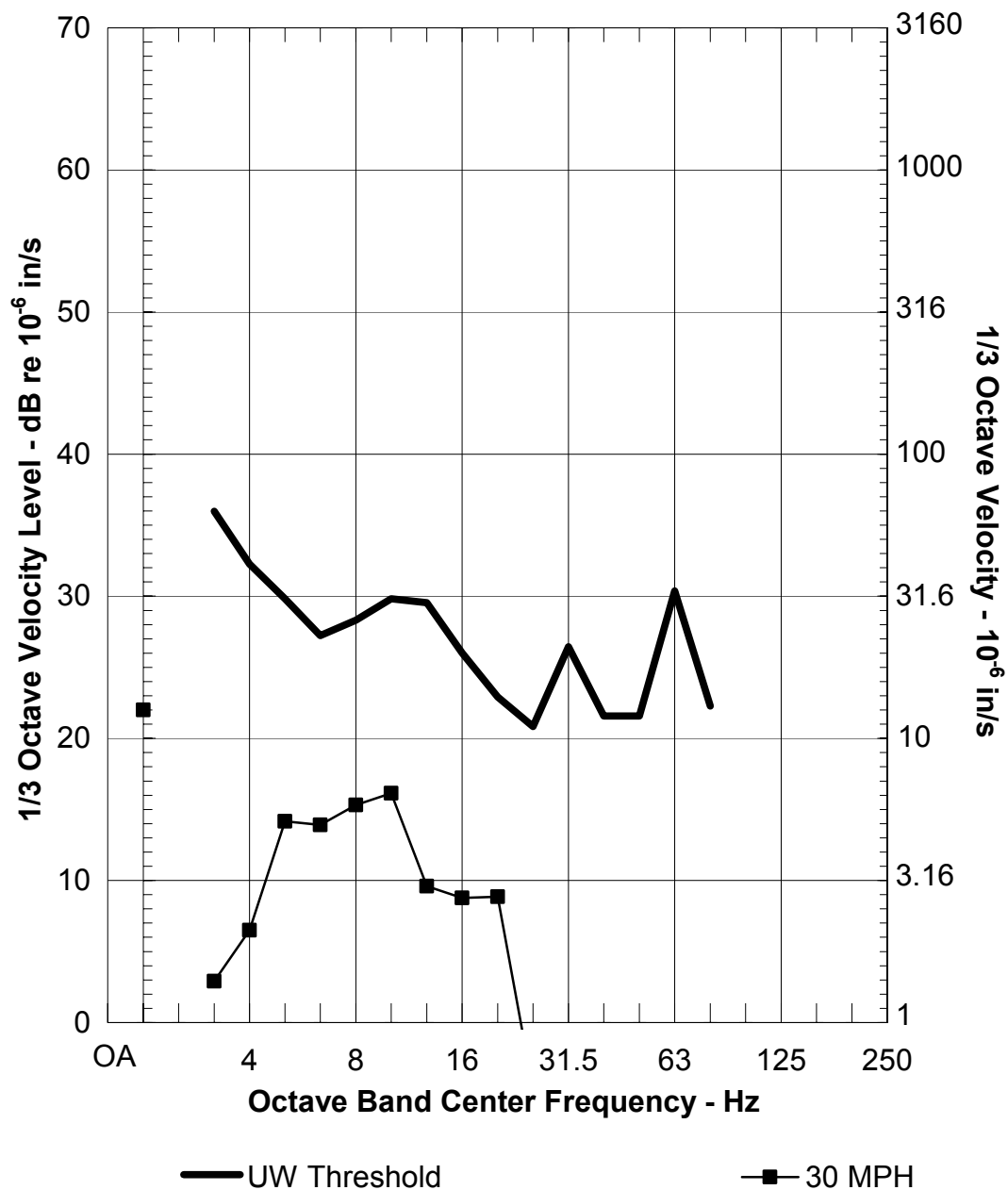
4) Chemistry Vibration At Ground Surface
Numerical Model Prediction
VTA FDL, Two Simultaneous Trains, 16 Hz Floating Slab
1008 ft Offset, 120 ft Predicted Depth

Figure E-4 Chemistry Building



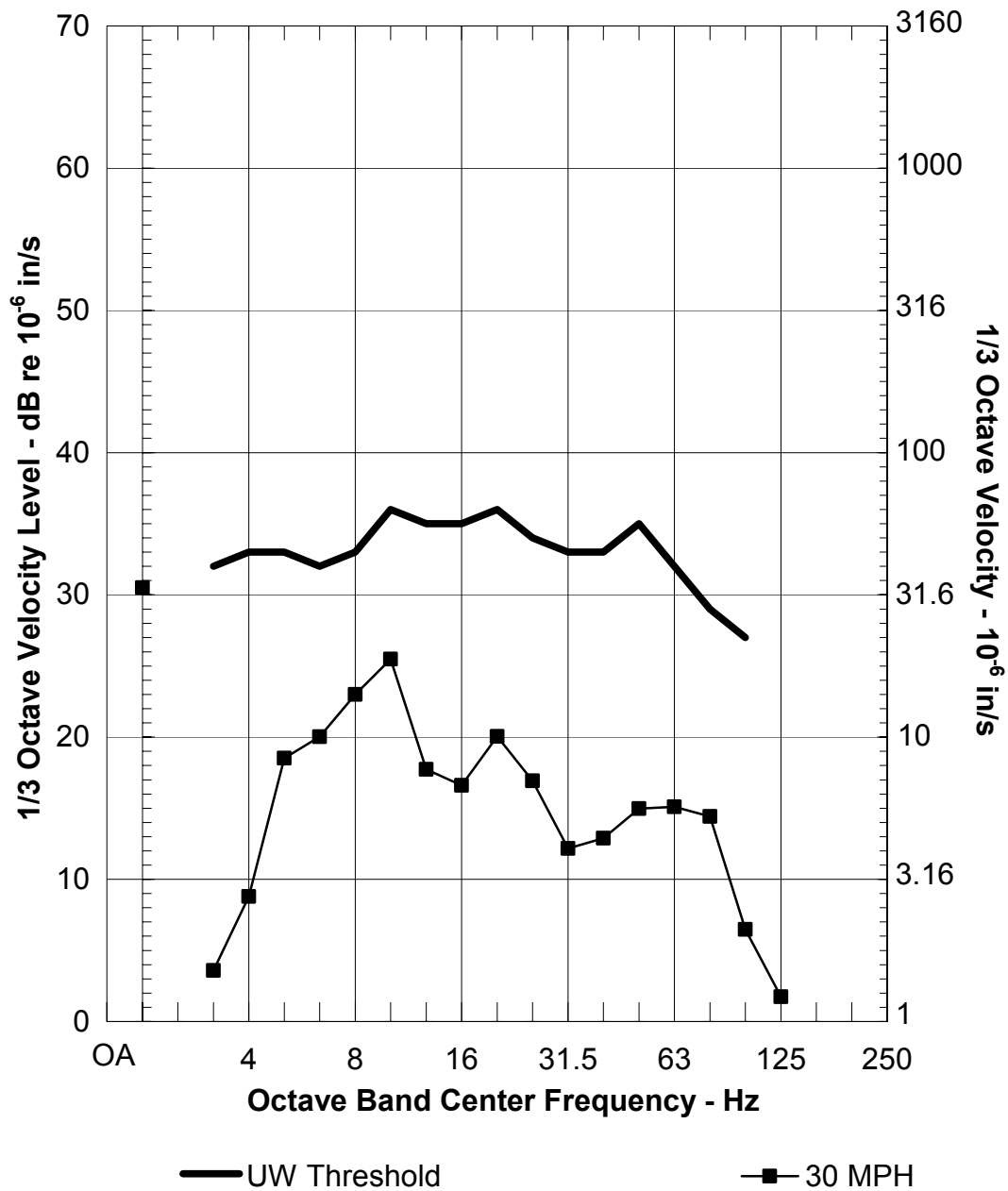
5) Wilcox Hall Vibration At Ground Surface
Global Quadratic LSR
VTA FDL, Two Simultaneous Trains, 16 Hz Floating Slab
110 ft Offset, 100 ft Predicted Depth

Figure E-5 Wilcox Hall



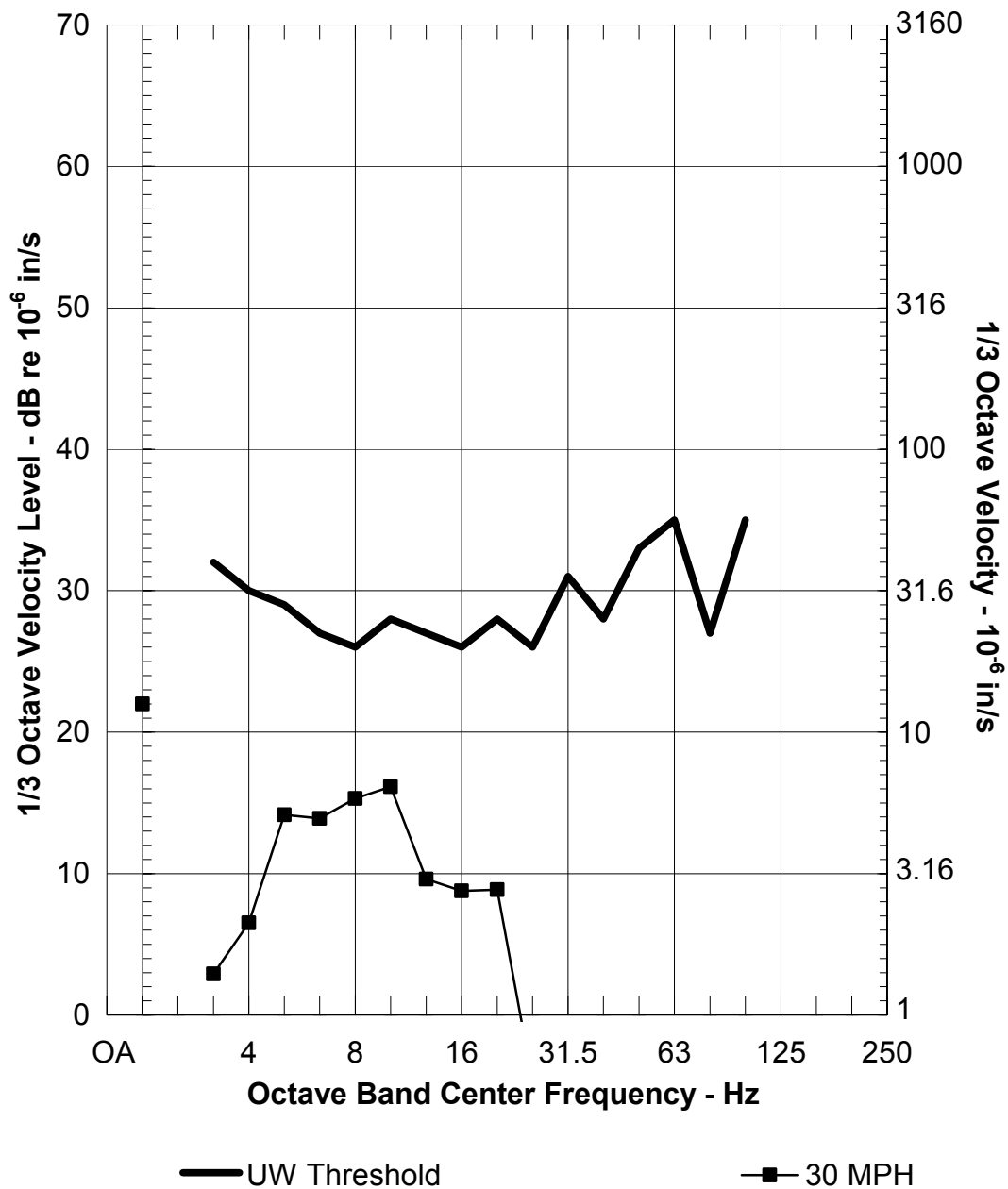
6) Physics & Astro. Vibration At Ground Surface
Numerical Model Prediction
VTA FDL, Two Simultaneous Trains, 16 Hz Floating Slab
1200 ft Offset, 120 ft Predicted Depth

Figure E-6 Physics and Astronomy



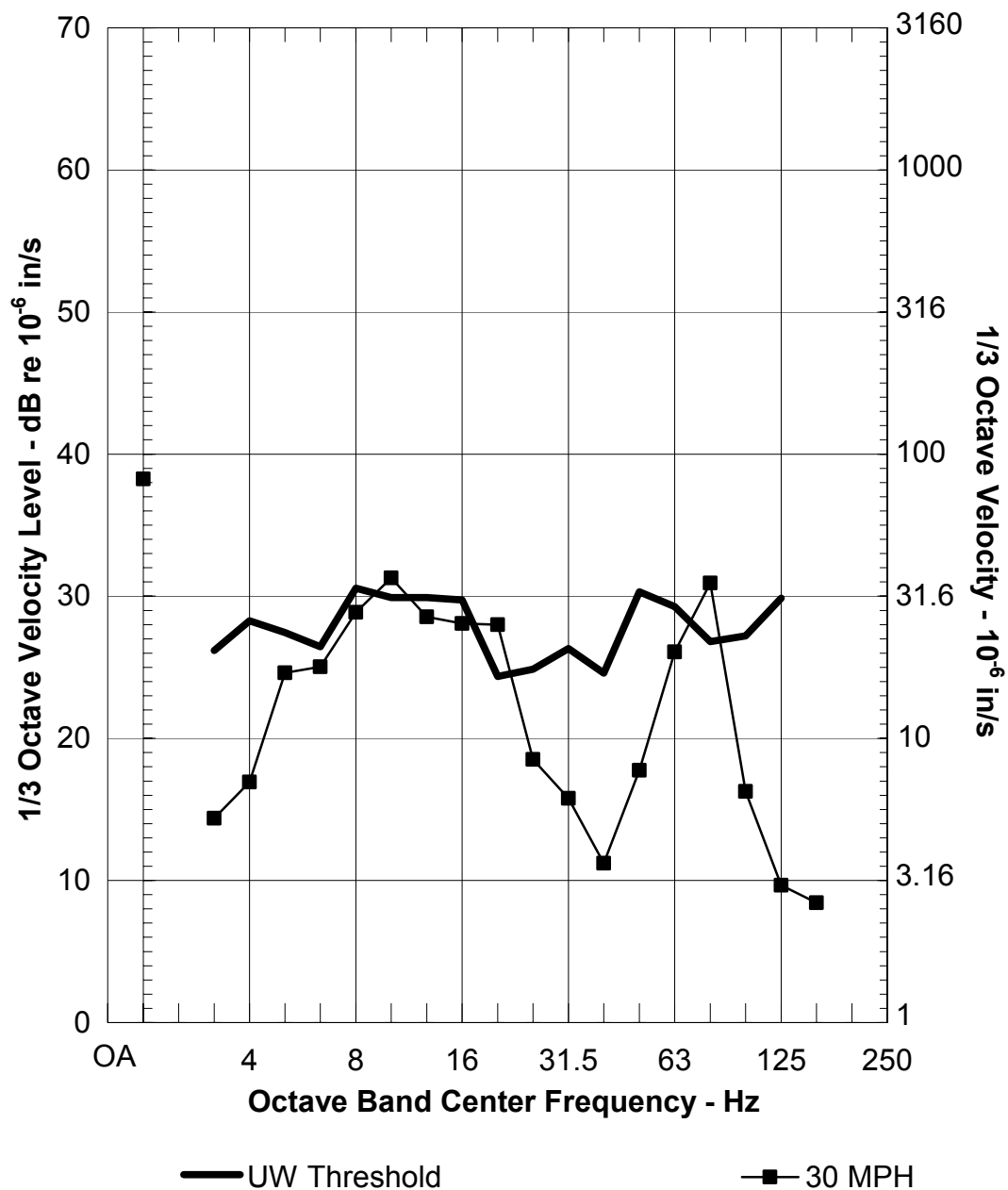
**7) Burke Museum Vibration At Ground Surface
Numerical Model Prediction
VTA FDL, Two Simultaneous Trains, HCDF Fastener
826 ft Offset, 80 ft Predicted Depth**

Figure E-7 Burke Museum



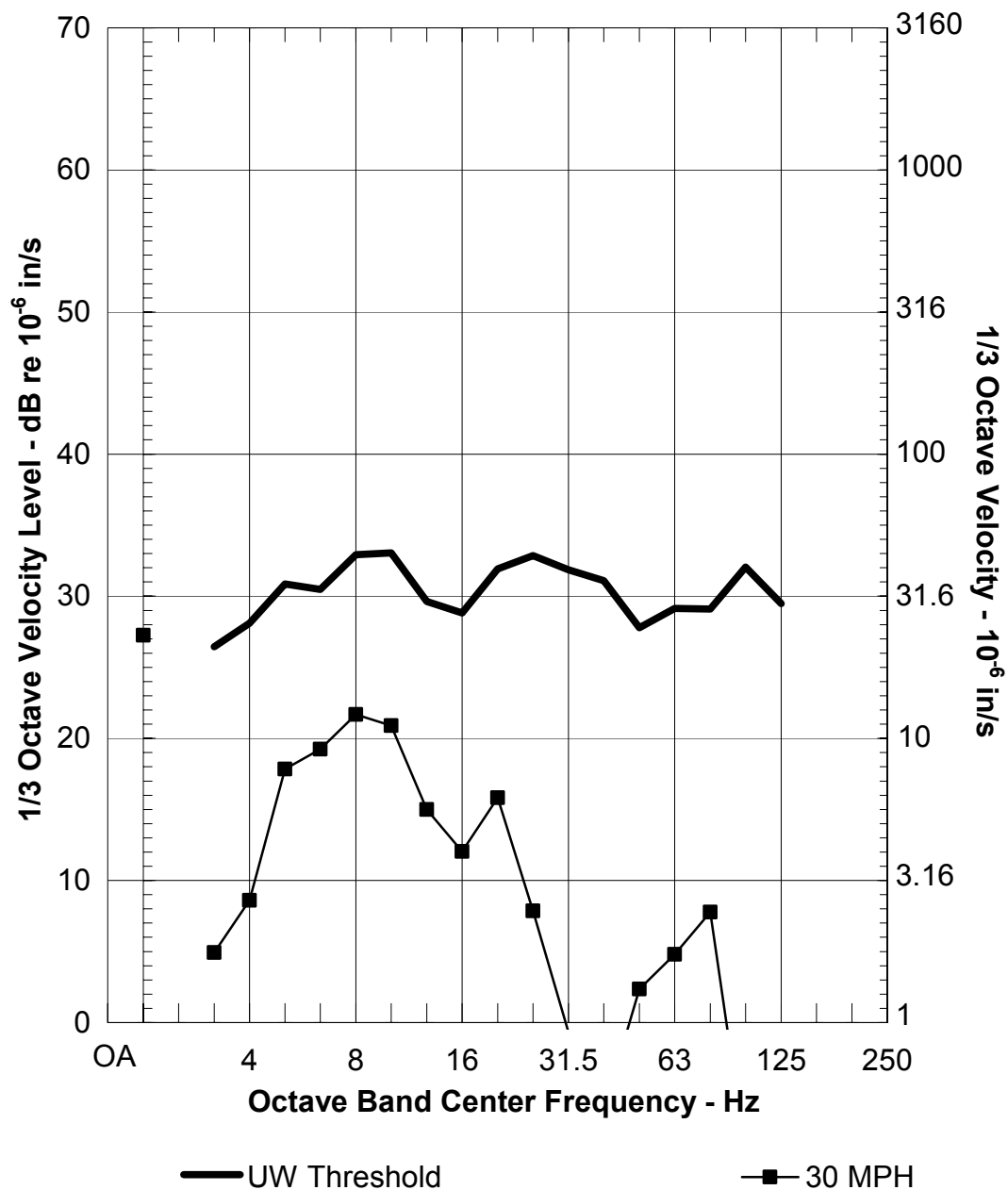
**8) Benson Hall Vibration At Ground Surface
Numerical Model Prediction
VTA FDL, Two Simultaneous Trains, 16 Hz Floating Slab
1269 ft Offset, 120 ft Predicted Depth**

Figure E-8 Benson Hall



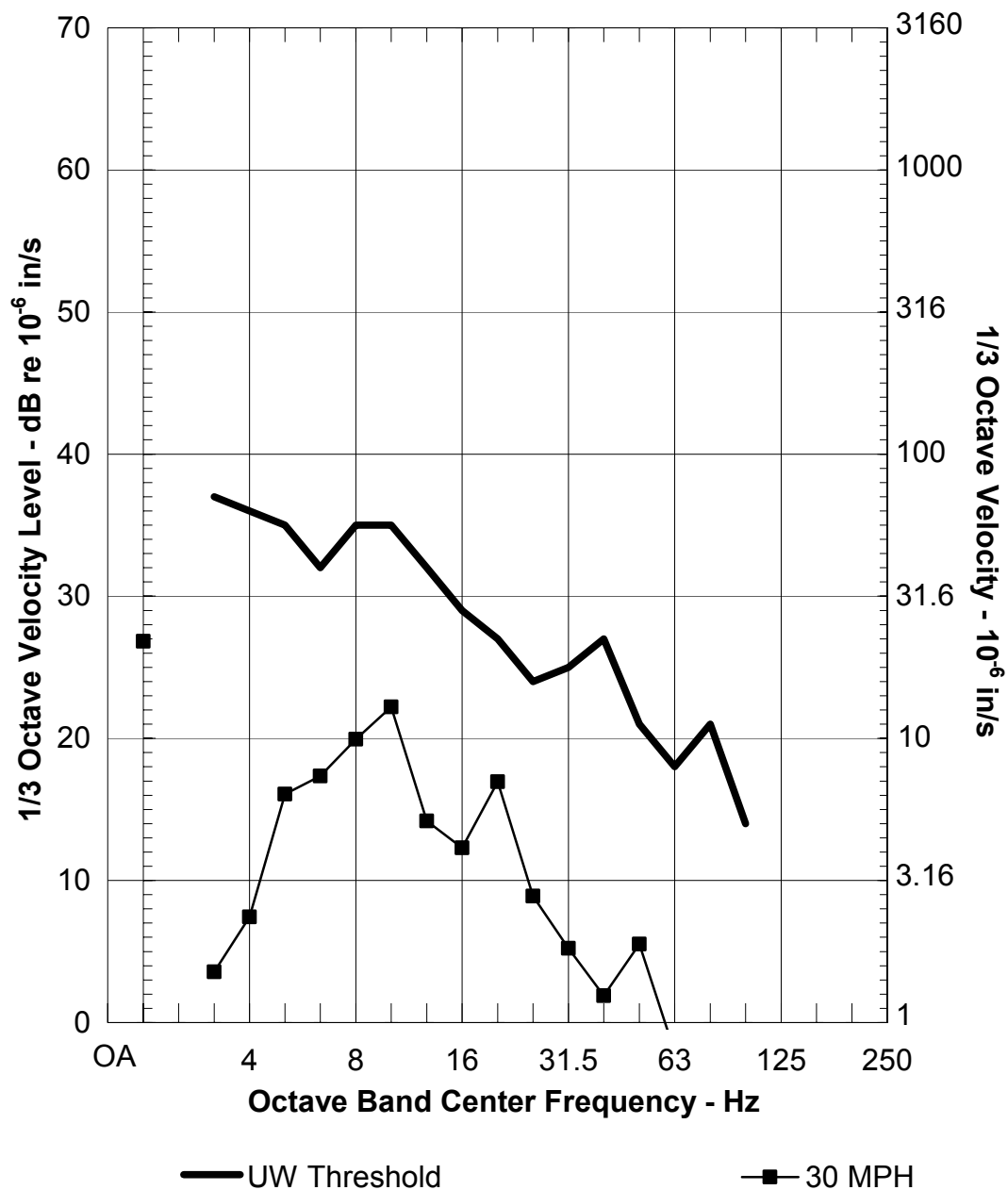
9) Roberts Hall Vibration At Ground Surface
Global Quadratic LSR
VTA FDL, Two Simultaneous Trains, 16 Hz Floating Slab
225 ft Offset, 115 ft Predicted Depth

Figure E-9 Roberts Hall



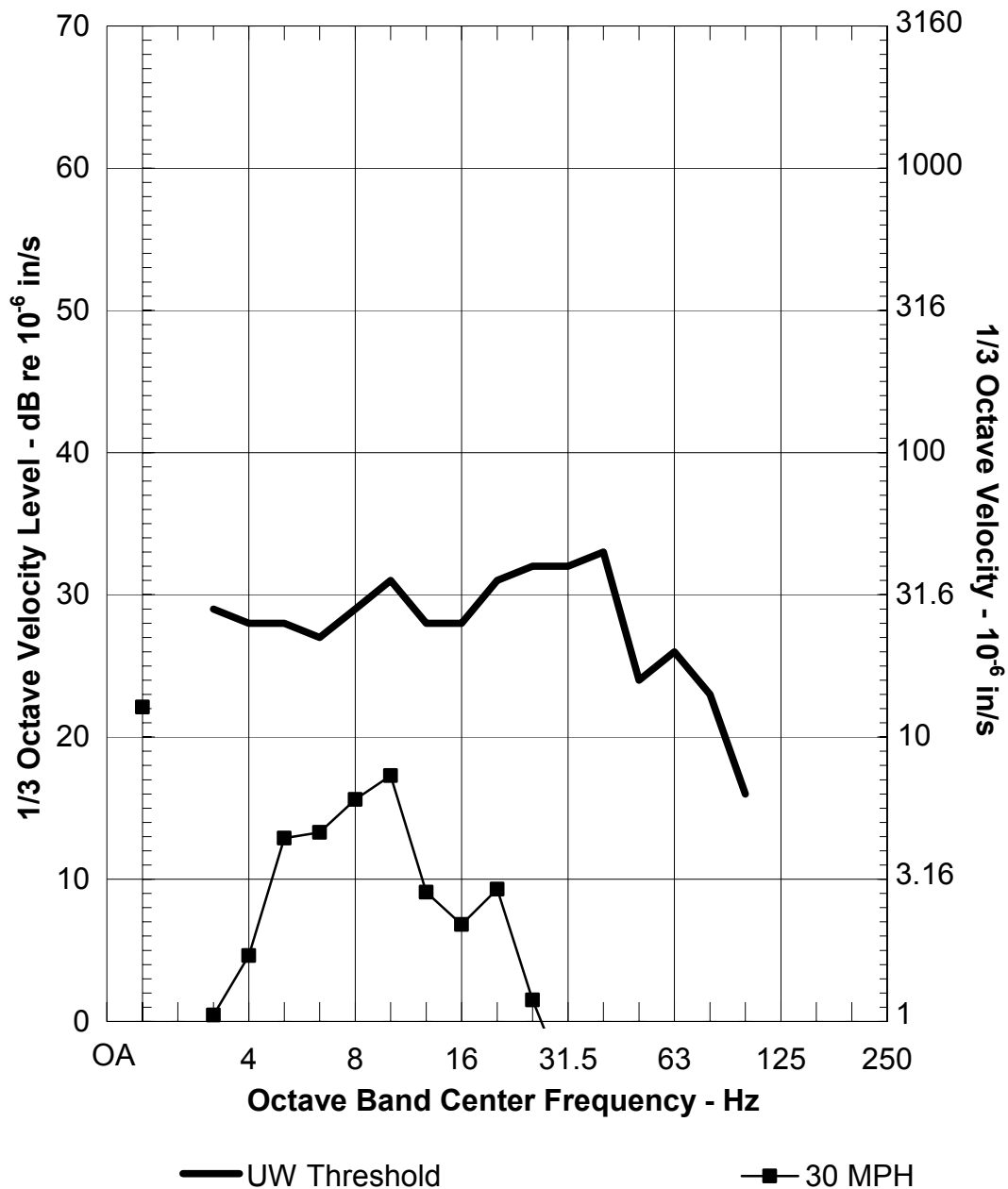
**10) Winkenwerder Hall Vibration At Ground Surface
Numerical Model Prediction
VTA FDL, Two Simultaneous Trains, 16 Hz Floating Slab
683 ft Offset, 100 ft Predicted Depth**

Figure E-10 Winkenwerder Hall



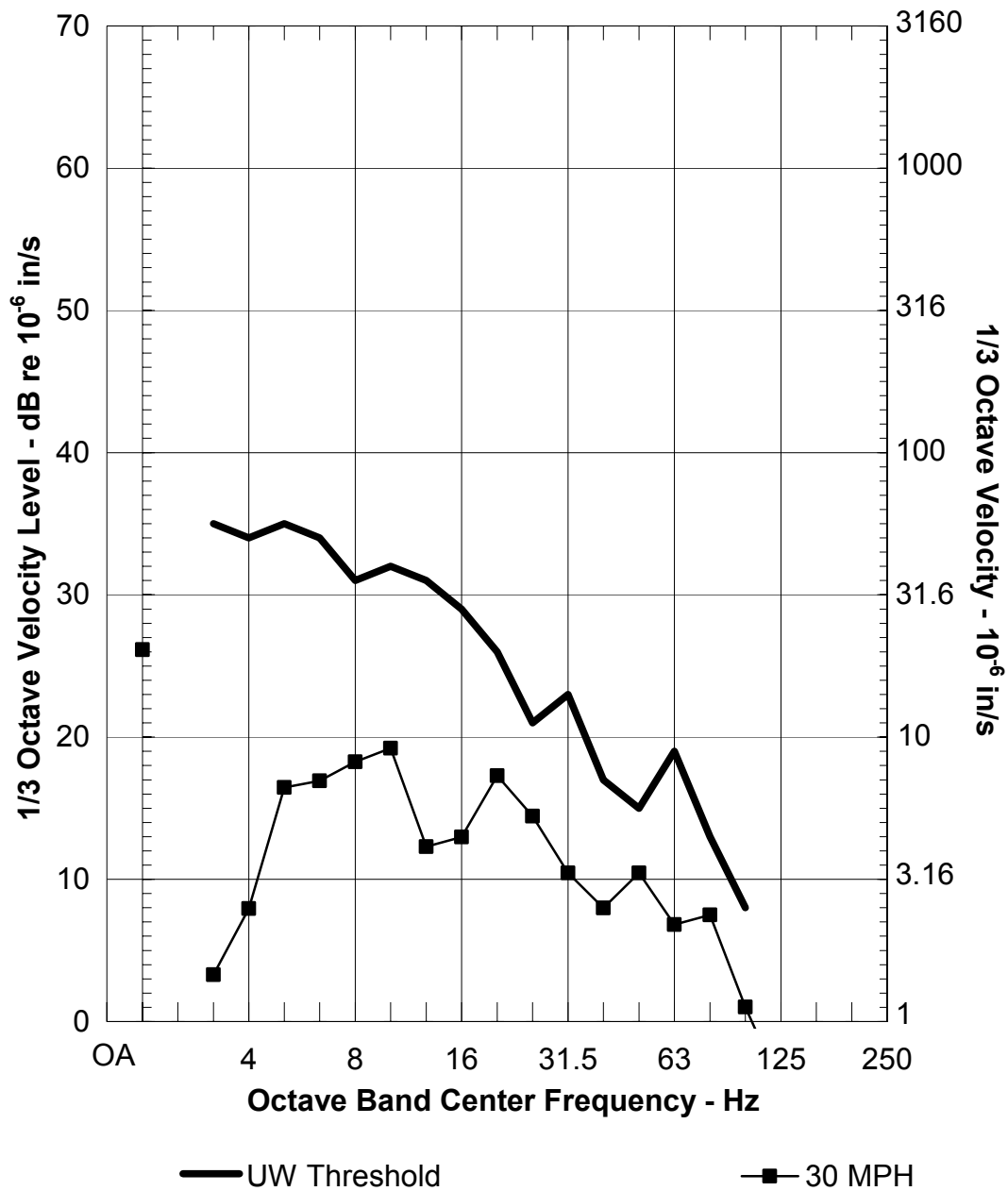
**11) Henderson Hall Vibration At Ground Surface
Numerical Model Prediction
VTA FDL, Two Simultaneous Trains, HCDF Fastener
1208 ft Offset, 80 ft Predicted Depth**

Figure E-11 Henderson Hall



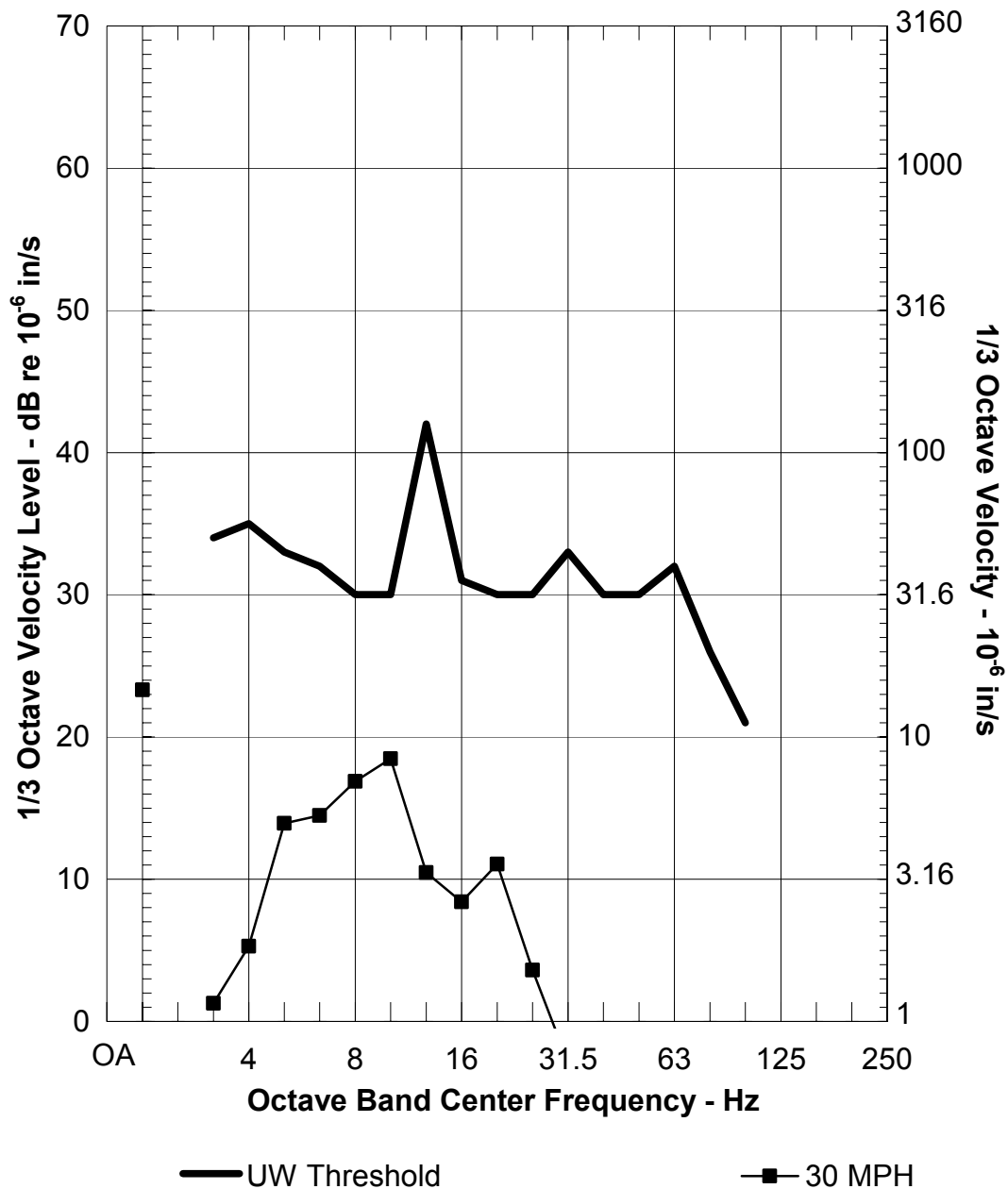
**12) Oceanography Research Vibration At Ground Surface
Numerical Model Prediction
VTA FDL, Two Simultaneous Trains, HCDF Fastener
1833 ft Offset, 80 ft Predicted Depth**

Figure E-12 Oceanography Research Building



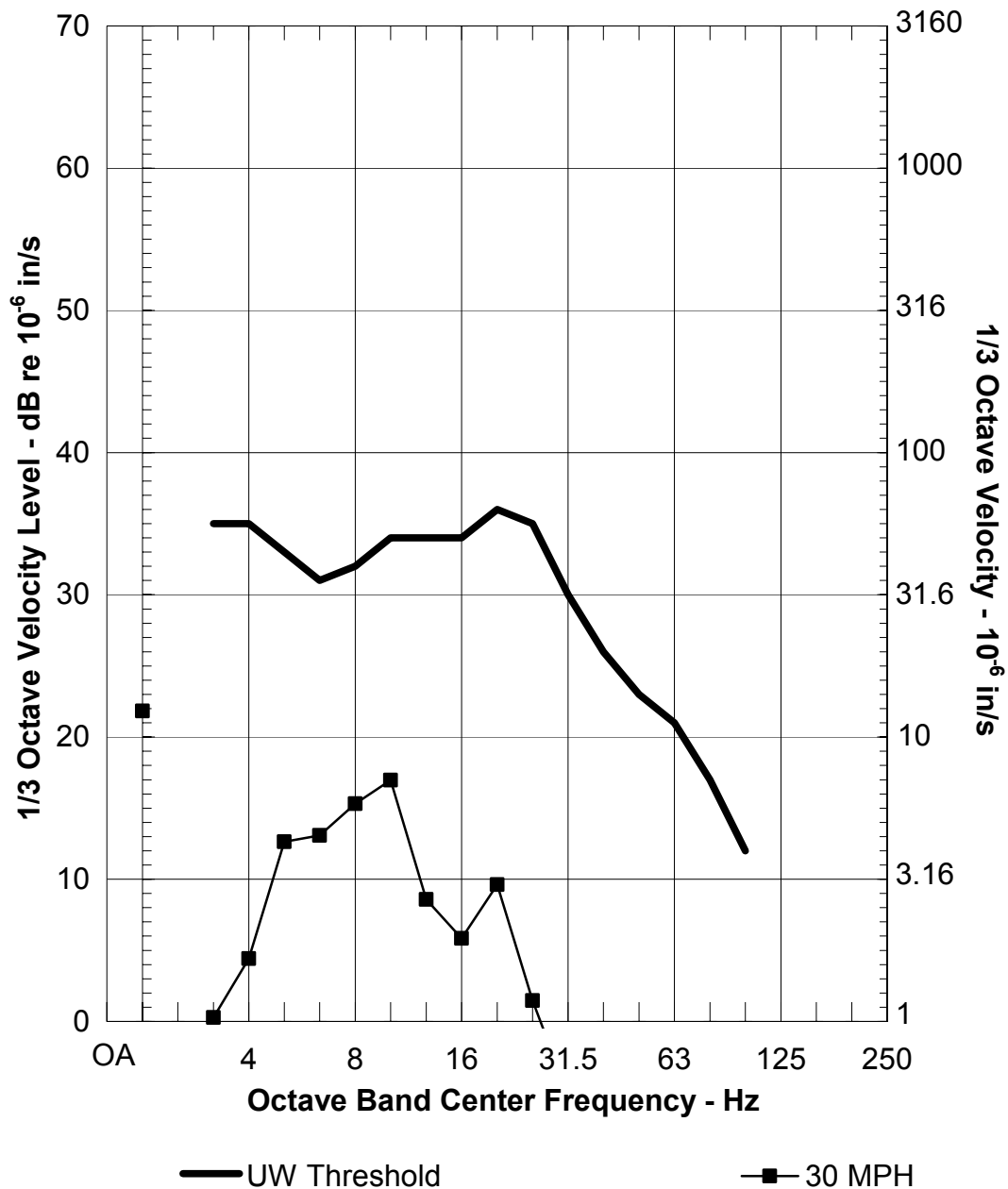
**13) Medical Center Vibration At Ground Surface
Numerical Model Prediction
VTA FDL, Two Simultaneous Trains, HCDF Fastener
910 ft Offset, 110 ft Predicted Depth**

Figure E-13 UW Medical Center



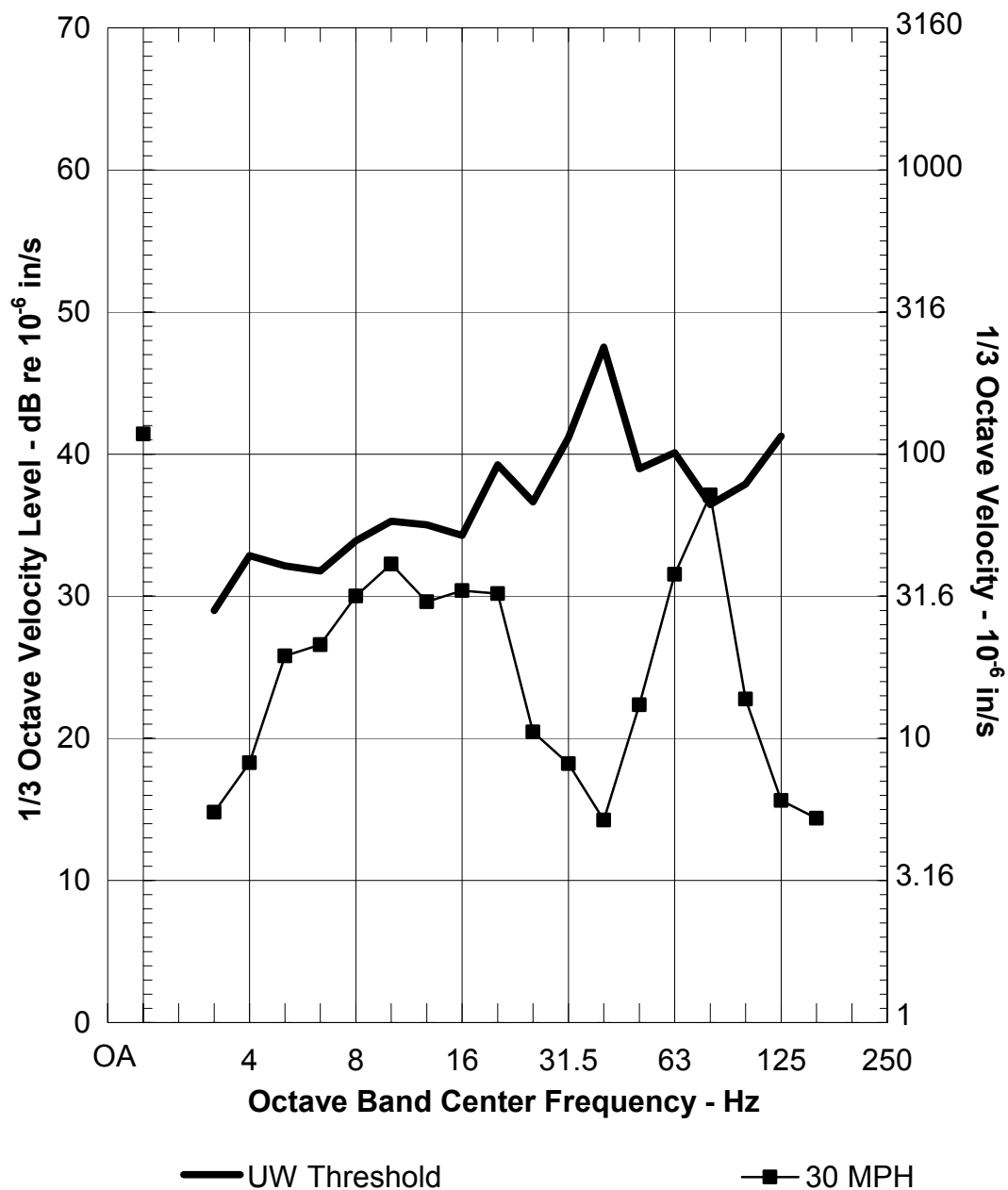
**14) Fisheries Sciences Vibration At Ground Surface
Numerical Model Prediction
VTA FDL, Two Simultaneous Trains, HCDF Fastener
1640 ft Offset, 80 ft Predicted Depth**

Figure E-14 Fisheries Sciences



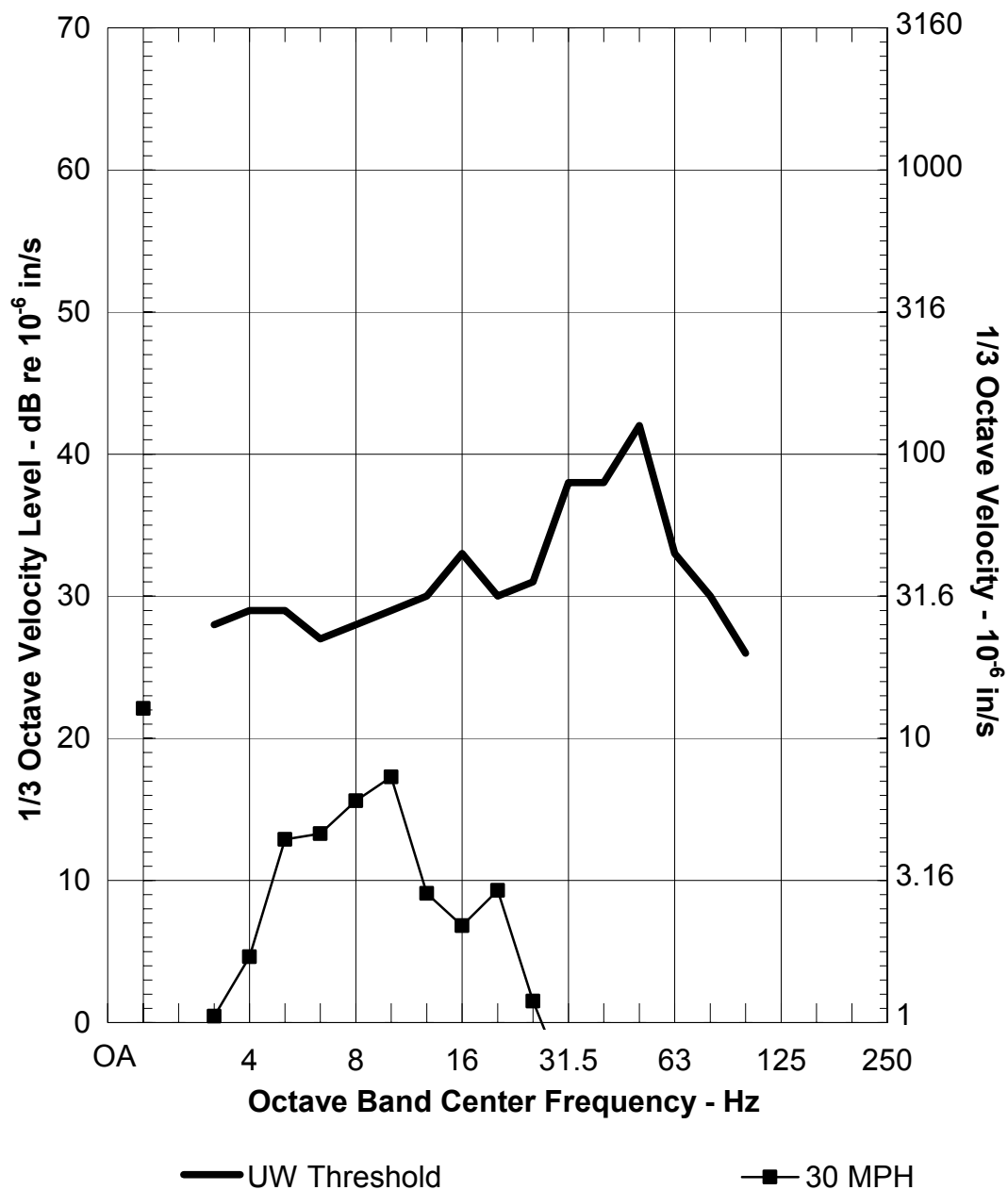
**15) Fisheries Teaching Vibration At Ground Surface
Numerical Model Prediction
VTA FDL, Two Simultaneous Trains, HCDF Fastener
1858 ft Offset, 80 ft Predicted Depth**

Figure E-15 Fisheries Teaching and Research Center



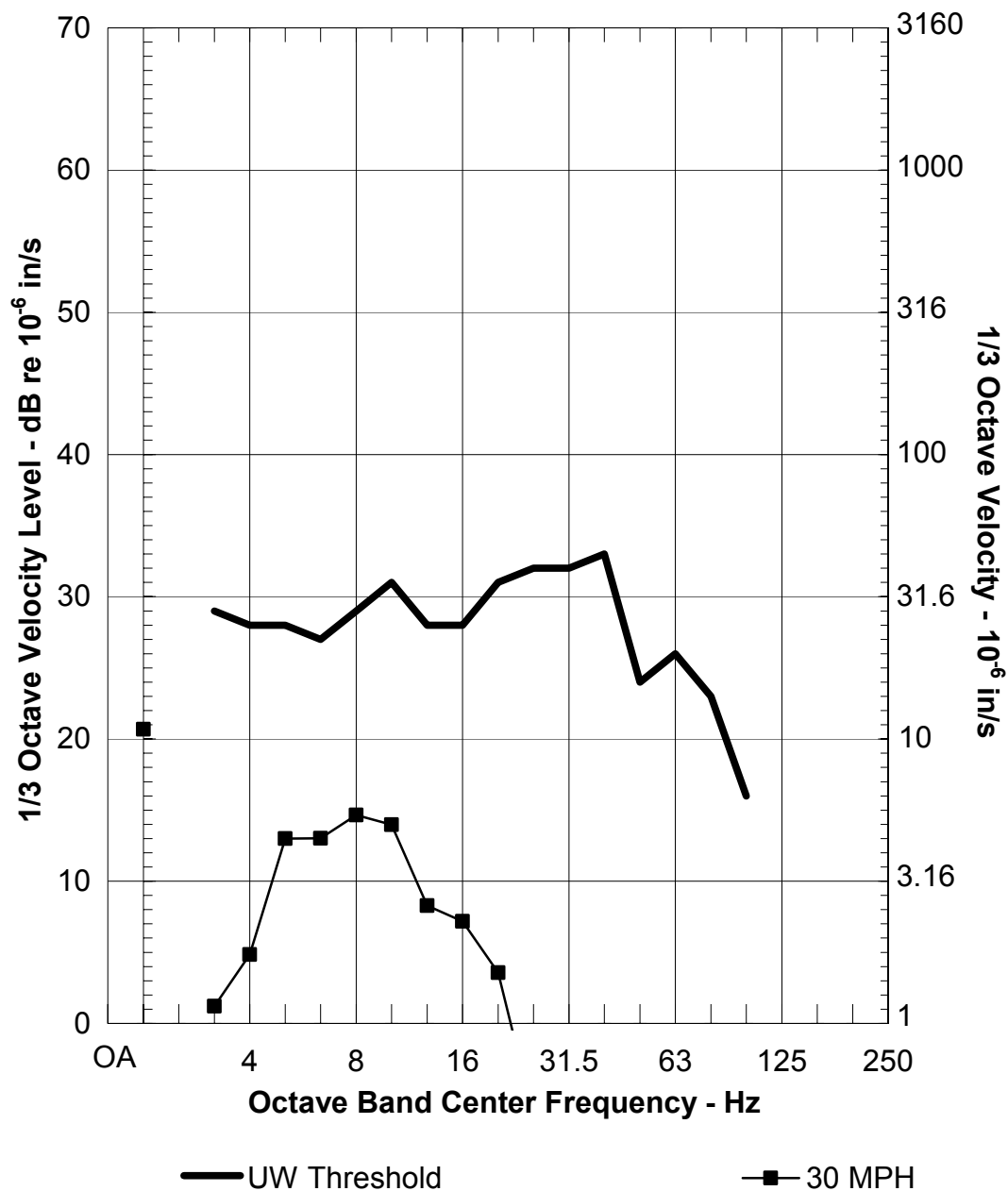
16) More Hall Vibration At Ground Surface
Global Quadratic LSR
VTA FDL, Two Simultaneous Trains, 16 Hz Floating Slab
137 ft Offset, 115 ft Predicted Depth

Figure E-16 More Hall



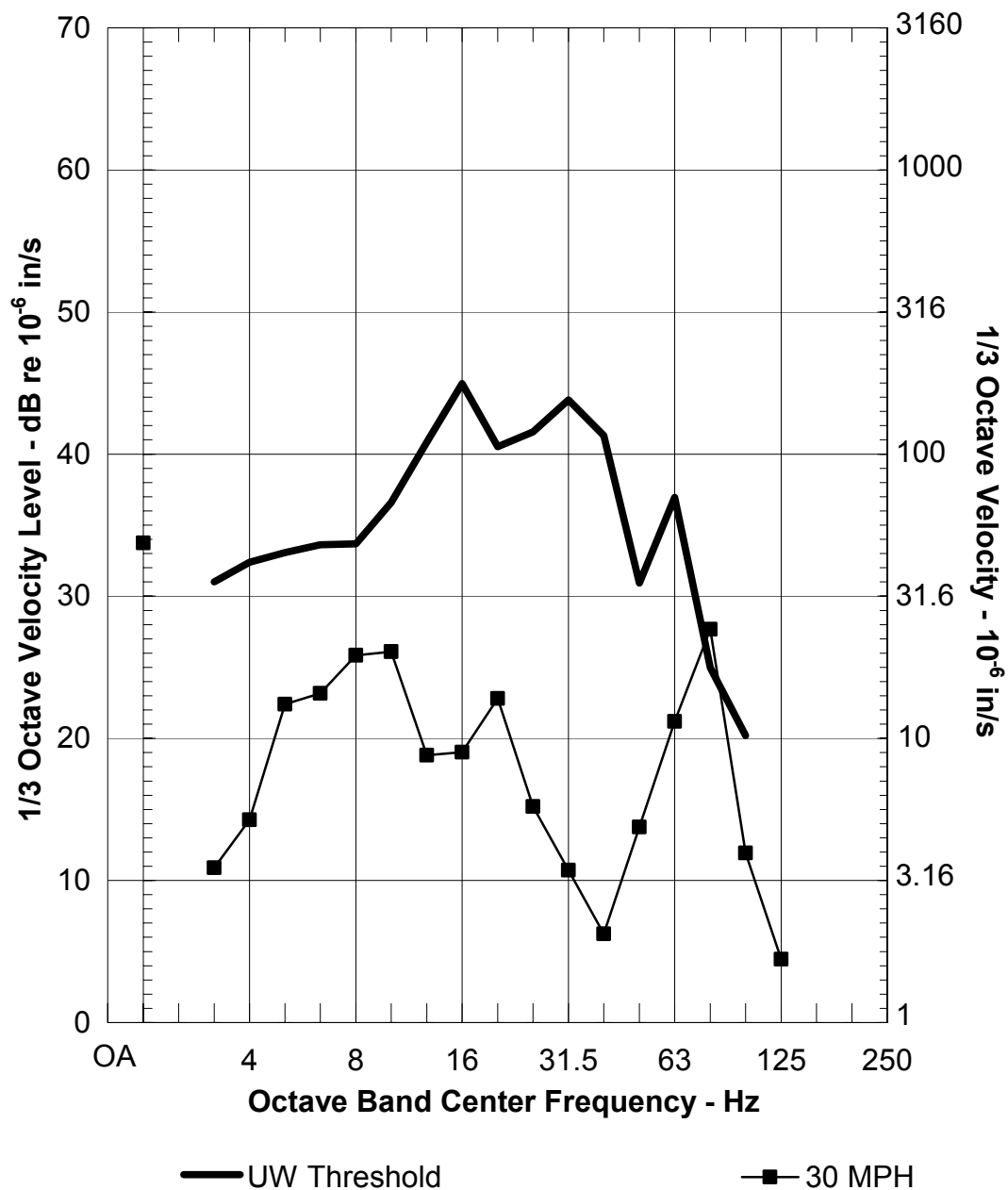
17) Marine Studies Vibration At Ground Surface
Numerical Model Prediction
VTA FDL, Two Simultaneous Trains, HCDF Fastener
1799 ft Offset, 80 ft Predicted Depth

Figure E-17 Marine Studies



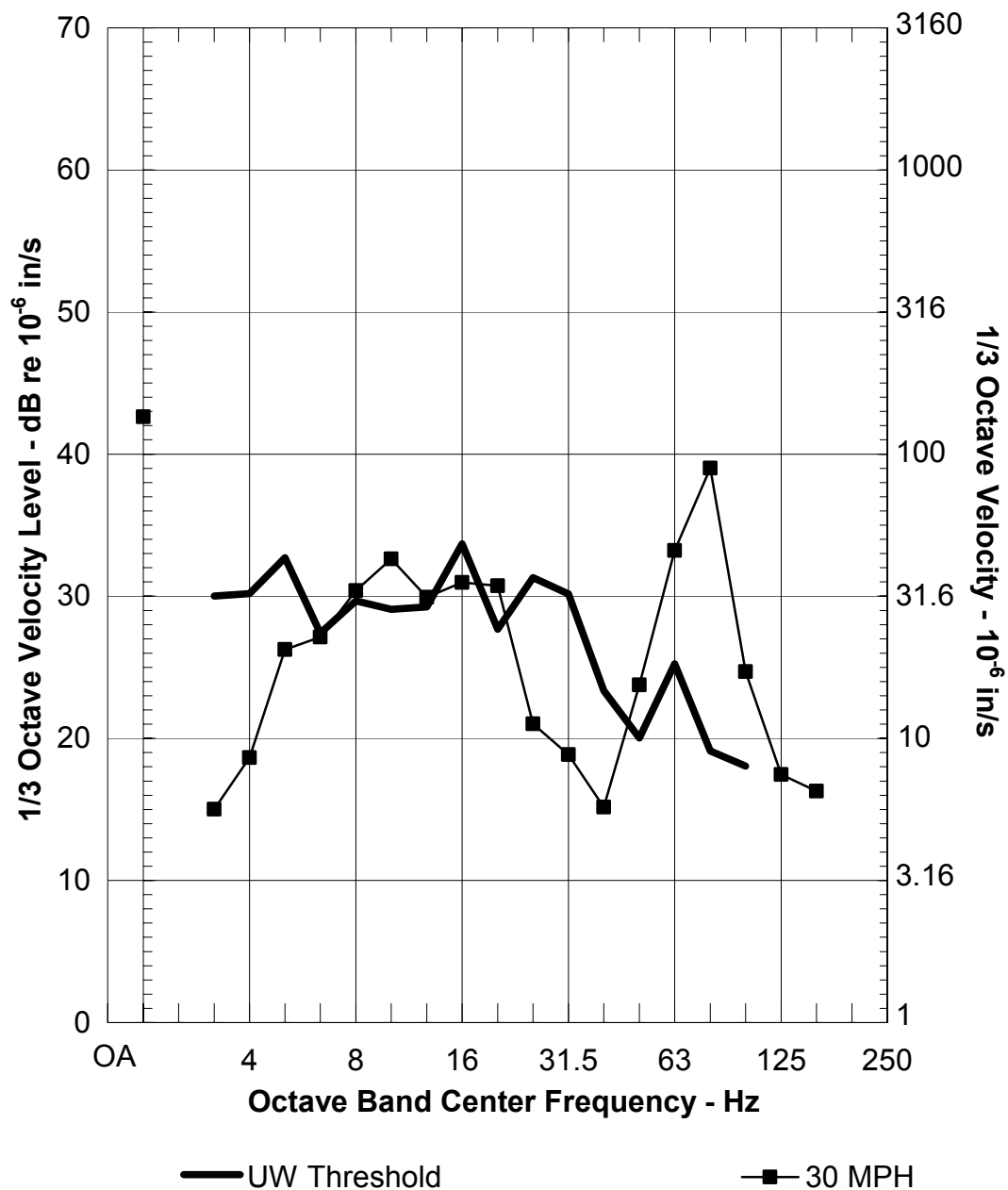
**18) Bioengineering Vibration At Ground Surface
Numerical Model Prediction
VTA FDL, Two Simultaneous Trains, 16 Hz Floating Slab
1612 ft Offset, 100 ft Predicted Depth**

Figure E-18 Bioengineering/Genomics



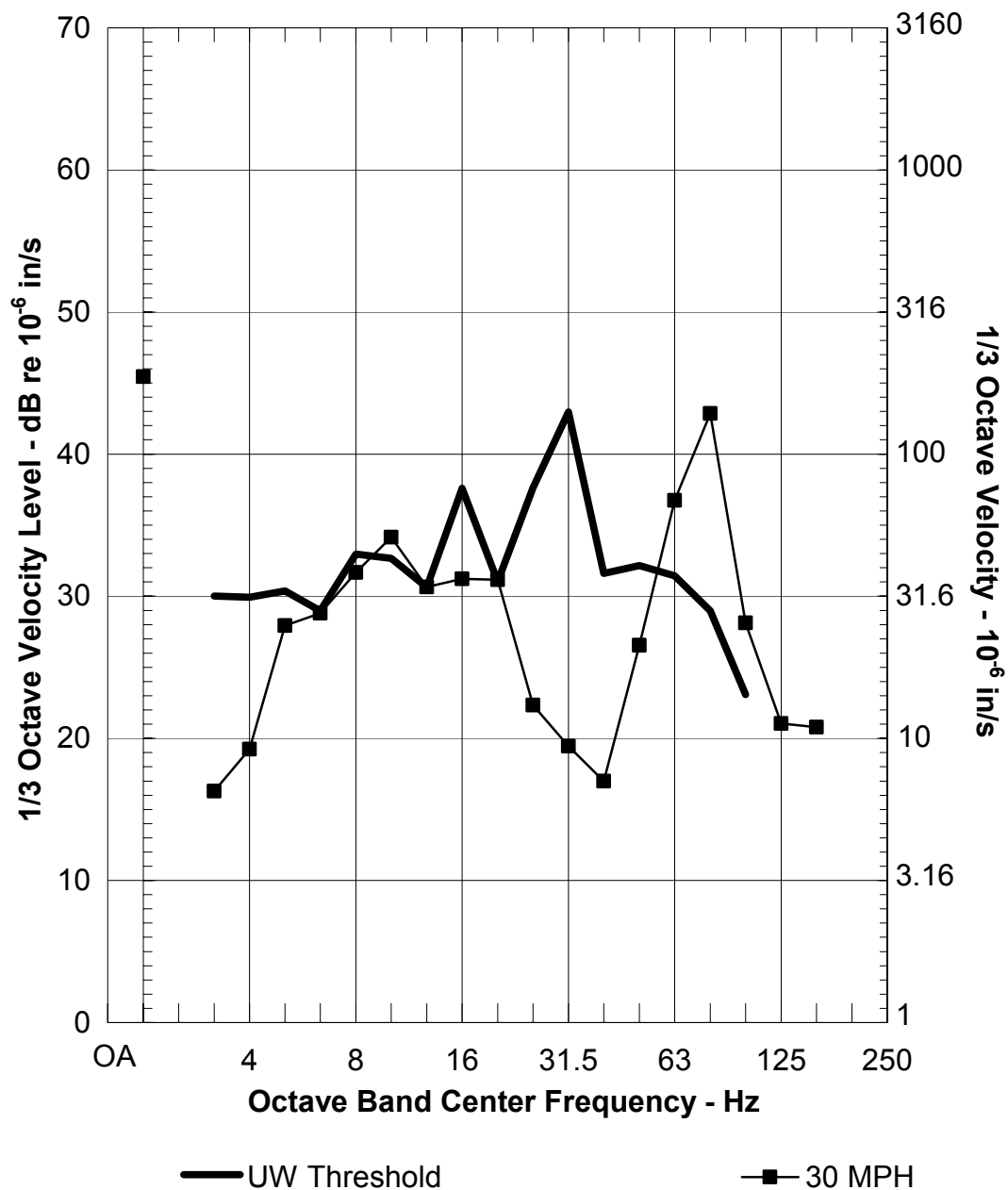
19) Fluke Hall Vibration At Ground Surface
Numerical Model Prediction
VTA FDL, Two Simultaneous Trains, 16 Hz Floating Slab
333 ft Offset, 100 ft Predicted Depth

Figure E-19 Fluke Hall



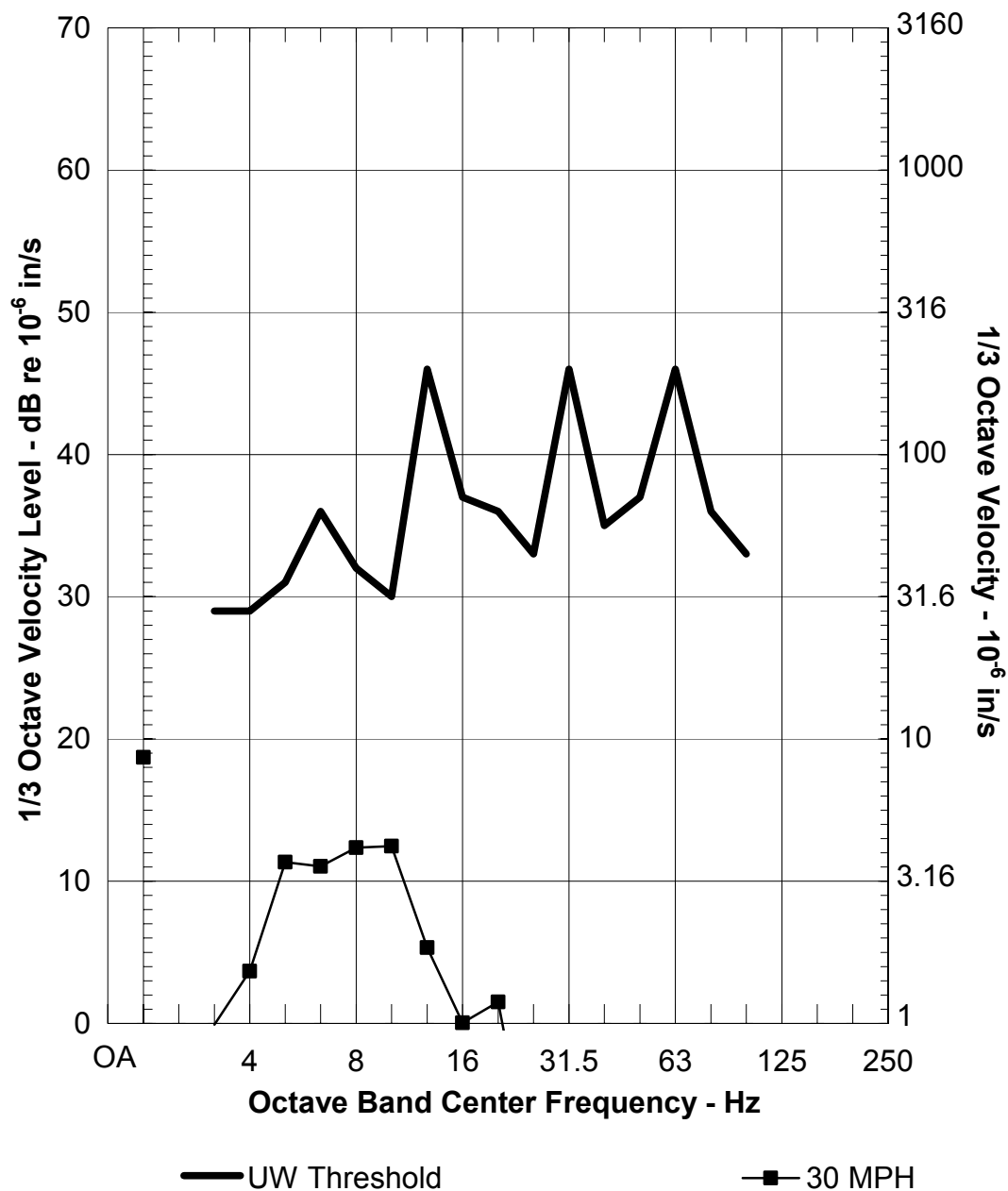
20a) ME Building Vibration At Ground Surface
Global Quadratic LSR
VTA FDL, Two Simultaneous Trains, 16 Hz Floating Slab
105 ft Offset, 115 ft Predicted Depth

Figure E-20 Mechanical Engineering Building



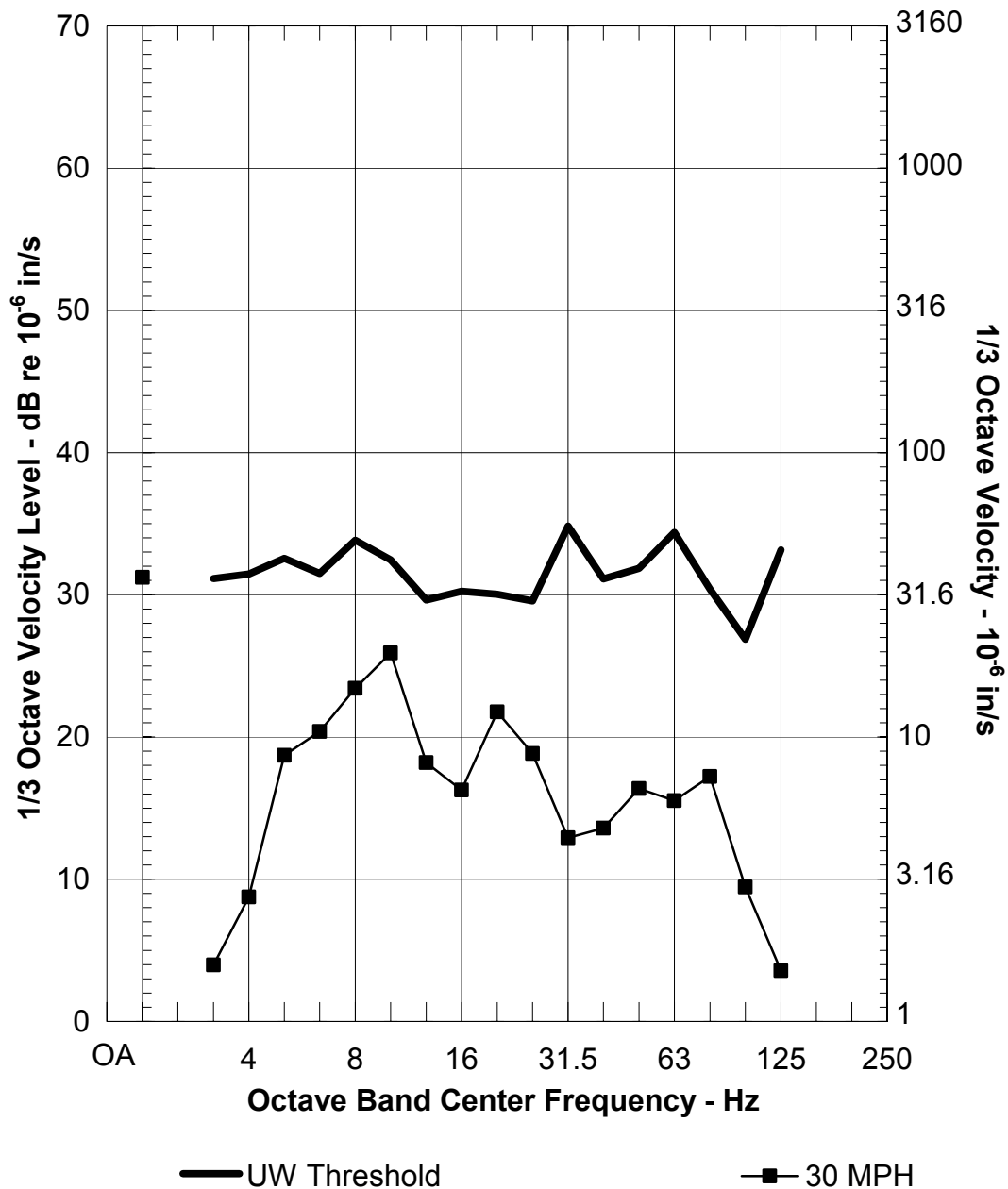
20b) ME Annex Vibration At Ground Surface
Physical Model LSR
VTA FDL, Two Simultaneous Trains, 16 Hz Floating Slab
9 ft Offset, 115 ft Predicted Depth

Figure E-21 Mechanical Engineering Annex



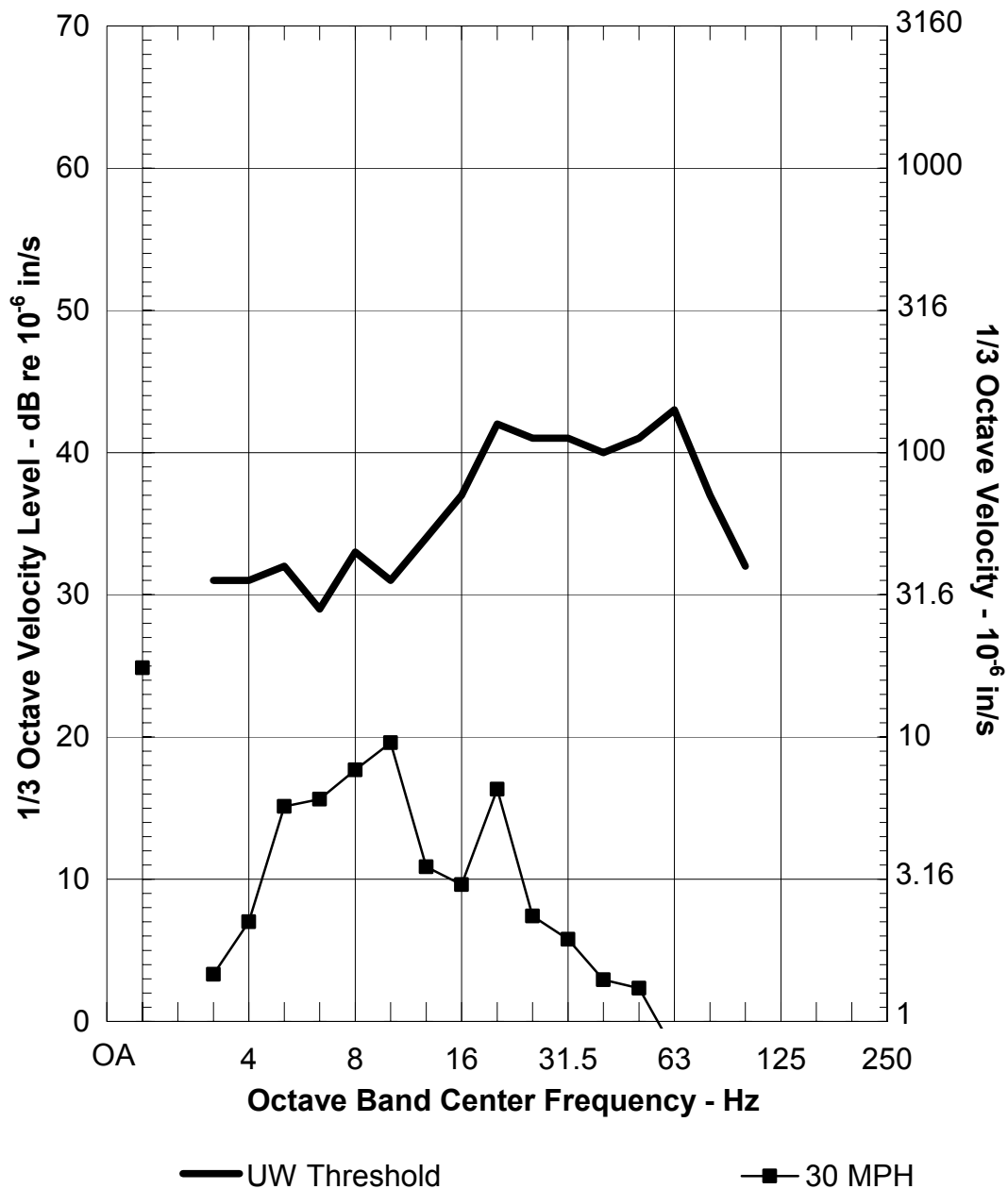
**21) Ocean Sciences Vibration At Ground Surface
Numerical Model Prediction
VTA FDL, Two Simultaneous Trains, 16 Hz Floating Slab
2056 ft Offset, 100 ft Predicted Depth**

Figure E-22 Ocean Sciences



22) CHDD Vibration At Ground Surface
Numerical Model Prediction
VTA FDL, Two Simultaneous Trains, HCDF Fastener
753 ft Offset, 100 ft Predicted Depth

Figure E-23 Center on Human Development and Disability



**23) Fisheries Center Vibration At Ground Surface
Numerical Model Prediction
VTA FDL, Two Simultaneous Trains, HCDF Fastener
1242 ft Offset, 100 ft Predicted Depth**

Figure E-24 Fisheries Center